Biochimica et Biophysica Acta 1861 (2017) 2942–2955

Contents lists available at ScienceDirect

Biochimica et Biophysica Acta

journal homepage: www.elsevier.com/locate/bbagen

Potential role of Apoptosis Inducing Factor in evolutionarily significant eukaryote, *Dictyostelium discoideum* survival

Ashlesha A. Kadam, Tina Jubin, Hina A. Mir, Rasheedunnisa Begum *

Department of Biochemistry, Faculty of Science, The Maharaja Sayajirao University of Baroda, Vadodara, 390 002, Gujarat, India

ARTICLE INFO

Article history:
Received 16 April 2016
Received in revised form 27 August 2016
Accepted 16 September 2016
Available online 20 September 2016

Keywords:
Apoptosis inducing factor
Reactive oxygen species
Mitochondrial membrane potential
Dictyostelium discoideum

ABSTRACT

Apoptosis Inducing Factor (AIF), a phylogenetically conserved mitochondrial inter-membrane space flavoprotein has an important role in caspase independent cell death. Nevertheless, AIF is also essential for cell survival. It is required for mitochondrial organization and energy metabolism. Upon apoptotic stimulation, AIF induces DNA fragmentation after its mitochondrio-nuclear translocation. Although it executes critical cellular functions in a coordinated manner, the exact mechanism still remains obscure. The present study aims to understand AIF's role in cell survival, growth and development by its down-regulation in an interesting unicellular eukaryote, *D. discoideum* which exhibits multicellularity upon starvation. Constitutive *AIF* down-regulated (dR) cells exhibited slower growth and delayed developmental morphogenesis. Also, constitutive *AIF* dR cells manifested high intracellular ROS, oxidative DNA damage and calcium levels with lower ATP content. Interestingly, constitutive *AIF* dR cells showed amelioration in cell growth upon antioxidant treatment, strengthening its role as ROS regulator. Under oxidative stress, *AIF* dR cells showed early mitochondrial membrane depolarization followed by AIF translocation from mitochondria to nucleus and exhibited necrotic cell death as compared to paraptoptic cell death of control cells. Thus, the results of this study provide an exemplar where AIF is involved in growth and development by regulating ROS levels and maintaining mitochondrial function in *D. discoideum*, an evolutionarily significant model organism exhibiting caspase independent apoptosis.

1. Introduction

Mitochondria play a major role in several cellular processes such as redox metabolism [1], energy production [2], ion homeostasis [3], steroid synthesis [4], apoptosis [5,6] etc. It acts as a reservoir of suicidal proteins involved in mitochondrial mediated apoptosis. The outer mitochondrial membrane gets disrupted followed by a loss of mitochondrial membrane potential ($\Delta\psi m$) in response to cell death signals [7,8]. This leads to the release of two vital pro-apoptogenic proteins from inter-membrane space into cytosol viz., cytochrome c and Apoptosis Inducing Factor (AIF) [9,10].

AIF is a phylogenetically ancient flavoprotein of 67 kDa, containing a mitochondrial localization sequence (MLS) at the N-terminus, two nuclear localization sequences (NLS), a FAD binding domain, a NADH binding domain and a C-terminal domain where the proapoptotic activity of the protein resides [11]. AIF displays functional but not structural similarity with bacterial ferredoxin reductase [12]. Interestingly, AIF has dual role in cell survival and cell death [11]. *AIF* up-regulation and down-regulation studies suggest that AIF might be essential for maintaining and organizing mitochondrial respiratory complex I assembly [13,14]. AIF deficiency also leads to growth arrest in *D. melanogaster*, which showed defective complex I function and reduced ATP levels [15].

Moreover, AIF due to its oxidoreductase and ROS scavenging activities [16,17] is involved in cell protection under stress conditions. Cerebella of harlequin mutant mice (80% loss in AIF) showed increased catalase and total glutathione levels, thus resulting in oxidative stress [14]. Nevertheless, AIF deficient embryonic stem cells and siRNA-treated HeLa cells failed to show oxidative stress suggesting AIF may not have antioxidant property [13]. Thus, the role of AIF in regulating ROS levels is still elusive.

In addition to its oxidoreductase function, AIF is also involved in apoptosis induction [18,19]. This apoptogenic activity is independent of its oxidoreductase function [20]. It was shown that the human colon cancer cells having mutation in N-terminal of PRG3 (AIF homologue) lacking oxidoreductase activity, preserves its apoptogenic activity [21]. Upon apoptotic insult, AIF translocates from mitochondria to nucleus where it interacts with DNA and disrupts chromatin structure leading to chromatinolysis (50 kbp) by recruiting nucleases or proteases [10,19]. The mitochondrio-nuclear translocation of AIF and large scale DNA fragmentation are the hallmark features of caspase independent cell death in mammalian and *D. discoideum* cells [22].

Our previous studies showed that AIF is a downstream effector in PARP and staurosporine induced caspase independent cell death in

* Corresponding author.
E-mail address: rasheedunnisab@yahoo.co.in (R. Begum).

http://dx.doi.org/10.1016/j.bbagen.2016.09.021
0304-4165/

D. discoideum [23,24]. *D. discoideum* is an evolutionarily conserved model organism showing both unicellular as well as multicellular forms in its life cycle [25,26], thus offering a model system to study the function of AIF in growth and development [27]. Also *D. discoideum*, being caspase independent, aids to study the mechanism of AIF in caspase independent paraptotic cell death. Arnoult et al., (2001) [28] reported that AIF (DdAIF) is required for cell death in *D. discoideum*, however, its role in cell survival and development are not yet understood. Hence, the present study aims to explore the involvement of AIF in *D. discoideum* growth, development and cell death. Our results suggest the importance of AIF in *D. discoideum* growth and development and reinstated its role in caspase independent cell death. Our results also strengthen AIF's role as a ROS regulator and in maintenance of the mitochondrial function.

2. Materials and methods

2.1. Cells and culture conditions

Dictyostelium discoideum (Ax-2 strain) which is an axenic derivative of Raper's wild type NC-4 was used. Unicellular *D. discoideum* cells were cultured in HL5 medium, pH 6.5 at 22 °C on a rotary shaker at 150 rpm. For maintenance of culture, these cells were grown on non-nutrient agar with *Klebsiella aerogenes* and harvested using standard procedures [29]. For induction of oxidative stress, 0.03 mM H_2O_2 (cumene H_2O_2) (paraptotic dose) and 0.05 mM H_2O_2 (necrotic dose) were used [23].

2.2. Antisense mediated down-regulation of AIF

In order to down-regulate the expression of *AIF*, constitutive and prestalk specific down-regulation of *AIF* was done by antisense strategy. Constitutive down-regulation of *AIF* was under actin promoter whereas prestalk specific down-regulation of *AIF* was under EcmB (inducible) promoter which is expressed only during slug stage of *D. discoideum*. 5′ region of *AIF* amplicon (390 bp) was directionally cloned into constitutive *D. discoideum* expression vector (pTX-GFP) by replacing GFP using *Xba*I and *Kpn*I enzymes and prestalk specific vector (pEcmB-Gal) using *Xho*I and *Cla*I enzymes. *D. discoideum* cells were electroporated with both confirmed clones (pTX-*AIF* and pEcmB-*AIF*) using *GenePulser* Xcell™ electroporator (BioRad, Hercules, CA, United States of America) [30] and transformants were selected using G418 (Geneticin) (100 μg/ml). For Dose dependent expressions of AIF, transformants were selected using various concentrations of G418 i.e. 20–100 μg/ml. pTX and pEcmB vector transformed cells were used as the respective vector controls for our further studies. *AIF* down-regulation was confirmed by monitoring gene specific expression of *AIF* by Real Time-PCR and *RNLA* was used as an internal control. Prestalk specific *AIF* down regulation was monitored during slug stage of *D. discoideum* development.

For mRNA expression and growth profile studies, both control (wild type *D. discoideum*) and vector control (pTX-control & pEcmB-control) cells were assessed; whereas for the rest of the experiments, pTX-control cells were used as the control.

2.3. Cell growth assay

To study growth profile of *AIF* dR cells, mid log phase cells at a density of 0.6×10^6 cells/ml were inoculated in HL5 medium. Cells were collected after every 2 h till 12 h and thereafter at 12 h interval till 144 h for cell count. The cell suspension was mixed with trypan blue solution [0.4% (*w*/*v*) in phosphate buffer] in the ratio of 2:1. After ~2 min. incubation, cell count was taken using haemocytometer [31]. To analyze the effect of antioxidant on cell growth, the experiment was done in the presence of 10 mM glutathione (GSH).

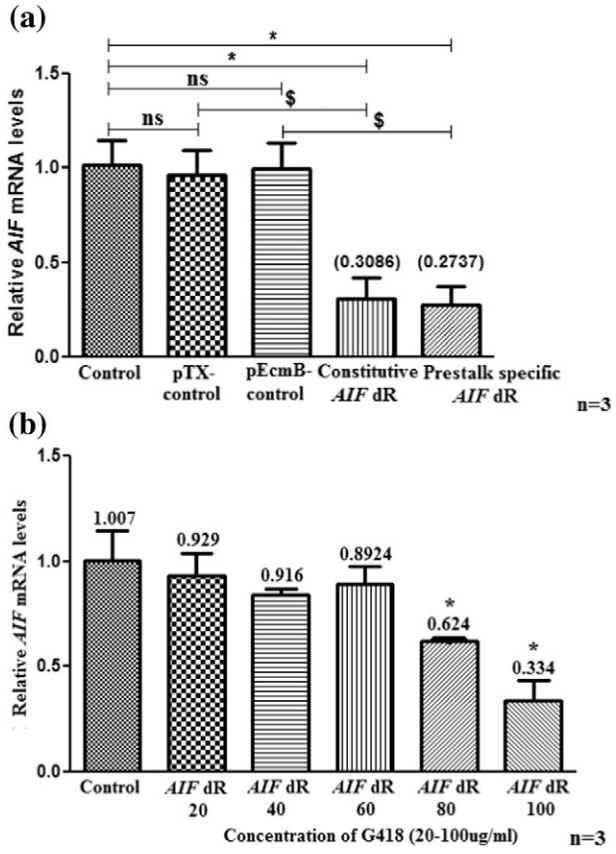

Fig. 1. (a) Functional characterization of *AIF* antisense. Real Time-PCR analysis showed ~70% & ~73% reduction in *AIF* transcript levels in constitutive and prestalk specific *AIF* dR cells respectively. Data are representative of three independent experiments which represented as mean ± S.E. ns- non significant; $^{*}p < 0.05$ compared to control; $^{\$}p < 0.05$ compared to respective vector controls (pTX-control & pEcmB-control). (**b**) **Dose dependent effect of G418 on expression *AIF*.** Real Time-PCR analysis showed dose dependent reduction in *AIF* transcript levels in constitutive *AIF* dR cells at 20, 40, 60, 80 and 100 μg/ml of G418 compared to control cells. Data are representation of SEM values of three independent experiments. $^{*}p < 0.05$ compared to control.

2.4. Cell cycle analysis

Cell cycle was analyzed by flow cytometry using Propidium Iodide (PI) (Sigma, USA). Mid log phase cells were fixed with drop wise addition of 70% ethanol and incubated at 4 °C overnight. Fixed cells were resuspended in staining solution (TritonX-100, DNase free RNase

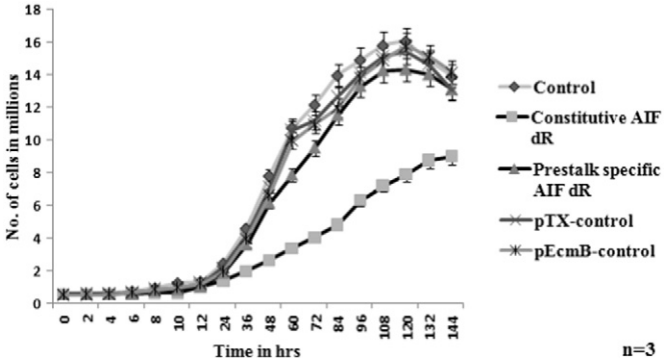

Fig. 2. Effect of *AIF* down-regulation on *D. discoideum* growth. Constitutive *AIF* dR cells exhibited slower growth rate whereas growth in prestalk specific *AIF* dR cells was comparable to control cells. pTX-control and pEcmB-control were used as respective vector controls. Data are representation of SEM values of three independent experiments. $^{**}p < 0.01$ compared to control and pTX-control.

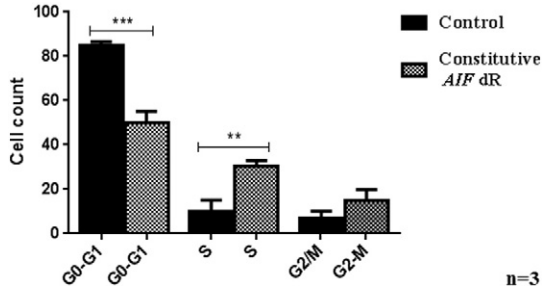

Fig. 3. Cell cycle analysis by FACS in constitutive *AIF* dR cells. Significant increase in percentage of cells in S phase and decrease in percentage of cells in G0-G1 phase was seen in constitutive *AIF* dR cells at 48 h. Data are representative of three independent experiments and represented as mean ± S.E. $^{**}p < 0.01$ compared to control, $^{***}p < 0.001$ compared to control.

and Propidium Iodide) and incubated for 30 min followed by FACS analysis [32]. Quantification was done by flow cytometry using FACS ARIA III (BD Biosciences) and data were analyzed with FACSDiva software.

2.5. Cell morphology

Transmission Electron Microscopy (TEM) was performed to observe morphology of *D. discoideum* vegetative cells. Log phase cells were fixed with 2.5% glutaraldehyde and 2.0% paraformaldehyde in 0.1 M phosphate buffer, pH 7.4, at 4^0 C for 6–8 h. The pellet was then stored in paraformaldehyde and 0.1 M phosphate buffer (1:1) and processed for microtomy [33]. Sections were obtained with a Reichert Ultracut E ultramicrotome, stained and examined with a Morgagni 268D Transmission Electron Microscope.

2.6. Development

To study the effect of *AIF* down-regulation on *D. discoideum* development, mid log phase cells were washed twice and resuspended in 1× Sorensen's Buffer (SB). This cell suspension was placed on 2% non-nutrient agar and incubated at 22 °C [34]. Images were taken every 2 h till 24 h and thereafter at 12 h interval till 48 h.

2.7. Estimation of NAD^+ and ATP levels

Intracellular NAD^+ levels were determined by enzymatic recycling method [35] using alcohol dehydrogenase to reduce NAD^+ to NADH. NAD^+ levels were estimated at 570 nm spectrophotometrically and protein concentration was estimated by Lowry method [36]. Total cellular and mitochondrial ATP levels were estimated by HPLC in aliquots extracted with alkali [37]. Mitochondria were isolated from log phase vegetative *D. discoideum* cells [38].

2.8. Glucose dependency

To study the dependency of glucose, mid log phase *D. discoideum* cells were washed once with 1× SB and allowed to grow in glucose free HL5 medium (GFM) and cell viability was monitored by trypan blue exclusion method [31].

2.9. Estimation of lactic acid

Lactic acid was estimated in culture medium by HPLC at 4th, 6th and 8th day of cell growth. Log phase vegetative cells (~3.5×10^6) were collected and washed with 1× SB. To measure the production of lactic acid, cells were subjected to freeze lysis and cell lysate was obtained by centrifugation [39]. This suspension was used to analyze lactic acid levels by HPLC [40].

2.10. Estimation of intracellular ROS generation

The production of ROS was measured using DCFDA (2′-7′ dichlorofluorescin diacetate) dye (1 μg/ml). 2.0×10^6 *D. discoideum* cells were washed twice with 1× SB followed by addition of membrane permeable dye, DCFDA and incubated for 15 min at 22 °C with shaking. Fluorescence was measured by Fluorimeter (F7000, Hitachi, Japan) and λ_{ex} and λ_{em} used for these studies were 480 nm and 525 nm respectively [41].

2.11. Electron Paramagnetic Resonance (EPR) spectroscopy

ROS formation was also detected using an EPR-based spin trapping system using POBN [(α-(4-Pyridyl N-oxide)-N-tert-butylnitrone) (Sigma-Aldrich) and Dimethyl Sulphoxide (DMSO) [42]. ~5.0×10^7 *D. discoideum* cells were mixed with POBN (200 mM) and DMSO (250 mM), and analyzed using an X band-EPR spectrometer (EMX series, Bruker, Germany). The spin trapping spectra were obtained by three signal-averaged scans at ambient temperature (25 ± 2 °C). The instrument settings were as follows: power, 15.94 mW; receiver gain, 1×10^5; modulation frequency, 100 kHz; modulation amplitude, 1.0 G; sweep width, 50 G; and sweep time, 40 ms.

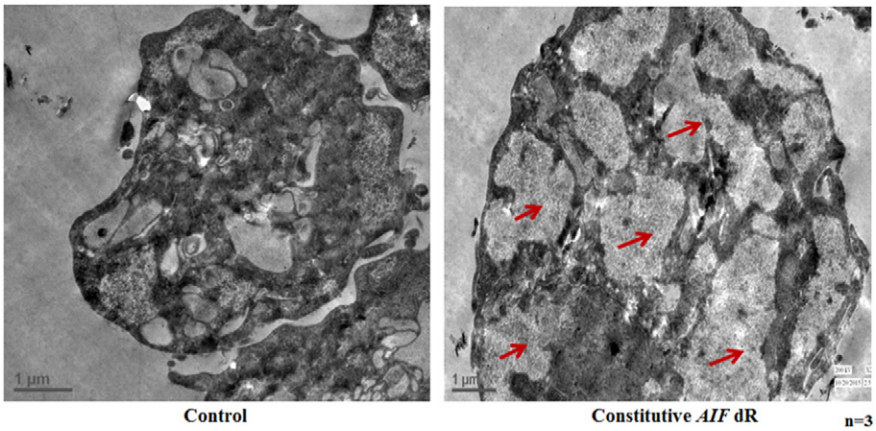

Fig. 4. TEM analysis of constitutive *AIF* dR cells. Vacuole like structures (shown by arrows) were observed in constitutive *AIF* dR cells compared to control cells.

2.12. Estimation of protein carbonyl (PC) content

Protein carbonyl content was estimated by spectrophotometric DNPH (2,4-dinitrophenylhydrazine) assay. 2.0×10^6 cells were washed once with 1× SB followed by its extraction in a final concentration of 10% (*w*/*v*) TCA. The precipitates were then treated with 0.2% DNPH and incubated at room temperature for 1 h. The cell pellets were washed 2–3 times with ethanol:ethyl acetate mixture and then finally dissolved in 6 M guanidine hydrochloride. The absorbance was measured at 370 nm and the protein carbonyl content was calculated [43].

2.13. Fluorimetric estimation of intracellular calcium $[Ca^{2+}]_i$ levels

Intracellular calcium levels were measured using Fura-2AM dye. 2.5×10^6 cells were washed with 1× SB and loaded with 5 μM Fura-2 AM (Molecular probe, USA) and 0.1% Pluronic F-127 (Molecular probe, USA) for 30 min at 22 °C followed by washing with 1× SB. The fluorescence intensities were recorded at 340/380 nm excitation and 510 nm emission by Fluorimeter (F7000, Hitachi, Japan). The ratio of peak amplitude at 340 nm and 380 nm was used to evaluate the calcium levels using the formula, $[Ca^{2+}]_i = K_d\,[(R - R_{min})/(R_{max}\text{-}R)]\beta$ [44].

2.14. DNA damage assay

DNA damage was analyzed using anti-human phospho-histone γ-H2AX (R&D Systems, Minneapolis, MN, USA; 2 μg/ml; rabbit polyclonal) [45]. Cells were incubated with anti-γ-H2AX for 7–8 h followed by secondary anti-rabbit IgG (whole molecule) TRITC conjugate (Sigma, St. Louis, MO, USA; 1:400 dilutions). The nucleus was counterstained with DAPI (1 μg/ml) for 5 min and fluorescence was analyzed by using confocal laser scan fluorescence-inverted microscope (LSM 710; Carl Zeiss, Jena, Germany).

2.15. Analysis of mitochondrial membrane potential (MMP)

Potential sensitive dye $DiOC_6$ (3,3′-dihexyloxacarbocyanine iodide) (Sigma, St. Louis, MO, United States of America) at a concentration of 5 nM was used to assess changes in MMP [46]. Cells were observed under fluorescence microscope (Nikon TE-2000S, Tokyo, Japan) and photographed. Results were expressed as mean fluorescence intensity that was proportional to MMP.

MMP was also measured by flow cytometry, by incubating *D. discoideum* cells ($1–2 \times 10^6$/ml) with 5,5′,6,6′-tetrachloro-1,1′,3,3′-tetraethylbenzimidazol carbocyanine iodide (JC-1) (Molecular Probe, USA) [47] and quantitated by flow cytometry using FACS ARIA (BD Biosciences, Franklin Lakes, New Jersey). Data were analyzed with FACSDiva software.

2.16. Assessment of cell death by AnnexinV-FITC/PI dual staining

2.5×10^6 cells/ml were exposed to different doses of H_2O_2 (0.03, 0.05 mM) in HL5 medium at 22 °C. To differentiate between apoptotic and necrotic cell death, dual staining with Annexin V-FITC (Fluorescein isothiocyanate)/PI was performed using apoptosis detection kit (Molecular Probes, USA) [48]. To distinguish apoptotic cells (Annexin V positive, PI negative) from necrotic cells (Annexin V positive, PI positive), cells were analyzed by Zeiss confocal laser scan fluorescence-inverted microscope (LSM 710; Carl Zeiss, Jena, Germany).

2.17. Monitoring AIF release

AIF translocation to the nucleus was monitored by immunofluorescence [49]. Rabbit anti-AIF polyclonal antibodies (1:1000 dilution) against amino acids 151–180 of human AIF (Cayman Chemical, USA) and anti-rabbit IgG (whole molecule) TRITC conjugate (Sigma, St. Louis, MO, United States of America), (1:400 dilution) were used. Nuclear counterstaining with DAPI (4′, 6 diamidino-2-phenylindole) (1 μg/ml) was performed for 5 min and was analyzed for fluorescence. Cell specimens were observed with confocal laser scan fluorescence-inverted microscope (LSM 710; Carl Zeiss, Jena, Germany).

2.18. Statistical analysis

Data are presented as a mean and standard error of mean (SEM) or standard deviation (SD) as appropriate. Statistical analyses were performed using GraphPad PRISM®6 software. Statistical significance was assessed by Student *t*-test for experiments with single

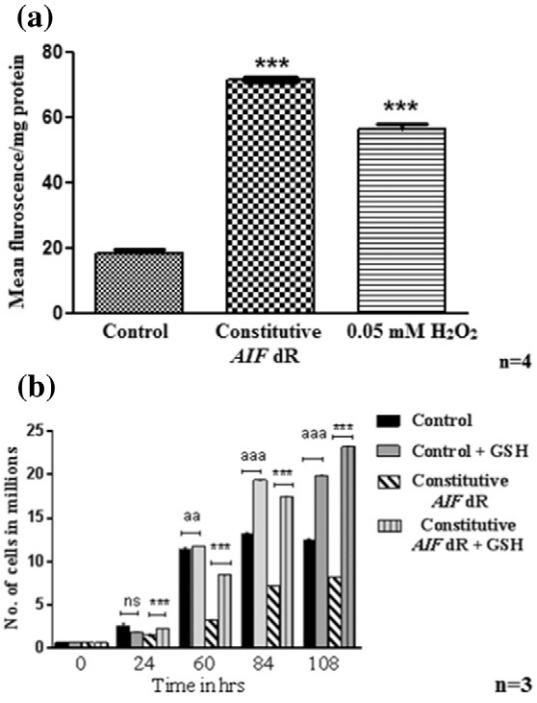

Fig. 5. Assessment of relation between AIF and ROS (a) Fluorimetric estimation of ROS using DCFDA dye. Significant increase in ROS levels was found in constitutive *AIF* dR cells compared to H_2O_2 treated control cells which was kept as a positive control. Data are representation of SEM values of four independent experiments. $^{***}p < 0.0001$ compared to control. **(b) Effect of GSH on growth of constitutive *AIF* dR cells.** 10 mM GSH partially restored the growth of constitutive *AIF* dR cells compared to untreated constitutive *AIF* dR cells. Data are representative of three independent experiments and represented as mean ± S.E. ns- non significant; $^{***}p < 0.0001$ compared to untreated *AIF* dR cells. **(c) EPR profile of *D. discoideum* cells**. The spin trapping spectra were obtained by three signal-averaged scans using EPR spectrometer. POBN adducts were observed in constitutive *AIF* dR cells but not in control cells. 0.05 mM treated control cells were kept as a positive control. **(d) DNA damage in constitutive *AIF* dR cells.** Immunofluorescence staining for DNA damage was done using γ-H2AX Ab (red) and DAPI (blue). Constitutive *AIF* dR cells exhibited γ-H2AX foci formation (pink) indicating DNA damage compared to control cells. 0.03 mM H_2O_2 treated cells were kept as a positive control. **(e) Spectrophotometric determination of Protein Carbonyl (PC) content by DNPH assay.** The PC content was observed to be significantly higher in constitutive *AIF* dR cells compared to control cells. Data are representative of four independent experiments which represented as mean ± S.E. $^{***}p < 0.0001$ compared to control. **(f) ROS levels by DCFDA dye.** Dose dependent increase in ROS levels was found in constitutive *AIF* dR compared to control cells. Data are representation of SEM values of three independent experiments. $^{**}p < 0.01$ compared to control; $^{***}p < 0.001$ compared to control; $^{\$}p < 0.05$ compared to constitutive *AIF* dR (100 μg/ml); $^{\$\$}p < 0.01$ compared to constitutive *AIF* dR (100 μg/ml); $^{\$\$\$}p < 0.01$ compared to constitutive *AIF* dR (100 μg/ml). **(g) Protein carbonyl (PC) content**. Significant increase in PC content was observed in constitutive *AIF* dR cells as concentration of G418 increased from 20–100 μg/ml. Data are representation of SEM values of three independent experiments. ns- non significant; $^{**}p < 0.01$ compared to control; $^{***}p < 0.001$ compared to control; $^{\$}p < 0.05$ compared to constitutive *AIF* dR (100 μg/ml); $^{\$\$}p < 0.01$ compared to constitutive *AIF* dR (100 μg/ml).

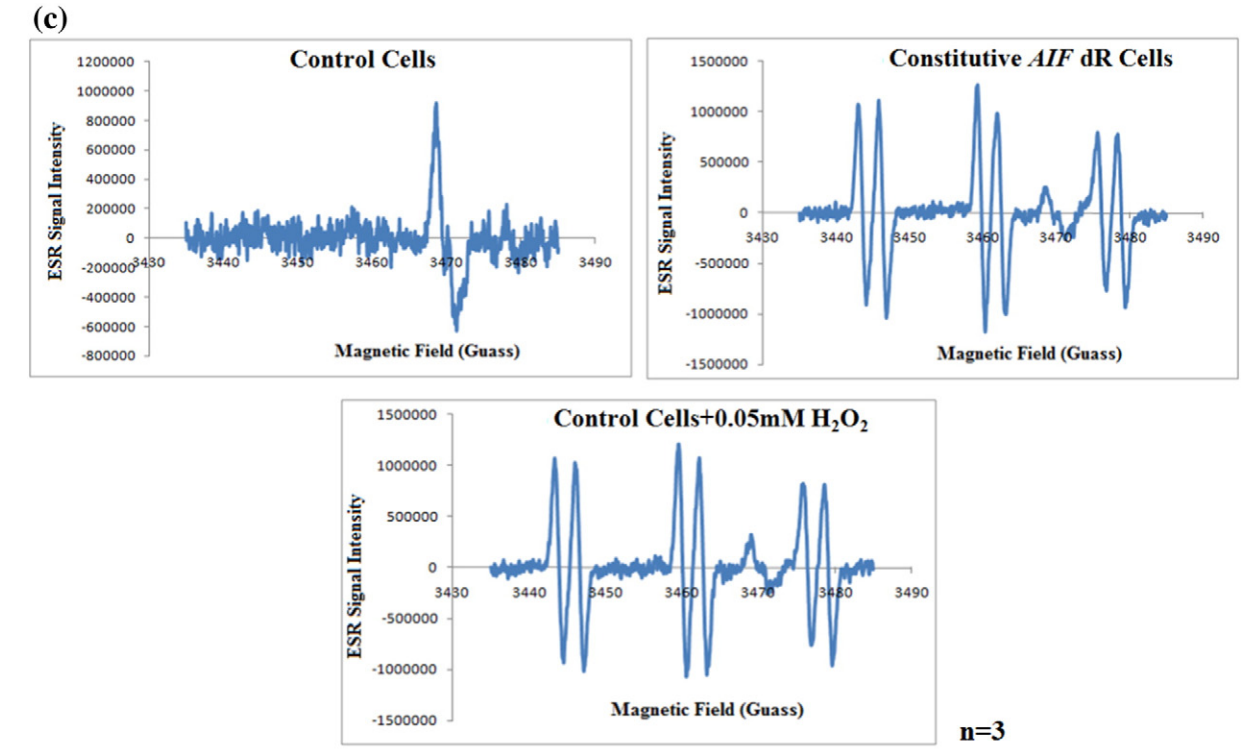

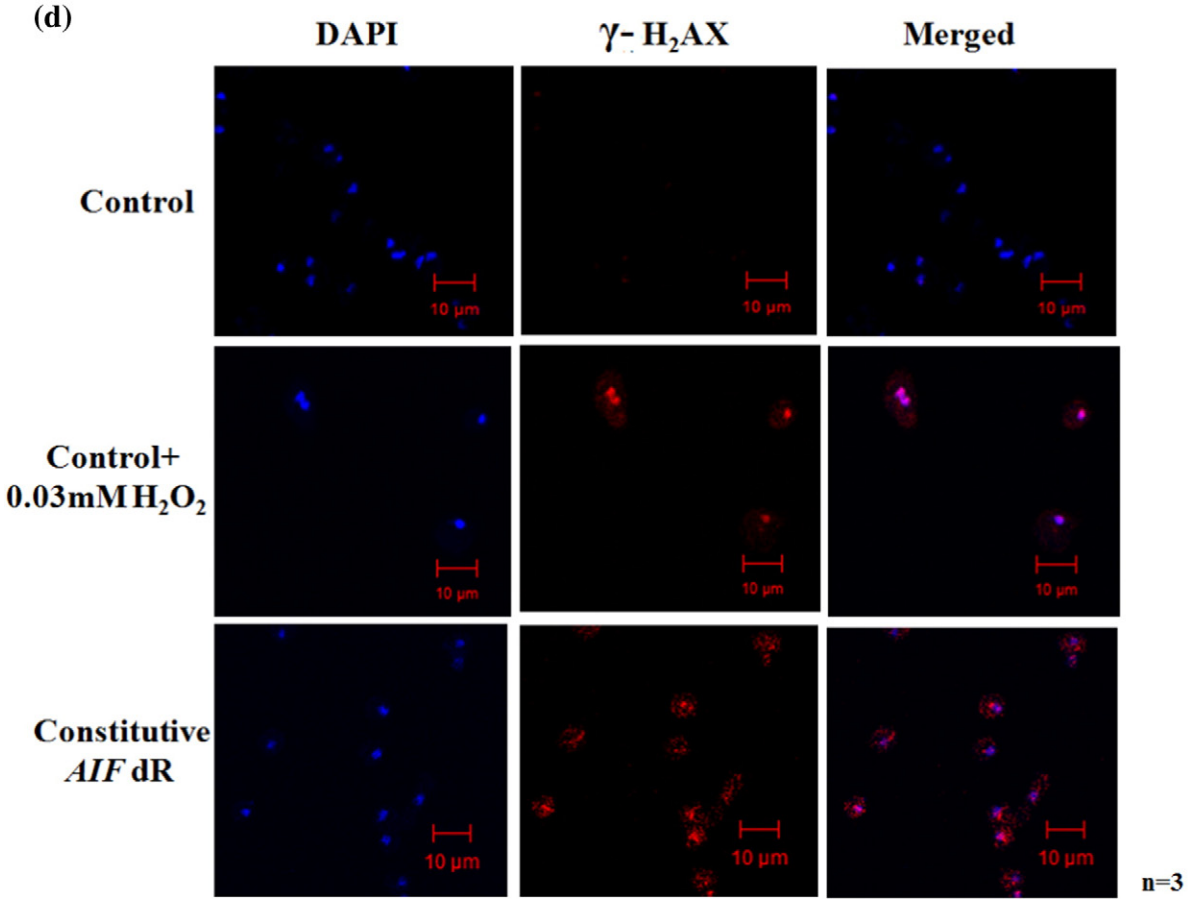

Fig. 5 (*continued*).

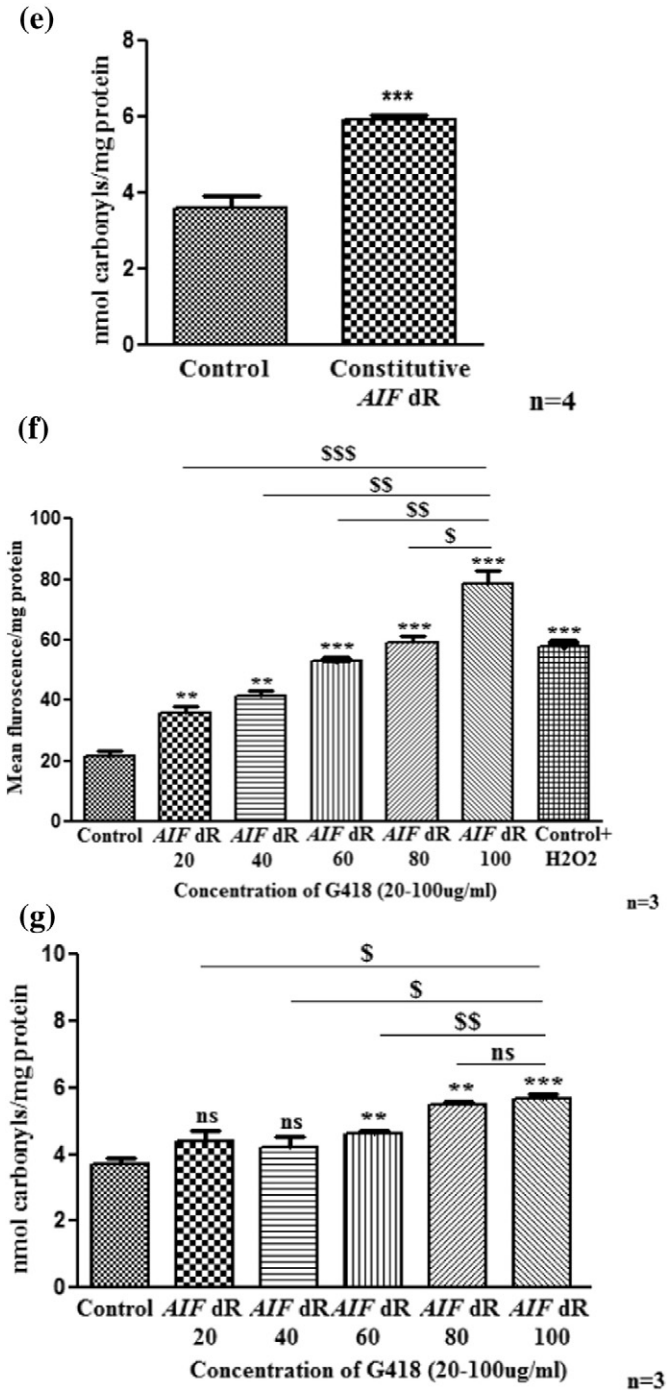

Fig. 5 (*continued*).

comparisons. Data were analyzed according to mean fluorescence intensity and plotted on dot plots or on graphs.

3. Results

3.1. Functional characterization of AIF antisense

Since, AIF knockout is lethal and there are no known inhibitors of AIF, down-regulation of *AIF* was carried out by using antisense strategy to establish constitutive and prestalk specific AIF antisense models. The rationale behind prestalk specific *AIF* antisense was to understand the role AIF in developmental cell death of *Dictyostelium*. *AIF* down-regulation was confirmed by monitoring gene specific expression of *AIF* using Real Time-PCR. *AIF* transcript levels displayed ~70% reduction in constitutive ($p = 0.0149$) and ~73% reduction in pre-stalk specific *AIF* dR cells ($p = 0.0109$) compared to control and the respective vector control cells (pTX-control & pEcmB-control) (Fig. 1a).

Expression of transgene was reported to be increased with increasing concentration of G418 in transformed *Dictyostelium* cells [50]. Hence dose dependent expression of *AIF* was studied under 20–100 μg/ml concentration of G418 by Real Time-PCR. As the concentration of G418 was increased from 20–100 μg/ml, significant reduction in *AIF* transcript levels were observed in constitutive *AIF* dR cells as shown in Fig. 1b.

3.2. To study the role of AIF in Cell Survival

3.2.1. Cell growth profile

Constitutive *AIF* down-regulated (dR) cells exhibited slower growth rate in logarithmic phase as compared to control cells ($p = 0.0016$) as well as pTX-control cells ($p = 0.0184$) (Fig. 2). However, prestalk specific *AIF* dR cells displayed no significant change in growth as compared to control cells ($p = 0.9524$) (Fig. 2). The doubling time of constitutive *AIF* dR cells and prestalk specific *AIF* dR cells were 25.71 ± 2.2 h and 14.37 ± 0.75 h respectively whereas control cells, pTX-control and pEcmB-control cells exhibited doubling time of 14.24 ± 0.77 h, 16.42 ± 2.22 h and 14.95 ± 0.80 respectively.

3.2.2. Analysis of cell cycle

Cell cycle analysis revealed significant decrease in the number of constitutive *AIF* dR cells in G0-G1 phase with a simultaneous increase in the number of cells in S phase at 48 h of growth compared to control cells (Fig. 3) upon constitutive *AIF* down-regulation. This change in the cell cycle profile as compared to control justifies the slower proliferation rate of constitutive *AIF* dR cells.

3.2.3. Cell morphology

In addition, constitutive *AIF* dR cells showed a stressed phenotype. This was confirmed by studying the cellular morphology of constitutive *AIF* dR cells under Transmission Electron Microscope (TEM). TEM analysis revealed vacuole like structures (shown by arrows) in constitutive *AIF* dR cells as compared to control which may be indicative of intrinsic stress in constitutive *AIF* dR cells (Fig. 4).

3.2.4. Assessment of relation between AIF and ROS

Cerebellar granule cells of Harlequin mutant mice demonstrated oxidative stress, suggesting that AIF may be playing a role in ROS homeostasis [14]. Hence, to study the same and also to understand the vacuolated phenotype, ROS levels were monitored. We found enhanced ROS levels in constitutive *AIF* dR cells as compared to control cells (Fig. 5a).

To strengthen this data, we monitored if supplementation of glutathione (GSH) could restore the growth of constitutive *AIF* dR cells by mimicking the function of AIF as GSH is known to maintain the redox status of the cell. Constitutive *AIF* dR cells in presence of 10 mM GSH showed rescue in growth (Fig. 5b) as compared to untreated constitutive *AIF* dR cells suggesting that AIF may be acting as a ROS regulator.

The presence of ROS was further monitored by EPR spectroscopy using POBN as a spin trap. Constitutive *AIF* dR cells exhibited triplet of POBN adducts which were absent in control cells, showing presence of hydroxyl radicals ($OH^{\cdot}$) in constitutive *AIF* dR cells (Fig. 5c).

Elevation in ROS levels may result oxidative damage to DNA and proteins. γ-H2AX foci formation was observed in constitutive *AIF* dR cells as compared to control cells indicating DNA damage (Fig. 5d). Protein carbonylation (PC) is also one of the oxidative stress markers [43] hence, PC content was estimated in constitutive *AIF* dR cells. The results showed that PC content was significantly higher ($p = 0.0004$) in constitutive *AIF* dR cells as compared to control cells (Fig. 5e).

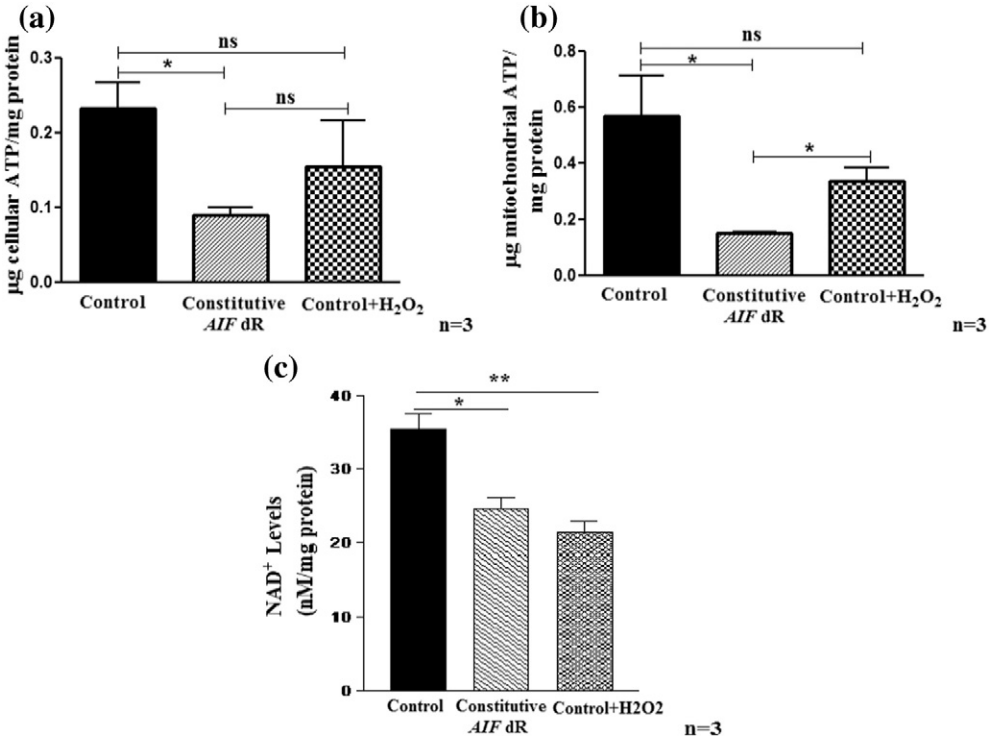

Fig. 6. Estimation of cellular & mitochondrial ATP and NAD^+ levels. (a) & (b) Significant decrease in both cellular & mitochondrial ATP levels respectively were observed in constitutive *AIF* dR cells compared to control cells. 0.03 mM H_2O_2 treated cells were used as positive control. Data are representative of three independent experiments and represented as mean ± S.E. ns- non significant; $^*p < 0.05$ compared to control. (c) Significant reduction in NAD^+ levels was detected in constitutive *AIF* dR cells compared to control cells. 0.03 mM H_2O_2 treated cells were kept as a positive control. Data are representation of SEM values of three independent experiments. $^*p < 0.05$ compared to control.

To study the correlation between AIF and ROS levels, ROS and protein carbonyl content were also measured in constitutive *AIF* dR cells with 20–100 µg/ml G418. Significant increase in ROS levels and protein carbonyl content was observed in constitutive *AIF* dR cells in a dose dependent manner of G418 as compared to control cells (Fig. 5f and g), explaining an inverse relation between reduction of AIF and ROS activity.

3.2.5. Total ATP and NAD^+ levels

Reduced AIF levels induced generation of more ROS due to impaired complex I function and thereby may lead to reduced ATP levels [15]. Hence, high ROS in constitutive *AIF* dR cells may also be suggestive of impaired mitochondrial functioning, which could be established by measuring the ATP and NAD^+ levels. Constitutive *AIF* dR cells exhibited ~60% depletion in cellular ATP levels (Fig. 6a) and ~75% depletion in mitochondrial ATP levels (Fig. 6b). Also, ~30% reduction in NAD^+ levels was observed in constitutive *AIF* dR cells compared to control cells (Fig. 6c). These results clearly indicate mitochondrial impairment and hence lower cellular energy supply owing to which proliferation rates were lower in constitutive *AIF* dR cells.

3.2.6. AIF down-regulation caused glucose dependency

As constitutive *AIF* dR cells have compromised energy production via oxidative phosphorylation, these cells might be dependent on glycolysis to compensate for the reduced mitochondrial ATP levels for survival. Hence, we checked glucose dependency of these cells. This was demonstrated by removal of glucose from growth medium. Constitutive *AIF* dR cells failed to grow in glucose free medium (GFM) compared to control cells indicating that constitutive *AIF* dR cells may be more dependent on glucose for energy production where mitochondrial functioning is intact (Fig. 7a). Production of lactic acid is a downstream metabolic change showing more utilization of glycolysis for energy production. Quantitation of lactic acid showed negligible difference in both control as well as constitutive *AIF* dR cells at 4th, 6th and 8th day

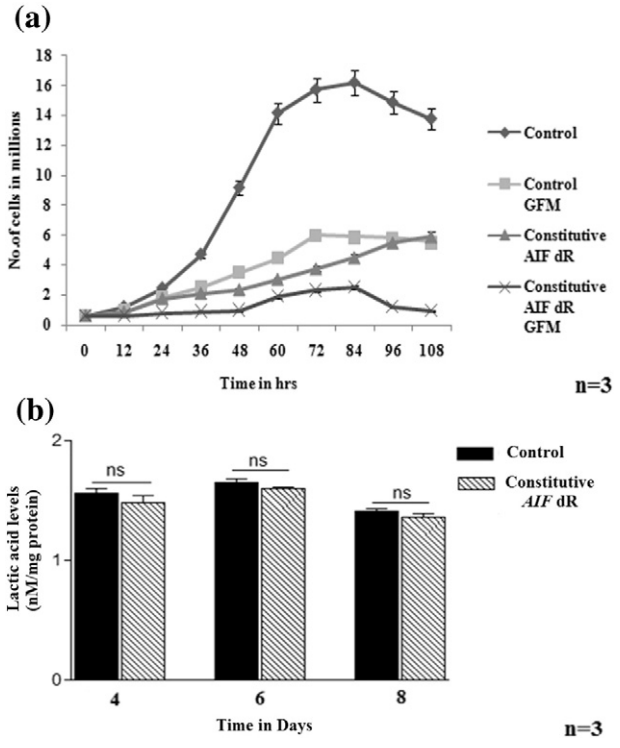

Fig. 7. Glucose dependency of constitutive *AIF* dR cells. (a) Growth profile of *D. discoideum* in glucose free medium (GFM). Constitutive *AIF* dR GFM cells showed arrest in growth in absence of glucose showing high glucose dependency whereas considerable growth was seen in control cells in GFM. Data is a representation of SEM values of three independent experiments. (b) Estimation of Lactic acid by HPLC in constitutive *AIF* dR cells. No significant difference was found in lactic acid levels produced by control and constitutive *AIF* dR cells at 4th, 6th and 8th day of cell growth. Data is a representation of SEM values of three independent experiments.

of cell growth ($p = 0.2927$, $p = 0.1193$ and $p = 0.244$ respectively) (Fig. 7b) because another metabolic pathway might be operating for taking care of the excess lactic acid production.

3.2.7. Free cytosolic calcium [Ca^{2+}] levels

AIF down-regulation and impaired mitochondrial function along with disrupted cellular ROS and ATP levels may affect cytosolic calcium homeostasis. Calcium estimation revealed enhanced free cytosolic calcium in constitutive *AIF* dR cells as compared to control cells (Fig. 8), suggesting the role of AIF in maintaining calcium homeostasis via maintaining potential and integrity of mitochondrial membrane.

3.2.8. Effect of AIF down-regulation on development

As seen above, *AIF* down-regulation led to significant effects in the unicellular stage of *D. discoideum*. Next, we intended to study its effect on developmental phase of the slime mold. Under starvation condition, *D. discoideum* cells aggregate and differentiate into multicellular structures like the loose aggregate, tight aggregate, the migrating slug and finally culminates into a fruiting body with spore case at the tip consisting of viable cells and a stalk composed of dead cells [34]. Constitutive and prestalk specific *AIF* down-regulation led to delayed morphogenesis as compared to control cells (Fig. 9a). Constitutive *AIF* down-regulation displayed a delay in initial stages of development i.e. tipped aggregate to migrating slug transition. Tipped aggregate and migrating slug were seen at 22 h and 36 h in constitutive *AIF* dR cells; while in control cells these stages were observed at 14 h and 18 h respectively. Mature fruiting bodies were formed only at 48 h in constitutive *AIF* dR cells which were smaller as compared to fruiting bodies of control cells at 24 h. Nevertheless, prestalk specific *AIF* down-regulated cells exhibited delayed development during migrating slug (36–38 h) and fruiting body formation (48 h) (Fig. 9a,b).

Regulated ROS levels were found to be essential during multicellular development in *D. discoideum* [51]. Hence defects due to increased ROS levels in constitutive *AIF* dR cells could be rescued by treating cells with an antioxidant, GSH. Supplementation with GSH led to rescue in the developmental delay further reinstating that AIF could behave as a regulator of the levels of ROS (Fig. 9b). Development was augmented by 12 h in GSH treated constitutive *AIF* dR cells as compared to untreated constitutive *AIF* dR cells, the former displaying mature fruiting bodies at 36 h (Fig. 9b) whereas untreated constitutive *AIF* dR cells exhibited at 48 h of treatment (Fig. 9a). Although control cells exhibited fruiting body formation at 24 h with or without GSH, the cells treated with GSH contained aberrant structures that were absent in control untreated cells (Fig. 9b), suggesting that quenched ROS might play a role in proper development [52].

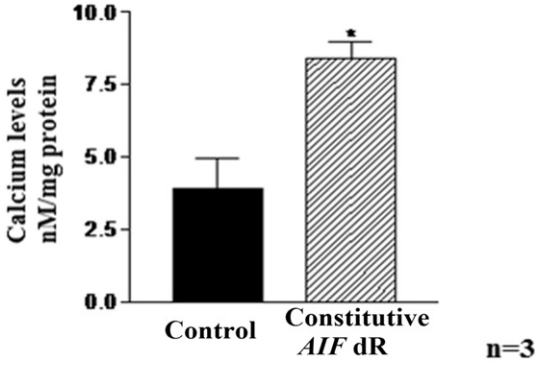

Fig. 8. Intracellular calcium levels in constitutive *AIF* dR cells. Fluorimetric measurement of intracellular calcium levels by Fura-2AM showed increase in $[Ca^{2+}]_i$ levels in constitutive *AIF* dR cells compared to control cells. Data are represented as mean ± S.E. of three independent experiments. $^*p < 0.01$ compared to control.

3.3. AIF in cell death

Cell death can be induced by a number of agents including hydrogen peroxide [53,54,55]. In addition to its cell survival function, AIF is known to be a pro-apoptotic factor that translocates from mitochondria to nucleus and causes large scale DNA fragmentation mainly via caspase independent pathway thus triggering cell death [19]. Next we examined the effect of *AIF* down-regulation on cell fate during oxidative stress.

3.3.1. Mitochondrial membrane potential (MMP)

Studies on MMP changes revealed that constitutive *AIF* dR cells exhibited reduced fluorescence i.e. lower $\Delta\psi m$, even without stress as compared to control cells indicating compromised mitochondrial membrane (Fig. 10a) which validates our earlier results of increased free calcium and lower ATP levels. Reduction in MMP was observed at 2 h post 0.03 mM H_2O_2 treatment with significant MMP loss occurring at 3 h (Fig. 10a) in constitutive *AIF* dR cells. On the contrary, 0.03 mM H_2O_2 treated control *D. discoideum* cells displayed MMP reduction at 3 h with significant reduction at 5 h.

Changes in MMP were confirmed by JC-1 staining. Healthy control cells displayed mitochondrial red JC-1 aggregates in FL2 channel while green JC-1 monomers in apoptotic cells are detectable in FL1 channel. Reduction in red fluorescence was seen in ~95.54% and 95.79% constitutive *AIF* dR cells indicating mitochondrial membrane depolarization at 3 h post 0.03 mM H_2O_2 and 0.05 mM H_2O_2 treatment respectively as compared to ~60% in control cells under both doses as shown in Fig. 10b. Constitutive *AIF* dR cells also showed significant reduction in red fluorescence in 95.42% cells compared to 1.67% control cells. These results were also supported by increased free cytosolic Ca^{2+} levels (Fig. 8).

3.3.2. AIF translocation under oxidative stress

Constitutive *AIF* down-regulated cells treated with 0.03 mM and 0.05 mM doses of H_2O_2 showed early translocation of AIF to nucleus within 3 h (Fig. 11). 0.03 mM H_2O_2 did not cause translocation of AIF whereas 0.05 mM H_2O_2 caused translocation of AIF at 3 h in control cells, suggesting constitutive *AIF* dR cells are more susceptible to oxidative stress induced cell death.

3.3.3. Annexin V-FITC and PI staining under oxidative stress

Based on our earlier results, control *D. discoideum* cells subjected to 0.03 mM H_2O_2 stress showed PS externalization (Annexin-V staining) at 5 h and PI staining at 12 h, while 0.05 mM H_2O_2 showed both Annexin-V staining and PI staining at 3 h [23] suggesting *D. discoideum* exhibits paraptotic cell death at lower dose and necrotic cell death at higher dose of H_2O_2. Nevertheless, 0.03 mM H_2O_2 caused Annexin-V as well as PI staining as early as 3 h in constitutive *AIF* dR cells suggesting that these cells exhibit necrotic cell death under 0.03 mM H_2O_2 treatment as compared to paraptosis in control cells (Fig. 12). Interestingly, constitutive *AIF* dR cells showed PS externalization even under non-oxidant conditions (Fig. 12) further establishing compromised mitochondrial membrane structure. In conclusion, constitutive *AIF* dR cells were more susceptible to oxidative stress.

4. Discussion

Although AIF is engaged in cell death and survival, its mechanism in the latter is not clearly understood. Hence, analyzing the role of AIF in cell survival appears quite promising. The present study investigates the function of AIF in survival as well as death of *Dictyostelium discoideum*.

Our findings suggest that diminution in AIF transcript (Fig. 1a) lead to reduced cell growth (Fig. 2) and delayed developmental morphogenesis (Fig. 9a) compared to control cells accentuating its crucial role in *D. discoideum* cell growth and development. Previous studies have

shown that loss of AIF causes reduction in growth of embryonic stem cells [13] and abortive embryogenesis in mice [56,57]. Our present study also suggests that reduced *AIF* levels in constitutive *AIF* dR cells impedes their growth with enhanced number of cells in S phase as compared to control (Fig. 3).

Mitochondria are the potent source of ROS [8]. AIF, being a mitochondrial inner membrane protein, may maintain the mitochondrial complex I assembly [58]. *AIF* knock-down studies in various cell lines show an increase in superoxide formation via impaired complex I function leading to oxidative stress [59]. High oxidative stress found in harlequin mice also suggests a novel function of AIF as an antioxidant [60,61,62]. On the contrary, studies failed to bolster AIF's ROS scavenging activity [13,63,64]. Increased ROS levels were observed in constitutive *AIF* dR cells as compared to control cells in our

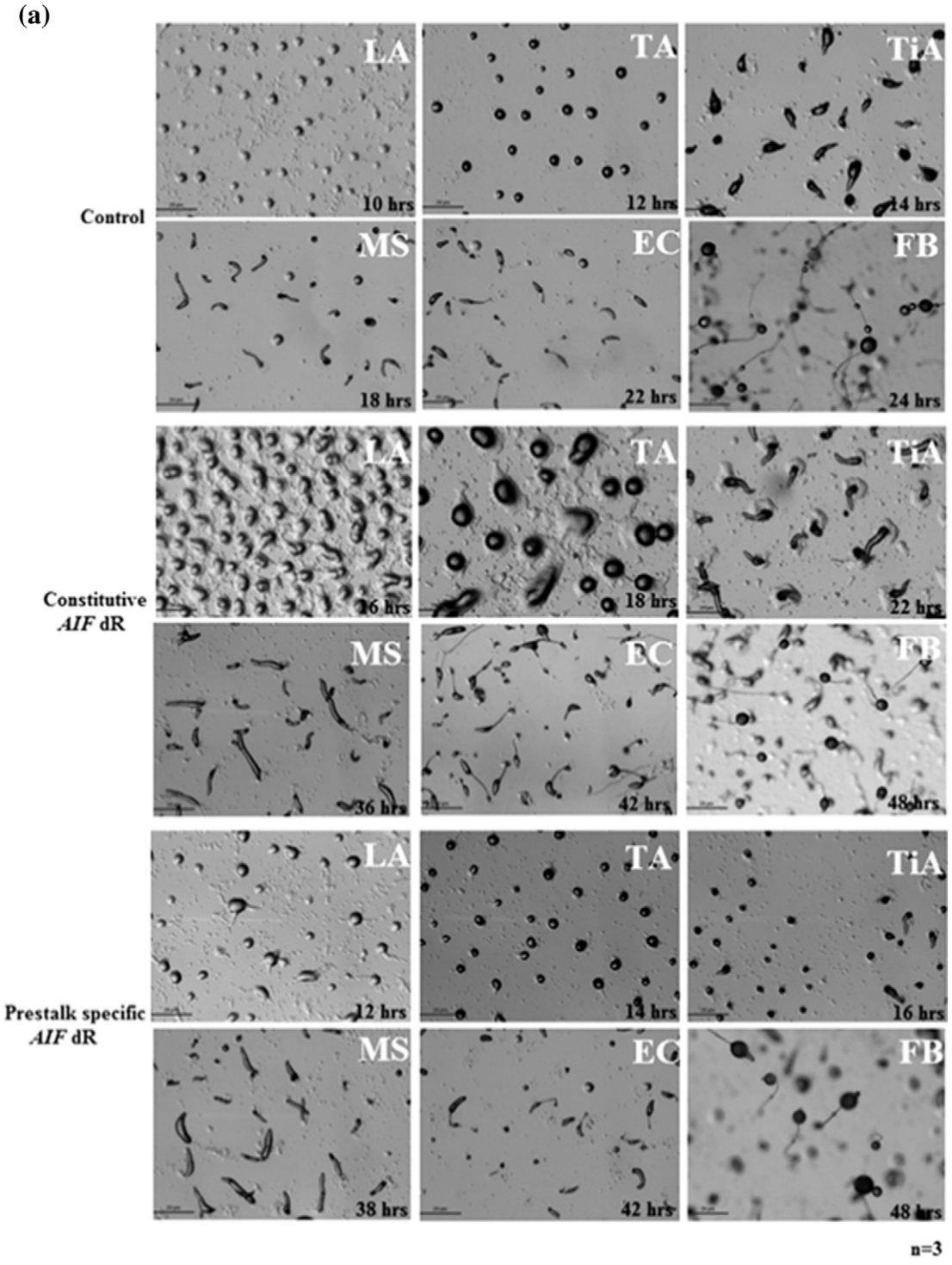

Fig. 9. (**a**) **Effect of *AIF* down-regulation on *D. discoideum* development**. Cells were starved and development was monitored till 48 h. Delayed development was observed in both, constitutive and pre-stalk specific *AIF* dR cells by 24 h and formation of fruiting bodies were observed by 48 h. The developmental stages are named on images (LA- Loose Aggregate, TA- Tight Aggregate, TiA- Tipped Aggregate, MS- Migrating Slug, EC- Early Culminant, FB- Fruiting Body). (Scale bar = 10 μm, Magnification = 4×). Data are representative of three independent experiments. (**b**) **Effect of GSH on development of constitutive *AIF* dR cells.** 10 mM GSH also caused rescue in development of constitutive *AIF* dR cells compared to untreated constitutive *AIF* dR cells (Scale bar = 10 μm, Magnification = 4×).

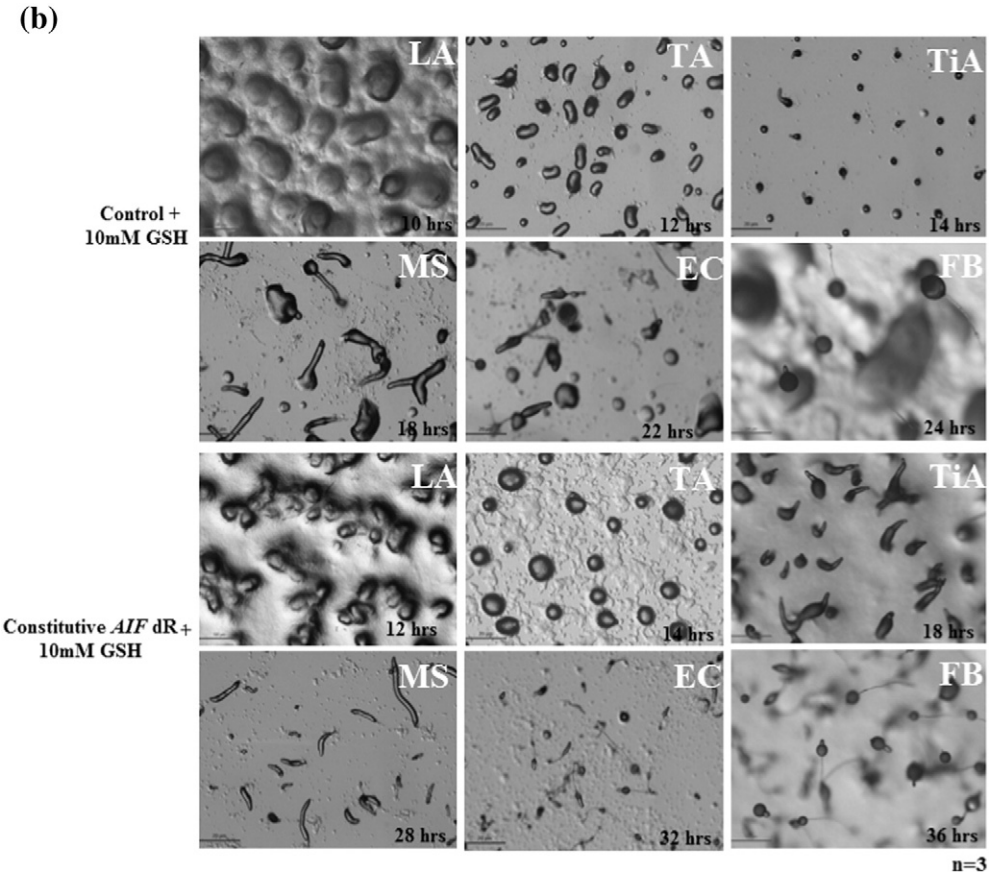

Fig. 9 (*continued*).

studies, confirming AIF as a ROS regulator (Fig. 5a, c, f, g). Perturbations in AIF levels hence may cause electrons (e^-) leakage during transport of electrons in Electron Transport Chain, thus generating ROS. Slower growth rate and development of constitutive *AIF* dR cells may be attributed to elevated ROS levels that were reversed by addition of GSH (Fig. 5b and Fig. 9b), a reducing agent suggesting that it might be mimicking AIF in reducing the reactive oxygen species. The oxido-reductase domain [NAD(P)H and FAD binding domain] of AIF can neutralize the ROS generated by mitochondrial complexes (mainly I and III), and depletion of the former, may weaken the function of these electron chain complexes, thereby increasing the intracellular ROS (Fig. 5a) which could result in oxidative DNA and protein damage (Fig. 5d, e) in constitutive *AIF* dR cells. Impaired mitochondrial activities might also cause disturbances in calcium homeostasis [65]. Since mitochondria is a reservoir of calcium, depolarization of MMP by enhanced ROS in constitutive *AIF* dR cells might also cause leakage of calcium reserves from mitochondria to cytosol, thus enhancing cytosolic calcium which was observed in the present study (Fig. 8).

Redox activity of AIF can stabilize the mitochondrial complex I &/III and reduction in AIF levels can impair their functioning resulting in compromised ATP production and elevated intracellular ROS. It has already been shown that AIF mutant mice turn their energy metabolism towards glycolysis instead of oxidative phosphorylation in order to comply with cellular energy demands [66] thus accumulating lactic acid in the cell [13]. Our studies reveal that constitutive *AIF* dR cells exhibit lower cellular and mitochondrial ATP pool (Fig. 6a, b), glucose dependency (Fig. 7a) and have enhanced glycolysis but fail to accumulate lactic acid (Fig. 7b). This discrepancy in our studies needs to be explored.

AIF is exclusively confined to mitochondria but apoptotic challenges trigger translocation of AIF from mitochondria to nucleus with depolarization of mitochondrial membrane [19]. Oxidative stress due to accumulation of excessive reactive oxygen species triggers cell death [67]. Furthermore, ~80% drop in expression of AIF protein leads to enhanced susceptibility to oxidative stress mediated cell death as observed in harlequin mutant mice [14]. Under oxidative stress, *AIF* down-regulation led to early loss of mitochondrial polarization compared to control cells (Fig. 10). AIF is also reported to be involved in maintenance of mitochondrial potential and morphology [11,68]. In line with these reports, constitutive *AIF* dR cells showed compromised mitochondrial membrane potential even under normal conditions (Fig. 10) implying AIF may be responsible for maintaining mitochondrial morphology. Mitochondrio-nuclear translocation of AIF and exposure of phosphatidylserine on outer leaflet of cell membrane are the characteristics of caspase independent cell death [22]. Our studies show early AIF release and translocation during oxidative stress induced cell death in constitutive *AIF* dR cells (Fig. 11). Annexin V and PI staining were noted positive as both Annexin-V, indicative of PS externalization and PI staining were observed in response to 0.03 mM and 0.05 mM H_2O_2 as early as 3 h. Annexin V staining was detected even in normal conditions in constitutive *AIF* dR cells (Fig. 12). Our outcomes are in agreement with previous findings that *AIF* down-regulation sensitizes the cells to oxidative stress induced apoptotic cell death [14,69,70].

In the current study, we enlighten the dual function of AIF in cell survival mainly assisting in growth and development, regulating free radicals and maintenance of mitochondrial function. However, on cell death signal, increased susceptibility due to AIF loss was demonstrated (Fig. 13).

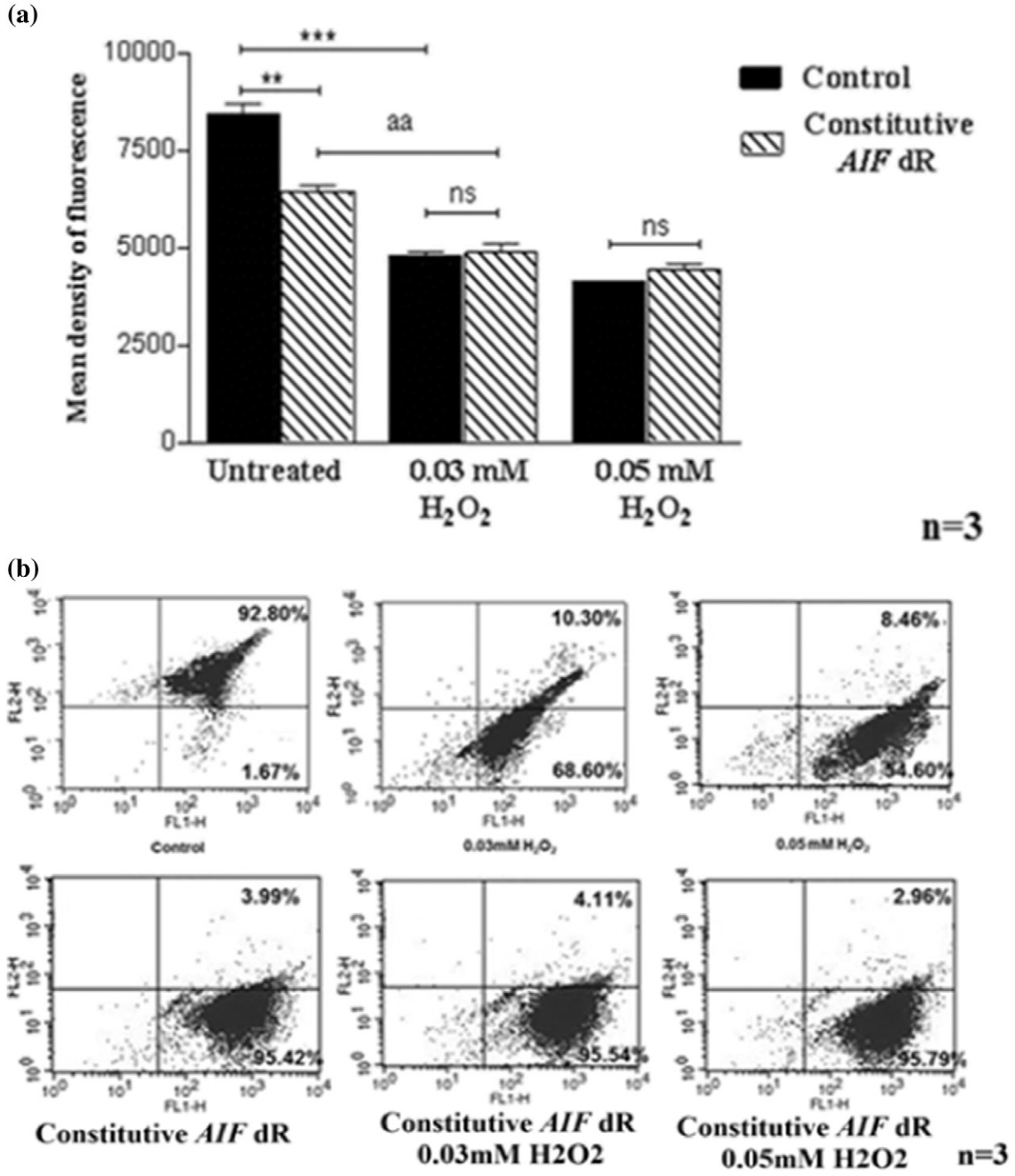

Fig. 10. Mitochondrial membrane potential changes induced by oxidative stress. (a) Densitometric analysis of MMP changes post 3 h treatments of 0.03 mM and 0.05 mM H_2O_2. $^{***}p < 0.001$ compared to oxidative stress; $^{**}p < 0.01$ compared to control; $^{aa}p < 0.01$ compared to oxidative stress. (b) A dot plot of red fluorescence (FL2) versus green fluorescence (FL1) resolved in control cells, constitutive *AIF* dR cells and 0.03 mM and 0.05 mM H_2O_2 treated (3 h) control and constitutive *AIF* dR cells. Constitutive *AIF* dR cells showed ~95% (FL1) cells with compromised mitochondrial membrane potential with and without oxidative stress as compared to 1.67% (FL1) without treatment and ~60% (FL1) in control cells under oxidative stress. Data are representative of three independent experiments. (For interpretation of the references to colour in this figure legend, the reader is referred to the web version of this article.)

5. Conclusion

D. discoideum is an excellent lower eukaryotic developmental model as it can switch from unicellular to multicellular phases. Although physiological role of AIF in *D. discoideum* cell death is well studied, its role in cell survival still remains elusive. We show that AIF is involved in growth and developmental morphogenesis of this organism. Our findings provide evidence for the protective function of AIF as ROS regulator and its essential role in regulation of mitochondrial function thereby affecting cell survival. This study opens new avenues to unravel role of AIF in mitochondrial integrity and functioning.

One of the intriguing facets of most common complex I mitochondriopathies is hypomorphic and/deletion *AIF* mutation

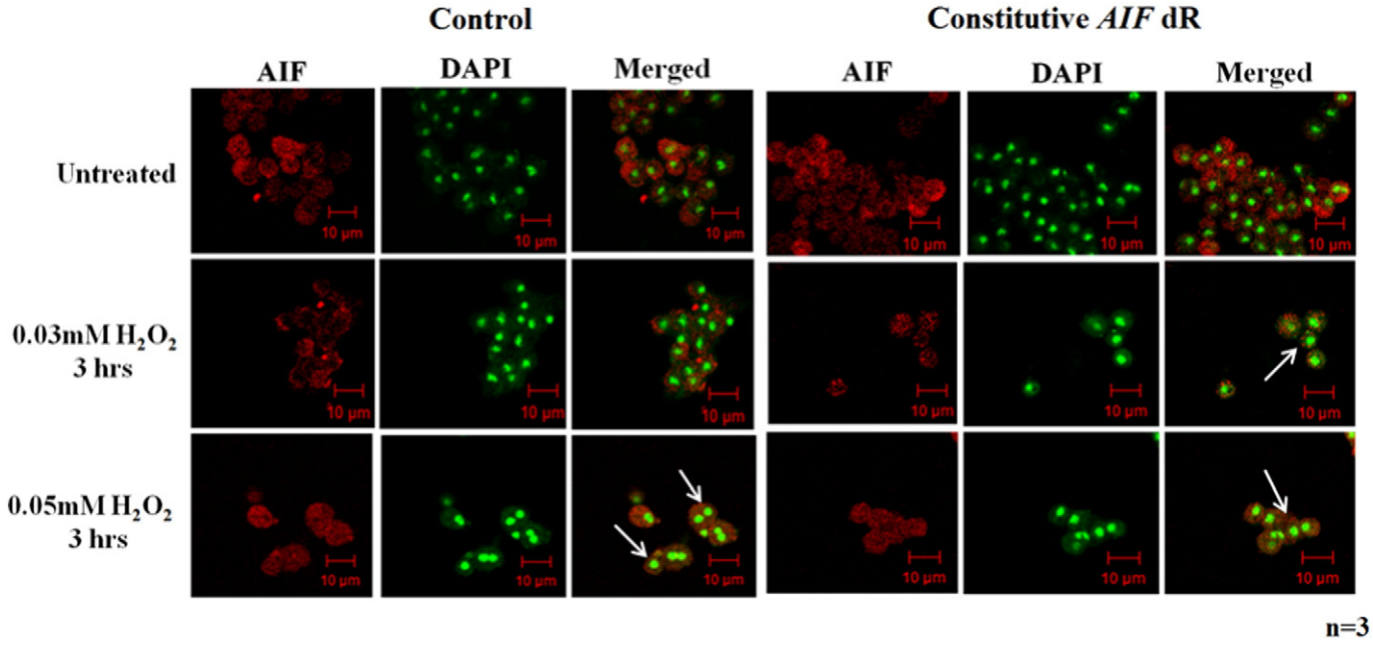

Fig. 11. Mitochondrio-nuclear translocation of AIF. Under oxidative stress, constitutive *AIF* dR cells exhibited AIF translocation from mitochondria to nucleus as early as 3 h. Red color: AIF, Green: DAPI (pseudo color), Fluorescent Green: Translocation of AIF to nucleus.

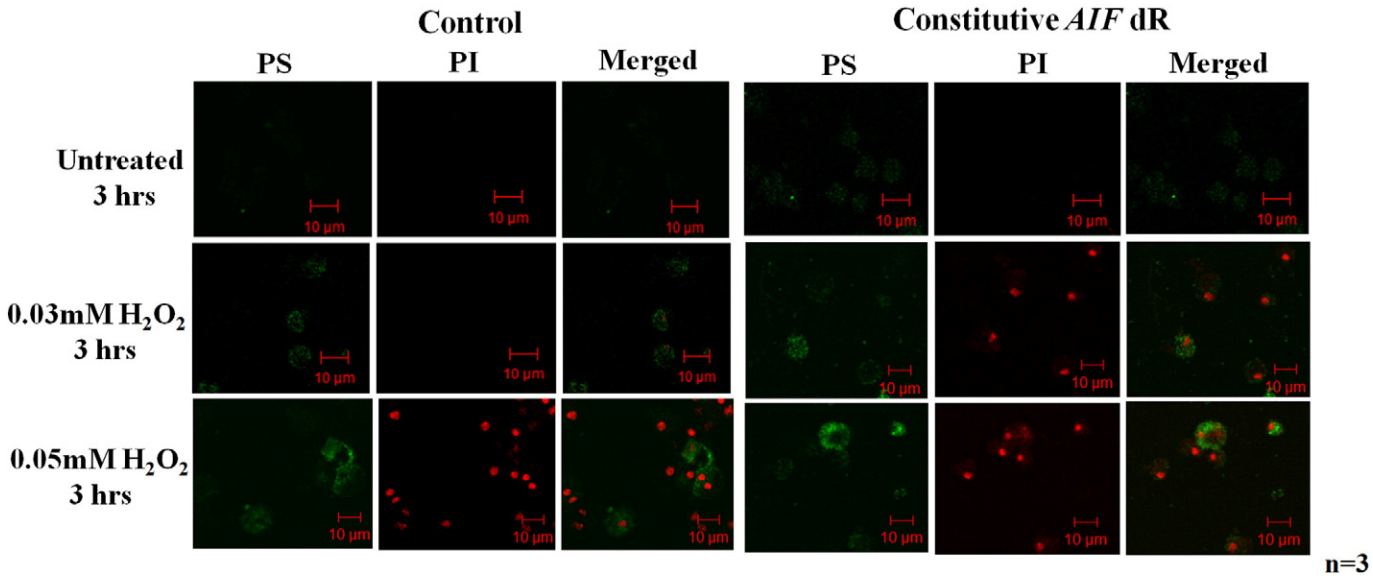

Fig. 12. Annexin V-PI dual staining of constitutive *AIF* dR cells under oxidative stress. Externalization of Phosphatidyl Serine (PS) was observed in constitutive *AIF* dR cells even in non-oxidant conditions. At 0.03 mM and 0.05 mM H_2O_2 doses, constitutive *AIF* dR cells exhibited Annexin V-PI dual positive cells as early as 3 h, while the same effect was found in control cells with 0.05 mM H_2O_2. Data are representative of three independent experiments. Photographs were taken with 60× objective.

which causes >30% of mitochondrial deficiencies. The *AIF* deficient models could be instrumental for therapeutic approaches in complex I and AIF deficiencies thus making it possible to identify target metabolic and stress-response pathways. In addition to this, various underlying mechanisms of AIF's mitochondrial activities would contribute to other diseases such as obesity, diabetes etc.

Transparency document

The Transparency document associated with this article can be found, in the online version.

Acknowledgments

RB thanks Department of Science and Technology, New Delhi (SR/SO/BB-03/2010), Department of Biotechnology, New Delhi (BT/PR4383/BRB/10/1014/2011) and Council of Scientific & Industrial Research, New Delhi [38(1383)/14/EMR-II] for financial support. We also thank DBT-MSUB-ILSPARE program and Dr. Shweta Saran for providing FACS and Confocal facilities. We acknowledge SAIF-AIIMS, New Delhi for TEM facility. We are indebted to Dr. S. Gautam, Dr. W. Surbhi, Dr. R. M. Kadam and Dr. Vinayak for providing EPR spectroscopy facility at Bhabha Atomic Research Center (BARC), Mumbai and helping in analyzing EPR spectroscopy data.

It is to be noted that none of the authors have any Conflict of Interest.

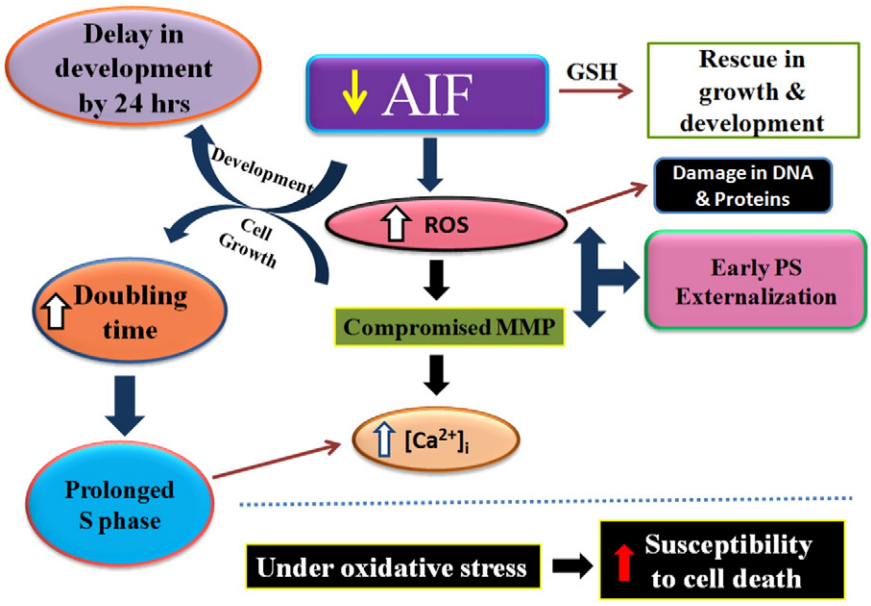

Fig. 13. Effect of *AIF* down-regulation in *D. discoideum*. Loss of AIF affects growth and development of *D. discoideum*. Under oxidative stress, *Dictyostelium* cells are susceptible to cell death upon *AIF* reduction. AIF could regulate ROS levels along with mitochondrial membrane potential and thereby mitochondrial function.

References

[1] R.B. Hamanaka, N.S. Chandel, Mitochondrial reactive oxygen species regulate cellular signaling and dictate biological outcomes, Trends Biochem. Sci. 35 (2010) 505–513.
[2] S. Passarella, A. Atlante, D. Valenti, L. de Bari, The role of mitochondrial transport in energy metabolism, Mitochondrion 2 (2003) 319–343.
[3] G. Hajnoczky, G. Csordas, S. Das, C. Garcia-Perez, M. Saotome, S.R. Sinha, M. Yi, Mitochondrial calcium signalling and cell death: approaches for assessing the role of mitochondrial Ca^{2+} uptake in apoptosis, Cell Calcium 40 (2006) 553–560.
[4] M.F. Rossier, T channels and steroid biosynthesis: in search of a link with mitochondria, Cell Calcium 40 (2006) 155–164.
[5] D.R. Green, Apoptotic pathways: the roads to ruin, Cell 94 (1998) 695–698.
[6] X. Liu, C.N. Kim, J. Yang, R. Jemmerson, X. Wang, Induction of apoptotic program in cell-free extracts: requirement for dATP and cytochrome c, Cell 86 (1996) 147–157.
[7] J.C. Goldstein, N.J. Waterhouse, P. Juin, G.I. Evan, D.R. Green, The coordinate release of cytochrome c during apoptosis is rapid, complete and kinetically invariant, Nat. Cell Biol. 2 (2000) 156–162.
[8] D.R. Green, J.C. Reed, Mitochondria and apoptosis, Science 281 (1998) 1309–1312.
[9] N. Joza, S.A. Susin, E. Daugas, W.L. Stanford, S.K. Cho, C.Y. Li, T. Sasaki, A.J. Elia, H.Y. Cheng, L. Ravagnan, K.F. Ferri, N. Zamzami, A. Wakeham, R. Hakem, H. Yoshida, Y.Y. Kong, T.W. Mak, J.C. Zuniga-Pflucker, G. Kroemer, J.M. Penninger, Essential role of the mitochondrial apoptosis-inducing factor in programmed cell death, Nature 410 (2001) 549–554.
[10] S.A. Susin, E. Daugas, L. Ravagnan, K. Samejima, N. Zamzami, M. Loeffler, P. Costantini, K.F. Ferri, T. Irinopoulou, M.C. Prevost, G. Brothers, T.W. Mak, J. Penninger, W.C. Earnshaw, G. Kroemer, Two distinct pathways leading to nuclear apoptosis, J. Exp. Med. 192 (2000) 571–580.
[11] I.F. Sevrioukova, Apoptosis inducing factor: structure, function and redox regulation, Antioxid. Redox Signal. 14 (2011) 2545–2579.
[12] M.J. Mate, M. Ortiz-Lombardia, B. Boitel, A. Haouz, D. Tello, S.A. Susin, J. Penninger, G. Kroemer, P.M. Alzari, The crystal structure of the mouse apoptosis-inducing factor AIF, Nat. Struct. Biol. 9 (2002) 442–446.
[13] N. Vahsen, C. Cande, J.J. Briere, P. Benit, N. Joza, N. Larochette, P.G. Mastroberardino, M.O. Pequignot, N. Casares, V. Lazar, O. Feraud, N. Debili, S. Wissing, S. Engelhardt, F. Madeo, M. Piacentini, J.M. Penninger, H. Schagger, P. Rustin, G. Kroemer, AIF deficiency compromises oxidative phosphorylation, EMBO J. 23 (2004) 4679–4689.
[14] J.A. Klein, C.M. Longo-Guess, M.P. Rossmann, K.L. Seburn, R.E. Hurd, W.N. Frankel, R.T. Bronson, S.L. Ackerman, The harlequin mouse mutation down-regulates apoptosis-inducing factor, Nature 419 (2002) 367–374.
[15] N. Joza, K. Galindo, J.A. Pospisilik, P. Benit, M. Rangachari, E.E. Kanitz, Y. Nakashima, G.G. Neely, P. Rustin, J.M. Abrams, G. Kroemer, J.M. Penninger, The molecular archaeology of a mitochondrial death effector: AIF in Drosophila, Cell Death Differ. 15 (2008) 1009–1018.
[16] M.D. Miramar, P. Costantini, L. Ravagnan, L.M. Saraiva, D. Haouzi, G. Brothers, J.M. Penninger, M.L. Peleato, G. Kroemer, S.A. Susin, NADH oxidase activity of mitochondrial apoptosis-inducing factor, J. Biol. Chem. 276 (2001) 16391–16398.
[17] C. Delettre, V.J. Yuste, R.S. Moubarak, M. Bras, N. Robert, S.A. Susin, Identification and characterization of AIFsh2, a mitochondrial apoptosis-inducing factor (AIF) isoform with NADH oxidase activity, J. Biol. Chem. 281 (2006) 18507–18518.
[18] H.K. Lorenzo, S.A. Susin, Mitochondrial effectors in caspase-independent cell death, FEBS Lett. 557 (2004) 14–20.
[19] S.A. Susin, H.K. Lorenzo, N. Zamzami, I. Marzo, B.E. Snow, G.M. Brothers, J. Mangion, E. Jacotot, P. Costantini, M. Loeffler, N. Larochette, D.R. Goodlett, R. Aebersold, D.P. Siderovski, J.M. Penninger, G. Kroemer, Molecular characterization of mitochondrial apoptosis-inducing factor, Nature 397 (1999) 441–446.
[20] M. Loeffler, E. Daugas, S.A. Susin, N. Zamzami, D. Metivier, A.-L. Nieminen, G. Brothers, J.M. Penninger, G. Kroemer, Dominant cell death induction by extramitochondrially targeted apoptosis-inducing factor, FASEB J. 15 (2001) 758–767.
[21] Y. Ohiro, I. Garkavtsev, S. Kobayashi, K.R. Sreekumar, R. Nantz, B.T. Higashikubo, S.L. Duffy, R. Higashikubo, A. Usheva, D. Gius, N. Kley, N. Horikoshi, A novel p53-inducible apoptogenic gene, PRG3, encodes a homologue of the apoptosis-inducing factor (AIF), FEBS Lett. 524 (2002) 163–171.
[22] C. Cande, I. Cohen, E. Daugas, L. Ravagnan, N. Larochette, N. Zamzami, G. Kroemer, Apoptosis-inducing factor (AIF): a novel caspase-independent death effector released from mitochondria, Biochimie 84 (2002) 215–222.
[23] J. Rajawat, H. Mir, T. Alex, S. Bakshi, R. Begum, Involvement of poly(ADP-ribose) polymerase in paraptotic cell death of *D. discoideum*, Apoptosis 19 (2014) 90–101.
[24] H. Mir, J. Rajawat, R. Begum, Staurosporine induced cell death in *D. discoideum* is independent of PARP, Indian J. Exp. Biol. 50 (2012) 80–86.
[25] A.M. Kawal, H. Mir, C.K. Ramniklal, J. Rajawat, R. Begum, Structural and evolutionary analysis of PARPs in *D. discoideum*, Am. J. Infect. Dis. 7 (2011) 67–74.
[26] B. Katoch, S. Sebastian, S. Sahdev, H. Padh, S.E. Hasnain, R. Begum, Programmed cell death and its clinical implications, Indian J. Exp. Biol. 40 (2002) 513–524.
[27] H. Mir, J. Rajawat, S. Pradhan, R. Begum, Signaling molecules involved in the transition of growth to development of *Dictyostelium discoideum*, Indian J. Exp. Biol. 45 (2007) 223–236.
[28] D. Arnoult, I. Tatischeff, J. Estaquier, M. Girard, F. Sureau, J.P. Tissier, A. Grodet, M. Dellinger, F. Traincard, A. Kahn, On the evolutionary conservation of the cell death pathway: mitochondrial release of an apoptosis-inducing factor during *Dictyostelium discoideum* cell death, Mol. Biol. Cell 12 (2001) 3016–3030.
[29] M. Sussman, Cultivation and synchronous morphogenesis of *Dictyostelium* under controlled experimental conditions, Methods Cell Biol. 28 (1987) 9–29.
[30] P. Gaudet, K.E. Pilcher, P. Fey, R.L. Chisholm, Transformation of *Dictyostelium discoideum* with plasmid DNA, Nat. Protoc. 2 (2007) 1317–1324.
[31] A. Kosta, C. Laporte, D. Lam, E. Tresse, M.F. Luciani, P. Golstein, How to assess and study cell death in *Dictyostelium discoideum*, Methods Cell Biol. 346 (2001) 535–550.
[32] G. Chen, G. Shaulsky, A. Kuspa, Tissue specific G1 phase cell cycle arrest prior to terminal differentiation in *Dictyostelium*, Development 131 (2004) 2619–2630.
[33] W.X. Ding, M. Li, J.M. Biazik, D.G. Morgan, F. Guo, H.M. Ni, M. Goheen, E.L. Eskelinen, X.M. Yin, Electron microscopic analysis of a spherical mitochondrial structure, J. Biol. Chem. 287 (2012) 42373–42378.
[34] W.F. Whittingham, K.B. Raper, Non-viability of stalk cells in *Dictyostelium*, Proc. Natl. Acad. Sci. U. S. A. 46 (1960) 642–649.
[35] C. Bernofsky, M. Swan, An improved cycling assay for nicotinamide adenine dinucleotide, Anal. Biochem. 53 (1973) 452–458.
[36] O.H. Lowry, N.J. Rosebrough, A.L. Farr, R.J. Randall, Protein measurement with the Folin phenol reagent, J. Biol. Chem. 193 (1951) 265–275.

[37] G. Leoncini, E. Buzzi, M. Maresca, M. Mazzel, A. Balbi, Alkaline extraction and reverse phase high-performance liquid chromatography of adenine and pyridine nucleotides in human platelets, Anal. Biochem. 165 (1987) 379–383.
[38] K. Nagayama, S. Itono, T. Yoshida, S. Ishiguro, H. Ochiai, T. Ohmachi, Antisense RNA inhibition of the b subunit of the *Dictyostelium discoideum* mitochondrial processing peptidase induces the expression of mitochondrial proteins, Biosci. Biotechnol. Biochem. 72 (2008) 1836–1846.
[39] W. Jang, O.G. Schwartz, R.H. Gomer, A cell number counting factor alters cell metabolism, Commun. Integr. Biol. 2 (2009) 293–297.
[40] J.F. Remme, A.K. Woll, A simple and rapid high performance liquid chromatography method for determination of lactic acid in blood serum from edible crab (*Cancer pagurus*). Møre Research, Ålesund, Norway, Report no. Å0160, 2006.
[41] O. Myhre, J.M. Andersen, H. Aarnes, F. Fonnum, Evaluation of the probes 2,7-dichlorofluorescein diacetate, luminol, and lucigenin as indicators of reactive species formation, Biochem. Pharmacol. 65 (2003) 1575–1582.
[42] S. Wadhawan, S. Gautam, A. Sharma, Metabolic stress-induced programmed cell death in *Xanthomonas*, FEMS Microbiol. Lett. 312 (2010) 176–183.
[43] T. Mekrungruangwong, P. Seenak, S. Luangaram, T. Thongsri, S. Kumphune, The serum protein carbonyl content level in relation to exercise stress test, Int. J. Health Allied Sci. 1 (2012) 200–203.
[44] I. Nakamura, Y. Nakai, H. Izumi, Use of Fura-2/AM to measure intracellular free calcium in *Selenomonas ruminantium*, J. Exp. Med. 179 (1996) 291–294.
[45] D.S. Roh, A.L. Cook, S.S. Rhee, A. Joshi, R. Kowalski, D.K. Dhaliwal, J.L. Funderburgh, DNA cross-linking, double-strand breaks, and apoptosis in corneal endothelial cells after a single exposure to mitomycin C, Invest. Ophthalmol. Vis. Sci. 49 (2008) 4837–4843.
[46] A.J. Koning, P.Y. Lum, J.M. Williams, R. Wright, $DiOC_6$ staining reveals organelle structure and dynamics in living yeast cells, Cell Motil. Cytoskeleton 25 (1993) 111–128.
[47] S.T. Smiley, M. Reers, C. Mottola-Hartshorn, M. Lin, A. Chen, T.W. Smith, G.D. Steele Jr., L.B. Chen, Intracellular heterogeneity in mitochondrial membrane potentials revealed by a J-aggregate-forming lipophilic cation JC-1, Proc. Natl. Acad. Sci. U. S. A. 88 (1991) 3671–3675.
[48] E. Miller, Apoptosis measurement by Annexin V staining, Methods Mol. Med. 9 (2004) 191–202.
[49] N. Bidere, H.K. Lorenzo, S. Carmona, M. Laforge, F. Harper, C. Dumont, A. Senik, Cathepsin D triggers Bax activation, resulting in selective apoptosis-inducing factor (AIF) relocation in T lymphocytes entering the early commitment phase to apoptosis, J. Biol. Chem. 278 (2003) 31401–31411.
[50] M.N. Simon, D. Driscoll, R. Mutzel, D. Part, J. Williams, M. Veron, Overproduction of the regulatory subunit of the cAMP–dependent protein kinase blocks the differentiation of *Dictyostelium discoideum*, EMBO J. 8 (1989) 2039–2043.
[51] G. Bloomfield, C. Pears, Superoxide signalling required for multicellular development of *Dictyostelium*, J. Cell Sci. 116 (2003) 3387–3397.
[52] L. Covarrubias, D. Hernández-García, D. Schnabel, E. Salas-Vidal, S. Castro-Obregón, Function of reactive oxygen species during animal development: Passive or active? Dev. Biol. 320 (2008) 1–11.
[53] S.E. Hasnain, T.K. Taneja, N.K. Sah, M. Mohan, N. Pathak, S. Sahdev, M. Athar, R. Begum, In vitro cultured *Spodoptera frugiperda* insect cells: model for oxidative stress-induced apoptosis, J. Biosci. 24 (1999) 13–19.
[54] N.K. Sah, T.K. Taneja, N. Pathak, R. Begum, M. Athar, S.E. Hasnain, The baculovirus anti-apoptotic p35 gene also functions via an oxidant dependent pathway, Proc. Natl. Acad. Sci. U. S. A. 96 (1999) 4838–4843.
[55] M. Mohan, T.K. Taneja, S. Sahdev, M. Krishnaveni, R. Begum, M. Athar, N.K. Sah, S.E. Hasnain, Antioxidants prevent UV induced apoptosis by inhibiting mitochondrial cytochrome c release and caspase activation in *Spodoptera frugiperda* (Sf9) cells, Cell Biol. Int. 27 (2003) 483–490.
[56] D. Brown, B.D. Yu, N. Joza, P. Benit, J. Meneses, M. Firpo, P. Rustin, J.M. Penninger, G.R. Martin, Loss of AIF function causes cell death in the mouse embryo, but the temporal progression of patterning is normal, Proc. Natl. Acad. Sci. U. S. A. 103 (2006) 9918–9923.
[57] A.G. Porter, A.G. Urbano, Does apoptosis-inducing factor (AIF) have both life and death functions in cells? BioEssays 28 (2006) 834–843.
[58] N. Modjtahedi, F. Giordanetto, F. Madeo, G. Kroemer, Apoptosis-inducing factor: vital and lethal, Trends Cell Biol. 16 (2006) 264–272.
[59] M. Varecha, D. Paclova, J. Prochazkova, P. Matula, D. Cmarko, M. Kozubek, Knockdown of apoptosis-inducing factor disrupts function of respiratory complex I, Biocell 36 (2012) 121–126.
[60] S. Krantic, N. Mechawar, S. Reix, R. Quirion, Apoptosis-inducing factor: a matter of neuron life and death, Prog. Neurobiol. 81 (2007) 179–196.
[61] S.A. Lipton, E. Bossy-Wetzel, Dueling activities of AIF in cell death versus survival: DNA binding and redox activity, Cell 111 (2002) 147–150.
[62] C. Zhu, X. Wang, Z. Huang, L. Qiu, F. Xu, N. Vahsen, M. Nilsson, P.S. Eriksson, H. Hagberg, C. Culmsee, N. Plesnila, G. Kroemer, K. Blomgren, Apoptosis-inducing factor is a major contributor to neuronal loss induced by neonatal cerebral hypoxia-ischemia, Cell Death Differ. 14 (2007) 775–784.
[63] S.J. Chinta, A. Rane, N. Yadava, J.K. Andersen, D.G. Nicholls, B.M. Polster, Reactive oxygen species regulation by AIF and complex I-depleted brain mitochondria, Free Radic. Biol. Med. 46 (2009) 939–947.
[64] J.A. Pospisilik, C. Knauf, N. Joza, P. Benit, M. Orthofer, P.D. Cani, T. Nakashima, R. Sarao, G. Neely, H. Esterbauer, A. Kozlov, C.R. Kahn, G. Kroemer, P. Rustin, R. Burcelin, J.M. Penninger, Targeted deletion of AIF decreases mitochondrial oxidative phosphorylation and protects from obesity and diabetes, Cell 131 (2007) 476–491.
[65] A.V. Gordeeva, R.A. Zvyagilskaya, Y.A. Labas, Cross-talk between reactive oxygen species and calcium in living cells, Biochemistry (Mosc) 68 (2003) 1077–1080.
[66] N. Joza, G.Y. Oudit, D. Brown, P. Benit, Z. Kassiri, N. Vahsen, L. Benoit, M.M. Patel, K. Nowikovsky, A. Vassault, P.H. Backx, T. Wada, G. Kroemer, P. Rustin, J.M. Penninger, Muscle-specific loss of apoptosis-inducing factor leads to mitochondrial dysfunction, skeletal muscle atrophy, and dilated cardiomyopathy, Mol. Cell. Biol. 25 (2005) 10261–10272.
[67] S. Elmore, Apoptosis: a review of programmed cell death, Toxicol. Pathol. 35 (2007) 495–516.
[68] E.C. Cheung, N. Joza, N.A. Steenaart, K.A. McClellan, M. Neuspiel, S. McNamara, J.G. MacLaurin, P. Rippstein, D.S. Park, G.C. Shore, H.M. McBride, J.M. Penninger, R.S. Slack, Dissociating the dual roles of apoptosis-inducing factor in maintaining mitochondrial structure and apoptosis, EMBO J. 25 (2006) 4061–4073.
[69] F.T. Schulthess, S. Katz, A. Ardestani, H. Kawahira, S. Georgia, D. Bosco, A. Bhushan, K. Maedler, Deletion of the mitochondrial flavoprotein apoptosis inducing factor (AIF) induces β-cell apoptosis and impairs β-cell mass, PLoS One 4 (2009), e4394.
[70] P.L. Liu, Y.L. Chen, Y.H. Chen, S.J. Lin, Y.R. Kou, Wood smoke extract induces oxidative stress-mediated caspase-independent apoptosis in human lung endothelial cells: role of AIF and EndoG, Am. J. Physiol. Lung Cell. Mol. Physiol. 289 (2005) L739–L749.

Contents lists available at ScienceDirect

BBA - Bioenergetics

journal homepage: http://ees.elsevier.com

Apoptosis inducing factor: Cellular protective function in *Dictyostelium discoideum*

Ashlesha Kadam, Darshan Mehta, Tina Jubin, Mohmmad Shoab Mansuri, Rasheedunnisa Begum *

Department of Biochemistry, Faculty of Science, The Maharaja Sayajirao University of Baroda, Vadodara 390002, Gujarat, India

ARTICLE INFO

Keywords
Apoptosis inducing factor
Mitochondrial respiration
Fusion-fission mechanism
mtDNA content
Dictyostelium discoideum

ABSTRACT

Apoptosis Inducing Factor (AIF), a nuclear encoded mitochondrial inter-membrane space flavoprotein with intrinsic NADH oxidase activity, plays an important role in inducing cell death mechanisms. In response to cell death signals, it undergoes mitochondrio-nuclear translocation leading to DNA fragmentation. In addition to its role in cell death, AIF has a pro-survival role, wherein it contributes to the maintenance of mitochondrial structure and function in a coordinated manner. However, its exact mechanism of controlling mitochondrial homeostasis is unclear. The current study aims to explore the protective functions of AIF by its downregulation and overexpression in *Dictyostelium discoideum*. Constitutive *AIF* downregulated (dR) cells exhibited compromised oxidative phosphorylation along with elevated levels of cellular ROS. Interestingly, constitutive *AIF* dR cells showed amelioration in the activity of the ETC complexes upon antioxidant treatment, strengthening AIF's role as an ROS regulator, by virtue of its oxidoreductase property. Also, constitutive *AIF* dR cells showed lower transcript levels of the various subunits of ETC. Moreover, loss of AIF affected mtDNA content and mitochondrial fusion-fission mechanism, which subsequently caused morphometric mitochondrial alterations. Constitutive *AIF* overexpressed (OE) cells also showed higher cellular ROS and mitochondrial fission genes transcript levels along with reduced mitochondrial fusion genes transcript levels and mtDNA content. Thus, the results of the current study provide a paradigm where AIF is implicated in cell survival by maintaining mitochondrial bioenergetics, morphology and fusion-fission mechanism in *D. discoideum*, an evolutionarily significant model organism for mitochondrial diseases.

1. Introduction

Apoptosis inducing factor (AIF) is a nuclear encoded mitochondrial inter-membrane space flavoprotein, recognised as an apoptotic effector molecule in caspase-independent cell death. Translocation of AIF from mitochondria to nucleus is a characteristic feature of Poly(ADP-ribose) polymerase (PARP) and staurosporine induced caspase independent cell death in *Dictyostelium discoideum* [1,2]. Its apoptotic function along with the underlying mechanism has been well documented [3–5]. The FAD and NADH binding domains of AIF distinguishes it from the pro-apoptotic proteins, imparting its dual role in cell death and cell survival. The strong structural and sequence homology to bacterial and plant ascorbate and ferredoxin reductases imply AIF has oxidoreductase activity [6]. Interestingly, its inherent NADH oxidase activity which is independent of its apoptotic activity [7] is linked to mitochondrial homeostasis maintenance [8]. A detailed mechanism of how AIF participates in mitochondrial metabolism and homeostasis remains obscure, but it is largely being attributed to its NADH dependent oxidoreductase activity. Our earlier study demonstrated that AIF is crucial for growth and development of *D. discoideum* [9]. Also, loss of AIF function in mice caused embryonic lethality owing to reduced complex I activity [10]. AIF-hypomorphic Harlequin (Hq) mice exhibited elevated Reactive Oxygen Species (ROS) that consequently led to T lymphocyte deficiency [11]. Tissue-specific deletion of *AIF* displayed severe mitochondrial dysfunction and aberrant cristae structures characterized by skeletal muscle atrophy and dilated cardiomyopathy [12]. AIF is proposed to be involved in cellular bioenergetics, assisting in the stabilization and/maintenance of assembly of the Electron Transport Chain (ETC) [13]. AIF mutation in humans has been associated with impaired ETC function that results in mitochondrial encephalomyopathy. The FAD binding pocket of AIF contains Arginine 201 (R201) residue that confers conformational stability to the flavoprotein. An inherited tri-nucleotide deletion in exon 5 of human AIF caused the ablation of the Arg201 (R201deletion) which showed abnormal FAD binding to AIF and consequently impaired structural stability, redox activities and oxidative phosphorylation (OXPHOS) functioning [14]. Hangen et al. [15] and Meyer et al. [16] showed that physical and functional interaction of AIF with CHCHD4/MIA40 is necessary for correct biogenesis of the respiratory chain (RC) complexes.

Mitochondrial metabolism is tightly linked to organelle structure and morphology. Interestingly, mitochondrial structure is dynamically regulated by two counteracting processes of fusion and fission [17

* Corresponding author.
E-mail address: rasheedunnisab@yahoo.co.in (R. Begum)

https://doi.org/10.1016/j.bbabio.2020.148158
Received 20 August 2019; Received in revised form 16 January 2020; Accepted 24 January 2020
Available online xxx
0005-2728/

]. Apart from stabilizing assembly of mitochondrial ETC complexes, AIF is suggested to play a role in the maintenance of mitochondrial DNA (mtDNA) pool and mitochondrial structure and morphology. *AIF* deficient neuronal mitochondria were found to be fragmented with aberrant cristae structure and altered mitochondrial respiration that ultimately reduced neuronal cell survival [18]. Moreover, Hq mice showed diminished levels of *Mitofusin1* (*MFN1*) in Purkinje cells, suggesting that loss of AIF disrupted mitochondrial fusion process [19]. Even though AIF is essential for maintaining mitochondrial function and structure, its underlying mechanism in cell survival remains enigmatic.

D. discoideum is a model organism as its life cycle exhibits both unicellular as well as multicellular forms [20,21], thus making it suitable to study AIF's role in growth and development [9,22]. Recently, it has also been widely used to study mitochondrial biogenesis and diseases [23]. Being caspase independent, it provides a better model to explore non-apoptotic functions of AIF without interference of caspases. Hence, we aim to explore the cellular protective functions of AIF, highlighting mitochondrial homeostasis during unicellular and multicellular phases of *D. discoideum.* Our study provides a deeper insight into the pro-survival functions of AIF, establishing its role in mitochondrial biology.

2. Materials and methods

2.1. D. discoideum culture, growth and development

Dictyostelium discoideum AX-2 strain, an axenic derivative of Raper's wild-type NC-4 was used. The unicellular cells were grown in HL-5 medium, pH 6.5 at 150 rpm shaking at 22 °C. *D. discoideum* was maintained on a solid substratum containing non-nutrient agar with *Klebsiella aerogenes* and harvested using standard procedures [24].

Under starvation, *D. discoideum* undergoes multicellular development. Mid log phase cells were washed twice and resuspended in 1× Sorensen's Buffer (SB). These cells were plated on 2% non-nutrient agar and incubated at 22 °C [24]. Then cells from the respective stages were collected for respiration studies, RNA isolation and gene expression analysis.

2.2. Downregulation of AIF

Downregulation of *AIF* was carried out by *AIF* antisense construct under constitutive actin promoter as described earlier and termed as constitutive *AIF* downregulated (*AIF* dR) cells [9]. *AIF* dR cells were grown in HL-5 medium supplemented with 100 μg/ml Geneticin and *AIF* downregulation was confirmed by monitoring *AIF* mRNA transcript levels by Real Time PCR with *RNLA* as an internal control [9].

2.3. Generation of AIF overexpression construct

Full length *AIFA* (*AIF*) (1.8 kbp) was PCR amplified from the genomic DNA of *D. discoideum* using *AIF* specific primers and cloned into act15-EYFP vector. Purified PCR product digested with *SacI* and *BamHI* was ligated into act15-EYFP. The positive clones, *AIF*-EYFP OE (*AIF* OE) and EYFP vector control were then transformed into *D. discoideum* cells by electroporation. EYFP-vector control cells were selected at 100 μg/mL G418. For selection of *AIF* OE, we went up to 30 μg/mL G418. However, these cells could not withstand 30 μg/mL concentration. Hence, we reduced G418 to 10 μg/mL. All the experiments were performed with 10 μg/mL G418.

2.4. Estimation of Oxygen Consumption Rate (OCR)

OCR was measured in saponin (5 mg/ml) permeabilized cells (~12×10^6 cells/ml) using Oxytherm Clark-type oxygen electrode (Hansatech Instruments, Norfolk, UK) containing respiration buffer (80 mM KCl, 0.1% BSA, 50 mM HEPES, 2 mM $MgCl_2$, and 2.5 mM KH_2PO_4; pH 7.2) [25]. Respiratory chain complexes I–IV activities were recorded using 100 mM Pyruvate & 800 mM Malate (complex I), 1 M Succinate (complex II), 10 mM α-glycerophosphate (complex III), 200 mM Ascorbate (complex IV) [26] and protein concentration was estimated by Lowry method [27]. Mitochondrial outer membrane integrity of saponin-treated cells was assessed by impermeability to exogenous Cytochrome-c which was consistently >95%. All chemicals were purchased from Sigma-Aldrich, USA. OCR was determined by measuring the amount of oxygen (nmol) consumed, divided by the time elapsed (min) and amount of protein present in the assay [26].

2.5. Blue Native-PAGE (BN-PAGE)

Assembly of mitochondrial respiratory chain complexes was analyzed by BN-PAGE. Mitochondria were isolated from vegetative *D. discoideum* cells and mitochondrial pellet was resuspended in solubilization buffer (50 mM NaCl, 50 mM Imidazole/HCl, 2 mM 6-aminohexanoic acid, 1 mM EDTA, pH 7) [28]. Amount of protein was quantified by Lowry method [27]. Mitochondrial pellet was then solubilized using Digitonin (5%) and the samples were centrifuged at 12,000 rpm for 20 min at 4 °C. Coomassie blue-G250 dye (5% in 750 mM 6-aminohexanoic acid) was added to the supernatant to set a detergent/Coomassie-dye ratio of 4 (g/g). This supernatant was then subjected to 1.0mm sample wells of BN-PAGE using 3–12% acrylamide gradient gels and run at 250 V for 2–3 h at RT [29].

2.6. Transcript analysis by Real Time PCR

Total RNA was isolated from *D. discoideum* cells and gene transcript (mRNA levels) analysis was performed using gene specific primers by Real time PCR using LightCycler® 480 SYBR Green I Master (Roche Diagnostics GmbH, Mannheim, Germany) in the LightCycler® 480 Real Time PCR (Roche Diagnostics GmbH, Mannheim, Germany). *RNLA* was used as an internal control. Fold change in the transcript levels ($2^{-\Delta\Delta Ct}$) was shown graphically [30]. Table 1 shows primer sequences used for gene expression analysis.

2.7. Estimation of mtDNA content (mtDNA/nDNA)

Total cellular DNA was isolated from *D. discoideum* [31] and mtDNA content was estimated by Real Time PCR using the SYBR Green PCR Master Mix. mtDNA content was calculated by taking the ratio of mtDNA to the nuclear DNA (nDNA). The relative mtDNA content was calculated as the difference in the numbers of threshold cycles (Ct) between the nuclear-specific glyceraldehyde 3-phosphate dehydrogenase (*GAPDH*) gene and the mitochondrial-specific cytochrome *c* oxidase subunit 1/2 (*COX1/2*) gene (ΔCt), in which the amount of mtDNA calculated per cell ($2^{-\Delta Ct}$) represents a relative measure of mtDNA content [32]. Table 2 shows primer sequences used for the estimation of mtDNA content.

2.8. Transmission electron microscopy (TEM)

TEM was performed to analyse the morphometric mitochondrial alterations in *D. discoideum*. Log phase cells were fixed with 2% glutaraldehyde in Phosphate Buffer Solution (PBS), pH 7.2 at 4 °C for 1 h and processed as described by Rajawat et al. [33] and Kosta et al. [34]. Sections were obtained with a Reichert Ultracut E ultramicrotome, stained and examined using TEM (Morgagni 268D, FEI electron optics company Philips, Hillsboro, Oregon, USA). Mitochondrial surface area was calculated using ImageJ software.

Table 1
Primers used for gene expression analysis.

Gene	Primer
NAD1	Forward Primer (FP): 5′-AAGAGGACCAAATGTAGTAGGG-3′
	Reverse Primer (RP): 5′-GCTGCTGATCGTAATCCTC-3′
NAD6	FP: 5′-GAGTCGTAGGTCTTCTGG-3′
	RP: 5′-CATTGTTCGTATATCTGTCG-3′
NDUFS3	FP: 5′-ACGGATTATGGATTTGTAGG-3′
	RP: 5′-TCT CCC CAT ACT GCT CC-3′
CYTB	FP: 5′-GGAATTTATGAAGCAGGCG-3′
	RP: 5′-GCTAAATCGACATGTGCCG-3′
COX1/2	FP: 5′-AGCAGAGAAAGAAGGAAAC-3′
	RP: 5′-TTGACCGTCTCCATCTAAC-3′
ATP6	FP: 5′-GGCAACCATAATAGGTGG-3′
	RP: 5′-AACCCCAAATTGTTATTCC-3′
NDUFA5	FP: 5′-GTTGAACCAAATGCAAGAC-3′
	RP: 5′-TCATGGACTAAATCGACAAC-3′
NDUFA9	FP: 5′-CTCGTAATTTCTCACTCGACG-3′
	RP:5′-CACCGATTGCTT TTGAACGTG-3′
CLUA	FP: 5′-TGTTACAGCATCAACTCAAGG-3′
	RP: 5′-ACTGGTAATACGCCTGGAAG-3′
DYMA	FP: 5′-CCAATTGCTGATGATGGATCAC-3′
	RP: 5′-GCTGGTGTCACTGCAACG-3′
DYMB	FP: 5′-GGTCAGAGATTACTCTACCAC-3′
	RP: 5′-GTCCAAATTCTCCCCATTCC-3
FSZA	FP: 5′-ACAAGAGGATTAGGAGCAGGAGC-3′
	RP: 5′-CAACTCTATCAAACCTTGTTCTGCCA-3′
FSZB	FP: 5′-TGGTGAAGCATCTGGTGAGGATAG-3′
	RP: 5′-ACGAAAACTTGAACATCAGGATCAGC-3′
AIF/AIFA	FP: 5′-CCAATCCTCATCAAAAGGAAG-3
	RP: 5′-AGCTGCTGTTCCACCACC-3′
AIFB	FP: 5′-TGTAATCAATGAGTCTGGAC-3′
	RP: 5′-AAAGACTAAGTATTGGACCTG-3′
AIFC	FP: 5′-TGGAGGTAGCCAAGTTG-3′
	RP: 5′-TTCTGGTTCAACTATTGCTC-3′
AIFD	FP: 5′-TTCAGGTAGTATTGTAGCAC-3′
	RP: 5′-TTGAGCCAGAGTTTATCA C-3′
RNLA	FP: 5′-TTACATTTATTAGACCCGAAACCAAGC-3′
	RP: 5′-TTCCCTTTAGACCTATGGACCTTAGCG-3′

Table 2
Primers used for estimation of mtDNA content.

Gene	Primer
GAPDH	FP: 5′-TCAACTGATGCCCCAATGTA-3′
	RP: 5′-CGTGAACGGTGGTCATTAAA-3′
COX1/2	FP: 5′-ACAAACTAAATGCGGGAACG-3′
	RP: 5′-TTAAATTTACGCCCCCACAG-3′

2.9. Estimation of cellular ROS levels

The generation of ROS was monitored using DCFDA (2′-7′ dichlorofluorescin diacetate) dye (1 μg/ml). ~2.0 × 10^6 *D. discoideum* cells were washed twice with 1× SB followed by exposure to membrane permeable dye, DCFDA and incubated for 15 min at 22 °C under shaking condition. Fluorescence intensity was measured by Fluorimeter (F7000, Hitachi, Japan) and λex and λem used for these studies were 480 nm and 525 nm respectively [35].

2.10. Statistical analysis

Data are presented as a mean and Standard Error of the Mean (SEM) or Standard Deviation (SD) as applicable. Statistical analysis was performed using GraphPad PRISM®6, GraphPad software Inc., USA. Student′s unpaired *t*-test assessed statistical significance for experiments with the single comparison.

3. Results

3.1. Relative expression of AIFA, AIFB, AIFC and AIFD

AIF/AIFA was downregulated by antisense mediated strategy and displayed ~70% reduction in *AIF* transcript levels in constitutive *AIF* downregulated (*AIF* dR) cells (Fig. 1a). Other than *AIF*, there are three more isoforms of *AIF* in *D. discoideum* i.e. *AIFB*, *AIFC* and *AIFD*. We further assessed their transcript levels in constitutive *AIF* dR cells to ensure that only *AIFA* was downregulated. No significant difference was observed in the transcript levels of *AIFB, AIFC* and *AIFD* in constitutive *AIF* dR cells compared to control and vector control cells (Fig. 1b,cand d), suggesting *AIFB, AIFC* and *AIFD* could not compensate the function of *AIFA*.

3.2. Estimation of OCR in constitutive AIF dR cells

In the presence of nutrients, *D. discoideum* cells multiply as unicellular amoebae (vegetative growth) while under nutrient deprivation, they enter into a developmental cycle to form mature fruiting bodies. In the present study, OCR was measured in both vegetative (unicellular phase) and starved (multicellular phase) constitutive *AIF* dR cells.

3.2.1. OCR studies during vegetative stage

As the rate of oxygen consumption is a vital indicator of mitochondrial respiration, OCR was measured. Reduced OCR at complex I, complex III and complex IV with increased OCR at complex II was found in constitutive *AIF* dR cells compared to control cells (Fig. 2a), indicating compromised mitochondrial respiration. CI/CII OCR ratio is also one of the parameters to confirm the impaired complex I function. CI/CII OCR ratio revealed that constitutive *AIF* dR cells exhibited ~50% reduction in CI dependent substrate oxidation relative to CII dependent substrate oxidation as compared to control cells (Fig. 2b).

3.2.2. OCR studies during developmental stages

Constitutive *AIF* dR cells exhibited delayed development, signifying AIF′s role in multicellular development of *D. discoideum* [9]. Hence, *AIF* dR cells were subjected to development and OCR was measured at the major developmental stages of *D. discoideum*, i.e. aggregate, slug and fruiting body. Constitutively *AIF* dR cells showed significantly diminished OCR at complex I at the aggregate stage compared to control cells (Fig. 3a). Also, reduced OCR was observed at complexes I, III and IV at slug stage (Fig. 3b) and at complex I and III activities at the fruiting body stage (Fig. 3c) of constitutive *AIF* dR compared to control cells. Taken together, these results indicate AIF′s role towards regulating the assembly and/ activities of mitochondrial respiratory chain complexes and thereby OXPHOS maintenance during developmental phase too in *D. discoideum*.

3.3. Investigating the effect of glutathione (GSH) on OCR

Previously it was shown that 10mM GSH could rescue the delay in *D. discoideum* growth and development regulating ROS levels in constitutive *AIF* dR cells [9]. To confirm the function of AIF as a ROS regulator, we monitored if exogenous treatment of GSH could restore activities of the ETC complexes in constitutive *AIF* dR cells as GSH is known to maintain the redox status of the cell. Constitutive *AIF* dR cells in the presence of 10mM GSH showed restoration of OCR at complexes I and III of constitutive *AIF* dR as compared to untreated cells suggesting that oxido-reductase property of AIF might be implicated in balancing the ROS levels (Fig. 4).

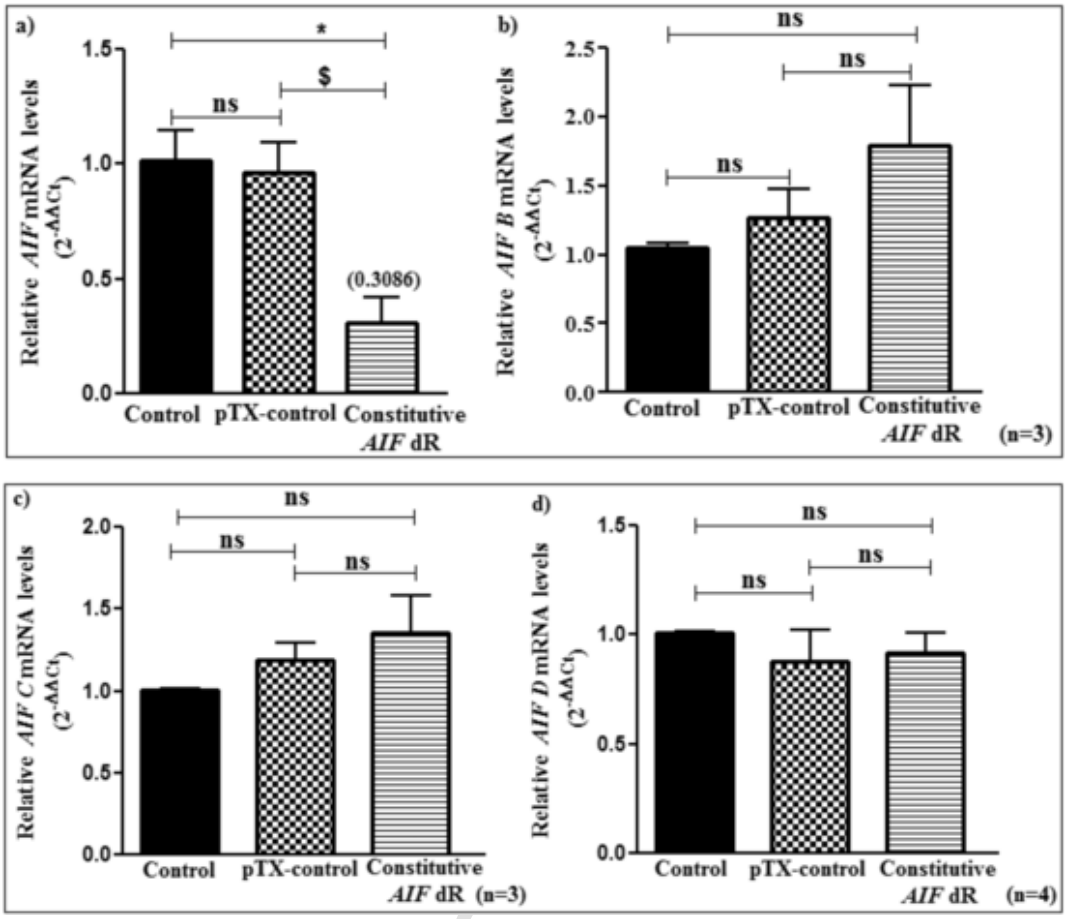

Fig. 1. Analysis of *AIFA*, *AIFB, AIFC* and *AIFD* transcript levels in constitutive *AIF* dR cells by Real Time PCR: a) Relative mRNA transcript levels of *AIF* were found be reduced in constitutive *AIF* dR cells compared to vector control and control cells. Data are representation of SEM values of three independent experiments. * $p < .05$ as compared to control. $ $p < .05$ as compared to pTX-control. b) Relative transcript levels of *AIFB* in constitutive *AIF* dR cells compared to vector control and control cells. Data are representation of SEM values of three independent experiments. c) Relative transcript levels of *AIFC* in constitutive *AIF* dR cells compared to vector control and control cells. Data are representation of SEM values of three independent experiments. d) Relative transcript levels of *AIFD* in constitutive *AIF* dR cells compared to vector control and control cells. Data are representation of SEM values of four independent experiments. *RNLA* used as an internal control. pTX-control used as a vector control. ns = non-significant.

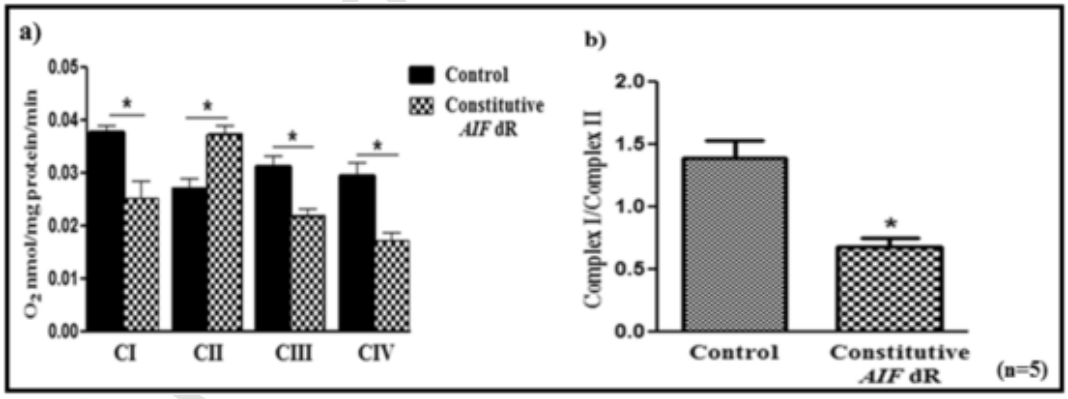

Fig. 2. Oxygen Consumption Rate (OCR) studies at vegetative stage of *D. discoideum*: a) Clark O_2 analysis showed reduced OCR at complex I ($p = .0243$), complex III ($p = .0211$) and complex IV ($p = .0127$) activity in constitutive *AIF* dR cells compared to control cells. b) CI/CII OCR ratio in constitutive *AIF* dR cells showed reduced CI dependent substrate oxidation relative to CII dependent substrate oxidation as compared to control cells ($p = .0102$). Data are representation of SEM values of five independent experiments. * $p < .05$ as compared to control.

3.4. Estimation of mtDNA content

As AIF is also involved in mtDNA maintenance [14], we estimated mitochondrial DNA content in *AIF* dR cells under both vegetative and developmental stages. mtDNA content relative to nuclear DNA content was observed to be significantly reduced in constitutive *AIF* dR compared to control cells at both stages of *D. discoideum* (Fig. 5a and b), implying AIF′s role in mtDNA maintenance.

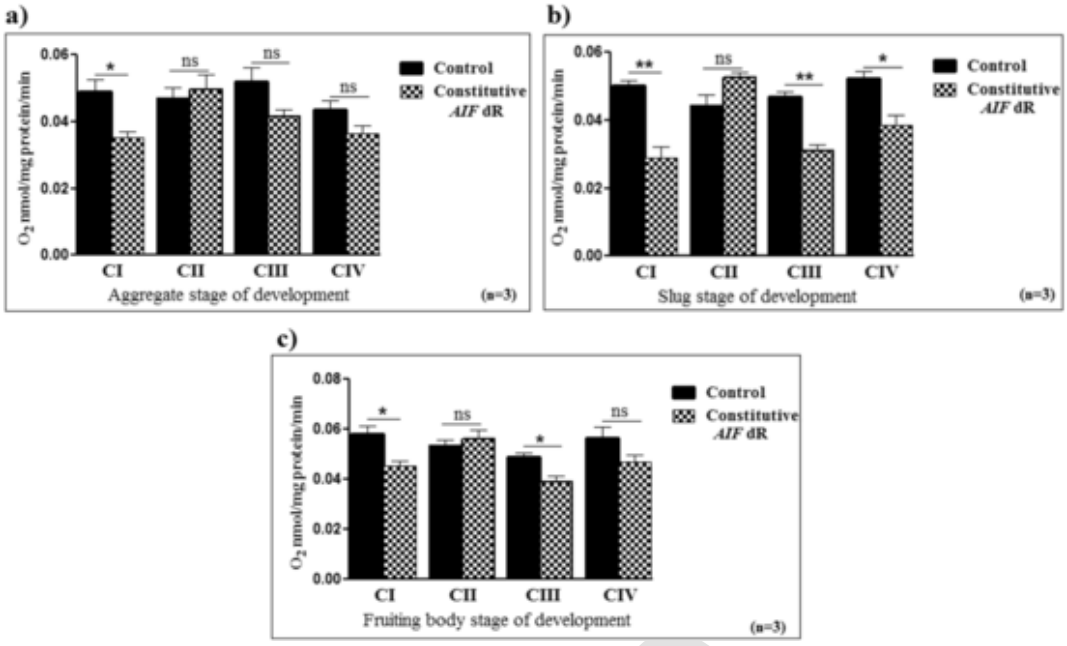

Fig. 3. Estimation of oxygen consumption rate (OCR) studies at developmental stages in *D. discoideum*: a) Constitutive *AIF* dR cells exhibited significantly reduced activities of complex I ($p = .0248$) compared to control cells during aggregate stage. b) Constitutive *AIF* dR cells exhibited significantly reduced activities of complexes I ($p = .0038$), III ($p = .0023$) and IV ($p = .0247$) compared to control cells during slug stage. c) Constitutive *AIF* dR cells showed significantly reduced activities at complexes I ($p = .0251$) and III ($p = .0198$) compared to control cells in fruiting body. Data are representation of SEM values of three independent experiments. * $p < .05$ and ** $p < .01$ as compared to control; ns = non-significant.

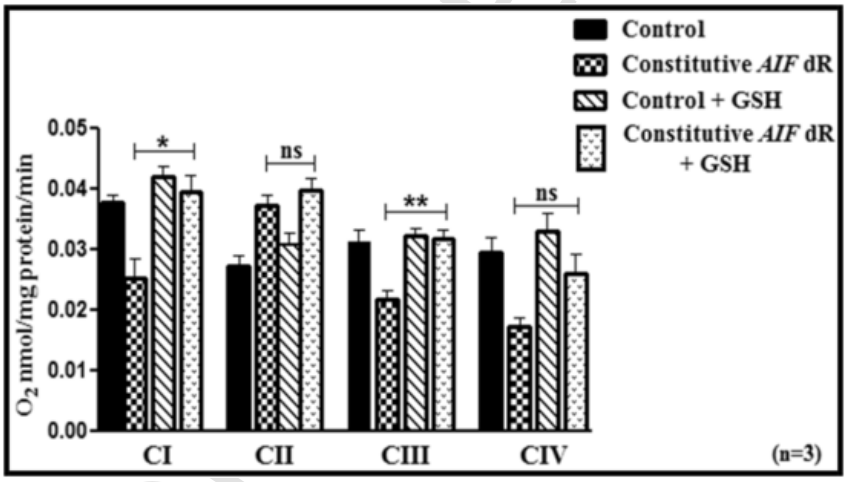

Fig. 4. Oxygen Consumption Rate (OCR) in constitutive *AIF* dR cells in the presence of 10 mM GSH: 10 mM GSH could restore the oxygen consumption rate of constitutive *AIF* dR cells at complexes I ($p = .0272$) and complex III ($p = .0079$) compared to untreated constitutive *AIF* dR cells. Data are representation of SEM values of three independent experiments. * $p < .05$ and ** $p < .01$ as compared to control; ns = non-significant.

3.5. Analysis of the assembly of electron transport chain complexes

In order to explore how AIF exerts its effect on the respiratory chain complexes, transcript levels of subunits of the affected complexes were analyzed by Real Time PCR. Constitutive *AIF* dR cells exhibited decreased transcript levels of *NAD1* (Fig. 6a), *NAD6* (Fig. 6b), *NDUFS3* (Fig. 6c), *NDUFA5* (Fig. 6d), *NDUFA9* (Fig. 6e), *CYTB* (complex III) (Fig. 6f), *COX1/2* (Fig. 6g) (complex IV) and *ATP6* (complex V) (Fig. 6h) subunits compared to control cells. The assembly of the ETC supercomplexes was observed by BN-PAGE. The abundance of complexes I, III and IV proteins were found to be reduced in constitutive *AIF* dR compared to control cells (Fig. 6i, j and supplementary fig. 1), suggesting assembly of ETC complexes is affected due to loss of *AIF*. Decreased ETC subunits′ transcript levels and defect in ETC assembly indicate that AIF may contribute in assembly, maintenance and/or stabilization of the mitochondrial ETC.

3.6. Effect of AIF downregulation in mitochondrial fusion-fission mechanism

3.6.1. Analysis of the transcript levels of mitochondrial fusion- fission genes in vegetative cells

Loss of AIF could result in compromised mitochondrial function in constitutive *AIF* dR cells. Knockdown of *AIF* led to fragmented mitochondria with aberrant cristae structure, indicating the role of AIF in maintaining mitochondrial structure [36]. Mitochondrial structure is maintained by the balanced processes of fusion and fission [37]. Hence, we further studied the effect of reduced *AIF* on mitochondrial structure by analysing the transcript levels of mitochondrial fusion-fission genes (*CLUA*, *DYMA*, *DYMB*, *FSZA*, and *FSZB*). Constitutive *AIF*

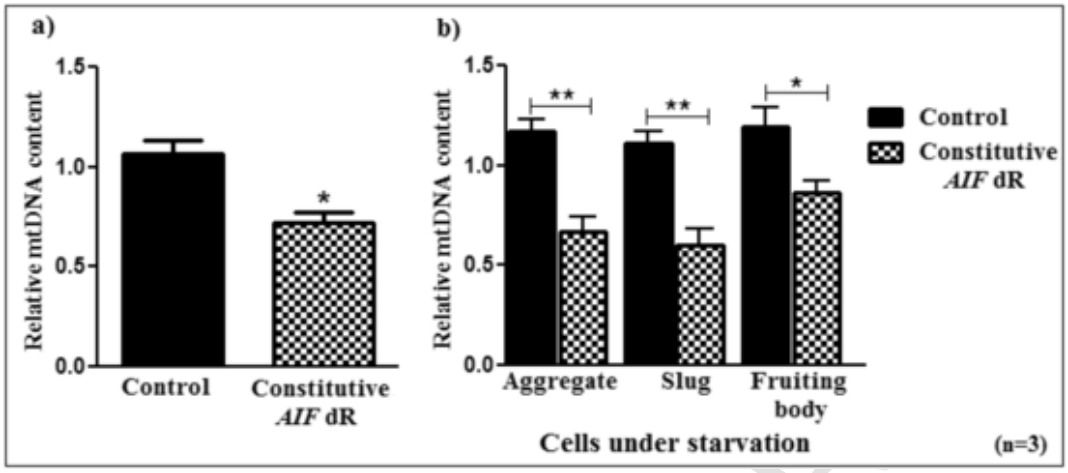

Fig. 5. Estimation of relative mtDNA content by Real Time PCR: a) Significant decrease in mtDNA content was found in vegetative constitutive *AIF* dR compared to control cells (p = .0140). b) Under starvation condition also, mtDNA content was found to be reduced significantly at the aggregate (p = .0058), slug (p = .0079) and fruiting body (p = .0442) stages of development in constitutive *AIF* dR compared to control cells. Data are representation of SEM values of three independent experiments. * $p < .05$ and ** $p < .01$ as compared to control; ns = non-significant.

dR cells exhibited reduced *CLUA* and elevated *DYMA*, *DYMB*, *FSZA* & *FSZB* transcript levels (Fig. 7). This altered fusion-fission balance in *AIF* dR cells uncovered the additional function of AIF in controlling mitochondrial morphology.

3.6.2. Analysis of transcript levels of mitochondrial fusion-fission genes in starving cells

As starved *AIF* dR cells exhibited impaired mitochondrial respiration, we were also interested to explore its effect on fusion-fission under starvation. Hence, the transcript levels of mitochondrial fusion-fission genes were analyzed at all developmental stages (aggregate, slug and fruiting bodies). *CLUA* transcript levels were observed to be significantly reduced at aggregate and slug stages (Fig. 8a) while *DYMA* and *FSZB* transcript levels were found to be significantly increased at slug stage of constitutive *AIF* dR compared to control cells (Fig. 8b and c). *FSZA* transcript levels were observed to be significantly elevated at aggregate and slug stages (Fig. 8d) whereas no significant difference was found in *DYMB* transcript levels of constitutive *AIF* dR compared to control cells (Fig. 8e). Altered fusion-fission process was demonstrated during developmental stages also due to absence of AIF in *D. discoideum.* Overall, our study suggested the importance of AIF in controlling the mitochondrial structure under both vegetative and development stages.

3.7. Mitochondrial morphology

Loss of respiratory capacity and altered mitochondrial fusion-fission mechanism might contribute to modulate the mitochondrial structure due to AIF deficiency [18]. In line with this report, perturbations in mitochondrial morphology were visualized by TEM. Mitochondria of constitutive *AIF* dR cells were defective with aberrant cristae and dilations. Interestingly, constitutive *AIF* dR mitochondria exhibited intra-mitochondrial 'holes' likely due to dilation of cristae which were absent in control cells (Fig. 9a). However, no significant difference was observed in mitochondrial average surface area in constitutive *AIF* dR compared to control cells (Fig. 9c). Constitutive *AIF* dR exhibited more number of mitochondria compared to control cells (Fig. 9b), corroborating increased mitochondrial fission and reduced mitochondrial fusion process (Fig. 7). These results highlight the prime role of AIF in maintaining mitochondrial structure and morphology.

3.8. Functional characterization of AIF overexpression

In order to study the role of AIF, we further overexpressed *AIF* and monitored its effect on total cellular ROS levels, mitochondrial fission-fusion profile and mtDNA content in *AIF* overexpressed (*AIF* OE) cells.

AIF overexpression was confirmed by monitoring gene specific expression of *AIF* using Real Time PCR. *AIF* OE cells showed ~36% higher expression of *AIF* transcript compared to control and vector control cells (EYFP-vector control) (Fig. 10).

3.8.1. Cellular ROS levels in AIF OE cells

As AIF is mainly involved in inducing cell death, higher *AIF* expression may lead to increase in ROS levels. Hence, ROS levels were estimated. A significant increase in ROS levels were observed in *AIF* OE cells as compared to control cells (Fig. 11), suggesting *AIF* OE cells exhibited high oxidative stress that might make the cells sensitive to oxidative stress mediated cell death.

3.8.2. Analysis of transcript levels of mitochondrial fusion-fission genes in AIF OE cells

To examine the functional state of mitochondria in *AIF* OE cells, we further monitored the effect of *AIF* overexpression on mitochondrial fusion-fission mechanism and mtDNA content. Interestingly, mitochondrial fusion-fission mechanism and mtDNA content were found to be affected upon *AIF* overexpression.

Significantly reduced *CLUA* transcript levels were seen in *AIF* OE cells, while *FSZA* and *FSZB* transcript levels were found to be significantly elevated in *AIF* OE cells compared to control cells (Fig. 12a, d and e). No significant difference was found in *DYMA* and *DYMB* expression levels of *AIF* OE cells compared to control cells (Fig. 12b and c).

Excessive oxidative stress can damage and affect mtDNA content [38]. Hence, we analyzed mtDNA content upon *AIF* overexpression. Significant reduction in mtDNA content was observed in *AIF* OE cells compared to control cells (Fig. 12f).

Overall, our *AIF* overexpression results suggest that fine tuning of *AIF* levels are crucial in maintaining the mitochondrial activities.

4. Discussion

Apart from AIF's role in cell death, its physiological role in cell survival highlights its importance in maintenance of mitochondrial structure and function. Nonetheless, the molecular mechanism of AIF in bio-

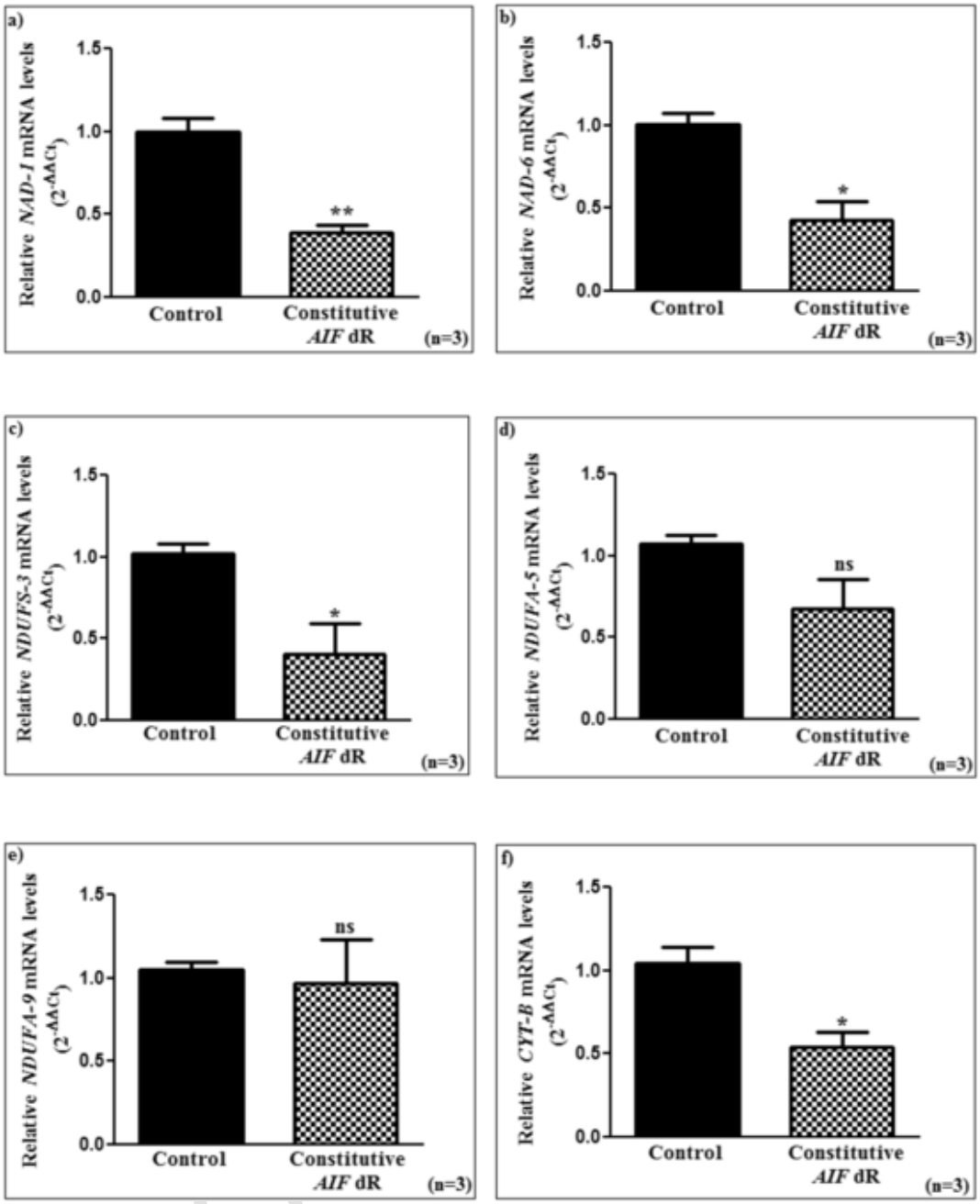

Fig. 6. Analysis of Electron transport chain complexes by Real Time PCR and BN-PAGE: a), b), c), d), e), f), g) and h) Real Time PCR analysis showed reduced relative mRNA transcript levels of *NAD1* ($p = .0024$), *NAD6* ($p = .0105$), *NDUFS3* ($p = .0348$), *NDUFA5* ($p = .1073$), *NDUFA9* ($p = .7656$), *CYTB* ($p = .0205$), *COX1/2* ($p = .0125$) and *ATP6* ($p = .0034$) in constitutive *AIF* dR compared to control cells. Data are representation of SEM values of three independent experiments. * $p < .05$ and ** $p < .01$ as compared to control; ns = non-significant. i) Representative gel image of BN-PAGE revealed reduced protein abundance of complexes I, III and IV in constitutive *AIF* dR cells. Lane 1: Native protein marker in kDa; Lane 2: control cells; Lane 3: constitutive *AIF* dR cells. j) Schematic representation of densitometric analysis of BN-PAGE gel by imageJ software. Data are representation of the SEM values of three independent experiments. * $p < .05$, ** $p < .01$ and *** $p < .001$ as compared to control; ns: non-significant.

genesis and protection of respiratory complexes is an enigma. Our present study focuses on the protective function of AIF in stabilizing assembly of the ETC and balancing mitochondrial fusion-fission process under vegetative and developmental stages of *D. discoideum*. Numerous *AIFM1* pathogenic mutations recognize mitochondrial dysfunction, with progressive encephalomyopathies, muscular atrophy and neuropathies [14,39,40]. *In vitro* and *in vivo* studies showed *AIF* deficiency led to loss in the assembly and/or maintenance of the respiratory chain complex I [13,41]. Interestingly, our study shows compromised OXPHOS function due to impairment not only in complex I but the entire ETC complex activities in both the vegetative and starved constitutive *AIF* dR cells (Fig. 2 and 3). Reduced complexes I, III & IV activities along with their lower subunits transcript and protein levels led to OXPHOS dysfunction (Fig. 2, 3 and 6), explaining further the reduced total cellular and mitochondrial ATP levels and hence metabolic switch to enhanced glycolysis in constitutive *AIF* dR cells for energy need [9]. Loss of *AIF* in heart and B cells also resulted in decrease in complex I along with increase in complex II activities [36]. Elevated complex II activity in constitutive *AIF* dR cells (Fig. 2) can be a compensatory mechanism that links mitochondrial reserve respiratory capacity to cellular survival under compromised complex I and III activities [42,43]. Oxidation OCR ratio are accurate indicators of partial respiratory

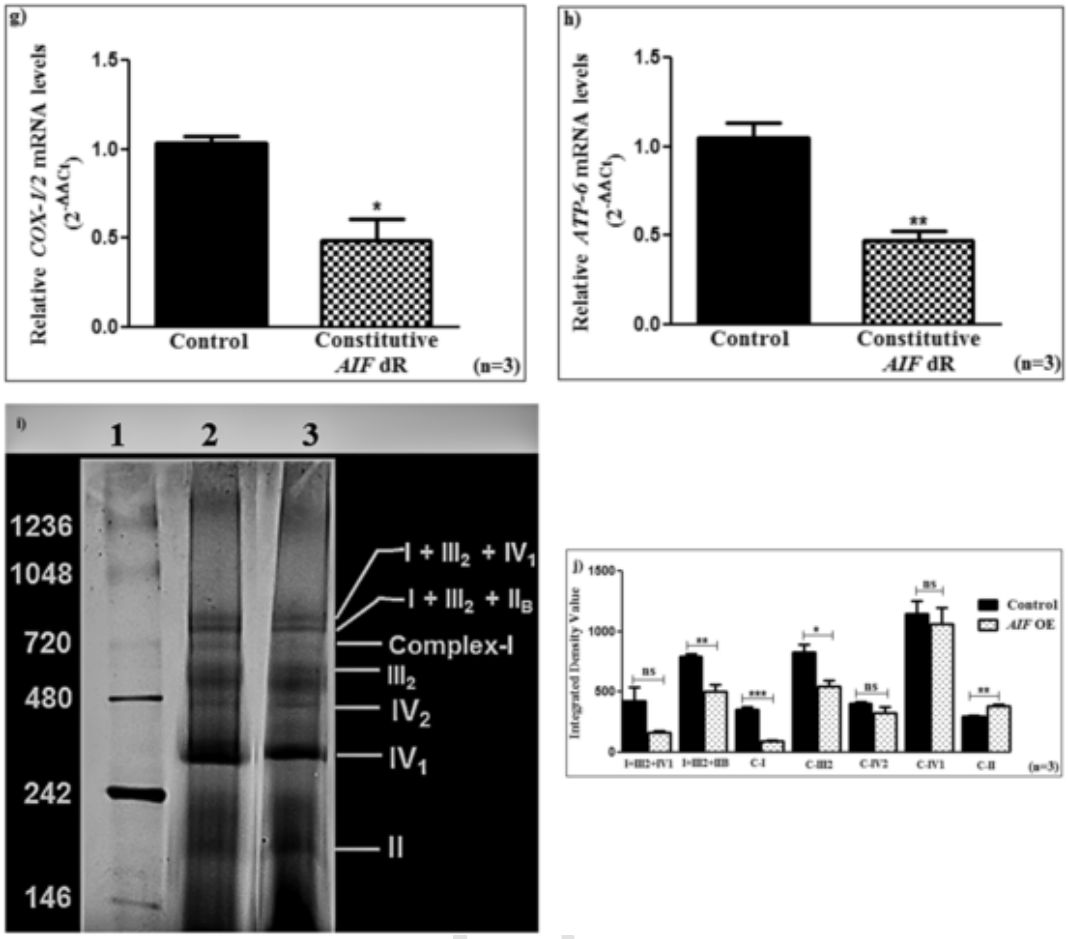

Fig. 6. *Continued*

chain deficiencies [44]. CI/CII OCR ratio in constitutive *AIF* dR cells confirmed the deficiency in CI relative to succinate oxidation (Fig. 2b). As AIF is neither an integral part of complex I of ETC or interacts with any ETC components [13,45], AIF is proposed to regulate mitochondrial biogenesis by interacting with proteins required for proper protein folding or recruitment of ETC subunits or stabilization of ETC assembly. NADH enhanced binding of AIF to oxido-reductase CHCHD4/MIA40 in Hq mutant mice stabilizes ETC subunits assembly and thereby OXPHOS maintenance [16]. MIA40 is a crucial component of the inter-membrane space (IMS) import and assembly machinery of complexes I & IV subunits. Loss of MIA40 protein was correlated with *AIF* deficiency. It acts downstream to AIF and is involved in proper folding of ETC subunits, confirming optimal mitochondrial function at the selected ETC complexes [16]. Another observed phenomenon of AIF loss is altered ROS generation as a consequence of respiratory chain dysfunction [46,47]. NADH- and two FAD-binding domains of AIF act as ROS regulator. They might be shielding the respiratory complexes from locally produced ROS [45] or modifying the electron flow through ETC complexes [48]. This hypothesis is corroborated by our study wherein GSH supplementation partially restore the complex I and complex III activities in constitutive *AIF* dR cells, mimicking the AIF′s function and strengthening the role of AIF as an oxidant regulator (Fig. 4). Our results are in agreement with a study that showed that antioxidant, MitoQ restored impaired respiration in *AIF* silenced cells [49]. Together, these observations suggest that AIF behaves as a ROS regulator and its redox activity is necessary for optimum functioning of mitochondrial bioenergetics.

Mitochondrial pathologies are the result of mutations of nuclear and mitochondrial genes encoding for proteins essential for mitochondrial homeostasis or the OXPHOS [50]. Human patients carrying Arginine deletion (R201) in AIF led to severe mitochondrial encephalomyopathy with reduced respiratory CIII and CIV levels and depleted mtDNA content in muscle biopsies, suggesting AIF′s involvement in mtDNA maintenance [14]. This was strengthened by reduced mtDNA copy number in EndoG knockout mice [51], where direct interaction of AIF with the mitochondrial endonuclease EndoG during cell death is established [5]. Troulinaki et al. [48] showed that the worm AIF homolog, WAH-1 dependent regulation of OXPHOS is functionally associated with the mtDNA homeostasis. In corroboration with these reports, we also observed diminished mtDNA content in vegetative and starved constitutive *AIF* dR cells (Fig. 5), confirming AIF′s regulatory role in mtDNA maintenance. Decrease in mtDNA pool could negatively affect the mitochondrial genes transcript as well as protein levels that eventually compromise the mitochondrial function [52]. However, the exact underlying mechanism linking AIF and mtDNA needs to be investigated further.

Apart from the role of AIF in mitochondrial respiration, a few evidences established the importance of AIF in modulating the mitochondrial structure and morphology which is balanced by fusion-fission. Telencephalon-specific *AIF* knockout mouse model (tel AIFΔ) was characterized by fragmented mitochondria with cristae malformation, while overexpression of *AIF* led to increased mitochondrial fusion [18]. Moreover, Hq mice demonstrated reduced levels of mitochondrial fusion protein, *MFN1*, indicating altered mitochondrial fusion that led to cerebellar degeneration [19]. Our present data also showed that loss of *AIF* alters mitochondrial fusion-fission process during vegetative and developmental stages of *D. discoideum* (Fig. 7 and 8). Constitutive *AIF* dR cells display decreased mitochondrial fusion and increased mito-

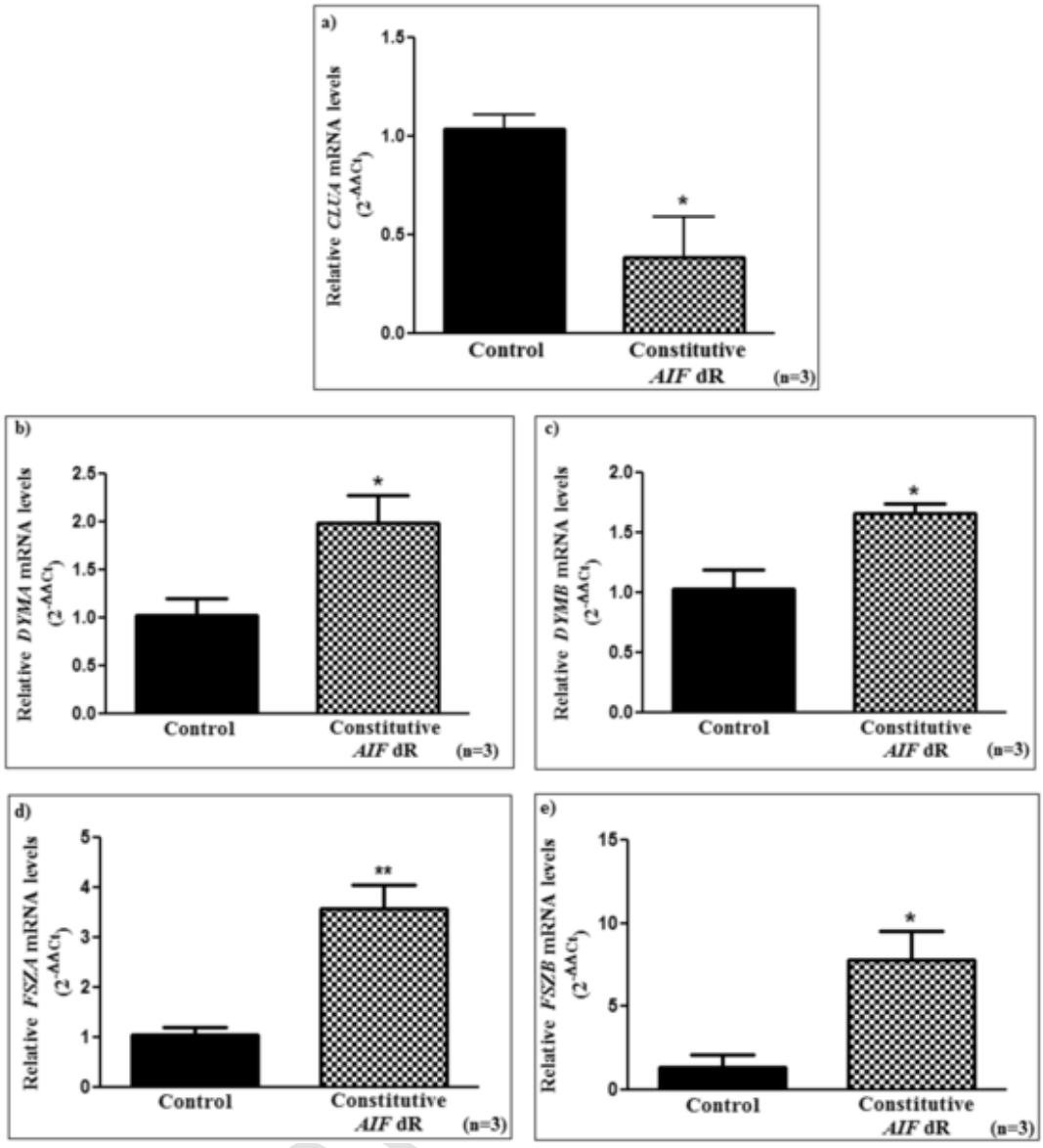

Fig. 7. Analysis of transcript levels of mitochondrial fusion-fission genes: a) Real Time PCR analysis showed significantly lower relative *CLUA* mRNA transcript levels in constitutive *AIF* dR cells as compared to control cells ($p = .0386$). b), c), d) & e) Relative *DYMA* ($p = .0453$), *DYMB* ($p = .0276$), *FSZA* ($p = .0067$) and *FSZB* ($p = .0277$) transcript levels were found to be significantly higher in constitutive *AIF* dR cells as compared to control cells. Data are representation of SEM values of three independent experiments. * $p < .05$ and ** $p < .01$ as compared to control; ns = non-significant.

chondrial fission (Fig. 7 and 8). The increase in fission was strengthened by our TEM results where more number of mitochondria in *AIF* deficient cells was observed (Fig. 9b). Loss of AIF caused defects in mitochondrial structure (Fig. 9a) which might be responsible for diminished respiratory capacity and bioenergetics failure in constitutive *AIF* dR cells. Physical interaction between AIF and mitochondrial fusion protein, Optic atrophy 1 (OPA-1) has already been established for proper cristae formation and stabilization of the ETC assembly [53]. OPA-1 lacking mitochondria showed similar metabolic defects as *AIF* deficient model. OPA-l and AIF may be part of a large multi protein complex consisting of ETC complexes and multiple structural proteins [54]. AIF's presence in the mitochondrial inter-membrane space (IMS) is requisite to maintain mitochondrial organization and morphology, possibly interacting with mitochondrial fusion-fission proteins.

Moreover, *AIF* overexpression resulted in elevated cellular ROS levels (Fig. 11), altered mitochondrial fusion-fission mechanism (Fig. 12a-e) and reduce mtDNA content (Fig. 12f). Excessive oxidative stress could damage and affect mtDNA content [38] in *AIF* OE cells. Our results corroborate with other studies suggesting *AIF* overexpression either strongly induces cell death or makes the cell sensitive to apoptosis [55,56].

Collectively, our findings enlighten the physiological role of AIF in mitochondrial homeostasis of both the vegetative and developmental stages of *D. discoideum*, controlling mitochondrial energy production by stabilizing respiratory chain complex assembly, maintaining mtDNA pool, mitochondrial structure and morphology via fusion-fission process, while its NADH activity functions as a redox regulator. Our results also suggest that fine tuning of *AIF* levels are crucial in maintaining the mitochondrial homeostasis.

5. Conclusion

Based on the existing literature, AIF is known to have two contradictory functions in cell death and cell survival. AIF acts as a survival protein possibly through its oxido-reductase property. The present study underscores the ability of mitochondria-localized AIF to influence the redox metabolism, thereby maintaining mitochondrial func-

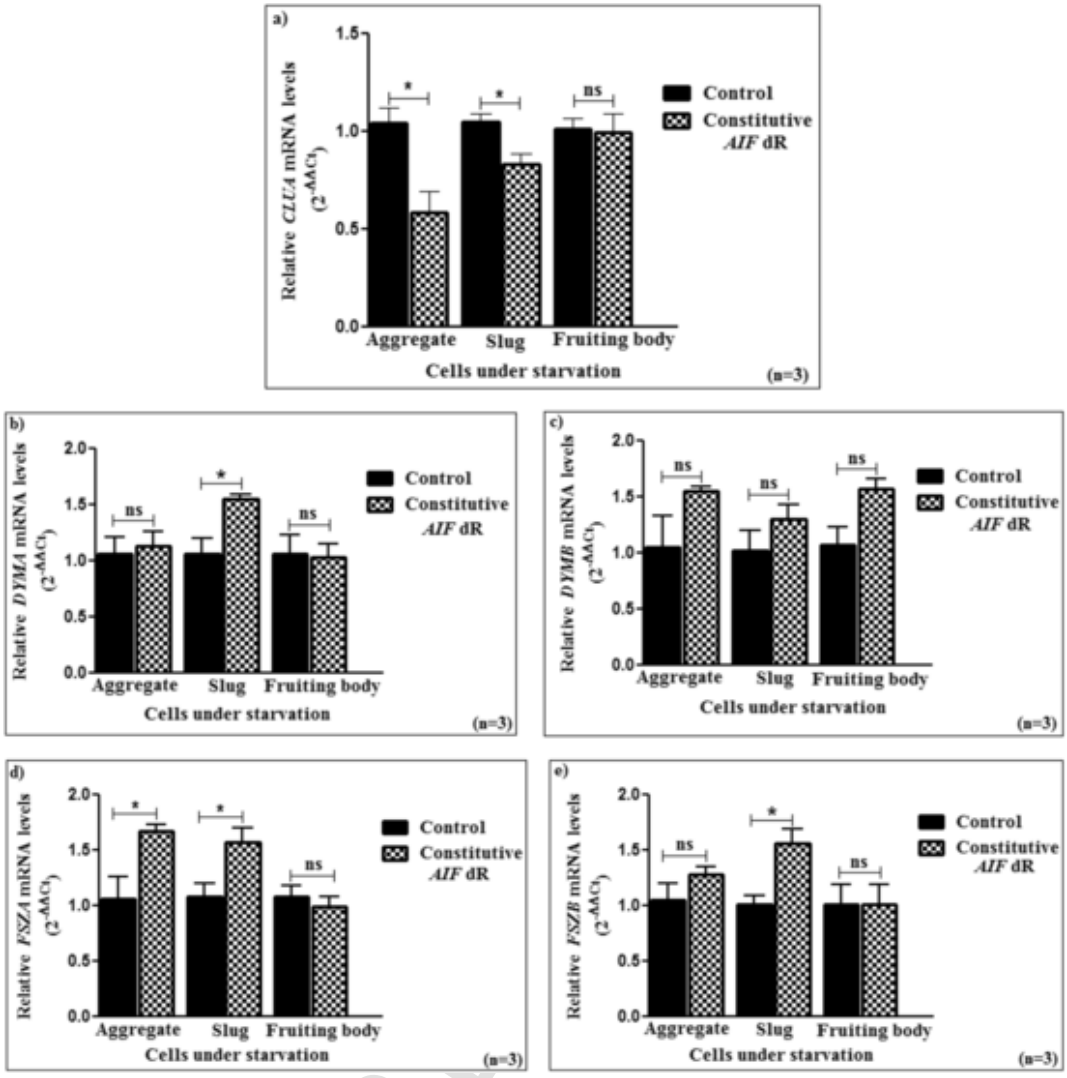

Fig. 8. Analysis of transcript levels of mitochondrial fusion-fission genes: a) Real Time PCR analysis showed significantly reduced relative *CLUA* mRNA transcript levels at the aggregate ($p = .0246$) and slug ($p = .0291$) stages of development in constitutive *AIF* dR as compared to control cells. b) Real Time PCR analysis showed significantly reduced relative *DYM A* transcript levels at slug stage ($p = .0284$) of development in constitutive *AIF* dR as compared to control cells. c) No significant difference was found in *DYM B* transcript levels of constitutive *AIF* dR cells under starvation. d) Significantly higher relative *FSZA* transcript levels were observed at the aggregate ($p = .0407$) and slug ($p = .0471$) stages of development in constitutive *AIF* dR as compared to control cells. e) Constitutive *AIF* dR cells exhibited significant elevated *FSZB* transcript levels at slug stage ($p = .0228$) of development compared to control cells. Data are representation of SEM values of three independent experiments. * $p < .05$ as compared to control; ns = non-significant.

tions and morphology in *D. discoideum* (Fig. 13). It would indeed be worthwhile to identify mitochondrial interacting targets of AIF to clarify whether it is an assembly factor of ETC or takes part in other mitochondrial activities in the inter-membrane space. In addition to this, it is useful to find out AIF inhibitors that may act as cyto-protective or cyto-toxic agents against AIF related diseases or mitochondrial diseases. This finding encompasses our understanding of molecular mechanisms underlying AIF related mitochondrial respiratory chain and redox balance diseases that may contribute to the development of new therapeutic targets.

Acknowledgments

RB thanks Department of Science and Technology (DST), New Delhi, India (SR/SO/BB-03/2010), Department of Biotechnology (DBT), New Delhi, India (BT/PR4383/BRB/10/1014/2011) and Council of Scientific and Industrial Research (CSIR), New Delhi, India [38(1383)/14/EMR-II] for financial support. We acknowledge Sophisticated Analytical Instrumentation Facility - All India Institute of Medical Sciences (SAIF-AIIMS), New Delhi for TEM facility. AK thanks CSIR, New Delhi for awarding Senior Research Fellowship (SRF).

Author contributions

Study design: AK and RB. Study conduct, data acquisition, analysis and its interpretation: AK, DM and RB. Manuscript drafting: AK and RB. Critical manuscript reviewing and editing: AK, DM, TJ, MSM and RB.

Declaration of competing interest

It is to be noted that none of the authors have any conflict of interest.

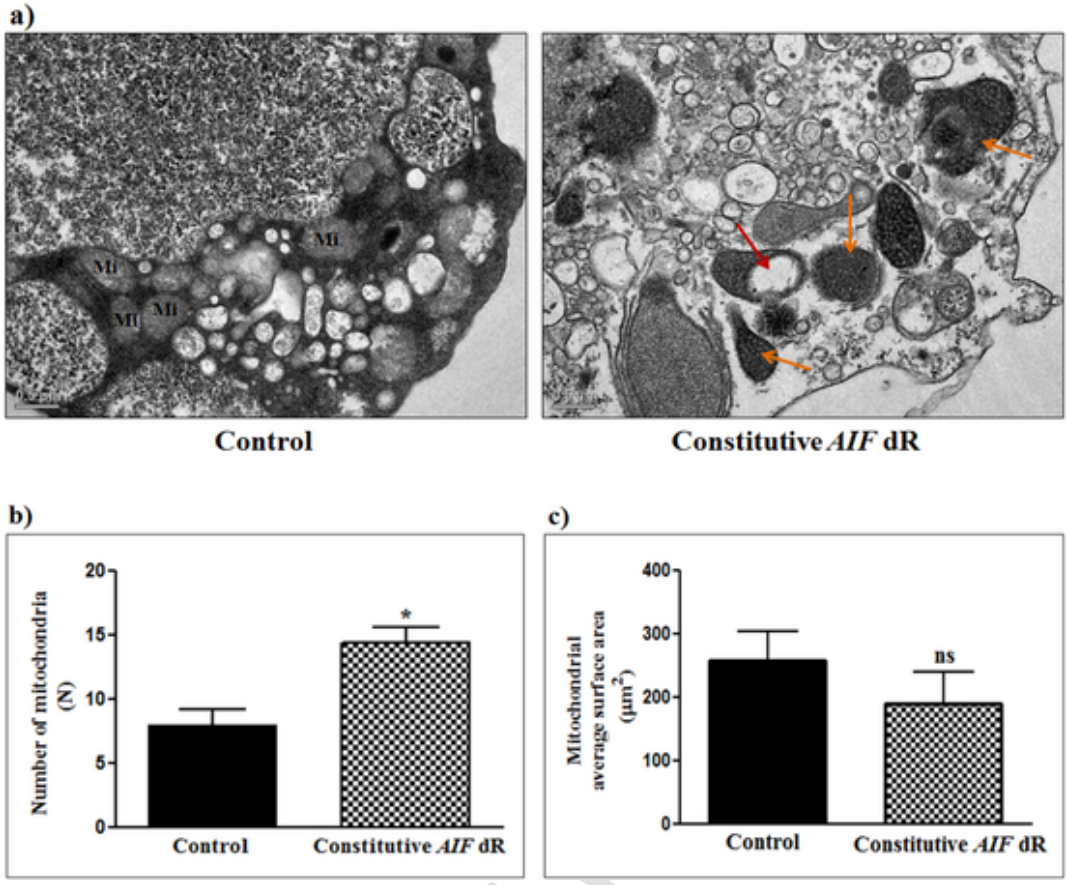

Fig. 9. Mitochondrial morphometric analysis by TEM: a) Representative electron micrographs showed compact Mitochondria (Mi) in control cells while defective (tubular and fragmented) mitochondria with a 'hole' in constitutive *AIF* dR cells. Red arrow indicates intra-mitochondrial 'hole' and orange arrow indicates defective mitochondria. Bar: 0.5 μm. b) Histogram showed significant increase in number of mitochondria in constitutive *AIF* dR compared to control cells ($p = .0191$). c) Non-significant difference was seen in mitochondrial average surface area of constitutive *AIF* dR compared to control cells. * $p < .05$ as compared to control; ns = non-significant. (For interpretation of the references to colour in this figure legend, the reader is referred to the web version of this article.)

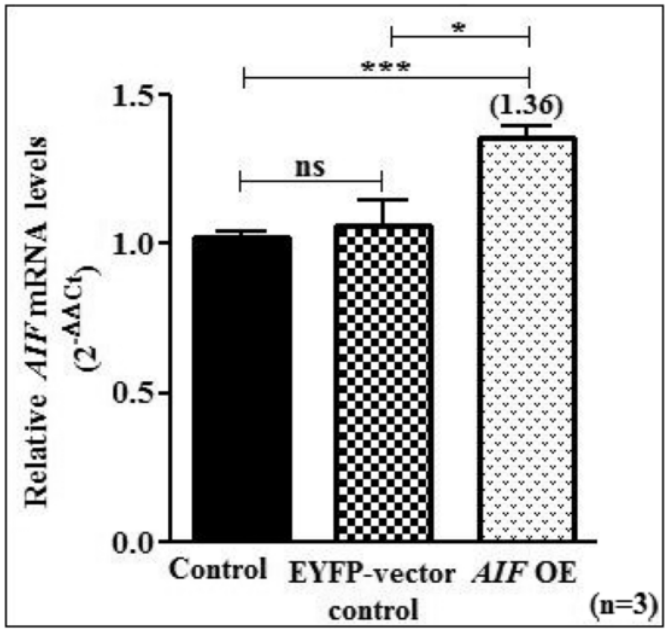

Fig. 10. Functional characterization of *AIF* overexpression by Real Time PCR: *AIF* OE cells exhibited significantly increased *AIF* transcript levels compared to control ($p < .0001$) and EYFP-vector control ($p = .0114$) cells. Data are representation of SEM values of three independent experiments. *$p < .0001$ as compared to control and *$p < .05$ as compared to EYFP-vector control; ns = non-significant.

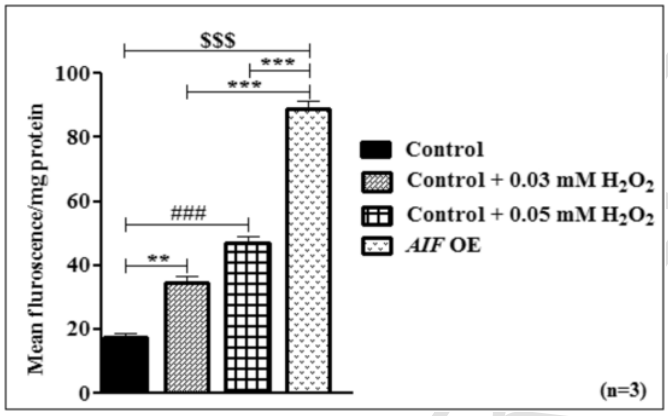

Fig. 11. Fluorimetric analysis of ROS levels using DCFDA dye: A significant rise in ROS levels was observed in *AIF* OE cells compared to control and 0.03 mM and 0.05 mM H_2O_2 treated control cells which were kept as positive controls. Data are representation of SEM values of three independent experiments. $^{\$}p < .0001$ as compared to control; *$p < .0001$ as compared to 0.03 mM and 0.05 mM H_2O_2 treated controls.

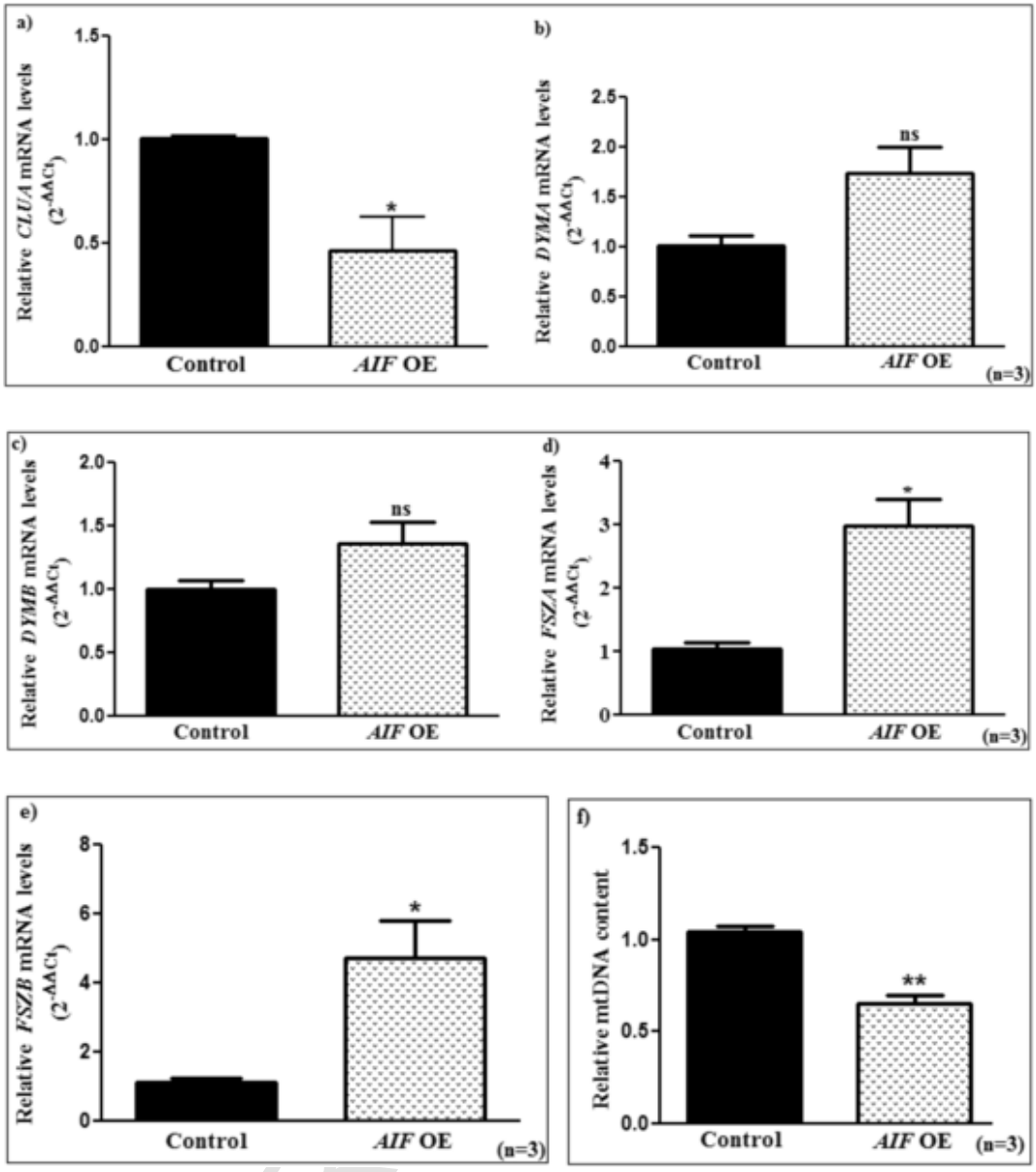

Fig. 12. Analysis of transcript levels of mitochondrial fusion-fission genes and mtDNA content by Real Time PCR: a) Significantly decreased *CLUA* transcript levels were seen in *AIF* OE cells as compared to control cells ($p = .0293$). b) and c) No significant difference was found in *DYMA* ($p = .0570$) and *DYMB* ($p = .1170$) expression of *AIF* OE cells as compared to control cells. d) and e) Significantly higher *FSZA* ($p = .0407$) and *FSZB* ($p = .0471$) transcript levels were found in *AIF* OE cells as compared to control cells. f) Estimation of relative mtDNA content: Significant diminution in mtDNA content was found in *AIF* OE cells compared to control cells ($p = .0014$). Data are representation of SEM values of three independent experiments. *$p < .05$ as compared to control; ns = non-significant.

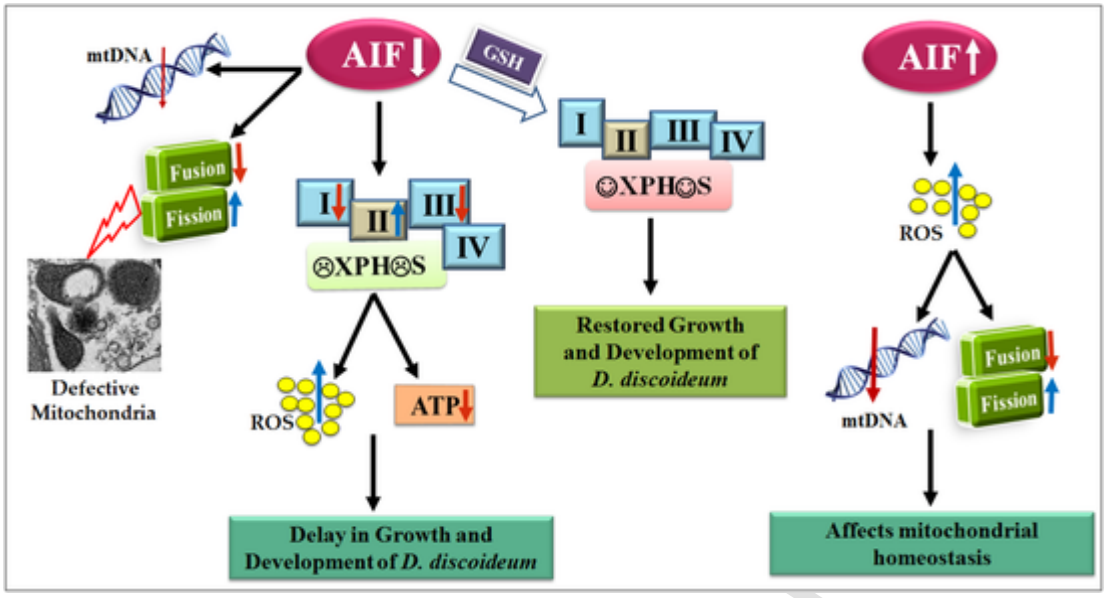

Fig. 13. Cyto-protective role of AIF in mitochondrial homeostasis maintenance.

References

[1] J. Rajawat, H. Mir, T. Alex, S. Bakshi, R. Begum, Involvement of poly(ADP-ribose) polymerase in paraptotic cell death of *D. discoideum*, Apoptosis 19 (2014) 90–101.

[2] H. Mir, J. Rajawat, R. Begum, Staurosporine induced poly (ADP-ribose) polymerase independent cell death in *Dictyostelium discoideum*, Indian J. Exp. Biol. 50 (2012) 80–86.

[3] H. Otera, S. Ohsakaya, Z. Nagaura, N. Ishihara, K. Mihara, Export of mitochondrial AIF in response to proapoptotic stimuli depends on processing at the intermembrane space, EMBO J. 24 (2005) 1375–1386.

[4] C. Cande, N. Vahsen, I. Kouranti, E. Schmitt, E. Daugas, C. Spahr, J. Luban, R.T. Kroemer, F. Giordanetto, C. Garrido, J.M. Penninger, G. Kroemer, AIF and cyclophilin a cooperate in apoptosis-associated chromatinolysis, Oncogene 23 (2004) 1514–1521.

[5] X. Wang, C. Yang, J. Chai, Y. Shi, D. Xue, Mechanisms of AIF-mediated apoptotic DNA degradation in *Caenorhabditis elegans*, Science 298 (2002) 158–1592.

[6] T. Senda, T. Yamada, N. Sakurai, M. Kubota, T. Nishizaki, E. Masai, M. Fukuda, Y. Mitsuidagger, Crystal structure of NADH-dependent ferredoxin reductase component in biphenyl dioxygenase, J. Mol. Biol. 304 (2000) 397–410.

[7] M.D. Miramar, P. Costantini, L. Ravagnan, L.M. Saraiva, D. Haouzi, G. Brothers, J.M. Penninger, M.L. Peleato, G. Kroemer, S.A. Susin, NADH oxidase activity of mitochondrial apoptosis-inducing factor, J. Biol. Chem. 276 (2001) 16391–16398.

[8] I.Y. Churbanova, I.F. Sevrioukova, Redox-dependent changes in molecular properties of mitochondrial apoptosis-inducing factor, J. Biol. Chem. 283 (2008) 5622–5631.

[9] A. Kadam, T. Jubin, H. Mir, R. Begum, Potential role of apoptosis inducing factor in evolutionarily significant eukaryote, *Dictyostelium discoideum* survival, Biochim. Biophys. Acta Gen. Subj. 1861 (1 Pt A) (2017) 2942–2955.

[10] D. Brown, B.D. Yu, N. Joza, P. Benit, J. Meneses, M. Firpo, P. Rustin, J.M. Penninger, G.R. Martin, Loss of AIF function causes cell death in the mouse embryo, but the temporal progression of patterning is normal, Proc. Natl. Acad. Sci. U. S. A. 103 (2006) 9918–9923.

[11] H. Banerjee, A. Das, S. Srivastava, H.R. Mattoo, K. Thyagarajan, J.K. Khalsa, S. Tanwar, D.S. Das, S.S. Majumdar, A. George, et al., A role for apoptosis-inducing factor in T cell development, J. Exp. Med. 209 (2012) 1641–1653.

[12] N. Joza, G.Y. Oudit, D. Brown, P. Benit, Z. Kassiri, N. Vahsen, L. Benoit, M.M. Patel, K. Nowikovsky, A. Vassault, P.H. Backx, T. Wada, G. Kroemer, P. Rustin, J.M. Penninger, Muscle-specific loss of apoptosis-inducing factor leads to mitochondrial dysfunction, skeletal muscle atrophy, and dilated cardiomyopathy, Mol. Cell. Biol. 25 (2005) 10261–10272.

[13] N. Vahsen, C. Cande, J.J. Briere, P. Benit, N. Joza, N. Larochette, P.G. Mastroberardino, M.O. Pequignot, N. Casares, V. Lazar, O. Feraud, N. Debili, S. Wissing, S. Engelhardt, F. Madeo, M. Piacentini, J.M. Penninger, H. Schagger, P. Rustin, G. Kroemer, AIF deficiency compromises oxidative phosphorylation, EMBO J. 23 (2004) 4679–4689.

[14] D. Ghezzi, I. Sevrioukova, F. Invernizzi, C. Lamperti, M. Mora, P. D'Adamo, F. Novara, O. Zuffardi, G. Uziel, M. Zeviani, Severe X-linked mitochondrial encephalomyopathy associated with a mutation in apoptosis-inducing factor, Am. J. Hum. Genet. 86 (2010) 639–649.

[15] E. Hangen, O. Feraud, S. Lachkar, H. Mou, N. Doti, G.M. Fimia, N.-V. Lam, C. Zhu, I. Godin, K. Muller, et al., Interaction between AIF and CHCHD4 regulates respiratory chain biogenesis, Mol. Cell 58 (2015) 1001–1014.

[16] K. Meyer, S. Buettner, D. Ghezzi, M. Zeviani, D. Bano, P. Nicotera, Loss of apoptosis-inducing factor critically affects MIA40 function, Cell Death Dis. 6 (2015) e1814.

[17] van der Bliek AM, Shen Q, Kawajiri S (2013) Mechanisms of mitochondrial fission and fusion. Cold Spring Harb. Perspect. Biol. 5:a011072.

[18] E.C. Cheung, N. Joza, N.A. Steenaart, K.A. McClellan, M. Neuspiel, S. McNamara, J.G. MacLaurin, P. Rippstein, D.S. Park, G.C. Shore, H.M. McBride, J.M. Penninger, R.S. Slack, Dissociating the dual roles of apoptosis-inducing factor in maintaining mitochondrial structure and apoptosis, EMBO J. 25 (2006) 4061–4073.

[19] S.H. Chung, M. Calafiore, J.M. Plane, D.E. Pleasure, W. Deng, Apoptosis inducing factor deficiency causes reduced mitofusion 1 expression and patterned Purkinje cell degeneration, Neurobiol. Dis. 41 (2011) 445–457.

[20] A.M. Kawal, H. Mir, C.K. Ramniklal, J. Rajawat, R. Begum, Structural and evolutionary analysis of PARPs in *D*, Discoideum. Am J Infect Dis 7 (2011) 67–74.

[21] B. Katoch, S. Sebastian, S. Sahdev, H. Padh, S.E. Hasnain, R. Begum, Programmed cell death and its clinical implications, Indian J. Exp. Biol. 40 (2002) 513–524.

[22] H. Mir, J. Rajawat, S. Pradhan, R. Begum, Signaling molecules involved in the transition of growth to development of *Dictyostelium discoideum*, Indian J. Exp. Biol. 45 (2007) 223–236.

[23] S.J. Annesley, P.R. Fisher, *Dictyostelium discoideum* –a model for many reasons, Mol. Cell. Biochem. 329 (2009) 73–91.

[24] D.J. Watts, J.M. Ashworth, Growth of myxamoebae of the cellular slime mould *Dictyostelium discoideum* in axenic culture, Biochem. J. 119 (1970) 171–174.

[25] G.N. Finner, P.C. Newell, GTP analogues stimulate inositol trisphosphate formation transiently in *Dictyostelium*, J. Cell Sci. 87 (1987) 513–518.

[26] Z. Li, B.H. Graham, Measurement of mitochondrial oxygen consumption using a Clark electrode, Methods Mol. Biol. 837 (2012) 63–72.

[27] O.H. Lowry, N.J. Rosebrough, A.L. Farr, R.J. Randall, Protein measurement with the Folin phenol reagent, J. Biol. Chem. 93 (1951) 265–275.

[28] K. Nagayama, S. Itono, T. Yoshida, S. Ishiguro, H. Ochiai, T. Ohmachi, Antisense RNA inhibition of the b subunit of the *Dictyostelium discoideum* mitochondrial processing peptidase induces the expression of mitochondrial proteins, Biosci. Biotechnol. Biochem. 72 (2008) 1836–1846.

[29] P. Jha, X. Wang, J. Auwerx, Analysis of mitochondrial respiratory chain supercomplexes using blue native polyacrylamide gel electrophoresis (BN-PAGE), Curr Protoc Mouse Biol 6 (2016) 1–14.

[30] K.J. Livak, T.D. Schmittgen, Analysis of relative gene expression data using real-time quantitative PCR and the 2(−Delta Delta C(T)) method, Methods 25 (2001) 402–408.

[31] K.E. Pilcher, P. Fey, P. Gaudet, A.S. Kowal, R.L. Chisholm, A reliable general purpose method for extracting genomic DNA from *Dictyostelium* cells, Nat. Protoc. 2 (2007) 1325–1328.

[32] H.L. Kim, Y.K. Choi, D.H. Kim, S.O. Park, J. Han, Y.S. Park, Tetrahydropteridine deficiency impairs mitochondrial function in *Dictyostelium discoideum* Ax2, FEBS Lett. 581 (2007) 5430–5434.

[33] J. Rajawat, T. Alex, H. Mir, A. Kadam, R. Begum, Proteases involved during oxidative stress induced poly(ADP-ribose) polymerase mediated cell death in *D. discoideum*, Microbiol 160 (2014) 1101–1111.

[34] A. Kosta, M.F. Luciani, W.J.C. Geerts, P. Golstein, Marked mitochondrial alterations upon starvation without cell death, caspases or Bcl-2 family members, Biochim. Biophys. Acta 1783 (2008) 2013–2019.

[35] O. Myhre, J.M. Andersen, H. Aarnes, F. Fonnum, Evaluation of the probes 2,7-dichlorofluorescein diacetate, luminol, and lucigenin as indicators of reactive species formation, Biochem. Pharmacol. 65 (2003) 1575–1582.

[36] S. Milasta, C.P. Dillon, O.E. Sturm, K.C. Verbist, T.L. Brewer, G. Quarato, S.A. Brown, S. Frase, L.J. Janke, S.S. Perry, P.G. Thomas, D.R. Green, Apoptosis-inducing-factor-dependent mitochondrial function is required for T cell but not B cell function, Immunity 44 (2016) 88–102.

[37] D.C. Chan, Mitochondrial fusion and fission in mammals, Annu. Rev. Cell Dev. Biol. 22 (2006) 79–99.
[38] B. Van Houten, S.E. Hunter, J.N. Meyer, Mitochondrial DNA damage induced autophagy, cell death, And Disease. Front Biosci (Landmark Ed) 21 (2016) 42–54.
[39] M. Kettwig, M. Schubach, F.A. Zimmermann, L. Klinge, J.A. Mayr, S. Biskup, et al., From ventriculomegaly to severe muscular atrophy: expansion of the clinical spectrum related to mutations in AIFM1, Mitochondrion 21 (2015) 12–18.
[40] C. Rinaldi, C. Grunseich, I.F. Sevrioukova, A. Schindler, I. Horkayne-Szakaly, C. Lamperti, et al., Cowchock syndrome is associated with a mutation in apoptosis-inducing factor, Am. J. Hum. Genet. 91 (2012) 1095–1102.
[41] J.A. Pospisilik, C. Knauf, N. Joza, P. Benit, M. Orthofer, P.D. Cani, et al., Targeted deletion of AIF decreases mitochondrial oxidative phosphorylation and protects from obesity and diabetes, Cell 131 (2007) 476–491.
[42] R. Dhingra, L.A. Kirshenbaum, Succinate dehydrogenase/complex II activity obligatorily links mitochondrial reserve respiratory capacity to cell survival in cardiac myocytes, Cell Death Dis. 6 (2015) e1956.
[43] C.L. Quinlan, A.L. Orr, I.V. Perevoshchikova, J.R. Treberg, B.A. Ackrell, M.D. Brand, Mitochondrial complex II can generate reactive oxygen species at high rates in both the forward and reverse reactions, J. Biol. Chem. 287 (2012) 27255–27264.
[44] P. Rustin, D. Chretien, T. Bourgeron, A. Wucher, J.M. Saudubray, A. Rotig, A. Munnich, Assessment of the mitochondrial respiratory chain, Lancet 338 (8758) (1991) 60.
[45] I.F. Sevrioukova, Apoptosis inducing factor: structure, Function and Redox Regulation. Antioxid Redox Signal 14 (2011) 2545–2579.
[46] A. Urbano, U. Lakshmanan, P.H. Choo, J.C. Kwan, P.Y. Ng, K. Guo, S. Dhakshinamoorthy, A. Porter, AIF suppresses chemical stress-induced apoptosis and maintains the transformed state of tumor cells, EMBO J. 24 (2005) 2815–2826.
[47] J.A. Klein, C.M. Longo-Guess, M.P. Rossmann, K.L. Seburn, R.E. Hurd, W.N. Frankel, R.T. Bronson, S.L. Ackerman, The harlequin mouse mutation down-regulates apoptosis-inducing factor, Nature 419 (2002) 367–374.
[48] K. Troulinaki, S. Büttner, A. Marsal Cots, S. Maida, K. Meyer, F. Bertan, A. Gioran, A. Piazzesi, A. Fornarelli, P. Nicotera, D. Bano, WAH-1/AIF regulates mitochondrial oxidative phosphorylation in the nematode *Caenorhabditis elegans*, Cell Death Discov 4 (2018) 2.
[49] N. Apostolova, A.M. Cervera, V.M. Victor, S. Cadenas, A. Sanjuan-Pla, A. Alvarez-Barrientos, J.V. Esplugues, K.J. McCreath, Loss of apoptosis-inducing factor leads to an increase in reactive oxygen species, and an impairment of respiration that can be reversed by antioxidants, Cell Death Differ. 13 (2006) 354–357.
[50] A.H. Schapira, Mitochondrial diseases, Lancet 379 (2012) 1825–1834.
[51] C. McDermott-Roe, J. Ye, R. Ahmed, X.M. Sun, A. Serafín, J. Ware, et al., Endonuclease G is a novel determinant of cardiac hypertrophy and mitochondrial function, Nature 478 (2011) 114–118.
[52] R. Barazzoni, K.R. Short, K.S. Nair, Effects of aging on mitochondrial DNA copy number and cytochrome c oxidase gene expression in rat skeletal muscle, liver, and heart, J. Biol. Chem. 275 (2000) 3343–3347.
[53] C. Zanna, A. Ghelli, A.M. Porcelli, M. Karbowski, R.J. Youle, S. Schimpf, et al., OPA1 mutations associated with dominant optic atrophy impair oxidative phosphorylation and mitochondrial fusion, Brain 131 (2008) 352–367.
[54] H. Chen, A. Chomyn, D.C. Chan, Disruption of fusion results in mitochondrial heterogeneity and dysfunction, J. Biol. Chem. 280 (2005) 26185–26192.
[55] C. Zhang, K.G. Csaky, Over expression apoptosis inducing factor (AIF) sensitizes human retinal pigment epithelium (HRPE) to oxidant induced cell death, Investig. Ophthalmol. Vis. Sci. 47 (2006) 1380.
[56] S. Wissing, P. Ludovico, E. Herker, S. Büttner, S.M. Engelhardt, T. Decker, A. Link, et al., An AIF orthologue regulates apoptosis in yeast, J. Cell Biol. 166 (2004) 969–974.

Biol. Cell (2019) **111,** 187–197 DOI: 10.1111/boc.201800056

Research article

Poly(ADP-ribose) polymerase-1 (PARP-1) regulates developmental morphogenesis and chemotaxis in *Dictyostelium discoideum*

Tina Jubin, Ashlesha Kadam and Rasheedunnisa Begum[1]

Department of Biochemistry, Faculty of Science, The Maharaja Sayajirao University of Baroda, Vadodara 390 002, India

Background information. Poly(ADP-ribose) polymerase-1 (PARP-1) has been attributed to varied roles in DNA repair, cell cycle, cell death, etc. Our previous reports demonstrate the role of PARP-1 during *Dictyostelium discoideum* development by its constitutive downregulation as well as by PARP-1 ortholog, *ADP ribosyl transferase 1 A* (*ADPRT1A*) overexpression. The current study analyses and strengthens the function of ADPRT1A in multicellular morphogenesis of *D. discoideum. ADPRT1A* was knocked out, and its effect was studied on cAMP signalling, chemotaxis and development of *D. discoideum*.

Results. We report that *ADPRT1A* is essential in multicellular development of *D. discoideum,* particularly at the aggregation stage. Genetic alterations of *ADPRT1A* and chemical inhibition of its activity affects the intracellular and extracellular cAMP levels during aggregation along with chemotaxis. Exogenous cAMP pulses could rescue this defect in the *ADPRT1A* knockout (*ADPRT1A* KO). Expression analysis of genes involved in cAMP signalling reveals altered transcript levels of four essential genes (*PDSA, REGA, ACAA* and *CARA*). Moreover, *ADPRT1A* KO affects prespore- and prestalk-specific gene expression and prestalk tendency is favoured in the *ADPRT1A* KO.

Conclusion. ADPRT1A plays a definite role in regulating developmental morphogenesis via cAMP signalling.

Significance. This study helps in understanding the role of PARP-1 in multicellular development and differentiation in higher complex organisms.

Introduction

Dictyostelium discoideum, a unicellular eukaryote exhibits multicellularity upon starvation [Raper, 1984). Under nutrient starvation conditions, cAMP acts not only as an intracellular second messenger but also as a secreted extracellular signal. Secreted cAMP signals to approximately 10,000 *D. discoideum* cells to chemotax and form a multicellular aggregate [Konijn et al., 1969]. The aggregate then forms a migrating slug and finally culminates into a fruiting body consisting of a slender dead stalk crowned by a cluster of viable spores enveloped by a spore case. Twenty per cent of cells at the anterior of the slug called 'prestalk cells' differentiate to form the stalk of the fruiting body, whereas 80% of the posterior 'prespore cells' form the spores [Raper, 1984; Williams, 2006]. These cell types can be identified by a set of molecular markers [Gaudet et al., 2008] namely *EcmA, EcmB* (prestalk specific) and *D19* (prespore specific). Secreted cAMP also binds to a G-protein-coupled cAMP receptor A (CARA) and activates adenylyl cyclase A (ACAA). Upon activation, ACAA catalyses the conversion of

[1]To whom correspondence should be addressed: (email: rasheedunnisab@yahoo.co.in)
Key words: cAMP signalling, cell differentiation, development.
Abbreviations: ACAA, adenylyl cyclase A; ADPRT1A KO, ADPRT1A knockout; ADPRT1A OE, ADPRT1A overexpression; ADPRT1A, ADP Ribosyl transferase 1 A; ADPRTs, ADP ribosyl transferases; cAMP, cyclic AMP; CARA, cAMP receptor A; NNA, non-nutrient agar; PARP dR, PARP downregulation; PARP, poly(ADP-ribose) polymerase; PARP-1, poly(ADP-ribose) polymerase-1; qPCR, quantitative PCR; SB, Sorensons's buffer.

ATP to cAMP, which is either secreted or used to initiate intracellular signalling events. cAMP levels are regulated, in part, by intracellular (REGA) and extracellular (PDSA and PDE4) phosphodiesterases, degrading excess intracellular and extracellular cAMP, respectively [Faure et al., 1990; Shaulsky et al., 1996; Bader et al., 2006; Garcia et al., 2009]. The organised generation of cAMP pulses and their relay is important for both initiating aggregation and formation of fruiting bodies [Gomer et al., 2011; Jaiswal et al., 2012].

D. discoideum possesses eight potential poly(ADP-ribose) polymerase (*PARP*) genes [Kawal et al., 2011]. *Drosophila* PARP has been reported to be involved in cytoskeletal organisation and the determination of tissue polarity during development [Uchida et al., 2002]. Moreover, it has been identified to regulate timely expression and silencing of both euchromatic and heterochromatic sequences during *Drosophila* development [Tulin and Spradling, 2003]. Hamazaki et al. [2015] have shown that inhibition of PARP catalytic activity led to inhibition of DNA de-methylation of *IL17d* promoter at the two-cell stage in mice leading to downregulation of the target mRNAs, which are essential for early embryogenesis. PARP proteins regulate cell proliferation [Colon-Otero et al., 1987; Jubin et al., 2016a] and cell differentiation [Exley et al., 1987; Jubin et al., 2016b] and repair DNA double strand breaks [Satoh and Lindahl, 1992; Couto et al., 2011, 2013; Pears and Lakin, 2014]. Poly(ADP-ribose) polymerase-1 (PARP-1) is a ~116-kDa ubiquitously expressed protein [D'amours et al., 1999]. PARP-1 activation has been reported to modify chromatin-associated proteins eventually regulating transcription [Beneke, 2012]. PARP-1 has also been shown to be involved in stress responses like oxidative stress and UV stress in *D. discoideum* [Couto et al., 2011; Rajawat et al., 2014a, 2014b; Mir et al., 2015; Jubin et al., 2016c]. Our previous studies on *ADPRT1A (ADP-ribosyl transferase-1A,* the PARP-1 ortholog in *D. discoideum)* overexpression indicated a link between ADPRT1A and cell growth along with multicellularity in *D. discoideum* [Jubin et al., 2016c]. Hence, the present study aims to confirm the role of ADPRT1A in developmental morphogenesis and cAMP signalling using a loss-of-function mutant; namely, *ADPRT1A* knockout. This is the first report, where the regulatory function of ADPRT1A in developmental morphogenesis via cAMP signalling and chemotaxis in *D. discoideum* is well documented.

Results

ADPRT1A and *D. discoideum* development

On subjecting *ADPRT1A* KO cells to starvation and subsequent development caused the initial aggregation process of development to be delayed significantly (Figure 1). Loose aggregates were seen only at 12 h in *ADPRT1A* KO, as compared to 6 h in the control cells (Figure 1A); ultimately leading to delayed developmental morphogenesis at 45 h, as compared to 24 h in the control cells (Figure 1C). In addition to the delay in aggregation, *ADPRT1A* KO cells yielded smaller and more aggregates, as compared to control cells (Figure 1A). As a result of forming small aggregates, fruiting bodies were smaller in size (smaller spore heads) and more in number, as compared to control cells (Figure 1C). It was also noted that *ADPRT1A* KO cells formed discontinuous streaming structures during aggregation, as compared to the control cells (Figure 1B). Thus, our results in the knockout background clearly point to a role of ADPRT1A in early development.

ADPRT1A and cAMP signalling, chemotaxis

cAMP acts as the signalling molecule during *Dictyostelium* development, particularly during aggregation and culmination [Kessin, 2001]. Thus, in order to explore whether delayed and defective aggregation in *ADPRT1A* KO is due to defective cAMP signalling, both intracellular and extracellular cAMP levels were estimated during development. Comparative analysis of *ADPRT1A* OE*, PARP* dR and PARP inhibited cells was also carried out along with *ADPRT1A* KO, and the results are shown in Figures 2A and 2B. *ADPRT1A* KO and *ADPRT1A* OE cells displayed significant reduction ($P < 0.001$) in cAMP levels as compared to control cells at 6 h of starvation (time point at which control cells initiate aggregate formation) (Figures 2A and 2B). *PARP* dR and PARP inhibition also showed decreased intracellular (Figure 2A) as well as extracellular cAMP levels (Figure 2B), suggesting regulated cAMP production is essential for initiation of development [Schulkes and Schaap, 1995]. Thus, alteration in cAMP levels may lead to a delay in the initiation of aggregation in ADPRT1A mutant phenotypes. In addition, we checked restoration in cAMP levels in these cells

Figure 1 | Role of *ADPRT1A* in *D. discoideum* development
(**A**) *ADPRT1A* KO cells (bottom panels) showed aggregation delay compared to control cells (top panels). Bar scale: 100 μm. Data are representative of three independent experiments. (**B**) Streaming structures of control and *ADPRT1A* KO cells developed on the NNA plates. Bar scale: 100 μm. (**C**) The fruiting body of control and *ADPRT1A* KO cells developed on the NNA plates. Bar scale: 100 μm.

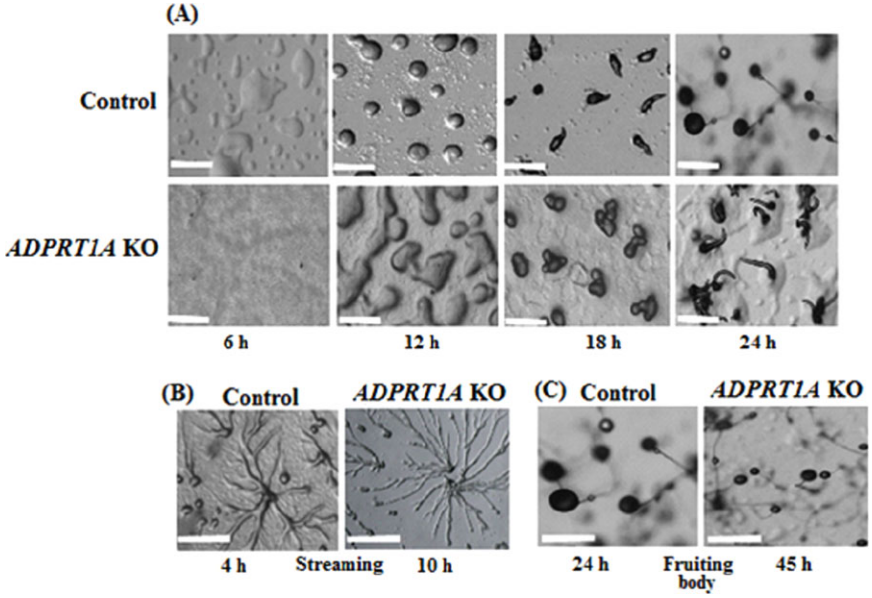

at a time point during loose aggregate formation (~12 h) and we observed a significant increase ($P < 0.05$) in cAMP levels upon ADPRT inhibition and downregulated cells compared to 6 h after starvation (Figure 2), but *ADPRT1A* KO and *ADPRT1A* OE showed no significant changes in cAMP levels. The partial restoration in cAMP levels at 12 h likely explains the delayed morphogenesis in *ADPRT1A* KO and *ADPRT1A* OE cells. Nevertheless, restoration in cAMP levels was not seen in PARP-inhibited and *PARP* dR cells consistent with a stall in development. This could be due to inhibition of all (ADP ribosyl transferase) ADPRT isoforms during downregulation (antisense against conserved catalytic domain) and chemical inhibition using benzamide (substrate analogue for ADPRTs), whereas other isoforms viz. ADPRT2 and ADPRT1B might have compensated for the ADPRT1A loss of function in *ADPRT1A* KO. In conclusion, both catalytic activity and the physical presence of ADPRT1A are essential for *D. discoideum* development as both gene loss and chemical inhibition of catalytic activity affected the cAMP levels.

Subsequent to cAMP estimation, we performed the droplet chemotaxis assay to explore the defective chemotactic response to cAMP. *ADPRT1A* KO and *PARP* dR cells displayed significant chemotaxis defects towards 1 μM cAMP as compared to 5 h in control cells (Figure 2C). Nevertheless, *ADPRT1A* OE and PARP-inhibited cells showed a few cells to chemotax towards cAMP, but it was not comparable to control cells (Figure 2C).

Thus, lack of both ADPRT1A and its catalytic activity leads to decreased cAMP levels and altered chemotaxis, which contributes to defective cAMP signalling. This was confirmed by pulsing the cells with 50 nM cAMP, whereupon pulsed *ADPRT1A* KO cells not only displayed rescued chemotaxis but also formed fruiting bodies at ~22 h, as opposed to 20 h in control cells (Figures 3A and 3B). Thus, ADPRT1A is involved in relaying cAMP signals as well as in regulating the synthesis and release of cAMP during the early developmental stages of *D. discoideum*.

ADPRT1A and cAMP signalling genes

We have reported diverse signalling molecules and regulatory components involved in the initiation and early developmental stages of *D. discoideum* [Mir et al.,

Figure 2 | cAMP estimation and chemotaxis assay

(**A**) Intracellular cAMP concentration after 6 h of nutrient starvation in control, *ADPRT1A* KO, *ADPRT1A* OE, PARP-inhibited and *PARP* dR cells and at the time point of loose aggregate formation in *ADPRT1A* KO, *ADPRT1A* OE, PARP-inhibited and *PARP* dR cells. $^{*}P < 0.05$, $^{**}P < 0.01$ and $^{***}P < 0.001$ as compared to intracellular cAMP in control cells at 6 h. Data are representative of SEM values of four independent experiments. (**B**) Extracellular cAMP concentration after 6 h of nutrient starvation and at the time point of loose aggregate formation in control, *ADPRT1A* KO, *ADPRT1A* OE, PARP-inhibited and *PARP* dR cells. $^{*}P < 0.05$, $^{**}P < 0.01$ and $^{***}P < 0.001$ as compared to extracellular cAMP in control cells at 6 h. Data are representative of SEM values of three independent experiments. (**C**) *ADPRT1A* KO, *ADPRT1A* OE, PARP-inhibited and *PARP* dR cells failed to move towards 1 μM cAMP. Photographs were captured 5 h after plating the cells at 40× magnification. Results are representative of three independent experiments.

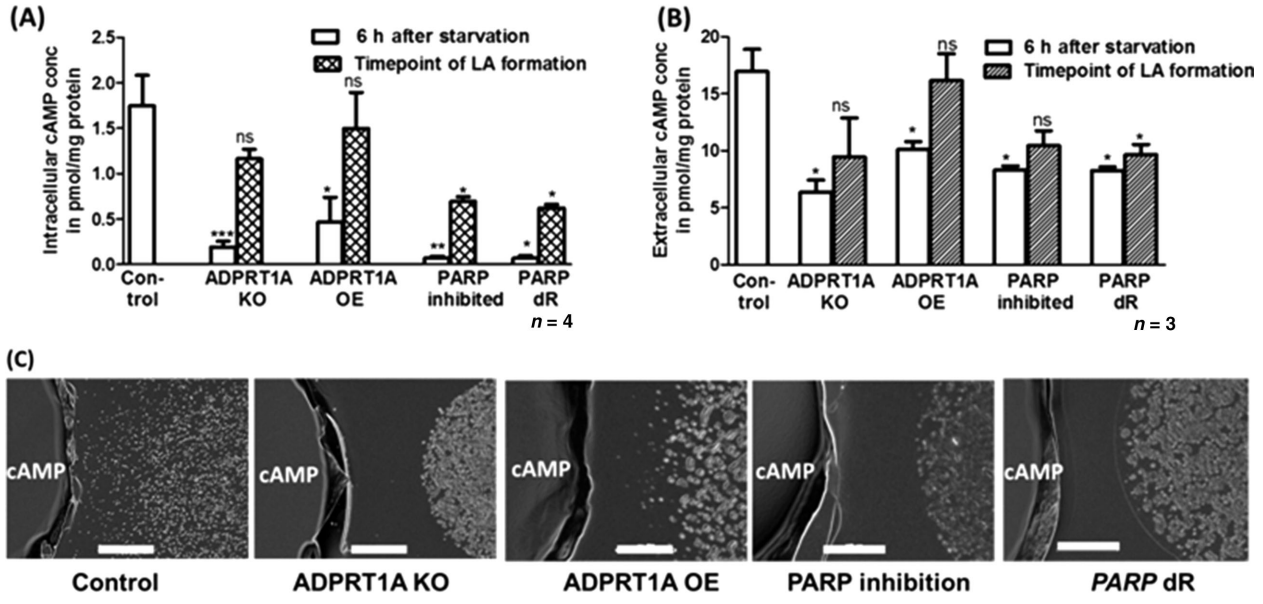

2007; Kadam et al., 2017]. cAMP is one of the important signalling molecules in *D. discoideum* developmental morphogenesis, particularly during aggregation and late developmental stages [Mir et al., 2007]. Mutants that exhibit defects in aggregate formation have been reported to show altered expression of *ACAA, CARA, PDSA* and, *REGA* genes [Hirose et al., 2000; Wu and Janetopoulos, 2013; Garciandia and Suarez, 2013]. The effect of *ADPRT1A* KO on cAMP signalling was addressed by analysing the transcript levels of the aforementioned genes involved in cAMP signal transduction. We examined extracellular and intracellular phosphodiesterases (*PDSA* and *REGA)*, adenylyl cyclase (*ACAA*) and cAMP receptor (*CARA*) transcript levels during early stages of development, that is 0–8 h of development. *ADPRT1A* KO cells showed decreased expression of *PDSA*, *REGA, ACAA* and *CARA* genes (Figures 4A, 4E, 4I and 4M), whereas *PARP* dR cells (Figures 4D, 4H, 4L and 4P) showed similar transcription profiles, but much reduced expression of genes involved in cAMP signalling as compared to control and *ADPRT1A* KO cells. Also, *ADPRT1A* OE (Figures 4B, 4F, 4J and 4N) and PARP-inhibited cells (Figures 4C, 4G, 4K and 4O) displayed a similar transcription profile. Overexpression of *ADPRT1A* may lead to overactivation of ADPRT1A, which in turn leads to higher auto ADP-ribosylation and hence inactivation of ADPRT1A, thereby mimicking ADPRT (PARP) inhibition. Additionally, transcript levels of *PDSA, ACAA* and *CARA* genes in *ADPRT1A* KO showed rescue during loose aggregate formation, which could be due to compensation of function by ADPRT isoforms. However, no rescue was seen even at a loose aggregate time point in *PARP* dR, which likely explains stalled development.

Figure 3 | Effect of exogenous cAMP pulsing on chemotaxis and development in *ADPRT1A* KO cells
(**A**) 2 x 10^7 cells/ml cells were starved with or without cAMP pulses every 6 min for 6 h. Droplets of pulsed cells were spotted next to 1 μM cAMP droplets on agar plates, and photographs were taken after 6 h. Results are representative of three independent experiments. Bar scale: 100 μm. (**B**) cAMP-pulsed *ADPRT1A* KO cells show normal aggregation in the absence of *ADPRT1A*. Cells were stimulated by 50 nM cAMP pulses every 6 min for 6 h and then were developed on NNA plates at 1 x 10^8 cells/ml. Time points on panels indicate time elapsed after cells were washed following the completion of cAMP pulsing. cAMP-pulsed *ADPRT1A* KO cells showed normal development without significant developmental delay. Results are representative of three independent experiments. Bar scale: 100 μm.

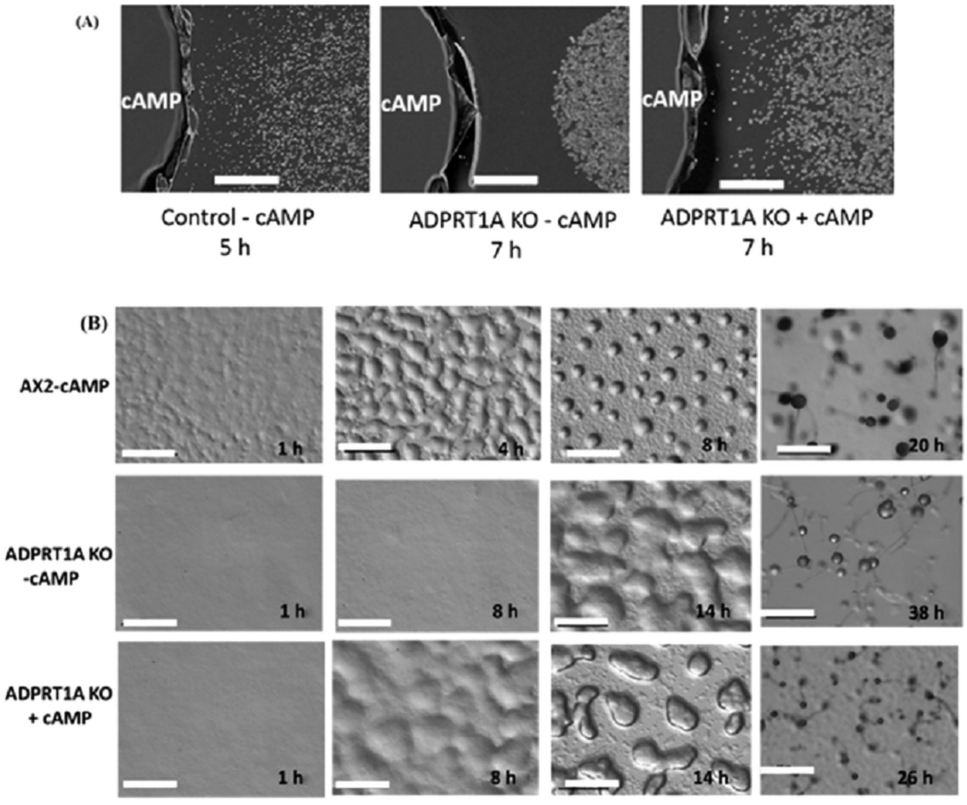

To further strengthen our hypothesis of compensatory function, we checked for *ADPRT2* (PARP-2 ortholog) transcript levels in *ADPRT1A* KO cells and *ADPRT2* levels were observed to be higher in *ADPRT1A* KO as compared to control cells at 8 h of starvation (Figures 5A and 5B). A delay was still observed, however as ADPRT2 might not be able to compensate for ADPRT1A function completely. Such results have been reported for *PARP-1* deficiency, where PARP-2 compensated for the loss of PARP-1, thus proving non-redundant functions [De Murcia et al., 2003].

Low *ACAA* and *CARA* levels explain the low intracellular cAMP levels in *ADPRT1A* KO, and *REGA* levels in *ADPRT1A* KO were significantly decreased (Figures 4I and 4M). On the contrary, *ADPRT1A* OE cells showed higher *ACAA* (Figure 4J) which might lead to higher cAMP levels which were further taken care of by the *REGA* levels seen in *ADPRT1A* OE cells, as observed in Figure 4F whereas *REGA* levels in *ADPRT1A* KO and *PARP* dR were significantly decreased (Figures 4E and 4H). Changes in transcript levels as seen in ADPRT-inhibited cells are due to decreased ADPRT/PARP activity of all isoforms, as the inhibitor used is an NAD^+ analogue that is the substrate for all ADPRTs. *ADPRT1A* KO, PARP inhibition and *PARP* dR showed similar transcript profiles for the aforementioned genes involved in regulating cAMP-signalling. *ADPRT1A* OE showed a different profile, as *CARA* levels were low, while an

Figure 4 | Expression patterns of cAMP signalling genes in *ADPRT1A* KO [A, E, I, M], *ADPRT1A* OE [B, F, J, N], PARP inhibited [C, G, K, O] and *PARP* dR [D, H, L, P] cells

Expression levels of each gene (*PDSA, REGA, ACAA and CARA*) at 6 h time point were analysed by qPCR. The levels were normalised to that of the endogenous control *RNLA* (mitochondrial large rRNA). Data are the representation of the SEM values of five independent experiments.

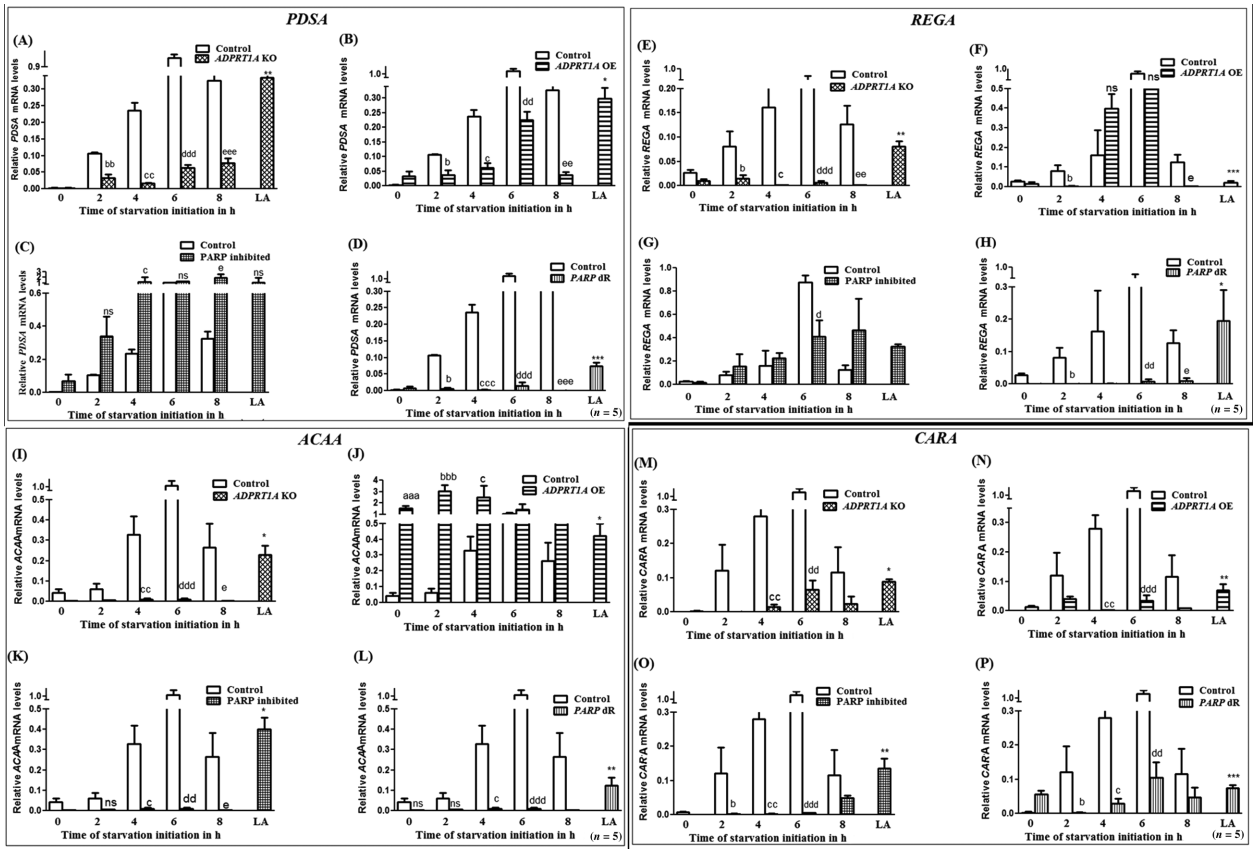

increase in *ACAA* and *PDSA* levels was seen. However, REGA remained unaffected. These phenotypes could be due to overexpression of *ADPRT1A* and hence higher ADPRT activity, which leads to auto-PARylation and regulation in ADPRT activity. In conclusion, the *ADPRT1A* KO profile gave us a much better understanding of the role of *ADPRT1A* KO due to its specificity unlike PARP inhibition and *PARP* dR, where all PARPs are likely to be affected. Also, *ADPRT1A* OE showed results like PARP inhibition leading to inactivation.

Furthermore, the aggregation and chemotaxis defects, which were seen due to an anomaly in cAMP-signalling, were validated by cAMP pulse which rescued defects in chemotaxis and development (Figures 3A and 3B, respectively). Thus, the above results in *ADPRT1A* KO, PARP-inhibited and *PARP* dR cells and other reports together suggest that PARP-1 interacts with histones and chromatin-modifying enzymes to control their activity at target gene promoters, ultimately affecting gene expression [Frizzell et al., 2009], emphasising ADPRT1A's role in regulation of transcription of genes involved in cAMP signal transduction.

ADPRT1A and differentiation

In order to explore the transcriptional regulatory role of ADPRT1A during cellular differentiation, we investigated prespore (*D19*) and prestalk markers (*ECMA* and *ECMB*) in *ADPRT1A* KO slugs by quantitative PCR (qPCR). *ADPRT1A* KO cells showed higher expression of the prestalk markers, *ECMA,*

Figure 5 | ADPRT isoforms in *ADPRT1A* KO

(**A**) qPCR analysis of *ADPRT1B* transcript levels in *ADPRT1A* KO cells. Data are the representation of the SEM values of three independent experiments. (**B**) qPCR analysis of *ADPRT2* transcript levels in *ADPRT1A* KO cells. Data are the representation of the SEM values of three independent experiments.

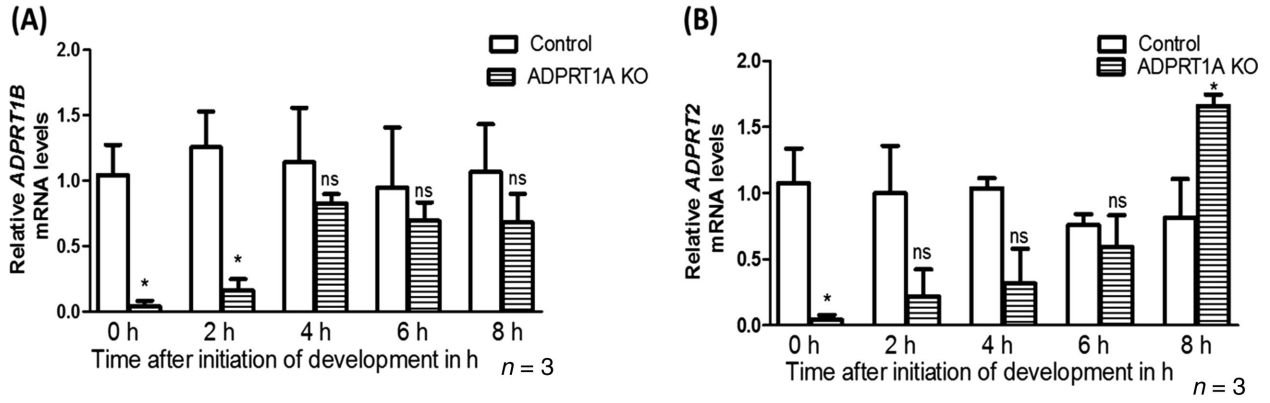

Figure 6 | Prespore and prestalk markers in *ADPRT1A* KO

(**A**) qPCR analysis of *ECMA, ECMB* and *D19* transcripts in *ADPRT1A* KO cells. Data are the representation of the SEM values of three independent experiments. (**B**) Neutral red stained slugs of control and *ADPRT1A* KO cells. Data are representative of three independent experiments. Bar scale: 100 μm.

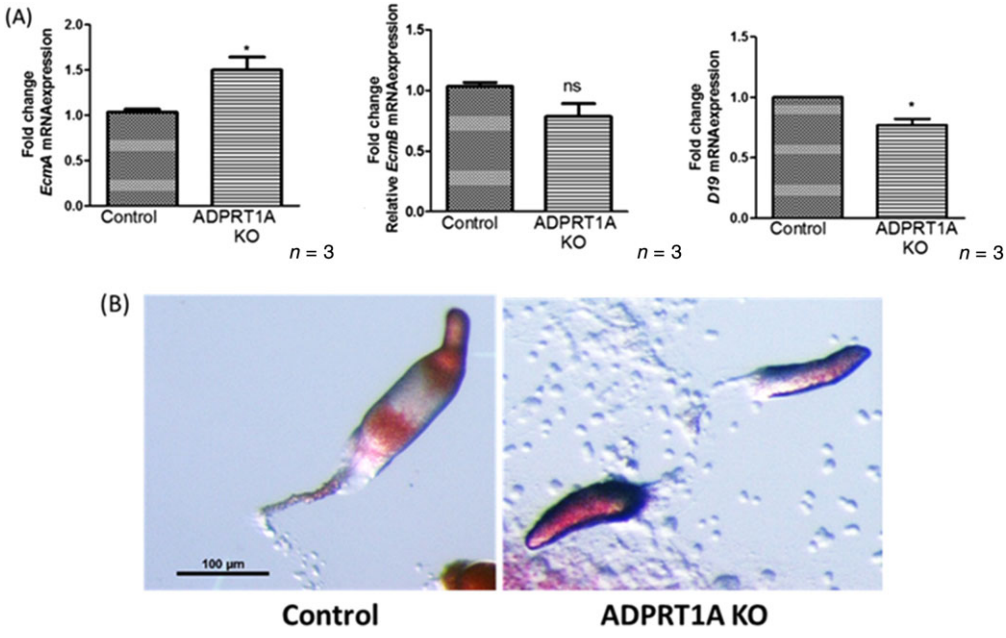

ECMB, and *D19* as compared to control cells as shown in Figure 6A. This was further substantiated by neutral red staining of control and *ADPRT1A* KO slugs, which also showed a higher proportion of prestalk cells (red) in *ADPRT1A* KO (Figure 6B). *ADPRT1A* OE and PARP-inhibited cells also showed similar transcriptional profile and neutral red staining (data not shown). Thus, these results suggest a role of ADPRT1A in cellular differentiation which needs to be further explored.

Discussion

Cell differentiation and developmental processes require the activation of various inducible genes, and *PARP-1* is one. A number of studies have shown the regulatory function of poly(ADP-ribosyl)ation and PARP1 in different cell types and at different developmental stages of organisms. AtPARP-1 and/or AtPARP-2 knockdown were reported to alter *Arabidopsis* development [De Block et al., 2005]. Furthermore, PARP-1 and PARP-2 double knockout mice were reported to exhibit embryonic lethality, suggesting PARP plays a crucial role in mouse development [De Murcia et al., 2003; Henrie et al., 2003]. PARP-1 also plays a crucial role in de-methylation of *IL17d* promoter, which in turn controls the genes required for early embryogenesis of mouse [Hamazaki et al., 2015]. Our previous studies also reported that *ADPRT1A* overexpression as well as PARP inhibition and downregulation affect *D. discoideum* development at the early aggregation stage [Rajawat et al., 2007, 2011; Jubin et al., 2016c]. Moreover, we have shown the highest *ADPRT1A* expression occurs during the aggregation stage of *D. discoideum* development [Jubin et al., 2016c]. Our results are corroborated by reports that *PARP-1* gene alterations in fungus result in defective development and decreased life span [Semighini et al., 2006; Kothe et al., 2010; Müller-Ohldach et al., 2011], strengthening the role of ADPRT1A in *D. discoideum* development (Figures 1A, 1B, and 1C).

cAMP is the signalling molecule that plays a critical role during the multicellular morphogenesis of *Dictyostelium,* particularly at aggregation and culmination stages [Kessin, 2001]. Defects in the cAMP synthesis and chemotaxis can lead to small aggregates and delayed aggregation [Tang and Gomer, 2008; Garciandia and Suarez, 2013]. Delay in development could be explained by chemotaxis defects in *D. discoideum* (Figure 2). *ADPRT1A* is involved in regulation of the synthesis and release of cAMP during early stage of development regulation (Figure 3). cAMP acts both as a secreted extracellular signal and an intracellular second messenger in signal transduction [Schaap, 2011]. Of the three isoforms, *ACAA* produces cAMP required for cell aggregation during early development [Pitt et al., 1992]. Binding of cAMP to *CARA* induces cAMP synthesis inside the cells by activating cAMP-dependent protein kinase A (PKA) [Firtel and Chung, 2000], thus leading to cAMP production (Maeda et al., 2004]. Disruption of any one of the genes involved in cAMP signalling such as *ACAA, CARA, PDSA* and *REGA* results in aggregation defects in *D. discoideum* [Pitt et al., 1992; Kim et al., 1998; Bader et al., 2006; Sawai et al., 2007]. *ADPRT1A* KO cells exhibited reduced levels of *PDSA*, *REGA, ACAA* and *CARA* (Figure 4), as previously demonstrated by Ogino et al. [2007]. However, transcript levels of *PDSA*, *REGA, ACAA* and *CARA* were found to be increased at loose aggregate stage of *ADPRT1A* KO cells, restoring their expression levels under starvation conditions (Figure 4). On the other hand, no rescue was observed even at loose aggregate stage in *PARP* dR cells, an observation supported by elevated levels of ADPRT2 in *ADPRT1A* KO cells (Figure 5). This goes in accordance with report, where the deficiency in DNA-dependent PARP-1 activity was not compensated by any other PARP family member during early development in mice [De Murcia et al., 2003]. Also, thick interrupted streams and smaller aggregates as seen in *ADPRT1A* KO cells (Figure 1A) were supported by the study that showed $PDSA^{-}$ cells to have unusually thick and transient streams at high cell densities [Garcia et al., 2009] and altered *REGA* levels [Wessels et al., 2000]. PARP-1 has also been reported to be involved in regulating cellular differentiation [Pavri et al., 2005; Jubin et al., 2016a]. The *Dictyostelium* developmental cycle exhibits cell differentiation into prespore and prestalk cells [Jeremyn et al., 1989]. Interestingly, *ADPRT1A* KO cells exhibited altered expression levels of prespore and prestalk marker genes consistent with ADPRT1A's role in cellular differentiation (Figure 6).

Conclusion

The current study indicates that ADPRT1A is involved in transcriptional regulation and in such a way controls chemotaxis, development as well as differentiation in *D. discoideum* (Figure 7), which adds a new facet to the multitasking functions of PARP-1. These results could help better in understanding the conserved signalling components in *Dictyostelium* and mammalian cells in leukocyte migration, cell differentiation, metastasis, DNA repair etc. igniting new ideas in the field of PARP-1 biology.

Figure 7 | ADPRT1A in chemotaxis and cellular differentiation of *D. discoideum*

ADPRT1A plays a crucial role in regulating multicellular development via cAMP signalling.

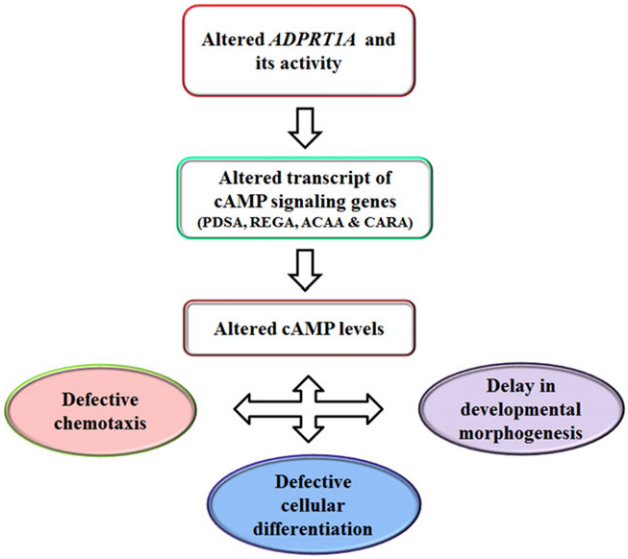

Materials and methods

Cell culture

D. discoideum Ax-2 strain was grown in HL-5 medium at 22°C [Watts and Ashworth, 1970]. The *ADPRT1A* knockout (*ADPRT1A* KO), *ADPRT1A* overexpression (*ADPRT1A* OE) [Jubin et al., 2016c], and *PARP* downregulation (*PARP* dR) [Rajawat et al., 2011] were grown in HL-5 medium supplemented with 10 μg/ml blasticidin S, 100 μg/ml geneticin and 20 μg/ml geneticin, respectively. PARP inhibition was obtained by treating the cells with 1 mM benzamide for 12 h.

Development

Log phase cells were washed twice and then resuspended in 1× Sorensons's buffer (SB). These cells were placed on 2% non-nutrient agar (NNA) and incubated at 22°C [Sussman, 1987]. Development was synchronised by incubating the cells at 4°C for 4–5 h followed by incubation at 22°C for further development. Images were taken every 2 h for the first 12 h and then at 12 h intervals using a stereo-microscope (Nikon SMZ 1000, Japan).

Generation of *ADPRT1A* KO strain

The *ADPRT1A* deletion mutant was generated via homologous recombination as described previously in Jubin et al. [2019]. The *ADPRT1A* KO was confirmed by qPCR and used for all downstream experiments.

cAMP estimation

Log phase cells were subjected to development for the indicated time points of developmental stages, and intracellular cAMP was estimated by ELISA according to the manufacturer's instructions (Calbiochem, Gibbstown, NJ, USA). Extracellular cAMP levels were estimated using the same kit, as described by Mir et al. [2015], and the protein concentration was estimated by the Lowry method [Lowry et al., 1951].

cAMP pulsing

Log phase cells were harvested and washed twice with 1× SB followed by stimulation with 50 nM cAMP pulses in 1× SB for every 6 min for 6 h, and then used for the chemotaxis assay [Mir et al., 2015].

Chemotaxis assay

Chemotaxis assay was performed as described by Mir et al. [2015] with a few modifications. Log phase cells were harvested and washed with 1× SB followed by starvation in 1× SB for 6 h. Three droplets of starved cells (2 μl) were placed on 2% NNA plate, and chemotaxis towards cAMP was tested by placing 1 μM of cAMP in a well at 3 mm distance from the droplet. The distribution of cells within the droplet was observed after 5 h, and images were captured using a stereo-microscope (Nikon, SMZ 1000, Japan). The relative number of cells and the distance moved was an indication of their chemotactic activity.

Gene expression analysis by qPCR

RNA extraction and cDNA synthesis: *D. discoideum* cells on NNA plates were harvested every 2 h for 8 h and RNA was isolated using TRIZOL reagent (Invitrogen, Carlsbad, CA, USA)) following the manufacturer's protocol. RNA integrity and purity were verified by 1.5% agarose gel electrophoresis and ethidium bromide staining and an O.D. 260/280 absorbance ratio 1.95, respectively. RNA was treated with DNase I (Ambion, Austin, TX, USA) before cDNA synthesis to avoid DNA contamination. cDNA synthesis was performed using the RevertAid First Strand cDNA Synthesis Kit (Fermentas, Vilnius, Lithuania) in the CG Palmcycler (Genetix, India).

The expression of transcripts was measured by qPCR using gene-specific primers (Eurofins, Bangalore, India). qPCR was performed using Light- CyclerH480 SYBR Green I Master (Roche Diagnostics, Mannheim, Germany) and carried out in the LightCyclerH480 Real-Time PCR (Roche Diagnostics, Mannheim, Germany). The thermal cycling conditions included an initial denaturation step at 95°C for 10 min followed by 45 cycles of denaturation, annealing and extension. The fluorescence data collection was performed during the extension step. At the end of the amplification phase, a melting curve analysis was carried out. The value of *Cp* was determined by the first cycle number at which fluorescence was greater than the set threshold value. Results of qPCR were analysed using the comparative CT method [Livak and Schmittgen, 2001] with the amplification of *RNLA* (mitochondrial large rRNA) as a control.

Neutral red staining

For development, log phase cells were washed twice and resuspended in 1× SB followed by incubation in 0.06% neutral red for 1 min. Slugs were obtained by placing drops of cells (1×10^8 cells/ml) on 1% NNA plates. The plates were then incubated in

dark for 24–48 h at 22°C and observed under a stereo-microscope (Nikon, SMZ-1000, Japan) with 4× objective.

Statistical analysis

Data are presented as a mean and standard error of the mean (SEM) or standard deviation (SD) as appropriate. Statistical analyses were performed by nonparametric unpaired *t*-test using GraphPad PRISM® 6 software Inc [San Diego CA, USA, 2003].

Author contribution

RB conceived the idea and designed the experiments. RB also did critical revision and approved the manuscript. TJ performed the experiments along with data acquisition, data analysis and manuscript writing. AK contributed in data acquisition.

Funding

RB thanks the Department of Biotechnology, New Delhi, India (BT/PR4383/BRB/10/1014/2011) and Council of Scientific and Industrial Research, New Delhi, India (38(1383)/14/EMR-II) for financial support.

Acknowledgements

Infrastructure facilities provided by The Maharaja Sayajirao University of Baroda, Vadodara are gratefully acknowledged. TJ thanks UGC-DRS for awarding JRF. We also thank Prof. Shweta Saran, Jawaharlal Nehru University, New Delhi, India, for assisting in *ADPRT1A* KO clone construction and Sandip Sutariya for capturing cAMP rescue images.

Conflict of interest statement

The authors have declared no conflict of interest.

References

Bader, S., Kortholt, A., Snippe, H. and Van Haastert, P.J. (2006) DdPDE4, a novel cAMP-specific phosphodiesterase at the surface of *Dictyostelium* cells. J. Biol. Chem **281**, 20018–20026

Beneke, S. (2012) Regulation of chromatin structure by poly(ADP-ribosyl)ation. Front. Genet. **3**, 169

Colon-Otero, G., Sando, J.J., Sims, J.L., McGrath, E., Jensen, D.E. and Quesenberry, P.J. (1987) Inhibition of hemopoietic growth factor-induced proliferation by adenosine diphosphate-ribosylation inhibitors. Blood **70**, 686–693

Couto, C.A.M., Hsu, D.W., Teo, R., Rakhimova, A., Lempidaki, S., Pears, C.J. and Lakin, N.D. (2013) Nonhomologous end-joining promotes resistance to DNA damage in the absence of an ADP-ribosyltransferase that signals DNA single strand breaks. J. Cell Sci. **126**(**Pt 15**), 3452–3461

Couto, C.A., Wang, H.Y., Green, J.C., Kiely, R., Siddaway, R., Borer, C., Pears, C.J. and Lakin, N.D. (2011) PARP regulates nonhomologous end joining through retention of Ku at double-strand breaks. J. Cell Biol. **194**, 367–375

D'amours, D., Desnoyers, S., D'Silva, I. and Poirier, G.G. (1999) Poly(ADP-ribosyl) ation reactions in the regulation of nuclear functions. Biochem. J. **342**, 249–268

De Block, M., Verduyn, C., Brouwer, D.D. and Cornelissen, M. (2005) Poly(ADP-ribose) polymerase in plants affects energy homeostasis, cell death and stress tolerance. Plant J. **41**, 95–106

De Murcia, J.M., Ricoul, M., Tartier, L., Niedergang, C., Huber, A., Dantzer, F., Schreiber, V., Amé, J.C., Dierich, A., LeMeur, M., Sabatier, L., Chambon, P. and de Murcia, G. (2003) Functional interaction between PARP-1 and PARP-2 in chromosome stability and embryonic development in mouse. EMBO J. **22**, 2255–2263

Exley, R., Gordon, J. and Clemens, M.J. (1987) Induction of B-cell differentiation antigens in interferon-or phorbol ester-treated Daudi cells is impaired by inhibitors of ADP-ribosyltransferase. Proc. Natl. Acad. Sci. U. S. A. **84**, 6467–6470

Faure, M., Franke, J., Hall, A.L., Podgorski, G.J. and Kessin, R.H. (1990) The cyclic nucleotide phosphodiesterase gene of *Dictyostelium discoideum* contains three promoters specific for growth, aggregation, and late development. Mol. Cell Biol. **10**, 1921–1930

Firtel, R.A. and Chung, C.Y. (2000) The molecular genetics of chemotaxis: sensing and responding to chemoattractant gradients. Bioessays **22**, 603–615

Frizzell, K.M., Gamble, M.J., Berrocal, J.G., Zhang, T., Krishnakumar, R., Cen, Y., Sauve, A.A. and Kraus, W.L. (2009) Global analysis of transcriptional regulation by poly(ADP-ribose) polymerase-1 and poly(ADP-ribose) glycohydrolase in MCF-7 human breast cancer cells. J. Biol. Chem. **284**, 33926–33938

Garcia, G.L., Rericha, E.C., Heger, C.D., Goldsmith, P.K. and Parent, C.A. (2009) The group migration of *Dictyostelium* cells is regulated by extracellular chemoattractant degradation. Mol. Biol. Cell **20**, 3295–3304

Garciandia, A. and Suarez, T. (2013) The NMRA/NMRAL1 homologue PadA modulates the expression of extracellular cAMP relay genes during aggregation in *Dictyostelium discoideum*. Dev. Biol. **381**, 411–422

Gaudet, P., Williams, J.G., Fey, P. and Chisholm, R.L. (2008) An anatomy ontology to represent biological knowledge in *Dictyostelium discoideum*. BMC Genomics **9**, 130

Gomer, R.H., Jang, W. and Brazill, D. (2011) Cell density sensing and size determination. Dev. Growth Differ. **53**, 482–494

Hamazaki, N., Uesaka, M., Nakashima, K., Agata, K. and Imamura, T. (2015) Gene activation-associated long noncoding RNAs function in mouse preimplantation development. Development **142**, 910–920

Henrie, M.S., Kurimasa, A., Burma, S., Ménissier de Murcia, J., de Murcia, G., Li, G.C. and Chen, D.J. (2003) Lethality in PARP-1/Ku80 double mutant mice reveals physiological synergy during early embryogenesis. DNA Repair (Amst) **2**, 151–158

Hirose, S., Inazu, Y., Chae, S. and Maeda, Y. (2000) Suppression of the growth/differentiation transition in *Dictyostelium* development by transient expression of a novel gene, dia1. Development **127**, 3263–3270

Jaiswal, P., Soldati, T., Thewes, S. and Baskar, R. (2012) Regulation of aggregate size and pattern by adenosine and caffeine in cellular slime molds. BMC Dev. Biol. **12**, 5

Jeremyn, K.A., Duffy, K.T.I. and Williams, J.G. (1989) A new anatomy of the prestalk zone in *Dictyostelium*. Nature **340**, 144–146

Jubin, T., Kadam, A., Gani, A.R., Singh, M., Dwivedi, M. and Begum, R. (2016b) Poly ADP-ribose polymerase-1: beyond transcription and towards differentiation. Semin. Cell Dev. Biol. **63**, 167–179

Jubin, T., Kadam, A., Jariwala, M., Bhatt, S., Sutariya, S., Gani, A.R., Gautam, S. and Begum, R. (2016a) The PARP family: insights into

the functional aspects of poly(ADP-ribose) polymerase-1 in cellular growth and survival. Cell Prolif. **49**, 421–437
Jubin, T., Kadam, A., Saran, S. and Begum, R. (2016c) Poly(ADP-ribose) polymerase1 regulates growth and multicellularity in *D. discoideum*. Differentiation **92**, 10–23
Jubin, T., Kadam, A., Saran, S. and Begum, R. (2019) Crucial role of poly(ADP-ribose) polymerase (PARP-1) in cellular proliferation of *Dictyostelium discoideum*. J. Cell Physiol. **234**, 7539–7547
Kadam, A., Jubin, T., Mir, H. and Begum, R. (2017) Potential role of apoptosis inducing factor in evolutionarily significant eukaryote, *Dictyostelium discoideum* survival. Biochim. Biophys. Acta Gen. Subj. **1861**(**1 Pt A**), 2942–2955
Kawal, A.M., Mir, H., Ramniklal, C.K., Rajawat, J. and Begum, R. (2011) Structural and evolutionary analysis of PARPs in *D. discoideum*. Am. J. Infect. Dis. **7**, 67–74
Kessin, R.H. (2001) *Dictyostelium - Evolution, Cell Biology, and the Development of Multicellularity*. Cambridge, UK: Cambridge University Press
Kim, J.Y., Borleis, J.A. and Devreotes, P.N. (1998) Switching of chemoattractant receptors programs development and morphogenesis in *Dictyostelium*: receptor subtypes activate common responses at different agonist concentrations. Dev. Biol. **197**, 117–128
Konijn, T.M., van de Meene, J.G.C., Chang, Y.Y., Barkley, D.S. and Bonner, J.T. (1969) Identification of adenosine-3′,5′-monophosphate as the bacterial attractant for myxamoebae of *Dictyostelium discoideum*. J. Bacteriol. **99**, 510–512
Kothe, G.O., Kitamura, M., Masutani, M., Selker, E.U. and Inoue, H. (2010) PARP is involved in replicative aging in Neurospora crassa. Fungal Genet. Biol. **47**, 297–309
Livak, K.J. and Schmittgen, T.D. (2001) Analysis of relative gene expression data using real-time quantitative PCR and the 2(-delta delta C(T)) method. Methods **25**, 402–408
Lowry, O.H., Rosebrough, N.J., Farr, A.L. and Randall, R.J. (1951) Protein measurement with the folin phenol reagent. J. Biol. Chem. **193**, 265–275
Maeda, M., Lu, J., Shaulsky, G., Miyazaki, Y., Kuwayama, H., Tanaka, Y., Kuspa, A. and Loomis, W.F. (2004) Periodic signaling controlled by and oscillatory circuit that includes protein kinases ERK2 and PKA. Science **304**, 875–878
Mir, H., Alex, T., Rajawat, J., Kadam, A. and Begum, R. (2015) Response of *D. discoideum* to UV-C and involvement of poly(ADP-ribose) polymerase. Cell Prolif. **48**, 363–374
Mir, H.A., Rajawat, J., Pradhan, S. and Begum, R. (2007) Signaling molecules involved in the transition of growth to development of *Dictyostelium discoideum*. Indian J. Exp. Biol. **45**, 223–236
Müller-Ohldach, M., Brust, D., Hamann, A. and Osiewacz, H.D. (2011) Overexpression of PaParp encoding the poly(ADP-ribose) polymerase of *Podospora anserina* affects organismal aging. Mech. Ageing Dev. **132**, 33–42
Ogino, H., Nozaki, T., Gunji, A., Maeda, M., Suzuki, H., Ohta, T., Murakami, Y., Nakagama, H., Sugimura, T. and Masutani, M. (2007) Loss of Parp-1 affects gene expression profile in a genome-wide manner in ES cells and liver cells. BMC Genomics **8**, 41
Pavri, R., Lewis, B., Kim, T., Dilworth, F.J., Erdjument-Bromage, H., Tempst, P., de Murcia, G., Evans, R., Chambon, P. and Reinberg, D. (2005) PARP-1 determines specificity in a retinoid signaling pathway via direct modulation of mediator. Mol. Cell **18**, 83–96
Pears, C. J. and Lakin, N. D. (2014) Emerging models for DNA repair: *Dictyostelium discoideum* as a model for nonhomologous end-joining. DNA Repair **17**, 121–131
Pitt, G.S., Milona, N., Borleis, J., Lin, K.C., Reed, R.R. and Devreotes, P.N. (1992) Structurally distinct and stage-specific adenylyl cyclase genes play different roles in *Dictyostelium* development. Cell **69**, 305–315
Rajawat, J., Alex, T., Mir, H., Kadam, A. and Begum, R. (2014b) Proteases involved during oxidative stress induced poly(ADP-ribose) polymerase mediated cell death in *D. discoideum*. Microbiology. **160**, 1101–1111
Rajawat, J., Mir, H. and Begum, R. (2011) Differential role of poly(ADP-ribose) polymerase (PARP) in *D. discoideum*. BMC Dev. Biol. **11**, 14
Rajawat, J., Mir, H., Alex, T., Bakshi, S. and Begum, R. (2014a) Involvement of poly(ADP-ribose) polymerase in paraptotic cell death of *D. discoideum*. Apoptosis **19**, 90–101
Rajawat, J., Vohra, I., Mir, H.A., Gohel, D. and Begum, R. (2007) Effect of oxidative stress and involvement of poly(ADP-ribose) polymerase (PARP) in *Dictyostelium discoideum* development. FEBS J. **274**, 5611–5618
Raper, K.B. (1935) *Dictyostelium discoideum*, a new species of slime mold from decaying forest leaves. J. Agri. Res. **50**, 135–147
Raper, K.B. (1984) *The Dictyostelids.* Princeton, NJ: Princeton University Press. 1–453 p
Satoh, M.S. and Lindahl, T. (1992) Role of poly(ADP-ribose) formation in DNA repair. Nature **356**, 356–358
Sawai, S., Guan, X.J., Kuspa, A. and Cox, E.C. (2007) High-throughput analysis of spatio-temporal dynamics in *Dictyostelium*. Genome Biol. **8**, R144
Schaap, P. (2011) Evolutionary crossroads in developmental biology: *Dictyostelium discoideum*. Development **138**, 387–396
Schulkes, C. and Schaap, P. (1995) cAMP-dependent protein kinase activity is essential for preaggregative gene expression in *Dictyostelium*. FEBS Lett. **368**, 381–384
Semighini, C.P., Savoldi, M., Goldman, G.H. and Harris, S.D. (2006) Functional characterization of the putative *Aspergillus nidulans* poly(ADP-ribose) polymerase homolog PrpA. Genetics **173**, 87–98
Shaulsky, G., Escalante, R. and Loomis, W.F. (1996) Developmental signal transduction pathways uncovered by genetic suppressors. Proc. Natl. Acad. Sci. U. S. A. **93**, 15260–15265
Sussman, M. (1987) Cultivation and synchronous morphogenesis of *Dictyostelium* under controlled experimental conditions. Methods Cell Biol. **28**, 9–29
Tang, Y. and Gomer, R.H. (2008) A protein with similarity to PTEN regulates aggregation territory size by decreasing cyclic AMP pulse size during *Dictyostelium discoideum* development. Eukaryot. Cell **7**, 1758–1770
Tulin, A. and Spradling, A. (2003) Chromatin loosening by poly(ADP)-ribose polymerase (PARP) at *Drosophila* puff loci. Science **299**, 560–562
Uchida, M., Hanai, S., Uematsu, N., Sawamoto, K., Okano, H., Miwa, M. and Uchida, K. (2002) Overexpression of poly(ADP-ribose) polymerase disrupts organization of cytoskeletal f-actin and tissue polarity in *Drosophila*. J. Biol. Chem. **277**, 6696–6702
Watts, D.J. and Ashworth, J.M. (1970) Growth of myxamoebae of the cellular slime mould *Dictyostelium discoideum* in axenic culture. Biochem. J. **119**, 171–174
Wessels, D.J., Zhang, H., Reynolds, J., Daniels, K., Heid, P., Lu, S., Kuspa, A., Shaulsky, G., Loomis, W.F. and Soll, D.R. (2000) The internal phosphodiesterase RegA is essential for the suppression of lateral pseudopods during *Dictyostelium* chemotaxis. Mol. Biol. Cell **11**, 2803–2820
Williams, J.G. (2006) Transcriptional regulation of *Dictyostelium* pattern formation. EMBO Reports **7**, 694–698
Wu, Y. and Janetopoulos, C. (2013) The G alpha subunit Gα8 inhibits proliferation, promotes adhesion and regulates cell differentiation. Dev. Biol. **380**, 58–72

Received: 11 August 2018; Revised: 5 March 2019; Accepted: 6 March 2019; Accepted article online: 13 March 2019

Received: 1 January 2018 | Accepted: 10 September 2018

DOI: 10.1002/jcp.27514

ORIGINAL RESEARCH ARTICLE

WILEY Journal of Cellular Physiology

Crucial role of poly (ADP-ribose) polymerase (PARP-1) in cellular proliferation of *Dictyostelium discoideum*

Tina Jubin[1] | Ashlesha Kadam[1] | Shweta Saran[2] | Rasheedunnisa Begum[1]

[1]Department of Biochemistry, Faculty of Science, The Maharaja Sayajirao University of Baroda, Vadodara, India

[2]School of Life Sciences, Jawaharlal Nehru University, New Delhi, India

Correspondence
Rasheedunnisa Begum, Department of Biochemistry, Faculty of Science, The Maharaja Sayajirao University of Baroda, Vadodara, Gujarat 390002, India.
Email: rasheedunnisab@yahoo.co.in

Funding information
Department of Biotechnology, Ministry of Science and Technology, Grant/Award Number: BT/PR4383/BRB/10/1014/2011; Council of Scientific and Industrial Research, Grant/Award Number: 38(1383)/14/EMR-II

Abstract

The unicellular, as well as multicellular stages of *Dictyostelium discoideum's* life cycle, make it an excellent model system for cell type determination, differentiation, development, and cell death studies. Our preliminary results show the involvement of poly (ADP-ribose) polymerase-1 (PARP-1) during *D. discoideum* growth by its constitutive downregulation as well as by its ortholog overexpression. The current study now analyzes and strengthens the role of the PARP-1 ortholog in cellular proliferation of *D. discoideum*. *ADPRT1A* was knocked out (KO) from *D. discoideum* and studied for its effect on cell growth, cell cycle, morphology, and oxidative stress. The present findings show that *ADPRT1A* KO (*A* KO) cells exhibited reduced cellular proliferation, stressed phenotype, and cell cycle arrest in G2-M phase. Under oxidative stress, *A* KO cells exhibited slower growth and DNA damage. This is the first report where the involvement of ADPRT1A in growth in *D. discoideum* is established.

KEYWORDS
ADPRT1A, cell cycle, cell proliferation, *Dictyostelium discoideum*

1 | INTRODUCTION

Cell differentiation and cell death during the developmental processes involve the action of a large network of inducible genes (Katoch et al., 2002). The compact eukaryotic chromatin provides a major hurdle to the transcriptional machinery. Chromatin modifiers work in conjunction with cellular signals, thus resolving the complex packaging and in turn controlling gene expression. One such well reported chromatin modifier is poly (ADP-ribose) polymerase-1 (PARP-1), a nuclear enzyme belonging to the PARP or ADP-ribosyl transferase (ART) family of proteins. It is a ~116 kDa ubiquitously expressed multifunctional protein, established majorly as a DNA damage response protein (D'amours, Desnoyers, D'Silva, & Poirier, 1999). PARP-1 is activated significantly in presence of a range of activators like DNA damage, non-B-DNA structures, and various protein-binding partners. DNA damage strongly activates PARP-1 activity (D'amours et al., 1999; Kim, Zhang, & Kraus, 2005; Kun, Kirsten, & Ordahl, 2002; Oei & Shi, 2001). Activated PARP-1 modifies it and other chromatin-associated proteins thereby regulate gene transcription (Beneke, 2012). However, emerging reports indicate that basal PARP-1 activity is crucial for regulation of gene expression during development (Ji & Tulin, 2010; Jubin, Kadam, Saran, & Begum, 2016a). Recently, Hamazaki, Uesaka, Nakashima, Agata, and Imamura (2015) have shown that PARP inhibition led to inhibition of DNA demethylation of interleukin 17 d (*IL17d*) promoter at the two-cell stage in mice leading to downregulation of the target messenger RNAs (mRNAs) which were essential for early embryogenesis. Moreover, PARP has also been shown to be involved in stress responses like oxidative stress via proteases, UV-C stress via nitric oxide and DNA repair in *Dictyostelium discoideum* (Couto et al., 2011; Mir, Alex, Rajawat, Kadam, & Begum, 2015; Rajawat, Alex, Mir, Kadam, & Begum, 2014a; Rajawat, Mir, Alex, Bakshi, & Begum, 2014b).

D. discoideum, a unicellular eukaryote exhibits multicellularity upon starvation (Raper, 1984). *D. discoideum* possesses eight potential *PARP* genes (Kawal, Mir, Ramniklal, Rajawat, & Begum, 2011). We have demonstrated PARP family role in *D. discoideum* by its downregulation by antisense wherein development was blocked at the initial aggregation stage without affecting growth (Rajawat, Mir, & Begum,

2011). Nevertheless, *ADPRT1A* (PARP-1 ortholog) overexpression led to a delay in growth and development in *D. discoideum*. ADPRT family of proteins is known to participate in cellular proliferation (Colon-Otero et al., 1987; Jubin, Kadam, Jariwala, et al., 2016b; Kaiser, Auer, & Schweiger, 1992) cell differentiation (Exley, Gordon, & Clemens, 1987; Jubin, Kadam, Gani, et al., 2016c) and DNA repair (Couto et al., 2011; Satoh & Lindahl, 1992). However, the role of ADPRT1A in other cellular processes is not clearly understood. Our studies on *ADPRT1A* overexpression (OE) indicated a certain link between ADPRT1A and cell growth along with multicellularity in *D. discoideum*. Hence, the current study aims to further strengthen the role of ADPRT1A in cellular proliferation of *D. discoideum* using loss-of-function mutant namely *ADPRT1A* knockout (KO). Our results suggest that ADPRT1A regulates cellular proliferation via regulation of cell cycle.

2 | MATERIALS AND METHODS

2.1 | Generation of *ADPRT1A* KO (*A* KO) strain

The *ADPRT1A* deletion mutant was generated from the Ax-2 strain via homologous recombination, using 5′ and 3′ regions of *ADPRT1A* flanking a blasticidin resistance cassette to generate the *ADPRT1A* deletion strain. For a generation of the *ADPRT1A* deletion mutant, homologous regions and primers were used that added *Not*I and *Xba*I sites to the 5′ fragment (forward primer: 5′-ACGGCGGCCGCGCAACAAAAAATACATCTC-3′ and reverse primer: 5′-AGCTCTAGAATCTTGCTCTTGTTCCTCCTC-3′) and a *Hin*dIII and *Bam*HI sites to the 3′ fragment (forward primer: 5′-ATCAAGCTTACACAGCTAATCCAAGTCG-3′ and reverse primer: 5′-AGTGGATCCTACTATGGAATGGATGTGGTGC-3′) of *ADPRT1A*. Polymerase chain reaction (PCR)-amplified fragments from Ax-2 genomic DNA were cloned into pDRIVE cloning vector with blasticidin cassette between *Hind*III and *Xba*I sites. The *Not*I and *Bam*HI fragment was then electroporated into *D. discoideum* cells and *A* KO cells were screened using PCR.

2.2 | Cell culture

The *D. discoideum* Ax-2 strain was grown in HL-5 medium at 22°C (Watts & Ashworth, 1970). The *A* KO was grown in HL-5 medium supplemented with 10 μg/ml blasticidin S.

2.3 | Functional characterization of *A* KO

A KO was confirmed by monitoring gene-specific expression of *ADPRT1A* by real-time PCR with *RNLA* as an internal control using Light-CyclerH480 SYBR Green I Master (Roche Diagnostics GmbH, Mannheim, Germany) following the manufacturer's instructions and carried out in the Light-CyclerH480 Real-Time PCR (Roche Diagnostics GmbH).

2.4 | Growth profile analysis of *A* KO

The growth profile was studied by inoculating mid-log phase cells at the density of 0.6×10^6 cells/ml in HL-5 medium. Cell viability was checked after every 2 hr initially till 12 hr and after 12 hr interval thereafter. The cell suspension was mixed with trypan blue solution (0.4% wt/vol) and cell count was taken using hemocytometer (Kosta et al., 2001).

2.5 | Estimation of NAD^+

Intracellular NAD^+ levels were determined by enzymatic recycling method (Bernofsky & Swan, 1973) using alcohol dehydrogenase to reduce NAD^+ to NADH. NAD^+ levels were estimated spectrophotometrically at 570 nm absorbance and protein concentration was estimated by the Lowry method (Lowry, Rosebrough, Farr, & Randall, 1951).

2.6 | Cell cycle analysis

The cell cycle was assessed by flow cytometry using propidium iodide (PI; Sigma-Aldrich, St. Louis, MO). Log-phase cells were fixed by dropwise addition of 70% ethanol and incubated at 4°C overnight. Fixed cells were resuspended in staining solution (Triton X-100, DNase-free RNase, and PI) and incubated for 30 min, followed by fluorescence-activated cell sorting (FACS) analysis (Chen, Shaulsky, & Kuspa, 2004). Quantification was performed using flow cytometry, with FACS ARIA III (BD Biosciences, San Jose, CA). Data were analyzed with FACS Diva software.

2.7 | Cell morphology

Transmission electron microscopy was done to observe the cellular morphology of *D. discoideum* cells. Log phase cells were fixed with 2.5% glutaraldehyde and 2.0% paraformaldehyde in 0.1 M phosphate buffer, pH 7.4, at 40°C for 6–8 hr. The pellet was then stored in paraformaldehyde and 0.1 M phosphate buffer (1:1) and processed for microtomy (Ding et al., 2012). Sections were obtained with a Reichert Jung/Leica UltraCut E ultramicrotome (70 17 04), stained and examined with a Transmission Electron Microscope (Morgagni 268D, FEI company Philips, Hillsboro, Oregon).

2.8 | Effect of oxidative stress on *A* KO

The growth profile of *A* KO in presence of 0.03 mM H_2O_2 was studied by inoculating mid log phase cells at the density of 2×10^6 cells/ml in HL5 medium. Cell viability was checked after every 12-hr interval thereafter till 120 hr. The cell suspension was mixed with trypan blue solution in the ratio of 2:1 and cell count was taken using hemocytometer (Kosta et al., 2001).

2.9 | DNA damage assay

DNA damage was studied by γ-H2AX staining as described in Kadam, Jubin, Mir, and Begum (2017) using anti-human phospho-histone γ-H2AX (S139) antibody (R&D Systems, Minneapolis, MN; 2 μg/ml; rabbit polyclonal) and secondary anti-mouse immunoglobin G (IgG;

whole molecule) tetramethylrhodamine (TRITC) conjugate (Sigma-Aldrich; 1:400 dilutions). The 4′,6-diamidino-2-phenylindole (DAPI; 1 μg/ml) was used to counterstain the nucleus and fluorescence was analyzed by using a confocal laser scan fluorescence-inverted microscope (LSM 710; Carl Zeiss, Jena, Germany).

2.10 | PARP activation

PARP was assayed by indirect immunofluorescence (Cole and Perez-Polo, 2002) using anti-PAR mouse mAb (10H; Calbiochem) at a concentration of 0.5 mg/ml and anti-mouse IgG (whole molecule) fluorescein isothiocyanate conjugate (Sigma-Aldrich) at a dilution of 1:200. Cells were observed for fluorescence which was monitored under 63X by Zeiss confocal laser scan fluorescence inverted microscope (LSM 710; Carl Zeiss).

2.11 | Transcript levels analysis by real-time PCR

Total RNA samples were extracted from *D. discoideum* Ax-2 cells and used for transcript analysis using gene-specific primers by real-time PCR using Light-CyclerH480 SYBR Green I Master (Roche Diagnostics GmbH) following the manufacturer's instructions and carried out in the Light-CyclerH480 Real-Time PCR (Roche Diagnostics GmbH). RNLA was used as an internal control. Fold change in transcript levels ($2^{-\Delta\Delta C_t}$) was shown graphically. Following genes' transcript levels were analyzed by real-time PCR:

Sr. no.	Gene	Primer details
1.	ADPRT1B	FP: TGGTCAAGAGGTTAAAAGATATCG RP: TGAATCTGAAATTGATAAAGCTG
2.	ADPRT2	FP: TTGCTATTGTATGTCACTTTCTGC RP: TTGGATCTGGTTCAACAGTACC
3.	CyclinA	FP: AAATGATCGGAGCCTGTGC' RP: GATGGTTGGAGTGCAAAGTG'
4.	CyclinB	FP: ACACATCAAACAACTGGAATGGC RP: TCCATTGGCATTTGGTAAAACTCC

2.12 | Statistical analysis

Data are presented as a mean and *SEM* or *SD* as appropriate. Statistical analyses were performed using GraphPad PRISM®6 (GraphPad Software Inc., La Jolla, CA). Statistical significance was assessed by the Student's *t* test for experiments with single comparisons. Data were analyzed according to mean fluorescence intensity and plotted on dot plots or on graphs.

3 | RESULTS

3.1 | Functional characterization of *A* KO

Overexpression of *ADPRT1A*, an ortholog of *Dictyostelium*'s PARP-1 affects both growth and development of *D. discoideum* (Jubin, Kadam, Saran, et al., 2016b; Rajawat et al., 2011; Rajawat, Mir, et al., 2014a). Thus, to understand the role of ADPRT1A in these processes, a loss of

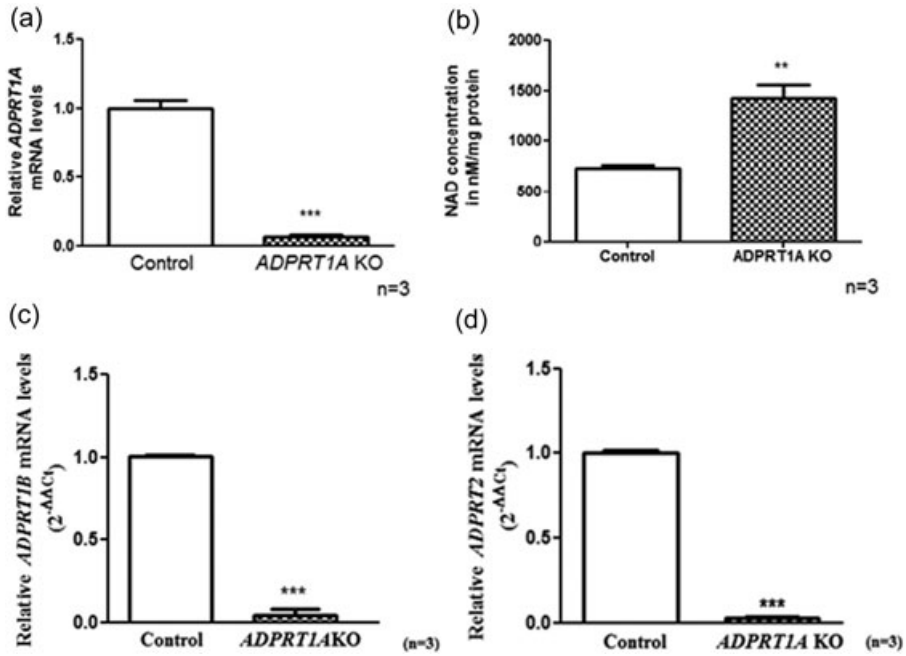

FIGURE 1 Functional characterization of *ADPRT1A* KO (*A KO*). (a) The real-time analysis in *A KO* cells showed significantly decreased (>90%) *ADPRT1A* transcript levels as compared with control. Data are the representation of SEM values of three independent experiments. (b) NAD^+ concentration in control and *A KO* cells using Bernofsky's enzymatic recycling method. Data are the representation of three independent experiments. $^{**}p < 0.01$ for *A* KO is compared with control. (c) Real-time analysis PCR showed reduced levels of *ADPRT1B* levels in *A* KO compared to control cells. $^{***}p < 0.001$ *A* KO is compared with control. (d) Real-time analysis PCR showed decreased levels of *ADPRT2* levels in *A* KO compared with control cells. $^{***}p < 0.001$ *A* KO is compared with control. PCR: polymerase chain reaction

function—*ADPRT1A* knockout was generated in *D. discoideum* by homologous recombination. *A* KO was confirmed by real-time PCR using *ADPRT1A* specific primers wherein transformed cells exhibited loss of ~93% expression of *ADPRT1A* as compared with control cells (Figure 1a).

In addition, NAD^+ levels in the knockout cells were found to be higher as compared with control cells ($p < 0.005$) due to lesser NAD^+ consumption in *A* KO cells (Figure 1b). Deletion or inhibition of PARP-1 has been reported to cause an increase in the NAD^+ levels in animal and cellular models (Bai et al., 2011). Thus, our results suggest that *ADPRT1A* has been successfully knocked out.

To understand the status of *ADPRT1B* and *ADPRT2* in *A* KO cells, their expression levels were estimated. Both the levels were found to be reduced in *A* KO cells as compared to control cells (Figure 1c,d).

3.2 | Effect of *ADPRT1A* knockout on growth

Cell growth profile was studied to check the effect of *ADPRT1A* knockout on the growth of *D. discoideum* was studied. Our results showed that *A* KO exhibited an extended lag phase (Figure 2a) as compared with control cells. *A* KO cells showed a doubling time of 24.95 ± 2.167 hr as compared with 12.26 ± 0.6703 hr for control cells, suggesting its role in unicellular growth. The difference in the doubling time of *A* KO cells further substantiates the effect of *A* KO and also nullifies any interference by the wild-type control cells as the presence of wild-type cells would not lead to significant difference in doubling time.

Moreover, microscopic images of *A* KO cells showed bigger cell size (Figure 2b), vacuoles like structures (shown by arrows; Figure 2c), indicating *A* KO cells exhibited stressed phenotype as compared with control cells. This illustrates loss of *ADPRT1A* affects cellular growth due to inherent stress.

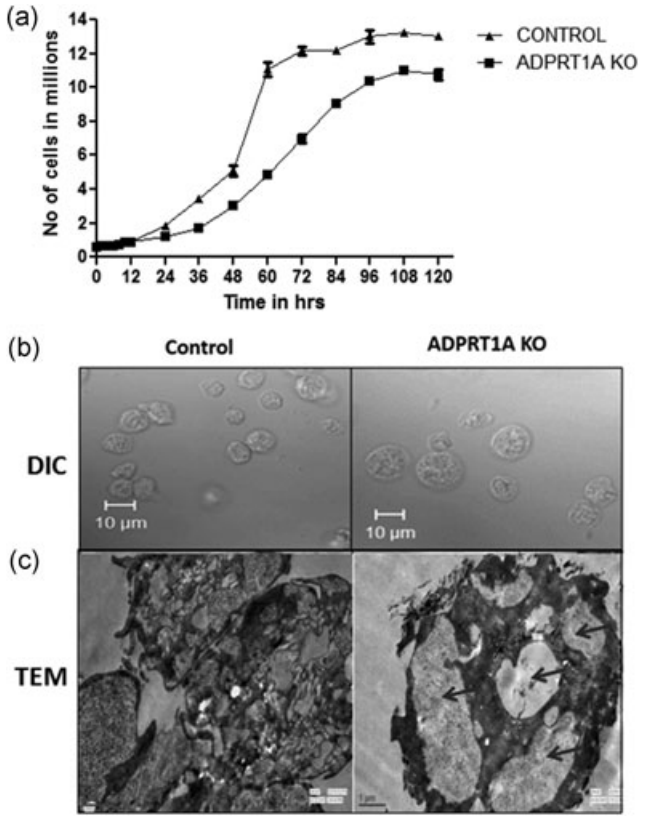

FIGURE 2 Growth analysis of control and *A* KO cells. (a) *A* KO cells showed a doubling time of 24.95 ± 2.167 hr as compared with 12.26 ± 0.6703 hr for control *Dictyostelium discoideum* cells. Data are representative of *SEM* values of five independent experiments. (b) DIC microscope images and (c) TEM images of control and *A* KO cells wherein the *A* KO cells show the stressed and vacuolar phenotype. Data are the representation of three independent experiments. *A* KO: ADPRT1A KO; DIC: differential interface contrast; TEM: transmission electron microscopic

3.3 | Cell cycle analysis and regulation

Further to explain the slow growth of *A* KO, cell cycle analysis was carried out in a time-dependent manner as PARP-1 is reported in the induction of G1 arrest and regulation of G2 arrest (Masutani, Nozaki, Wakabayashi, & Sugimura, 1995). *A* KO cells showed significant cells in G2/M phase at 48 hr of growth (Figure 3a). However, this G2/M arrest continued till 72 hr, wherein a significant number of cells was stalled at G2/M phase as compared with control *D. discoideum* cells (Figure 3b).

Additionally, PARP-1 has been reported to regulate cell cycle regulating proteins such as CyclinA and CyclinB (Simbulan-Rosenthal et al., 2000). Therefore, to understand the G2/M arrest exhibited by *A* KO cells, *CyclinA* and *CyclinB* (mitotic promoting factor) transcript levels were monitored in these cells and interestingly, both the transcript levels were found to be significantly lower as compared with control cells (Figure 3c,d). PARP-1 may regulate *CyclinA* and *CyclinB* expression, thus controlling cell cycle which eventually affects cellular proliferation.

3.4 | ADPRT1A and response to oxidative stress

The absence of ADPRT1A leading to stressed and vacuolar phenotype intrigued us to extend our study on stress response of *A* KO cells. To understand the effect of *ADPRT1A* deficiency in *D. discoideum* to oxidative stress, growth profile was studied in presence of apoptotic dose of cumene H_2O_2 for 120 hr. Interestingly, *A* KO cells under oxidative stress showed comparable growth as control cells till 48 hr (Figure 4a), suggesting the absence of ADPRT1A could make the *A* KO cells insensitive to DNA damage. Nevertheless, ADPRT isoforms in the cell may compensate for ADPRT1A function.

Interestingly, it was observed that after 48 hrs, the growth rate of H_2O_2 exposed *A* KO cells reduced significantly as compared to control which could be due to accumulated DNA damage as demonstrated by γ-H2AX staining, the marker of DNA damage which was significantly higher in H_2O_2 exposed *A* KO cells (Figure 4b) as compared with *A* KO as well as control cells.

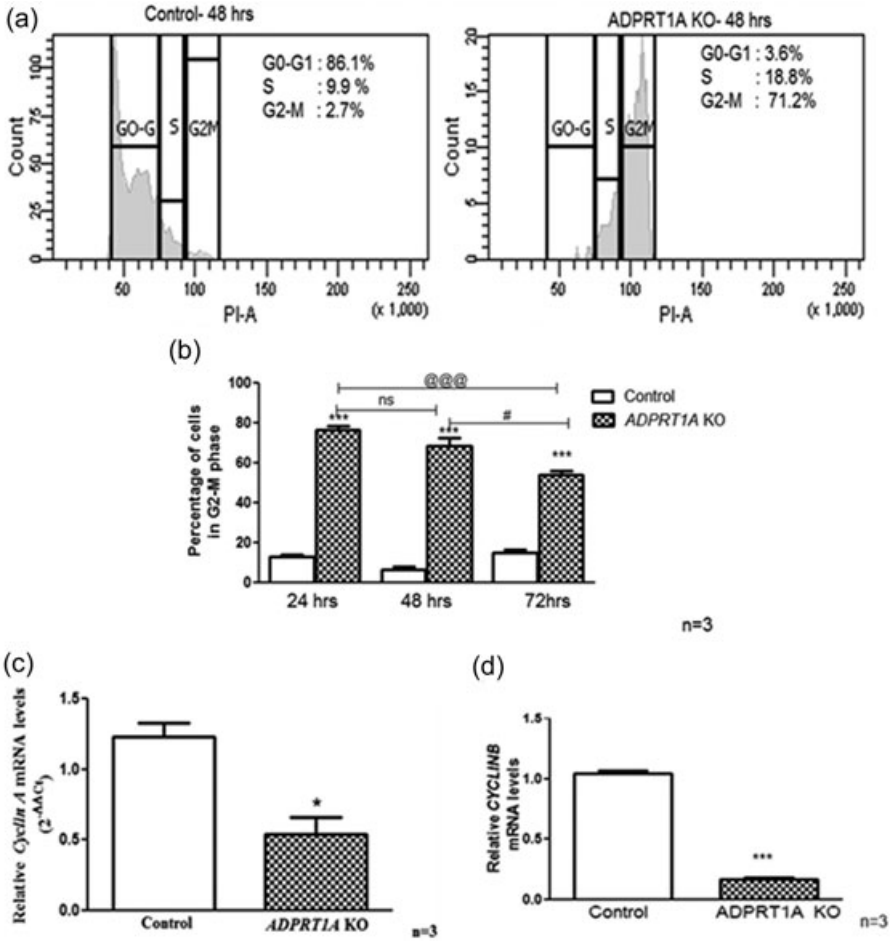

FIGURE 3 Cell cycle analysis and *CyclinA* and *CyclinB* transcript levels in *A* KO cells. (a) Analysis of cells cycle by FACS using propidium iodide. *A* KO cells show a marked population of cells G2/M phase as compared with control, both at 48 hr of growth. Data are representative of three independent experiments. (b) Time-dependent cell cycle analysis of *A* KO cells show cells arrested in G2-M phase till 72 hr of growth. ***$p < 0.001$ for *A KO* as compared with control. (c) *A KO* cells exhibited significant reduced *CyclinA* transcript levels as compared with control. Data are the representation of *SEM* values of three independent experiments. *$p < 0.05$ as compared with control. (d) Real-time analysis of *CyclinB* transcript levels showed significant decrease in *A KO* cells as compared with control. Data are representation of *SEM* values of three independent experiments. ***$p < 0.001$ as compared with control

Thus, *ADPRT1A* deficiency could result in the initial (till 48 hr) resistance to oxidative stress in *D. discoideum*.

3.5 | PARP activation in *A* KO

PARP activity was checked under 0.03 mM H_2O_2 treatment at 5 and 10 min in *A* KO cells. Upon oxidative stress, control cells showed peak PARP activity while *A* KO cells showed some PARP activity at 10 min due to the presence of other PARPs in *A* KO cells (Figure 5).

4 | DISCUSSION

PARP-1 is a major ADP-ribosylating enzyme involved in various biological pathways namely, DNA repair, cell death, mitotic apparatus function, transcriptional regulation and so forth (Kashima et al., 2012; Krishnakumar et al., 2008; Soldani & Scovassi, 2002; Virág & Szabó, 2002). In addition to this, PARP-1 has been reported, to be involved in cell growth and survival (Jubin, Kadam, Jariwala, et al., 2016b). Our previous study also showed that ADPRT1A OE hampered the cell growth in *Dictyostelium*. Thus, this study would help us to strengthen the function of ADPRT1A in growth. PARP-1 (ADPRT1A ortholog) is PARylated by itself, PARP-2, and possibly other PARPs; autoPARylation of PARP-1 inhibits its catalytic activity (Kauppinen et al., 2006). In *ADPRT1A* OE, due course leads to extensive autoPARylation finally causing inhibition. Hence, the results are not very clear in OE, for example, there is no distinct G2/M arrest seen in *ADPRT1A OE* as seen in *A KO*. In contrast, *A* KO results are due to the direct reduction of *ADPRT1A* levels hence leading to confirm results indicating the exact role of ADPRT1A. Approximately 93% loss of ADPRT1A expression-caused reduction in cell growth. ADPRT1a, being a NAD^+ consumer, depletion in NAD^+ levels was found *A* KO cells. In mouse, PARP-1 and PARP-2 double knockouts exhibit embryonic lethality (Henrie et al., 2003), suggesting that PARP proteins play a crucial role in growth and development. The slower growth rate was substantiated by the arrest in G2-M phase of cell cycle and decrease in *CyclinA* and *CyclinB* levels, indicating ADPRT1A may have a regulatory function in the cell cycle. In line with the other result, PARP inhibitors or PARP-1 siRNA treatment significantly affected the growth of hepatoma cells and induced G0/G1 cell cycle arrest in hepatoma cells (Yang et al., 2013). Furthermore, reports suggest that *Cyclin B* mRNA, as well as protein levels, fluctuate throughout growth of *Dictyostelium* with the highest accumulation at G2/M boundary (Evans, Rosenthal, Youngblom,

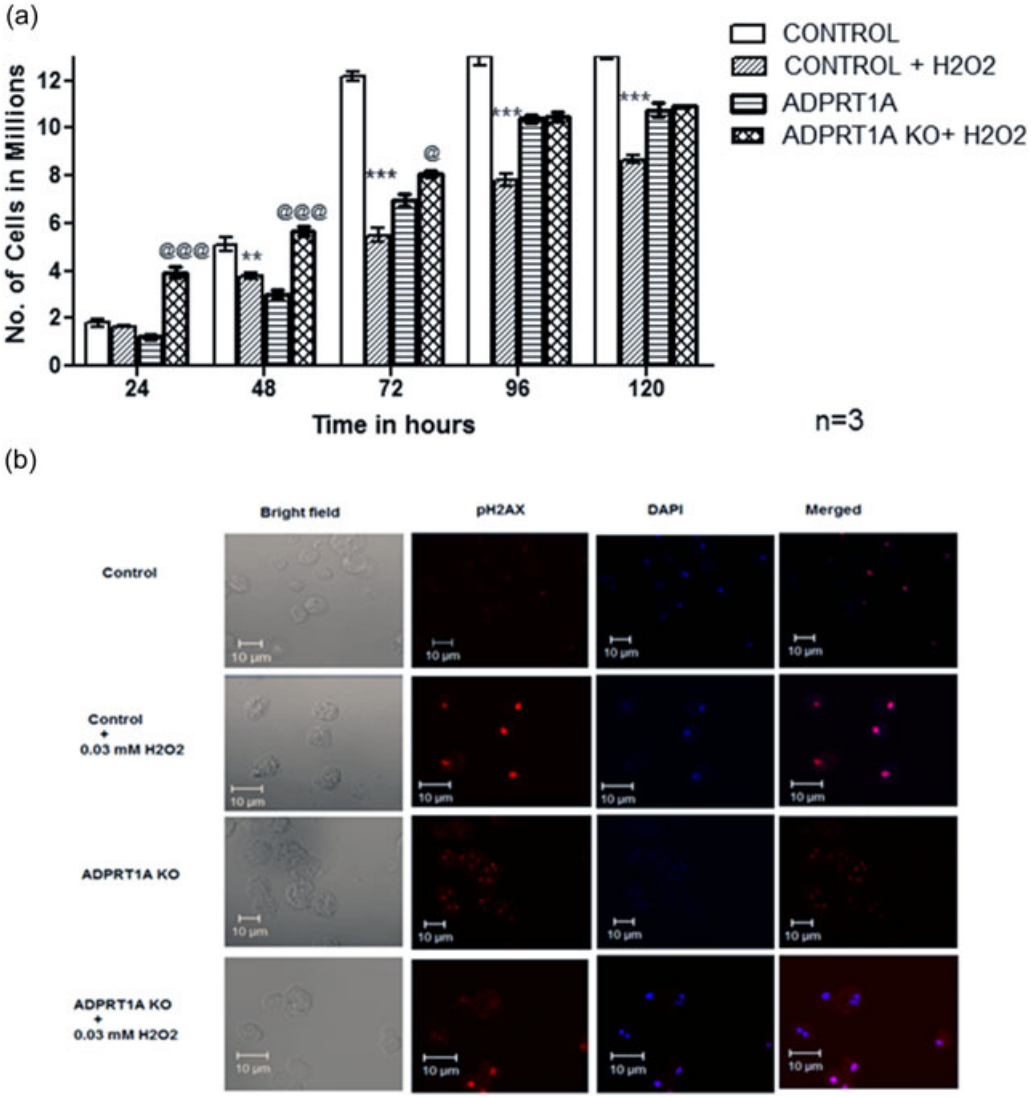

FIGURE 4 Effect of oxidative stress on *A KO* cells. (a) Growth analysis in presence of 0.03 mM H_2O_2. *A KO* cells show significant growth in presence of oxidative stress as compared with untreated *A KO* cells till 72 hr exhibiting a resistant phenotype. $^{**}p$ Value for treated control cells <0.01; $^{***}p$ value for treated control cells <0.001 as compared with untreated control cells; $^{@}p$ value for treated *A KO* <0.05; $^{@@@}p$ value for treated *A KO* <0.001 as compared with untreated *A KO* cells. (b) DNA damage analysis was carried out in control and *A KO* post 5 min of 0.03 mM cumene H_2O_2 stress by immunofluorescence using an antibody against γ-H2AX. Data are the representation of three independent experiments. Magnification: ×60; Scale bar: 10 μm [Color figure can be viewed at wileyonlinelibrary.com]

Distel, & Hunt, 1983; Luo, Michaelis, & Weeks, 1994) and G2M-transition was prevented by inhibition of *CyclinB* transcription (Innocente, Abrahamson, Cogswell, & Lee, 1999). *A* KO cells also exhibited stressed morphological characteristics indicating intrinsic stress due to loss of ADPRT1A.

A number of agents such as UV rays, H_2O_2 lead to cell death (Hasnain et al., 1999; Katoch & Begum, 2003; Mohan et al., 2003; Sah et al., 1999). Evidence demonstrate *PARP-1* KO to confer resistance to endotoxic shock (Oliver et al., 1999), while reports also suggest sensitivity to environmental cues (Wang et al., 1997). Interestingly, absence of ADPRT1A rendered cells resistant to oxidative stress till 48 hr of growth and further cell growth was reduced which could be due to accumulation of DNA damage. It is to be noted that *ADPRT1A* knockout is not lethal to the cell. This is explained by reports wherein ADPRT isoforms in the cell may compensate for ADPRT1A function. Similar results were seen in which significant poly (ADP-ribose) polymers(PAR) were observed due to PARP-2 in PARP-1 mouse knockout models following genotoxic stimulation (Ame et al., 1999; Couto et al., 2013; Shieh et al., 1998). However, it was found that these knockouts present several phenotypes associated with genomic instability (Trucco et al., 1999), demonstrating that PARP-2 could not completely compensate for the loss of PARP-1. Thus, it reinstates crucial role of ADPRT1A in cell survival.

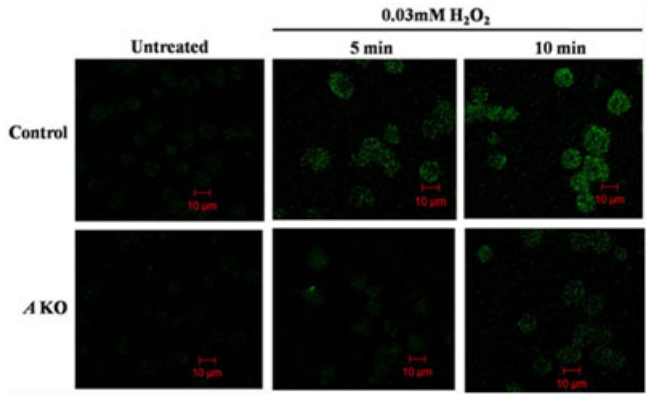

FIGURE 5 PARP activation in *A KO* cells: PARP activation was observed post 0.03 mM cumene H_2O_2 treatment using anti-PAR antibodies in control and *A KO* cells by confocal microscopy. *A KO* cells exhibited some PARP activity while peak PARP activity was seen at 10 min post 0.03 mM cumene H_2O_2 stress in control cells. Data are representative of three independent experiments. Magnification: ×60; Scale bar = 10 μm [Color figure can be viewed at wileyonlinelibrary.com]

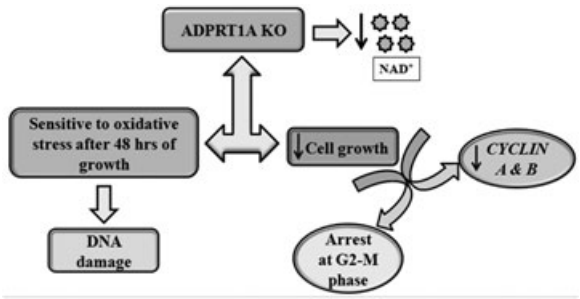

FIGURE 6 Effect of *ADPRT1A* knockout on growth of *D. discoideum*

5 | CONCLUSION

This report thus provides the first evidence wherein ADPRT1A, PARP-1 ortholog is specifically shown to be involved in controlling cell growth and cell cycle in *D. discoideum* (Figure 6). This adds a new dimension to the multitasking functions of PARP-1. These results could be exploited to understand the conserved signaling modules in *Dictyostelium* and the mammalian system thereby opening new research avenues in the field of PARP-1 biology.

ACKNOWLEDGMENTS

Infrastructure facilities were provided by The Maharaja Sayajirao University of Baroda, Vadodara, DBT-MSUB ILSPARE, JNU Life sciences, and AIIMS SAIF–DST electron microscopy facility are gratefully acknowledged. R. B. thanks the Department of Biotechnology, New Delhi (BT/PR4383/BRB/10/1014/2011) and Council of Scientific and Industrial Research (38(1383)/14/EMR-II) for financial support. T. J. thanks UGC-DRS for awarding JRF.

CONFLICTS OF INTEREST

The authors declare that there are no conflicts of interest.

AUTHOR CONTRIBUTIONS

T. J. and R. B.: study design; T. J., A. K., S. S., and R. B.: study conduct, data analysis, and its interpretation; T. J., A. K., and R. B.: manuscript drafting.

ORCID

Rasheedunnisa Begum http://orcid.org/0000-0003-3446-0980

REFERENCES

Amé, J. C., Rolli, V., Schreiber, V., Niedergang, C., Apiou, F., Decker, P., … de Murcia, G. (1999). PARP-2, a novel mammalian DNA damage-dependent poly(ADP-ribose) polymerase. *Journal of Biological Chemistry*, *274*, 17860–17868.

Bai, P., Cantó, C., Oudart, H., Brunyánszki, A., Cen, Y., Thomas, C., … Auwerx, J. (2011). PARP-1 inhibition increases mitochondrial metabolism through SIRT1 activation. *Cell Metabolism*, *13*, 461–468.

Beneke, S. (2012). Regulation of chromatin structure by poly (ADP-ribosyl) ation. *Frontiers in Genetics*, *3*, 169.

Bernofsky, C., & Swan, M. (1973). An improved cycling assay for nicotinamide adenine dinucleotide. *Analytical Biochemistry*, *53*, 452–458.

Chen, G., Shaulsky, G., & Kuspa, A. (2004). Tissue-specific G1-phase cell-cycle arrest prior to terminal differentiation in *Dictyostelium*. *Development*, *131*, 2619–2630.

Cole, K. K., & Perez-Polo, J. R. (2002). Poly(ADP-ribose) polymerase inhibition prevents both apoptotic-like delayed neuronal death and necrosis after H2O2 injury. *Journal of Neurochemistry*, *82*, 19–29.

Colon-Otero, G., Sando, J. J., Sims, J. L., McGrath, E., Jensen, D. E., & Quesenberry, P. J. (1987). Inhibition of hemopoietic growth factor-induced proliferation by adenosine diphosphate-ribosylation inhibitors. *Blood*, *70*, 686–693.

Couto, C. A. M., Hsu, D. W., Teo, R., Rakhimova, A., Lempidaki, S., Pears, C. J., & Lakin, N. D. (2013). Nonhomologous end-joining promotes resistance to DNA damage in the absence of an ADP-ribosyltransferase that signals DNA single strand breaks. *Journal of Cell Science*, *126*, 3452–3461.

Couto, C. A. M., Wang, H. Y., Green, J. C. A., Kiely, R., Siddaway, R., Borer, C., … Lakin, N. D. (2011). PARP regulates nonhomologous end joining through retention of Ku at double-strand breaks. *Journal of Cell Biology*, *194*, 367–375.

D'amours, D., Desnoyers, S., D'Silva, I., & Poirier, G. G. (1999). Poly (ADP-ribosyl) ation reactions in the regulation of nuclear functions. *Biochemical Journal*, *342*, 249–268.

Ding, W. X., Li, M., Biazik, J. M., Morgan, D. G., Guo, F., Ni, H. M., … Yin, X. M. (2012). Electronmicroscopic analysis of a sphericalmitochondrial structure. *Journal of Biological Chemistry*, *287*, 42373–42378.

Evans, T., Rosenthal, E. T., Youngblom, J., Distel, D., & Hunt, T. (1983). Cyclin: A protein specified by maternal mRNA in sea urchin eggs that is destroyed at each cleavage division. *Cell*, *33*, 389–396.

Exley, R., Gordon, J., & Clemens, M. J. (1987). Induction of B-cell differentiation antigens in interferon- or phorbol ester-treated Daudi cells is impaired by inhibitors of ADP-ribosyltransferase. *Proceedings of the National Academy of Sciences of the United States of America*, *84*, 6467–6470.

Hamazaki, N., Uesaka, M., Nakashima, K., Agata, K., & Imamura, T. (2015). Gene activation-associated long noncoding RNAs function in mouse preimplantation development. *Development*, *142*, 910–920.

Hasnain, S. E., Taneja, T. K., Sah, N. K., Mohan, M., Pathak, N., Sahdev, S., … Begum, R. (1999). In vitro cultured *Spodoptera frugiperda* insect cells: Model for oxidative stress-induced apoptosis. *Journal of Biosciences*, *24*, 13–19.

Henrie, M. S., Kurimasa, A., Burma, S., Ménissier-de Murcia, J., de Murcia, G., Li, G. C., & Chen, D. J. (2003). Lethality in PARP-1/Ku80 double mutant mice reveals physiological synergy during early embryogenesis. *DNA Repair*, *2*, 151–158.

Innocente, S. A., Abrahamson, J. L. A., Cogswell, J. P., & Lee, J. M. (1999). p53 regulates a G2 checkpoint through cyclin B1. *Proceedings of the National Academy of Sciences of the United States of America*, *96*, 2147–2152.

Ji, Y., & Tulin, A. V. (2010). The roles of PARP1 in gene control and cell differentiation. *Current Opinion in Genetics & Development*, *20*, 512–518.

Jubin, T., Kadam, A., Gani, A. R., Singh, M., Dwivedi, M., & Begum, R. (2016c). Poly ADP-ribose polymerase-1: Beyond transcription and towards differentiation. *Seminars in Cell and Developmental Biology*, *63*, 167–179.

Jubin, T., Kadam, A., Jariwala, M., Bhatt, S., Sutariya, S., Gani, A. R., … Begum, R. (2016b). The PARP family: Insights into the functional aspects of Poly (ADP-ribose) polymerase-1 in cellular growth and survival. *Cell Proliferation*, *49*, 421–437.

Jubin, T., Kadam, A., Saran, S., & Begum, R. (2016a). Poly (ADP-ribose) polymerase1 regulates growth and multicellularity in *D. discoideum*. *Differentiation*, *92*, 10–23.

Kadam, A. A., Jubin, T., Mir, H. A., & Begum, R. (2017). Potential role of apoptosis inducing factor in evolutionarily significant eukaryote, *Dictyostelium discoideum* survival. *BBA-General Subjects*, *1861*, 2942–2955.

Kaiser, P., Auer, B., & Schweiger, M. (1992). Inhibition of cell proliferation in *Saccharomyces cerevisiae* by expression of human NAD^+ ADP-ribosyltransferase requires the DNA binding domain ("zinc fingers"). *Molecular and General Genetics*, *232*, 231–239.

Kashima, L., Idogawa, M., Mita, H., Shitashige, M., Yamada, T., Ogi, K., … Tokino, T. (2012). CHFR protein regulates mitotic checkpoint by targeting PARP-1 protein for ubiquitination and degradation. *Journal of Biological Chemistry*, *287*, 12975–12984.

Katoch, B., & Begum, R. (2003). Biochemical basis of the high resistance to oxidative stress in *Dictyostelium discoideum*. *Journal of Biosciences*, *28*, 581–588.

Katoch, B., Sebastian, S., Sahdev, S., Padh, H., Hasnain, S. E., & Begum, R. (2002). Programmed cell death and its clinical implications. *Indian Journal of Experimental Biology*, *40*, 513–524.

Kauppinen, T. M., Chan, W. Y., Suh, S. W., Wiggins, A. K., Huang, E. J., & Swanson, R. A. (2006). Direct phosphorylation and regulation of poly (ADP-ribose) polymerase-1 by extracellular signal regulated kinases 1/2. *Proceedings of the National Academy of Sciences of the United States of America*, *103*, 7136–7141.

Kawal, A. M., Mir, H., Ramniklal, C. K., Rajawat, J., & Begum, R. (2011). Structural and evolutionary analysis of PARPs in *D. discoideum*. *American journal of infectious diseases*, *7*, 67–74.

Kim, M. Y., Zhang, T., & Kraus, W. L. (2005). Poly (ADP-ribosyl) ation by PARP-1: 'PAR-laying' NAD^+ into a nuclear signal. *Genes and Development*, *19*, 1951–1967.

Kosta, A., Laporte, C., Lam, D., Tresse, E., Luciani, M. F., & Golstein, P. (2001). How to assess and study cell death in *Dictyostelium discoideum*. *Methods in Cell Biology*, *346*, 535–550.

Krishnakumar, R., Gamble, M. J., Frizzell, K. M., Berrocal, J. G., Kininis, M., & Kraus, W. L. (2008). Reciprocal binding of PARP-1 and histone H1 at promoters specifies transcriptional outcomes. *Science*, *319*, 819–821.

Kun, E., Kirsten, E., & Ordahl, C. P. (2002). Coenzymatic activity of randomly broken or intact double-stranded DNAs in auto and histone H1 trans-poly (ADP-ribosylation), catalyzed by poly (ADP-ribose) polymerase (PARP I). *Journal of Biological Chemistry*, *277*, 39066–39069.

Lowry, O. H., Rosebrough, N. J., Farr, A. L., & Randall, R. J. (1951). Protein measurement with the Folin phenol reagent. *Journal of Biological Chemistry*, *93*, 265–275.

Luo, Q. I. A. N., Michaelis, C., & Weeks, G. (1994). Overexpression of a truncated cyclin B gene arrests *Dictyostelium* cell division during mitosis. *Journal of Cell Science*, *107*, 3105–3114.

Masutani, M., Nozaki, T., Wakabayashi, K., & Sugimura, T. (1995). Role of poly (ADP-ribose) polymerase in cell-cycle checkpoint mechanisms following γ-irradiation. *Biochimie*, *77*, 462–465.

Mir, H., Alex, T., Rajawat, J., Kadam, A., & Begum, R. (2015). Response of *D. discoideum* to UV-C and involvement of poly(ADP-ribose) polymerase. *Cell Proliferation*, *48*, 363–374.

Mohan, M., Taneja, T. K., Sahdev, S., Krishnaveni, M., Begum, R., Athar, M., … Hasnain, S. E. (2003). Antioxidants prevent UV induced apoptosis by inhibiting mitochondrial cytochrome c release and caspase activation in Spodoptera frugiperda (Sf9) cells. *Cell Biology International*, *27*, 483–490.

Oei, S. L., & Shi, Y. (2001). Poly (ADP-ribosyl) ation of transcription factor Yin Yang 1 under conditions of DNA damage. *Biochem Biophys Res Commu*, *285*, 27–31.

Oliver, F. J., Ménissier-de Murcia, J., Nacci, C., Decker, P., Andriantsitohaina, R., Muller, S., … de Murcia, G. (1999). Resistance to endotoxic shock as a consequence of defective NF-κB activation in poly (ADP-ribose) polymerase-1 deficient mice. *EMBO Journal*, *18*, 4446–4454.

Rajawat, J., Alex, T., Mir, H., Kadam, A., & Begum, R. (2014b). Proteases involved during oxidative stress induced poly(ADP-ribose) polymerase mediated cell death in *D. discoideum*. *Microbiol*, *160*, 1101–1111.

Rajawat, J., Mir, H., Alex, T., Bakshi, S., & Begum, R. (2014a). Involvement of poly(ADP-ribose) polymerase in paraptotic cell death of *D. discoideum*. *Apoptosis*, *19*, 90–101.

Rajawat, J., Mir, H., & Begum, R. (2011). Differential role of poly(ADP-ribose) polymerase (PARP) in *D. discoideum*. *BMC Developmental Biology*, *11*, 14.

Raper, K. B. (1984). *The Dictyostelids* (1–453). Princeton, NJ: Princeton University Press.

Sah, N. K., Taneja, T. K., Pathak, N., Begum, R., Athar, M., & Hasnain, S. E. (1999). The baculovirus anti-apoptotic p35 gene also functions via an oxidant dependent pathway. *Proceedings of the National Academy of Sciences of the United States of America*, *96*, 4838–4843.

Satoh, M. S., & Lindahl, T. (1992). Role of poly (ADP-ribose) formation in DNA repair. *Nature*, *356*, 356–358.

Shieh, W. M., Amé, J. C., Wilson, M. V., Wang, Z. Q., Koh, D. W., Jacobson, M. K., & Jacobson, E. L. (1998). Poly(ADP-ribose) polymerase null mouse cells synthesize ADP-ribose polymers. *Journal of Biological Chemistry*, *273*, 30069–30072.

Simbulan-Rosenthal, C. M., Ly, D. H., Rosenthal, D. S., Konopka, G., Luo, R., Wang, Z. Q., … Smulson, M. E. (2000). Misregulation of gene expression in primary fibroblasts lacking poly (ADP-ribose) polymerase. *Proceedings of the National Academy of Sciences of the United States of America*, *97*, 11274–11279.

Soldani, C., & Scovassi, A. I. (2002). Poly (ADP-ribose) polymerase-1 cleavage during apoptosis: An update. *Apoptosis*, *7*, 321–328.

Trucco, C., Rolli, V., Oliver, F. J., Flatter, E., Masson, M., Dantzer, F., … de Murcia, G. (1999). A dual approach in the study of poly (ADP-ribose) polymerase: In vitro random mutagenesis and generation of deficient mice. *Molecular and Cellular Biochemistry*, *193*, 53–60.

Virág, L., & Szabó, C. (2002). The therapeutic potential of poly (ADP-ribose) polymerase inhibitors. *Pharmacol Reviews*, *54*, 375–429.

Wang, Z. Q., Stingl, L., Morrison, C., Jantsch, M., Los, M., Schulze-Osthoff, K., & Wagner, E. F. (1997). PARP is important for genomic stability but dispensable in apoptosis. *Genes and Development*, *11*, 2347–2358.

Watts, D. J., & Ashworth, J. M. (1970). Growth of myxamoebae of the cellular slime mould *Dictyostelium discoideum* in axenic culture. *Biochemical Journal*, *119*, 171–174.

Yang, L., Huang, K., Li, X., Du, M., Kang, X., Luo, X., … Huang, D. (2013). Identification of poly(ADP-Ribose) polymerase-1 as a cell cycle regulator through modulating Sp1 mediated transcription in human hepatoma cells. *PLOS One*, *8*(12), e82872.

How to cite this article: Jubin T, Kadam A, Saran S, Begum R. Crucial role of poly (ADP-ribose) polymerase (PARP-1) in cellular proliferation of *Dictyostelium discoideum*. *J Cell Physiol*. 2019;234:7539–7547. https://doi.org/10.1002/jcp.27514

Seminars in Cell & Developmental Biology 63 (2017) 167–179

Contents lists available at ScienceDirect

Seminars in Cell & Developmental Biology

journal homepage: www.elsevier.com/locate/semcdb

Review

Poly ADP-ribose polymerase-1: Beyond transcription and towards differentiation

Tina Jubin[a], Ashlesha Kadam[a,1], Amina Rafath Gani[a,b,1], Mala Singh[a], Mitesh Dwivedi[a,c], Rasheedunnisa Begum[a,*]

[a] Department of Biochemistry, Faculty of Science, The Maharaja Sayajirao University of Baroda, Vadodara, Gujarat 390002, India
[b] Department of Biochemistry, School of Life Sciences, University of Hyderabad, Hyderabad, 500046 Telangana, India
[c] C.G. Bhakta Institute of Biotechnology, Faculty of Science, Uka Tarsadia University, Surat, Gujarat 394350, India

ARTICLE INFO

Article history:
Received 29 June 2016
Accepted 27 July 2016
Available online 28 July 2016

Keywords:
PARP-1
DNA independent activation
Gene regulation
Differentiation
Therapeutics

ABSTRACT

Gene regulation mediates the processes of cellular development and differentiation leading to the origin of different cell types each having their own signature gene expression profile. However, the compact chromatin structure and the timely recruitment of molecules involved in various signaling pathways are of prime importance for temporal and spatial gene regulation that eventually contribute towards cell type and specificity. Poly (ADP-ribose) polymerase-1 (PARP-1), a 116-kDa nuclear multitasking protein is involved in modulation of chromatin condensation leading to altered gene expression. In response to activation signals, it adds ADP-ribose units to various target proteins including itself, thus regulating various key cellular processes like DNA repair, cell death, transcription, mRNA splicing etc. This review provides insights into the role of PARP-1 in gene regulation, cell differentiation and multicellular morphogenesis. In addition, the review also explores involvement of PARP-1 in immune cells development and therapeutic possibilities to treat various human diseases.

Contents

* Corresponding author.
E-mail address: rasheedunnisab@yahoo.co.in (R. Begum).
[1] These authors contributed equally to the work as second authors.

http://dx.doi.org/10.1016/j.semcdb.2016.07.027
1084-9521/

1. Introduction

Innumerable studies over decades have illustrated the most fundamental concepts in gene regulation [1,2]. Cell growth and differentiation involve cellular transition from one type to the other, a process that is tightly modulated by gene regulatory networks that involve activation and recruitment of specific transcription factors, chromatin remodeling, histone regulation, post translational modifications, alternative splicing, epigenetics etc. Multiple molecular systems involving an array of gene regulatory machinery initiate, promote and execute various processes involved in maintaining these complex cellular signaling pathways. Poly (ADP-ribose) polymerase-1 (PARP-1) is a ubiquitously expressed highly conserved protein in mammalian tissues with predominant nuclear localization. Exploration of several molecular events governed by PARP-1 to regulate gene expression, cell differentiation and development pathways may lead to new therapeutic possibilities for several human diseases. The article focuses on the unaccounted roles of PARP-1 in gene regulation, differentiation, development, morphogenesis, and multicellularity along with its therapeutic potential in immune cell development.

2. Poly ADP-ribose polymerases (PARP-1)

One of the emerging families of proteins involved in gene regulation for development and differentiation is the Poly ADP-ribose polymerase family. Poly ADP-ribose polymerase belongs to the ADP-ribosyltransferase (ART) family [3,4]. These transferases utilize nicotinamide adenine dinucleotide (NAD^+) as its substrate for the synthesis of mono or poly (ADP-ribose) polymers on target acceptor proteins and this process is termed as poly (ADP-ribosylation) or PARylation [5,6]. The negatively charged ADP-ribose units are degraded by poly(ADP-ribose) glycohydrolase (PARG) and ADP-ribosylhydrolase 3 (ARH3) [7,8]. However, macro domain containing proteins and NUDIX hydrolases have also been shown to degrade ADP-ribose polymers [9]. In the due process of PARylating target proteins, PARP-1 itself becomes a prime target for PARylation- this process is called as auto- modification. PARylation and PARP proteins have been identified across various domains of life from plants to animals as well as lower life forms like bacteria, double-stranded DNA viruses etc. [10,11]. The human PARP family comprises of 17 members with either mono- or poly-ADP-ribosyltransferase activity possessing a conserved PARP signature motif in their catalytic domain [3]. PARP-1, recently termed as ADP-ribosyltransferase diphtheria toxin-like (ARTD-1), is one of the most abundant nuclear enzymes responsible for ~90% of the PARylation activity [12,13]. Although PARP-1 is one of the well-studied and characterized members of the PARP protein family, yet many of its features still remain unexplored. PARP-1 is a 116-kDa nuclear protein with well characterized structural domains [3,4] viz., (1) the N-terminal DNA binding domain comprising of three zinc finger motifs, a nuclear localization signal (NLS) and a zinc binding domain [15,14] (2) an auto-modification domain with a BRCA1 C-terminus (BRCT) motif, for protein–protein interactions [4] (3) a WGR (Trp-Gly-Arg) motif with a plausible role in nucleic acid binding, and (4) a C-terminal catalytic domain comprising of the PARP regulatory domain (PRD), and the highly conserved PARP signature motif with acceptor site for adenosine and donor site for nicotinamide [4]. PARP-1 acts as a DNA damage sensor molecule and participates in various DNA repair processes involved in protection against cell death [16,17]. Conversely, a hyper-activated PARP-1 is destructive [18]. Accumulating evidences demonstrate that the activity of PARP-1 is also linked to cellular signaling pathways wherein they regulate gene expression, interactions of RNA/protein and protein/protein, recruitment of proteins and the location and activity of proteins involved in signaling responses [19].

3. PARP-1 in regulation of gene expression

The regulation of gene expression by PARP-1 is a crucial aspect for cell differentiation and development in many organisms. The underlying mechanisms for PARP-1 dependent gene expression or transcriptional regulation are well established. However, its activation and signaling are prerequisites to execute these important processes.

3.1. Activation of PARP-1: Kicking signals up a notch

Varied endogenous and exogenous genotoxic stress cues have been implicated in PARP-1 activation. Genotoxic stress can arise due to; (a) Endogenous agents such as reactive oxygen and nitrogen species that are generated during various metabolic activities and cellular processes [20,21]. Conditions including hypoxia [22], elevated extracellular glucose concentration [23,24] and angiotensin II [25,26] are known to produce rampant reactive oxygen species (ROS) within the cell endangering the cellular genomic integrity. (b) Exogenous agents involving different environmental factors that can be harmful for the genome. (c) non B-DNA structures, DNA breaks like cruciform, protein-protein interactions, nuclear nicotinamide mononucleotide adenylyl transferase 1 (NMNAT1), hormone secretion etc. [27–31] are also known to activate PARP-1. Auto-modification domain of PARP-1 is implicated in protein-protein interactions along with PARP-1 homodimerization [32], an indispensable factor for its higher enzymatic activity. As per other reports, N-terminal region of PARP-1 is important for its dimerization and activation [33]. However, the basis and importance of PARP-1 dimerization for its activity is yet unclear.

Previous research established that formation of a compact PARP-1–DNA complex is imperative for its catalytic activity [15]. The helical subdomain in the catalytic domain of PARP-1 is auto-inhibitory in nature and regulates productive binding of NAD^+ [34]. In addition, the N-terminal tail of histone H4 can also induce PARP-1 activation to a higher degree than damaged DNA [35]. Upon genomic insult, maximal PARP-1 activation is achieved by phosphorylation of PARP-1 by the mitogen-activated protein kinase (MAPK) and extracellular-signal-regulated kinase (ERK) 1/2 [36]. This in turn stimulates transcription of genes implicated in cell development and proliferation through phosphorylation of transcription factor, Elk1 [37]. Also, NMNAT-1 modulates PARP-1 by binding to auto-modified PARP-1, triggering its enzymatic activity and allosterically regulating both the PAR synthesis activity and PAR chain elongation of PARP-1. NMNAT-1 is shown to

stimulate PARP-1 in the absence of ongoing NAD^+ biosynthesis, suggesting that NAD^+ synthesis and PARP-1 activation are two separable biochemical functions displayed by NMNAT-1 [31]. Furthermore, kinase-PARP-1 interaction is crucial for gene regulation during cellular differentiation. Reports have proposed that calcium-dependent protein kinase, CamKIIδ stimulates PARP-1 activation through its phosphorylation during neuronal development [38]. This cross talk between PARP-1 and kinase is important for fibroblast growth factor (FGF)-stimulated neuronal differentiation of embryonic stem cells and cell death (JNK, p38, Akt, Erk etc.). Another post-translational modification that activates PARP-1 is acetylation; upon coactivation of NF-κB by interaction with subunits of NF-κB (p65 and p50) and p300 [39]. In addition, developmental or environmental (exogenous) cues, such as steroids or thermal shock also stimulate PARP-1. dPARP (*Drosophila* homolog of PARP-1) plays a pivotal role in chromatin decondensation during heat shock of polytene chromatin [40,41]. Upon heat shock, PARP-1 activation occurs at heat-shock-responsive loci which alters or loosens nucleosome assembly in a PAR-dependent manner to enhance RNA polymerase II dependent transcription [40,42]. SIRT6, a member of another NAD^+ utilizing enzyme *i.e* Sirtuins, possesses either mono-ADP-ribosyltransferase, or deactylase activity and is identified to activate PARP-1 by mono-ADP-ribosylating PARP-1 in response to DSB's [43]. SIRT1 is also reported to inhibit PARP, and in the absence of SIRT1, hyperactivated PARP leads to AIF mediated cell death [44]. Also, Kinesin superfamily protein 4 (KIF4) interacts with PARP-1 via its C terminal domain, and keeps it inactive. Thus, it is evident that DNA damage alone does not induce PARP-1 activation but environmental, developmental cues and certain post-translational modifications can also activate PARP-1, thereby supporting the multifunctional roles of PARP-1 in different aspects of cell biology.

3.2. Signaling of PARP-1: Sensing the nicks

PARP-1 identifies the genomic lesions such as SSBs, DSBs, non-BDNA structures etc., gets activated, and recruits itself at the deformed site, forming homodimers and triggering the transfer of an ADP-ribosyl moiety from NAD^+ to aspartate or glutamate residues of its target substrates in the chromatin, mainly linker histone H1. This leads to structural changes involving unwinding of the highly condensed chromatin that renders the DNA easily accessible to transcription and repair enzymes [45,46,40]. This entire process commences with NAD^+ which is synthesized from nicotinic acid (NA). NA phosphoribosyltransferase (NAPRT) initiates the reaction, which uses phosphoribosyl pyrophosphate (PRPP) to form phosphoribosyl pyrophosphate (NAMN). Together with ATP, NAMN is then converted into (NA adenine dinucleotide) NAAD by the NMNAT1-3 enzymes. Finally, NAAD is transformed to NAD^+ through an amidation reaction catalyzed by the NAD^+ synthetase (NADSYN) enzyme. PARPs catalyze the polymerization of ADP-ribose units from donor NAD^+ molecules on accepter proteins, resulting in the addition of linear or branched polymers. Covalently attached PAR gets hydrolyzed by PARG and ARH3, both of which possess both endoglycosidic and exoglycosidic activities [47].

The different mechanisms of PARP-1 dependent regulation of gene expression are explained here.

3.3. PARP-1 dependent gene expression by chromatin remodeling: Revamping the DNA

Several *in vivo* and *in vitro* studies have revealed the transcriptional regulatory mechanism of PARP-1 for shaping the chromatin architecture. Binding of PARP-1 to nucleosomes facilitates compaction or loosening of the chromatin structure and regulates gene expression at both splicing and transcriptional levels [48,49]. PARP-1 interacts with chromatin based on nucleosome complexity such as histone variants and modifications of histones. It has the ability to recruit chromatin architectural/remodeling proteins, histones or histone variants by PARylating them [50,51] or it can compete with histone H1 to bind to nucleosomes [52].

The histone H2A variant, macroH2A, inhibits PARP-1, leading to silencing of inactive X chromosome [53]. In *Drosophila*, the conformational changes of core nucleosome due to replacement of H2A with variant H2Av assist the binding of PARP-1 to H3 and H4 [54] through C-terminal domain of PARP-1 for chromatin structure rearrangement [35]. H4 activates whereas H2A completely inhibits PARP-1 enzymatic activity. Acetylation of H2A at 5th lysine residue activates PARP-1 by removing the inhibitory effects of H2A (Fig. 1). Phosphorylation of H2Av histone variant at Ser137 by JL1 kinase in *Drosophila* activates PARP-1 and increases the interaction between PARP-1 and H4 causing H4 to get polyADP-ribosylated (Fig. 1). This in turn induces JL-1 dependent phosphorylation of H3Ser10 causing nucleosomal shifts and conformational changes leading to chromatin loosening and transcriptional initiation [55].

Local chromatin loosening by PARP-1 has also been reported at the puff loci in *Drosophila* which assists transcription and chromatin remodeling during development [40]. Interaction of nucleosome remodeling or histone modifying enzymes with PARP-1 can modulate their localization and activities. SMARCA5, the catalytic subunit of ISWI chromatin remodeling complex, gets recruited to DNA damage site in PARP-1 dependent manner, which then interacts with RNF168, E3 Ubiquitin ligase. This implies that spatial organization of PARylated RNF168-driven response to DNA damage depends on the activity of PARP-1 [56]. Previous reports by Meyer-Ficca et al., have shown that PARP inhibition results in aberrant chromatin condensation and histone retention by removing histone H1 during spermiogenesis, linking PAR metabolism with the integrity of mice sperm chromatin [57,58]. The same group further revealed that PARP-1 and PARP-2 activities modulate the chromatin structure through DNA Topoisomerase II beta (TOP2B) during spermiogenesis in mice [59]. Recently, it is reported that PARP-1 may act as a chaperone of histone molecules, recruiting or directly binding to histones or other proteins. PARylation of PARP-1 itself can bind to free histones to assist assembly of nucleosomes [60]. This association of PARP-1 and histones is summarized in Fig. 1.

In addition to this, PARP-1 can bind between linker DNA and nucleosome to open nucleosome structure, allowing regulatory proteins to access DNA [61,62]. It has been demonstrated that lipopolysaccharide (LPS) stimulation enhances PARP-1 enzymatic activity and PARylation of histones at nucleosome-occupied promoters which increases the promoter accessibility to facilitate NF-κB recruitment followed by gene transcription in macrophages [63]. Izhar et al., [64] also discovered amyotrophic lateral sclerosis (ALS) factor-TAF15 that gets recruited at the DNA lesion in a PARP-1 dependent manner thus emphasizing the critical role of PARP-1 in mediating DNA damage response.

3.4. PARP-1 dependent gene expression by splicing (alternative/pre-mRNA/co-transcriptional): Sp(li)cing up the genome

Another indispensible function of PARP-1 is alternative splicing by PARylating splicing factors or modulating RNAs. PARP-1 has been found in association with mRNA, human pre-mRNA 3′-end-processing complex factor and noncoding pRNA (promoter-associated RNA) [65,66], chromatin and splicing factors suggesting its role in co-transcriptional splicing [67]. The components involved in PARP-1 mediated splicing are shown in Fig. 2. In addition, heterogeneous nuclear ribonucleoproteins (hnRNPs) have been identified to be PARylated by PARP-1 during alternative splicing [68]. This is substantiated by presence of conserved PAR binding motif in

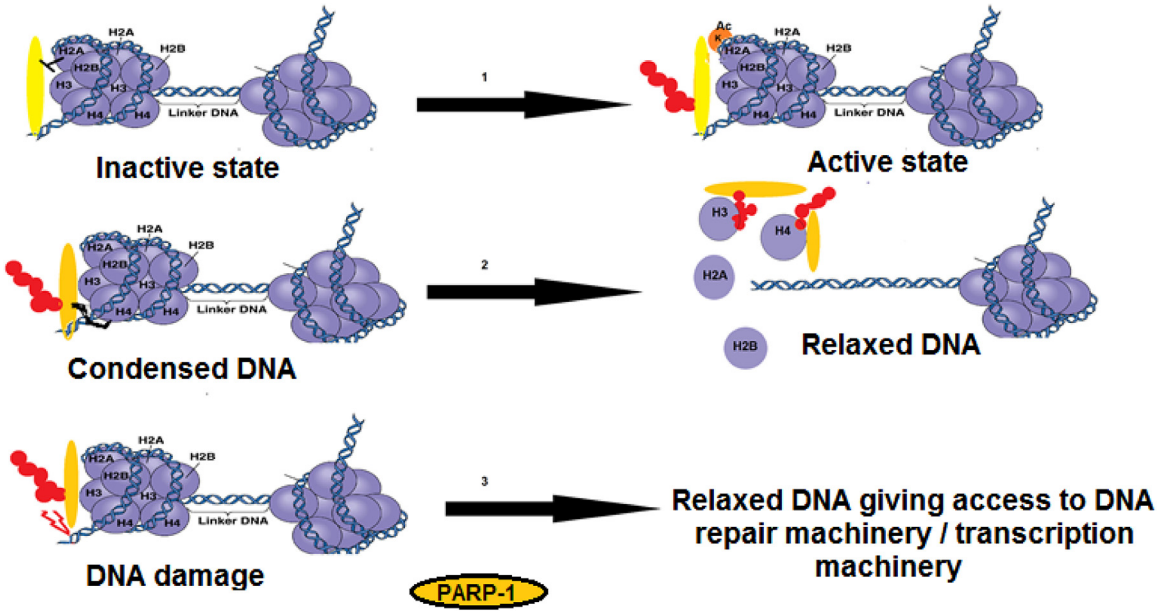

Fig. 1. PARP-1 and histones: (1) Under normal physiological state, histone H2A interacts with PARP-1 inhibiting PARP-1 activity. However, acetylation of the 5th lysine residue of H2A relieves the inhibition allowing functioning of PARP-1 (2) DNA-independent PARP-1 activation. Developmental or environmental cues cause changes in the "histone core" and consequently the N-terminal tail of histone H4 is exposed followed by H4-dependent PARP-1 activation. (3) Stress-dependent PARP1 activation: The N-terminal domain of PARP-1 protein serves as a sensor of the damaged DNA. Upon binding to such structures, it mediates conformational changes leading to disruption of interaction with histones and subsequently relaxed DNA giving access to DNA repair proteins or transcription machinery.

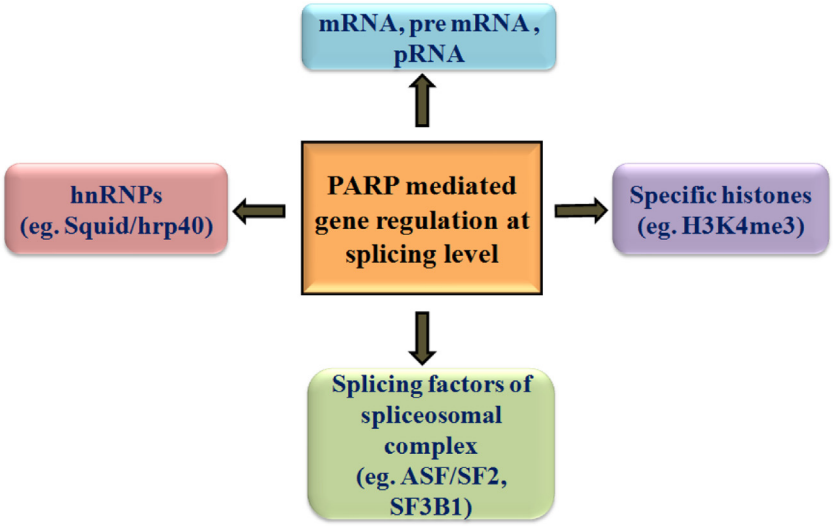

Fig. 2. Components of PARP mediated regulation of splicing: PARP-1 can interact or form a complex with mRNA, pre mRNA, noncoding pRNA (promoter-associated RNA), hnRNPs and splicing factors by PARylating or modulating them, proving its importance in splicing for regulation of gene expression.

human hnRNPs such as A1, G, H, K etc. [69]. PARylation of *Drosophila* hnRNPs (Squid/hrp40 and Hrb98DE/hrp38) decreases their RNA-binding activity subsequently altering their alternative splicing activities [68]. Assembly of Cajal Bodies (CB) involved in pre-mRNA splicing, spliceosome formation and RNPs maturation [70], are maintained by PARP-1 autoPARylation too. During splicing, the PAR moieties interact with coilin and fibrillarin and get localized in Cajal Bodies (CBs) in a PARP-1 dependent manner. Not only PARP-1 but PAR molecules also behave as a regulator of gene expression. PAR molecules form a complex with alternative splicing factor/splicing factor 2 (ASF/SF2) to control topoisomerase I mediated gene regulation [71]. Collectively, all these findings strongly support the regulatory role of PAR and PARP-1 in alternative splicing and co-transcriptional mechanism. Further studies are needed to decipher the gene regulatory mechanism of PARP-1.

3.5. PARP-1 dependent gene expression through transcriptional regulation: Managing the chromatin dynamics

PARP-1 can stimulate transcription positively with co-activators or negatively with repressors [72], on the basis of DNA binding transcription factors' sequence specificity [49]. Activated PARP-1

gets auto-PARylated followed by its dissociation from nucleosome assembly which in turn decondenses the chromatin to initiate/enhance transcription [35]. Actively transcribed sites (promoters) are found to be enriched with PARP-1 [49]. PARP-1 acts as a co-activator for the Nrf2 genes, enhancing their expression through interaction with antioxidant response elements (ARE) [73]. Recently, it has been investigated that stimulation-induced Erk-PARP-1 synergism in chromatin of cerebral neurons is essential for immediate early gene expression involved in long-term memory [74]. Repression of transcriptional activities by incorporation of PARP-1 into chromatin structure leads to compaction of chromatin and inhibition of transcription [75,14]. Peng et al., have reported that PARP-1 and linker histone H1.2 proteins serve a crucial role in the transcriptional regulation of EPHX1 (mEH gene). PARP-1 stimulates EPHX1 transcription, a process which was inhibited by heterozygous mutations in the proximal promoter region of EPHX1 [76]. Kotova et al., [75] have disclosed PARP-1 induced silencing of retro-transposable genes and formation of heterochromatin structures in *Drosophila*. Pharmacological inhibition of PARP-1 with Olaparib results in global gene deregulation through polycomb repressive complex 2 (PRC2) member, EZH2 in a lymphoblastoid B cell line [77]. Recent studies are drawing attention towards rDNA silencing by PARP-1 in cell division. TIP5 (component of NoRC chromatin remodeling complex) combines with PARP-1 to maintain rDNA silencing after replication and represses transcription in a chromatin dependent manner [78].

3.6. PARP-1 dependent gene expression by DNA methylation: Silencing the genome

Methylation is one of most key post-translational modifications of histone proteins which can alter chromatin structure and thereby regulate gene expression. PARP-1 and PAR molecules play an important role in maintaining DNA methylation patterns by regulating the activity as well as expression levels of DNA methyl transferases (Dnmt)1 [79–81]. Functional interaction of PARP-1 with methylcytosine dioxygenase, Tet2 stimulates formation of 5-hydroxymethylcytosine (5hmC) from 5-methylcytosine (5mc). This interaction plays an important role in epigenetic programming of somatic cells during their transition to pluripotency [82]. Demethylase activity of histone lysine demethylase was shown to be maintained by PARP-1, PARylating it and hence inhibiting binding of KDM5 to chromatin, influencing alterations in chromatin structure. This study explains the co-ordination of PARP-1 with histone modification for controlling transcription [83]. CTCF (CCCTC-binding factor) is considered to be a vital protein through which PARylation conserves the unmethylated pattern of a few DNA sequences [84]. Irrespective of DNA damage, CTCF stimulates PARylation activity of PARP-1. Moreover, CCCTC-binding factor (CTCF) loses its nuclear localization due to PAR depletion eventually resulting in changes in the chromatin arrangement. This work underlined the link between CTCF and PARylation to uphold chromatin architecture and DNA methylation patterns [85] as also shown in Fig. 3 .

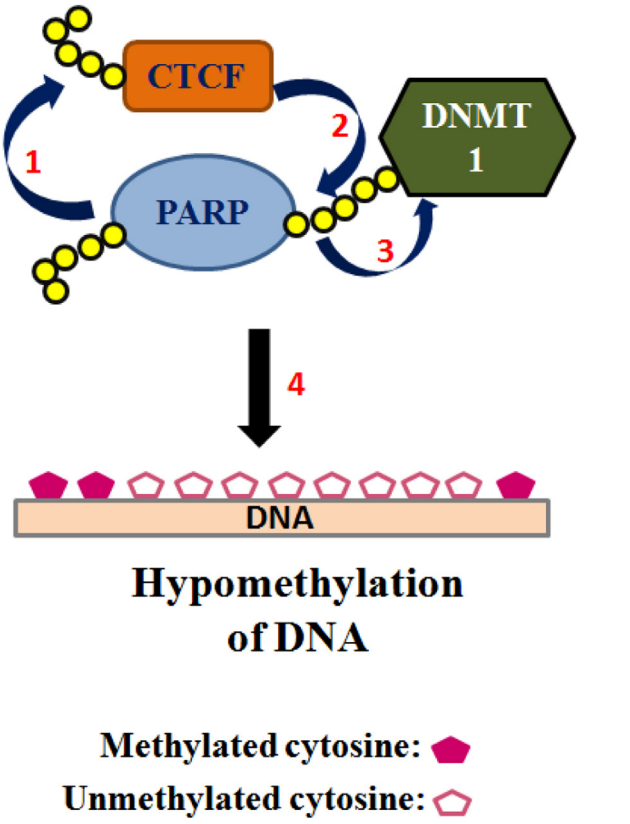

Fig. 3. DNA methylation control by PARP-1: PARP-1 PARylates N-terminal end of transcription factor, CTCF, which in turn stimulates auto-PARylation of PARP-1. This CTCF-PARP-1 interaction inhibits the catalytic activity of DNA methyl transferase 1 (DNMT1) through non covalent binding between PAR-DNMT1 due to which DNA methylation is inhibited thereby maintaining the methylation pattern.

4. PARP-1 in development: From the cradle to the grave

4.1. PARP-1 in embryonic development

Accumulating evidences suggest a role of PARP-1 in driving cell differentiation and cell fate commitment. PARylation by PARP-1 is developmentally regulated. PARP-1 and PARP-2 have been established to play an important role in mouse embryogenesis and development. de Murcia et al. (2003) reported that PARP-1 and PARP-2 double mutant mice died at the onset of gastrulation [86]. Moreover, female embryonic lethality is found to be associated with specific X-chromosome instability in *PARP* knock out (KO) mice [86]. An early post implantation embryonic lethality is observed in mouse having double mutation in both ATM and PARP-1 genes at embryonic day 8.0. The synergistic effect of these genes may be responsible for either monitoring or repairing DNA damage during embryo development [87]. PARP-1–Ku80 interaction is vital for early developmental stage, as suggested by Henrie et al., [88]. They show that PARP-1$^{-/-}$Ku80$^{-/-}$ embryos fail to repair DNA damage in early embryogenesis developmental stage generating an embryonic lethal phenotype of these double KO mice. The Wnt signaling pathway is considered to be a central pathway for embryogenesis wherein T-cell factor-4 (TCF-4) combines with nuclear B-catenin to form a complex [89]. Earlier studies show that transcriptional activity of TCF-4 and B-catenin complex is enhanced by interaction with PARP-1 [90]. The same group further revealed the competitive interaction between PARP-1 and Ku70 to control TCF-4 and B-catenin complex mediated gene trans-activation [91]. Moreover, the loss of SSBR/BER and DSB repair pathways' component led to massive apoptosis of the embryo as a result of defect in DNA-damage signaling. *DYX1C1* is a known candidate gene for dyslexia susceptibility. PARP-1 is also reported to be essential in migration of neurons during embryogenesis, forming a complex with TFII-I and SFPQ proteins to control transcription of *DYX1C1* [92]. *Drosophila* has been used as a model system to illustrate the role of PARP-1 during larval development. Higher PARP enzymatic activity is found at the prepupal stage of development in *Drosophila* [93]. These reports are indicative of role of PARP-1 in embryogenesis *via* different pathways wherein DNA repair is identified to be PARP-1's primary role.

4.2. PARP-1 in germline development

Germ cells play an important role in reproduction; development and evolution and therefore transfer of conserved genetic information from these cells to the next progeny is a matter of prime importance. PARP-1 *via* its multifunctional roles in DNA repair, gene transcription, chromatin remodeling and epigenetic modification proves to be an important candidate in germline development. The temporal and spatial expression of few PARP-1 target genes, along with their molecular interactions, is ultimately responsible for germ cell differentiation [94]. PARylation regulates the key events in epigenetics, chromatin structure modulation and transcription in germ line differentiation and development. It was reported that PARP inhibition in mice ovaries increases oogenesis and folliculogenesis by regulating expression of transforming growth factor (TGF) super-family members and other genes involved in oogenesis pathways [95]. *PARP-1* KO was found to be more sensitive to genotoxic stress due to its compromised DNA repair ability. PARP1$^{-/-}$ mice embryonic fibroblast displayed tetraploid population with an unstable genome [96] and immortalized embryonic fibroblasts showed hyperploidy in *PARP-1* KO conditions [97]. Partial KO of PARP (*PARP-1*$^{+/-}$) and complete KO of PARP-2$^{-/-}$ was found to be associated with X chromosome instability conferring specifically female lethality [86]. PARP-1 null oocytes exhibit defects in meiosis like persistent H2AX phosphorylation, suggesting a role of PARP-1 in chromatin modification during oogenesis [98]. The expression of PARP-1 is restricted to the peripheral cellular layer which contains proliferating spermatogonia, whereas the PARP-2 is evenly distributed all over the seminiferous tubules, suggesting a crucial role of PARP for different aspects of spermatogenesis [32]. Dantzer et al., [99] have reported a decline in fertility potential of males in PARP-2 deficient mice that relates to defects in spermiogenesis and meiosis-I. GATA3 regulates cell growth and tumorigenesis by favoring G1/S transition and transcriptional regulation of the CCND1 (coding Cyclin D1 protein). PARP-1, a transcriptional coactivator for GATA3, interacts with the later and this interactome in turn transactivates the CCND1 gene [100]. Mouse PARP-1 is found to be enriched and is suggestive of a role in gene silencing of inactive X chromosome [53]. Thus, it will be interesting to further probing the roles of PARP-1 in X chromosome inactivation and germ cell development.

4.3. Mechanism of gene regulation for development/differentiation by PARP-1

PARP-1 has been shown to regulate growth and development of variety of cells [37,30] through transcriptional regulation [101]. Although PARP-1's role in differentiation had been detected long back, only recently it has grabbed the interest of researchers. It has been demonstrated that mouse myeloid leukemia cells treated with purified poly (ADP-ribose) differentiated into mature macrophages and granulocytes [102]. ADP-ribosylation mediates formation of a complex between PARP-1 and PPARγ at the promoter regions of target genes, a process that increases ligand binding and aids ligand induced co-factor exchange. ADP-ribosylated PARP-1 then stabilizes the PPAR ligand binding. Torsional stress created during TopoII cleavage further recruits and activates PARP-1. The modified PARP-1 interacts with PPARγ and stabilizes PPARγ ligand binding, which permits an exchange of the NCoR1 co-repressor with the p300 co-activator at PPARγ promoter sites. Further, the PAR formation favors ligand binding and p300 recruitment to PPARγ response elements (PPREs) and thus leading to PPARγ dependent gene expression [103].

PARP-1 is also reported to have role in differentiation of neuroectoderm. Yoo et. al., discovered that FGF-ERK1/2 orchestrates neural specification via regulating PARP-1 activity, thus reinforcing role of PARP-1 in neural induction from human embryonic stem cells [104,36,37]. Recently, PARP-1 has been reported to regulate osteoclastogenesis *via* inhibition of recruitment of p65/RelA to the IL-1β promoter subsequently affecting IL-1β expression [105].

The transforming growth factor beta (TGFB) signaling pathway is another pathway in which PARP-1 plays a crucial role. TGFB signaling pathway is implicated in both the adult organisms and the developing embryo. The TGFB regulates cellular proliferation, differentiation, and migration during embryonic development and adult tissue homeostasis. Smad proteins mediate signals by the TGFB family of morphogens. PARP-1 has been shown to dissociate the Smad complexes from DNA and attenuate Smad mediated transcription [106]. However, Huang et al., [107] demonstrated PARP-1 to be a requisite for TGFB1 induced Smad3 activation. The TGFB1 promotes PARylation of Smad3 resulting in enhanced Smad-Smad binding element [SBE] complex formation and increased DNA binding activity and eventually resulting in transcription of its target genes.

Recent report have further illustrated that PARP-2 assists PARP-1 in negatively regulating Smad function while PARG is a positive regulator [108]. Reports indicate that PARP-1 can act either as a negative regulator of responses to TGFB, as seen in epithelial cells [106] and CD4^{+}T cells [109], or as a positive regulator of TGFB responses, as seen in vascular smooth muscle cells [107] to TGFB signaling. Poly ADP-ribosylation has also been strongly implicated to regulate TGF super family members during oogenesis and folliculogenesis in mice [95]. Moreover, reports also illustrate role of PARP-1 in white adipocyte differentiation and lipid metabolism by regulating PPARγ dependent gene expression [110,111].

Switching on and off of gene expression in response to temporal and spatial patterns is essential in normal development. PARP-1 has been demonstrated to play such a pivotal role in neuronal differentiation. Activated PARP-1 as a part of the groucho/TLE-co-repressor complex drives the dismissal of the poly ADP-ribosylated components of the co-repressor complex from HES1 regulated promoters followed by CAMKIIδ phosphorylating HES1 thereby permitting neurogenic gene activation [38]. PARP-1 has also been recently associated with HIF [Hypoxia inducible factors] in hypoxic response. HIFs control induction of genes involved in cellular metabolism, cell growth, metastasis, apoptosis, and others [112]. PARP-1 is also suggested as an essential co-regulator for retinoic acid [RA] induced gene expression *in vivo* and thus a requisite of RA dependent growth and developmental pathways [113]. In addition, role of poly (ADP-ribosyl)ation by the PARP family member, tankyrase has also been established in the regulation of Wnt-β-catenin signaling pathway which plays a fundamental role during embryonic development and adult tissue homeostasis [114]. On similar lines, PARP-1 also regulates embryonic stem cell differentiation *via* PARylation of SOX2 protein levels and regulation of *FGF4* expression [115]. However, poly ADP-ribosylation of the target proteins finally leading to gene regulation may not be the only mode of regulating gene expression by PARP-1. PARP-1 is reported to regulate *Nrf2* transcription by neither PARylating Nrf2 nor physically interacting with it. Rather, PARP-1 interacts directly with small Maf proteins and ARE of Nrf2 target genes, which amplifies ARE-specific DNA-binding of Nrf2 and enhances the transcription of Nrf2 target genes thereby maintaining intracellular redox homeostasis [73]. Rajawat et al., also showed impediment of development of *Dictyostelium discoideum* when PARP was down-regulated, showcasing its importance during developmental program of the organism [116]. In view of the above literature, it is evident that PARP-1 through its modes of transcriptional regulation as discussed above regulates many signaling pathways in the cell thereby controlling important cellular processes like differentiation which are summarized in Fig. 4.

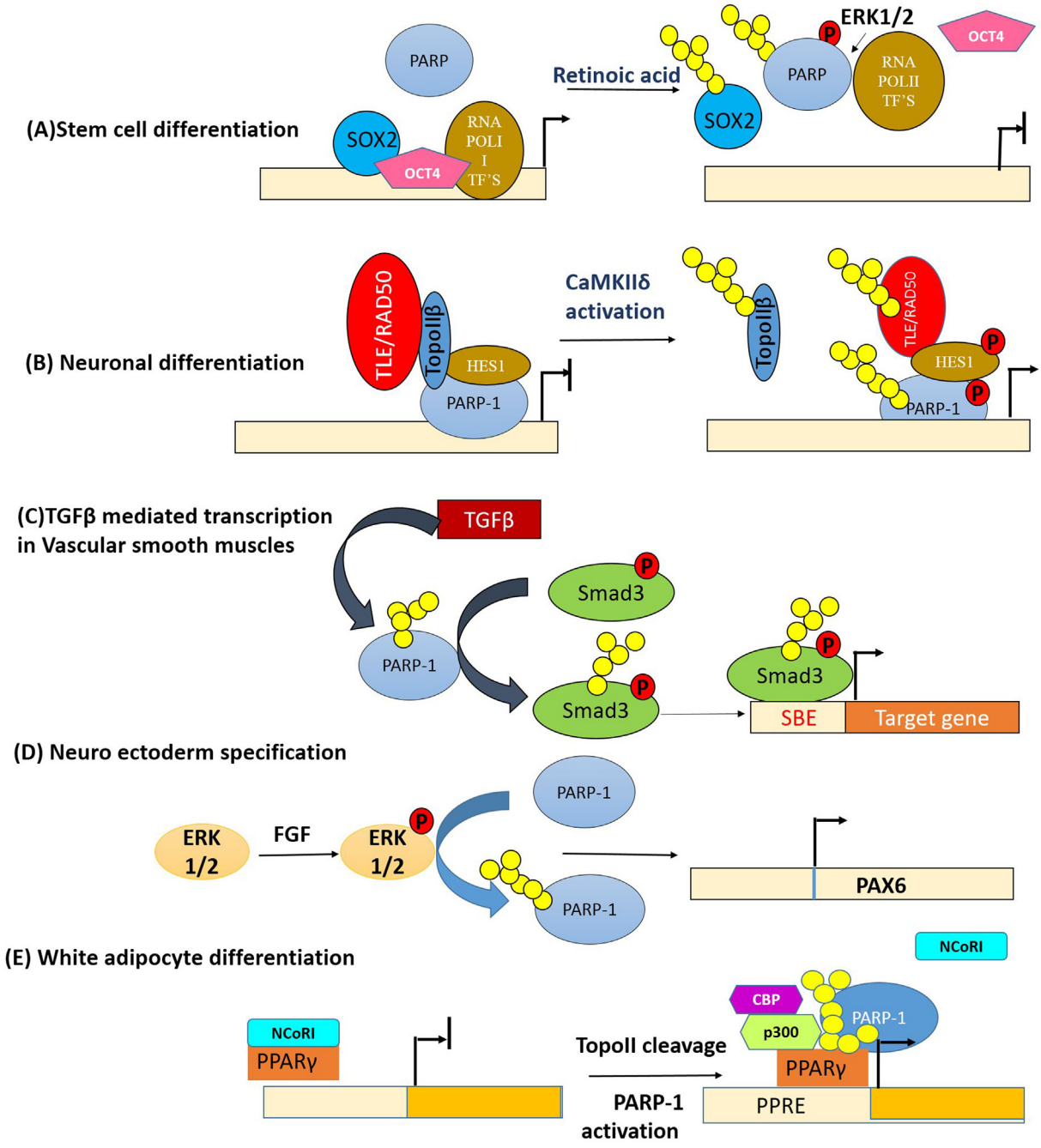

Fig. 4. PARP-1 in differentiation: (A) PARP-1 in regulation of stem cell differentiation: Phosphorylation of PARP-1 by kinase ERK1 leads to auto-modification of PARP-1. PARylated PARP-1 abolishes SOX2 DNA-binding and dimerization with OCT4 leading to transcription inhibition of target genes involved in differentiation. (B) PARP-1 in neuronal differentiation: Treatment of neuronal stem cells with PDGF (platelet derived growth factor) induces activity of the kinase CaMKIIδ. Activated CaMKIIδ leads to phosphorylation of PARP-1, which in turn leads to PARylation resulting in disruption of co-repressor complex including TLE, RAD50, TopoIIβ, PARP-1 and HES1 at promoter. Auto-modified PARP-1 and HES1 recruit histone acetyl-transferase CBP, and also subsequent phosphorylation of repressor protein HES1 by CaMKIIδ initiates transcription. (C) PARP-1 in TGFβ mediated transcription: TGFβ promoted PARylation of Smad3 ensuing into stronger Smad-Smad binding element [SBE] complex formation and increased DNA binding activity and eventually transcription of its target genes (D) PARP-1 in neuro ectoderm specification: FGF-ERK1/2 coordinates PARP-1 activation which eventually facilitates transcription of genes involved in neural differentiation from human embryonic stem cells. (E) PARP-1 in white adipocyte differentiation: ADP-ribosylated PARP-1 stabilizes PPAR ligand binding. Torsional stress created during TopoII cleavage leads to PARP-1 activation. Modified PARP-1 interacts with PPARγ and stabilizes PPARγ ligand binding, which allows an exchange of the NCoR1 co-repressor with the p300 co-activator at the PPARγ response elelments (PPREs) and thereby ensured continuous expression of PPARγ target genes.

5. PARP-1 in cell differentiation/multicellularity in different organisms: Translating time

Cell growth and differentiation processes involve transcriptional activation of a variety of genes in response to specific developmental and environmental stimuli. PARP-1 has also been reported to engage in transcriptional control during development as well [93]. Evidences across domains of life substantiate the role of PARP-1 from unicellular to multicellular forms [117]. The differentiation from preadipocytes to adipocytes triggered by the nuclear receptor PPARγ is an illustration of the involvement of PARP-1 [111] in cellular differentiation. Many such recent accumulating

evidences enlisted below propose a strong association of PARP-1 in differentiation and multicellularity.

5.1. *PARP-1 in* Dictyostelium discoideum *development*

D. discoideum is a unicellular eukaryote exhibiting multicellularity upon starvation [118] and has eight potential *PARP* genes [119]. Our previous study showed that *D. discoideum* exhibits basal PARP activity and inhibition of PARP by benzamide delays the development [120]. Our further study demonstrated PARP's role in development by down-regulation and no effect is observed on the growth profile of unicellular amoebae. On the contrary, development was blocked at the initial aggregation stage, signifying the involvement of PARP-1 during development of *D. discoideum* [116]. In addition, PARP-1 has also shown to be involved in stress responses like oxidative stress via proteases, UV-C stress *via* nitric oxide and DNA repair in *D. discoideum* whereas it has been shown to play no role in staurosporine induced cell death [121–125]. Moreover, our recent lab report shows association of ADPRT1A (PARP-1 ortholog in *D. discoideum*) with cell survival and development [126]. In addition, *ADPRT1A* knockout resulted in altered levels of genes essential for cAMP production and signaling as well as markers of differentiation (Unpublished data). These findings clearly establish the importance of ADPRT1A in *D. discoideum* life cycle.

5.2. *PARP-1 in fungus development*

The presence of PARP in only multicellular eukaryotes is suggestive of the association between PARP function and a multicellular lifestyle. It has been reported that PARP homologs exist in fungi that have multicellular hyphae and organized developmental structures and lack yeast-like unicellular growth pattern. However, PARP homologs are notably absent in *S. cerevisiae* and *S. pombe* while they are found in all other eukaryotes [127]. Semighini et al., [128] reported that the disruption of the *PrpA* gene (PARP-1 ortholog) in filamentous fungus *Aspergillus nidulans* was found to be lethal in haploid strains, whereas *PrpA* overexpression led to fluffy phenotype caused by defect in conidiation while generation of $PrpA^{-}/^{-}$ failed.

Interestingly, PARP overexpression in *P. anserina* led to reduced number of ascospores and fruiting body and also decreased the growth rate and life span whereas complete deletion failed thereby suggesting a vital role of PARP-1 in growth and development [129]. Furthermore, Neurospora PARP-1 orthologue [NPO] mutant strain also exhibited an accelerated aging in mycelia [130]. All these reports are suggestive of PARP-1 role in multicellularity and how its regulated expression is quintessential in the correct development and cellular processes.

5.3. *PARP-1 in plant development*

In plants, the roles of PARP-1 orthologs in development remain obscure. Unlike in mammals, plants lack the variety of PARP superfamily members. However, plants encode a group of PARP-like proteins belonging to the SRO family. Plants PARP family members and/or poly [ADP-ribosyl] ation have been linked to various processes like DNA repair, innate immunity, mitosis, and stress responses. In addition, SRO family members have been also shown to be essential for normal sporophyte development [131]. Moreover, PARP super-family members have been found to be crucial for stress responses in *Arabidopsis thaliana* [131]. In *Arabidopsis*, AtPARP3 is reported to be expressed specifically in seed development signifying its potential role [132]. In addition, AtPARP-1 and/or AtPARP2 knockdown were reported to alter *Arabidopsis* development [133]; however, AtPARP2 ortholog in oilseed rape (*Brassica napus*) did not affect its development [134]. These reports suggest that further research is necessary to establish the role of PARP in plant development.

5.4. *PARP-1 in* Drosophila melanogaster *development*

Role of PARP-1 in differentiation and development is well studied in the model organism *Drosophila melanogaster*. In *Drosophila*, PARP activity is found to be developmentally regulated [135]. Also, the expression levels of PARP in *Drosophila* are shown to be the highest in embryos whereas reduced expression was seen in larvae, pupae, and adults [136]. Moreover, PARP overexpression hampers the cytoskeletal organization (F-actin) and disrupts tissue polarity, suggesting its participation in *Drosophila* development [137].

Previous literature strengthens the importance of PARP as a transcriptional co-activator [138], implicating that PARP may regulate the expression of a few genes involved in determining tissue polarity or cytoskeleton in *Drosophila*. Miwa et al., [139] reported that *PARP* deletion mutant failed to grow into an adult fly suggesting PARP's involvement in larval metamorphosis since 50% of mutant larvae were arrested at this stage. In addition, PARP activation is a prerequisite for viability and organization of chromatin, heterochromatin, and other sequences during development [140]. Studies have been shown PARP to be vital for purparium formation and metamorphosis [40,141]. Thus, PARP-1 also plays an important role during the *Drosophila* development.

5.5. *PARP-1 in mice development*

PARP-1 and PARP-2 have been implicated in playing an important role in mouse embryogenesis and development over the past couple of decades. In particular, PARP-1 and PARP-2 double mutations in mice were found to be lethal as the embryos died at the onset of gastrulation [86]. This result is further supported from ATM and Ku80 deficient mice in PARP-1 knockout background [142,88]. It has been suggested that both PARP-1 and ATM act synergistically during mouse development [142]. Moreover, the loss of SSBR/BER and DSB repair pathway components lead to massive apoptosis of the embryo as a result of defect in DNA-damage signaling. PARP-1 is involved in germline development wherein PARP-1 deficient oocyctes were found to exhibit defective meiosis [98]. In addition, PARP-1 knockout mice also demonstrate altered gene expression of cytoskeletal elements [143]. Furthermore, PARP-1 has been reported to contribute to DNA demethylation in pre-implantation embryos of mice [144]. Authors report that the mean life span of *PARP-1*$^{-/-}$ knockout mice was significantly reduced while these mice also showed accelerated aging of the reproductive function as compared to wild type mice. PARP-1 and PARP-2 have been reported to be a requisite for the differentiation of mouse embryonic carcinoma F9 cells into endodermal cells via recruitment of the transcriptional intermediary factor (TIFIβ) for the expression of the endoderm specific gene during endodermal differentiation [145]. Similarly, adipogenic differentiation is reduced in adipose derived stromal cells isolated from *PARP-1* knockout mice. Recently it has been reported that PARP-1 deficiency notably reduce bone mass in mice as a result of increased osteoclast differentiation [105]. Zhou et al., report that PARP-1 inhibition by PJ-34 induces angiogenesis in diabetic and ischemic conditions. Thus, PARP-1 plays a very important role in cell differentiation and development in mice [146].

5.6. *PARP-1 in immune cells development*

Recently, growing body of reports indicate that PARP-1 engages in inflammatory/immune responses as well. PARP-1 controls cell functions in many types of immune cells, including dendritic cells, macrophages, and T and B lymphocytes [147–150]. It has been sug-

gested that *PARP-1* KO T cells stimulated in the absence of antigen presenting cells exhibit a lower cellular proliferation rate [151]. Moreover, V(D)J recombination deficient T cells can be partially rescued by knocking out PARP-1, implicating its role in T-cell maturation too. Several studies demonstrate that *PARP-1* KO cells display a reduced ability to differentiate in Th2 cells. In immune cell differentiation, PARP-1 genetic ablation decreases specifically Th2 cell differentiation and enhances regulatory [$CD4^+CD25^+FoxP3^+$] T cells population [152,153]. PARP-1 is also reported to play a role in differentiation to plasma cells *via* transcriptional repression of Bcl-6 [154].

Apart from erratic environmental genomic insults, certain cellular processes such as lymphocyte development and antibodies production involve spontaneous DNA damage wherein PARylation and PARPs/ARTDs play a crucial role in combating the insults. B lymphocytes undergo a course of rigorous genomic rearrangements and recombination along with somatic mutations, to generate B cells that produce related antibodies possessing varying degrees of specificity and diverse functions due to class switching and affinity/maturation. Thus, during the B cell development, differentiation, and maturation, the genome in question undergoes lesions and damages, that eventually activates the DNA repair machinery and cell cycle check points to initiate genomic repair. Moreover, NF-κB signaling plays a crucial role in immature B cell development and differentiation and mature B cell survival. Earlier evidences suggest a crosstalk between intrinsic NF-κB activity of B cells and spontaneous DNA damage/repair for proper B cell function. Stilmann et al., demonstrate the importance of PARylation by PARP1/ARTD1 in bridging the nuclear sensing of DNA damage with cytoplasmic activation of the IKK (IκB kinases) complex [155]. Upon DNA damage, the PAR- modified PARP-1 dissociates from damage sites, and orchestrates the assembly of transient multiprotein PARP1/ARTD1-IKKγ–PIASy-ATM signalosome complex which in turn trigger stimulation of IKKγ via its sumoylation by PIASy (protein inhibitor of activated STAT superfamily), leading to IKKγ induced NF-kB activation of survival pathways [155,156]. These findings suggest the importance of PARP-1 in immune cells differentiation and maturation, implicating PARP as a therapeutic target for several immune mediated diseases.

6. PARP-1 and immune mediated diseases:Diss(ease)ing the alter ego

PARP-1 is expressed in almost all cells and plays a central role in inflammation and immunity [157]. Its enzymatic inhibition confers protection in several models of immune-mediated diseases, mostly through an inhibitory effect on NF-κB (and NFAT) activation [153]. PARP inhibitors ameliorate immune mediated diseases in several experimental models, including colitis, rheumatoid arthritis, allergy and experimental autoimmune encephalomyelitis [158]. Previously, *PARP-1* KO mice have been suggested to display a decreased severity of rheumatoid arthritis due to lower IL-1β and MCP-1 expression which led to decreased destruction of bone and cartilage in arthritic joints [159]. Rosado et al., [158] demonstrate that PARP-1 have involvement in the differentiation of $Foxp3^+$ regulatory T (Treg) cells, suggesting it's role in tolerance induction. Also ARTs is involved in regulating Treg cell homeostasis by promoting Treg cell apoptosis during inflammatory responses, thus rendering it a crucial target for immune suppressive therapy.

Several studies show that PARP-1 deficiency and PARP inhibition confer resistance to inflammatory bowel disease (IBD) in rodent models of dinitrobenzene/trinitrobenzene sulphonic acid (DNBS/TNBS)-induced colitis by dampening AP-1 and NF-κB activation, inflammatory cytokine production and apoptosis, with consequent reduction of colon damage [160,161]. Together, these findings show that PARP-1 plays a pivotal role in the regulation of immune responses and may represent a good target for new therapeutic interventions in immune-mediated diseases.

PARP-1 also changes the responsiveness of dendritic cells, T-cell activation and antibody production via alteration in gene regulation and secretion of various cytokines and adhesion molecules [150]. PARP-1 inhibition targeting the enzymatic site reduces the secretion of pro-inflammatory cytokines and ameliorates various autoimmune and inflammatory diseases like heart and brain inflammatory processes, rheumatoid arthritis, inflammatory bowel disease, colitis, autoimmune encephalomyelitis etc. [162–168]. Furthermore, PARP-1 acts as a crucial mediator in maintaining the balance between pro-inflammatory/effector and anti-inflammatory/regulatory responses, suggesting possible therapeutic perspectives of PARP inhibition [150]. Studies demonstrate that PARP-1 sustains NF-kB induced transcription of several genes involved in inflammation, including cytokines, such as TNFα, IL1-B, IL6, IFN and CCL3, and inducible nitric-oxide synthase (iNOS) [169,170]. In view of these studies, PARP inhibitors can be proposed as a potent future therapeutant for various autoimmune disorders. Moreover, role of PARP-1 has been suggested in adaptive immune response as it gets stimulated during T-cell activation. In addition,PARP-1 regulates NFAT function as well, which is involved in T-cell differentiation and functions [171,172], and modulates the expression of Th1/Th2 cytokines [151].

The promising results of various studies including animal models emphasize the urgency of introducing PARP inhibitors into clinical trials for various autoimmune diseases exhibiting cytokine imbalance, upregulation of adhesion molecules, dysregulation in antibody production etc., implicating the multi targeting effects of PARP-1 in attenuation of such diseases.

7. Conclusion

A wealth of reports over the past decades have drawn the attention of researchers towards PARP-1 from being just a 'DNA damage sensor', to a multitasking protein in the cell with prime roles such as gene regulation, chromatin remodelling, differentiation etc. Structural evidences now explain the multidomain structure of PARP-1 and the process of poly ADP-ribosylation in response to various stimuli. PARP-1 is well demonstrated to be activated not just by damaged DNA but also by various developmental and environmental cues. PARP-1 PARylates numerous chromatin-remodeling factors, resulting in chromatin modification and regulation of gene expression. In addition, PARP-1 also regulates splicing and DNA methylation processes. All these functions of PARP-1 in gene regulation are mirrored in its association with developmental and differentiation processes in the cell, including embryogenesis, germline development and cell differentiation. Thus, instead of just being merely treated as a DNA damage sensing protein, PARP-1 should be explored for its role in differentiation that has been highlighted in the present review. Nonetheless, the role of PARP in gene regulation, cell differentiation and development also makes it suitable and promising target for therapeutic armenatrium to treat several human diseases.

Acknowledgements

RB thanks the Department of Biotechnology, New Delhi (BT/PR4383/BRB/10/1014/2011) and Council of Scientific and Industrial Research (38 (1383)/14/EMR-II) for financial support. TJ thanks UGC-SAP DRS for fellowship. MS thanks CSIR for fellowship. RB also thanks DBT-MSUB ILSPARE. It is to be noted that none of the authors have any conflict of interest.

References

[1] A.M. Näär, B.D. Lemon, R. Tjian, Transcriptional coactivator complexes, Annu. Rev. Biochem. 70 (2001) 475–501.
[2] D. Reinberg, G. Orphanides, R. Ebright, S. Akoulitchev, J. Carcamo, H. Cho, The RNA polymerase II general transcription factors: past, present, and future, Cold Spring Harb. Symp. Quant. Biol. 63 (1998) 83–103.
[3] J.C. Ame, C. Spenlehauer, G. de Murcia, The PARP superfamily, Bioessays 26 (2004) 882–893.
[4] V. Schreiber, F. Dantzer, J.C. Ame, G. de Murcia, Poly(ADP-ribose): novel functions for an old molecule, Nat. Rev. Mol. Cell. Biol. 7 (2006) 517–528.
[5] D. Lautier, J. Lagueaux, J. Thibodeau, L. Ménard, G.G. Poirier, Molecular and biochemical features of poly (ADP-ribose) metabolism, Mol. Cell Biochem. 122 (1993) 171–193.
[6] S. Smith, The world according to PARP, Trends Biochem. Sci. 26 (2001) 174–179.
[7] W. Min, Z.Q. Wang, Poly (ADP-ribose) glycohydrolase (PARG) and its therapeutic potential, Front. Biosci. 14 (2009) 1619–1626.
[8] S. Oka, J. Kato, J. Moss, Identification and characterization of a mammalian 39-kDa poly(ADP-ribose) glycohydrolase, J. Biol. Chem. 281 (2006) 705–713.
[9] F. Rosenthal, K.L.H. Feijs, E. Frugier, M. Bonalli, A.H. Forst, R. Imhof, et al., Macrodomain-containing proteins are new mono-ADP-ribosylhydrolases, Nat. Struct. Mol. 20 (2013) 502–509.
[10] M. Citarelli, S. Teotia, R.S. Lamb, Evolutionary history of the poly(ADP-ribose) polymerase gene family in eukaryotes, BMC Evol. Biol. 10 (2010) 308.
[11] D. Perina, A. Mikoč, J. Ahel, H. Ćetković, R. Žaja, I. Ahel, Distribution of protein poly(ADP-ribosyl)ation systems across all domains of life, DNA Repair 23 (2014) 4–16.
[12] M.O. Hottiger, P.O. Hassa, B. Luscher, H. Schuler, F. Koch-Nolte, Toward a unified nomenclature for mammalian ADP-ribosyltransferases, Trends Biochem. Sci. 35 (2010) 208–219.
[13] M. Rouleau, A. Patel, M.J. Hendzel, S.H. Kaufmann, G.G. Poirier, PARP inhibition: PARP1 and beyond, Nat. Rev. Cancer 10 (2010) 293–301.
[14] M.F. Langelier, D.D. Ruhl, J.L. Planck, W.L. Kraus, J.M. Pascal, The Zn3 domain of human poly(ADP-ribose) polymerase-1 (PARP-1) functions in both DNA-dependent poly(ADP-ribose) synthesis activity and chromatin compaction, J. Biol. Chem. 285 (2010) 18877–18887.
[15] M.F. Langelier, K.M. Servent, E.E. Rogers, J.M. Pascal, A third zinc-binding domain of human poly(ADP-ribose) polymerase-1 coordinates DNA dependent enzyme activation, J. Biol. Chem. 283 (2008) 4105–4114.
[16] P. Jagtap, C. Szabo, Poly(ADP-ribose) polymerase and the therapeutic effects of its inhibitors, Nat. Rev. Drug Discov. 4 (2005) 421–440.
[17] C. Herceg, Z.Q. Wang, Functions of poly(ADP-ribose) polymerase (PARP) in DNA repair, genomic integrity and cell death, Mutat. Res. 477 (2001) 97–110.
[18] Y. Wang, V.L. Dawson, T.M. Dawson, Poly(ADP-ribose) signals to mitochondrial AIF: a key event in parthanatos, Exp. Neurol. 218 (2009) 193–202.
[19] B.A. Gibson, W.L. Kraus, New insights into the molecular and cellular functions of poly(ADP-ribose) and PARPs, Nat. Rev. Mol. Cell. Biol. 13 (2012) 411–424.
[20] R.J. Aitken, G.N. De Iuliis, Origins and consequences of DNA damage in male germ cells, Reprod. Biomed. Online 14 (2007) 727–733.
[21] I. Amiri, N. Sheikh, R. Najafi, Nitric oxide level in seminal plasma and its relation with sperm DNA damages, Iran. Biomed. J. 11 (2007) 259–264.
[22] E. Gilad, B. Zingarelli, A.L. Salzman, C. Szabó, Protection by inhibition of poly(ADP-ribose) synthetase against oxidant injury in cardiac myoblasts in vitro, J. Mol. Cell. Cardiol. 29 (1997) 2585–2597.
[23] F. Garcia Soriano, L. Virág, P. Jagtap, E. Szabó, J.G. Mabley, L. Liaudet, et al., Diabetic endothelial dysfunction: the role of poly(ADP-ribose) polymerase activation, Nat. Med. 7 (2001) 108–113.
[24] P. Pacher, L. Liaudet, F.G. Soriano, J.G. Mabley, E. Szabó, C. Szabó, The role of poly(ADP-ribose) polymerase activation in the development of myocardial and endothelial dysfunction in diabetes, Diabetes 51 (2002) 514–521.
[25] C. Szabo, P. Pacher, Z. Zsengellér, A. Vaslin, K. Komjáti, R. Benkö, et al., Angiotensin II-mediated endothelial dysfunction: role of poly(ADP-ribose) polymerase activation, Mol. Med. 10 (2004) 28–35.
[26] J.B. Pillai, M. Gupta, S.B. Rajamohan, R. Lang, J. Raman, M.P. Gupta, Poly(ADP-ribose) polymerase-1-deficient mice are protected from angiotensin II induced cardiac hypertrophy, Am. J. Physiol. Heart Circ. Physiol. 291 (2006) H1545–H1553.
[27] D. D'Amours, S. Desnoyers, I. D'silva, G.G. Poirier, Poly(ADP-ribosyl)ation reactions in the regulation of nuclear functions, Biochem. J. 342 (1999) 249–268.
[28] S.L. Oei, Y. Shi, Poly (ADP-ribosyl)ation of transcription factor Y in Yang 1 under conditions of DNA damage, Biochem. Biophys. Res. Commun. 285 (2001) 27–31.
[29] E. Kun, E. Kirsten, C.P. Ordahl, Coenzymatic activity of randomly broken or intact double-stranded DNAs in auto and histone H1 trans-poly(ADP-ribosylation), catalyzed by poly(ADP-ribose) polymerase (PARP I), J. Biol. Chem. 277 (2002) 39066–39069.
[30] M.Y. Kim, T. Zhang, W.L. Kraus, Poly(ADP-ribosyl)ation by PARP-1: 'PARlaying' NAD^+ into a nuclear signal, Genes Dev. 19 (2005) 1951–1967.
[31] T. Zhang, J.G. Berrocal, J. Yao, M.E. DuMond, R. Krishnakumar, D.D. Ruhl, Regulation of poly(ADP-ribose) polymerase-1-dependent gene expression through promoter-directed recruitment of a nuclear NAD^+ synthase, J. Biol. Chem. 287 (2012) 12405–12416.
[32] V. Schreiber, J.C. Ame, P. Dolle, I. Schultz, B. Rinaldi, V. Fraulob, Poly(ADP-ribose) polymerase-2 (PARP-2) is required for efficient base excision DNA repair in association with PARP-1 and XRCC1, J. Biol. Chem. 277 (2002) 23028–23036.
[33] E. Pion, G.M. Ullmann, J.C. Ame, D. Gerard, G. de Murcia, E. Bombarda, DNA-induced dimerization of poly(ADP-ribose) polymerase-1 triggers its activation, Biochemistry 44 (2005) 14670–14681.
[34] J.M. Dawicki-McKenna, M.F. Langelier, J.E. DeNizio, A.A. Riccio, C.D. Cao, K.R. Karch, et al., PARP-1 activation requires local unfolding of an autoinhibitory domain, Mol. Cell 60 (2015) 755–768.
[35] A. Pinnola, N. Naumova, M. Shah, A.V. Tulin, Nucleosomal core histones mediate dynamic regulation of poly(ADP-ribose) polymerase 1 protein binding to chromatin and induction of its enzymatic activity, J. Biol. Chem. 282 (2007) 32511–32519.
[36] T.M. Kauppinen, W.Y. Chan, S.W. Suh, A.K. Wiggins, E.J. Huang, R.A. Swanson, Direct phosphorylation and regulation of poly(ADP-ribose) polymerase-1 by extracellular signal regulated kinases ½, Proc. Natl. Acad. Sci. U. S. A. 103 (2006) 7136–7141.
[37] M. Cohen-Armon, L. Visochek, D. Rozensal, A. Kalal, I. Geistrikh, R. Klein, et al., DNA-independent PARP-1 activation by phosphorylated ERK2 increases Elk1 activity: a link to histone acetylation, Mol. Cell 25 (2007) 297–308.
[38] B. Ju, D. Solum, E.J. Song, K. Lee, D.W. Rose, C.K. Glass, et al., Activating the PARP-1 sensor component of the Groucho/TLE1 corepressor complex mediates a CaMKinase IIdelta-dependent neurogenic gene activation pathway, Cell 119 (2004) 815–829.
[39] P.O. Hassa, S.S. Haenni, C. Buerki, N.I. Meier, W.S. Lane, H. Owen, Acetylation of poly(ADP-ribose) polymerase-1 by p300/CREB-binding protein regulates coactivation of NF-kappaB-dependent transcription, J. Biol. Chem. 280 (2005) 40450–40464.
[40] A. Tulin, A. Spradling, Chromatin loosening by poly(ADP-ribose) polymerase (PARP) at Drosophila Puff Loci, Science 299 (2003) 560–562.
[41] S.J. Petesch, J.T. Lis, Rapid, transcription-independent loss of nucleosomes over a large chromatin domain at Hsp70 loci, Cell 134 (2008) 74–84.
[42] S.J. Petesch, J.T. Lis, Activator-induced spread of poly (ADP-ribose) polymerase promotes nucleosome loss at Hsp70, Mol. Cell 45 (2012) 64–74.
[43] Z. Mao, C. Hine, X. Tian, M. Van Meter, M. Au, A. Vaidya, et al., SIRT6 promotes DNA repair under stress by activating PARP-1, Science 332 (2011) 1443–1446.
[44] U. Kolthur-Seetharam, F. Dantzer, M.W. McBurney, G. de Murcia, P. Sassone-Corsi, Control of AIF-mediated cell death by the functional interplay of SIRT1 and PARP-1 in response to DNA damage, Cell Cycle. 5 (2006) 873–877.
[45] W.L. Kraus, J.T. Lis, PARP goes transcription, Cell 113 (2003) 677–683.
[46] I. Rouleau, J. Chiquette, M. Plante, J. Simard, M. Dorval, Changes in health-related behaviours following BRCA 1/2 genetic testing: the case of hormone replacement therapy, J. Obstet. Gynaecol. Can. 26 (2004) 1059–1066.
[47] C. Cantó, K.J. Menzies, J. Auwerx, NAD+ metabolism and the control of energy homeostasis: a balancing act between mitochondria and the nucleus, Cell Metab. 22 (2015) 31–53.
[48] L.I. Gomez Acuna, A. Fiszbein, M. Allo, I.E. Schor, A.R. Kornblihtt, Connections between chromatin signatures and splicing, Wiley Interdiscip. Rev. RNA 4 (2013) 77–91.
[49] R. Krishnakumar, W.L. Kraus, PARP-1 regulates chromatin structure and transcription through a KDM5B-dependent pathway, Mol. Cell 39 (2010) 736–749.
[50] A.J. Gottschalk, G. Timinszky, S.E. Kong, J. Jin, Y. Cai, S.K. Swanson, et al., Poly(ADP-ribosyl)ation directs recruitment and activation of an ATP-dependent chromatin remodeler, Proc. Natl. Acad. Sci. U. S. A. 106 (2009) 13770–13774.
[51] G. Timinszky, S. Till, P.O. Hassa, M. Hothorn, G. Kustatscher, B. Nijmeijer, et al., A macrodomain-containing histone rearranges chromatin upon sensing PARP1 activation, Nat. Struct. Mol. Biol. 16 (2009) 923–929.
[52] R. Krishnakumar, M.J. Gamble, K.M. Frizzell, J.G. Berrocal, M. Kininis, W.L. Kraus, Reciprocal binding of PARP-1 and histone H1 at promoters specifies transcriptional outcomes, Science 319 (2008) 819–821.
[53] D.A. Nusinow, I. Hernández-Muñoz, T.G. Fazzio, G.M. Shah, W.L. Kraus, B. Panning, Poly(ADP-ribose) Polymerase 1 is inhibited by a histone H2A variant MacroH2A, and contributes to silencing of the inactive X chromosome, J. Biol. Chem. 282 (2007) 12851–12859.
[54] E. Kotova, N. Lodhi, M. Jarnik, A.D. Pinnola, Y. Ji, A.V. Tulin, Drosophila histone H2A variant (H2Av) controls poly (ADP-ribose) polymerase1 (PARP1) activation in chromatin, Proc. Nat. Acad. Sci. U. S. A. 108 (2011) 6205–6210.
[55] C.J. Thomas, E. Kotova, M. Andrake, J. Adolf-Bryfogle, R. Glaser, C. Regnard, et al., Kinase-mediated changes in nucleosome conformation trigger chromatin decondensation via poly (ADP-ribosyl) ation, Mol. Cell 53 (2014) 831–842.
[56] G. Smeenk, W.W. Wiegant, J.A. Marteijn, M.S. Luijsterburg, N. Sroczynski, T. Costelloe, et al., Poly(ADP-ribosyl)ation links the chromatin remodeler SMARCA5/SNF2H to RNF168-dependent DNA damage signalling, J. Cell Sci. 126 (2013) 889–903.

[57] M.L. Meyer-Ficca, J. Lonchar, C. Credidio, M. Ihara, Y. Li, Z.Q. Wang, et al., Disruption of poly(ADP-ribose) homeostasis affects spermiogenesis and sperm chromatin integrity in mice, Biol. Reprod. 81 (2009) 46–55.
[58] M.L. Meyer-Ficca, H. Scherthan, A. Burkle, R.G. Meyer, Poly(ADPribosyl)ation during chromatin remodeling steps in rat spermiogenesis, Chromosoma 114 (2005) 67–74.
[59] M.L. Meyer-Ficca, M. Ihara, J.D. Lonchar, M.L. Meistrich, C.A. Austin, W. Min, et al., Poly(ADP-ribose) metabolism is essential for proper nucleoprotein exchange during mouse spermiogenesis, Biol. Reprod. 84 (2011) 218–228.
[60] U.M. Muthurajan, M.R. Hepler, A.R. Hieb, N.J. Clark, M. Kramer, T. Yao, et al., Automodification switches PARP-1 function from chromatin architectural protein to histone chaperone, Proc. Natl. Acad. Sci. U. S. A. 111 (2014) 12752–12757.
[61] N.J. Clark, M. Kramer, U.M. Muthurajan, K. Luger, Alternative modes of binding of poly(ADP-ribose) polymerase 1 to free DNA and nucleosomes, J. Biol. Chem. 287 (2012) 32430–32439.
[62] M.Y. Kim, S. Mauro, N. Gévry, J.T. Lis, W.L. Kraus, NAD+-dependent modulation of chromatin structure and transcription by nucleosome binding properties of PARP-1, Cell 119 (2004) 803–814.
[63] R. Martinez-Zamudio, H.C. Ha, Histone ADP-Ribosylation facilitates gene transcription by directly remodeling nucleosomes, Mol. Cell. Biol. 32 (2012) 2490–2502.
[64] L. Izhar, B. Adamson, A. Ciccia, J. Lewis, L. Pontano-Vaites, Y. Leng, et al., A systematic analysis of factors localized to damaged chromatin reveals PARP-dependent recruitment of transcription factors, Cell Rep. 11 (2015) 1486–1500.
[65] A. Castello, B. Fischer, K. Eichelbaum, R. Horos, B.M. Beckmann, C. Strein, et al., Insights into RNA biology from an atlas of mammalian mRNA-binding proteins, Cell 149 (2012) 1393–1406.
[66] D.C. Di Giammartino, Y. Shi, J.L. Manley, PARP1 represses PAP and inhibits polyadenylation during heat shock, Mol. Cell 49 (2013) 7–17.
[67] E. Matveeva, J. Maiorano, Q. Zhang, A.M. Eteleeb, P. Convertini, J. Chen, et al., Involvement of PARP1 in the regulation of alternative splicing, Cell Discov. 2 (2015) 15046, http://dx.doi.org/10.1038/celldisc.2015.46.
[68] Y. Ji, A.V. Tulin, Poly(ADP-ribosyl)ation of heterogeneous nuclear ribonucleoproteins modulates splicing, Nucleic Acids Res. 37 (2009) 3501–3513.
[69] Y. Ji, A.V. Tulin, Post-transcriptional regulation by poly(ADP-ribosyl)ation of the RNA-binding proteins, Int. J. Mol. Sci. 14 (2013) 16168–16183.
[70] G.E. Morris, The Cajal body, Biochim. Biophys. Acta 1783 (2008) 2108–2115.
[71] M. Malanga, A. Czubaty, A. Girstun, K. Staron, F.R. Althaus, Poly(ADP-ribose) binds to the splicing factor ASF/SF2 and regulates its phosphorylation by DNA topoisomerase I, J. Biol. Chem. 283 (2008) 19991–19998.
[72] K.M. Frizzell, M.J. Gamble, J.G. Berrocal, T. Zhang, R. Krishnakumar, Y. Cen, Global analysis of transcriptional regulation by poly (ADP-ribose) polymerase-1 and poly (ADP-ribose) glycohydrolase in MCF-7 human breast cancer cells, J. Biol. Chem. 284 (2009) 33926–33938.
[73] T. Wu, X.J. Wang, W. Tian, M.C. Jaramillo, A. Lau, D.D. Zhang, Poly(ADP-ribose) polymerase-1 modulates Nrf2-dependent transcription, Free Radic. Biol. Med. 67 (2014) 69–80.
[74] L. Visochek, G. Grigoryan, A. Kalal, H. Milshtein-Parush, N. Gazit, I. Slutsky, et al., A PARP1-ERK2 synergism is required for the induction of LTP, Sci. Rep. 6 (2016) 24950.
[75] E. Kotova, M. Jarnik, A.V. Tulin, Uncoupling of the transactivation and transrepression functions of PARP1 protein, Proc. Natl. Acad. Sci. U. S. A. 107 (2010) 6406–6411.
[76] H. Peng, Q. Zhu, S. Zhong, D. Levy, Transcription of the human microsomal epoxide hydrolase gene (EPHX1) is regulated by PARP-1 and Histone H1.2. Association with sodium-dependent bile acid transport, PLoS One 10 (2015) e0125318.
[77] K.A. Martin, M. Cesaroni, M.F. Denny, L.N. Lupey, I. Tempera, Global transcriptome analysis reveals that Poly(ADP-Ribose) Polymerase 1 regulates gene expression through EZH2, Mol. Cell. Biol. 35 (2015) 3934–3944.
[78] C. Guetg, F. Scheifele, F. Rosenthal, M.O. Hottiger, R. Santoro, Inheritance of silent rDNA chromatin is mediated by PARP1 via noncoding RNA, Mol. Cell 45 (2012) 790–800.
[79] P. Caiafa, T. Guastafierro, M. Zampieri, Epigenetics: poly(ADP-ribosyl)ation of PARP-1 regulates genomic methylation patterns, FASEB J. 23 (2009) 672–678.
[80] P. Caiafa, J. Zlatanova, CCCTC-binding factor meets poly(ADP-ribose) polymerase-1, J. Cell. Physiol. 219 (2009) 265–270.
[81] A. Reale, G.D. Matteis, G. Galleazzi, M. Zampieri, P. Caiafa, Modulation of DNMT1 activity by ADP-ribose polymers, Oncogene 24 (2005) 13–19.
[82] C.A. Doege, K. Inoue, T. Yamashita, R.B. David, S. Travis, R. Fujita, et al., Early-stage epigenetic modification during somatic cell reprogramming by PARP-1 and Tet2, Nature 488 (2012) 652–655.
[83] R. Krishnakumar, W.L. Kraus, The PARP side of the nucleus: Molecular actions, physiological outcomes, and clinical targets, Mol. Cell 39 (2010) 8–24.
[84] M. Zampieri, T. Guastafierro, R. Calabrese, F. Ciccarone, M.G. Bacalini, A. Reale, et al., ADP-ribose polymers localized on Ctcf–Parp1–Dnmt1 complex prevent methylation of Ctcf target sites, Biochem. J. 441 (2012) 645–652.
[85] T. Guastafierro, A. Catizone, R. Calabrese, M. Zampieri, O. Martella, M.G. Bacalini, et al., ADP-ribose polymer depletion leads to nuclear Ctcf re-localization and chromatin rearrangement, Biochem. J. 449 (2013) 623–630.
[86] J.M. De Murcia, M. Ricoul, L. Tartier, C. Niedergang, A. Huber, F. Dantzer, et al., Functional interaction between PARP-1 and PARP-2 in chromosome stability and embryonic development in mouse, EMBO J. 22 (2003) 2255–2263.
[87] J. Ménisser-de Murcia, M. Mark, O. Wendling, A. Wynshaw-Boris, G. de Murcia, Early embryonic lethality in PARP-1 Atm double-mutant mice suggests a functional synergy in cell proliferation during development, Mol. Cell. Biol. 21 (2001) 1828–1832.
[88] M.S. Henrie, A. Kurimasa, S. Burma, J. Ménissier-de Murcia, G. de Murcia, G.C. Li, et al., Lethality in PARP-1/Ku80 double mutant mice reveals physiological synergy during early embryogenesis, DNA Repair (Amst.) 2 (2003) 151–158.
[89] M. Peifer, P. Polakis, Wnt signaling in oncogenesis and embryogenesis-a look outside the nucleus, Science 287 (2000) 1606–1609.
[90] M. Idogawa, T. Yamada, K. Honda, S. Sato, K. Imai, S. Hirohashi, Poly(ADP-ribose) polymerase-1 is a component of the oncogenic T-cell factor-4/h-catenin complex, Gastroenterology 128 (2005) 1919–1936.
[91] M. Idogawa, M. Masutani, M. Shitashige, K. Honda, T. Tokino, Y. Shinomura, et al., Ku70 and poly(ADP-Ribose) polymerase-1 competitively regulate B-catenin and T-cell factor-4-mediated gene transactivation: possible linkage of DNA damage recognition and Wnt signaling, Cancer Res. 67 (2007) 911–918.
[92] I. Tapia-Páez, K. Tammimies, S. Massinen, A.L. Roy, J. Kere, The complex of TFII-I, PARP1 and SFPQ proteins regulates the DYX1C1 gene implicated in neuronal migration and dyslexia, FASEB J. 22 (2008) 3001–3009.
[93] Y. Ji, A.V. Tulin, The roles of PARP1 in gene control and cell differentiation, Curr. Opin. Genet. Dev. 20 (2010) 512–518.
[94] B. Ewen-Campen, E.E. Schwager, C.G. Extavour, The molecular machinery of germ line specification, Mol. Reprod. Dev. 77 (2010) 3–18.
[95] H. Qian, J. Xu, M.D. Lalioti, K. Gulle, D. Sakkas, Oocyte numbers In the mouse increase after treatment with 5-minoisoquinolinone: a potent inhibitor of poly[ADP-ribosyl]ation, Biol. Reprod. 82 (2010) 1000–1007.
[96] C.M. Simbulan-Rosenthal, D.S. Rosenthal, R. Luo, M.E. Smulson, Poly(ADP-ribose) polymerase up regulates E2F-1 promoter activity and DNA pol alpha expression during early s phase, Oncogene 18 (1999) 5015–5023.
[97] T. Nozaki, H. Fujihara, N. Kamada, O. Ueda, T. Takato, H. Nakagama, et al., Hyperploidy of embryonic fibroblasts derived from Parp-1 knockout mouse, Proc. Jpn. Acad. Ser. B 77 (2001) 121–124.
[98] F. Yang, C. Baumann, R. De La Fuente, Persistence of histone H2AX phosphorylation after meiotic chromosome synapsis and abnormal centromere cohesion in poly (ADP-ribose) polymerase (Parp-1) null oocytes, Dev. Biol. 331 (2009) 326–338.
[99] F. Dantzer, M. Mark, D. Quenet, H. Scherthan, A. Huber, B. Liebe, et al., Poly(ADP-ribose) polymerase-2 contributes to the fidelity of male meiosis I and spermiogenesis, Proc. Natl. Acad. Sci. U. S. A. 103 (2006) 14854–14859.
[100] L. Shan, X. Li, L. Liu, X. Ding, Q. Wang, Y. Zheng, et al., GATA3 cooperates with PARP1 to regulate CCND1 transcription through modulating histone H1 incorporation, Oncogene 33 (2014) 3205–3216.
[101] H.C. Ha, L.D. Hester, S.H. Snyder, Poly[ADP-ribose] polymerase-1 dependence of stress-induced transcription factors and associated gene expression in glia, Proc. Natl. Acad. Sci. U. S. A 99 (2002) 3270–3275.
[102] M. Yamada, T. Shimada, M. Nakayasu, H. Okada, T. Sugimura, Induction of differentiation of mouse myeloid leukemia cells by poly(ADP-ribose), Biochem. Biophys. Res. Commun. 83 (1978) 1325–1332.
[103] M. Lehmann, E. Pirinen, A. Mirsaidi, F.A. Kunze, P.J. Richards, J. Auwerx, M.O. Hottiger, ARTD1-induced poly-ADP-ribose formation enhances PPARγ ligand binding and co-factor exchange, Nucleic Acids Res. 43 (2015) 129–142.
[104] Y.D. Yoo, C.T. Huang, X. Zhang, T.M. Lavaute, S. Zhang, Fibroblast growth factor regulates human neuroectoderm specification through Erk1/2-Parp-1 pathway, Stem Cells 29 (2011) 1975–1982.
[105] C. Robaszkiewicz, E. Qu, T. Wisnik, A. Ploszaj, A. Mirsaidi, F.A. Kunze, et al., ARTD1 regulates osteoclastogenesis and bone homeostasis by dampening NF-κB-dependent transcription of IL-1β, Sci. Rep. 6 (2016) 21131.
[106] P. Lonn, L.P. van der Heide, M. Dahl, U. Hellman, C.H. Heldin, A. Moustakas, PARP-1 attenuates smad-mediated transcription, Mol. Cell 40 (2010) 521–532.
[107] D. Huang, Y. Wang, L. Wang, F. Zhang, S. Deng, R. Wang, et al., Poly[ADP-ribose] polymerase 1 is indispensable for transforming growth factor-b induced smad3 activation in vascular smooth muscle cell, PLoS One 6 (2011) e27123.
[108] M. Dahl, V. Maturi, P. Lönn, P. Papoutsoglou, A. Zieba, M. Vanlandewijck, et al., Fine-tuning of smad protein function by poly[ADP-Ribose] polymerases and poly[ADPRibose] glycohydrolase during transforming growth factor b signaling, PLoS One 9 (2014) e103651.
[109] P. Zhang, H. Nakatsukasa, E. Tu, S. Kasagi, K. Cui, M. Ishikawa, et al., PARP-1 regulates expression of TGF-β receptors in T cells, Blood 122 (2013) 2224–2232.
[110] S. Erener, A. Mirsaidi, M. Hesse, A.N. Tiaden, H. Ellingsgaard, R. Kostadinova, et al., ARTD1 deletion causes increased hepatic lipid accumulation in mice fed a high-fat diet and impairs adipocyte function and differentiation, FASEB J. 26 (2012) 2631–2638.
[111] S. Erener, M. Hesse, R. Kostadinova, M.O. Hottiger, Poly(ADP-ribose)polymerase-1 (PARP1) controls adipogenic gene expression and adipocyte function, Mol. Endocrinol. 26 (2012) 79–86.

[112] A. Gonzalez-Flores, R. Aguilar-Quesada, E. Siles, S. Pozo, M.I. Rodriguez-Lara, L. López-Jiménez, F.J. Oliver, Interaction between PARP-1 and HIF-2α in the hypoxic response, Oncogene 33 (2014) 891–898.
[113] R. Pavri, B. Lewis, T. Kim, F.J. Dilworth, H. Erdjument-Bromage, P. Tempst, et al., PARP-1 determines specificity in a retinoid signaling pathway via direct modulation of mediator, Mol. Cell 18 (2005) 83–96.
[114] Y. Zhang, S. Liu, C. Mickanin, Y. Feng, O. Charlat, G.A. Michaud, et al., RNF146 is a poly[ADP-ribose]-directed E3 ligase that regulates axin degradation and Wnt signalling, Nat. Cell. Biol. 13 (2011) 623–629.
[115] F. Gao, S.W. Kwon, Y. Zhao, Y. Jin, PARP-1 poly[ADP-ribosyl]ates sox2 to control sox2 protein levels and FGF4 expression during embryonic stem cell differentiation, J. Biol. Chem. 284 (2009) 22263–22273.
[116] J. Rajawat, H. Mir, R. Begum, Differential role of poly(ADP-ribose) polymerase (PARP) in *D. discoideum*, BMC Dev. Biol. 11 (2011) 14.
[117] T. Jubin, A. Kadam, M. Jariwala, S. Bhatt, S. Sutariya, A.R. Gani, et al., The PARP family: insights into the functional aspects of Poly (ADP-ribose) polymerase-1 in cellular growth and survival, Cell Prolif. (2016), http://dx.doi.org/10.1111/cpr.12268.
[118] K.B. Raper, The Dictyostelids, Princeton University Press, Princeton, New Jersey, 1984, pp. 1–453.
[119] A.M. Kawal, H. Mir, C.K. Ramniklal, J. Rajawat, R. Begum, Structural and evolutionary analysis of PARPs in *D. discoideum*, Am. J. Infect. Dis. 7 (2011) 67–74.
[120] J. Rajawat, I. Vohra, H. Mir, D. Gohel, R. Begum, Effect of oxidative stress and involvement of poly(ADP-ribose) polymerase (PARP) in *Dictyostelium discoideum* development, FEBS J. 274 (2007) 5611–5618.
[121] J. Rajawat, T. Alex, H. Mir, A. Kadam, R. Begum, Proteases involved during oxidative stress induced poly(ADP-ribose) polymerase mediated cell death in *D. discoideum*, Microbiology 160 (2014) 1101–1111.
[122] J. Rajawat, H. Mir, T. Alex, S. Bakshi, R. Begum, Involvement of poly(ADP-ribose) polymerase in paraptotic cell death of *D. discoideum*, Apoptosis 19 (2014) 90–101.
[123] H. Mir, T. Alex, J. Rajawat, A. Kadam, R. Begum, Response of *D. discoideum* to UV-C and involvement of poly(ADP-ribose) polymerase, Cell Prolif. 48 (2015) 363–374.
[124] C.A. Couto, H.Y. Wang, J.C. Green, R. Kiely, R. Siddaway, C. Borer, et al., PARP regulates nonhomologous end joining through retention of Ku at double-strand breaks, J. Cell Biol. 194 (2011) 367–375.
[125] H. Mir, J. Rajawat, R. Begum, Staurosporine induced cell death in *D. discoideum* is independent of PARP, Indian J. Exp. Biol. 50 (2012) 80–86.
[126] T. Jubin, A. Kadam, S. Saran, R. Begum, Poly (ADP-ribose) polymerase1 regulates growth and multicellularity in *D. discoideum*, Differentiation (2016), http://dx.doi.org/10.1016/j.diff.2016.03.002, pii: S0301-4681(15)30081-5.
[127] S. Beneke, A. Burkle, Poly(ADP-ribosyl)ation, PARP and aging, Sci. Aging Knowledge Environ. 49 (2004) res9.
[128] C.P. Semighini, M. Savoldi, G.H. Goldman, S.D. Harris, Functional characterization of the putative Aspergillus nidulans poly(ADP-ribose) polymerase homolog PrpA, Genetics 173 (2006) 87–98.
[129] M. Müller-Ohldach, D. Brust, A. Hamann, H.D. Osiewacz, Overexpression of PaParp encoding the poly(ADP-ribose) polymerase of Podospora anserina affects organismal aging, Mech. Ageing Dev. 132 (2011) 33–42.
[130] G.O. Kothe, M. Kitamura, M. Masutani, E.U. Selker, H. Inoue, PARP is involved in replicative aging in *Neurospora crassa*, Fungal Genet. Biol. 47 (2010) 297–309.
[131] R.S. Lamb, M. Citarelli, S. Teotia, Functions of the poly [ADP-ribose] polymerase superfamily in plants, Cell. Mol. Life Sci. 69 (2012) 175–189.
[132] C. Becerra, P. Puigdomenech, C.M. Vicient, Computational and experimental analysis identifies Arabidopsis genes specifically expressed during early seed development, BMC Genomics 7 (2006) 38.
[133] M. De Block, C. Verduyn, D. De Brouwer, M. Cornelissen, Poly(ADP-ribose) polymerase in plants affects energy homeostasis, cell death and stress tolerance, Plant J. 41 (2005) 95–106.
[134] S. Vanderauwera, M. De Block, N. Van de Steene, B. van de Cotte, M. Metzlaff, F. Van Breusegem, Silencing of poly[ADPribose] polymerase in plants alters abiotic stress signal transduction, Proc. Natl. Acad. Sci. U. S. A. 104 (2007) 15150–15155.
[135] E. Kotova, M. Jarnik, A.V. Tulin, Poly (ADP-ribose) polymerase 1 is required for protein localization to Cajal body, PLoS Genet. 5 (2009) e1000387.
[136] S. Hanai, M. Uchida, S. Kobayashi, M. Miwa, K. Uchida, Genomic organization of Drosophila poly(ADP-ribose) polymerase and distribution of its mRNA during development, J. Biol. Chem. 273 (1998) 11881–11886.
[137] M. Uchida, S. Hanai, N. Uematsu, K. Sawamoto, H. Okano, M. Miwa, et al., Overexpression of poly(ADP-ribose) polymerase disrupts organization of cytoskeletal F-actin and tissue polarity in Drosophila, J. Biol. Chem. 277 (2002) 6696–6702.
[138] M.N. Cervellera, A. Sala, Poly(ADP-ribose) polymerase is a B-MYB coactivator, J. Biol. Chem. 275 (2000) 10692–10696.
[139] M. Miwa, S. Hanai, P. Poltronieri, M. Uchida, K. Uchida, Functional analysis of poly(ADP-ribose)polymerase in *Drosophila melanogaster*, Mol. Cell. Biochem. 193 (1999) 103–108.
[140] A. Tulin, D. Stewart, A.C. Spradling, The Drosophila heterochromatic gene encoding poly [ADP-ribose] polymerase [PARP] is required to modulate chromatin structure during development, Genes Dev. 16 (2002) 2108–2119.
[141] J.C. Fletcher, K.C. Burtis, D.S. Hogness, C.S. Thummel, The Drosophila E74 gene is required for metamorphosis and plays a role in the polytene chromosome puffing response to ecdysone, Development 121 (1995) 1455–1465.
[142] A. Huber, P. Bai, J.M. de Murcia, G. de Murcia, PARP-1, PARP-2 and ATM in the DNA damage response: functional synergy in mouse development, DNA Repair 3 (2004) 1103–1108.
[143] C.M. Simbulan-Rosenthal, D.H. Ly, D.S. Rosenthal, G. Konopka, R. Luo, Z.Q. Wang, et al., Misregulation of gene expression in primary fibroblasts lacking poly(ADP-ribose) polymerase, Proc. Natl. Acad. Sci. 97 (2000) 11274–11279.
[144] P. Hajkova, S.J. Jeffries, C. Lee, N. Miller, S.P. Jackson, M.A. Surani, Genome-wide reprogramming in the mouse germ line entails the base excision repair pathway, Science 329 (2010) 78–82.
[145] D. Quénet, V. Gasser, L. Fouillen, F. Cammas, S. Sanglier-Cianferani, R. Losson, et al., The histone subcode: poly (ADP-ribose) polymerase-1 (Parp-1) and Parp-2 control cell differentiation by regulating the transcriptional intermediary factor TIF1β and the heterochromatin protein HP1α, FASEB J. 22 (2008) 3853–3865.
[146] X. Zhou, D. Patel, S. Sen, V. Shanmugam, A. Sidawy, L. Mishra, B.N. Nguyen, Poly-ADP-ribose polymerase inhibition enhances ischemic and diabetic wound healing by promoting angiogenesis, J. Vasc. Surg. (2016), http://dx.doi.org/10.1016/j.jvs.2016.03.407, pii: S0741-5214(16)00820-X.
[147] S. Hauschildt, P. Scheipers, W. Bessler, K. Schwarz, A. Ullmer, H.D. Flad, et al., Role of ADP-ribosylation in activated monocytes/macrophages, Adv. Exp. Med. Biol. 419 (1997) 249–252.
[148] C. Szabo, L.H. Lim, S. Cuzzocrea, S.J. Getting, B. Zingarelli, R.J. Flower, et al., Inhibition of poly (ADP-ribose) synthetase attenuates neutrophil recruitment and exerts antiinflammatory effects, J. Exp. Med. 186 (1997) 1041–1049.
[149] M.F. Farez, F.J. Quintana, R. Gandhi, G. Izquierdo, M. Lucas, H.L. Weiner, Toll-like receptor 2 and poly(ADP-ribose) polymerase 1 promote central nervous system neuroinflammation in progressive EAE, Nat. Immunol. 10 (2009) 958–964.
[150] F. Laudisi, M. Sambucci, C. Pioli, Poly (ADP-ribose) polymerase-1 (PARP-1) as immune regulator, Endocr. Metab. Immune Disord. Drug Targets 11 (2011) 326–333.
[151] L. Saenz, J.J. Lozano, R. Valdor, A. Baroja-Mazo, P. Ramirez, P. Parrilla, et al., Transcriptional regulation by poly(ADP-ribose) polymerase-1 during T cell activation, BMC Genomics 9 (2008) 171.
[152] F. Nasta, F. Laudisi, M. Sambucci, M.M. Rosado, C. Pioli, Increased Foxp3$^+$ regulatory T cells in poly(ADP-ribose) polymerase-1 deficiency, J. Immunol. 184 (2010) 3470–3477.
[153] M. Sambucci, F. Laudisi, F. Novelli, E. Bennici, M.M. Rosado, C. Pioli, Effects of PARP-1 deficiency on Th1 and Th2 cell differentiation, Sci. World J. (2013) 375024.
[154] H.E. Ambrose, V. Papadopoulou, R.W. Beswick, S.D. Wagner, Poly-(ADP-ribose) polymerase-1 (Parp-1) binds in a sequence-specific manner at the Bcl-6 locus and contributes to the regulation of Bcl-6 transcription, Oncogene 26 (2007) 6244–6252.
[155] M. Stilmann, M. Hinz, S.C. Arslan, A. Zimmer, V. Schreiber, C. Scheidereit, A nuclear poly(ADP-ribose)-dependent signalosome confers DNA damage-induced IκB kinase activation, Mol. Cell 36 (2009) 365–378.
[156] J.J. Lasola, A. Hodgson, X. Sun, F. Wan, The PARP1/ARTD1-mediated poly-ADP-ribosylation and DNA damage repair in B cell diversification, Antibodies 3 (2014) 37–55.
[157] P. Bai, L. Virág, Role of poly (ADP-ribose) polymerases in the regulation of inflammatory processes, FEBS Lett. 586 (2012) 3771–3777.
[158] M.M. Rosado, E. Bennici, F. Novelli, C. Pioli, Beyond DNA repair: the immunological role of PARP-1 and its siblings, Immunology 139 (2013) 428–437.
[159] S. Garcia, A. Bodano, A. Gonzalez, J. Forteza, J.J. Gomez-Reino, C. Conde, Partial protection against collagen antibody-induced arthritis in PARP-1 deficient mice, Arthritis Res. Ther. 8 (2006) R14.
[160] E. Mazzon, L. Dugo, J.H. Li, R. Di Paola, T. Genovese, A.P. Caputi, J. Zhang, S. Cuzzocrea, GPI 6150 a PARP inhibitor, reduces the colon injury caused by dinitrobenzene sulfonic acid in the rat, Biochem. Pharmacol. 64 (2002) 327–337.
[161] B. Zingarelli, P.W. Hake, T.J. Burroughs, G. Piraino, M. O'Connor, A. Denenberg, Activator protein-1 signalling pathway and apoptosis are modulated by poly(ADP-ribose) polymerase-1 in experimental colitis, Immunology 113 (2004) 509–517.
[162] P. Pacher, C. Szabó, Role of poly(ADP-ribose) polymerase 1 (PARP-1) in cardiovascular diseases: the therapeutic potential of PARP inhibitors, Cardiovasc. Drug. Rev. 25 (2007) 235–260.
[163] F. Moroni, A. Chiarugi, Post-ischemic brain damage: targeting PARP-1 within the ischemic neurovascular units as a realistic avenue to stroke treatment, FEBS J. 276 (2009) 36–45.
[164] E. Gonzalez-Rey, R. Martínez-Romero, F. O'Valle, R. Aguilar-Quesada, C. Conde, M. Delgado, et al., Therapeutic effect of a poly(ADP-ribose) polymerase-1 inhibitor on experimental arthritis by downregulating inflammation and Th1 response, PLoS One 2 (2007) e1071.
[165] H.B. Jijon, T. Churchill, D. Malfair, A. Wessler, L.D. Jewell, H.G. Parsons, et al., Inhibition of poly(ADP-ribose) polymerase attenuates inflammation in a model of chronic colitis, Am. J. Physiol. Gastrointest. Liver Physiol. 279 (2000) G641–651.
[166] B. Zingarelli, M. O'Connor, P.W. Hake, Inhibitors of poly (ADP-ribose) polymerase modulate signal transduction pathways in colitis, Eur. J. Pharmacol. 469 (2003) 183–194.

[167] G.S. Scott, R.B. Kean, T. Mikheeva, M.J. Fabis, J.G. Mabley, C. Szabó, et al., The therapeutic effects of PJ34 [*N*-(6-oxo-5,6-dihydrophenanthridin-2-yl)-*N*,*N*-dimethylacetamide.HCl], a selective inhibitor of poly(ADP-ribose) polymerase, in experimental allergic encephalomyelitis are associated with immunomodulation, J. Pharmacol. Exp. Ther. 310 (2004) 1053–1061.
[168] A. Chiarugi, Inhibitors of poly(ADP-ribose) polymerase-1 suppress transcriptional activation in lymphocytes and ameliorate autoimmune encephalomyelitis in rats, Br. J. Pharmacol. 137 (2002) 761–770.
[169] P.O. Hassa, C. Buerki, C. Lombardi, R. Imhof, M.O. Hottiger, Transcriptional coactivation of nuclear factor-kB dependent gene expression by p300 is regulated by poly(ADP)-ribose polymerase-1, J. Biol. Chem. 278 (2003) 45145–45153.
[170] D. Huang, C.Z. Yang, L. Yao, Y. Wang, Y.H. Liao, K. Huang, Activation and overexpression of PARP-1 in circulating mononuclear cells promote TNF and IL-6 expression in patients with unstable angina, Arch. Med. Res. 39 (2008) 775–784.
[171] O.A. Olabisi, N. Soto-Nieves, E. Nieves, T.T. Yang, X. Yang, R.Y. Yu, et al., Regulation of transcription factor NFAT by ADP-ribosylation, Mol. Cell. Biol. 28 (2008) 2860–2871.
[172] R. Valdor, V. Schreiber, L. Saenz, T. Martínez, A. Muñoz-Suano, M. Dominguez-Villar, P. Ramírez, P. Parrilla, E. Aguado, F. García-Cózar, J. Yélamos, Regulation of NFAT by poly(ADP-ribose) polymerase activity in T cells, Mol. Immunol. 45 (2008) 1863–1871.

Differentiation 92 (2016) 10–23

Contents lists available at ScienceDirect

Differentiation

journal homepage: www.elsevier.com/locate/diff

Poly (ADP-ribose) polymerase1 regulates growth and multicellularity in *D. discoideum*

Tina Jubin [a], Ashlesha Kadam [a], Shweta Saran [b], Rasheedunnisa Begum [a,*]

[a] Department of Biochemistry, Faculty of Science, The Maharaja Sayajirao University of Baroda, Vadodara, Gujarat 390002, India
[b] School of Life Sciences, Jawaharlal Nehru University, New Delhi 110067, India

ARTICLE INFO

Article history:
Received 24 November 2015
Received in revised form
9 March 2016
Accepted 15 March 2016
Available online 26 March 2016

Keywords:
ADPRT1A
Overexpression
Cell cycle
Cell death
Development
D. discoideum

ABSTRACT

Poly (ADP-ribose) polymerase (PARP)-1 regulates various biological processes like DNA repair, cell death etc. However, the role of PARP-1 in growth and differentiation still remains elusive. The present study has been undertaken to understand the role of PARP-1 in growth and development of a unicellular eukaryote, *Dictyostelium discoideum*. *In silico* analysis demonstrates *ADPRT1A* as the ortholog of human PARP-1 in *D. discoideum*. The present study shows that *ADPRT1A* overexpression (A OE) led to slow growth of *D. discoideum* and significant population of AOE cells were in S and G2/M phase. Also, AOE cells exhibited high endogenous PARP activity, significant NAD^+ depletion and also significantly lower ADPRT1B and ADPRT2 transcript levels. Moreover, AOE cells are intrinsically stressed and also exhibited susceptibility to oxidative stress. AOE also affected development of *D. discoideum* predominantly streaming, aggregation and formation of early culminant which are concomitant with reports on PARP's role in *D. discoideum* development. In addition, under developmental stimuli, increased PARP activity was seen along with developmentally regulated transcript levels of *ADPRT1A* during *D. discoideum* multicellularity. Thus the present study suggests that PARP-1 regulates growth as well as the developmental morphogenesis of *D. discoideum*, thereby opening new avenues to understand the same in higher eukaryotes.

1. Introduction

Poly (ADP-ribose) polymerase (PARP)-1 is a multifunctional nuclear protein belonging to the transferase family that catalyzes the formation of both linear and branched poly ADP-ribose polymers (PAR) on target proteins by utilizing NAD^+ as its substrate (Ame et al., 2004). In higher eukaryotes, PARylation is reversible through the action of PAR glycohydrolases (PARG) (Uchida et al., 1993). Poly (ADP-ribosyl) ation is a widely used post translational modification in eukaryotes and the presence of PARPs has been reported in all major eukaryotic groups (Citarelli et al., 2010; Perina et al., 2014). PARP-1 and PARylation impacts a variety of biological processes like DNA repair, transcriptional regulation, cell growth, differentiation and programmed cell death (Hottiger et al., 2010; Messner and Hottiger, 2011; Quenet et al., 2009; Mir et al., 2012). PARP-1 influences ~60–70% of genes controlling important processes like cell cycle and transcription (Chaitanya et al., 2010). The role of PARP-1 is majorly identified as NAD^+ dependent modifying enzyme that mediates important steps in DNA damage response, transcription etc., however, its role during development and differentiation is yet to be fully understood. PARP homologs have been identified in plants, metazoans, protists and filamentous fungi with the notable exception of unicellular fungi, *Saccharomyces cerevisiae* and *Schizosaccharomyces pombe* (Citarelli et al., 2010).There are a few reports suggesting that PARP-1 regulates critical gene transcription and cellular events during development. Regulated expression of prpA (PARP ortholog) was reported for *Aspergillus nidulans* asexual development (Semighini et al., 2006). Although, PARP-1 is constitutively expressed, its enzyme activity is also reported to be developmentally regulated (Ji and Tulin, 2010). Moreover, regulated expression of PARP was found to be essential for conidiospore development (Semighini et al., 2006). Also maximum accumulation of pADPr was observed at the pre-pupal stage of Drosophila development (Kotova et al., 2009). Thus the absence of PARP in unicellular eukaryote, yeast and above reports on essentiality of PARP for development connotes plausible role of PARP in multicellularity and development.

Dictyostelium discoideum is the simplest studied eukaryote that exhibits multicellularity (Raper, 1984) and it has eight potential *parp* genes (Kawal et al., 2011). As per studies from our lab and Couto et al. (2013); out of the eight isoforms, three are reported to

* Corresponding author.
E-mail addresses: alex.tina1901@gmail.com (T. Jubin), ashleshakadam@rediffmail.com (A. Kadam), ssaran@mail.jnu.ac.in (S. Saran), rasheedunnisab@yahoo.co.in (R. Begum).

http://dx.doi.org/10.1016/j.diff.2016.03.002
Join the International Society for Differentiation (www.isdifferentiation.org)
0301-4681/

be active (Rajawat et al., 2011; Couto et al., 2013). However, all eight isoforms show structural features for poly ADP-ribosylation but no studies show presence of mono ADP-ribosyltransferase activity (Fey et al., 2004; Citarelli et al., 2010). *D. discoideum,* being at the transition point from unicellular to multicellular forms, offers to be an excellent model system to study the role of PARP in growth and multicellular development. We have investigated the role of PARP in stress induced cell death in *D. discoideum* (Rajawat et al., 2007). We have also showed PARP's role in *D. discoideum* development by inhibiting its basal PARP activity with Benzamide (PARP inhibitor), delayed development was observed. We have also demonstrated that constitutive *parp* down-regulation did not affect the growth of *D. discoideum,* nevertheless its development was found to be blocked at initial aggregation stage (Rajawat et al., 2011). Delayed development due to UV-C stress was also found to be rescued in *D. discoideum* via PARP inhibitor (Mir et al., 2015). Thus, our reports suggest that PARP plays an important role in *D. discoideum* development and cell death. We are interested to further explore the role of PARP-1 in *D. discoideum* growth and development.

In the present study, we have analyzed the role of PARP-1 ortholog viz., *ADPRT1A* in growth and development of *D. discoideum. In silico* analysis of *ADPRT1A* showed that it possesses all major domains that define PARP-1. Our results substantiate that *ADPRT1A* is essential for the growth of *D. discoideum* and its regulated expression is essential for the proper cellular metabolism. We have also demonstrated *ADPRT1A* activity during *D. discoideum* development and substantiate its role in multicellularity.

2. Materials and methods

2.1. D. discoideum culturing

D. discoideum (Ax-2 strain) cells were grown in HL5 medium, pH 6.5 with 150 rpm shaking at 22 °C and also maintained on nutrient agar with *Klebsiella aerogenes* and harvested using standard procedures (Watts and Ashworth, 1970). All the experiments were carried out with the *D. discoideum* cells at mid-log phase at a cell density of 2×10^6 cells/ml with $>$ 95% viability (tested with Trypan blue exclusion).

2.2. Sequence similarity, domain and phylogenetic analysis

The *ADPRT1A* protein was aligned by Clustal W. The aligned sequences were analyzed by the maximum likelihood method (Dereeper et al., 2008). The treefile was constructed by TreeView. Domain analyses were done using Pfam and Prosite and the alignment of *ADPRT1A* from *D. discoideum* and similar PARP-1 proteins in other model organisms were made using ClustalW.

2.3. Generation of ADPRT1A overexpression construct

Full length *ADPRT1A* (3046 bp) was amplified from the genomic DNA and cloned in act15/Acg-Eyfp vector using *ADPRT1A* specific primers. Purified PCR product digested with *Sac*I and *BamH*I was inserted in to act15/Acg-Eyfp (Saran and Schaap, 2004) from which the Acg was replaced by *ADPRT1A*. The positive constructs were then transformed into *D discoideum* Ax-2 cells by electroporation and selected till 100 μg/mL G418 and were labeled as *ADPRT1A-Eyfp OE* (AEOE).

A second construct lacking EYFP (as EYFP interferes with FITC tagged antibodies used in our cell death studies) was made by restriction digestion of PCR product and act15/Acg-Eyfp with enzymes *Sac*I and *Xba*I. The positive constructs were then transformed into Ax-2 cells by electroporation and selected till 100 μg/mL of G418 and were labeled as *ADPRT1A OE* (AOE).

2.4. Functional characterization of ADPRT1A overexpression

ADPRT1A overexpression was confirmed by monitoring gene specific expression of *ADPRT1A* by Real time-PCR with *RNLA* as an internal control.

2.4.1. Cellular localization of ADPRT1A

To determine cellular localization of *ADPRT1A*, AEOE (YFP-tagged) was stained with DAPI and images were captured under 63X by Zeiss confocal laser scan fluorescence-inverted microscope (LSM 710; Carl Zeiss). Data are representative image of three independent experiments.

2.4.2. Estimation of NAD^+ levels

Intracellular levels of NAD^+ were determined by enzymatic recycling method by Bernofsky and Swan (1973) using alcohol dehydrogenase to reduce NAD^+ to NADH. NAD^+ levels were estimated at 570 nm and protein concentration was estimated by Lowry method (Lowry et al., 1951).

2.5. Growth profile analysis of ADPRT1A-Eyfp OE and ADPRT1A OE

The growth profile of AEOE and AOE were studied by inoculating mid log phase cells at the density of 0.6×10^6 cells/ml in HL5 medium. Cell viability was checked after every 2 h initially till 12 h and after 12 h interval thereafter. The cell suspension was mixed with trypan blue solution [0.4% (w/v) in Phosphate Buffer] in the ratio of 2:1 and cell count was taken using haemocytometer (Kosta et al., 2001).

Similar growth profile studies were also done in presence of Benzamide, a PARP inhibitor (1 mM) and NAC, an antioxidant (2.5 mM).

2.5.1. Cell cycle analysis

Cell cycle was analyzed by Flow cytometry using Propidium Iodide. Mid log phase cells were fixed with drop wise addition of 70% ethanol and incubation at 4 °C overnight. Fixed cells were resuspended in staining solution (TritonX-100, DNase free RNase and Propidium Iodide) and incubated for 30 min followed by FACS analysis (Chen et al., 2004). Quantification was done by flow cytometry using FACS ARIA III (BD Biosciences) and data were analyzed with FACSDiva software.

2.5.2. Induction of oxidative stress

Oxidative stress was induced in *D. discoideum* cells by exogenous addition of cumene H_2O_2 (Sigma). Log phase cells at a density of $\sim 2.5 \times 10^6$ cells/ml were exposed to paraptotic (0.03 mM) and necrotic (0.05 mM) doses of cumene H_2O_2 as described in (Rajawat et al., 2014) in HL-5 medium at 22 °C in a sterile flask.

2.6. ROS estimation (Degli Esposti, 2002)

In order to observe the formation of reactive oxygen species, a fluorescent dye 2′,7′ dichlorodihydrofluorescein diacetate (H2DCFDA-AM) was used. Oxidation of H2DCFDA by ROS converts the molecule to 2′,7′ dichlorodihydrofluorescein (DCF), which is highly fluorescent. Upon stimulation, the resultant production of ROS causes an increase in fluorescence over time.

2×10^6 cells were harvested and washed with 1X KK2 twice. DCFDA (50 nM) was added to cells and was incubated for 15 min at 22 °C with shaking, followed by two washes with 1X SB. Fluorescence was measured by fluorimeter (F7000, Hitachi, Japan) using 200 μl sample diluted 5 times using KK2 buffer. Excitation (λ_{ex})

and emission (λ_{em}) wavelengths used for fluorimetric studies were 480 and 525 nm respectively.

2.6.1. Monitoring stress induced DNA damage by immunofluorescence (Minami et al., 2005)

Phospho-Histone H2AX (S139) antibody at a concentration of 2 ug/ml (R&D systems) and anti-mouse IgG (whole molecule) TRITC conjugate (Sigma) at a dilution of 1:400 were used to study DNA damage. Cells were pelleted and washed once with phosphate buffered saline (PBS) pH 7.4, fixed in 70% chilled methanol for 10 min at −20 °C and then washed with blocking solution (1.5% BSA with 0.05% Tween 20 in PBS), incubated for 8 h in primary antibody. After incubation the cells were washed 2–3 times with blocking solution and further incubated for 1 h with TRITC labeled secondary antibody. Followed by 2 PBS washes, cells were observed for fluorescence which was monitored under 63X by Zeiss confocal laser scan fluorescence-inverted microscope (LSM 710; Carl Zeiss).

2.7. PARP activation

PARP was assayed by indirect immunofluorescence (Cole and Perez-Polo, 2002) using anti-PAR mouse mAb (10H) (Calbiochem) at a concentration of 0.5 μg/ml and anti-mouse IgG (whole molecule) FITC conjugate (Sigma) at a dilution of 1:200. Cells were observed for fluorescence which was monitored under 63X by Zeiss confocal laser scan fluorescence-inverted microscope (LSM 710; Carl Zeiss).

2.7.1. Evaluation of mitochondrial membrane potential

Potential sensitive dye $DiOC_6$ (3,3′-dihexyloxacarbocyanine iodide) (Sigma) was used to evaluate changes in mitochondrial membrane potential (MMP) (Koning et al., 1993). $\sim 2.0 \times 10^6$ cells were pelleted and washed twice with 1X SB. Cells were stained with $DiOC_6$ (400 nM) for 15 min in dark and then washed once with 1X SB and fluorescence was monitored under 63X by Zeiss confocal laser scan fluorescence-inverted microscope (LSM 710; Carl Zeiss).

MMP was also and quantitated by flow cytometry using a FACS ARIA (BD Biosciences). Data were analyzed with FACSDiva software.

2.7.2. Assessment of cell death by AnnexinV-FITC/PI dual staining

To differentiate between apoptotic and necrotic cell death, dual staining with Annexin V-FITC/PI (Miller, 2004) was performed using apoptosis detection kit (Molecular Probes). $\sim 2.0 \times 10^6$ cells were pelleted and washed twice with 1X Sorenson's buffer (SB). *D. discoideum* cells were then suspended in binding buffer provided in the kit and incubated with Annexin V for 10 min and then with PI for 5 min in dark at 22 °C. Fluorescence was monitored under 63X by Zeiss confocal laser scan fluorescence-inverted microscope (LSM 710; Carl Zeiss).

2.7.3. Development

For development, mid log phase cells were washed twice and resuspended in 1X SB at a density of 1×10^8 cells/ml. This cell suspension was spotted on 2% non-nutrient agar and incubated at 22 °C (Sussman, 1987). Images were taken every 2 h initially till 12 h and then at 12 h interval. Development was synchronized by incubating the cells at 4 °C for 4–5 h and then transferring them to 22 °C for further development.

2.7.4. Transcript analysis of ADPRT1A during development

Total RNA samples extracted from *D. discoideum* Ax- 2 cells during the growth and developmental phases were used for *ADPRT1A* transcript analysis using *ADPRT1A* specific primers by Real time PCR. Amplification of *RNLA* was carried out as an internal control. Fold change in transcript levels in developmental phases ($2^{-\Delta\Delta Ct}$) as compared to growth (vegetative) phase is shown graphically.

3. PARP activation on initiation of development

Cells were subjected to development as explained above followed by collection of cells at 0, 2, 4 and 6 h of development. PARP activity was monitored by indirect immunofluorescence (Cole and Perez-Polo, 2002) using anti-PAR mouse mAb (10H) (Calbiochem) at a concentration of 0.5 μg/ml and anti-mouse IgG (whole molecule) FITC conjugate (Sigma) at a dilution of 1:200. Cells were observed for fluorescence which was monitored under 63X by Zeiss confocal laser scan fluorescence-inverted microscope (LSM 710; Carl Zeiss). Mean density of fluorescence was plotted for quantification.

3.1. Data analysis and statistics

Flow cytometry and colorimetric assay experiments were repeated at least three times. Data were analyzed according to mean fluorescence intensity or optical density and plotted on histograms or on graphs. Statistical analysis was performed by *t* test for experiments with single comparisons.

4. Results

4.1. Sequence similarity, domain and phylogenetic analysis

ADP-ribosylation is a reversible post-translational modification that is involved in many cellular processes, including various signaling cascades, DNA repair, gene regulation and cell death (Gibson and Kraus, 2012). However, studies on its roles in growth and differentiation remain elusive. Several aspects of the life cycle of *D. discoideum* make it an attractive model to investigate the possible physiological role(s) of ADP-ribosylation in growth and differentiation. PARP-1 contributes to 80% of PARylation in cells. Thus, with this aim to identify the PARP-1 isoform in *Dictyostelium*, protein sequences of known PARPs in *Dictyostelium* were obtained from *D. discoideum* database by searching for proteins containing the PARP catalytic domain. Eight protein sequences were retrieved from dictyBase and the phylogenetic tree was constructed by maximum likelihood method to identify the isoform closest to human PARP-1. Of the eight isoforms identified, *ADPRT2*, *ADPRT1A* and *ADPRT1B* displayed maximum similarity to human PARP-1 (Fig. 1A). Further, domain-wise analysis was carried out to identify the closest ortholog of human PARP-1 in *D. discoideum* using the Pfam and Prosite. Unlike *ADPRT2* and *ADPRT1B*, the predicted domain analysis of *ADPRT1A* shows presence of a 2 zinc fingers, pADPR1 domain, BRCT domain, WGR domain, PARP regulatory domain; which are the key features of human PARP-1 (Fig. 1B). Also, multiple alignments of *ADPRT1A* with PARP-1 from *Homo sapiens, Drosophila melanogaster, Arabidopsis thaliana, Mus musculus* by Clustal W indicate that the protein encoded by *ADPRT1A* transcript has the definitive features of human PARP-1 i.e., the metal binding residues of zinc finger 1 (Eustermann et al., 2011), WGR motif, D loop residues (Wahlberg et al., 2012), K893 for poly ADP initiation (Simonin et al., 1993) and E988, the catalytic active site except a canonical caspase cleavage site (DEVD) [Fig. 1C]. *ADPRT1A* is thus identified as human PARP-1 ortholog in *D. discoideum*.

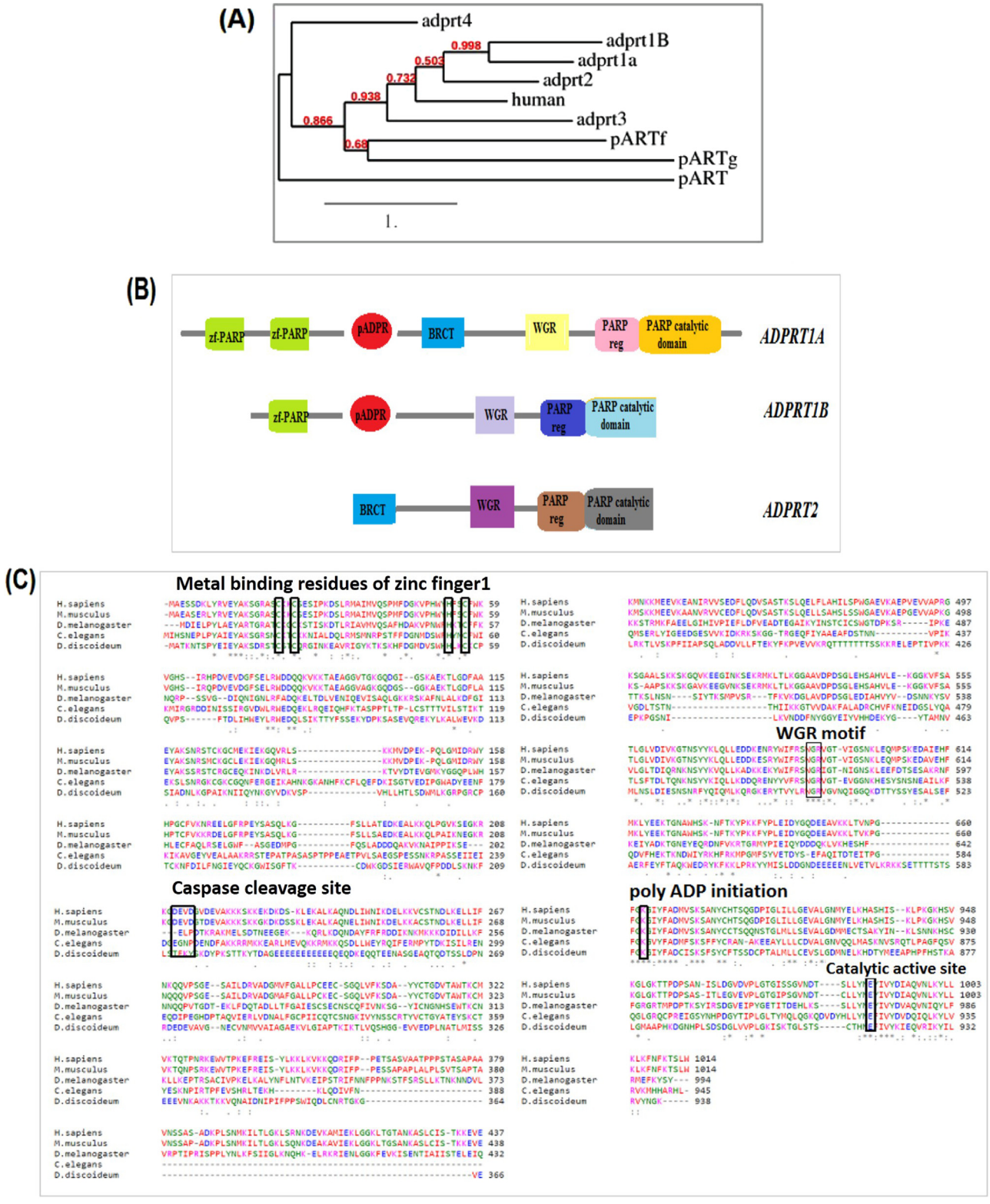

Fig. 1. *In silico* analysis of PARP1 ortholog in *D. discoideum*. (A) Phylogenetic analysis of PARP isoforms in *D. discoideum* and human PARP by maximum likelihood method. (B) Domain organization of ADPRT1A, ADPRT1B and ADPRT2 by Pfam and Prosite. ADPRT1A shows all domains like human PARP1 protein. (C) Multiple alignment of protein sequences of PARP1 protein from human and its orthologs from *M. musculus*, *D. melanogaster*, *C. elegans* and *D. discoideum* (ADPRT1A). ADPRT1A displays key features – CCHC– type zinc finger, WGR motif, poly ADP-initiation residues K893 and the catalytic active site.

4.2. Functional characterization and localization of ADPRT1A over expressing cells

In order to unravel the novel role of ADPRT1A in growth and multicellularity, we studied the effect of overexpressed *ADPRT1A* in AEOE cell lines. Semi quantitative Reverse Transcriptase PCR (Fig. 2A) showed significantly higher *ADPRT1A* transcript levels in AEOE cells which were further confirmed by qPCR studies wherein 61.10 ± 7.354 fold higher expression of *ADPRT1A* transcripts were observed in AEOE cells as compared to control (Fig. 2B). ADPRT1A

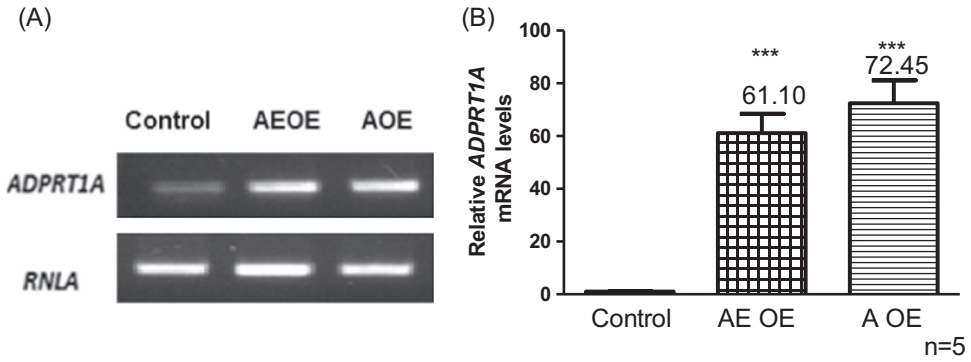

Fig. 2. Functional characterization of ADPRT1A overexpression AE OE and A OE. (A) Semi-quantitative RT-PCR of *ADPRT1A* in AE OE and AOE. AE OE and AOE exhibited increased ADPRT1A transcript levels as compared to control. (B) Real time analysis in AE OE and A OE cells showed 61.10 ± 7.354 and 72.45 ± 8.678 fold overexpression of *ADPRT1A* transcripts as compared to control. Data is a representation of SEM values of three independent experiments.

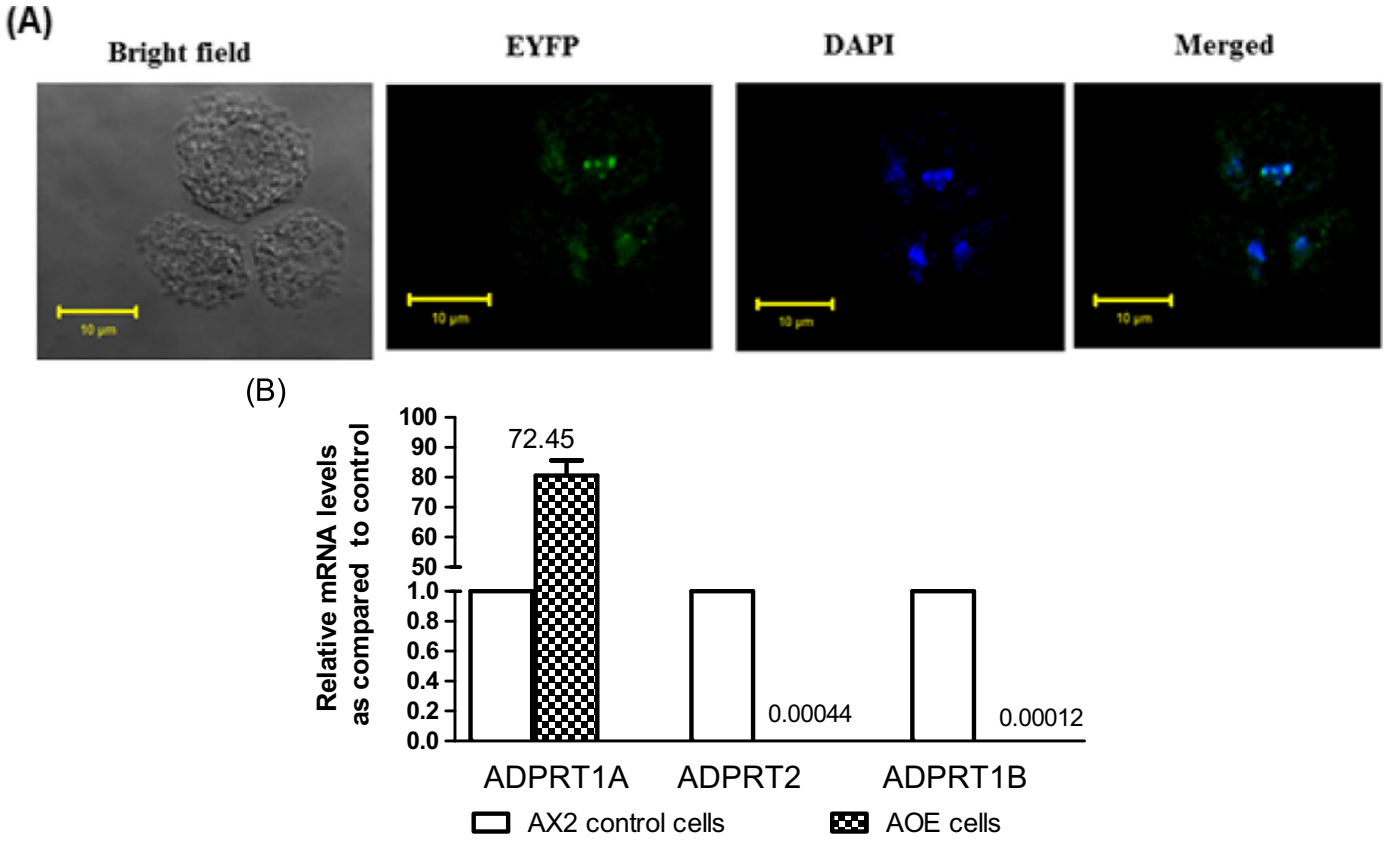

Fig. 3. Localization of ADPRT1A-EYFP in *D. discoideum* cells and transcript analysis of ADPRT isoforms in A OE. (A)Localization of ADPRT1A-EYFP in *D. discoideum* cells: EYFP merges with the DAPI stain demonstrating ADPRT1A to be a nuclear protein. Scale: 10 µm. Data are representative of three independent experiments (Photographs were taken at 63X objective). (B) Relative mRNA levels of PARP isoforms – *ADPRT1A*, *ADPRT2* and *ADPRT1B* in AOE cells as compared to their respective levels in control cells. Data is a representation of SEM values of three independent experiments.

OE (untagged- AOE) also showed 72.45 ± 8.678 fold higher *ADPRT1A* transcript levels. AOE was used for all our fluorescence based studies in order to avoid interference of YFP tag. In addition, the localization of cloned ADPRT1A was confirmed to be nuclear as YFP was colocalized with that of DAPI indicating that *ADPRT1A* is a nuclear localizing protein (Fig. 3A). As per *in silico* analysis, ADPRT2 and 1B also show homology to human PARP-1. Hence, to ensure that only ADPRT1A was overexpressed, ADPRT2 and 1B transcript levels were compared to their respective levels in control cells. Fig. 3B shows that ADPRT1A transcript levels are 72.45 fold higher in AOE cells as compared to control cells. On the contrary, there is significant decrease in ADPRT2 and 1B transcripts in AOE cells as compared to their respective expression in control cells. Thus, re-establishing that only ADPRT1A is overexpressed.

4.3. NAD^+ estimation in ADPRT1A over expression cell line

Further, it was essential to confirm the activity of the over-expressed ADPRT1A. Activation of PARP can lead to depletion of cellular NAD^+ pools which it uses as its substrate (Szabó and Dawson, 1998). Interestingly, the overexpressing cells show 60% reduction in NAD^+ levels in AEOE as well as AOE as compared to control cells, confirming the ADPRT-1 activation in ADPRT1A overexpressing *D. discoideum* cells. (Fig. 4).

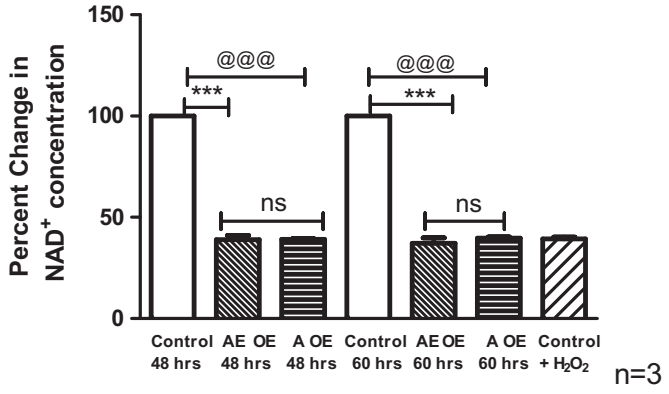

Fig. 4. Percent change of NAD^+ concentration in control and AE OE and AOE cells using Bernofsky's Enzymatic recycling method. Data are representative of three independent experiments. ***p value for AE OE < 0.001 as compared to control, $^{@@@}p$ value for AOE < 0.001 as compared to control.

4.4. *Effect of ADPRT1A overexpression on growth and cell cycle of D. discoideum*

Followed by NAD^+ estimation, the effect of *ADPRT1A* overexpression on cellular proliferation of *D. discoideum* cells was studied. AEOE *D. discoideum* cells were significantly slow growing with doubling time of approximately 18.48 ± 1.65 h while AOE cells showed a doubling time of approximately 17.84 ± 1.45 h (Fig. 5A) while control cells and EYFP vector control cells divided at approximately every 12.41 ± 0.5166 h and 12.89 ± 1.126 h respectively. Thus, ADPRT1A overexpression significantly reduced cellular proliferation in *D. discoideum* cells.

Since PARP-1 is known to be involved in regulation of cell-cycle (Yang et al., 2013), we studied its effects on cell growth and cell cycle using Propidium Iodide staining. We found that AEOE *D. discoideum* cells exhibited predominant population of cells in S and G2/M phases as compared to population of cells in G2/M phase in control cells at 48 h and 60 h (log-phase cells) respectively (Fig. 5B). Similar growth pattern and cell cycle profile was exhibited by AOE *D. discoideum* cells. These results suggest that PARP-1 homeostasis is indispensable for proper cell-cycle regulation and maintenance.

Since the redox status of the cell, influences various cellular activities including growth and cell death, the decreased cellular proliferation in AOE cells may be a consequence of ROS generation (Suzuki et al., 1997). Our studies showed higher endogenous ROS in AOE cells as compared to that of control (Fig. 6A). Interestingly we found that presence of Benzamide, a PARP inhibitor, alone rescued the delay in growth of AOE cells while N-Acetyl Cysteine

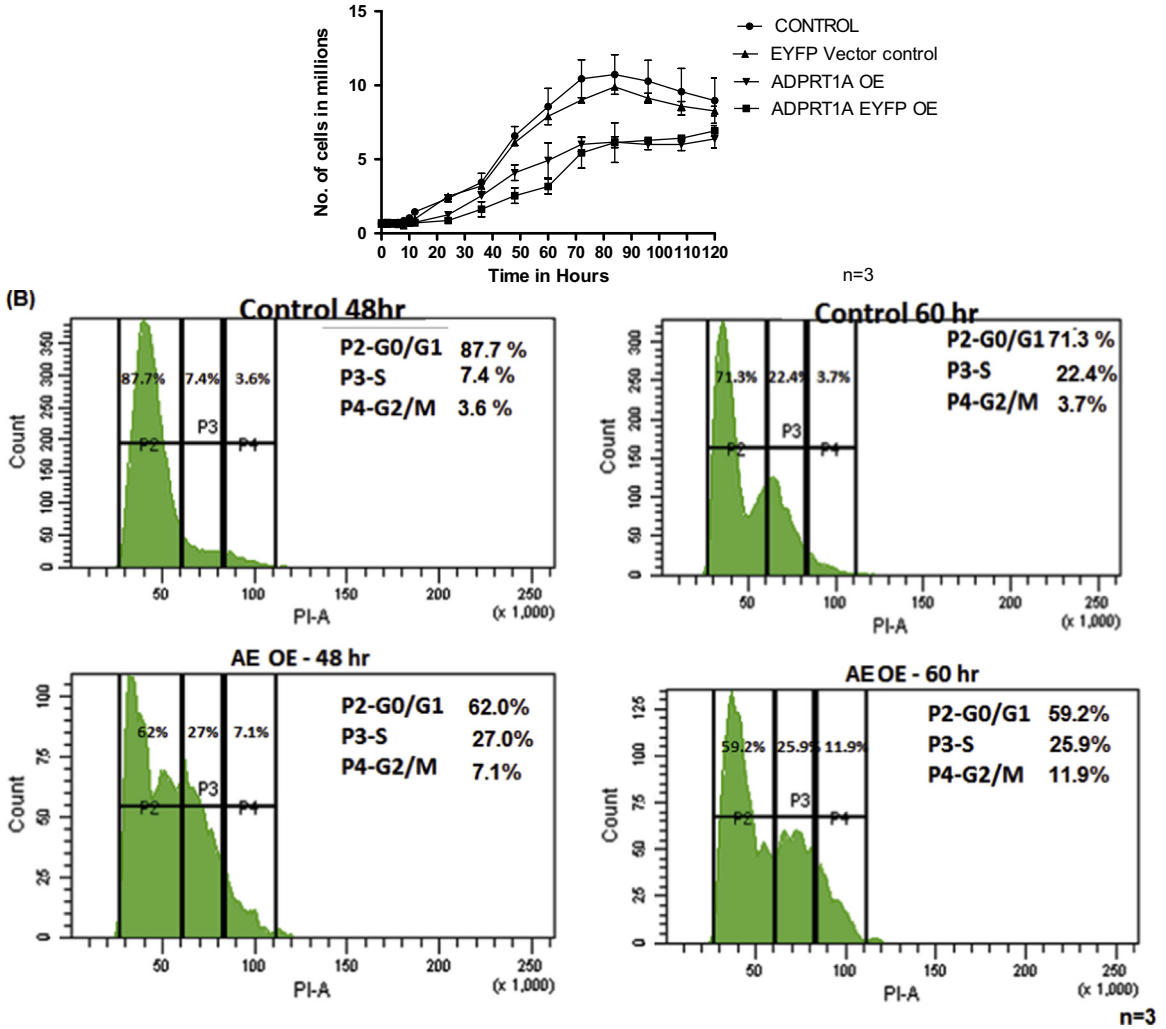

Fig. 5. Growth analysis of Control, AE OE , AOE and EYFP vector control cells. (A) Doubling Time in exponential phase for control cells was 12.41 ± 0.5166 h, EYFP vector control cells showed 12.89 ± 1.126 h while that of AE OE cells and A OE were 18.48 ± 1.65 h and 17.84 ± 1.45 h respectively. Data are representative of three independent experiments. (B) Analysis of cells cycle by FACS using Propidium Iodide. AE OE cells show marked population of cells in S and G2/M phase as compared to control, both at 48 and 60 h of growth. Data are representative of three independent experiments.

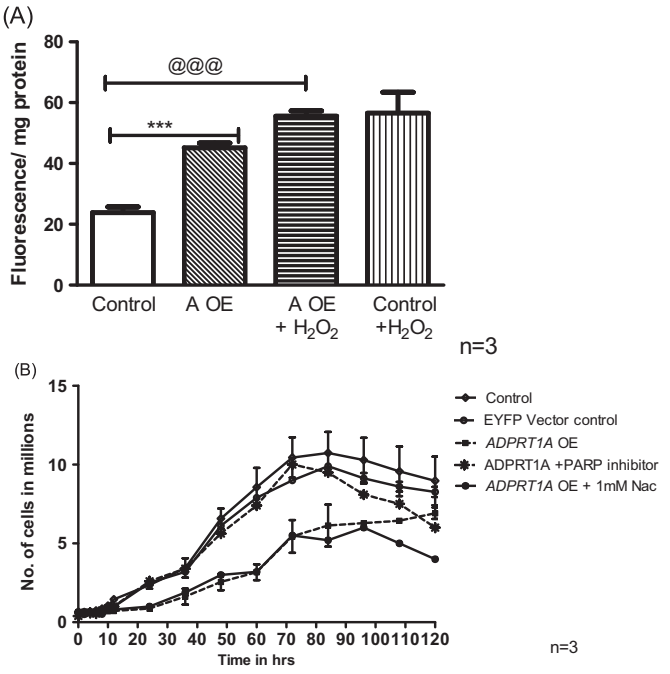

Fig. 6. ROS and PARP inhibition in AOE. (A) Fluorimetric analysis of ROS levels using DCFDA dye in control and AOE cells. AOE shows significantly higher ROS levels as compared to control. Data are representative of three independent experiments. $^{***}p$ value for AOE <0.001 as compared to control, $^{@@@}p$ value for A OE$+H_2O_2<0.001$ as compared to control. (B) Rescue in slow growth of AOE on treatment with PARP inhibitor benzamide as compared to untreated AOE and control cells. However no change was seen in growth when AOE were treated with antioxidant N-acetyl cysteine NAC as compared to untreated AOE and control cells. Data are representative of three independent experiments.

(NAc), an antioxidant did not have any significant effect on growth of AOE cells, thus indicating that decrease in NAD^+ levels or the accumulation of poly-ADP-ribose product could account for the phenotypes observed in *ADPRT1A* overexpressing cells (Fig. 6B).

4.5. Effect of ADPRT1A overexpression on cell death of D. discoideum

Depending on the signal, PARP-1 either favors cell survival or triggers cell death during extensive DNA damage, thus deciding cell fate. We were interested to study the effect of overexpressed ADPRT1A on cell survival during oxidative stress.

4.6. ROS estimation and DNA damage

ROS generation causes DNA lesions; the most abundant being base modification and phosphorylation of gamma H2AX protein (Minami et al., 2005). ROS levels in AOE cells peaked within 10 min after 0.03 mM H_2O_2 treatment (Fig. 7A) while in control cells the peak was obtained at 30 min. The effect of ROS on DNA damage in treated and untreated AOE cells was confirmed using pH2AX (Fig. 7B). AOE cells treated with 0.03 mM H_2O_2 showed significant DNA damage as compared to untreated control. However, it was lesser as compared to control cells treated with similar H2O2 dose.

4.7. PARP activation under oxidative stress

Subsequent to ROS estimation, PARP activation was checked after 0.03 mM H_2O_2 treatment at 2 min, 5 min and 10 min in AOE cells as well as control cells. AOE cells showed higher basal levels of poly ADP-ribosylation activity (Fig. 7C) as compared to control without any oxidant treatment. On subjecting cells to oxidative stress, the significant increase in fluorescence indicating PARP activation was seen within 5 min (Fig. 7C). However, in control cells highest PARP activation signals were observed at 10 min (Fig. 7C). It was thus observed that endogenous PAR levels were higher in AOE cells. Moreover, under oxidative stress AOE cells showed faster PARP activation as opposed to control cells.

4.8. Mitochondrial membrane potential

Mitochondrial membrane potential (MMP) loss is a characteristic feature of cell death and as PARP-1 has a major role to play in cell death, overexpression of *ADPRT1A* was hypothesized to change the MMP in *D. discoideum* cells. MMP loss was monitored using $DiOC_6$ dye after subjecting AOE cells to oxidative stress of 0.03 mM H_2O_2 dose after 3 h and 5 h. AOE cells showed marked decrease in fluorescence within 3 h (Fig. 8A) suggesting significant loss of mitochondrial membrane potential while in control cells loss of MMP was observed at 5 h of 0.03 mM H_2O_2 dose as opposed to PARP inhibitor treated cells wherein there was no significant loss of mitochondrial membrane potential even at 5 h.

MMP changes were also quantified using $DiOC_6$ dye by FACS. Population of cells showing MMP loss post 3 h of 0.03 mM H_2O_2 dose in AOE cells were observed to be ~81% (P1+P2), out of which 40.1% (P1: lowest fluorescence) cells (Fig. 8B) had very less fluorescence intensity suggesting significant mitochondrial membrane potential loss. Control cells after 3 h of 0.03 mM H_2O_2 dose did not show complete mitochondrial membrane potential loss while PARP inhibitor treated control showed no significant loss in MMP.

4.9. Annexin V FITC-PI

PARP-1 on over activation causes severe NAD^+ and ATP depletion resulting in energy crisis and thus results in necrotic cell death (Edinger and Thompson, 2004). However moderate PARP-1 activation favors programmed cell death or apoptosis. Above cell death parameters illustrated ADPRT1A OE cells to demonstrate an oxidative stress sensitive phenotype. Nevertheless, mode of cell death under ADPRT1A overexpression background remains to be studied. AOE and control cells after 0.03 mM H_2O_2 treatment exhibited both Annexin V-FITC and Propidium Iodide (PI) staining, however, AOE cells showed early Annexin V-FITC staining (due to early exposure of phosphatidylserine) as well as early PI staining (1 h and 3 h respectively) (Fig. 9). Control cells, on the other hand, showed Annexin V-FITC and PI staining at 3 h and 12 h respectively (Fig. 9). Together, these results indicate that AOE cells are susceptible to oxidative stress as 0.03 mM H_2O_2 dose led to paraptotic cell death in control cells nevertheless, AOE cells exhibited necrotic cell death at the same dose.

4.10. Effect of ADPRT1A overexpression on development of D. discoideum

Morphogenesis during developmental program involves large scale changes in gene expression. PARP-1 is reported to regulate gene expression via transcriptional control thereby controlling growth and differentiation (Ji and Tulin, 2010). To pin down the role of *ADPRT1A* during *D. discoideum* development, control and AOE cells were subjected to starvation and then developmental morphogenesis was studied. Interestingly, AOE cells showed delay at aggregation stage. Streaming started in these cells at around 8 h thereby forming loose aggregates at 10 h and tight aggregates at 14 h, tipped aggregates at 18 h followed by slug formation at 22 h. However, AOE cells remained in the slug stage until 28 h and also showed much delay in fruiting body formation at 38 h as opposed

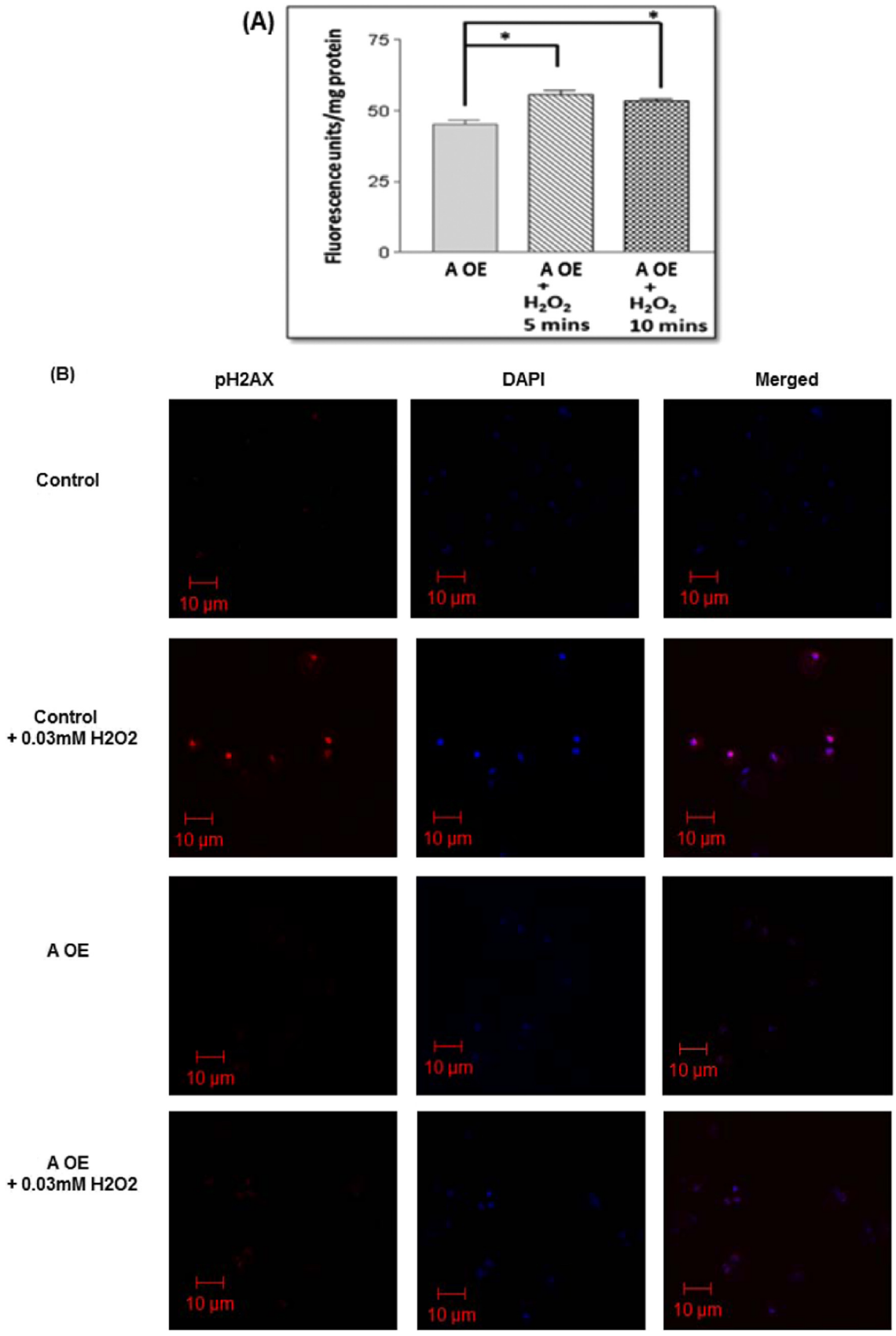

Fig. 7. ROS estimation, DNA damage and PARP activation post 0.03 mM cumene H_2O_2 treatment in control and ADPRT1A OE (A OE). (A) Fluorimetric analysis of ROS levels using DCFDA dye in control and ADPRT1A OE (A^{OE}) cells. Data are representative of three independent experiments. $^*p$ value < 0.05 as compared to control. (B) DNA damage was observed in control and A OE 5 min post 0.03 mM cumene H_2O_2 stress by immunofluorescence using antibody against H2AX. Data are representative of three independent experiments. Scale: 10 μm. (C) PARP activation post 0.03 mM cumene H_2O_2 treatment using anti-PAR antibodies in control, PARP inhibitor control and A OE cells by confocal microscopy at 63X magnification. Peak PARP activity was observed at 10 min post 0.03 mM cumene H_2O_2 stress in control cells as opposed to 5 min in A OE cells. Data are representative of three independent experiments. Scale: 10 μm.

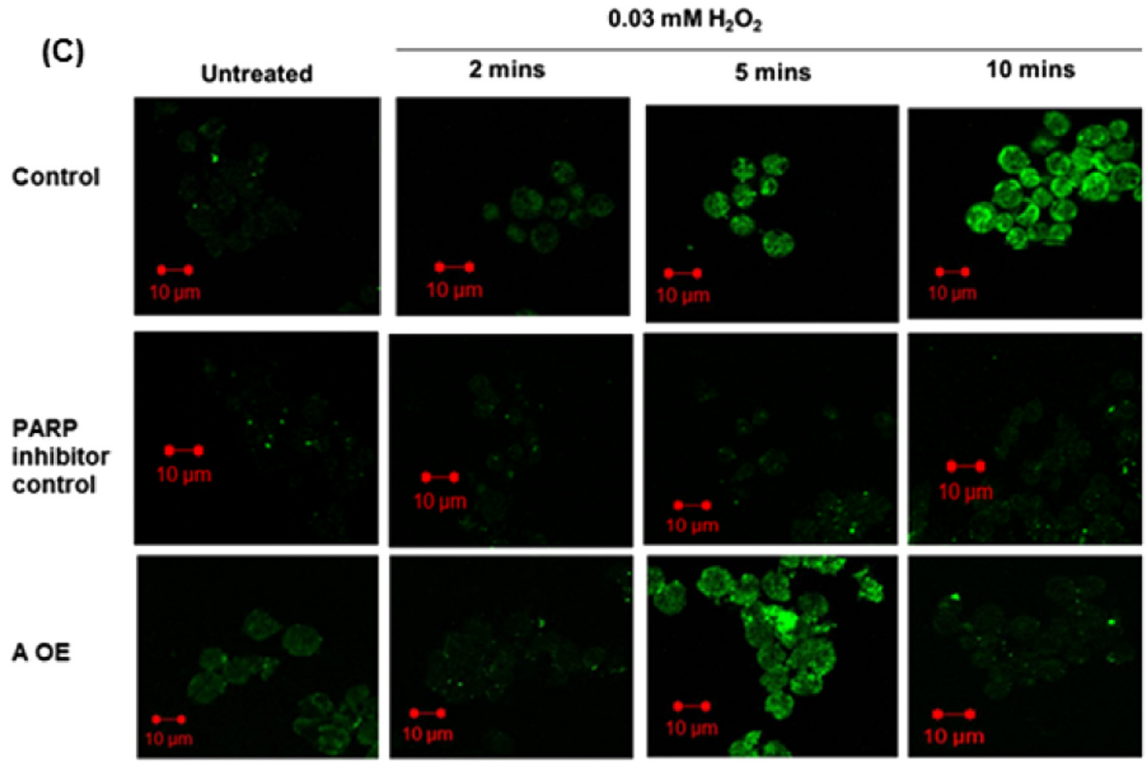

Fig. 7. (*continued*)

to 24 h in control cells (Fig. 10A). Thus the aggregation stage seems to be affected in *ADPRT1A* OE cells, hence these cells required prolonged time to form the culminants.

4.11. ADPRT1A transcript levels and PARP activation during D. discoideum development

Additionally, to understand whether ADPRT1A is developmentally regulated in *D. discoideum,* the expression pattern of *ADPRT1A* during the growth and developmental phases were monitored by Real Time PCR. Interestingly, *ADPRT1A* transcript levels were highest at the loose aggregate stage followed by significant reduction at the tight aggregate stage after which an increase was seen at the migrating slug stage. The fruiting body of *D. discoideum* showed the lowest transcript levels of *ADPRT1A* (Fig. 10B). However, during development there is a significant decrease in *ADPRT1A* mRNA levels as compared to vegetative stage. Although the expression was seen to drop at the onset of development, PARP activity was found to be significantly higher in cells subjected to nutrient starvation from 2 h till 6 h than the vegetative stage implicating a strong role of PARP during developmental morphogenesis of *Dictyostelium* and specifically during aggregation (Fig. 10C). Also, these results are consistent with the above results wherein aggregation stage seems to be affected more due to ADPRT1A overexpression. These results along with existing literature suggest ADPRT1A homeostasis may be essential for the aggregation process in *Dictyostelium.*

In conclusion, the above results illustrate a definite role of *ADPRT1A* in *D. discoideum* growth and multicellularity.

5. Discussion

PARP-1 is an abundant and ubiquitous nuclear enzyme involved in many diverse functions like DNA repair, chromatin modulation, transcription regulation, cell death etc. In addition, recent reports suggest a novel function of PARP-1 in multicellularity and differentiation as well. PARP deletion mutants in Drosophila develop only up to larval stages due to defects in chromatin remodeling and regulation of gene expression (Tulin and Allan, 2003), suggesting that poly (ADP-ribosyl)ation is essential for normal development. In addition, overexpression of *PrpA* leads to increased spore production and fluffy colonies largely consisting of aerial hyphae, reflecting PARP's role in regulating the expression and/or activity of proteins essential in its development (Semighini et al., 2006). Interestingly, our earlier reports are also suggestive of a role of PARP-1 in *D. discoideum* multicellularity since downregulation of PARP using antisense against catalytic domain resulted in stalled development at aggregate stage of *D. discoideum* (Rajawat et al., 2007). Thus, an understanding of how *ADPRT1A*, an ortholog of human PARP-1 in *D. discoideum*, functions in growth and multicellularity of *D. discoideum* would help us identify some of its unknown functions that still remain obscure.

The *Dictyostelium* genome encodes eight PARP proteins (Kawal et al., 2011). The *in silico* analysis by phylogenetic tree construction and domain analysis identified ADPRT1A as the PARP-1 ortholog in *D. discoideum*. This analysis is in accordance with *ADPRT1A* domains defined by Couto et al. (2011) using InterProScan. In addition, multiple alignment studies clearly confirm that *D. discoideum* may be a suitable model system to study PARP proteins (Fig. 1C).

It is already known that PARP activation results in drop of NAD^+ levels upon excessive DNA damage (Berger, 1985) and hence triggering NAD^+ turnover (Houtkooper et al., 2010). Similar results were obtained in ADPRT1A overexpressed cells wherein there was significant NAD^+ depletion (Fig. 4). This suggests that PARP is indeed activated in ADPRT1A overexpressed cells. This result is consistent with our PARP activation results where basal level of PARP activation was higher as compared to control cells (Fig. 7A). Higher basal levels of PAR were observed during hPARP overexpression in transfected hamster cell lines thus indicating PARP activation (Van Gool et al., 1997). Also, it was seen that

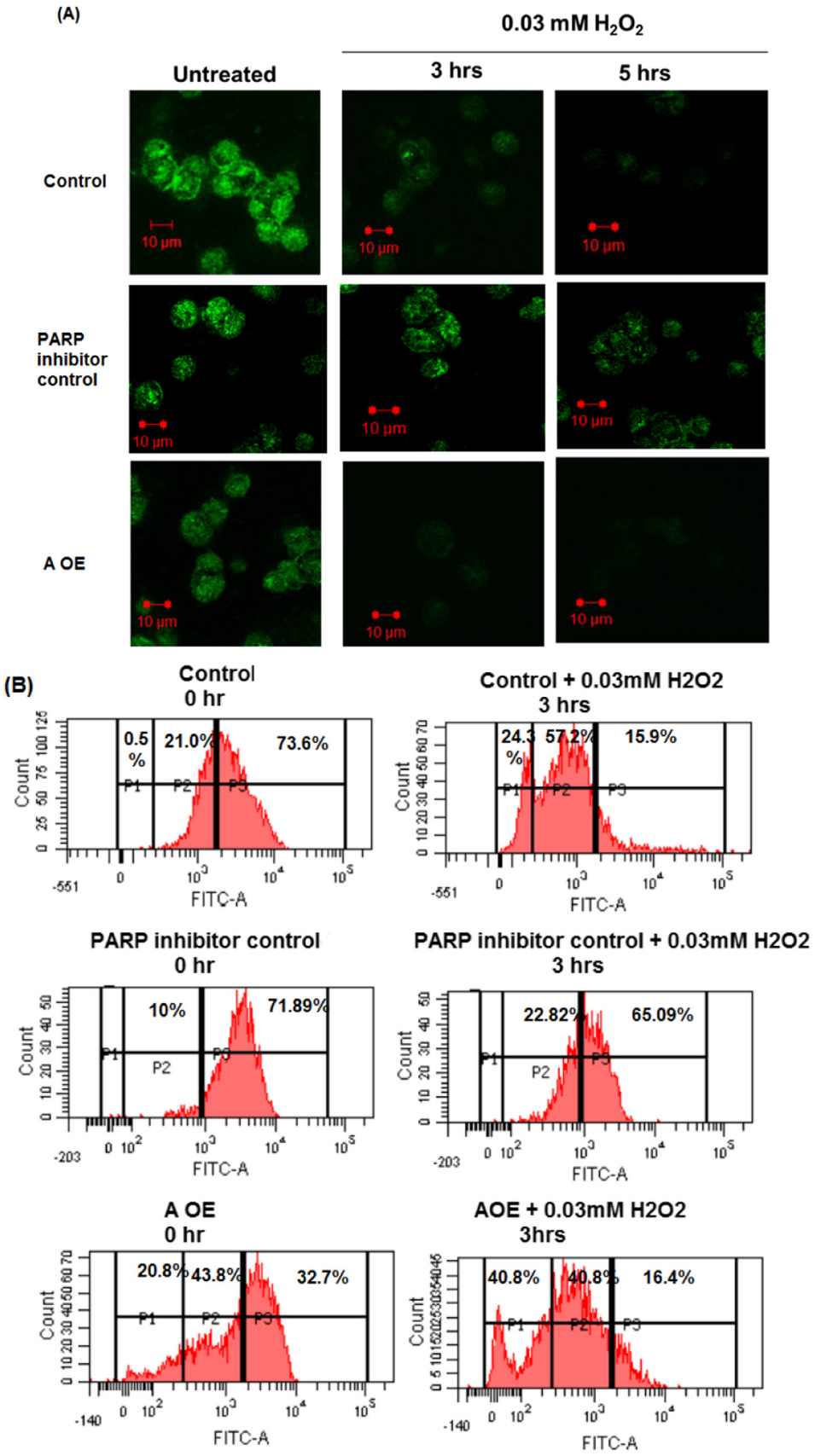

Fig. 8. Mitochondrial membrane potential changes in control, PARP inhibitor treated and ADPRT1A OE (AOE) cells at 3 h and 5 h post 0.03 mM cumene H_2O_2 treatment. (A) Mitochondrial membrane potential changes by $DiOC_6$ staining in control, PARP inhibitor treated cells and ADPRT1A OE (A OE) cells by confocal microscopy at 63X magnification. Data are representative of five independent experiments. Scale: 10 µm. (B) FACS analysis of mitochondrial membrane potential change in A OE and control cells post 3 h of 0.03 mM cumene H_2O_2 treatment using $DiOC_6$ dye Data are representative of three independent experiments.

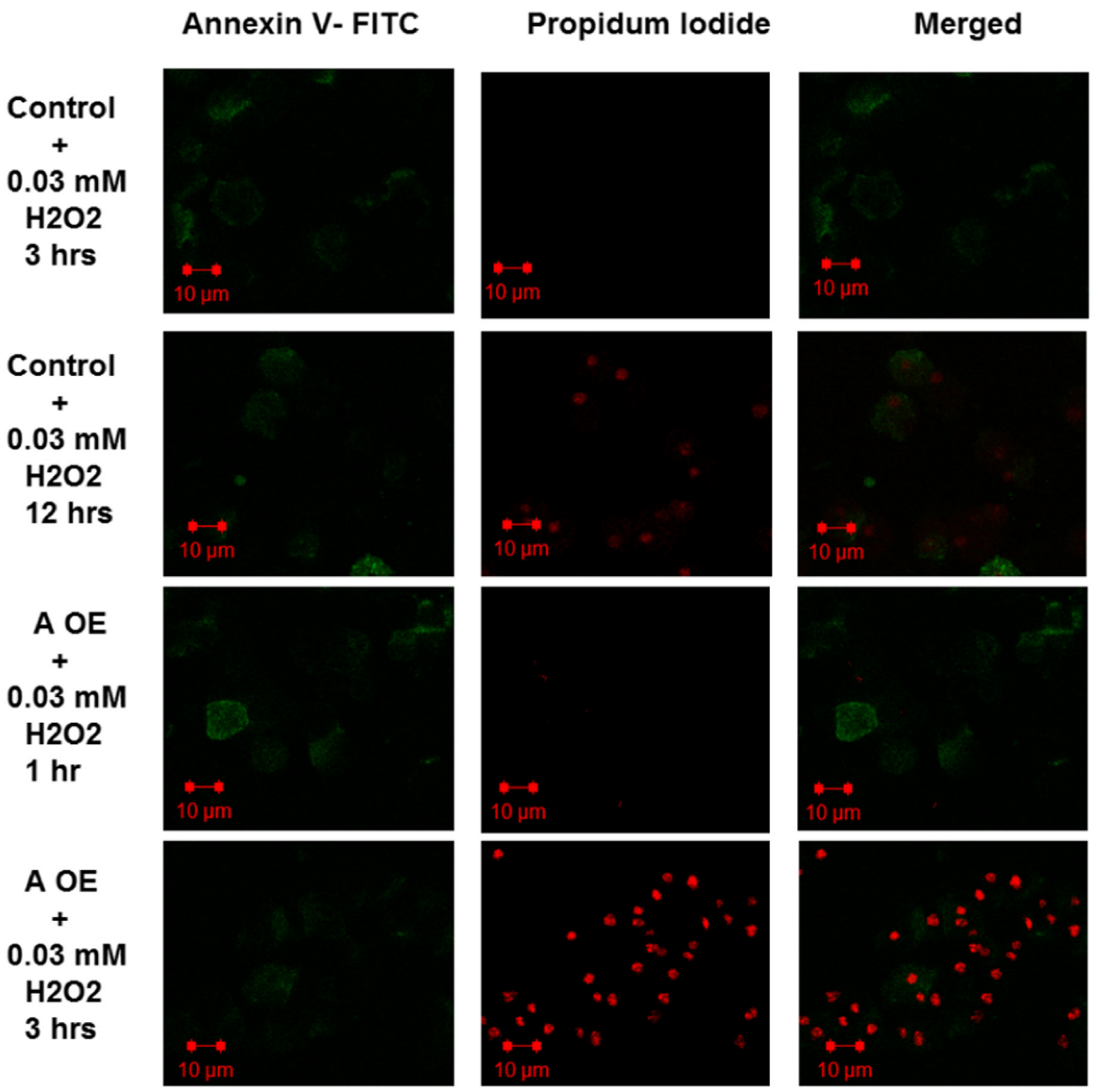

Fig. 9. Phosphatidylserine (PS) exposure (Annexin V-FITC Staining) and PI staining in control and ADPRT1A OE (AOE). Cells were by confocal microscopy at 63X magnification. A OE cells showed both PS (green - Annexin V FITC staining) and PI (red) positive cells as early as 3 h post 0.03 mM cumene H_2O_2 treatment indicating necrotic mode of cell death while control cells showed only PS (green) positive cells at 3hrs indicating paraptotic mode of cell death under the same oxidative stress. Data are representative of three independent experiments. Scale: 10 µm.

overexpression of ADPRT1A led to downregulation of the other PARP isoforms ADPRT1B and ADPRT2 (Fig. 3B). This decrease in ADPRT2 and 1B levels could be the cells' mechanism to circumvent the further reduction of the common substrate for all the isoforms i.e NAD^+, thereby keeping the cell viable. This is supported by the growth profile of the A OE cells wherein in spite of the high NAD^+ consumption, the cells are viable but show delayed growth. There are reports wherein overexpression of the Na^+/K^+ATPase α2 elicited downregulation of the other isoform α1 isoform in a manner that preserved total levels of Na^+/K^+ATPases (Correll et al., 2014).

NAD^+ and ATP depletion can be seen as a result of PARP activation in response to DNA damage due to ROS (Cantó et al., 2013). Our results are consistent with the fact that despite having high ROS levels (Fig. 6A), AOE cells showed negligible cell death. This could be due to the presence of more PARP molecules in ADPRT1A overexpressed cells as compared to control, making the cells more equipped to combat the increased DNA damage caused by ROS as seen in Fig. 7B wherein untreated AOE do not show significant DNA damage. Reports suggest that ADPRT1A is involved in double stranded break repair while ADPRT1B and ADPRT2 are required for tolerance to single stranded breaks (Tulin and Allan, 2003). Couto et al., also explain that in absence of ADPRT2, ADPRT1A signals single strand DNA lesions to promote resistance of cells to DNA damage (Couto et al., 2013). Our results clearly indicate lower ADPRT1B and ADPRT2 levels in AOE cells as compared control cells (Fig. 3B). Hence, overexpressed ADPRT1A may compensate for the other isoforms. Together, these results suggest that ADPRT1A homeostasis is very important, and any disruption/change in ADPRT1A levels and activated PARP levels may disturb normal functioning of the cell.

Higher NAD^+ and ATP reduction along with high basal ROS thus justify increased doubling time (~18 h) in *ADPRT1A* overexpressed cells (Fig. 5A). Therefore, decreased energy availability, would result in slow growth of *ADPRT1A* overexpressed cells. Apart from NAD^+ and ATP reduction, cell cycle analysis by FACS also revealed that population of cells in S and G2/M phase was higher in *ADPRT1A* OE cells as compared to control (Fig. 5B). Thus ADPRT1A also seems to affect cell-cycle regulation in *ADPRT1A* OE cells. This goes in accordance with reports suggesting that PARP-1

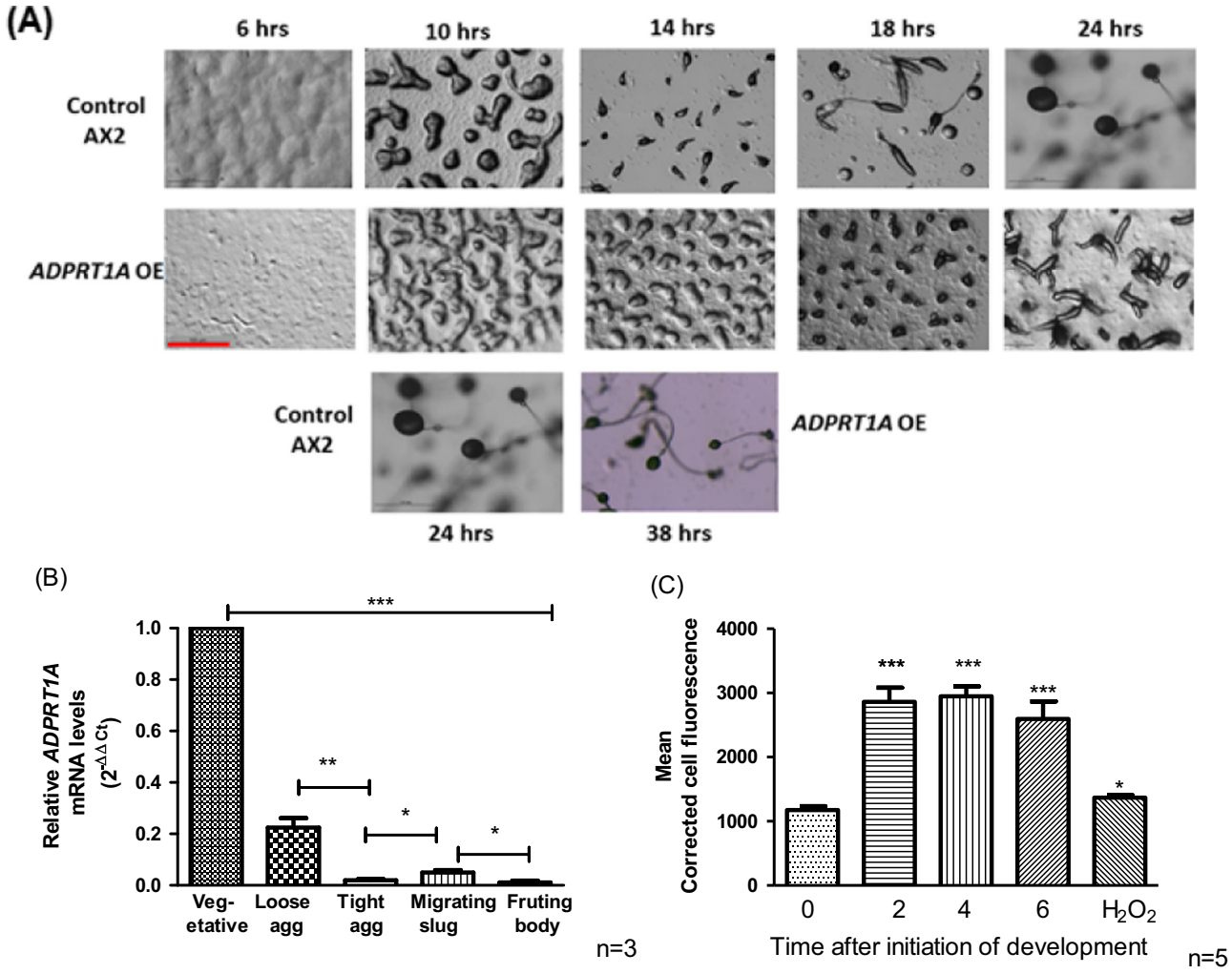

Fig. 10. Role of ADPRT1A in *D. discoideum* development. (A) Development of Control Ax-2 and *ADPRT1A*-OE cells were plated on nutrient-free agar and allowed to develop at 22 °C followed by synchronization. Photographs were taken at various time points. Scale: 100 μm. Data are representative of three independent experiments. (B) Developmental expression pattern of *ADPRT1A*. Change in gene expression was analyzed by Real time PCR using total RNA samples extracted from *D. discoideum* Ax-2 cells in the growth and developmental phases as templates. Relative mRNA levels ($2^{-\Delta\Delta Ct}$) as compared to vegetative phase *ADPRT1A* transcript levels were plotted graphically. Data are representative of three independent experiments. (C) Densitometric analysis of PARP activation up to 6 h of nutrient starvation. Mean corrected fluorescence was plotted for confocal microscopic pictures of PARP activity checked using FITC labeled Anti-PAR antibodies. ***p value < 0.001, *p value < 0.05 as compared to control. Data are representative of five independent experiments.

over-expression results in an increase in the number of cells in the diploid population (Bhatia et al., 1996). Moreover, PARP-1 is critical for the induction of G1 arrest and is also involved in the regulation of G2 arrest (Masutani et al., 1995). PARP-2 is reported to regulate cell cycle-related genes independently of poly (ADP-ribosyl)ation (Liang et al., 2013). The present study thus provides the first report in *Dictyostelium* wherein ADPRT1A, ortholog of PARP-1 is involved in cell cycle control via poly (ADP-ribosyl)ation.

PARP-1 is a well-established mediator of necrotic cell death (Edinger and Thompson, 2004; Rajawat et al., 2014). It is known that in *D. discoideum*, high oxidative stress causes DNA damage and PARP activation (Fey et al., 2004). PARP-1 depletes cellular NAD^+ and ATP levels leading to necrotic cell death instead of apoptosis (Ha and Snyder, 1999). Similarly *ADPRT1A* overexpressed *D. discoideum* cells showed susceptibility to oxidative stress during 0.03 mM H_2O_2 insult resulting in necrosis (Fig. 9).

In addition to PARP's role in growth, evidences also suggest that it might be playing a key role in development and differentiation. PARP-1 and PARP-2 double knockouts in mice exhibit embryonic lethality (Henrie et al., 2003) suggesting the role of PARP in development. Constitutive *PARP* downregulation inhibits development at aggregate stage (Rajawat et al., 2007). Interestingly, *ADPRT1A* OE cells showed delayed streaming, loose aggregate stage and early culminant stage (Fig. 10A). Aggregation defective phenotypes of *D. discoideum* display disruption in cAMP signaling. (Sawai et al., 2007; Bader et al., 2006). PARP-1 is known to interact with histones and other chromatin modifying enzymes to control their activity at target gene promoters, eventually influencing gene expression (Frizzell et al., 2009).

Thus, our results show that analysis of endogenous *ADPRT1A* transcript level in *D. discoideum* cells subjected to starvation display highest *ADPRT1A* transcript levels at aggregation stage (Fig. 10B). Furthermore, the developmental stimulus of nutrient starvation not only causes increased transcript levels but also a significant increase in PARP activity in the aggregation stages (Fig. 10C). Masutani et al., also report significant change in PARP mRNA expression throughout the developmental stages of *Sarcophaga peregrina* (Masutani et al., 2004). Overall, it could be concluded that *ADPRT1A* has a definite role in development and may affect the cAMP signaling which is quintessential for aggregation. Our results for the first time reveal that there is increased PARP activity and developmentally regulated transcript profile of *ADPRT1A* during *D. discoideum* development. Thus, it would be of great interest to further explore how ADPRT1A affects *D. discoideum* developmental morphogenesis.

6. Conclusion

The current study shows that PARP-1 is essential for differentiation and its function may be linked to multicellularity. This new finding will give us an insight into the role of PARP-1 in differentiation and developmental cell death in higher complex organisms. It would add one more feather to the multitasking functions of PARP-1 thereby igniting new ideas to understand the manner in which this multifunctional protein can be tapped for therapeutic purposes.

Acknowledgment

Infrastructure facilities provided by The Maharaja Sayajirao University of Baroda, Vadodara and DBT-MSUB ILSPARE are gratefully acknowledged. RB thanks the Department of Biotechnology, New Delhi (BT/PR4383/BRB/10/1014/2011) and Council of Scientific and Industrial Research (38(1383)/14/EMR-II) for research support; and TJ thanks the UGC-DRS (Grant number: F.3 -13/2012(SAP-II)) for awarding JRF.

References

Ame, J.C., Spenlehauer, C., de Murcia, G., 2004. The PARP superfamily. Bioessays 26, 882–893.
Bader, S., Kortholt, A., Snippe, H., Van Haastert, P.J., 2006. DdPDE4, a novel cAMP-specific phosphodiesterase at the surface of *Dictyostelium* cells. J. Biol. Chem. 281, 20018–20026.
Berger, N.A., 1985. Poly(ADP-ribose) in the cellular response to DNA damage. Radiat. Res. 101, 4–15.
Bernofsky, C., Swan, M., 1973. An improved cycling assay for nicotinamide adenine dinucleotide. Anal. Biochem. 53, 452–458.
Bhatia, M., Kirkland, J.B., Meckling-Gill, K.A., 1996. Overexpression of poly (ADP-ribose) polymerase promotes cell cycle arrest and inhibits neutrophilic differentiation of NB4 acute promyelocytic leukemia cells. Cell Growth Differ. 7, 91–100.
Cantó, C., Sauve, A.A., Bai, P., 2013. Crosstalk between poly (ADP-ribose) polymerase and sirtuin enzymes. Mol. Asp. Med. 34, 1168–1201.
Chaitanya, G.V., Alexander, J.S., Babu, P.P., 2010. PARP-1 cleavage fragments: signatures of cell-death proteases in neurodegeneration. Cell. Commun. Signal 8, 31.
Chen, G., Shaulsky, G., Kuspa, A., 2004. Tissue-specific G1-phase cell-cycle arrest prior to terminal differentiation in *Dictyostelium*. Development 131, 2619–2630.
Citarelli, M., Teotia, S., Lamb, R.S., 2010. Evolutionary history of the poly (ADP-ribose) polymerase gene family in eukaryotes. BMC Evol. Biol. 10, 308.
Cole, K.K., Perez-Polo, J.R., 2002. Poly (ADP-ribose) polymerase inhibition prevents both apoptotic-like delayed neuronal death and necrosis after H_2O_2 injury. J. Neurochem. 82, 19–29.
Correll, R.N., Eder, P., Burr, A.R., Despa, S., Davis, J., Bers, D.M., Molkentin, J.D., 2014. Overexpression of the Na+/K+ATPase α2 but not α1 isoform attenuates pathological cardiac hypertrophy and remodeling. Circ. Res. 114, 249–256.
Couto, C.A., Wang, H.Y., Green, J.C., Kiely, R., Siddaway, R., Borer, C., Pears, C.J., Lakin, N.D., 2011. PARP regulates nonhomologous end joining through retention of Ku at double-strand breaks. J. Cell. Biol. 194, 367–375.
Couto, C.A.M., Hsu, D.W., Teo, R., Rakhimova, A., Lempidaki, S., Pears, C.J., Lakin, N.D., 2013. Nonhomologous end-joining promotes resistance to DNA damage in the absence of an ADP-ribosyltransferase that signals DNA single strand breaks. J. Cell Sci. 126, 3452–3461.
Degli Esposti, M., 2002. Measuring mitochondrial reactive oxygen species. Methods 26, 335–340.
Dereeper, A., Guignon, V., Blanc, G., Audic, S., Buffet, S., Chevenet, F., Dufayard, J.F., Guindon, S., Lefort, V., Lescot, M., Claverie, J.M., Gascuel, O., 2008. Phylogeny.fr: robust phylogenetic analysis for the non-specialist. Nucleic Acids Res. 1, 36.
Edinger, A.L., Thompson, C.B., 2004. Death by design: apoptosis, necrosis and autophagy. Curr. Opin. Cell Biol. 16, 663–669.
Eustermann, S., Videler, H., Yang, J.C., Cole, P.T., Gruszka, D., Veprintsev, D., Neuhaus, D., 2011. The DNA-binding domain of human PARP-1 interacts with DNA single-strand breaks as a monomer through its second zinc finger. J. Mol. Biol. 407, 149–170.
Fey, P., Gaudet, P., Just, E.M., Pilcher, K.E., Dyck, P.A., Kibbe, W.A., Chisholm, R.L., 2004. Dictybase.
Frizzell, K.M., Gamble, M.J., Berrocal, J.G., Zhang, T., Krishnakumar, R., Cen, Y., Sauve, A.A., Kraus, W.L., 2009. Global analysis of transcriptional regulation by poly (ADP-ribose) polymerase-1 and poly (ADP-ribose) glycohydrolase in MCF-7 human breast cancer cells. J. Biol. Chem. 284, 33926–33938.
Gibson, B.A., Kraus, W.L., 2012. New insights into the molecular and cellular functions of poly(ADP-ribose) and PARPs. Nat. Rev. Mol. Cell. Biol. 13, 411–424.
Ha, H.C., Snyder, S.H., 1999. Poly(ADP-ribose) polymerase is a mediator of necrotic cell death by ATP depletion. Proc. Natl. Acad. Sci. USA 96, 13978–13982.
Henrie, M.S., Kurimasa, A., Burma, S., Ménissier de Murcia, J., de Murcia, G., Li, G.C., Chen, D.J., 2003. Lethality in PARP-1/Ku80 double mutant mice reveals physiological synergy during early embryogenesis. DNA Repair 2, 151–158.
Hottiger, M.O., Hassa, P.O., Luscher, B., Schuler, H., Koch-Nolte, F., 2010. Toward a unified nomenclature for mammalian ADP-ribosyltransferases. Trends Biochem. Sci. 35, 208–219.
Houtkooper, R.H., Williams, R.W., Auwerx, J., 2010. Metabolic networks of longevity. Cell 142, 9–14.
Ji, Y., Tulin, A.V., 2010. The roles of PARP1 in gene control and cell differentiation. Curr. Opin. Genet. Dev. 20, 512–518.
Kawal, A.M., Mir, H., Ramniklal, C.K., Rajawat, J., Begum, R., 2011. Structural and evolutionary analysis of PARPs in *D. discoideum*. Am. J. Infect. Dis. 7, 67–74.
Koning, A.J., Lum, P.Y., Williams, J.M., Wright, R., 1993. $DiOC_6$ staining reveals organelle structure and dynamics in living yeast cells. Cell. Motil. Cytoskelet. 25, 111–128.
Kosta, A., Laporte, C., Lam, D., Tresse, E., Luciani, M.F., Golstein, P., 2001. How to assess and study cell death in *Dictyostelium discoideum*. Methods Cell Biol. 346, 535–550.
Kotova, E., Jarnik, M., Tulin, A., 2009. Poly (ADP-Ribose) polymerase1 is required for protein localization to Cajal body. PloS Genet. 5, e1000387.
Liang, Y.C., Hsu, C.Y., Yao, Y.L., Yang, W.M., 2013. PARP-2 regulates cell cycle-related genes through histone deacetylation and methylation independently of poly (ADP-ribosyl) ation. Biochem. Biophys. Res. Commun. 431, 58–64.
Lowry, O.H., Rosebrough, N.J., Farr, A.L., Randall, R.J., 1951. Protein measurement with the Folin phenol reagent. J. Biol. Chem. 193, 265–275.
Masutani, M., Nozaki, T., Wakabayashi, K., Sugimura, T., 1995. Role of poly(ADP-ribose) polymerase in cell-cycle checkpoint mechanisms following gamma-irradiation. Biochimie 77, 462–465.
Masutani, M., Ikejima, M., Mariotto, S., Nozaki, T., Kurata, S., Natori, S., Esumi, H., Sugimura, T., 2004. Developmental changes of poly (ADP-ribose) polymerase expression in *Sarcophaga peregrina*. Proc. Jpn. Acad. 80, 336–341.
Messner, S., Hottiger, M.O., 2011. Histone ADP-ribosylation in DNA repair, replication and transcription. Trends Cell Biol. 21, 534–542.
Miller, E., 2004. Apoptosis measurement by Annexin V staining. Methods Mol. Med. 88, 191–202.
Minami, T., Adachi, M., Kawamura, R., Zhang, Y., Shinomura, Y., Imai, K., 2005. Sulindac enhances the proteasome inhibitor bortezomib-mediated oxidative stress and anticancer activity. Clin. Cancer Res. 11, 5248–5256.
Mir, H., Rajawat, J., Begum, R., 2012. Staurosporine induced poly (ADP-ribose) polymerase independent cell death in *Dictyostelium discoideum*. Indian J. Exp. Biol. 50, 80–86.
Mir, H., Alex, T., Rajawat, J., Kadam, A., Begum, R., 2015. Response of *Dictyostelium discoideum* to UV-C and involvement of poly (ADP-ribose) polymerase. Cell Prolif. 48, 363–374.
Perina, D., Mikoč, A., Ahel, J., Ćetković, H., Žaja, R., Ahel, I., 2014. Distribution of protein poly (ADP-ribosyl) ation systems across all domains of life. DNA Repair (Amst.) 23, 4–16.
Quenet, D., El Ramy, R., Schreiber, V., Dantzer, F., 2009. The role of poly(ADPribosyl) ation in epigenetic events. Int. J. Biochem. Cell Biol. 41, 60–65.
Rajawat, J., Mir, H., Begum, R., 2011. Differential role of poly (ADP-ribose) polymerase in *D. discoideum* growth and development. BMC Dev. Biol. 11, 14.
Rajawat, J., Vohra, I., Mir, H., Gohel, D., Begum, R., 2007. Effect of oxidative stress and involvement of poly (ADP-ribose) polymerase (PARP) in *Dictyostelium discoideum* development. FEBS J. 274, 5611–5618.
Rajawat, J., Mir, H., Alex, T., Bakshi, S., Begum, R., 2014. Involvement of poly (ADP-ribose) polymerase in paraptotic cell death of *D. discoideum*. Apoptosis 19, 90–101.
Rajawat, J., Alex, T., Mir, H., Kadam, A., Begum, R., 2014. Proteases involved during oxidative stress-induced poly (ADP-ribose) polymerase-mediated cell death in *Dictyostelium discoideum*. Microbiology 160, 1101–1111.
Raper, K.B., 1984. The Dictyostelids. Princeton University Press, Princeton, New Jersey, pp. 1–453.
Saran, S., Schaap, P., 2004. Adenylyl cyclase G is activated by an intramolecular osmosensor. Mol. Biol. Cell 15, 1479–1486.
Sawai, S., Guan, X.J., Kuspa, A., Cox, E.C., 2007. High-throughput analysis of spatio-temporal dynamics in *Dictyostelium*. Genome Biol. 8, R144.
Semighini, C.P., Savoldi, M., Goldman, G.H., Harris, S.D., 2006. Functional characterization of the putative *Aspergillus nidulans* poly (ADP-ribose) polymerase homolog PrpA. Genetics 173, 87–98.
Simonin, F., Poch, O., Delarue, M., de Murcia, G., 1993. Identification of potential active-site residues in the human poly(ADP-ribose) polymerase. J. Biol. Chem. 268, 8529–8535.
Sussman, M., 1987. Cultivation and synchronous morphogenesis of *Dictyostelium* under controlled experimental conditions. Methods Cell. Biol. 28, 9–29.
Suzuki, Y.J., Forman, H.J., Sevanian, A., 1997. Oxidants as stimulators of signal transduction. Free Radic. Biol. Med. 22, 269–285.
Szabó, C., Dawson, V.L., 1998. Role of poly (ADP-ribose) synthetase in inflammation and ischaemia–reperfusion. Trends Pharmacol. Sci. 19, 287–298.
Tulin, A., Allan, S., 2003. Chromatin loosening by poly(ADP)-ribose polymerase (PARP) at *Drosophila* puff loci. Science 299, 560–562.
Uchida, K., Suzuki, H., Maruta, H., Abe, H., Aoki, K., Miwa, M., Tanuma, S., 1993. Preferential degradation of protein-bound (ADP-ribose)n by nuclear poly(ADP-ribose) glycohydrolase from human placenta. J. Biol. Chem. 268, 3194–3200.

Van Gool, L., Meyer, R., Tobiasch, E., Cziepluch, C., Jauniaux, J.C., Mincheva, A., Lichter, P., Poirier, G.G., Burkle, A., Küpper, J.H., 1997. Overexpression of human poly (ADP-ribose) polymerase in Transfected hamster cells leads to increased poly (ADP-ribosyl)ation and cellular sensitization to gamma irradiation. Eur. J. Biochem. 244, 15–20.

Wahlberg, E., Karlberg, T., Kouznetsova, E., Markova, N., Macchiarulo, A., Thorsell, A. G., Pol, E., Frostell, Å., Ekblad, T., Öncü, D., Kull, B., Robertson, G.M., Pellicciari, R., Schüler, H., Weigelt, J., 2012. Family-wide chemical profiling and structural analysis of PARP and tankyrase inhibitors. Nat. Biotechnol. 30, 283–288.

Watts, D.J., Ashworth, J.M., 1970. Growth of myxamoebae of the cellular slime mould *Dictyostelium discoideum* in axenic culture. Biochem. J. 119, 171–174.

Yang, L., Huang, K., Li, X., Du, M., Kang, X., Luo, X., Lu, G., Cheng, W., Yanqing, Z., Zhang, C., 2013. Identification of poly(ADP-ribose) polymerase-1 as a cell cycle regulator through modulating Sp1 mediated transcription in human hepatoma cells. PloS One 8 (12), e82872.

Cell Proliferation

Cell Prolif., 2015, **48**, 363–374 doi: 10.1111/cpr.12182

Response of *Dictyostelium discoideum* to UV-C and involvement of poly (ADP-ribose) polymerase

H. Mir, T. Alex, J. Rajawat, A. Kadam and R. Begum

Department of Biochemistry, Faculty of Science, The Maharaja Sayajirao University of Baroda, Vadodara, Gujarat 390002, India

Received 2 June 2014; revision accepted 5 December 2014

Abstract

Objectives: Radiation and chemical mutagens are direct DNA-damaging agents and ultraviolet (UV) radiation is frequently used in biological studies. Consequent to ozone depletion, UV-C could become a great challenge to living organisms on earth, in the near future. The present study has focused on the role of poly (ADP-ribose) polymerase (PARP) during UV-C-induced growth and developmental changes in *Dictyostelium discoideum,* a phylogenetically important unicellular eukaryote.

Materials and methods: *Dictyostelium discoideum* cells were exposed to different doses of UV-C and PARP activity, and effects of its inhibition were studied. Expression of developmentally regulated genes *yakA*, *car1*, *aca*, *csA*, *regA*, *ctnA*, *ctnB*, *gp24*, *hspD* and *dsn* were analysed using semi-quantitative RT-PCR.

Results: We report that the *D. discoideum* cells displayed PARP activation within 2 min of UV-C irradiation and there was increase in NO levels in a dose-dependent manner. UV-C-irradiated cells had impaired growth, delayed or blocked development and delayed germination compared to control cells. In our previous studies we have shown that inhibition of PARP recovered oxidative stress-induced changes in *D. discoideum*; however, intriguingly PARP inhibition did not correct all defects as effectively in UV-C-irradiated cells. This possibly was due to interplay with increased NO signalling.

Conclusions: Our results signify that UV-C and oxidative stress affected growth and development in *D. discoideum* by different mechanisms; these studies could provide major clues to complex mechanisms of growth and development in higher organisms.

Abbreviations

Ax-2: axenic 2

FITC: fluorescein isothiocyanate

HA: hydroxylamine

iNOS: inducible nitric oxide synthase

NO: nitric oxide

PAR: poly-ADP ribose

PARP: poly(ADP-ribose) polymerase

PBA: phosphate-buffered agar

SB: Sorenson's buffer

G0, G1, G2, M, S: phases of the cell cycle

L-NIO: iNOS inhibitor

Introduction

Dictyostelium discoideum is a unicellular organism that feeds on bacteria and divides (under favourable environmental conditions) approximately every 4 h. It divides every 8–12 h in axenic media. During starvation, cells become chemotactically sensitive to cAMP pulses and initiate their developmental program to ultimately form a multicellular fruiting body, consisting of spores within a sorocarp, and a stalk. Spores germinate to form unicellular amoebae under favourable conditions. *Dictyostelium discoideum,* being a eukaryote that stands at the transition point of unicellularity and multicellularity, is an exceptional model system to study various signal transduction pathways (1) that can be extrapolated to mammalian systems. The unicellular stage is known to be highly resistant to DNA-damaging agents and oxidative stress (2,3).

Ionising radiation and chemical mutagens are direct DNA-damaging agents. Ultraviolet (UV) radiation, of a

Correspondence: R. Begum, Department of Biochemistry, Faculty of Science, The Maharaja Sayajirao University of Baroda, Vadodara, Gujarat – 390002, India. Tel.: +91 265 2795594; Fax: +91 265-2795594; E-mail: rasheedunnisab@yahoo.co.in

broad band of energy extending from 200 to 400 nm, is one of the frequently used types of radiation in biological studies. UV wavelengths of the solar electromagnetic spectrum can be subdivided into three regions: UV-C (200–280 nm), UV-B (280–315 nm) and UV-A (315–400 nm). Of these, UV-C is the most harmful although its rays do not reach the surface earth, due to the protective ozone layer. All UV-C and approximately 90% UV-B radiation is absorbed by ozone, water vapour, oxygen and carbon dioxide [WHO] as sunlight passes through the atmosphere. However, consequent to ozone depletion, UV-C could become a great challenge to living organisms in the future. Oxidative stress induced by ionizing radiation and alkylating agent accounts for DNA damage induced by these agents. UV-C can cause formation of thymine glycol (4) but the main lesions are caused by cyclobutane pyrimidine dimers (CPDs) and pyrimidine-(6-4)-pyrimidone photoproducts (5). In double-stranded DNA, these lesions lead to generation of SSBs (single-strand breaks) when they are repaired by NER (nucleotide excision repair) (6). They also lead to distortion in the DNA double helical structure which is sufficient to activate the nuclear enzyme, poly(ADP-ribose) polymerase (PARP) (7). PARP uses NAD^+ as donor of poly(ADP-ribose) and catalyses poly(ADP ribosylation) (PARylation), of itself and of a variety of other proteins. Numerous substrates list PARP and link it to a wide range of physiological processes. Primarily, it is involved in chromatin remodelling, DNA repair and maintenance of genomic integrity (8–13). PARP contributes to cellular homoeostasis under conditions of basal DNA damage, wherein it is involved in cell cycle arrest (14). During conditions of moderate/severe cell stress, PARP over-activation leads to cell death resulting in various pathological conditions (15). PARP inhibition during moderate/severe cellular stress is beneficial (16) and we have reported long-term consequences of PARP inhibition and down-regulation (17) in oxidative stressed *D. discoideum* cells (18,19). Also, staurosporine-induced cell death has been studied in *D. discoideum* (20). In the present study, the role of PARP in UV-C-induced growth and developmental changes in *D. discoideum* has been addressed by inhibiting its activity with benzamide, and also long-term effects of PARP inhibition for two successive generations and interplay with nitric oxide (NO) have been explored.

Materials and methods

Cell death after UV-C stress

Dictyostelium discoideum cells (Ax-2 strain) were grown in suspension in HL5 medium (21), with shaking at 3 g, at 22 °C. All experiments were carried out with *D. discoideum* cells at mid log phase expansion, cell density 2.5×10^6 cells/ml. Cells were washed in 1× SB (1× Sorenson's buffer from 50× SB, 2 mM Na_2HPO_4, 15 mM KH_2PO_4, pH 6.4) by centrifugation, at 300 ***g*** for 5 min, then exposed to different doses of UV-C (254 nm) (10.4 J/m^2, 13 J/m^2, 65 J/m^2 and 130 J/m^2). Cells were then resuspended in HL5 after pelleting, and incubated at 22 °C, with shaking at 150 rpm, for 24 h.

Growth curve studies

For growth curve studies after UV-C irradiation, 1% inoculations (50 µl from ~2.5×10^6 cells/ml into 5 ml) were performed in HL5 medium, and cell viability was assayed using the trypan blue exclusion technique, every 24 h until death (22).

Cell cycle analysis

The cell cycle was analysed by flow cytometry using propidium iodide. Mid-log-phase cells were fixed by drop wise addition of 70% ethanol, and incubated at 4 °C overnight. Fixed cells were resuspended in staining solution (TritonX-100, DNase-free RNase and propidium iodide) and incubated for 30 min, followed by FACS analysis (23). Quantification was performed using flow cytometry, with FACS ARIA (BD Biosciences, San Jose, CA, USA). Data were analysed with FACSDiva software.

Developmental studies

2.5×10^6 cells were harvested and processed as described above for UV-C treatment (10.4 J/m^2, 13 J/m^2, 65 J/m^2 and 130 J/m^2), then were resuspended in 100 µl 1× SB and spread on non-nutrient agar plates (2% agar in 1× SB) kept at 22 °C, and different stages of development were studied.

Chemotactic assay

Chemotactic studies were performed according to the method of Wallace and Fraizier (24). Exponentially growing cells were washed free of medium with 1× SB and starved for 5–6 h after treatment. Of the cell suspension, 5 µl were placed on 2% agar surfaces at a distance of 2 mm from wells containing 1 µM cAMP. Movement of cells towards wells was observed using phase contrast microscopy (Nikon TE-2000S, Tokyo, Japan) and was photographed. Relative number and distance moved by cells was an indication of their chemotactic activity.

cAMP pre-treatment. Exogenous (1 μM) cAMP was added 2.5 h prior to UV-C treatment to *D. discoideum* cells in 1× SB. Plates were then kept at 22 °C to observe different stages of development, or cells were harvested to study developmental gene expression, at various time points.

cAMP estimation in UV-C-irradiated cells

5×10^6 cells were harvested by centrifugation at 300 ***g***/5 min/4 °C and subjected to UV-C irradiation and they were resuspended in Sorenson's buffer for 6 h. Cells were then collected, and extracellular cAMP was estimated in the buffer, using an ELISA kit method according to the manufacturer's instructions (Calbiochem, Gibbstown, NJ, USA). A total of 200 μM L-NIO (iNOS inhibitor) pre-treated cells were also collected, and extracellular cAMP was estimated.

Nitric oxide estimation

NO generation was estimated according to the method of Green *et al.* (25). 5×10^6 cells were suspended in 1 ml 1× SB and incubated at 22 °C for 20 min, to allow for accumulation of NO. 1 ml Griess reagent was added and mixed in well. Incubation was again carried out at 22 °C for 15–30 min. Absorbance was measured at 546 nm.

PARP activation under UV-C stress

Cells treated with different doses of UV-C were processed for PARP assay (19). Data were analysed using Image Proplus software to calculate mean intensity of fluorescence from different fields and ~50 cells were examined for each dose. PARP was inhibited by 12 h pre-treatment with 1 mM benzamide (Sigma Aldrich, St Louis, MO, USA), prior to UV-C irradiation.

Expression analysis of developmentally regulated genes, by RT-PCR

RNA extraction and cDNA synthesis. Dictyostelium discoideum cells were exposed to UV-C stress as mentioned above. After specific pre-treatment, cells were pelleted and washed in 1× SB before finally being resuspended in 1× SB. Total RNA was isolated from cells at two time points (as specified in figure 4) using TRIZOL reagent (Invitrogen, Carlsbad, CA, USA). RNA integrity was verified by 1.5% agarose gel electrophoresis and 260/280 absorbance ratio >1.95. RNA was treated with DNase I (Ambion Inc., Austin, TX, USA) before cDNA synthesis, to avoid DNA contamination. Reactions were performed by reverse transcriptase using RevertAid First Strand cDNA Synthesis Kit (Fermentas, Vilnius, Lithuania) according to the manufacturer's instructions, in MJ Research Thermal Cycler (Model PTC-200, Watertown, MA, USA).

Second strand synthesis. First-strand cDNA was used as a template with gene-specific primers to synthesize second strand DNA by conventional PCR. Expression kinetics of DYRK family protein kinase (*yakA*), cAMP receptor-1 (*car1*), adenylyl cyclase (*aca*),cell adhesion molecule–contact site A protein (*csA*), component of the counting factor complex–countin A (*ctnA*) and countin B (*ctnB*), calcium-dependent cell adhesion molecule-1 (*gp24*), cAMP phosphodiesterase (*regA*), a heat shock protein of Hsp90 family (*hspD*) and discoidin (*dsn*) genes were analysed. *rnlA* was used as internal control (Table 1). Reactions were performed according to the manufacturer's instructions (Fermentas, Burlington, ON, Canada). DNA fragments were amplified for 24 cycles and signal intensities were analysed on 2% agarose gel stained with ethidium bromide. Densitometric analysis was performed using AlphaImager software, and mean density for respective genes with respect to *rnlA*, was plotted.

Fate of spores formed under UV-C stress. Spores formed from cells irradiated with 10.4 J/m^2 UV-C in the presence and absence of benzamide (Sigma Aldrich)

Table 1. Primer sequences used for gene expression analysis.

Gene	Primer sequence
*yak*A Forward	5′-GCTTAGAGGACTTTCAACCAATTT-3′
*yak*A Reverse	5′-GATTTTTCATAACAAGCAGATCCA-3′
*cAR*1 Forward	5′-TGTGGACTTTATGTCTTGCAATTAG-3′
*cAR*1 Reverse	5′-CCAATACTGCTGAAATTGCCC-3′
aca Forward	5′-GTGATACTGCCAATACCGCC-3′
aca Reverse	5′-ACCCAAGAGAGTTCCAGATAATGG-3′
*cs*A Forward	5′-ATAGTGCACATTCAGCTCC-3′
*cs*A Reverse	5′-AAGAACTTTGCCATACTTTGG-3′
*ctn*A Forward	5′-ATGAATAAATTATTTTCATTAATTTTAG CTTTATTCCTTGTCAACTCCGC-3′
*ctn*A Reverse	5′-TTAAAATAAAGCAAAACCTGAACCTGA ACCAGAGGCGGCACC-3′
*ctn*B Forward	5′-GTGGTGCCGTTTGTTCATTACTCCC-3′
*ctn*B Reverse	5′-CCAGTTGGGTCAGTTACCATAACAGCAAC-3′
*gp*24 Forward	5′-CCAGGAGCTTTTCAATGGGCAGTTGATG-3′
*gp*24 Reverse	5′-GTGTAACAGTCATATTCTTTGGGAATGTCTC-3′
dsn Forward	5′-CCACCCATTAACCTGGAATG-3′
dsn Reverse	5′-TGGTGGCATCAGTACAATCG-3′
*hsp*D Forward	5′-ACATTCCAAGCTGAAATTAATCAGC-3′
*hsp*D Reverse	5′-GTGTAAGAGTTTTGGCAGTCTTATC-3′
*reg*A Forward	5′-AATTGTTGGGGATACTGAATCAGC-3′
*reg*A Reverse	5′-ATAAAGTGCGGTGATATTTC-3′
*rnl*A Forward	5′-TTACATTTATTAGACCCGAAACCAAGCG-3′
*rnl*A Reverse	5′-TTCCCTTTAGACCTATGGACCTTAGCG-3′

were picked from different areas, with the aid of sterilized nichrome loops, and added to 5 ml HL5 medium. Flasks were kept shaking at 150 rpm/22 °C. After germination, cells were counted using a haemocytometer, every 12 h, for growth curve experiments.

Assessment of DNA damage in cells germinated from spores (26). Histones become phosphorylated during oxidative stress. Hence, presence of phosphorylated histone indicates oxidative stress-induced DNA damage. Anti-H2AX at 0.5 μg/ml, and anti-mouse IgG (whole molecule)–TRITC conjugate (Sigma, St. Louis, MO, USA), 1:200, were used to study presence of oxidative stress. Cells were pelleted and washed once in phosphate-buffered saline (PBS) pH 7.4, fixed in 70% chilled methanol for 10 min at −20 °C, then washed in blocking solution (1.5% BSA with 0.05% Tween 20 in PBS) and incubated for 1 h in primary antibody. After incubation, cells were washed 2–3 times in blocking solution and further incubated for 1 hr with TRITC-labelled secondary antibody. Then, they were washed 2–3 times in PBS and fluorescence was observed under 60× magnification. Data were analysed using Image Proplus software to calculate mean density of fluorescence and graphs were plotted using Graphpad prism software.

Results

Cell death and PARP activation after UV-C irradiation

Cell death was monitored after different doses of UV-C irradiation. UV-C dose (10.4 J/m^2 and 13 J/m^2) led to less than 10% cell death (Fig. 1a). UV-C is a potent DNA damage inducer and is well reported to activate PARP (7,15). PARP was assayed at various time points post UV-C stress. 10.4 J/m^2 and 13 J/m^2 UV-C-treated cells had highest PARP activity at 2 min (Fig. 1b), which then declined, and reached basal levels after 5 min. Benzamide pre-treated cells had reduced activation of PARP (Fig. 1b).

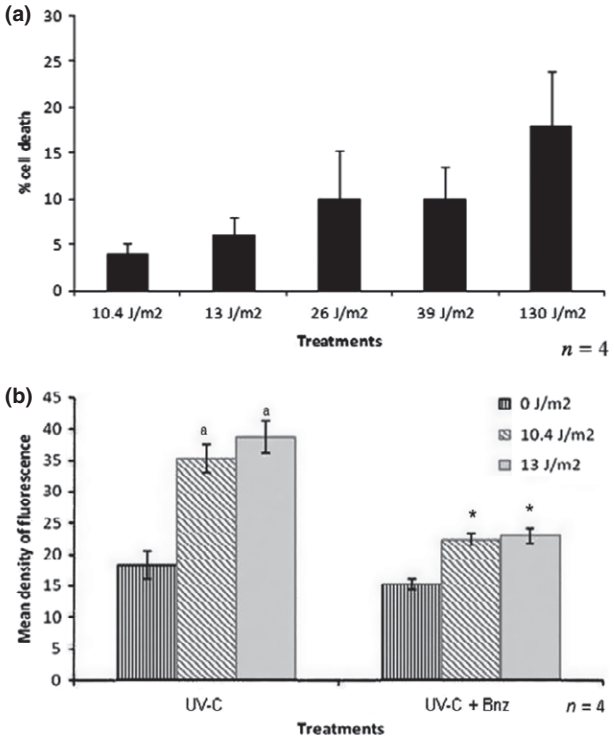

Figure 1. Cell death and PARP activation in UV-C-irradiated cells. (a) UV-C induced dose-dependent cell death as monitored by the trypan blue exclusion method. Results are mean ± SE of four independent experiments. (b) Peak PARP activity induced by UV-C irradiation was intercepted by benzamide. Benzamide inhibited PARP activity at 2 min post 10.4 J/m^2 and 13 J/m^2 irradiation respectively. Data (mean ± SE) are from four independent experiments. *$P < 0.05$ compared to control; $^a P < 0.05$ compared to respective dose of UV-C irradiation, without benzamide pre-treatment.

Dictyostelium discoideum *growth and development under UV-C stress*

Growth analysis revealed dose-dependent increase in lag phase with UV-C dose. As can be seen from Fig. 2a, with increase in UV-C dose, there was increase in lag phase and consequently late entry into the log phase. Also, the stationary phase was achieved at lower density compared to control cells. Pre-treatment of cells with benzamide reseulted in partial rescue in UV-C-induced changes in growth (Fig. 2a). Lag phase growth of UV-C-stressed cells can be clearly explained by cell cycle analysis studies, wherein UV-C-stressed cells were seen to be arrested in G0/G1 (~77%) as opposed to untreated control cells (~68%), at 48 h growth (Fig. 2b). Also, marked reduction is seen in percentage of cells in S phase after UV-C irradiation at 10 J/m^2 (13.6%) and 13 J/m^2 (12.1%) compared to untreated control cells (22.1%) (Fig. 2b), explaining the slower growth in stressed cells.

Effects of UV-C on development also reflected dose dependency as seen in growth (Fig. 3); however, it was more drastic. Cells exposed to 13 J/m^2 (Fig. 3) and higher doses (65 J/m^2 and 130 J/m^2) (data not shown) UV-C failed to undergo complete development. 10.4 J/m^2 UV-C-treated cells displayed development that was delayed compared to control cells. Delay in development induced by 10.4 J/m^2 was rescued when cells were pretreated with benzamide (Fig. 3). Interestingly after 12 h, benzamide-pretreated cells exposed to higher doses (65 J/m^2) of UV developed streaming structures and incompetence to form aggregates, compared to untreated control and UV-C-exposed cells.

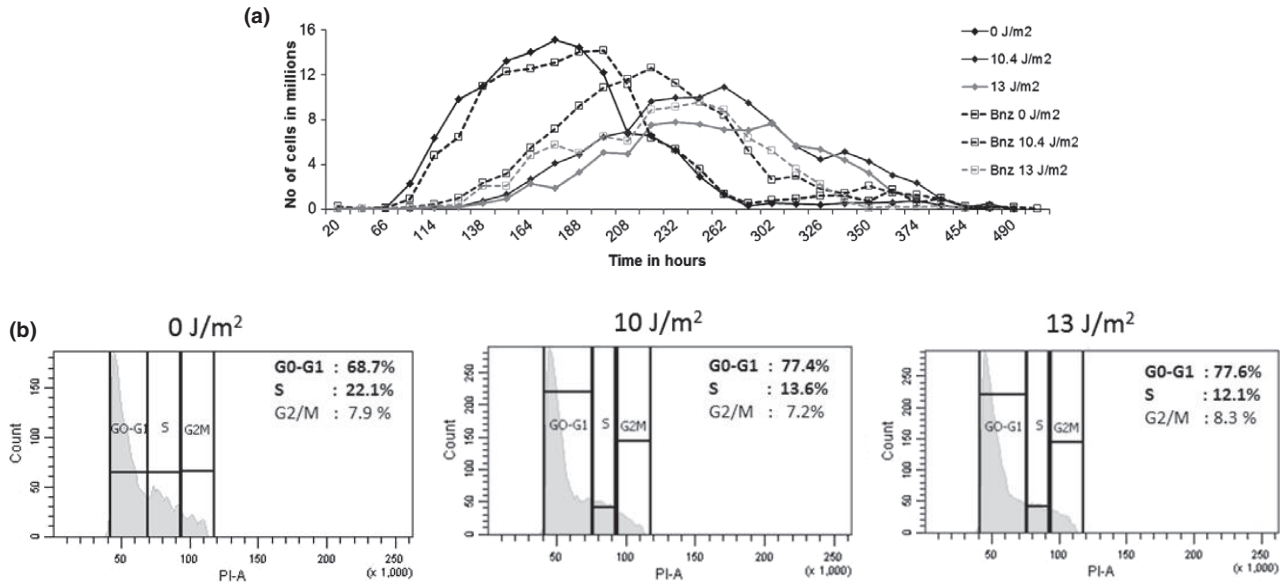

Figure 2. Effect of PARP inhibition on UV-C induced growth changes and fate of spores in *Dictyostelium discoideum.* (a) Effect of PARP inhibition on UV-C induced growth changes Benzamide rescued UV-C-induced changes as shown in the growth curve. The stationary phase was achieved at higher cell density in benzamide pre-treated cells compared to respective control. Results are mean of four independent experiments. (b) Cell cycle analysis of UV-C-irradiated cells by propidium iodide staining. The 10.4 J/m^2 and 13 J/m^2 UV-C-treated cells had G0/G1 arrest, i.e. ~77% cells were in G0/G1 phase in contrast to ~68% untreated control cells. This figure is a representative picture of three independent experiments performed.

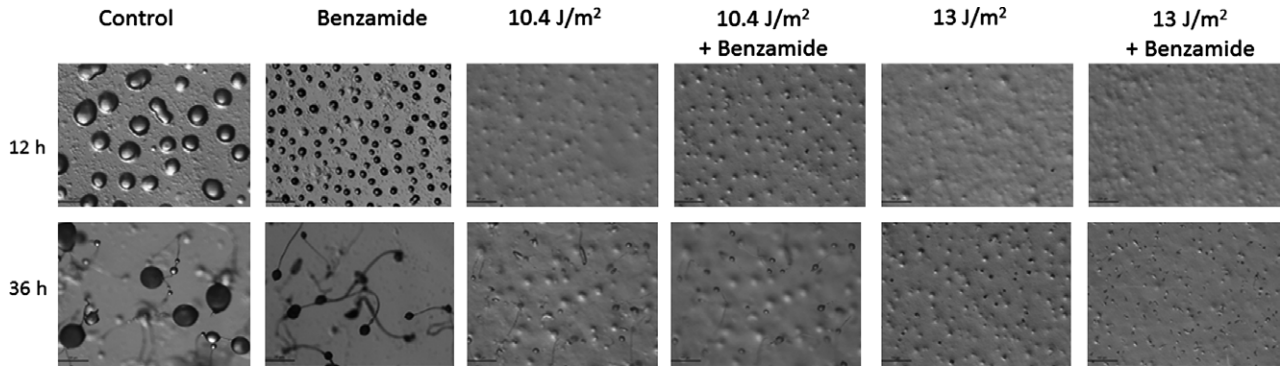

Figure 3. Development of *Dictyostelium discoideum* cells under UV-C stress. *Dictyostelium discoideum* cells after UV-C treatment were allowed to develop on nutrient-free agar medium and were observed at various time intervals. Benzamide pre-treatment restored the delay induced by 10.4 J/m^2 but did not lead the 13 J/m^2 UV-C-treated cells to complete development, though the cells entered it. Photographs taken with 4× objective. Scale = 100 μm.

Also, developing fruiting bodies formed after 10.4 J/m^2 UV-C stress were smaller and ~40% greater in number. Cells subjected to UV-C stress formed less compact aggregates (Fig. 3). This observation led us to assess expression profile of development-related genes such as *ctnA*, *ctnB*, *dsn1*, *hspD*, *csA* and *gp24*. These are associated with regulation of aggregate size (27–29). Expression profiles of *yakA*, *car1*, *aca* and *regA* were also studied as these genes are important for growth to differentiation transition and cAMP-mediated signalling, respectively (1,30). As shown in Fig. 4a and 4b, UV-C affected levels of *ctnA*, *yakA*, *car1*, *aca, csA* and *regA* mRNA. Benzamide pre-treatment prevented UV-C-induced changes in expression of *ctnA* and *regA*; however, *yakA*, *car1*, *aca* and *csA* expression levels could not be restored. Altered expression levels of *yakA, car1, aca, csA* and *regA* during UV-C stress indicated that the finely tuned cAMP signalling network of development was affected, which was re-established by *yakA, car1* and *aca* restoration in presence of exog-

enous cAMP. To probe effects on cAMP signalling, chemotactic assay and cAMP estimations were undertaken**.** Control amoebae moved toward 1 μM cAMP wells, while UV-C-irradiated cells failed to sense cAMP in cups (Fig. 5a). These results justify effects of exogenous cAMP on altered expression profiles of developmentally regulated genes (Fig. 4a, b) and on developmental arrest (Fig. 5b). Also cAMP levels were found reduced in UV-C-irradiated cells (Fig. 6). Spores developed after 10.4 J/m^2 UV-C irradiation were delayed by around 27 h in revival (111 h ± 6.0) compared to control cells (81 h ± 6.658) (Fig. 7a). These spores also had longer lag phases compared to controls. However, benzamide pre-treatment had no effect on revival of spores formed after 10.4 J/m^2 UV-C exposures as shown in (Fig. 7a). Also this second generation of UV-C-exposed cells did not differ from that of control cells with respect to damage in DNA (Fig. 7b); ensuring that partial inhibition of PARP did not interfere with basal repair of the cells.

UV-C-induced developmental changes restored by iNOS inhibition

UV-C radiation, unlike oxidative stress, leads to increased NO generation which may further interfere with *D. discoideum* development. Hence, we monitored effects of inducible nitric oxide synthase inhibitor (L-NIO) on UV-C-induced developmental changes. UV-C dose of 13 J/m^2 caused arrested development. However, 200 μM L-NIO (iNOS inhibitor) pre-treated cells exhibited partial rescue in developmental delay due to UV-C treatment (Fig. 8a). These results were further confirmed by monitoring NO production under UV-C stress (Fig. 8b). Results clearly suggest that *D. discoideum* cells exposed to UV-C irradiation had dose-dependent increase in production of nitric oxide, and NO levels decreased significantly ($P < 0.05$) on benzamide pre-treatment. Also inhibition of iNOS partially restored cAMP levels (Fig. 6). Thus, increased NO generation affected signalling in UV-C-exposed cells, thereby impeding their development.

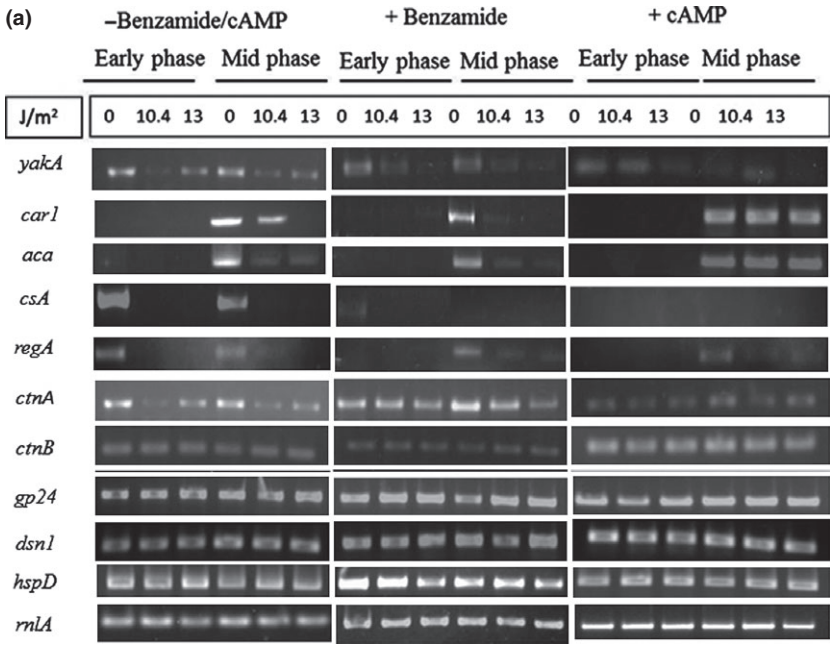

Figure 4. (a) Irradiation with UV-C affected mRNA expression of various genes involved in *Dictyostelium discoideum* development. Expression of *yakA*, coding for cell cycle arrest protein; cAMP receptor – *cAR1*, *aca* coding for adenyl cyclase A, countin, coding for a protein involved in cell counting mechanism, *csA*, a cell adhesion molecule and *regA*, a phosphodiesterase were found to be reduced in UV-C-treated cells compared to internal control *rnlA* (mitochondrial rRNA IG7). Benzamide pre-treatment restored expression levels of countin, however, it did not affect *yakA* and *cAR1* mRNA levels. Levels of countin (another protein of cell counting mechanism) mRNA were found increased in benzamide pre-treated cells. Exogenous cAMP restored *cAR1* without affecting *yakA* and *csA*. Expression of *dsn,* a gene coding for a protein which helps cells to adhere to the substratum, *hspD*, a heat shock protein and *gp24* (intercellular contacts and aggregation) were not affected. mRNA levels of *yakA*, *cAR1, aca*, *csA* and *regA* were assayed at 0 and 9 h, while the rest of the genes were assayed at 6 and 10 h of development induction. (b) Densitometric analysis of various genes involved in *D. discoideum* development. $*^{**,aaa,+++,\$\$\$,\#\#\#,\&\&\&}P < 0.001$ compared to respective controls; $*^{*,aa,++,\$\$,\#\#,\&\&}P < 0.05$ compared to respective controls and $*^{,a,+,\$,\#,\&}p < 0.05$ compared to respective controls. For benzamide pre-treated and 13 J/m^2 UV-C-treated cells, $^{bbb}P < 0.001$, $^{bb}P < 0.01$ compared to 13 J/m^2 UV-C-treated cells (-benzamide/-cAMP). For cAMP pre-treated and 13 J/m^2 UV-C-treated cells, $^{qqq}P < 0.001$, $^{qq}P < 0.01$ compared to 13 J/m^2 UV-C-treated cells (benzamide/cAMP).

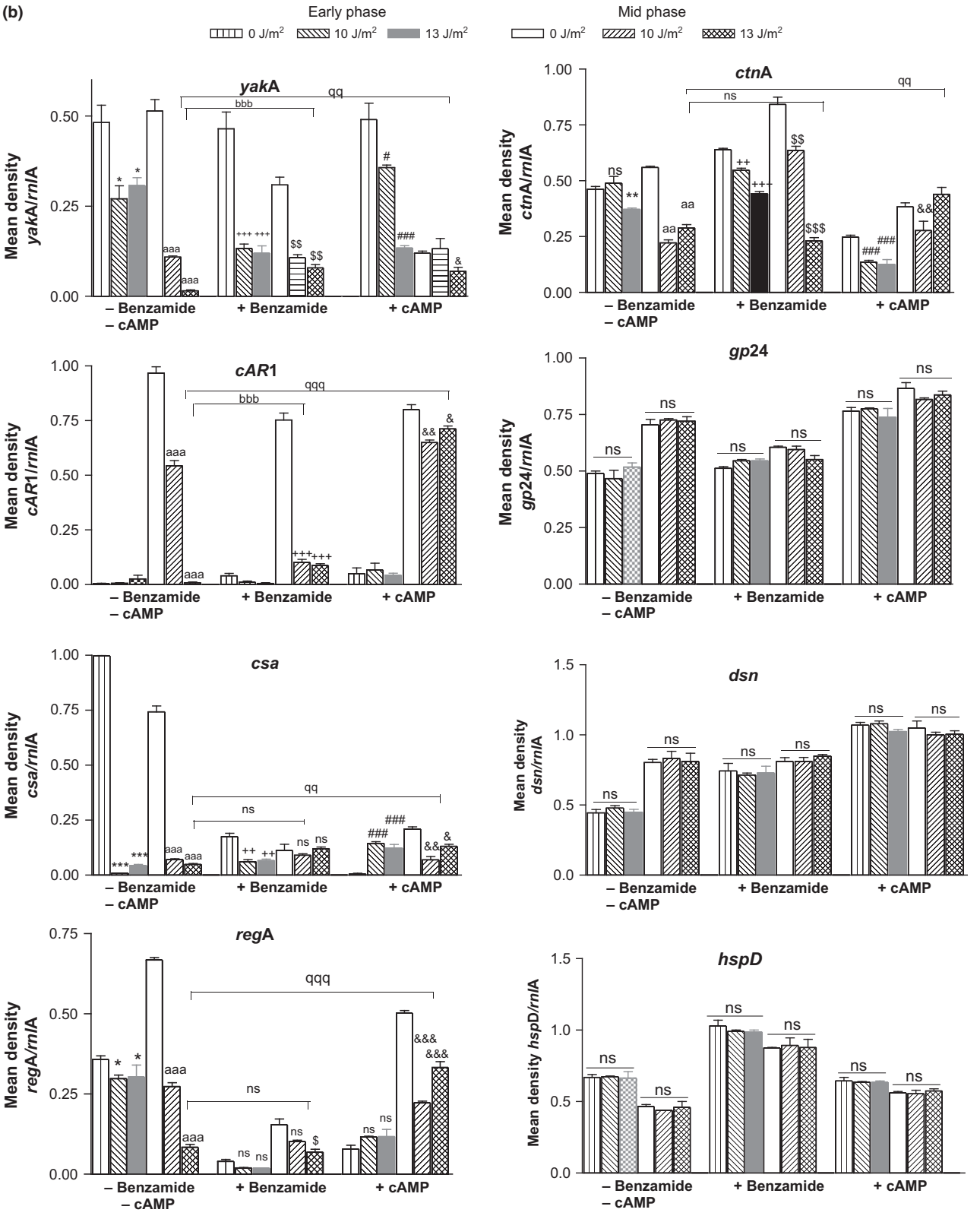

Figure 4. (Continued).

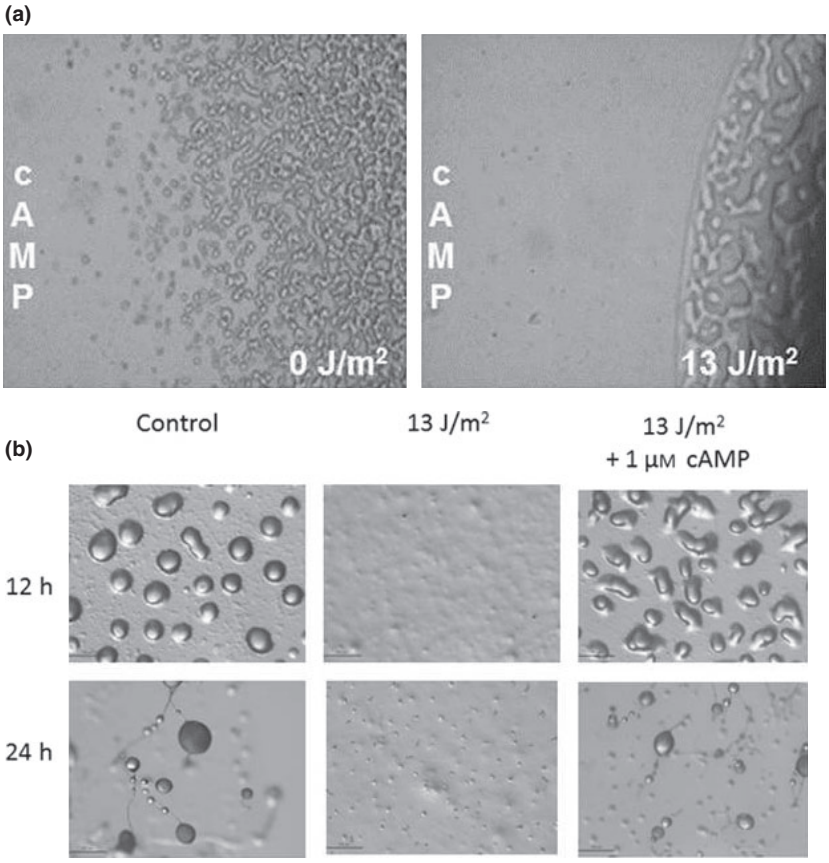

Figure 5. Effect of UV-C irradiation on chemotaxis in *Dictyostelium discoideum.* (a) UV-C-exposed *D. discoideum* cells failed to move towards cAMP. Wells were formed on PBA plates using a cup borer and were filled with 100 µl of 1 µM cAMP; cells were placed at a distance of 2 mm from wells. Photographs were captured 6 h after plating the cells at 4× magnification. Results are representative of three independent experiments. (b) Exogenous cAMP resumed development of UV-C-exposed *D. discoideum* cells. Exposure to 13 J/m^2 UV-C blocked initiation of development; however supplementation with cAMP (1 µM) restored development. Photographs were captured at 4× magnification. Results representative of three independent experiments. Scale = 100 µm

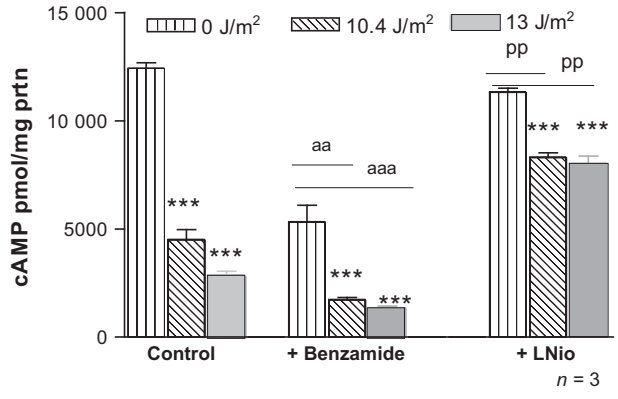

Figure 6. cAMP levels in UV-C irradiated *Dictyostelium discoideum* were reduced in NO-dependent manner. UV-C irradiated *D. discoideum* cells had reduced cAMP levels. Cells pre-treated with iNOS inhibitor, L-NIO, retained levels of cAMP even after UV-C exposure. Results are mean ± SE of three independent experiments. $^{*}P < 0.05$, $^{***}P < 0.001$ compared to control (0 J/m^2), $^{a}P < 0.05$ and $^{aa}P < 0.01$ compared to benzamide pre-treated cells and $^{PP}P < 0.01$ compared to L-NIO pre-treated cells.

Discussion

PARP characteristics render it an ideal candidate for participation in cell responses to UV stress (31). UV-C induces direct DNA lesions such as CPDs (e.g. T-T, T-C or C-C) or 6,4-photoproducts. These lesions distort DNA structure. DNA strand breaks generated during excision repair of such lesions activate PARP (32–35). Using elegant techniques that allow visualization of events occurring in UV-C-irradiated zone, Vodenicharov *et al.,* (36) demonstrated that UV-C causes immediate PARP activation within the first 15 s to 5 min. Our results corroborate these reports. UV-C treatment lead to both dose-dependent cell death and PARP activation within 2 min (Fig. 1). Cells exposed to higher doses of UV-C (130 J/m^2) had a longer lag phase (~100 h) than at milder doses, which could be due to seized cell cycle (Fig. 2b). This is in accordance with the finding that UV-C lead to cell cycle arrest after activation of the repair machinery (37). PARP inhibition allowed cells exposed to 10.4 J/m^2 UV-C to enter the log phase earlier than UV-C-only exposed cells. These also attained higher cell density compared to10.4 J/m^2 UV-C-only irradiated cells, suggesting that PARP played a role in cell cycle arrest and DNA repair.

Dictyostelium discoideum, during its unicellular vegetative phase, exhibits higher resistance to oxidative stress (3) and other DNA-damaging agents (2,20). Very high doses of hydroxylamine (4 mM) leading to ~90%

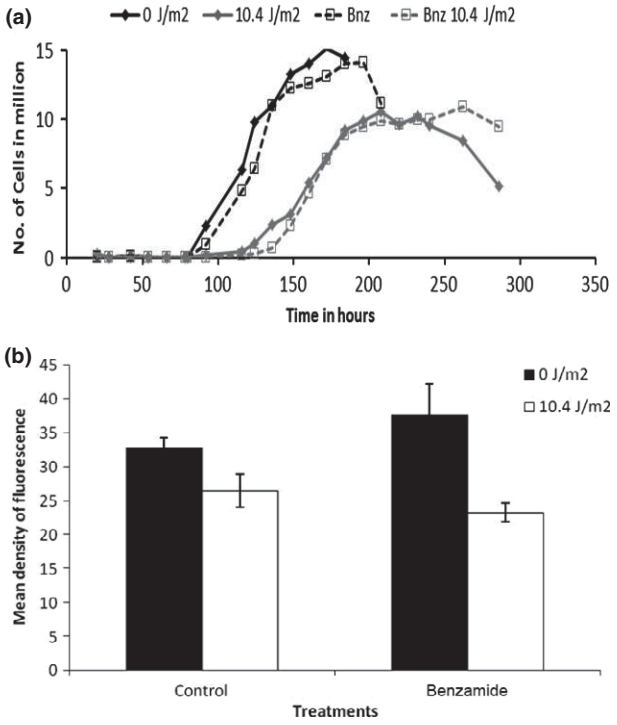

Figure 7. (a) Effect of PARP inhibition on fate of spores developed under UV-C stress. Spores of control cells revived within 81 h whereas spores formed after 10.4 J/m^2 UV-C stress exhibited ~27 h of delay in spore revival, which could not be rescued by benzamide pre-treatment. Data are mean of four independent experiments. (b) DNA damage monitored in second-generation *Dictyostelium discoideum* cells. No significant damage was observed in second-generation cells.

cell death, is required to block *D. discoideum* development (17,18). Surprisingly, the effect of UV-C is more drastic on *D. discoideum* development. Doses of UV-C equivalent to 13 J/m^2 (~6% cell death) or higher, completely arrested *D. discoideum* development at the loose aggregate stage, whereas 10.4 J/m^2 UV-C-irradiated cells completed development albeit delayed (Fig. 3). Benzamide pre-treatment of 13 J/m^2 UV-C-exposed cells had streaming structures indicating a definite role of PARP in development. This is supported by work previously published (19) from our laboratory, where we showed that both constitutive and slug stage-specific down-regulation of PARP lead to blocked or arrested development respectively. Protective effects of PARP inhibition were not seen at doses higher than 13 J/m^2, as cells died (38).

Azzam *et al.* (39) demonstrated cell type-specific effect of UV-C irradiation on expression of connexin 43 native isoform, in human fibroblasts and AG1522 cells. Experiments performed with UV-C irradiation in human skin fibroblasts (37) showed that UV-C reduced transcription of certain proteins involved in adhesion and motility. Hence, expression of certain genes crucial to various aspects of *Dictyostelium* development were assessed. Our results indicate that heat shock protein D, a cytosolic protein was required for early developmental stages. Discoidin-1, a marker of growth to differentiation transition that aids differentiating cells adhere to the substratum and gp24, required for filopodia formation and

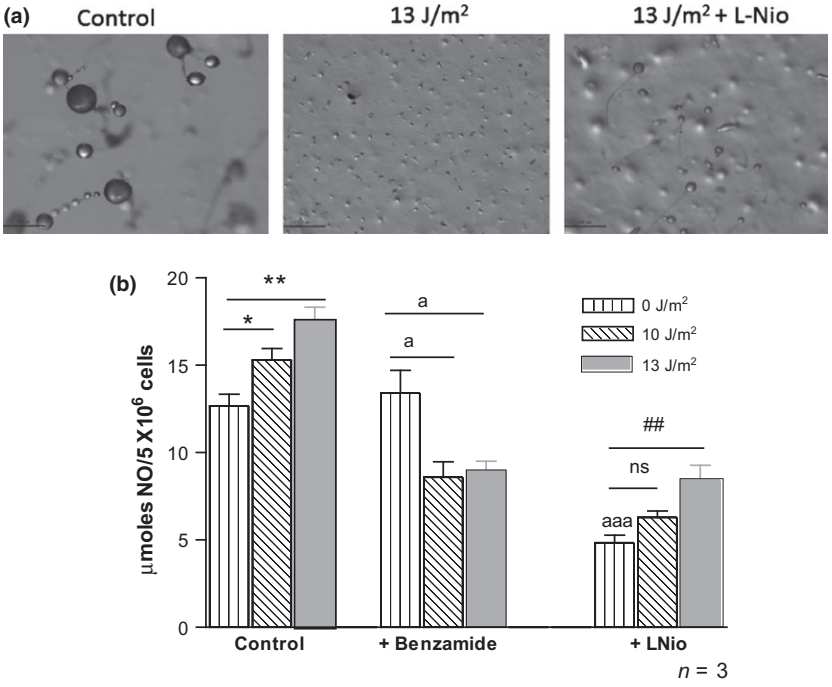

Figure 8. Effect of UV-C on development of *Dictyostelium discoideum* under iNOS inhibition and nitric oxide generation. (a) Development of UV-C-irradiated cells pre-treated with iNOS inhibitor. L-NIO-treated cells developed like control untreated *D. discoideum* cells within 24 h. Photographs were captured at 4× magnification 24 h after plating the cells. Results are representative of three independent experiments. Scale = 100 µm. (b) Nitric oxide generation increased in UV-C-treated *D. discoideum* cells. NO generation was estimated 30 min after UV-C treatment by the Griess method and was found to increase with increasing doses of UV-C. Results are the mean ± SE of three independent experiments. $^{*}P < 0.05$, $^{**}P < 0.01$, $^{***}P < 0.001$ compared to untreated control cells, $^{a}P < 0.05$ compared to benzamide pre-treated cells and $^{\#\#\#}P < 0.001$ compared to L-NIO pre-treated cells.

aggregation, was not affected in UV-C-treated cells. Nevertheless, expression of *csA* and *ctnA* was markedly reduced without great alteration in *ctnB* mRNA levels (Fig. 4a, b). *csA* is involved in Ca^{2+} independent cell–cell adhesion during aggregation, and countin and countin 2 along with at least three other polypeptides form a > 450 kDa counting factor complex, involved in maintaining aggregate size. *ctn* null cells had increased group size (40) similar to larger aggregate size seen in UV-C-treated cells (Fig. 3), unable to progress to fruiting bodies. Such cells have been reported to have reduced cAMP-induced cAMP pulse, and decrease in cAMP-stimulated Akt/PKB membrane translocation and kinase activity, which in turn lower cell motility (40–42). This is substantiated by reduced expression of *cAR1* and *aca* (Fig. 4a, b) and lower cAMP levels (Fig. 6), quintessential for cAMP signalling. In addition to this, reduced *regA* expression underlay compromised motility of UV-C-irradiated cells (Fig. 5a), as the protein is a phosphodiesterase that regulates PKA activity *via* reducing cAMP levels during chemotactic aggregation. cAMP addition was capable of restoring UV-C-induced changes in *car1* and *aca* expression (Fig. 4a, b). This explains that some UV-C-induced developmental defects were *via* modulating cAMP signalling to alter expression of genes associated with growth to differentiation transition, chemotaxis and aggregate size regulation (43–45).

Interfering PARP activity partly rescued development of UV-C-irradiated cells. It restored countin levels to normal but failed to affect expression of *car1, aca, yakA,* crucial for regulating cell cycle exit and growth to differentiation transition, and *csA*. Also, expression of *gp24*, a cell adhesion protein, increased in the presence of benzamide. PARP activity has previously been associated with expression of adhesion proteins (46). As increased adhesion proteins are known to hinder chemotaxis (47), the effect of benzamide on the gp(s) may mask its effect on development *via* restoration of countin levels.

On the other hand, UV irradiation induces NO generation in keratinocytes; this serves as a signal for melanogenesis (48). NO functions as a signalling molecule for *D. discoideum* cells also. NO-treated cells transiently activate their adenylyl cyclase and produce pulses of cAMP when stimulated with exogenously applied cAMP (49). However, physiological or environmental conditions that enhance external NO levels delay initiation of cAMP pulses, which are essential for cell differentiation (50). Estimation of NO (Fig. 8b) during development with L-NIO, iNOS (inducible nitric oxide synthase) inhibitor, showed NO generation *via* iNOS in *D. discoideum* after UV-C irradiation. Also, this NO production (Fig. 8b) was dependent on PARP. Activated PARP-1 up-regulates iNOS expression (51,52) and further iNOS byproducts may modulate PARP-1 enzymatic activity by nitration (53) making PARP activity and NO production interdependent. In *D. discoideum* cells, UV-C irradiation affects expression of certain developmentally important genes (*yakA*, *aca, car1*) and hence affects cAMP pulses *via* PARP activation and NO production. This has also been hinted at by increase in levels of cAMP with iNOS inhibition after UV-C exposure. An alternative sequence of events in which UV-C induces NO production prior to PARP activation is also possible. Further experiments need to be performed to pinpoint the affected pathways. Nevertheless, our results suggest interplay between PARP and NO with respect to regulation of gene expression during developmental defects induced by UV-C. Delayed revival of spores could be attributed to down-regulation of certain genes involved in spore revival, by UV-C. PARP may not be involved in increasing dormancy of spores induced by UV-C, as benzamide pre-treatment did not show any significant change in the revival of spores compared to UV-C-only treated cells. Cells germinated from spores did not show any significant damage (Fig. 7b) signifying that reduced activity of PARP (Fig. 1b) may be sufficient to repair DNA damage induced by 10.4 J/m^2 UV-C.

Interestingly, effects of PARP inhibition on UV-C-induced changes in *D. discoideum* growth and development also differed from our oxidative stress response results (17,18). Spores formed under oxidative stress exhibited delayed revival compared to benzamide-pretreated cells suggesting that PARP inhibition during oxidative stress not only resumed delayed development but also retained normal spore revival (17). However, the present study suggests that PARP inhibition and UV-C treatment did not have any effect on spore development of second-generation cells. This, in addition to the observation that lower doses of UV-C caused developmental defects in *D. discoideum* cells, a few of which were unaffected by PARP inhibition, raises a question concerning therapeutic significance of PARP inhibition in various DNA damage-related diseases. Thus, the concept of PARP inhibition being beneficial in various DNA associated diseases should be considered cautiously.

On a different note, *D. discoideum* despite being a lower eukaryote shows differential effects of oxidative and UV-C stress on development and spore germination. Hence, this organism has the complex signalling machinery to deal with different stresses such as oxidative stress and UV-C, in diverse ways. This fact emphasizes the importance of signalling pathway studies in *D.*

discoideum, which is simple and easy to handle compared to mammalian cell lines. Proteases involved in *D. discoideum* cell death downstream of PARP have been identified in oxidative stress-induced cell death (54). Further work needs to be performed to explore downstream targets of PARP during *D. discoideum* development for understanding the role of this multifunctional enzyme, in developmental cell death.

Acknowledgements

Infrastructure facilities provided by The Maharaja Sayajirao University and FACS facility provided by DBT-MSUB ILSPARE are gratefully acknowledged. RB thanks the Department of Biotechnology, New Delhi (BT/PR4383/BRB/10/1014/2011), Department of Science and Technology, New Delhi (SR/SO/BB-03/2010) and Council of Scientific and Industrial Research (38 (1383)/14/EMR-II) for research support; JR thanks the Council of Scientific and Industrial Research (New Delhi) for awarding SRF and TA thanks UGC- SAP DRS for fellowship.

References

1 Mir HA, Rajawat J, Pradhan S, Begum R (2007) Signaling molecules involved in the transition of growth to development of *Dictyostelium discoideum*. *Indian J. Exp. Biol.* **45**, 223–236.
2 Welker DL, Deering RA (1978) Genetic analysis of radiation-sensitive mutations in the slime mould *Dictyostelium discoideum*. *J. Gen. Microbiol.* **109**, 11–23.
3 Katoch B, Begum R (2003) Biochemical basis of the high resistance to oxidative stress in *Dictyostelium discoideum*. *J. Biosci.* **28**, 581–588.
4 Demple B, Linn S (1982) 5,6-Saturated thymine lesions in DNA: production by ultraviolet light or hydrogen peroxide. *Nucleic Acids Res.* **10**, 3781–3789.
5 Gentil A, Le Page F, Margot A, Lawrence CW, Borden A, Sarasin A (1996) Mutagenicity of a unique thymine-thymine dimer or thymine-thymine pyrimidine pyrimidone (6-4) photoproduct in mammalian cells. *Nucleic Acids Res.* **24**, 1837–1840.
6 Friedberg EC (1996) Relationships between DNA repair and transcription. *Annu. Rev. Biochem.* **65**, 15–42.
7 Rouleau M, Poirier GG (2004) Potential role of PARP inhibitors in cancer treatment and cell death. In: Panasci L. C., Alaoui-Jamali M.A., eds. DNA Repair in Cancer Therapy, pp. 197–210. Humana Press, Clifton, N.J.
8 de Murcia G, Menissier de Murcia J (1994) Poly(ADP-ribose) polymerase: a molecular nick-sensor. *Trends Biochem. Sci.* **19**, 172–176.
9 de Murcia G, Schreiber V, Molinete M, Saulier B, Poch O, Masson M *et al.* (1994) Structure and function of poly(ADP-ribose) polymerase. *Mol. Cell. Biochem.* **138**, 15–24.
10 de Murcia JM, Niedergang C, Trucco C, Ricoul M, Dutrillaux B, Mark M *et al.* (1997) Requirement of poly(ADP-ribose) polymerase in recovery from DNA damage in mice and in cells. *Proc. Natl Acad. Sci. USA* **94**, 7303–7307.
11 Schreiber V, Hunting D, Trucco C, Gowans B, Grunwald D, de Murcia G *et al.* (1995) A dominant–negative mutant of human poly(ADP-ribose) polymerase affects cell recovery, apoptosis and sister chromatid exchange following DNA damage. *Proc. Natl Acad. Sci. USA* **92**, 4753–4757.
12 Chatterjee S, Berger SJ, Berger NA (1999) "Poly (ADP-ribose) polymerase: a guardian of the genome that facilitates DNA repair by protecting against DNA recombination." ADP-Ribosylation Reactions: From Bacterial Pathogenesis to Cancer. Springer US. pp. 23–30.
13 Shall S, de Murcia G (2000) Poly (ADP-ribose) polymerase-1: what have we learned from the deficient mouse model? *Mutat. Res.* **460**, 1–15.
14 Masutani M, Nozaki T, Wakabayashi K, Sugimura T (1995) Role of poly (ADP-ribose) polymerase in cell-cycle checkpoint mechanisms following γ-irradiation. *Biochimie* **77**, 462–465.
15 D'Amours D, Desnoyers S, D'Silvaoxidat I, Poirier GG (1999) Poly(ADPribosyl)ation reactions in the regulation of nuclear functions. *Biochem J.* **342**, 249–268.
16 Virag L, Szabo C (2002) The therapeutic potential of poly(ADP-ribose) polymerase inhibitors. *Pharmacol. Rev.* **54**, 375–429.
17 Rajawat J, Mir H, Begum R (2011) Differential Role of poly(ADP-ribose) polymerase in *D. discoideum* growth and development. *BMC Dev. Biol.* **11**, 14.
18 Rajawat J, Vohra I, Mir H, Gohel D, Begum R (2007) Effect of oxidative stress and involvement of poly(ADP-ribose) polymerase (PARP) in *Dictyostelium discoideum* development. *FEBS J.* **274**, 5611–5618.
19 Rajawat J, Mir H, Alex T, Bakshi S, Begum R (2014) Involvement of poly(ADP-ribose) polymerase in paraptotic cell death of *D. discoideum*. *Apoptosis* **19**, 90–101.
20 Mir HA, Rajawat J, Begum R (2012) Staurosporine induced poly (ADP-ribose) polymerase independent cell death in *Dictyostelium discoideum*. *Indian J. Exp. Biol.* **50**, 80–86.
21 Watts DJ, Ashworth JM (1970) Growth of myxamoebae of the cellular slime mould *Dictyostelium discoideum* in axenic culture. *Biochem J.* **119**, 171–174.
22 Kosta A, Laporte C, Lam D, Tresse E, Luciani MF, Golstein P (2001) How to assess and study cell death in *Dictyostelium discoideum*. *Methods Cell Biol.* **346**, 535–550.
23 Chen G, Shaulsky G, Kuspa A (2004) Tissue specific G1 phase cell cycle arrest prior to terminal differentiation in *Dictyostelium*. *Development* **131**, 2619–2630.
24 Wallace LJ, Frazier WA (1979) Photoaffinity labeling of cyclic-AMP- and AMP binding proteins differentiating *Dictyostelium discoideum* cells. *Proc. Natl Acad. Sci. USA* **76**, 4250–4254.
25 Green LC, Wagner DA, Glogowski J, Skipper PL, Wishnok JS, Tannenbaum SR (1982) Analysis of nitrate, nitrite, and [15N] nitrate in biological samples. *Anal. Biochem.* **126**, 131–138.
26 Minami T, Adachi M, Kawamura R, Zhang Y, Shinomura Y, Imai K (2005) Sulindac enhances the proteasome inhibitor bortezomib-mediated oxidative stress and anticancer activity. *Clin. Cancer Res.* **11**, 5248–5256.
27 Okuwa T, Katayama T, Takano A, Kodaira K, Yasukawa H (2001) Two cell counting factors regulate the aggregate size of the cellular slime mold *Dictyostelium discoideum*. *Dev. Growth Differ.* **43**, 735–744.
28 Barondes SH, Haywood RPL, Cooper DNW (1985) Discoidin I, an endogenous lectin, is externalized from *Dictyostelium discoideum* in multilamellar bodies. *J. Cell Biol.* **100**, 1825–1833.
29 Kamboj RK, Lam TY, Siu CH (1990) Regulation of slug size by the cell adhesion molecule gp80 in *Dictyostelium discoideum*. *Cell Regul.* **1**, 715–729.

30 Souza GM, Lu S, Kuspa A (1998) *YAK*A, a protein kinase required for the transition from growth to development in *Dictyostelium*. *Development* **125**, 2291–2302.
31 Jacobson EL, Giacomoni PU, Roberts MJ, Wondrak GT, Jacobson MK (2001) Optimizing the energy status of skin cells during solar radiation. *J. Photochem. Photobiol., B* **63**, 141–147.
32 Alvarez-Gonzalez R, Althaus FR (1989) Poly(ADP-ribose) catabolism in mammalian cells exposed to DNA damaging agents. *Mutat. Res.* **218**, 67–74.
33 Berger NA, Sikorski GW (1980) Nicotinamide stimulates repair of DNA damage in human lymphocytes. *Biochem. Biophys. Res. Commun.* **95**, 67–72.
34 McCurry LS, Jacobson MK (1981) Unscheduled synthesis of DNA and poly(ADP-ribose) in human fibroblasts following DNA damage. *J. Supramol. Struct. Cell Biochem.* **17**, 87–90.
35 Yoon YS, Kim JW, Kang KW, Kim YS, Choi KH, Joe CO (1996) Poly (ADP-ribosyl) ation of histone H1 correlates with internucleosomal DNA fragmentation during apoptosis. *J. Biol. Chem.* **271**, 9129–9134.
36 Vodenicharov MD, Ghodgaonkar MM, Halappanavar SS, Shah RG, Shah GM (2005) Mechanism of early biphasic activation of poly(ADP-ribose) polymerase-1 in response to ultraviolet B radiation. *J. Cell Sci.* **118**, 589–599.
37 Gentile M, Latonen L, Laiho M (2003) Cell cycle arrest and apoptosis provoked by UV radiation-induced DNA damage are transcriptionally highly divergent responses. *Nucleic Acids Res.* **31**, 4779–4790.
38 Mir HA (2011) Involvement of poly(ADP-ribose) polymerase and Apoptosis Inducing Factor in *Dictyostelium discoideum* Cell Death and Development. PhD thesis, The MS University of Baroda, Vadodara.
39 Azzam EI, de Toledo SM, Little JB (2003) Expression of connexin43 is highly sensitive to ionizing radiation and other environmental stresses. *Cancer Res.* **63**, 7128–7135.
40 Gao T, Knecht D, Tang L, Hatton RD, Gomer RH (2004) A cell number counting factor regulates Akt/protein kinase B to regulate *Dictyostelium discoideum* group size. *Eukaryot. Cell* **3**, 1176–1184.
41 Tang L, Gao T, McCollum C, Jang W, Vicker MG, Ammann RR *et al.* (2002) A cell number-counting factor regulates the cytoskeleton and cell motility in *Dictyostelium*. *Proc. Natl Acad. Sci. USA* **99**, 1371–1376.
42 Brock DA, Ehrenman K, Ammann RR, Tang Y, Gomer RH (2003) Two components of a secreted cell number-counting factor bind to cells and have opposing effects on cAMP signal transduction in *Dictyostelium*. *J. Biol. Chem.* **278**, 52262–52272.
43 Jaiswal P, Soldati T, Thewes S, Baskar R (2012) Regulation of aggregate size and pattern by adenosine and caffeine in cellular slime molds. *BMC Dev. Biol.* **12**, 5.
44 Chisholm RL, Hopkinson S, Lodish HF (1987) Superinduction of the *Dictyostelium discoideum* cell surface cAMP receptor by pulses of cAMP. *Proc. Natl Acad. Sci. USA* **84**, 1030–1034.
45 Klein P, Vaughan R, Borleis J, Devreotes P (1987) The surface cyclic AMP receptor in *Dictyostelium*. *J. Biol. Chem.* **262**, 358–364.
46 Franke J, Podgorski GJ, Kessin RH (1987) The expression of two transcripts of the phosphodiesterase gene during the development of *Dictyostelium discoideum*. *Dev. Biol.* **124**, 504–511.
47 Jang W, Gomer RH (2008) Combining experiments and modelling to understand size regulation in *Dictyostelium discoideum*. *J. R. Soc. Interface* **5**, S49–S58.
48 Romero-Graillet C, Aberdam E, Clement M, Ortonne JP, Ballotti R (2008) Nitric oxide produced by ultraviolet-irradiated keratinocytes stimulates melanogenesis. *J. Clin. Invest.* **99**, 635–642.
49 Freeman SL, MacNaughton WK (2004) Nitric oxide inhibitable isoforms of adenylate cyclase mediates epithelial secretory dysfunction following exposure to ionising radiation. *Gut* **53**, 214–221.
50 Tao Y, Howlett A, Klein C (1996) Nitric oxide inhibits the initiation of cAMP pulsing in *D.discoideum* without altering receptor-activated adenylate cyclase. *Cell. Signal.* **8**, 26–34.
51 Romero MR, Cañuelo A, Siles E, Javier F, Oliver Martínez-Lara E (2012) Nitric oxide modulates hypoxia-inducible factor-1 and poly (ADP-ribose) polymerase-1 cross talk in response to hypobaric hypoxia. *J. Appl. Physiol.* **112**, 823–826.
52 Park EM, Cho S, Frys K, Racchumi G, Zhou P, Anrather J *et al.* (2004) Interaction between inducible nitric oxide synthase and poly (ADP-ribose) polymerase in focal ischemic brain injury. *Stroke* **35**, 2896–2901.
53 Yu SW, Andrabi SA, Wang H, Kim NS, Poirier GG, Dawson TM *et al.* (2006) Apoptosis-inducing factor mediates poly(ADP-ribose) (PAR) polymer induced cell death. *Proc. Natl Acad. Sci. USA* **103**, 18 314–18319.
54 Rajawat J, Alex T, Mir H, Kadam A, Begum R (2014) Proteases involved during oxidative stress induced poly (ADP-ribose) polymerase mediated cell death in *D. discoideum*. *Microbiology* **160**, 1101–1111.

Received: 9 March 2016 | Accepted: 4 May 2016

DOI: 10.1111/cpr.12268

REVIEW ARTICLE

WILEY Cell Proliferation

The PARP family: insights into functional aspects of poly (ADP-ribose) polymerase-1 in cell growth and survival

T. Jubin[1] | A. Kadam[1] | M. Jariwala[1] | S. Bhatt[1] | S. Sutariya[1] | A.R. Gani[1] | S. Gautam[2] | R. Begum[1]

[1]Department of Biochemistry, Faculty of Science, The Maharaja Sayajirao University of Baroda, Vadodara, Gujarat, India

[2]Food Technology Division, Bhabha Atomic Research Centre, Mumbai, India

Correspondence
Rasheedunnisa Begum, Department of Biochemistry, Faculty of Science, The Maharaja Sayajirao University of Baroda, Vadodara, Gujarat, India.
Email: rasheedunnisab@yahoo.co.in

Abstract

PARP family members can be found spread across all domains and continue to be essential molecules from lower to higher eukaryotes. Poly (ADP-ribose) polymerase 1 (PARP-1), newly termed ADP-ribosyltransferase D-type 1 (ARTD1), is a ubiquitously expressed ADP-ribosyltransferase (ART) enzyme involved in key cellular processes such as DNA repair and cell death. This review assesses current developments in PARP-1 biology and activation signals for PARP-1, other than conventional DNA damage activation. Moreover, many essential functions of PARP-1 still remain elusive. PARP-1 is found to be involved in a myriad of cellular events *via* conservation of genomic integrity, chromatin dynamics and transcriptional regulation. This article briefly focuses on its other equally important overlooked functions during growth, metabolic regulation, spermatogenesis, embryogenesis, epigenetics and differentiation. Understanding the role of PARP-1, its multidimensional regulatory mechanisms in the cell and its dysregulation resulting in diseased states, will help in harnessing its true therapeutic potential.

1 | INTRODUCTION

Poly (ADP-ribose) polymerase (PARP) enzymes are a family of proteins involved in a number of cellular processes including gene regulation, chromatin remodelling, DNA repair and apoptosis.[1] These enzymes are present in all eukaryotes except yeast.[2] PARPs can either transfer a single unit of (ADP-ribose) or more than one (ADP-ribose) moieties from NAD^+onto substrates yielding poly (ADP-ribose) (PAR) chains, which can be of varying length and branch content. ADP-ribosyltransferase D-type 1 (ARTD-1 or PARP-1) falls in the latter category.[1,3] The PAR polymers are rapidly degraded by poly (ADP-ribose) glycohydrolase (PARG)[4] possessing both endoglycosidic and exoglycosidic activities,[5] and PAR hydrolase (ARH3), which also shares catalytic domain similarity with PARG.[6] However, ARH3 does not hydrolyse ADP-ribose-arginine, -cysteine, -diphthamide or -asparagine bonds.[6] Another set of enzymes known as macro domain-containing proteins and NUDIX hyrolases have also been reported to be involved in PAR degradation.[7,8] There are 17 different homologues of PARP that have a conserved catalytic domain with various domains like zinc finger, BRCT, SAM, SAP, ankyrin and macro domain.[9] Though PARP-1 has been demonstrated as a key player in DNA repair and cell death, many of its equally vital cellular functions have been overlooked. In this review, we discuss the distribution of PARP homologues across all organisms and the role of PARP-1 in various cellular functions like transcription, spermatogenesis, epigenetics and the most novel in differentiation and multicellularity.

2 | THE PARP FAMILY

Based on new proposed nomenclature by Hottiger et al.,[10] the human PARP (hPARP) family is classified into three groups depending on their motifs and functions: (1) PARP 1-5: have a conserved glutamate residue (Glu988); (2) PARP 6-8, 10-12 and 14-16: are putative mono-(ADP-ribose) polymerases and (3) PARP 9 and 13 which do not have PARP signature motif that binds NAD^+nor do they have Glu988 implying that they are inactive.[10] PARP superfamily can be subdivided into six clades which are shown in Table 1.

Out of 17 members, PARP-1 (113 kDa) was the first characterized and extensively studied enzyme recognized to play an essential role in DNA repair.[11] PARP-1 and PARP-2 share ~69% homology in the catalytic domain and they are documented as vital proteins in DNA repair system,[2] while PARP-3 is reported to be a mono-ADP-ribosylating enzyme by Loseva and group.[12] PARP-2 and PARP-3 were considered as a subgroup of PARP-1 as they all carry out synthesis of branched polymers.[13] PARP-4 also known as Vault PARP, is a ribonucleoprotein complex having PARylation activity and it is thought to be involved in multidrug resistance of tumour and intracellular transport.[14] Tankyrase-1 (TRF-1-interacting ankyrin-related ADP-ribose polymerase-1), also known as PARP5a, is identified to enhance telomere elongation by telomerase.[15] Other PARP homologues show structural and functional differences. Tankyrase-2 lacks N-terminal HPS (His-Pro-Ser) domain, but it may share some overlapping functions with tankyrase-1.[16] Other PARP family members like tiPARP, PARP-12 and PARP-13 share PARP catalytic, WWE and CX8CX5CX3-like zinc finger domains.[2] PARP-13 has been reported to be an important regulator of cellular mRNA via regulation of miRNA activity.[17] The next subgroup which includes PARP-9/BAL1, PARP-14/BAL2/CoaSt6 and PARP-15/BAL3 are macro-PARPs, characterized by macro domains positioned before the PARP domain. This domain is found to be involved in transcriptional repression and X-chromosome inactivation, suggesting it as a transcription factor.[18] The RNA recognition motif (RRM) and the Gly-rich domain of PARP-10 are known to help in binding of RNA with proto-oncoprotein c-Myc.[2] Other PARP family members such as PARP-6, PARP-8, PARP-11 and PARP-16 have been identified but their functions are still elusive, though PARP-8 and 16 have been recently shown to be involved in assembly or maintenance of membranous organelles.[19]

3 | DISTRIBUTION OF PARP ACROSS LIFE

3.1 | PARP in lower life forms

3.1.1 | PARP in bacteria

Numerous PARP-like proteins are detected in several bacterial genomes.[20,21] Till now, around 28 PARP homologues have been suggested across 27 bacterial species.[22] However, only a few bacteria possess the entire machinery required for PARP metabolism. Some also show the conserved histidine-tyrosine-glutamate (H-Y-E) catalytic triad which is essential for its activity.[21] PARP from *Herpetosiphon aurantiacus* has been reported to have conserved catalytic triad having the same characteristics as human PARP-1 enzyme.[21]

3.1.2 | PARP in archaea

Archaea do show the presence of PARP homologues. PARP-like thermozymes have been identified from *Sulfolobus solfataricus*. This PARP-like protein shows oligo (ADP-ribosyl) transferase activity and DNA-binding activity.[23]

3.1.3 | PARP in viruses

PARP-like proteins have also been identified in a few double-stranded DNA viruses [24] such as *Aeromonas* phage—Aeh1, *Anticarsia gemmatalis* nucleopolyhedro virus, invertebrate iridescent virus 6 and cellulophagaphage phi4:1. All these viral PARPs have been found to possess the conserved catalytic triad H-Y-E with an exception of one which has an aspartate instead of glutamate suggesting that these PARPs are active ADP-ribosyl transferases. Some viruses such as Herpes simplex virus and Epstein-Barr virus have also been reported to use PAR metabolism for their replication.[25,26]

3.2 | PARP in higher eukaryotes

PARPs are found in a divergent group of eukaryotes.[9,10] PARP expression has been identified in nearly all eukaryotic cells ranging from plants to vertebrates.[27] PARP-1 was long assumed to be the single enzyme with PARylation function until two PARP isoforms were discovered in plants.[28] Citarelli et al.[29] investigated at least two more PARP proteins in the last common extant ancestor of eukaryotes.

In conclusion, it is clear that the complexity of PARP proteins is augmented with the evolutionary level of the species. Vyas et al.[19] evidently illustrated that this domain complexity confers the diversity in functions to the PARP family.

PARP-1 is best studied out of this 17-member family of hPARPs. PARP has been implicated in development and cell differentiation from lower life forms to higher eukaryotes.[30] However, it is involved in a plethora of functions and many of its functions in spermatogenesis, epigenetics and differentiation remain unclear. Thus, understanding PARP-1 and its role in the above processes is the focus of this review.

4 | PARP-1: STRUCTURE, ACTIVATION SIGNALS AND ITS DIVERSE CELLULAR ROLES

4.1 | Gene organization of PARP-1 and its modifications

PARP-1 (EC 2.4.2.30) is a prominent member of the PARP family. It is a nuclear enzyme with approximately 10^6 molecules per cell [31] and accounts for 80%–90% of total cellular PARylation. Gene structure of PARP-1 mainly consists of DNA binding, an auto modification and a catalytic domain (Fig. 1). (1) The N-terminal DNA-binding domain has three zinc fingers and a nuclear localization sequence (NLS). The two homologous zinc finger proteins (Zn1 and Zn2) are characterized by a CCHC ligand pattern.[32,33] (2) The auto modification domain has BRCA1 C terminus (BRCT) motif and it is involved in protein-protein interaction.[2,10,34] (3) The catalytic domain at C terminus comprises of PARP signature motif (six β-strands and one α-helix) that binds to $NAD^+$and glutamate residue at its 988 position.[2]

TABLE 1 Distribution of PARP. PARP has been divided into six clades depending on the domains present[22,29] and [30]

Clade	Clade sub group	Class	Key features
Clade 1	Clade 1A	Amoebozoa (*Dictyostelium*) Opisthokonta (Fungi) Chromalveolates	Ankyrin repeats, WGR PRD, PARP catalytic domains.
	Clade 1B	Opisthokonta (animals and *Choanoflagellata*) and the Excavata (the *Heterolobosea* member Naegleria)	three N-terminal zinc fingers that contribute to DNA binding, a BRCT domain and a PADR1 domain in addition to WGR, PRD and the catalytic domain
	Clade 1C	Oomyocete Phytophtora species (within the Excavata) and one basal animal.	WGR, PRD and PARP catalytic domains and mostly do not contain other functional domains.
	Clade1D	Opisthokonta, the animals *Xenopus laevis* (Q566G1) and *Schistosoma japonicum* (Q5DAZ0) and the fungus *Batrachochytrium dendrobatidis* and Plantae (land plants) as well as ciliate members of the Chromalveolates.	WGR, PRD and PARP catalytic domains and mostly do not contain other functional domains.
	Clade 1E	most of the fungal members of Clade 1	BRCT domains N-terminal to WGR, PRD and PARP catalytic domains.
	Clade 1F	the Excavata	—
	Clade 1G	Opisthokonta (both animals and the Choanoflagellate *Monosiga brevicollis*)	only WGR, PRD and PARP catalytic domains
	Clade 1H	Two *Caenorhabditis elegans (C. elegans)* proteins	PADR1, WGR, PRD and PARP
Clade2	Clade 2A	—	an N-terminal WWE domain, the PARP signature and a C-terminal extension
	Clade 2B	—	only the PARP signature and the C-terminal extension
Clade 3	Clade 3A	—	RRM RNA-binding domain, a glycine-rich region (GRD), and a UIM domain
	Clade 3B	*Trichoplax adhaerens*	Macro domain N-terminal to their C-terminal catalytic domain
	Clade 3C	—	Macro domain N-terminal to their C-terminal catalytic domain
	Clade 3D	two *Dictyostelium discoideum* and four *Tetrahymena thermophila* proteins	—
	Clade 3E	—	one to two WWE domains, alone or in combination with zinc fingers (either CCCH or CCCH types) in front of their PARP catalytic domains
	Clade3F	—	PARP9
Clade 4	Clade 4	—	15–18 ankyrin repeats followed by a sterile alpha motif (SAM) and the PARP catalytic domain
Clade 5	Clade 5A	Opishthokonts (animals)	the PARP signature is found in the middle of the protein, rather than at the C terminus
	Clade 5B	Amoebozoa	—
Clade 6	Clade 6A	Opisthokonts (animals and fungi), Excavates (Parabasalids and Heterolobosa), and Plantae (chlorophyta and bryophytes)	N termini with no known functional domains and C-terminal extensions beyond the PARP catalytic domain of varying lengths
	Clade 6B		PfamB_2311 domains as well as the PARP catalytic domain
	Clade 6C		PfamB_2311 domain and a PARP catalytic domain
	Clade 6D	Deuterostomes with the exception of the mollusc *Lottia gigantean*	PfamB_2311 domain and the PARP catalytic domain
	Clade 6E	seven proteins encoded by *Trichomonas vaginalis*	PfamB_2311 domain and the PARP catalytic domain

The next important component of this enzyme is the PARP signature motif (PSM). It has two sites, acceptor site for adenosine and donor site for nicotinamide wherein ADP residues from $NAD^+$are transferred to target site.[35] His-862 and Glu-988 play important role in NAD^+binding.[36] In addition to this, WGR domain also contains highly conserved amino acid sequence i.e. Trp, Gly and Arg, but its role

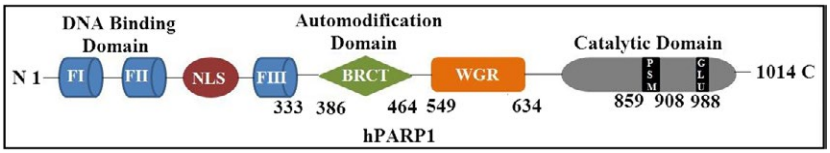

FIGURE 1 **Structural organization of human PARP-1 (hPARP-1):** It is characterized by FI, FII: Zinc finger motifs, FIII: Zinc ribbon domain (1-333 aa); NLS: Nuclear localization sequence; BRCT: BRCA1 C terminal motif (386-464 aa); WGR domain (549-634 aa) and the most conserved catalytic domain with PARP signature motif (PSM) between 859-908 aa and Glutamate (Glu) at 988 position.

TABLE 2 Post-translational Modifications of Poly (ADP-ribose) polymerase 1

Modification in PARP-1	Source	Residue modified	Activator	Result	References
Auto modification Poly (ADP-ribosylation)	PARP	K498, K521 and K524	Intact and damaged DNA	Regulation of PARP activity	Altmeyer et al.[38]
Mono-ADP-ribosylation	SIRT6	K521	dsDNA damage	Enhances double-strand break repair under oxidative stress	Mao et al.[42]
Sumolyation small ubiquitin-related modifier (SUMO)	SUMO-2 SUMO 3	K203, K486 and K512	Heat shock intact DNA	Transcriptional co-activator of hypoxia-responsive genes and promotes induction of the heat shock-induced HSP70.1 promoter	Zilio et al.[43]
Acetylation	p300/CREB-binding protein	K498, K505, K508, K521 and K524	Inflammatory stimuli	NF-κB-dependent gene activation	Hassa et al.[40]
Phosphorylation	ERK1/2 Protein Kinase C	S372 and T373	DNA damage	Neuronal cell death Decreased PARP-1 DNA-binding and catalytic activity	Kauppinen et al.,[41] Beckert et al.[39]

is yet to be identified.[2,34] However, Langelier et al.[37] showed that Zn3 along with Zn1 and WGR domain of PARP-1 together bind to the DNA damage leading to structural changes eventually abridging DNA damage site to its catalytic domain.

Other than auto modification by PARylation, PARP-1 itself undergoes various other modifications enlisted in Table 2 that has various cellular effects.[38–43]

4.2 | Mechanism of PARP-1 activation

The enzymatic activity of PARP-1 is stimulated significantly in the presence of a range of activators like damaged DNA, non-B-DNA structures, nucleosomes and various protein-binding partners.[1,44–46] Lonskaya et al.[47] reported that DNA bent, cruciform DNA or stably unpaired DNA regions can also stimulate PARylation. The activation signal for PARP-1 is DNA damage although several reports illustrate that PARP-1 may also be activated in the absence of DNA damage. The best characterized ligands for PARP-1 are single-strand and double-strand breaks (SSBs and DSBs).

There are reports suggesting that PARP-1 activation by SSBs requires presence of both the zinc fingers while only Zn1 is required for DSBs.[33] Zn1 has been demonstrated to relay the signals to the catalytic domain for formation of PAR molecules,[33,48] while Zn2 has been shown to be majorly involved in DNA binding as compared to Zn1 due to its higher affinity to DNA.[49] Eustermann et al.[50] have demonstrated very recently how the two zinc fingers recognize SSBs and coordinate domain folding in PARP-1 to control the activity of the C-terminal catalytic domain. PARP-1 has been reported to have affinity for intact DNA structures and recognizes specific octamer motif "RNNWCAAA" found in various gene promoters.[51]

Another mode of alternative DNA-independent mode of PARP-1 activation is based on kinase cascades. Phosphorylated ERK2 has been shown to significantly enhance and maximize PARP-1 catalytic activity in the presence and absence of damaged DNA.[41,52] Interaction between PARP-1 and a pre-phosphorylated kinase has also been shown to mediate PARP-1 activation.[52,53] Likewise, phosphorylation by activated calcium-dependent protein kinase (CaMKII) is also capable of activating PARP-1 enzyme during neuronal development thereby promoting the nuclear export of its negative regulator KIF4.[54] Moreover, overexpression of protein phosphatase 5 (PP5) led to increase in PARP-1 enzymatic activity in response to double-stranded DNA breaks.[55] Nuclear nicotinamide mononucleotide adenylyl transferase 1 (NMNAT1), an enzyme involved in NAD^+synthesis, also associates with PAR to enhance PARP-1 enzyme activity.[56] Other proteins regulating PARP-1 activity include Ku,[55] histone variant macroH2A1.1[57] and KIF4.[58] Protein-protein interactions also seem to activate PARP-1. Mao et al.[42] have demonstrated that SIRT6 activates PARP-1 by mono-ADP-ribosylating it in position Lys521. Developmental or environmental stimuli induce PARP-1 activation and the PAR-dependent nucleosome loosening leading to histone stripping and hence opening of the chromatin structure. This process allows

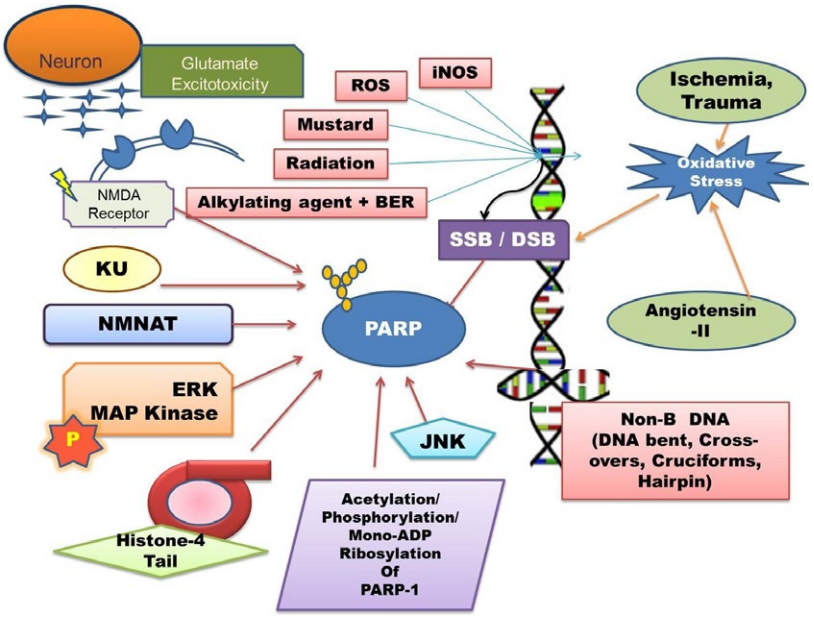

FIGURE 2 Mechanism of PARP-1 Activation. The nuclear enzyme PARP-1 can bind to DNA breaks resulting in the activation of the enzyme. DNA breaks are caused either by ROS, RNS or radiation or indirectly by DNA repair machinery where breaks are introduced into the DNA strands as in the case of alkylating DNA damage. Binding to special non-B-DNA structures such as bent or cruciform DNA or four-way junctions may culminate into PARP-1 activation. Protein-protein interactions or covalent modifications (e.g. mono-ADP-ribosylation, acetylation or phosphorylation) have also been described as activation mechanisms for PARP-1 which are DNA-independent. Other proteins activating PARP include nuclear NMNAT, Ku and phosphorylated ERK2 and Histone-4 tail

transcriptional activation. This PAR-mediated chromatin loosening phenomenon is detected at larval salivary-gland polytene chromosome puffs.[59] Hence, PARP-1 can be activated by DNA-dependent and -independent manner which is summarized in Fig. 2.

4.3 | PARP-1: single protein with varied roles

4.3.1 | PARP-1 in DNA repair

ADP-ribosylation activity of PARP-1 is an instantaneous biochemical response to DNA damage induced by ionizing radiations, alkylations etc. At low levels of DNA damage, it detects DNA damage followed by repair and cell survival, whereas at high levels of DNA damage, it activates the cell death pathway.[60] Upon DNA damage, PARP-1's zinc finger FI/Zn1, FII/Zn2 and FIII/Zn3 motifs have been reported to relay binding signal to catalytic domain followed by the recruitment of proteins involved in repair mechanism such as base excision repair (BER), single-strand breaks (SSBs) and double-strand breaks (DSBs) repair.[1,61] It is also indicated to act as a DNA damage sensor [62] and help in chromatin remodelling at DNA damage sites.[63] A variety of proteins like ALC1, histone mH2A1.1, scaffold attachment factor SAFB1 have been illustrated to be recruited to DNA damage sites via PARP-1 thus proving its indispensable role in DNA repair.[64–66] Evidences show presence of PAR-binding zinc finger motifs in DNA damage response and checkpoint regulation proteins.[67,68] PARP-2 was also shown to be involved in the later steps of BER/single-strand break repair.[69] In nucleotide excision repair, PARP-1 inhibition or depletion has also shown to cause low efficiency of removal of UV-induced DNA damage.[70] Among mammalian DNA repair pathways, PARP-1 has been also implicated in homologous recombination[71] and non-homologous end-joining pathways.[72] PARP-1 has been reported to interact with replication fork protein (Timeless) in a PAR-independent manner thereby allowing its recruitment to DSB sites to promote homologous recombination.[73] Thus, it is clearly illustrated that PARP-1 plays a vital role in DNA damage response.

4.3.2 | PARP-1 in cell death

Under normal physiological conditions, cell morphology, numbers, pattern and injury are taken care of by the process of apoptosis.[74] The mode of cell death depends on the extent of DNA damage. Low DNA damage can activate PARP-1 resulting in cell survival via DNA repair mechanisms. At moderate levels of DNA damage, cell undergoes apoptosis and PARP-1 activation results into cleavage of PARP-1 by caspases-3 and -7 into two fragments (89 kDa and 24 kDa)[75] which is believed to be a key feature of apoptosis.[76] N-terminal 24 kDa fragment remains in nucleolus and other 89 kDa fragment translocates from nucleus to cytosol wherein it acts as a target for autoimmunity.[77] Severe DNA damage leads to programmed necrotic cell death through over-activation of PARP-1.[78] Ring finger protein 146 (RNF146), a cytoplasmic E3-ubiquitin ligase, acts as a direct interactor of PARP-1 during this process and elicits release of PARP-1 from the nucleus. This has been demonstrated during myocardial ischaemia-reperfusion injury.[79] On the other side, in caspase-independent cell death, it plays an important role in the release of apoptosis-inducing factor (AIF) from mitochondria to nucleus. Yu et al.[80] have studied the dependence of PARP-1 and AIF in caspase-independent cell death which is termed as 'parthanatos'. PARP-1 has been reported to play a very crucial role in initiation and regulation of this type of cell death.[81] Parthanatos has been detected in many disease conditions like stroke, Parkinsons, diabetes, etc.[82] Upon PARP-1 activation stimulated with various DNA-damaging agents like NMDA, H_2O_2, etc., AIF translocates from mitochondria to nucleus and finally culminates into cell death.[83–85] On the contrary, Mir et al. showed that staurosporine-induced cell death did not involve PARP.[86]

PARP-1 is also reported to be involved in autophagy induced by DNA damage.[87] PARP-1 via autophagy displays a cytoprotective role in oxidative stress-induced necrotic cell death.[88] Moreover, Son et al.[89] have also reported that cadmium-mediated ROS generation leads to PARP-1 activation and energy (ATP) reduction, eventually culminating into autophagy in skin epidermal cells. Wyrsch et al.[90] have found that PARP-1 and PARP-2 control cytosolic Ca^{2+}shifts from extracellular and intracellular sources during oxidative stress. The different Ca^{2+}signals arise from the transient receptor potential melastatin 2 (TRPM2) channels located in the cellular and lysosomal membranes. This Ca^{2+}overload induces specific stress kinase response which leads to autophagy or cell death. Under mild oxidative stress conditions, PARP-1 operates as an autophagy suppressor after oxidative stress leading to cell death by activating downstream of extracellular signal-regulated kinase 1/2 (ERK1/2) and AKT. Under severe oxidative conditions, PARP-2 induces Ca^{2+}shifts from lysosomes, while PARP-1 becomes completely inactive. The cytosolic Ca^{2+}overload leads to phosphorylation of p38, stress-activated protein kinase/Jun amino-terminal kinase (SAPK/JNK), and cyclic AMP response element-binding protein (CREB) with its activating transcription factor (ATF-1), further activating autophagy markers leading to cell survival.

PARP-1 and related PARP family members are at the intersection of conversing stress signalling pathways. Oxidative stress causes disruption in redox potential that extends to the ER, causing accumulation of misfolded proteins, finally stimulating the unfolded protein response (UPR).[91] It would be interesting to know if PARP-1 has a role in ER stress-mediated cell death as it is upstream to autophagy, where PARP-1 is demonstrated to play an essential role. Hence, it is clear that PARP-1 is an essential regulator in many of the cell death pathways and this has been demonstrated in many tissues. However, a very interesting work by Jog and Caricchio[92] illustrates a characteristic difference in PARP-1-mediated necrosis in males and females. Male mice were shown to be prone to PARP-1-mediated necrosis while female mice showed PARP-1-independent cell death.[92] Understanding the role of PARP-1 in different stress conditions and even in different sexes would help us dissect out pathomechanisms of various disease conditions.

4.3.3 | PARP-1 and epigenetics

The poly (ADP-ribosyl)ation of histones leading to open chromatin conformation at DNA damage sites was the first indication to the function of PAR as an epigenetic modification.[2] Recent evidence has shown that PAR has an important role in the epigenetic regulation of chromatin structure and in gene expression under physiological conditions wherein DNA integrity is maintained.[93] Lodhi et al.[94] have demonstrated PARP-1 as a genome-wide epigenetic memory mark in mitotic chromatin. They report that PARP-1 establishes stable epigenetic marks at the transcription start sites in metaphase chromatin and these marks are a prerequisite for transcriptional restart after mitosis. Moreover, PARP-1 activity epigenetically regulates mitochondrial DNA repair and transcription.[95] PARP-1 also associates with genome-wide epigenetic regulatory elements suggesting a functional interplay between PARP-1 and DNA methylation.[96] Previous studies have shown that PARP-1 can affect the genomic DNA methylation pattern via DNA methyl transferase, Dnmt1, both by regulating its expression as well as activity.[93,97] Furthermore, the role of PARP-1 in DNA methylation events has been explored in induced pluripotent stem cells (iPSCs).[98] Recently, PARP-1 has been shown to be associated epigenetically with Tet2 (a methyl cytosine dioxygenase) during somatic cell reprogramming which leads to transcriptional induction at the pluripotency loci.[99] PARP-1 has also been demonstrated to interact with TIP5 via non-coding RNA, thereby playing a role in maintenance of silent rDNA chromatin in mid-late S phase.[100] Though, these studies suggest the possible epigenetic involvement of PARP-1; its mechanistic role in epigenetic control is still elusive and remains to be an area of great interest to researchers.

4.3.4 | PARP-1 as a chromatin modulator

Chromatin consists of genomic DNA, linker histones (H1), core histones (H2A, H2B, H3 and H4) and other chromatin-associated proteins. Early reports have shown that purified PARP-1 could ADP-ribosylate chromatin proteins (e.g. mainly H1), by decondensation of chromatin and destabilization of nucleosomes.[101] Also proven in recent reports, PARP-1 binding to chromatin can change the conformation and composition of nucleosome.[32,102] In addition, it has also been demonstrated that PARP-1 interacts with core histone variants resulting in the recruitment and integration of histone variants to specific sites in the genome.[57] Local chromatin loosening by PARP-1 has also been demonstrated well at the puff loci in *Drosophila* facilitating transcription and eventually helping chromatin remodelling during development.[59] Nalabothula et al.[96] discussed the possible mechanisms of chromatin structure remodelling by PARP-1 as: a) it binds between entry and exit sites between nucleosomes and linker DNA, b) it PARylates histones, linker histone H1, etc. thus modifying chromatin architecture and c) it competes with histone H1 for nucleosome binding. All the above reports strengthen the role of PARP-1 in chromatin remodelling.

4.3.5 | PARP-1 in transcription

It is well studied that PARP-1 behaves as chromatin modifier at transcriptional level with a number of in vitro and in vivo experiments. Electrostatic repulsion between DNA and histones due to transfer of negatively charged PAR molecules onto accepter proteins promotes transcription by recruiting transcriptional machinery.[103] PARP-1 is observed to be more localized at the promoter regions of most actively transcribed genes.[104] The transcriptional regulatory roles of PARP-1 are manifested mainly through two processes, modulating chromatin structure and acting as a part of enhancer/promoter-binding complexes. Based on the cell type, it can enhance transcription with co-activators or inhibit transcription by repressors.[105] Chromatin-dependent gene expression is controlled by

PARP-1 interacting with histones at promoter.[104] The type of histone modification (acetylation, phosphorylation and methylation) is very essential for interaction between PARP-1 and DNA because it can add structural changes into histones.[106] Phosphorylation of histone variant, H2Av, promotes activity of PARP-1 in *Drosophila* at specific promoter regions.[107] PARP-1 is also found to be localized at DNA repair sites after binding to other histone variant, macroH2A.[108] Also, macroH2A1-stimulated H2B acetylation was seen in cancer progression which was PARP-1-dependent.[109] Depletion of PARP-1 activity resulted into ineffective loading of RNA polymerase II transcriptional machinery implying its role in gene regulation.[110]

Recent studies suggest that PARP-1 functions as a co-activator, which upregulates the transcription of Nrf2, promoting the interaction among Nrf2 and ARE (antioxidant response elements).[111] Reduced expression of CCN2 was found in tubular epithelial cells of kidney upon knockdown of PARP-1.[112] In addition to this, PARP-1 also functions as an insulator that organizes the genome into distinct regulatory units by controlling the effects of enhancers on promoters, or by preventing the spread of heterochromatin.[113] In vivo and in vitro binding studies of PARP-1 and transcription factor Yin Yang 1 (YY1) suggested that PARP-1 plays a promoter regulatory role and inhibits the transcription of Cxcl12. In addition, changes in PARP-1-CTCF interactions due to serum shock induced recruitment of circadian loci to the lamina leading to transcriptional attenuation.[114] PARP-1 is also known to be acting as an exchange factor thereby controlling transcription. Recently, it has been demonstrated that PARP-1 functions in remodelling of promoter-associated nucleosomes by replacing H2A.Z by H2A from *FOS* promoter to allow transcriptional activation in response to ERK signalling.[115] Thus, the underlying mechanism of PARP-1-mediated transcriptional regulation is very complex and extensive and hence more studies are required to explore the transcriptional role of PARP-1.

4.3.6 | PARP and spermatogenesis

Both PARP-1 and PARP-2 have been found to have a significant role in spermatogenesis.[116] It has been observed that there is significant PARP expression during the earlier stages of spermatogenesis and its transcription declines during late stages of maturation.[117,118] The levels of PARP-1, PARP-2 and PARP-9 were found to be increased in mature sperms as compared to immature sperms [116] and interestingly PARP-1 was also found to be downregulated during the haploid stage of meiosis.[119] The presence of PARG in the nuclei of rat primary spermatocytes also suggests that the levels of poly (ADP-ribose) in these germ cells are highly regulated.[117] Moreover, Meyer-Ficca et al.[120] reported the presence of PAR polymerization by PARP-1 and PARP-2 in rat spermatids, highest during the phase of chromatin condensation.

Studies demonstrating an increase in DNA strand breaks in all population of elongating spermatids in human testis [121] and the presence of higher levels of PARP-1, PARP-2 and PARP-9 in ejaculated sperm from fertile men compared to infertile men indicate a possible relationship between PARP expression and male infertility.

4.3.7 | PARP-1 in cell differentiation/multicellularity

Out of the various roles of PARP-1, its role in cell differentiation and multicellularity has yet to be unravelled. However, accumulating reports in different model systems suggest a definite role of PARP-1 in growth and multicellularity. For example, Drosophila PARP has been shown to act in ectodermal specification and neural crest development in zebrafish.[122] Our laboratory studies are indicative of PARP's role in *D.discoideum* development wherein its downregulation led to arrested development.[123] Recent studies from our laboratory show PARP-1 involvement in *D. discoideum* growth and multicellularity by ADPRT1A (PARP-1 orthologue) overexpression which led to delayed growth and developmental morphogenesis.[124] We have also reported that PARP may be essential in combating stress conditions in *D. discoideum*.[83–85,125,126] Genetic studies on PARP-1 orthologues in fungus demonstrated defective development and decreased life span.[127–129] As we move to the higher life forms like plants, it was seen that AtPARP-1 and/or AtPARP2 knockdown reported to alter *Arabidopsis* development [130] and AtPARP2 orthologue in oilseed rape (*Brassica napus*) did not affect its development.[131] However, further work is mandatory to explore the role of PARP in plant development. In addition, studies in Drosophila also suggest importance of PARP in chromatin loosening at ecdysone-inducible regions thereby inducing purparium formation and metamorphosis.[59,132] These results are also substantiated by mice studies wherein PARP-1 and PARP-2 double-mutant mice were found to be not viable and die at the onset of gastrulation, establishing the importance of both the PARPs during early embryogenesis.[133] Recently, Hamazaki et al.[134] have shown that PARP inhibition caused inhibition of DNA demethylation of the *IL17d* promoter region at the two-cell stage leading to downregulation of genes essential for early embryogenesis. Thus it is clear from the above that a strong association of PARP-1 exists in differentiation and multicellularity, which is yet to be explored in detail.

4.3.8 | PARP-1 in metabolic regulation

PARP-1 has been known for its role in DNA repair as discussed in above sections. However, recent data suggest a role for PARP-1 in metabolic regulation by influencing mitochondrial function and oxidative metabolism. Mouse knockout studies showed that PARP-1 deletion led to increased food intake.[135,136] PARP-1$^{-/-}$ mice showed an increased metabolic rate.[137] PARP-1 has also been associated with reduction in the glycolytic rate which has been linked to a reduction in NAD^+availability over the years.[138] Over-activation of PARP activity can lead to metabolic perturbations through reduction in ATP, NAD^+/NADH levels, which is enough to impair carbohydrate metabolism.[139] It also changes the flow of glycolytic metabolites into Krebs cycle and thereby compromised energy production in mitochondria.[140] However, recent evidence indicates that PARP-1 may be responsible for reduction in hexokinase activity and hence affects the

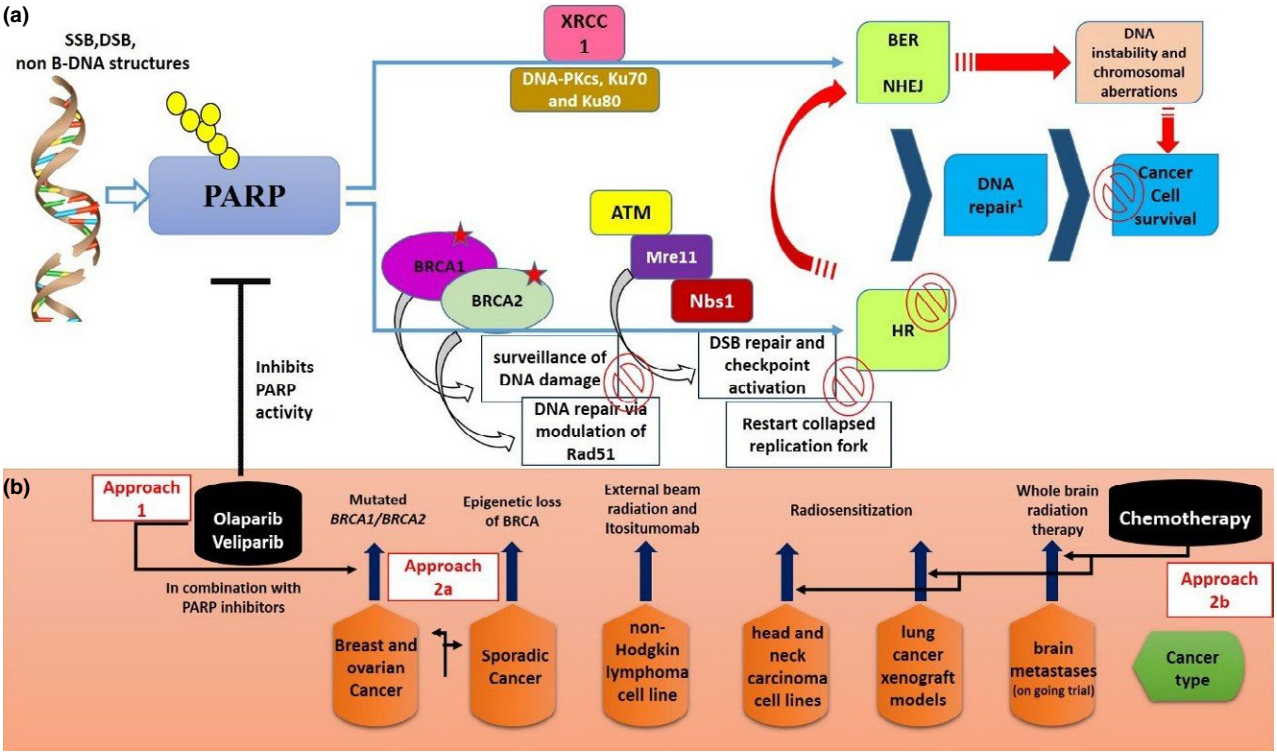

FIGURE 3 PARP-1 and cancer therapy. (a) In normal cells, upon DNA damage like SSB, DSB and non-B-DNA structures, PARP-1 gets activated and thereby aids in the recruitment of DNA repair proteins such as the scaffolding protein XRCC1 to sites of SSBs through BER, whereas DNA-PKcs, Ku70 and Ku80 to sites of DSBs through NHEJ. It also aids HR via recruitment of factors like ATM, Mre11 and Nbs1 to sites of DSBs. Another very essential process of HR repair involves localization of BRCA-1 and BRCA-2 to sites of double-stranded DNA damage. In cancer cells bearing BRCA1/2 mutations or deficiency (red star), cells are rendered faulty in HR repair (red no symbol) and thus there is complete dependence on NHEJ (error-prone) for DSB DNA repair and SSB for BER (red arrows); both of which are PARP-1-dependent. Thus, PARP inhibition serves as an excellent approach for therapy. BRCA1/2 mutations or deficiency along with PARP-1 inhibition leads to amplification of DNA instability due to impairment in BER-, NHEJ- and ATM-mediated HR repair and chromosomal aberrations results in cell death. (b) PARP-1 inhibitors like Olaparib, Veliparib, etc. have been promising therapeutic candidates in case of breast cancer and ovarian cancer—Approach 1. Approach 2a uses PARP-1 inhibitors in case of epigenetic modulation or artificial inactivation of BRCA pathway in case of sporadic cancers, whereas approach 2b involves use of chemotherapy and radiation along with PARP-1 inhibitor depending on the cancer type

cellular glycolytic rate via poly (ADP-ribosyl)ation of hexokinase directly.[141] PARP-1 and PARP-2 activation have also been demonstrated to affect mitochondrial activity negatively.[142] Hence, PARP inhibition arises as therapeutant to treat mitochondrial dysfunction.

In addition, PARP-1 also plays a crucial role in the circadian entrainment and regulates feeding behaviour. Asher et al.[143] demonstrated that CLOCK (Circadian transcription factor)–BMAL1-dependent gene expression was altered in PARP-1-knockout mice, in response to changes in feeding times. In contrast, the deletion of PARP-2 did not affect food intake or daily behaviour.[135] Moreover, both PARP-1$^{-/-}$ and PARP-2$^{-/-}$ mice displayed enhanced energy expenditure.[135,138] PARP-1$^{-/-}$ mice showed an increased mitochondrial content in their brown adipose tissue (BAT),[138] which physiologically renders them to be able to maintain their body temperature during cold exposure. Interestingly, PARP-2 deletion does not influence mitochondrial biogenesis in BAT.[138] Furthermore, it has been suggested that PARP-1 acts as a positive regulator of adipogenesis and adipocyte function resulting in fat deposition.[144] Studies have confirmed that PARP-1 regulates adipogenic gene expression and is required selectively for adipocyte function.[145] PARP-1$^{-/-}$ and PARP-2$^{-/-}$ mice also displayed an increased glucose clearance [135,138] suggesting the increased insulin sensitivity. Thus, these reports suggest the metabolic involvement of PARP-1 and PARP-2; however, more studies are needed to confirm these findings and to explore new metabolic regulatory functions of PARP.

4.3.9 | PARP-1 and cancer

Errors in replication process, production of ROS and UV radiations result in DNA damage which includes single-strand breaks (SSBs), double-strand breaks (DSBs), etc. Cells then signal DNA repair pathways such as nucleic acid excision repair (NER), base excision repair (BER), mismatch repair (MMR), non-homologous end-joining (NHEJ) and homologous recombination (HR) resulting into cell survival with an exception of tumour cells. PARP-1 and PARP-2 are key regulators for the function of DNA repair mechanisms; however, genetic disorders, such as BRCA1 and BRCA2 mutations, prevent

TABLE 3 PARP inhibitors—Olaparib and Veliparib in various disorders

Mode of administration	Disease/disorder	Nature of disorder	Clinical trial status and results	Dosage (mg)	Side effects/toxicity	Reference
(a) PARP inhibitor Olaparib in various cancers						
Oral, monotherapy	Ovarian cancer	Recurrent; with *BRCA1* or *BRCA2* mutation	Phase II; positive	200; Twice a day	Anaemia and Vomiting	Kaye et al.,[167] Mateo et al.[168]
				300; Twice a day	Anaemia	Mateo et al.[168]
				400; Twice a day	Fatigue, nausea, vomiting and decreased appetite	Gelmon et al.,[169] Kaye et al.,[167] Ledermann et al.,[170] Kaufman et al.[171]
		Advanced; without *BRCA1/2* mutation	Phase II; negative	400; Twice a day	—	Gelmon et al.[169]
	Triple-negative breast cancer	Advanced; with *BRCA1* or *BRCA2* mutation	Phase II; positive	100; Twice a day	Fatigue and nausea	Tutt et al.[172]
	Breast cancer	Advanced; with *BRCA1* or *BRCA2* mutation	Phase II; positive	400; Twice a day	Fatigue, nausea and vomiting	Tutt et al.[172]
Oral, Combination therapy with Cediranib	Ovarian cancer	Recurrent; with *BRCA1* or *BRCA2* mutation	Phase I; positive	200/400 mg twice daily plus Cediranib 30 mg daily	Bowel obstruction, fatigue, hypertension, thrombocytopenia	Liu et al.[173]
Oral, Combination therapy with Cediranib	Ovarian fallopian tube, or primary peritoneal cancer	Recurrent; platinum-sensitive, or with *BRCA1/2* mutations	Phase II; Positive compared to monotherapy (400 mg)	200 mg twice daily plus Cediranib 30 mg daily vs 400 mg Olaparib	Fatigue, diarrhoea and hypertension	Liu et al.[174]
Oral, Combination therapy with Cediranib	Triple-negative breast cancer	Metastatic	Phase I; Negative	200/400 mg twice daily plus Cediranib 30 mg daily	—	Liu et al.[173]
Oral, Triple combination therapy with carboplatin and paclitaxel	Ovarian cancer	Advanced, with or w/o *BRCA1* or *BRCA2 mutations*, relapsed	Phase Ib/II; Positive	200 mg twice daily plus carboplatin and paclitaxel, followed by olaparib 400 mg	Neutropenia and anaemia	Oza et al.,[175] Rivkin et al.[176]
Oral, Triple combination therapy with carboplatin+paclitaxel and Chemo therapy	Ovarian cancer	Advanced, with or without *BRCA1* or *BRCA2 mutations*, relapsed	Phase I; Positive	200 mg twice daily plus carboplatin and paclitaxel, followed by olaparib 400 mg	Alopecia, nausea, neutropenia, diarrhoea, headache, peripheral neuropathy and dyspepsia	Oza et al.[175]
Oral; with Chemo therapy	Ewing sarcoma	Refractory	Phase II; Negative	400; Twice a day	Anaemia and thrombocytopenia	Choy et al.[177]
Oral, monotherapy	Pancreatic cancer	With germline BRCA1/2 mutation	Phase II; Positive	400; Twice a day	Fatigue, nausea, anaemia and vomiting	Kaufman et al.[171]
Oral, monotherapy	Prostate cancer	With germline BRCA1/2 mutation	Phase II; Positive	400; Twice a day	Fatigue, nausea, anaemia and vomiting	Kaufman et al.[171]
Intravenous; Combined with cetuximab (cet) and intensity modulated radiation therapy	Head and neck squamous cell carcinoma	Heavy smokers, locally advanced	Phase I; Uncertain/ ongoing	400 mg/m^2+cet 250 mg/ m^2 IV.	Mucositis, dermatitis, clinically insignificant lymphopenia, and hypomagnesaemia	Waxweiler et al.[178]

TABLE 3 (continued)

Mode of administration	Disease/disorder	Nature of disorder	Clinical trial status and results	Dosage (mg)	Side effects/toxicity	Reference
Oral; with temozolomide	Glioblastoma	Relapsed	Phase I; Positive penetration	400	—	Chalmers et al.[179]
Oral; with topotecan	Advanced solid tumours	—	Phase I; Negative	100 mg twice daily	— events	Samol et al.[180]
(b) PARP inhibitor Veliparib in various cancers						
Oral, monotherapy	Epithelial ovarian cancer	Recurrent or persistent; With germline BRCA1/2 mutation	Phase II; Negative; discontinued	400	Grade 3-fatigue, nausea, leukopenia, neutropenia, dehydration, and ALT. Grade 2 events-nausea, fatigue, vomiting and anaemia	Coleman et al.[181]
Oral; monotherapy	Serous ovarian cancer	Without BRCA1/2 mutation	Phase I; Negative	400	Nausea/vomiting, fatigue and leukopenia	Pahuja et al.[182]
Oral; monotherapy	Triple-negative breast cancer	Without BRCA1/2 mutation	Phase I; Negative	400	—	Pahuja et al.[182]
Oral; monotherapy	Castration-resistant prostate cancer	BRCA2-mutated metastatic	Phase I; Positive	400	—	Pahuja et al.[182]
Oral; with irinotecan	Triple-negative breast cancer	Without BRCA1/2 mutation With BRCA1/2 mutation	Phase I; Negative Phase I; positive	40 mg+irinotecan 100 mg/m^2	Leukopenia, neutropenia, nausea, diarrhoea, fatigue, anaemia and vomiting	LoRusso et al.[183]
Oral; Combined with Cisplatin and etoposide	Small cell lung cancer	Previously untreated	Phase I; positive	100+Cisplatin 75 mg/m^2+etoposide 100 mg/m^2	Dehydration, diarrhoea, fatigue, febrile neutropenia, heart failure, leukopenia, lymphopenia, nausea, neutropenia, respiratory failure and thrombocytopenia	Owonikoko et al.[184]
Oral, Combined with carboplatin and paclitaxel	Squamous (Sq) non-small cell lung cancer	Untreated advanced/metastatic	Phase III;	120 mg+carboplatin AUC 6 mg/mL/m IV and paclitaxel 200 mg/m^2 IV	—	McKee et al.[185]
Oral; with metronomic Cyclophosphamide	Solid tumours and lymphomas	Advanced	Phase I; Positive	60 mg+cyclophosphamide 50 mg	—	Kummar et al.[186]
Oral; with cisplatin and gemcitabine	Pancreas adenocarcinoma	Potential BRCA/PABL2 mutated	Phase Ib; Positive	80 mg+C 25 mg/m^2 IV, G 600 mg/m^2 IV	Anaemia, neutropenia, thrombocytopenia, haematologic toxicity and fatigue	O'Reilly et al.[187]
Oral; With Temozolomide (TMZ)	Castration-resistant prostate cancer	Docetaxel-pretreated patients with metastatic	Phase I; positive	40 mg+TMZ 150 mg/m^2	Thrombocytopenia, anaemia, fatigue, neutropenia, nausea and constipation	Hussain et al.[188]

DNA repair mechanism and increase the risk of malignancies.[146] Inhibition of DNA repair process may lead to cell death and this brings PARP-1 as a perfect target for anti-cancer therapy. PARylation of targeted proteins by PARP-1 on activation by SSBs and DSBs facilitates the recruitment of DNA repair proteins such as XRCC1 to sites of damage.[147,148] PARP-1 may also facilitate HR via recruitment of factors like ataxia telangiectasia-mutated (ATM, Ataxia Telangiectasia Mutated), Nijmegen breakage syndrome 1 (Nbs1) and mitotic recombination 11 (Mre11) to sites of DSBs.[149] However, major role in HR repair involves localization of BRCA-1 and BRCA-2. BRCA-1 plays an essential role in the surveillance of DNA damage and transduction of DNA repair responses, while BRCA-2 is directly involved in double-stranded DNA repair, *via* modulation of Rad51 by HR.[150]

PARP-1 inhibition does not cause cell lethality by itself, as the cell has an intact HR pathway for DNA repair. Cells that have a mutated *BRCA1* or *BRCA2* genes as in the case of breast cancer or those that are deficient in BRCA1 or BRCA2 proteins like sporadic cancers are found to be defective in their ability to repair DNA through HR and henceforth depend on error-prone NHEJ. This results in amplification of DNA instability and chromosomal aberrations eventually causing cell death (Fig. 3a). This synergistic effect has been very well demonstrated by Arun et al.,[151] wherein PARPi AZD2281 showed more promising results in BRCA1- and BRCA2-bearing mutants *via* induction of autophagy. This concept of synthetic lethality has been implemented upon in cancer therapeutics. In cases of breast and ovarian cancer, treatment with PARP-1 inhibitors Olaparib and Veliparib (Approach A) has found positive clinical results.[152] Epigenetic modulation or artificial inactivation of BRCA pathway (Approach 2a) in cases of sporadic cancer along with the use of PARPi plays a key to therapeutics. This synergistic inhibition of DNA repair poses as a double-hit mechanism for cancer cell death. PARPi can also be used in combination with chemotherapy and radiation (Approach 2b) to render the cells prone to cell death under enhanced damaged conditions as in cases of non-Hodgkin lymphoma cell line, use of PARPi in combination with both external beam radiation and ^{131}I-tositumomab; radio sensitization with veliparib in head and neck carcinoma cell lines and lung cancer xenograft models; or with niraparib in neuroblastoma cell lines, and whole brain radiation in cases of brain metastases [153] (Fig. 3b). In addition, Table 3 compiles various drug combinations with Olaparib (Table 3a) and Veliparib (Table 3b) which are being currently extensively used in various cancers along with its side effects.

The transcriptional role of PARP-1 in cancer includes chromatin modulation of tumour suppressor and oncogene function, regulation of the metastatic processes, alteration of cell survival and adaptation. For example, in liver cancer, ATPases activity of ALC1 (amplified in liver cancer 1) was found to be dependent upon both PARP-1 and NAD^{+}.[154] Furthermore, various tumour cell lines exhibited overexpression of PARP-1 with malignancy progression.[155] One of the recent studies indicated that following irradiation, PARP-1 activation plays a critical role in prostate cancer cell lines (LNCaP and DU145).[156]

PARP-1 is also thought to be an important modulator of tumour suppressor gene, p53.[157] In addition, PARP-1 is known to regulate organ site-specific tumour suppressors as explained by tumour

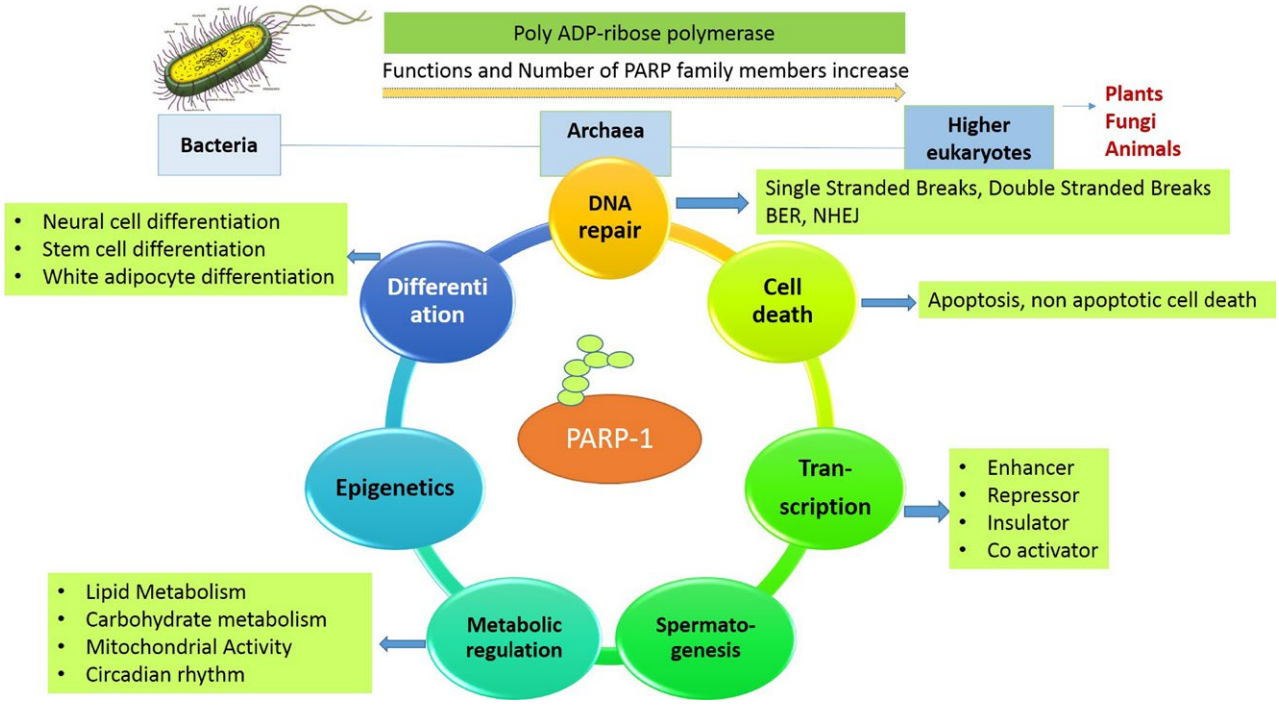

FIGURE 4 PARP-multifunctional protein. Poly ADP-ribose polymerase family of proteins are detected from prokaryotes to eukaryotes. The number of PARP family members and their involvement in various cellular processes increases with the complexity of the organism. PARP-1, the most studied PARP family member is involved a wide range of processes like DNA repair, cell death, transcription, spermatogenesis, metabolic regulation, epigenetics and differentiation

suppressor gene, APC (adenomatous polyposis coli). The loss of this gene was associated with sporadic colorectal cancer (CRC). Collective reports suggest that PARP-1 controls activity of T-cell factor (TCF)/lymphoid enhancer factor (LEF), i.e. TCF/LEF complex in CRC with higher expression levels of PARP-1.[158,159] In addition, Schiewer et al. [160] showed that PARP-1 controls androgen receptor (AR) association and functions with chromatin using in vitro and in vivo systems. In particular, reduction in AR activity was correlated with significant anti-tumour response to PARP-1 inhibition, indicating the dependence of prostate cancer on PARP-1 activity.[160] Thus, these studies suggest that inhibition of PARP-1 has potential as a cancer therapeutic through at least two mechanisms: (1) by potentiating chemotherapeutic agents that damage DNA and increasing tumour sensitivity; and (2) by inducing "synthetic lethality" in cells that are highly dependent on PARP-1, due to deficiency in homologous recombination such as BRCA1 mutants.

4.3.10 | Clinical implications of PARP-1 in other diseases

Dysfunctional PARP-1 has been linked to the onset and progression of myriad of diseases including cancer, ageing, diabetes, neurological diseases, etc. Several evidences point out the role of PARP-1 in cancer. In addition, PARP-1 has also been associated in neuronal pathology. PARP-1 inhibition has been proven to play a protective role in Parkinsons and Alzheimer's disease.[161] Moroni et al. also illustrated PARP-1 inhibitor HYDAMTIQ to be very effective in conferring neuroprotection post stroke.[162] In addition, PARP-1 activation plays a role in diabetic nephropathy, neuropathy and retinopathy. Studies in experimental models reflect the role of PARP-1 in inflammatory responses by promoting inflammation-relevant gene expression. Moreover, activation of NF-κB, AP-1 and heat shock factor protein-1 transcription factors, classically known to signal inflammatory gene expression are mediated by PARP-1.[163,164] PARP-1 also controls immunosuppressive function of regulatory T cells by destabilizing Foxp3.[165] Also, an increase in Foxp3^{+}T regulatory cells has been observed in PARP-1 deficiency.[166] PARP-1 has thus emerged as a very important therapeutic target not only in cancer but also in several other diseases which can be further probed for its therapeutic potential.

5 | CONCLUSION

The current research in PARP-1 biology unravels the role of PARP-1 beyond DNA repair and its involvement in several biological/cellular processes, such as epigenetics, transcriptional regulation, spermatogenesis, differentiation, etc. (Fig. 4). The role of PARP-1 as a transcriptional regulator has shed light on the broader aspect of PARP-1 in the cell. Recent studies have also highlighted the multifaceted role of PARP-1 in transcriptional regulation and provided new insights into how PARP-1 plays a very important role in signalling pathways in the cell. In addition, PARP-1's potential in therapeutics for diverse disease conditions require more animal-based clinical studies. Much work needs to be done to understand how PARP-1 works in conjunction with the other PARP family members. Moreover, PARP-1 inhibitors have been a promising therapeutic for a wide range of pathological conditions. Inhibiting PARP activity uncovers potential of PARP inhibitors as promising candidates for cancer therapy, particularly in BRCA1/2-mutated cancers, alone or in combination with cytotoxic drugs. p53-deficient breast cancer cells treated with a PARP inhibitor happen to lose resistance to an apoptosis promoting, clinically active anti-tumour agent called doxorubicin. However, these PARP inhibitors have several side effects that are toxic to the cell as the reports clearly show PARP-1's role in physiological conditions. Hence, to harness the therapeutic potential of PARP-1, studies are required to find out new inhibitors with least side effects. Thus, PARP-1 has now opened new avenues for researchers to understand PARP-1's multifunctional role in the cell which would eventually aid to further expand the utility of PARP family and its inhibition in therapeutics.

ACKNOWLEDGEMENTS

RB thanks Council of Scientific and Industrial Research, New Delhi (38 (1383)/14/EMR-II) Department of Biotechnology, New Delhi (BT/PR4383/BRB/10/1014/2011) and Department of Science and Technology, New Delhi (SR/SO/BB-03/2010) and for financial support. TJ thanks UGC-SAP DRS for fellowship. RB thanks Dr. Mitesh Dwivedi for his critical suggestions. It is to be noted that none of the authors have any conflict of interest.

REFERENCES

1. D'Amours D, Desnoyers S, D'Silva I, Poirier GG. Poly(ADP-ribosyl)ation reactions in the regulation of nuclear functions. *Biochem J*. 1999;342:249–268.
2. Schreiber V, Dantzer F, Ame JC, de Murcia G. Poly(ADP-ribose): novel functions for an old molecule. *Nat Rev Mol Cell Biol*. 2006;7:517–528.
3. Lautier D, Lagueaux J, Thibodeau J, Ménard L, Poirier GG. Molecular and biochemical features of poly (ADP-ribose) metabolism. *Mol Cell Biochem*. 1993;122:171–193.
4. Meyer-Ficca ML, Meyer RG, Coyle DL, Jacobson EL, Jacobson MK. Human poly(ADP-ribose) glycohydrolase is expressed in alternative splice variants yielding isoforms that localize to different cell compartments. *Exp Cell Res*. 2004;297:521–532.
5. Min W, Wang ZQ. Poly (ADP-ribose) glycohydrolase (PARG) and its therapeutic potential. *Front Biosci (Landmark Ed)*. 2009;14:1619–1626.
6. Oka S, Kato J, Moss J. Identification and Characterization of a Mammalian 39-kDa Poly(ADP-ribose) Glycohydrolase. *JBC*. 2006;281:705–713.
7. Dunn CA, O'Handley SF, Frick DN, Bessman MJ. Studies on the ADP-ribose pyrophosphatase subfamily of the nudix hydrolases and tentative identification of trgB, a gene associated with tellurite resistance. *J Biol Chem*. 1999;274:32318–32324.
8. Rosenthal F, Feijs KLH, Frugier E, et al. Macrodomain-containing proteins are new mono-ADP-ribosylhydrolases. *Nat Struct Mol*. 2013;20:502–509.
9. Ame JC, Spenlehauer C, de Murcia G. The PARP superfamily. *BioEssays*. 2004;26:882–893.
10. Hottiger MO, Hassa PO, Luscher B, Schuler H, Koch-Nolte F. Toward a unified nomenclature for mammalian ADP-ribosyltransferases. *Trends Biochem Sci*. 2010;35:208–219.

11. Morales J, Li L, Fattah FJ, et al. Review of poly(ADP-Ribose) polymerase (PARP) mechanisms of action and rationale for targeting in cancer and other diseases. *Crit Rev Eukaryot Gene Expr*. 2014;24:15–28.
12. Loseva O, Jemth AS, Bryant HE, et al. PARP-3 is a mono-ADP-ribosylase that activates PARP-1 in the absence of DNA. *J Biol Chem*. 2010;285:8054–8060.
13. Hassa PO, Haenni SS, Elser M, Hottiger MO. Nuclear ADP-ribosylation reactions in mammalian cells: where are we today and where are we going? *Microbiol Mol Biol Rev*. 2006;70:789–829.
14. Kickhoefer VA, Siva AC, Kedersha NL, et al. The 193-kD vault protein, VPARP, is a novel poly(ADP-ribose) polymerase. *J Cell Biol*. 1999;146:917–928.
15. Smith S, Giriat I, Schmitt A, de Lange T. Tankyrase, a poly(ADP-ribose) polymerase at human telomeres. *Science*. 1998;282:1484–1487.
16. Seimiya H. The telomeric PARP, tankyrases, as targets for cancer therapy. *Br J Cancer*. 2006;94:341–345.
17. Leung AK, Vyas S, Rood JE, Bhutkar A, Sharp PA, Chang P. Poly(ADP-Ribose) Regulates Stress Responses and MicroRNA Activity in the Cytoplasm. *Mol Cell*. 2011;42:489–499.
18. Ma Q, Baldwin KT, Renzelli AJ, McDaniel A, Dong L. TCDD-inducible poly(ADP-ribose) polymerase: a novel response to 2,3,7,8-tetrachlo rodibenzo-p-dioxin. *Biochem Biophys Res Commun*. 2001;289:499–506.
19. Vyas S, Chesarone-Cataldo M, Todorova T, Huang YH, Chang P. A systematic analysis of the PARP protein family identifies new functions critical for cell physiology. *Nat Commun*. 2013;4:2240.
20. Barkauskaite E, Jankevicius G, Ladurner AG, Ahel I, Timinszky G. The recognition and removal of cellular poly(ADP-ribose) signals. *FEBS J*. 2013;280:3491–3507.
21. Slade D, Dunstan MS, Barkauskaite E, et al. The structure and catalytic mechanism of a poly(ADP-ribose) glycohydrolase. *Nature*. 2011;477:616–620.
22. Perina D, Mikoč A, Ahel J, Ćetković H, Žaja R, Ahel I. Distribution of protein poly(ADP-ribosyl)ation systems across all domains of life. *DNA Repair*. 2014;23:4–16.
23. Faraone-Mennella MR, Gambacorta A, Nicolaus B, Farina B. Purification and biochemical characterization of a poly(ADP-ribose) polymerase-like enzyme from the thermophilic archaeon Sulfolobus solfataricus. *Biochem J*. 1998;335:441–447.
24. Otto H, Reche PA, Bazan F, Dittmar K, Haag F, Koch-Nolte F. In silico characterization of the family of PARP-like poly(ADP-ribosyl) transferases (pARTs). *BMC Genom*. 2005;6:139.
25. Li Z, Yamauchi Y, Kamakura M, et al. Herpes simplex virus requires poly(ADP-ribose) polymerase activity for efficient replication and induces extracellular signal-related kinase-dependent phosphorylation and ICP0-dependent nuclear localization of tankyrase 1. *J Virol*. 2012;86:492–503.
26. Mattiussi S, Tempera I, Matusali G, Mearini G, Lenti L, Fratarcangeli S. Inhibition of poly(ADP-ribose)polymerase impairs Epstein Barr Virus lytic cycle progression. *Infect Agent Cancer*. 2007;2:18.
27. Ogura T, Takenouchi N, Yamaguchi M, Matsukage A, Sugimura T, Esumi H. Striking similarity of the distribution patterns of the poly(ADP-ribose) polymerase and DNA polymerase beta among various mouse organs. *Biochem Biophys Res Commun*. 1990;172:377–384.
28. Babiychuk E, Cottrill PB, Storozhenko S, Fuangthong M, Chen Y, O'Farrell MK. Higher plants possess two structurally different poly(ADP-ribose) polymerases. *Plant J*. 1998;15:635–645.
29. Citarelli M, Teotia S, Lamb RS. Evolutionary history of the poly(ADP-ribose) polymerase gene family in eukaryotes. *BMC Evol Biol*. 2010;10:308.
30. Kawal AM, Mir H, Ramniklal CK, Rajawat J, Begum R. Structural and evolutionary analysis of PARPs in *D. discoideum*. *Am J Infect Dis*. 2011;7:67–74.
31. Kameshita I, Matsuda Z, Taniguchi T, Shizuta Y. Poly(ADP-ribose) synthetase. Separation and identification of three proteolytic fragments as the substrate-binding domain, the DNA-binding domain and the automodification domain. *J Biol Chem*. 1984;259:4770–4776.
32. Langelier MF, Ruhl DD, Planck JL, Kraus WL, Pascal JM. The Zn3 domain of human poly(ADP-ribose) polymerase-1 (PARP-1) functions in both DNA-dependent poly(ADP-ribose) synthesis activity and chromatin compaction. *J Biol Chem*. 2010;285:18877–18887.
33. Langelier MF, Servent KM, Rogers EE, Pascal JM. A third zinc-binding domain of human poly(ADP-ribose) polymerase-1 coordinates DNA dependent enzyme activation. *J Biol Chem*. 2008;283:4105–4114.
34. Ye'lamos J, Farres J, Llacuna L, Ampurdanes C, Martin-Caballero J. PARP-1 and PARP-2: new players in tumour development. *Am J Cancer Res*. 2011;1:328–346.
35. Kinoshita T, Nakanishi I, Warizaya M, et al. Inhibitor-induced structural change of the active site of human poly(ADP-ribose) polymerase. *FEBS Lett*. 2004;556:43–46.
36. Masson MV, Rolli FD, Dantzer F, et al. Poly(ADP-ribose) polymerase: structure-function relationship. *Biochimie*. 1995;77:456–461.
37. Langelier MF, Planck JL, Roy S, Pascal JM. Structural basis for DNA damage–dependent poly (ADP-ribosyl)ation by human PARP-1. *Science*. 2012;336:728–732.
38. Altmeyer M, Messner S, Hassa PO, Fey M, Hottiger MO. Molecular mechanism of poly(ADP-ribosyl)ation by PARP1 and identification of lysine residues as ADP-ribose acceptor sites. *Nucleic Acids Res*. 2009;37:3723–3738.
39. Beckert S, Farrahi F, Perween GQ, et al. IGF-I-induced VEGF expression in HUVEC involves phosphorylation and inhibition of poly(ADP-ribose) polymerase. *Biochem Biophys Res Commun*. 2006;341:67–72.
40. Hassa PO, Haenni SS, Buerki C, Meier NI, Lane WS, Owen H. Acetylation of poly(ADP-ribose) polymerase-1 by p300/CREB-binding protein regulates coactivation of NF-kappaB-dependent transcription. *J Biol Chem*. 2005;280:40450–40464.
41. Kauppinen TM, Chan WY, Suh SW, Wiggins AK, Huang EJ, Swanson RA. Direct phosphorylation and regulation of poly(ADP-ribose) polymerase-1 by extracellular signal regulated kinases 1/2. *Proc Natl Acad Sci USA*. 2006;103:7136–7141.
42. Mao Z, Hine C, Tian X, et al. SIRT6 promotes DNA repair under stress by activating PARP-1. *Science*. 2011;332:1443–1446.
43. Zilio N, Williamson CT, Eustermann S, et al. DNA-dependent SUMO modification of PARP-1. *DNA Repair*. 2013;12:761–773.
44. Kim MY, Zhang T, Kraus WL. Poly(ADP-ribosyl)ation by PARP-1: 'PARlaying' NAD^+into a nuclear signal. *Genes Dev*. 2005;19:1951–1967.
45. Kun E, Kirsten E, Ordahl CP. Coenzymatic activity of randomly broken or intact double-stranded DNAs in auto and histone H1 trans-poly(ADP-ribosylation), catalyzed by poly(ADP-ribose) polymerase (PARP I). *J Biol Chem*. 2002;277:39066–39069.
46. Oei SL, Shi Y. Poly (ADP-ribosyl)ation of transcription factor Y in Yang 1 under conditions of DNA damage. *Biochem Biophys Res Commun*. 2001;285:27–31.
47. Lonskaya I, Potaman VN, Shlyakhtenko LS, Oussatcheva EA, Lyubchenko YL, Soldatenkov VA. Regulation of poly(ADP-ribose) polymerase-1 by DNA structure-specific binding. *J Biol Chem*. 2005;280:17076–17083.
48. Eustermann S, Videler H, Yang JC, et al. The DNA-binding domain of human PARP-1 interacts with DNA single-strand breaks as a monomer through its second zinc finger. *J Mol Biol*. 2011;407:149–170.
49. Langelier MF, Planck JL, Roy S, Pascal JM. Crystal structures of poly (ADP-ribose) polymerase-1 (PARP-1) zinc fingers bound to DNA structural and functional insights into DNA-dependent PARP-1 activity. *J Biol Chem*. 2011;286:10690–10701.

50. Eustermann S, Wu WF, Langelier MF, et al. Structural Basis of Detection and Signaling of DNA Single-Strand Breaks by Human PARP-1. *Mol Cell* 2015;60:742–754.
51. Ko HL, Ren EC. Novel poly(ADP-ribose) polymerase 1 binding motif in hepatitis B virus core promoter impairs DNA damage repair. *Hepatology*. 2011;54:1190–1198.
52. Cohen-Armon M, Visochek L, Rozensal D, et al. DNA-independent PARP-1 activation by phosphorylated ERK2 increases Elk1 activity: a link to histone acetylation. *Mol Cell*. 2007;25:297–308.
53. Cohen-Armon M. PARP-1 activation in the ERK signaling pathway. *Trends Pharmacol Sci*. 2007;28:556–560.
54. Ju B, Solum D, Song EJ, et al. Activating the PARP-1 sensor component of the Groucho/TLE1 corepressor complex mediates a CaMKinase IIdelta-dependent neurogenic gene activation pathway. *Cell*. 2004;119:815–829.
55. Dong F, Soubeyrand S, Haché RJ. Activation of PARP-1 in response to bleomycin depends on the Ku antigen and protein phosphatase 5. *Oncogene*. 2010;29:2093–2103.
56. Zhang T, Berrocal JG, Yao J, DuMond ME, Krishnakumar R, Ruhl DD. Regulation of poly(ADP-ribose) polymerase-1-dependent gene expression through promoter-directed recruitment of a nuclear NAD^+synthase. *J Biol Chem*. 2012;287:12405–12416.
57. Ouararhni K, Hadj-Slimane R, Ait-Si-Ali S, Robin P, Mietton F, Harel-Bellan A. The histone variant mH2A1.1 interferes with transcription by down-regulating PARP-1 enzymatic activity. *Genes Dev*. 2006;20:3324–3336.
58. Midorikawa R, Takei Y, Hirokawa N. KIF4 motor regulates activity-dependent neuronal survival by suppressing PARP-1 enzymatic activity. *Cell*. 2006;125:371–383.
59. Tulin A, Spradling A. Chromatin loosening by poly(ADP-ribose) polymerase (PARP) at Drosophila Puff Loci. *Science*. 2003;299:560–562.
60. Virág L, Szabó C. The therapeutic potential of poly(ADP-ribose) polymerase inhibitors. *Pharmacol Rev*. 2002;54:375–429.
61. Masutani M, Nakagama H, Sugimura T. Poly(ADP-ribose) and carcinogenesis. *Genes Chromosom Cancer*. 2003;38:339–348.
62. Dantzer F, de La Rubia G, Menissier-De MJ, Hostomsky Z, de Murcia G, Schreiber V. Base excision repair is impaired in mammalian cells lacking poly(ADP-ribose) polymerase-1. *Biochemistry*. 2000;39:7559–7569.
63. Izhar L, Adamson B, Ciccia A, et al. A systematic analysis of factors localized to damaged chromatin reveals PARP-dependent recruitment of transcription factors. *Cell Rep*. 2015;11:1486–1500.
64. Ahel D, Hořejší Z, Wiechens N, et al. Poly (ADP-ribose) dependent regulation of DNA repair by the chromatin remodeling enzyme ALC1. *Science*. 2009;325:1240–1243.
65. Altmeyer M, Toledo L, Gudjonsson T, et al. The chromatin scaffold protein SAFB1 renders chromatin permissive for DNA damage signaling. *Mol Cell*. 2013;52:206–220.
66. Timinszky G, Till S, Hassa PO, et al. A macrodomain-containing histone rearranges chromatin upon sensing PARP1 activation. *Nat Struct Mol Biol*. 2009;16:923–929.
67. Ahel I, Ahel D, Matsusaka T, et al. Poly (ADP-ribose)-binding zinc finger motifs in DNA repair/checkpoint proteins. *Nature*. 2008;451:81–85.
68. Rulten SL, Cortes-Ledesma F, Guo L, Iles NJ, Caldecott KW. APLF (C2orf13) is a novel component of poly (ADP-ribose) signaling in mammalian cells. *Mol Cell Biol*. 2008;28:4620–4628.
69. Mortusewicz O, Amé JC, Schreiber V, Leonhardt H. Feedback-regulated poly(ADP-ribosyl)ation by PARP-1 is required for rapid response to DNA damage in living cells. *Nucleic Acids Res*. 2007;35:7665–7675.
70. Robu M, Shah RG, Petitclerc N, Brind'Amour J, Kandan-Kulangara F, Shah GM. Role of poly(ADP-ribose) polymerase-1 in the removal of UV-induced DNA lesions by nucleotide excision repair. *Proc Natl Acad Sci USA* 2013;110:1658–1663.
71. Adamson B, Smogorzewska A, Sigoillot FD, King RW, Elledge SJ. A genome-wide homologous recombination screen identifies the RNA-binding protein RBMX as a component of the DNA-damage response. *Nat Cell Biol*. 2012;14:318–328.
72. Patel AG, Sarkaria JN, Kaufmann SH. Nonhomologous end joining drives poly(ADP-ribose) polymerase (PARP) inhibitor lethality in homologous recombination-deficient cells. *Proc Natl Acad Sci USA*. 2011;108:3406–3411.
73. Xie S, Mortusewicz O, Ma HT, et al. Timeless interacts with PARP-1 to promote homologous recombination repair. *Mol Cell*. 2015;60:163–167.
74. Galluzzi L, Joza N, Tasdemir E, et al. No death without life: vital functions of apoptotic effectors. *Cell Death Differ*. 2008;15:1113–1123.
75. Soldani C, Scovassi AI. Poly(ADP-ribose) polymerase-1 cleavage during apoptosis: an update. *Apoptosis*. 2002;7:321–328.
76. Tewari M, Quan LT, O'Rourke K, et al. Yama/CPP32 beta, a mammalian homolog of CED-3, is a CrmA inhibitable protease that cleaves the death substrate poly(ADP-ribose) polymerase. *Cell*. 1995;81:801–809.
77. Scovassi AI, Diederich M. Modulation of poly(ADP-ribosylation) in apoptotic cells. *Biochem Pharmacol*. 2004;68:1041–1047.
78. Sosna J, Voigt S, Mathieu S, et al. TNF-induced necroptosis and PARP-1-mediated necrosis represent distinct routes to programmed necrotic cell death. *Cell Mol Life Sci*. 2014;71:331–348.
79. Gerö D, Szoleczky P, Chatzianastasiou A, Papapetropoulos A, Szabo C. Modulation of Poly (ADP-Ribose) Polymerase-1 (PARP-1)-Mediated Oxidative Cell Injury by Ring Finger Protein 146 (RNF146) in Cardiac Myocytes. *Mol Med*. 2014;20:313.
80. Yu SW, Andrabi SA, Wang H, et al. Apoptosis-inducing factor mediates poly(ADP-ribose) (PAR) polymer-induced cell death. *Proc Natl Acad Sci USA*. 2006;103:18314–18319.
81. Donizy P, Halon A, Surowiak P, Pietrzyk G, Kozyra C, Matkowski R. Correlation between PARP-1 immunoreactivity and cytomorphological features of parthanatos, a specific cellular death in breast cancer cells. *Eur J Histochem*. 2013;57:35.
82. Andrabi SA, Dawson TM, Dawson VL. Mitochondrial and nuclear cross talk in cell death. *Ann NY Acad Sci*. 2008;1147:233–241.
83. Rajawat J, Alex T, Mir H, Kadam A, Begum R. Proteases involved during oxidative stress induced poly(ADP-ribose) polymerase mediated cell death in *D. discoideum*. *Microbiology*. 2014;160:1101–1111.
84. Rajawat J, Mir H, Alex T, Bakshi S, Begum R. Involvement of poly(ADP-ribose) polymerase in paraptotic cell death of *D. discoideum*. *Apoptosis*. 2014;19:90–101.
85. Rajawat J, Vohra I, Mir H, Gohel D, Begum R. Effect of oxidative stress and involvement of poly(ADP-ribose) polymerase (PARP) in *Dictyostelium discoideum* development. *FEBS J*. 2007;274:5611–5618.
86. Mir H, Rajawat J, Begum R. Staurosporine induced cell death in *D. discoideum* is independent of PARP. *Indian J Exp Biol*. 2012;50:80–86.
87. Muñoz-Gámez JA, Rodríguez-Vargas JM, Quiles-Pérez R, et al. PARP-1 is involved in autophagy induced by DNA damage. *Autophagy*. 2009;5:61–74.
88. Huang Q, Shen HM. To die or to live: the dual role of poly(ADP-ribose) polymerase-1 in autophagy and necrosis under oxidative stress and DNA damage. *Autophagy*. 2009;5:273–276.
89. Son YO, Wang X, Hitron JA, et al. Cadmium induces autophagy through ROS-dependent activation of the LKB1–AMPK signaling in skin epidermal cells. *Toxicol Appl Pharmacol*. 2011;255:287–296.
90. Wyrsch P, Blenn C, Bader J, Althaus FR. Cell death and autophagy under oxidative stress: roles of poly(ADP-Ribose) polymerases and Ca(2+). *Mol Cell Biol*. 2012;32:3541–3553.
91. Mansuri MS, Singh M, Jadeja SD, et al. Could ER stress be a major link between oxidative stress and autoimmunity in Vitiligo? *Pigmentary Disord*. 2014;1:123.

92. Jog NR, Caricchio R. Differential regulation of cell death programs in males and females by Poly (ADP-Ribose) Polymerase-1 and 17β estradiol. *Cell Death Dis*. 2013;4:e758.
93. Caiafa P, Guastafierro T, Zampieri M. Epigenetics: poly(ADP-ribosyl) ation of PARP-1 regulates genomic methylation patterns. *FASEB J*. 2009;23:672–678.
94. Lodhi N, Kossenkov AV, Tulin AV. Bookmarking promoters in mitotic chromatin: poly(ADP-ribose) polymerase-1 as an epigenetic mark. *Nucleic Acids Res*. 2014;42:7028–7038.
95. Lapucci A, Pittelli M, Rapizzi E, Felici R, Moroni F, Chiarugi A. Poly(ADP-ribose) polymerase-1 is a nuclear epigenetic regulator of mitochondrial DNA repair and transcription. *Mol Pharmacol*. 2011;79:932–940.
96. Nalabothula N, Al-jumaily T, Eteleeb AM, Flight RM, Xiaorong S, Moseley H, et al. Genome-wide profiling of PARP1 reveals an interplay with gene regulatory regions and DNA methylation. *PLoS ONE*. 2015;10:e0135410.
97. Caiafa P, Zlatanova J. CCCTC-binding factor meets poly(ADP-ribose) polymerase-1. *J Cell Physiol*. 2009;219:265–270.
98. Vitale AM, Wolvetang E, Mackay-Sim A. Induced pluripotent stem cells: a new technology to study human diseases. *Int J Biochem Cell Biol*. 2011;43:843–846.
99. Doege CA, Inoue K, Yamashita T, et al. Early-stage epigenetic modification during somatic cell reprogramming by PARP-1 and Tet2. *Nature*. 2012;488:652–655.
100. Guetg C, Scheifele F, Rosenthal F, Hottiger MO, Santoro R. Inheritance of silent rDNA chromatin is mediated by PARP1 via noncoding RNA. *Mol Cell*. 2012;45:790–800.
101. Huletsky A, de Murcia G, Muller S, et al. The effect of poly(ADP-ribosyl)ation on native and H1-depleted chromatin. A role of poly(ADP-ribosyl)ation on core nucleosome structure. *J Biol Chem*. 1989;264:8878–8886.
102. Wacker DA, Ruhl DD, Balagamwala EH, Hope KM, Zhang T, Kraus WL. The DNA binding and catalytic domains of poly(ADP-ribose) polymerase 1 cooperate in the regulation of chromatin structure and transcription. *Mol Cell Biol*. 2007;27:475–7485.
103. Pinnola A, Naumova N, Shah M, Tulin AV. Nucleosomal Core Histones Mediate Dynamic regulation of Poly(ADP-ribose) Polymerase 1 Protein Binding to Chromatin and Induction of Its enzymatic Activity. *J Biol Chem*. 2007;282:32511–32519.
104. Krishnakumar R, Gamble MJ, Frizzell KM, Berrocal JG, Kininis M, Kraus WL. Reciprocal binding of PARP-1 and histone H1 at promoters specifies transcriptional outcomes. *Science*. 2008;319:819–821.
105. Frizzell KM, Gamble MJ, Berrocal JG, Zhang T, Krishnakumar R, Cen Y. Global analysis of transcriptional regulation by poly (ADP-ribose) polymerase-1 and poly (ADP-ribose) glycohydrolase in MCF-7 human breast cancer cells. *J Biol Chem*. 2009;284:33926–33938.
106. Berger SL. Thecomplex language of chromatin regulation during transcription. *Nature*. 2007;447:407–412.
107. Kotova E, Lodhi N, Jarnik M, Pinnola AD, Ji Y, Tulin AV. Drosophila histone H2A variant (H2Av) controls poly (ADP-ribose) polymerase1 (PARP1) activation in chromatin. *Proc Natl Acad Sci*. 2011;108:6205–6210.
108. Kraus WL. New functions for an ancient domain. *Nat Struct Mol Biol*. 2009;16:904–907.
109. Chen H, Ruiz PD, Novikov L, Casill AD, Park JW, Gamble MJ. MacroH2A1.1 and PARP-1 cooperate to regulate transcription by promoting CBP-mediated H2B acetylation. *Nat Struct Mol Biol*. 2014;21:981–989.
110. Krishnakumar R, Kraus WL. PARP-1 regulates chromatin structure and transcription through a KDM5B-dependent pathway. *Mol Cell*. 2010;39:736–749.
111. Wu T, Wang XJ, Tian W, Jaramillo MC, Lau A, Zhang DD. Poly (ADP-ribose) polymerase-1 modulates Nrf2-dependent transcription. *Free Radic Biol Med*. 2014;67:69–80.
112. Okada H, Inoue T, Kikuta T, et al. Poly(ADP-ribose) polymerase-1 enhances transcription of the profibrotic CCN2 gene. *J Am Soc Nephrol*. 2008;19:933–942.
113. Ong CT, Van Bortle K, Ramos E, Corces VG. Poly(ADP-ribosyl)ation regulates insulator function and intrachromosomal interactions in *Drosophila*. *Cell*. 2013;155:148–159.
114. Zhao H, Sifakis EG, Sumida N, et al. PARP1-and CTCF-mediated interactions between active and repressed chromatin at the lamina promote oscillating transcription. *Mol Cell*. 2015;59:984–997.
115. O'Donnell A, Yang SH, Sharrocks AD. PARP1 orchestrates variant histone exchange in signal-mediated transcriptional activation. *EMBO J*. 2013;14:1084–1091.
116. Agarwal A, Mahfouz RZ, Sharma RK, Sarkar O, Mangrola D, Mathur PP. Potential biological role of poly(ADP-ribose) polymerase (PARP) in male gametes. *Reprod Biol Endocrinol*. 2009;7:143.
117. Di Meglio S, Denegri M, Vallefuoco S, Tramontano F, Scovassi AI, Quesada P. Poly(ADPR) polymerase-1 and poly(ADPR) glycohydrolase level and distribution in differentiating rat germinal cells. *Mol Cell Biochem*. 2003;248:85–91.
118. Quesada P, Atorino L, Cardone A, Ciarcia G, Farina B. Poly(ADP-ribosyl)ation system in rat germinal cells at different stages of differentiation. *Exp Cell Res*. 1996;226:183–190.
119. Schreiber V, Ame JC, Dolle P, Schultz I, Rinaldi B, Fraulob V. Poly(ADP-ribose) polymerase-2 (PARP-2) is required for efficient base excision DNA repair in association with PARP-1 and XRCC1. *J Biol Chem*. 2002;277:23028–23036.
120. Meyer-Ficca ML, Scherthan H, Burkle A, Meyer RG. Poly(ADP-ribosyl)ation during chromatin remodeling steps in rat spermiogenesis. *Chromosoma*. 2005;114:67–74.
121. Marcon L, Boissonneault G. Transient DNA strand breaks during mouse and human spermiogenesis new insights in stage specificity and link to chromatin remodeling. *Biol Reprod*. 2004;70:910–918.
122. Rouleau M, Saxena V, Rodrigue A, et al. A key role for poly(ADP-ribose) polymerase 3 in ectodermal specification and neural crest development. *PLoS ONE*. 2011;6:e15834.
123. Rajawat J, Mir H, Begum R. Differential role of poly(ADP-ribose) polymerase (PARP) in *D. discoideum*. *BMC Dev Biol*. 2011;11:14.
124. Jubin T, Kadam A, Saran S, Begum R. Poly (ADP-ribose) polymerase1 regulates growth and multicellularity in D. discoideum. *Differentiation* 2016;pii:S0301-4681(15)30081-5. doi:10.1016/j.diff.2016.03.002.
125. Couto CA, Wang HY, Green JC, et al. PARP regulates nonhomologous end joining through retention of Ku at double-strand breaks. *J Cell Biol*. 2011;194:367–375.
126. Mir H, Alex T, Rajawat J, Kadam A, Begum R. Response of *D. discoideum* to UV-C and involvement of poly(ADP-ribose) polymerase. *Cell Prolif*. 2015;48:363–374.
127. Kothe GO, Kitamura M, Masutani M, Selker EU, Inoue H. PARP is involved in replicative aging in Neurospora crassa. *Fungal Genet Biol*. 2010;47:297–309.
128. Müller-Ohldach M, Brust D, Hamann A, Osiewacz HD. Overexpression of PaParp encoding the poly(ADP-ribose) polymerase of Podospora anserina affects organismal aging. *Mech Ageing Dev*. 2011;132:33–42.
129. Semighini CP, Savoldi M, Goldman GH, Harris SD. Functional characterization of the putative Aspergillus nidulans poly(ADP-ribose) polymerase homolog PrpA. *Genetics*. 2006;173:87–98.
130. De Block M, Verduyn C, De Brouwer D, Cornelissen M. Poly(ADP-ribose) polymerase in plants affects energy homeostasis, cell death and stress tolerance. *Plant J*. 2005;41:95–106.
131. Vanderauwera S, De Block M, Van de Steene N, van de Cotte B, Metzlaff M, Van Breusegem F. Silencing of poly(ADP-ribose) polymerase in plants alters abiotic stress signal transduction. *Proc Natl Acad Sci USA*. 2007;104:15150–15155.
132. Fletcher JC, Burtis KC, Hogness DS, Thummel CS. The Drosophila E74 gene is required for metamorphosis and plays a role in the

polytene chromosome puffing response to ecdysone. *Development*. 1995;121:1455–1465.
133. De Murcia JM, Ricoul M, Tartier L, et al. Functional interaction between PARP-1 and PARP-2 in chromosome stability and embryonic development in mouse. *EMBO J*. 2003;22:2255–2263.
134. Hamazaki N, Uesaka M, Nakashima K, Agata K, Imamura T. Gene activation-associated long noncoding RNAs function in mouse preimplantation development. *Development*. 2015;142:910–920.
135. Bai P, Canto C, Brunyanszki A, et al. PARP 1 regulates SIRT1 expression and whole body energy expenditure. *Cell Metab*. 2011a;13:450–460.
136. Devalaraja-Narashimha K, Padanilam BJ. PARP1 deficiency exacerbates diet-induced obesity in mice. *J Endocrinol*. 2010;205:243–252.
137. Wang ZQ, Auer B, Stingl L, et al. Mice lacking ADPRT and poly(ADP-ribosyl)ation develop normally but are susceptible to skin disease. *Genes Dev*. 1995;9:509–520.
138. Bai P, Canto C, Oudart H, et al. PARP-1 inhibition increases mitochondrial metabolism through SIRT1 activation. *Cell Metab*. 2011b;13:461–468.
139. Houtkooper RH, Williams RW, Auwerx J. Metabolic networks of longevity. *Cell*. 2010;142:9–14.
140. Ying W, Chen Y, Alano CC, Swanson RA. Tricarboxylic acid cycle substrates prevent PARP-mediated death of neurons and astrocytes. *J Cereb Blood Flow Metab*. 2002;22:774–779.
141. Andrabi SA, Umanah GKE, Chang C, et al. Poly(ADP-ribose) polymerase-dependent energy depletion occurs through inhibition of glycolysis. *Proc Natl Acad Sci USA*. 2014;111:10209–10214.
142. Bai P, Nagy L, Fodor T, Liaudet L, Pacher P. Poly (ADP-ribose) polymerases as modulators of mitochondrial activity. *Trends Endocrinol Metab*. 2015;26:75–83.
143. Asher G, Reinke H, Altmeyer M, Gutierrez-Arcelus M, Hottiger MO, Schibler U. Poly(ADP-ribose) polymerase 1 participates in the phase entrainment of circadian clocks to feeding. *Cell*. 2010;142:943–953.
144. Erener S, Mirsaidi A, Hesse M, et al. ARTD1 deletion causes increased hepatic lipid accumulation in mice fed a high-fat diet and impairs adipocyte function and differentiation. *FASEB J*. 2012b;26:2631–2638.
145. Erener S, Hesse M, Kostadinova R, Hottiger MO. Poly(ADP-ribose) polymerase-1 (PARP-1) controls adipogenic gene expression and adipocyte function. *Mol Endocrinol*. 2012a;26:79–86.
146. Hennessy BT, Timms KM, Carey MS, Gutin A, Meyer LA, Flake DD 2nd. Somatic mutations in BRCA1 and BRCA2 could expand the number of patients that benefit from poly(ADP-ribose) polymerase inhibitors in ovarian cancer. *J Clin Oncol*. 2010;28:3570–3576.
147. El-Khamisy SF, Masutani M, Suzuki H, Caldecott KW. A requirement for PARP-1 for the assembly or stability of XRCC1 nuclear foci at sites of oxidative DNA damage. *Nucleic Acids Res*. 2003;31:5526–5533.
148. Houtgraaf JH, Versmissen J, van der Giessen WJ. A concise review of DNA damage checkpoints and repair in mammalian cells. *Cardiovasc Revasc Med*. 2006;7:165–172.
149. Haince JF, McDonald D, Rodrigue A, et al. PARP-1 dependent kinetics of recruitment of MRE11 and NBS1 proteins to multiple DNA damage sites. *J Biol Chem*. 2008;283:1197–1208.
150. Tutt A, Ashworth A. The relationship between the roles of BRCA genes in DNA repair and cancer predisposition. *Trends Mol Med*. 2002;8:571–576.
151. Arun B, Akar U, Gutierrez-Barrera AM, Hortobagyi GN, Ozpolat B. The PARP inhibitor AZD2281 (Olaparib) induces autophagy/mitophagy in BRCA1 and BRCA2 mutant breast cancer cells. *Int J Oncol*. 2015;47:262–268.
152. Fong PC, Yap TA, Boss DS, et al. Poly(ADP-ribose) polymerase inhibition: frequent durable responses in BRCA carrier ovarian cancer correlating with platinum-free interval. *J Clin Oncol*. 2010;28:2512–2519.
153. Do K, Chen AP. Molecular Pathways: targeting PARP in cancer treatment. *Clin Cancer Res*. 2013;19:977–984.
154. Gottschalk AJ, Timinszky G, Kong SE, et al. Poly(ADP-ribosyl)ation directs recruitment and activation of an ATP-dependent chromatin remodeler. *Proc Natl Acad Sci USA*. 2009;106:13770–13774.
155. Zaremba T, Ketzer P, Cole M, Coulthard S, Plummer ER, Curtin NJ. Poly(ADP-ribose) polymerase-1 polymorphisms, expression and activity in selected human tumour cell lines. *Br J Cancer*. 2009;101:256–262.
156. Espinoza LA. *The Role of PARP Activation in Prostate Cancer*. Advances in Prostate Cancer, Dr. Gerhard Hamilton (Ed.). Croatia: InTech, 2013.
157. Mendoza-Alvarez H, Alvarez-Gonzalez R. Regulation of p53 sequence-specific DNA-binding by covalent poly(ADP-ribosyl)ation. *J Biol Chem*. 2001;276:36425–36430.
158. Idogawa M, Masutani M, Shitashige M, et al. Ku70 and poly(ADP-ribose) polymerase-1 competitively regulate beta-catenin and T-cell factor-4-mediated gene transactivation: possible linkage of DNA damage recognition and Wnt signaling. *Cancer Res*. 2007;67:911–918.
159. Idogawa M, Yamada T, Honda K, Sato S, Imai K, Hirohashi S. Poly(ADP-ribose) polymerase-1 is a component of the oncogenic T-cell factor-4/beta-catenin complex. *Gastroenterology*. 2005;128:1919–1936.
160. Schiewer MJ, Goodwin JF, Han S, Brenner JC, Augello MA, Dean JL. Dual Roles of PARP-1 Promote Cancer Growth and Progression. *Cancer Discov*. 2012;2:1134–1149.
161. Martire S, Mosca L, d'Erme M. PARP-1 involvement in neurodegeneration: A focus on Alzheimer's and Parkinson's diseases. *Mech Ageing Dev*. 2015;146–148:53–64.
162. Moroni F, Cozzi A, Chiarugi A, et al. Long-lasting neuroprotection and neurological improvement in stroke models with new, potent and brain permeable inhibitors of poly(ADP-ribose) polymerase. *British J Pharmacol*. 2012;165:1487–1500.
163. Ba X, Gupta S, Davidson M, Garg NJ. Trypanosoma cruzi induces the reactive oxygen species-PARP-1-RelA pathway for up-regulation of cytokine expression in cardiomyocytes. *J Biol Chem*. 2010;285:11596–11606.
164. Beneke S. Poly(ADP-ribose) polymerase activity in different pathologies: the link to inflammation and infarction. *Exp Gerontol*. 2008;43:605–614.
165. Zhang P, Maruyama T, Konkel JE, et al. PARP-1 controls immunosuppressive function of regulatory T cells by destabilizing Foxp3. *PLoS ONE*. 2013;8:e71590.
166. Nasta F, Laudisi F, Sambucci M, Rosado MM, Pioli C. Increased Foxp3$^+$regulatory T cells in poly(ADP-ribose) polymerase-1 deficiency. *J Immunol*. 2010;184:3470–3477.
167. Kaye SB, Lubinski J, Matulonis U, et al. Phase II, open-label, randomized, multicenter study comparing the efficacy and safety of olaparib, a poly (ADP-ribose) polymerase inhibitor, and pegylated liposomal doxorubicin in patients with BRCA1 or BRCA2 mutations and recurrent ovarian cancer. *J Clin Oncol*. 2011;30:372–379.
168. Mateo J, Friedlander M, Sessa C, et al. Administration of continuous/intermittent olaparib in ovarian cancer patients with a germline BRCA1/2 mutation to determine an optimal dosing schedule for the tablet formulation. *Eur J Cancer*. 2013;49:S161.
169. Gelmon KA, Tischkowitz M, Mackay H, et al. Olaparib in patients with recurrent high-grade serous or poorly differentiated ovarian carcinoma or triple-negative breast cancer: a phase 2, multicentre, open-label, non-randomised study. *Lancet Oncol*. 2011;12:852–861.
170. Ledermann J, Harter P, Gourley C, et al. Olaparib maintenance therapy in platinum-sensitive relapsed ovarian cancer. *N Engl J Med*. 2012;366:1382–1392.
171. Kaufman B, Shapira-Frommer R, Schmutzler RK, et al. Olaparib monotherapy in patients with advanced cancer and a germline BRCA1/2 mutation. *J Clin Oncol*. 2015;33:244–250.

172. Tutt A, Robson M, Garber JE, et al. Oral poly (ADP-ribose) polymerase inhibitor olaparib in patients with BRCA1 or BRCA2 mutations and advanced breast cancer: a proof-of-concept trial. *Lancet*. 2010;376:235–244.
173. Liu JF, Tolaney SM, Birrer M, et al. A Phase 1 trial of the poly(ADP-ribose) polymerase inhibitor olaparib (AZD2281) in combination with the anti-angiogenic cediranib (AZD2171) in recurrent epithelial ovarian or triple-negative breast cancer. *Eur J Cancer*. 2013;49:2972–2978.
174. Liu JF, Barry WT, Birrer M, et al. Combination cediranib and olaparib versus olaparib alone for women with recurrent platinum-sensitive ovarian cancer: a randomised phase 2 study. *Lancet Oncol*. 2014;15:1207–1214.
175. Oza AM, Cibula D, Benzaquen AO, et al. Olaparib combined with chemotherapy for recurrent platinum-sensitive ovarian cancer: a randomised phase 2 trial. *Lancet Oncol*. 2015;16:87–97.
176. Rivkin SE, Iriarte D, Sloan H, Wiseman C, Moon J. Phase Ib/II with expansion of patients at the MTD study of olaparib plus weekly (metronomic) carboplatin and paclitaxel in relapsed ovarian cancer patients. *ASCO Annu Meet Proc* 2014;15(Suppl):5527.
177. Choy E, Butrynski JE, Harmon DC, et al. Phase II study of olaparib in patients with refractory Ewing sarcoma following failure of standard chemotherapy. *BMC Cancer*. 2014;14:813.
178. Waxweiler TV, Bowles D, Reddy K, et al. Safety and feasibility update of olaparib, an orally bioavailable PARP inhibitor, with concurrent cetuximab and radiation therapy in heavy smokers with stage III-IVB squamous cell carcinoma of the head/neck: a phase 1 trial. *Int J Radiation Oncol Biol Phys*. 2014;90:S559.
179. Chalmers AJ, Jackson A, Swaisland H, et al. Results of stage 1 of the oparatic trial: a phase I study of olaparib in combination with temozolomide in patients with relapsed glioblastoma. *J Clin Oncol*. 2014;32:5S.
180. Samol J, Ranson M, Scott E, et al. Safety and tolerability of the poly(ADP-ribose) polymerase (PARP) inhibitor, olaparib (AZD2281) in combination with topotecan for the treatment of patients with advanced solid tumors: a phase I study. *Invest New Drugs*. 2012;30:1493–1500.
181. Coleman RL, Sill MW, Bell-McGuinn K, et al. A phase II evaluation of the potent, highly selective PARP inhibitor veliparib in the treatment of persistent or recurrent epithelial ovarian, fallopian tube, or primary peritoneal cancer in patients who carry a germline BRCA1 or BRCA2 mutation-An NRG Oncology/Gynecologic Oncology Group study. *Gynecol Oncol*. 2015;137:386–391.
182. Pahuja S, Appleman LJ, Belani CP, et al. Preliminary activity of veliparib (V) in BRCA2-mutated metastatic castration-resistant prostate cancer (mCRPC). *J Clin Oncol*. 2015;33.
183. LoRusso PM, Tolaney SM, Wong S, et al. Combination of the PARP inhibitor veliparib (ABT888) with irinotecan in patients with triple negative breast cancer: Preliminary activity and signature of response. *Cancer Res*. 2015;75:CT325.
184. Owonikoko TK, Dahlberg SE, Khan SA, et al. A phase 1 safety study of veliparib combined with cisplatin and etoposide in extensive stage small cell lung cancer: A trial of the ECOG–ACRIN Cancer Research Group (E2511). *Lung Cancer*. 2015;89:66–70.
185. McKee MD, Bondarenko I, Guclu SZ, et al. Veliparib (ABT-888) or placebo combined with carboplatin and paclitaxel in patients with previously untreated advanced/metastatic squamous (Sq) non-small cell lung cancer (NSCLC): a randomized phase 3 trial. *J Clin Oncol*. 2015;33.
186. Kummar S, Ji J, Morgan R, et al. A Phase I Study of Veliparib in Combination with Metronomic Cyclophosphamide in Adults with Refractory Solid Tumors and Lymphomas. *Clin Cancer Res*. 2012;18:1726–1734.
187. O'Reilly EM, Lowery MA, Segal MF, et al. Phase IB trial of cisplatin (C), gemcitabine (G), and veliparib (V) in patients with known or potential BRCA or PALB2-mutated pancreas adenocarcinoma (PC). *ASCO Annual Meeting Proceedings* 2014;32(15 suppl):4023.
188. Hussain M, Carducci MA, Slovin S, et al. Targeting DNA repair with combination veliparib (ABT-888) and temozolomide in patients with metastatic castration-resistant prostate cancer. *Invest New Drugs*. 2014;32:904–912.

Microbiology (2014), **160**, 1101–1111 **DOI** 10.1099/mic.0.076620-0

Proteases involved during oxidative stress-induced poly(ADP-ribose) polymerase-mediated cell death in *Dictyostelium discoideum*

Jyotika Rajawat, Tina Alex, Hina Mir, Ashlesha Kadam and Rasheedunnisa Begum

Correspondence
Rasheedunnisa Begum
rasheedunnisab@yahoo.co.in

Department of Biochemistry, Faculty of Science, Maharaja Sayajirao University of Baroda, Vadodara-390002, Gujarat, India

Apoptosis involves a cascade of caspase activation leading to the ordered dismantling of critical cell components. However, little is known about the dismantling process in non-apoptotic cell death where caspases are not involved. *Dictyostelium discoideum* is a good model system to study caspase-independent cell death where experimental accessibility of non-apoptotic cell death is easier and molecular redundancy is reduced compared with other animal models. Poly(ADP-ribose) polymerase (PARP) is one of the key players in cell death. We have previously reported the role of PARP in development and the oxidative stress-induced cell death of *D. discoideum. D. discoideum* possesses nine PARP genes and does not have a caspase gene, and thus it provides a better model system to dissect the role of PARP in caspase-independent cell death. The current study shows that non-apoptotic cell death in *D. discoideum* occurs in a programmed fashion where proteases cause mitochondrial membrane potential changes followed by plasma membrane rupture and early loss of plasma membrane integrity. Furthermore, the results suggest that calpains and cathepsin D, which are instrumental in dismantling the cell, act downstream of PARP. Thus, PARP, apoptosis inducing factor, calpains and cathepsin D are the key players in *D. discoideum* caspase-independent cell death, acting in a sequential manner.

Received 4 January 2014
Accepted 6 April 2014

INTRODUCTION

Cells contain a specific death-governing network associated with different effector and/or dismantling mechanisms. Apoptosis consists of events occurring via a cascade of caspase activation leading to ordered dismantling of critical cell components and pathways. At the end of apoptosis, the cell is fragmented into apoptotic bodies that undergo phagocytosis by neighbouring cells (Katoch *et al.*, 2002). Thus, these morphological changes are the manifestation of the cell undergoing systematic dismantling and further packaging itself into membrane-bound vesicles to be taken up by neighbouring cells. Because cellular contents are not released, apoptosis occurs without inflammation. However, little is known about the dismantling process in non-apoptotic cell death where caspases are not involved. A major task, for the less well-known non-apoptotic types of cell death, will be the identification and study of cell death types, which reflect dismantling events of effector mechanisms. *Dictyostelium discoideum* is a good model system to study dismantling events where it shows poly(ADP-ribose) polymerase (PARP)-mediated caspase-independent cell death (Rajawat *et al.*, 2014). The evolutionary aspects of programmed cell death would be illuminated by studying cell death mechanisms in *D. discoideum* (Mir *et al.*, 2007; Kawal *et al.*, 2011).

Oxidative stress has been shown to be associated with cell death in most systems (Hasnain *et al.*, 1999; Sah *et al.*, 1999; Mohan *et al.*, 2003). We have reported the high resistance of the unicellular stage of *D. discoideum* to oxidative stress (Katoch & Begum, 2003). *D. discoideum* devoid of caspases exhibits non-apoptotic cell death mediated by several proteins or factors, PARP being one of them (Rajawat *et al.*, 2014). We have established the role of PARP during development (Rajawat *et al.*, 2007, 2011) and staurosporine- (Mir *et al.*, 2012) and oxidative stress-induced cell death (Rajawat *et al.*, 2014) along with the downstream effects. Our results suggest that PARP and apoptosis inducing factor (AIF) may be the key players in regulating caspase-independent cell death. In the current study we have explored the biochemical events occurring during oxidative stress-induced cell death in *D. discoideum*.

Abbreviations: AIF, apoptosis inducing factor; ALLN, N-Acetyl-L-leucyl-L-leucyl-L-norleucinal; AMC, 7-amino-4-methyl-coumarin; $DiOC_6$, 3,3′-dihexyloxacarbocyanine iodide; DPH, 1,6-diphenyl-1,3,5-hexatriene; HA, hydroxylamine; MMP, mitochondrial membrane potential; PARP, poly(ADP-ribose) polymerase; PI, propidium iodide; PIC, protease inhibitor cocktail; PS, phosphatidylserine; zVAD-fmk, N-Benzyloxycarbonyl-Val-Ala-Asp(O-Me) fluoromethyl ketone.

In mammalian systems, probable candidates involved in cell dismantling could be lysosomal proteases or cytosolic protease, namely calpain. Partial destabilization of lysosomal membrane leads to release of cathepsin D in the cytosol. Cathepsin D triggers Bax activation, which induces the release of AIF into the cytosol (Bidère *et al.*, 2003). Cathepsin D also induces generalized proteolysis leading to caspase-independent cell death. Calpains are believed to participate in intracellular signal processing via limited proteolysis of their targets. Calpains have been shown to act downstream of caspase activation and contribute to the degradation phase of campthotecin-induced apoptosis in HL-60 cells (Wood *et al.*, 1998; Wood & Newcomb, 1999). Sanvicens *et al.* (2004) have shown that both caspases and calpains contribute to oxidative stress-induced apoptosis in retinal photoreceptor cells. Thus, to explore the role of proteases in *D. discoideum* dismantling, we initiated our study with protease inhibitor cocktail (PIC) to inhibit most of the proteases and then used specific inhibitors for calpain and cathepsin D.

METHODS

***D. discoideum* culture conditions.** *D. discoideum* strain Ax-2, which is an axenic derivative of Raper's wild-type NC-4, was used. *D. discoideum* was grown under different culture conditions. Growing cells (unicellular) were maintained in a liquid suspension (HL5 medium). *D. discoideum* cells were grown in HL5 medium, pH 6.5, with shaking (150 r.p.m.) at 22 °C (Watts & Ashworth, 1970). Exponential phase cells at a density of ~2.5×10^6 cells ml^{-1} were used for experiments.

Induction of oxidative stress. Oxidative stress was induced in *D. discoideum* cells by *in situ* generation of H_2O_2 upon addition of hydroxylamine (HA; Sigma), a catalase inhibitor (Kono & Fridovich, 1983), or by exogenous addition of cumene hydroperoxide (Sigma). Exponential phase cells at a density of ~2.5×10^6 cells ml^{-1} were exposed to different doses of HA (0, 1, 2.5 mM) and paraptotic (0.03 mM) and necrotic (0.05 mM) doses of cumene H_2O_2 as described by Rajawat *et al.* (2014) in HL-5 medium at 22 °C in a sterile flask.

Assessment of cell death by Annexin V-FITC/propidium iodide (PI) dual staining. To differentiate between apoptotic and necrotic cell death, dual staining with Annexin V-FITC/PI (Miller, 2004) was performed using an apoptosis detection kit (Molecular Probes). Then, ~2.0×10^6 cells were pelleted and washed twice with 1× Sorenson's buffer (SB). *D. discoideum* cells were then suspended in binding buffer provided in the kit and incubated with Annexin V for 10 min and then with PI for 5 min in the dark at 22 °C. Fluorescence was monitored at ×63 using a Zeiss confocal laser scanning fluorescence-inverted microscope (LSM 710; Carl Zeiss) and quantified by flow cytometry using a FACS ARIA cytometer (BD Biosciences). Data were analysed with FACSDiva software. A dose- and time-dependent study was done to standardize the paraptotic and necrotic doses of HA for further experiments.

Evaluation of mitochondrial membrane potential (MMP). The potential sensitive dye 3,3′-dihexyloxacarbocyanine iodide ($DiOC_6$; Sigma) was used to evaluate changes in MMP (Koning *et al.*, 1993). To observe the change in MMP, a time-dependent study was done using paraptotic and necrotic doses of HA as standardized by Annexin V–PI dual staining. Approximately 2.0×10^6 cells were pelleted and washed twice with 1× SB. Cells were stained with $DiOC_6$ (400 nM) for 15 min in the dark and then washed once with 1× SB and monitored for fluorescence using a Nikon Eclipse TE2000S fluorescence microscope.

MMP was also measured by flow cytometry, by incubating *D. discoideum* cells (1×10^6 ml^{-1}) with 5,5′,6,6′-tetrachloro-1,1′,3,3′-tetraethylbenzimidazol carbocyanine iodide (JC-1; Molecular Probes) (Cossarizza & Salvioli, 2001), and quantified by flow cytometry using a FACS ARIA cytometer. Data were analysed with CellQuest software.

Monitoring AIF release by immunofluorescence. Release of AIF from mitochondria to cytosol and its translocation to nucleus were monitored by detecting immunofluorescence (Bidère *et al.*, 2003) at different time intervals. *D. discoideum* cells were pelleted and washed once with PBS (pH 7.4), fixed in 70 % chilled methanol for 10 min at −20 °C and then washed with blocking solution (1.5 % BSA with 0.05 % Tween 20 in PBS) followed by incubation for 1 h in primary antibody using rabbit anti-AIF polyclonal antibodies raised against amino acids 151–180 of human AIF (Cayman Chemical) at 1 : 1000 dilution and then anti-rabbit IgG (whole molecule) TRITC conjugate (Sigma) at 1 : 400 dilution. Nuclear counterstaining with DAPI (1 μg ml^{-1}) for 5 min was performed after the removal of excess secondary antibody and observed for fluorescence.

Detection of caspase activity. The substrate DEVD-AMC is an oligopeptide that is covalently linked with the fluorophore 7-amino-4-methylcoumarin (AMC). DEVD is the cleavage site for caspases (3 and 7). Cleavage takes place at the C terminus of the last aspartate residue, thus liberating the fluorophore AMC, which can be estimated and/or visualized under the fluorescence microscope (AMC λ_{ex}=380 nm; λ_{em}=420 nm).

Approximately 2.0×10^6 cells were harvested and washed with PBS. Cells were resuspended in 1 ml PBS and an aliquot of 100 μl was taken from it and 10 μl of DEVD-AMC substrate (1 mg ml^{-1}) was added. After incubation for 1 h, cells were observed under the Nikon Eclipse TE2000S fluorescence microscope. AMC liberated from the fluorogenic substrate was measured at 380 nm using a UV filter (Olie *et al.*, 1998). Caspase activity as a function of AMC fluorescence was monitored at different time intervals. The entire procedure was carried out using a caspase-3 assay kit (Sigma) as per the manufacturer's instructions. The effect of caspases on cell death was also studied by using a broad caspase inhibitor (zVAD-fmk, Sigma).

Characterization of vesicles formed during paraptotic cell death. Isolation of vesicles was performed from *D. discoideum* culture after 16 h of 1 mM HA stress as mentioned by Gautam & Sharma (2002a). The culture was centrifuged at 1000 ***g*** for 4 min at 4 °C; the supernatant was collected and centrifuged at 21 000 ***g*** for 45 min at 4 °C. The pellet obtained was washed once with 1× SB and used for further analysis. Formation of these vesicles was monitored at different time intervals. Isolated vesicles were stained separately with a fluorescent membrane probe, 1,6-diphenyl-1,3,5-hexatriene (DPH), at a concentration of 1 μM, DAPI and Annexin V–PI and then observed using a confocal laser scanning fluorescence-inverted microscope (LSM 710; Carl Zeiss) and fluorimeter (F7000; Hitachi).

Vacuolization in paraptotic cell death. Cultured exponential-phase cells exposed to 0.03 mM H_2O_2 were rinsed in 0.1 M phosphate buffer, and fixed in 2.5 % glutaraldehyde and 2.0 % paraformaldehyde in 0.1 M phosphate buffer, pH 7.4, at 4 °C for 6–8 h. The pellet was then stored in paraformaldehyde and 0.1 M phosphate buffer (1 : 1) and processed for microtomy. Sections were obtained with a Reichert Ultracut E ultramicrotome, stained and examined with a Morgagni 268D transmission electron microscope.

Investigation of proteases involved in cell death. Cells were pre-incubated with PIC (Sigma) followed by oxidative stress, and MMP change was monitored. Similarly, MMP change, phosphatidylserine

(PS) exposure and vesicle formation were followed in oxidative stress-treated cells pre-incubated for 12 h with 7.5 μM pepstatin A, a cathepsin D inhibitor, and 10 μM N-acetyl-L-leucyl-L-leucyl-L-norleucinal (ALLN), a calpain inhibitor.

Calpain activity. Calpain activity present in total cell lysates of 2.0×10^6 cells of control and oxidative stressed *D. discoideum* was determined by cleavage of the fluorescent substrate *N*-succinyl-LLVY-AMC (Calbiochem). Calcium-dependent fluorescence was measured after 30 min incubation at 37 °C in buffer containing 63 mM imidazole-HCl, pH 7.3, 10 mM β-mercaptoethanol and 5 mM $CaCl_2$ (Moubarak *et al.*, 2007). Fluorescence was recorded in a fluorimeter. Data were normalized per milligram of protein, as estimated by the Lowry method (Lowry *et al.*, 1951).

RESULTS

Induction of cell death in *D. discoideum* cells by oxidative stress

Experiments were designed to establish the ability of *D. discoideum* to undertake cell death as a function of oxidative stress. This was achieved by intracellular build up of H_2O_2 by HA treatment. Cells were treated with different concentrations of HA (0, 1, 2.5, 3, 4 mM), a known inhibitor of catalase, leading to intracellular accumulation of reactive oxygen species, and cell death was measured by the trypan blue exclusion method (Fig. 1a). The LD_{50}, i.e. the concentration of HA inducing 50 % cell death at 12 h post-treatment, was 2.5 mM.

Staining with Annexin V-FITC in conjunction with vital dyes such as PI allows us to distinguish apoptotic cells (Annexin V-positive, PI-negative) from necrotic cells (Annexin V-positive, PI-positive). Thus, based on Annexin V–PI dual staining results, 2.5 mM HA was necrotic as cells exhibited both Annexin V staining due to PS exposure and PI staining at 3 h. In contrast, 1 mM HA was paraptotic as Annexin V staining due to PS exposure was exhibited by cells after 5 h while PI was observed at 12 h of oxidant treatment (Fig. 1b, c). Paraptotic and necrotic doses of cumene H_2O_2 were also used for further experiments, as described previously (Rajawat *et al.*, 2014).

Oxidative stress-induced cell death in *D. discoideum* is caspase-independent

Oxidative stress was generated with HA or cumene H_2O_2. Caspase-3 activity was monitored during oxidative stress-induced cell death. No significant change in caspase activity was seen in basal fluorescence in control and 1 mM HA-treated cells at 1 and 6 h post-stress. A caspase-3-specific inhibitor (DEVD-CHO) could not inhibit the observed caspase activity (Fig. 2a), suggesting absence of caspase activation during oxidative stress-induced cell death in *D. discoideum*. HA at 2.5 mM also exhibited non-significant caspase activity (Fig. 2a).

To demonstrate that the cytotoxicity effect is not due to a caspase-dependent pathway, cell death study was carried out with a broad caspase inhibitor (zVAD-fmk). Our previous reports show that MMP changes following post-oxidative stress. zVAD-fmk had no effect on MMP changes (Fig. 2b) induced by oxidative stress and also on plasma membrane integrity as monitored by PI staining (Fig. 2c). In the presence of 10 μM zVAD-fmk, the cytotoxicity induced by oxidative stress was not inhibited, indicating that *D. discoideum* cells take up a caspase-independent pathway. Further increasing the concentration of zVAD-fmk up to 25 μM did not change the results.

Characterization of vesicles formed during non-apoptotic cell death

To examine the fate of dying paraptotic cells, paraptotic vesicle formation was assessed. We could observe the formation of vesicles at a later stage after loss of plasma membrane integrity. Our results suggest that the vesicles formed by paraptotic doses of HA and cumene H_2O_2 were membranous in nature (Fig. 3a, b) and contain DNA (Fig. 3c). PS staining could not be seen, suggesting that vesicles did not exhibit PS exposure (data not shown). Interestingly such vesicles were not observed with 2.5 mM HA/0.05 mM cumene H_2O_2 stress, which is the necrotic dose.

Vacuolization in paraptotic cell death

Under the electron microscope, vegetatively growing *D. discoideum* cells showed a highly developed cytoplasmic system of small vacuoles. After 16–22 h of oxidative stress-induced paraptotic cell death (1 mM HA/0.03 mM cumene H_2O_2), vacuoles were more abundant in stressed cells than in control cells. After 12 h in the presence of 1 mM HA/0.03 mM cumene H_2O_2, the cell borders were altered. The most prominent difference was the presence of large cytoplasmic vacuoles, either appearing empty or containing residual material (Fig. 3d).

Proteases involved in *D. discoideum* caspase-independent cell death

Effect of PIC on caspase-independent cell death. PIC had no effect at 3 h while partial rescue in MMP changes was observed at 5 h (Fig. 4a). Protease inhibition results showed that MMP changes were unaffected, suggesting that lysosomal proteases are not involved in the early phase of paraptotic cell death. However, during the late phase of paraptotic cell death lysosomes seem to be involved in dismantling events, as caspases are absent in *D. discoideum*.

Calpain activity during caspase-independent cell death

To explore a possible role of calpain in oxidative stress-induced cell death we examined the effect of HA and H_2O_2 on calpain activity. The kinetics of calpain activity was studied using the fluorescent calpain peptide substrate *N*-succinyl-leu-leu-val-tyr-7-amino-4-methylcoumarin. Our results suggest an increase in calpain activity by 3 h during 1 mM HA and 0.03 mM cumene H_2O_2 treatments (Fig. 4b).

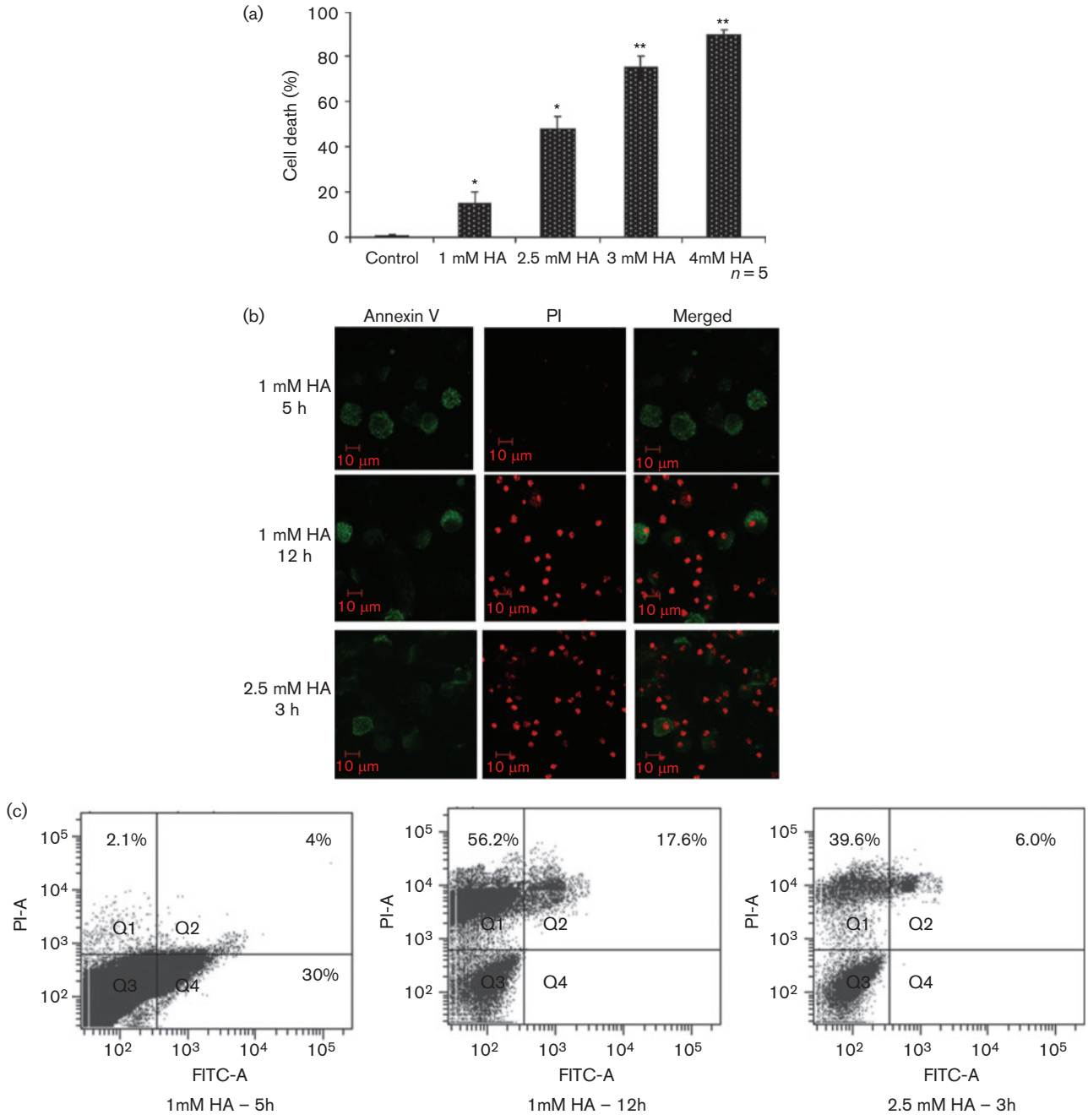

Fig. 1. HA induces dose-dependent cell death. (a) Dose-dependent increase in cell death was observed with HA, as monitored by trypan blue exclusion. Results are the mean ± SEM of five independent experiments. $^{**}P<0.01$, $^{*}P<0.05$ compared with control. (b) 2.5 mM HA-treated cells showed Annexin V–PI dual positive cells as early as 3 h. Annexin V–PI dual staining of 1 mM HA-stressed *D. discoideum* cells. Annexin V staining due to PS externalization was seen at 5 h and PI staining at 12 h with 1 mM HA. Data are representative of three independent experiments. Photographs were taken using a ×60 objective. (c) Annexin V–PI staining for *D. discoideum* cells subjected to 1 mM HA and 2.5 mM HA quantified by flow cytometry.

Effect of calpain and cathepsin D inhibition on MMP changes during oxidative stress-induced cell death

To further identify the specific protease(s) involved during oxidative stress-induced cell death we used ALLN, a calpain inhibitor, and pepstatin A, a cathepsin D inhibitor, and monitored their effects on MMP changes and PS–PI staining. To study the effect of calpain and cathepsin D inhibition during oxidative stress-induced cell death, cells were pre-incubated with 10 µM calpain inhibitor (ALLN)

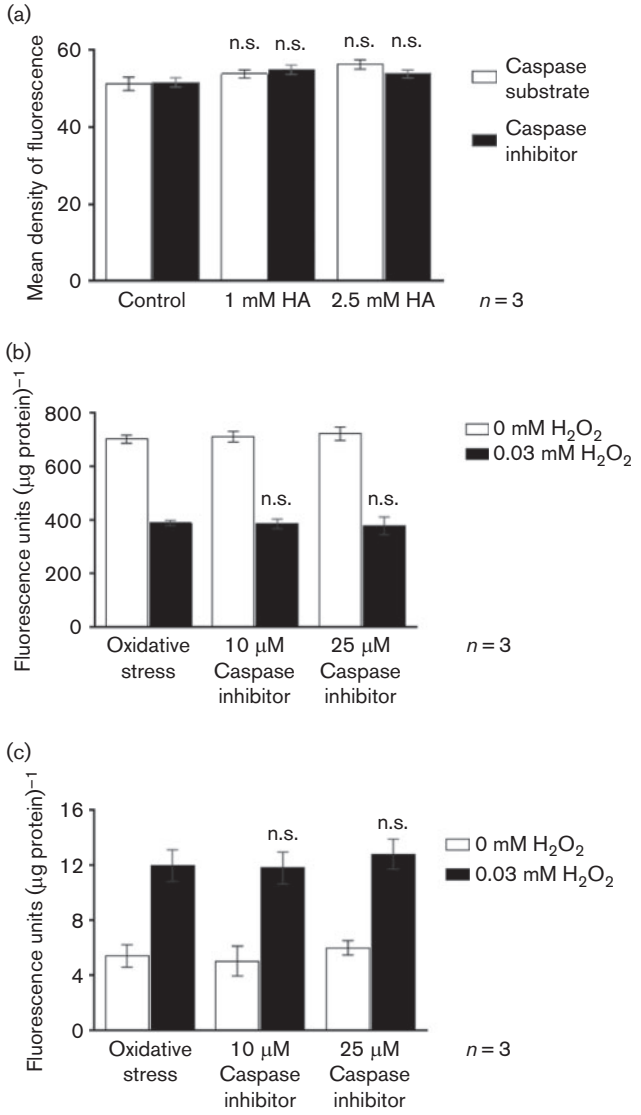

Fig. 2. Caspase-independent cell death in *D. discoideum.* (a) Caspase activity during paraptotic cell death. *D. discoideum* cells were treated with HA stress and caspase activity was assayed at 6 h in the form of DEVD-AMC cleavage and also in the presence of a caspase-3 inhibitor. Caspase activity was non-significant (n.s.). (b) MMP changes in the presence of a broad caspase inhibitor during paraptosis. Data (mean ± SE) are from three independent experiments. No significant (n.s.) effect was observed. (c) Propidium iodide staining in the presence of a broad caspase inhibitor during paraptosis. Data (mean ± SE) are from three independent experiments.

and 7.5 μM pepstatin A before inducing oxidative stress. No significant effect was observed on MMP with pepstatin alone (Fig. 5a). Nevertheless, calpain inhibitor (ALLN) alone could partially retrieve the changes in MMP induced during stress with 1 mM HA and 0.03 mM H_2O_2. Further combinatorial effects of both inhibitors on cell death were also monitored. The resultant MMP changes as monitored using $DiOC_6$ are shown in Fig. 5(b, c). As can be seen, calpain inhibitor and pepstatin A pretreatment together gave significant rescue in MMP changes as compared with pepstatin A or ALLN alone on 1 mM HA- and 0.03 mM H_2O_2-induced MMP changes. To confirm the change in MMP, JC-1 staining was performed. Mitochondria containing red JC-1 aggregates in healthy cells are detectable in the FL2 channel, and green JC-1 monomers in apoptotic cells are detectable in the FITC channel (FL1). JC-1 staining also showed a reduction in red fluorescence in ~64 % of cells, indicating mitochondrial membrane depolarization at 3 h post-1 mM HA treatment, which showed marked rescue by the calpain inhibitor ALLN and pepstatin A pretreatment: an ~37 % increase in red fluorescence as opposed to 5.6 % with pepstatin A or 12.56 % with ALLN (Fig. 5d). As pepstatin alone could not rescue MMP changes, cathepsin D probably does not have a major role in inducing cell death.

As shown in Fig. 6, cells pre-incubated with calpain inhibitor (ALLN) and cathepsin D inhibitor (pepstatin A) subjected to 1 mM HA stress exhibited only PS exposure at 12 h but no PI staining, indicating that plasma membrane integrity remains intact upon treatment with calpain and cathepsin inhibitors during oxidative stress.

Effect of calpain inhibition on AIF translocation

AIF translocation to nucleus was observed at 6 h of 1 mM HA treatment (cells exhibited pink fluorescence). Pretreatment of ALLN and pepstatin A partially prevented the translocation of AIF to nucleus in 1 mM HA-stressed *D. discoideum* cells (Fig. 7).

Vesicle formation in the presence of calpain and cathepsin D inhibitors

The vesicles were formed by 16 h with a paraptotic dose of oxidative stress. As can be seen from the fluorescence images, the vesicles are membranous in nature and contain DNA as indicated by staining with DPH and DAPI, respectively. Cells pretreated with cathepsin D and calpain inhibitors, then exposed to 1 mM HA and 0.03 mM H_2O_2 stress showed no vesicle formation while pre-incubation with calpain inhibitor alone followed by treatment with 1 mM HA and 0.03 mM H_2O_2 showed vesicle formation (Fig. 8) although less than under oxidative stress alone.

Proteases involved during oxidative stress-induced necrotic cell death

Calpain activity during necrosis. A significant increase in calpain activity was observed in cells subjected to 2.5 mM HA and 0.05 mM H_2O_2 treatments as compared with control at 3 h (Fig. 9a).

Effect of PIC on necrosis

Partial rescue in MMP was seen at 2 h with PIC during necrotic cell death, confirming that lysosomal proteases are involved in MMP changes (Fig. 9b).

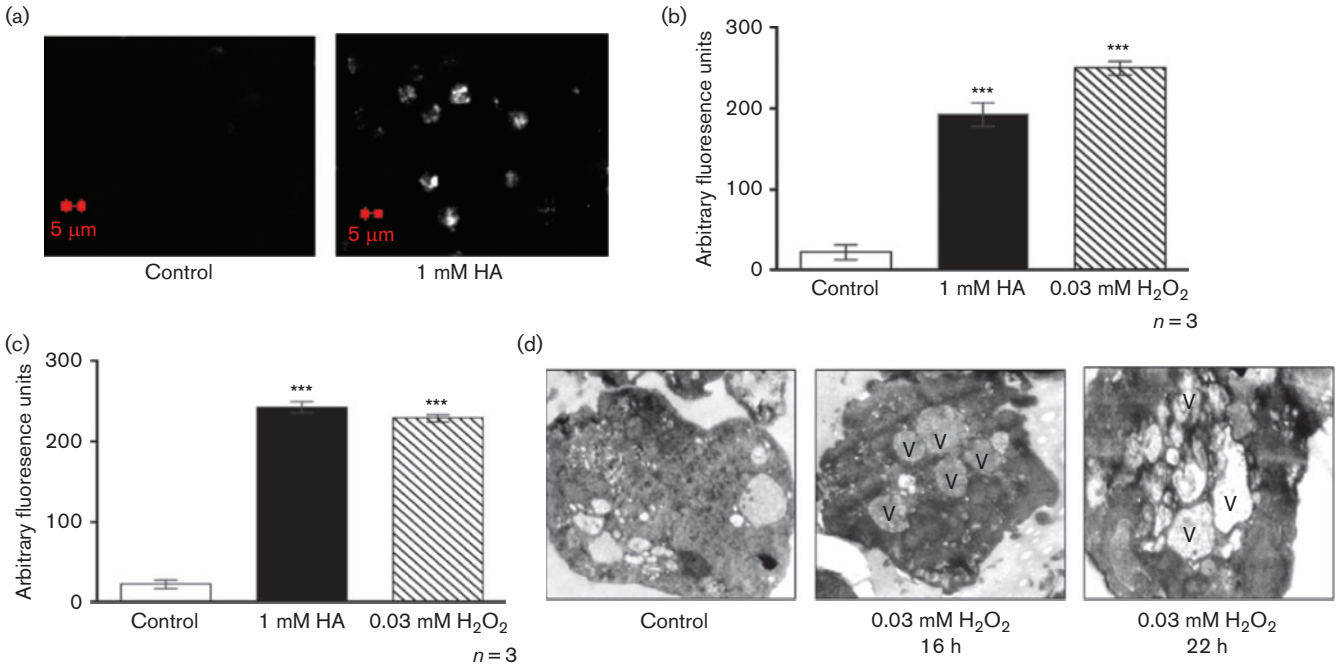

Fig. 3. Vesicle formation and vacuolization during oxidative stress-induced paraptosis. (a) Characterization of paraptotic vesicles formed during oxidative stress using the membrane probe DPH by confocal microscopy. Data are representative of at least three independent experiments. Photographs were taken using a ×63 objective. (b) Fluorimetric analysis of paraptotic vesicles using DPH staining. ***$P<0.001$ compared with control. Error bars, ±SEM. (c) Characterization of paraptotic vesicles formed during oxidative stress using the DNA binding dye DAPI. Data are representative of at least three independent experiments. ***$P<0.001$ compared with control. Error bars, ±SEM. (d) Electron microscopy of 0.03 mM H_2O_2-stressed *D. discoideum* Ax-2 cells at 16 and 22 h. Cells exhibit an irregular shape with a highly developed vacuolar system (V) under oxidative stress.

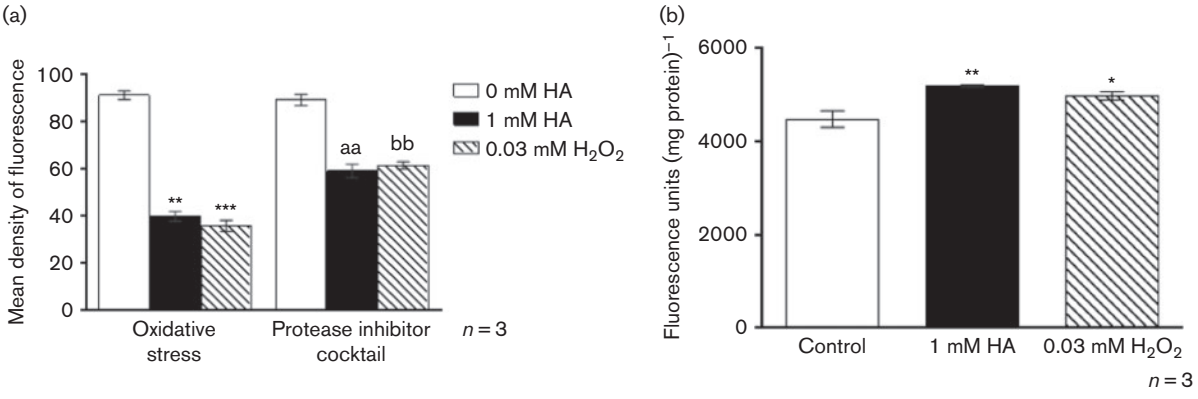

Fig. 4. Effect of PIC on MMP changes and calpain activity during paraptotic cell death. (a) PIC exhibited partial restoration of MMP changes at 5 h. Results are the mean of three independent experiments ± SEM. ***$P<0.001$, **$P<0.01$ compared with control; ^{aa}, $^{bb}P<0.01$ compared with the respective treatments. (b) Calpain activity measured by using its substrate succinyl-AMC during paraptosis at 3 h post-oxidative stress. **$P<0.001$, *$P<0.01$ compared with control.

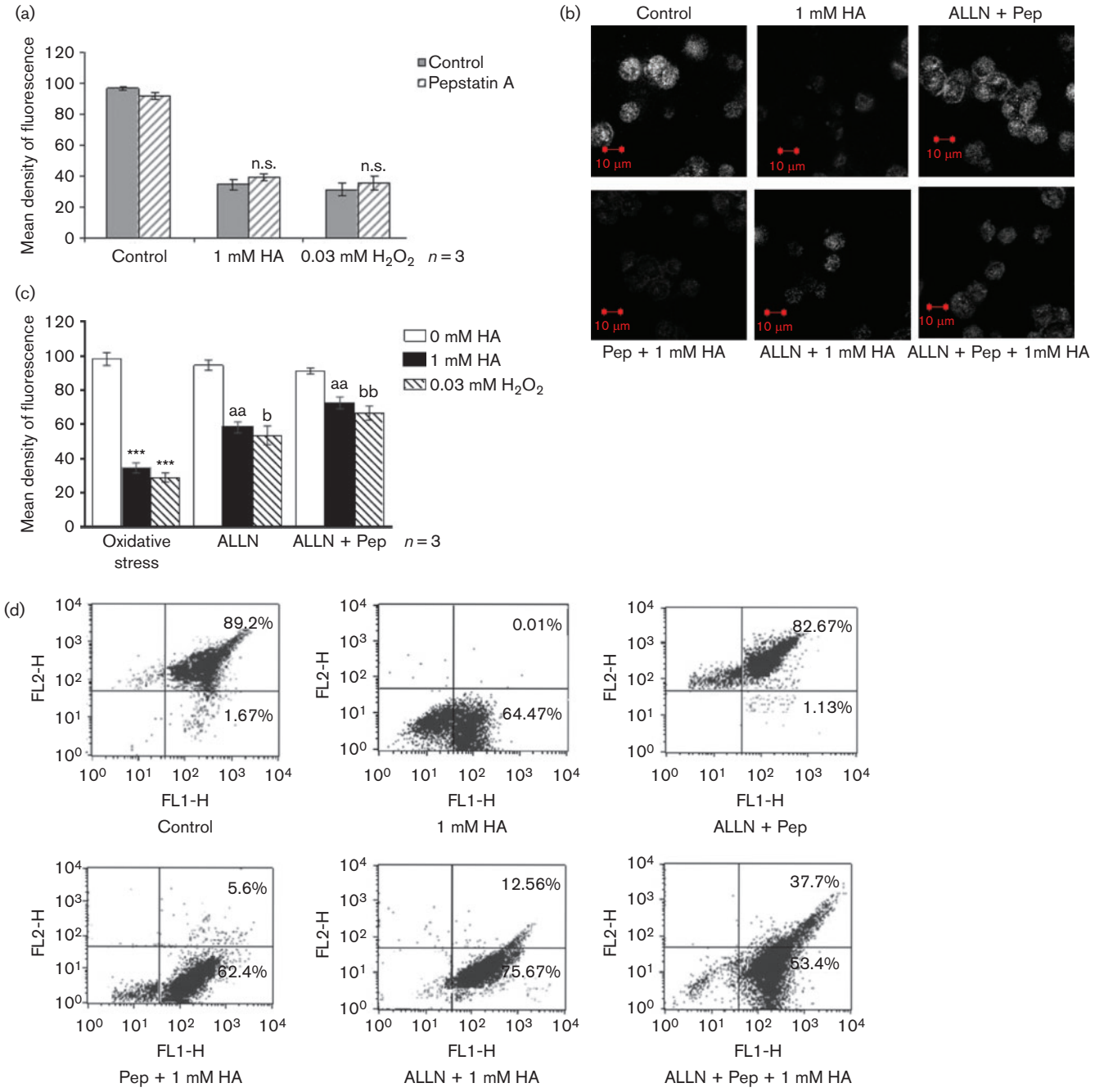

Fig. 5. MMP changes during paraptosis in *D. discoideum*. (a) Effect of cathepsin D inhibition on MMP changes during oxidative stress. No significant changes were observed with cathepsin D inhibitor, pepstatin A. Results are the mean of three independent experiments ± SEM. (b) Fluorescence images of MMP changes monitored using $DiOC_6$ dye. Data are representative of three independent experiments. Photographs were taken using a ×60 objective. (c) Densitometric analysis of fluorescence data. Calpain inhibition partially intercepts the MMP changes at both 1 mM HA and 0.03 mM H_2O_2. ***$P<0.001$ compared with untreated control; $^{aa,\ bb}P<0.01$ compared with the respective treated controls; $^{b}P<0.05$ compared with H_2O_2 treatment. Error bars, ± SEM. (d) Dot plot of red fluorescence (FL2) versus green fluorescence (FL1) resolved in live cells with intact MMP and from 1 mM HA-treated cells (in the presence of ALLN, pepstatin and ALLN + pepstatin) with loss of MMP. Mitochondria containing red JC-1 aggregates in healthy cells are detectable in the FL2 channel, and green JC-1 monomers in apoptotic cells are detectable in the FITC channel (FL1).

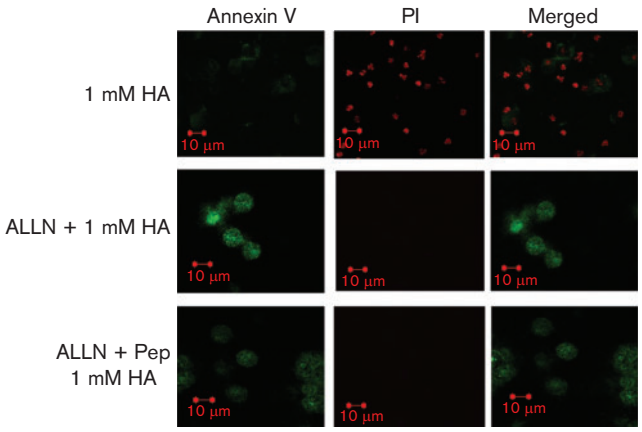

Fig. 6. Effect of calpain and cathepsin D inhibition on plasma membrane integrity as monitored by PS–PI dual staining. Both ALLN and pepstatin A delayed the PS exposure during paraptosis. Photographs were taken using a ×60 objective.

Effect of calpain and cathepsin D inhibition on MMP changes during oxidative stress-induced necrotic cell death

No effect was observed on 2.5 mM HA- and 0.05 mM H_2O_2-induced MMP changes by ALLN, a calpain inhibitor, alone. Calpain and cathepsin D inhibition collectively prevented the MMP changes during necrosis (Fig. 9c).

DISCUSSION

Caspase activation is the hallmark feature of apoptotic cell death seen in all multicellular eukaryotes (Saraste & Pulkki, 2000). Interestingly, caspase activation has also been reported during prokaryotic cell death (Gautam & Sharma,

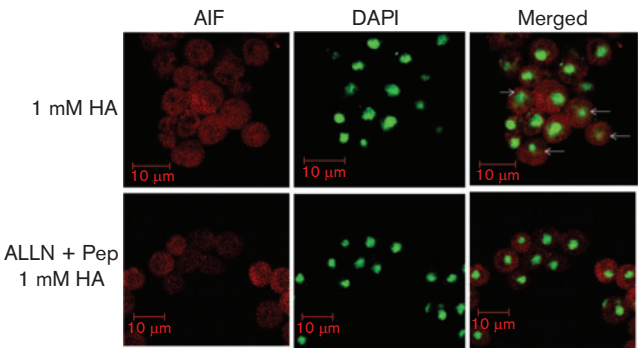

Fig. 7. Effect of calpain inhibition on AIF translocation. Intensity of green fluorescence was monitored after 6 h of oxidative stress-induced paraptotic cell death. Red colour: AIF; fluorescent green: DAPI (pseudo colour); green: AIF translocated to nucleus (indicated by arrow). Photographs were taken using a ×60 objective.

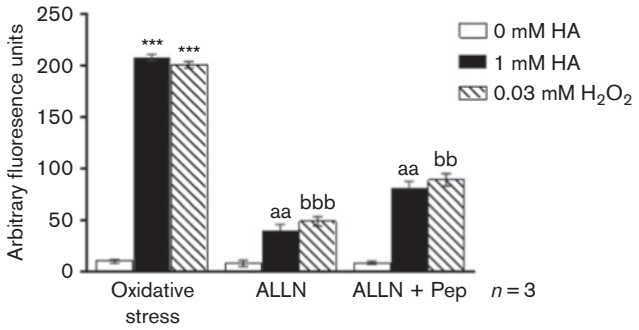

Fig. 8. Paraptotic vesicles stained with membrane probe DPH. Vesicles collected after 12 h of HA and H_2O_2 treatments were incubated with DPH and fluorescence was observed by fluorimetry. ***$P<0.001$ compared with control; $^{aa,\ bb}P<0.01$ compared with the respective treatments; $^{bbb}P<0.001$ compared with H_2O_2 treatment. Error bars, ± SEM.

2002a, b) and also during oxidative stress-induced cell death in yeast (Madeo *et al.*, 2002). We have characterized the oxidative stress-mediated cell death in *D. discoideum*, which was found to be PARP- and AIF-mediated but caspase-independent. Reports suggest that developmental cell death is caspase-independent (Roisin-Bouffay *et al.*, 2004). However, Olie *et al.* (1998) reported that extracts from vegetative Ax-2 cells showed labelling with z-EK(bio)D-aomk, which labels activated caspases and caspase inhibitor, blocked morphogenesis and not cell death. Nevertheless, caspase activation could not be seen in *D. discoideum* under oxidative stress (Fig. 2a), strengthening caspase independence during oxidative stress-induced cell death in *D. discoideum* unlike the yeast system which showed caspase activation during oxidative stress-induced cell death (Madeo *et al.*, 2002). The absence of caspases led us to characterize caspase-independent cell dismantling mechanisms. The sequence of events between oxidative insult and cell dismantling remain unclear. Along with caspase independence, vacuolization continues to be a morphological change in non-apoptotic PARP-mediated death called 'paraptosis' (Sperandio *et al.*, 2000). Vacuolization observed under oxidative stress indicates paraptotic cell death (Fig. 3).

To explore the possibility of lysosomal involvement during oxidative stress-induced cell death in *D. discoideum*, PIC was used to monitor MMP changes, which exhibited partial rescue, suggesting that proteases could be acting upstream of MMP changes (Fig. 4a). Cathepsin D and calpain inhibition studies were performed to further elucidate the involvement of specific proteases in dismantling during paraptosis. Cathepsin D, being a lysosomal protease known to be active at cytosolic pH (Zong & Thompson, 2006), could serve as the protease in dismantling the cell (Turk & Stoka, 2007) during oxidative stress-induced cell death. In addition, calpain, a cytosolic protease known to affect MMP (Polster & Fiskum, 2004), and further downstream events during caspase-independent cell death could be involved. Hence

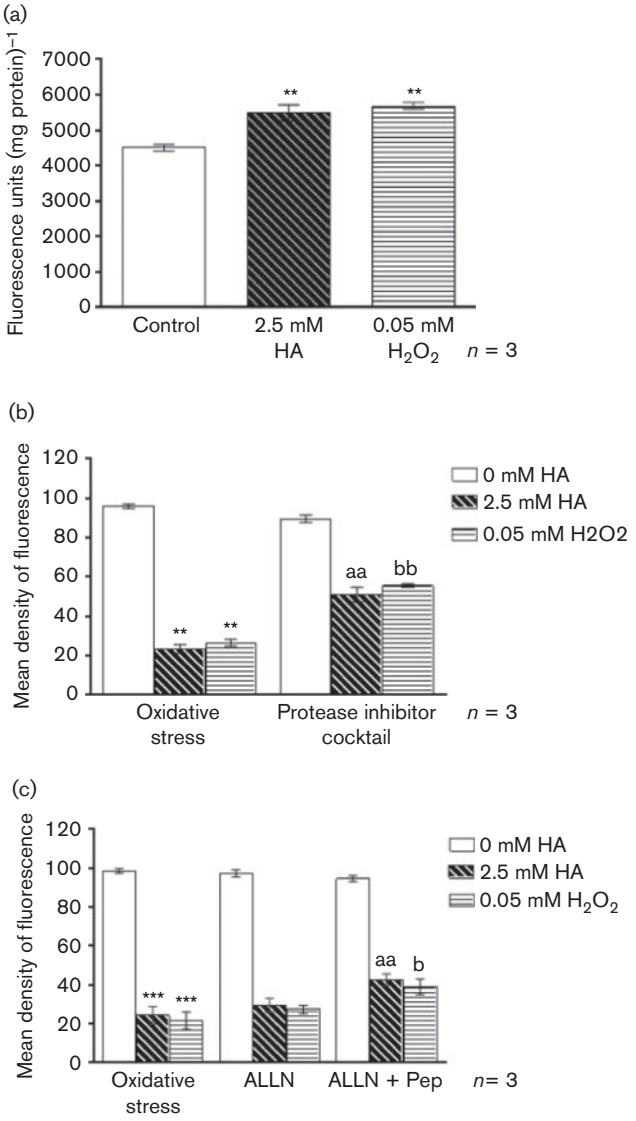

Fig. 9. Programmed necrosis exhibited at higher oxidative stress in *D. discoideum*. (a) Calpain activity measured during necrosis. $^{**}P<0.01$ compared with control. (b) Effect of PIC on MMP changes during necrosis. Results are the mean of three independent experiments. $^{**}P<0.01$ compared with control; $^{aa,\ bb}P<0.01$ compared with the respective treatments. (c) Effect of calpain and cathepsin D inhibition on MMP changes during necrosis. MMP changes during necrosis are partially rescued by both calpain and cathepsin D inhibition. $^{***}P<0.001$ compared with control; $^{aa}P<0.01$ compared with the respective treatments; $^{b}P<0.05$ compared with H_2O_2 treatment. Error bars, ± SEM.

experiments were done using a cathepsin D inhibitor (pepstatin A) and calpain inhibitor (ALLN).

Calpain inhibition studies showed a partial rescue in caspase-independent cell death while cathepsin D inhibition alone could not delay death of the cell. When pre-incubated with the calpain inhibitor ALLN, cells showed rescue in MMP changes at 3 h (Fig. 5b, c), while pepstatin A did not show any effect on MMP (Fig. 5a). During necrosis MMP change was partially rescued by PIC (Fig. 9b) and by both calpain and cathepsin D inhibition at 3 h (Fig. 9c). Inhibition of these two proteases also prevented the loss of plasma membrane integrity (Fig. 6). It has been reported that calpain inhibitor is able to block translocation of AIF and further cell death both *in vivo* and *in vitro* (Sanges *et al.*, 2006). AIF translocation to the nucleus was also partially rescued upon calpain inhibition (Fig. 7). Thus, our results imply that calpains function upstream while lysosomal proteases function downstream of mitochondrial changes during oxidative stress-induced cell death.

Cells pre-incubated with both cathepsin D and calpain inhibitors showed complete inhibition of vesicle formation (Fig. 8), suggesting that cathepsin D and calpains facilitate cell dismantling during oxidative stress-induced cell death. Calpain activation as well as its blockade during PARP-mediated cell death was confirmed by using a fluorescent substrate for calpain in the total cell lysate (Figs 4b and 9a), and our results suggest that calpain regulates AIF release during oxidative stress-induced PARP-mediated cell death in *D. discoideum*. Hence, protection observed with protease inhibitors could be attributed mainly to calpains as caspases are absent in *D. discoideum* (Olie *et al.*, 1998). Our data suggest that oxidative stress promotes calpain activity in *D. discoideum*. We have also shown that proteases are involved in causing MMP changes and downstream events including cell dismantling in the absence of caspases. Our studies suggest that proteases, particularly calpains and cathepsin D, could be the main players involved in the downstream events during oxidative stress-induced cell death as their inhibition prevented dismantling of the cell and thus delayed cell death in *D. discoideum*.

Mitochondrial uncoupling leads to plasma membrane rupture in necrotic cell death induced by DIF in *D. discoideum*, whereas exogenous glucose delays it non-glycolytically (Laporte *et al.*, 2007). Our study suggests that necrosis occurs in a programmed fashion with MMP changes manifested by proteases followed by plasma membrane rupture. Proteolysis during oxidative stress-induced necrotic cell death involves calpains and lysosomal proteases. While the pathways for apoptosis and necrosis are distinct, they nonetheless overlap and cross talk *in vivo* (Hasnain *et al.*, 2003). It would be of interest to explore if such cross talk exists.

Thus, from the above results we suggest an alternative cell death programme that may be regulated by PARP, AIF, calpains and cathepsin D as key players, where PARP may activate calpains by bringing a change in calcium homeostasis, as shown by Moubarak *et al.* (2007). Activated calpains would cause the release of AIF from mitochondria and cathepsin D from lysosomes. In this context we have revealed two proteases that could be orchestrating cell dismantling. This pathway opens the possibility to further

characterize the mechanism involved in cell dismantling during caspase-independent cell death. Moreover, *D. discoideum* can thus be used as a model to study the molecular mechanisms involved in non-apoptotic and programmed necrosis, which can then be substantiated in mammalian cells.

ACKNOWLEDGEMENTS

R. B. thanks the Department of Biotechnology, New Delhi (BT/PR9496/BRB/10/562/2007) and Department of Science and Technology, New Delhi (SR/SO/BB-03/2010) for research support. J. R. thanks the Council of Scientific and Industrial Research, New Delhi, for JRF/SRF awards. We thank the DBT-MSUB-ILSPARE program and Dr Shweta Saran, JNU, for providing the FACS and confocal microscopy facilities. We acknowledge SAIF-AIIMS for use of their electron microscopy facility.

REFERENCES

Bidère, N., Lorenzo, H. K., Carmona, S., Laforge, M., Harper, F., Dumont, C. & Senik, A. (2003). Cathepsin D triggers Bax activation, resulting in selective apoptosis-inducing factor (AIF) relocation in T lymphocytes entering the early commitment phase to apoptosis. *J Biol Chem* **278**, 31401–31411.

Cossarizza, A. & Salvioli, S. (2001). Flow cytometric analysis of mitochondrial membrane potential using JC-1. *Curr Protoc Cytom* **Chapter 9**, 9. 14.

Gautam, S. & Sharma, A. (2002a). Involvement of caspase-3-like protein in rapid cell death of *Xanthomonas*. *Mol Microbiol* **44**, 393–401.

Gautam, S. & Sharma, A. (2002b). Rapid cell death in *Xanthomonas campestris* pv. *glycines*. *J Gen Appl Microbiol* **48**, 67–76.

Hasnain, S. E., Taneja, T. K., Sah, N. K., Mohan, M., Pathak, N., Sahdev, S., Athar, M. & Begum, R. (1999). *In vitro* cultured *Spodoptera frugiperda* insect cells: model for oxidative stress-induced apoptosis. *J Biosci* **24**, 13–19.

Hasnain, S. E., Begum, R., Ramaiah, K. V. A., Sahdev, S., Shajil, E. M., Taneja, T. K., Mohan, M., Athar, M., Sah, N. K. & Krishnaveni, M. (2003). Host–pathogen interactions during apoptosis. *J Biosci* **28**, 349–358.

Katoch, B. & Begum, R. (2003). Biochemical basis of the high resistance to oxidative stress in *Dictyostelium discoideum*. *J Biosci* **28**, 581–588.

Katoch, B., Sebastian, S., Sahdev, S., Padh, H., Hasnain, S. E. & Begum, R. (2002). Programmed cell death and its clinical implications. *Indian J Exp Biol* **40**, 513–524.

Kawal, A. M., Mir, H., Ramniklal, C. K., Rajawat, J. & Begum, R. (2011). Structural and evolutionary analysis of PARPs in *D. discoideum*. *Am J Infect Dis* **7**, 67–74.

Koning, A. J., Lum, P. Y., Williams, J. M. & Wright, R. (1993). $DiOC_6$ staining reveals organelle structure and dynamics in living yeast cells. *Cell Motil Cytoskeleton* **25**, 111–128.

Kono, Y. & Fridovich, I. (1983). Isolation and characterization of the pseudocatalase of *Lactobacillus plantarum*. *J Biol Chem* **258**, 6015–6019.

Laporte, C., Kosta, A., Klein, G., Aubry, L., Lam, D., Tresse, E., Luciani, M. F. & Golstein, P. (2007). A necrotic cell death model in a protist. *Cell Death Differ* **14**, 266–274.

Lowry, O. H., Rosebrough, N. J., Farr, A. L. & Randall, R. J. (1951). Protein measurement with the Folin phenol reagent. *J Biol Chem* **193**, 265–275.

Madeo, F., Herker, E., Maldener, C., Wissing, S., Lächelt, S., Herlan, M., Fehr, M., Lauber, K., Sigrist, S. J. & other authors (2002). A caspase-related protease regulates apoptosis in yeast. *Mol Cell* **9**, 911–917.

Miller, E. (2004). Apoptosis measurement by annexin v staining. *Methods Mol Med* **88**, 191–202.

Mir, H. A., Rajawat, J., Pradhan, S. & Begum, R. (2007). Signaling molecules involved in the transition of growth to development of *Dictyostelium discoideum*. *Indian J Exp Biol* **45**, 223–236.

Mir, H., Rajawat, J. & Begum, R. (2012). Staurosporine induced cell death in *D. discoideum* is independent of PARP. *Indian J Exp Biol* **50**, 80–86.

Mohan, M., Taneja, T. K., Sahdev, S., Mohareer, K., Begum, R., Athar, M., Sah, N. K. & Hasnain, S. E. (2003). Antioxidants prevent UV-induced apoptosis by inhibiting mitochondrial cytochrome *c* release and caspase activation in *Spodoptera frugiperda* (*Sf*9) cells. *Cell Biol Int* **27**, 483–490.

Moubarak, R. S., Yuste, V. J., Artus, C., Bouharrour, A., Greer, P. A., Menissier-de Murcia, J. & Susin, S. A. (2007). Sequential activation of poly(ADP-ribose) polymerase 1, calpains, and Bax is essential in apoptosis-inducing factor-mediated programmed necrosis. *Mol Cell Biol* **27**, 4844–4862.

Olie, R. A., Durrieu, F., Cornillon, S., Loughran, G., Gross, J., Earnshaw, W. C. & Golstein, P. (1998). Apparent caspase independence of programmed cell death in *Dictyostelium*. *Curr Biol* **8**, 955–958.

Polster, B. M. & Fiskum, G. (2004). Mitochondrial mechanisms of neural cell apoptosis. *J Neurochem* **90**, 1281–1289.

Rajawat, J., Vohra, I., Mir, H. A., Gohel, D. & Begum, R. (2007). Effect of oxidative stress and involvement of poly(ADP-ribose) polymerase (PARP) in *Dictyostelium discoideum* development. *FEBS J* **274**, 5611–5618.

Rajawat, J., Mir, H. & Begum, R. (2011). Differential role of poly(ADP-ribose) polymerase in *D. discoideum* growth and development. *BMC Dev Biol* **11**, 14.

Rajawat, J., Mir, H., Alex, T., Bakshi, S. & Begum, R. (2014). Involvement of poly(ADP-ribose) polymerase in paraptotic cell death of *D. discoideum*. *Apoptosis* **19**, 90–101.

Roisin-Bouffay, C., Luciani, M. F., Klein, G., Levraud, J. P., Adam, M. & Golstein, P. (2004). Developmental cell death in *Dictyostelium* does not require paracaspase. *J Biol Chem* **279**, 11489–11494.

Sah, N. K., Taneja, T. K., Pathak, N., Begum, R., Athar, M. & Hasnain, S. E. (1999). The baculovirus antiapoptotic p35 gene also functions via an oxidant-dependent pathway. *Proc Natl Acad Sci U S A* **96**, 4838–4843.

Sanges, D., Comitato, A., Tammaro, R. & Marigo, V. (2006). Apoptosis in retinal degeneration involves cross-talk between apoptosis-inducing factor (AIF) and caspase-12 and is blocked by calpain inhibitors. *Proc Natl Acad Sci U S A* **103**, 17366–17371.

Sanvicens, N., Gómez-Vicente, V., Masip, I., Messeguer, A. & Cotter, T. G. (2004). Oxidative stress-induced apoptosis in retinal photoreceptor cells is mediated by calpains and caspases and blocked by the oxygen radical scavenger CR-6. *J Biol Chem* **279**, 39268–39278.

Saraste, A. & Pulkki, K. (2000). Morphologic and biochemical hallmarks of apoptosis. *Cardiovasc Res* **45**, 528–537.

Sperandio, S., de Belle, I. & Bredesen, D. E. (2000). An alternative, nonapoptotic form of programmed cell death. *Proc Natl Acad Sci U S A* **97**, 14376–14381.

Turk, B. & Stoka, V. (2007). Protease signalling in cell death: caspases versus cysteine cathepsins. *FEBS Lett* **581**, 2761–2767.

Watts, D. J. & Ashworth, J. M. (1970). Growth of myxameobae of the cellular slime mould *Dictyostelium discoideum* in axenic culture. *Biochem J* **119**, 171–174.

Wood, D. E. & Newcomb, E. W. (1999). Caspase-dependent activation of calpain during drug-induced apoptosis. *J Biol Chem* **274**, 8309–8315.

Wood, D. E., Thomas, A., Devi, L. A., Berman, Y., Beavis, R. C., Reed, J. C. & Newcomb, E. W. (1998). Bax cleavage is mediated by calpain during drug-induced apoptosis. *Oncogene* **17**, 1069–1078.

Zong, W. X. & Thompson, C. B. (2006). Necrotic death as a cell fate. *Genes Dev* **20**, 1–15.

Edited by: N. L. Glass

Chemistry SELECT

www.chemistryselect.org

A journal of ChemPubSoc Europe

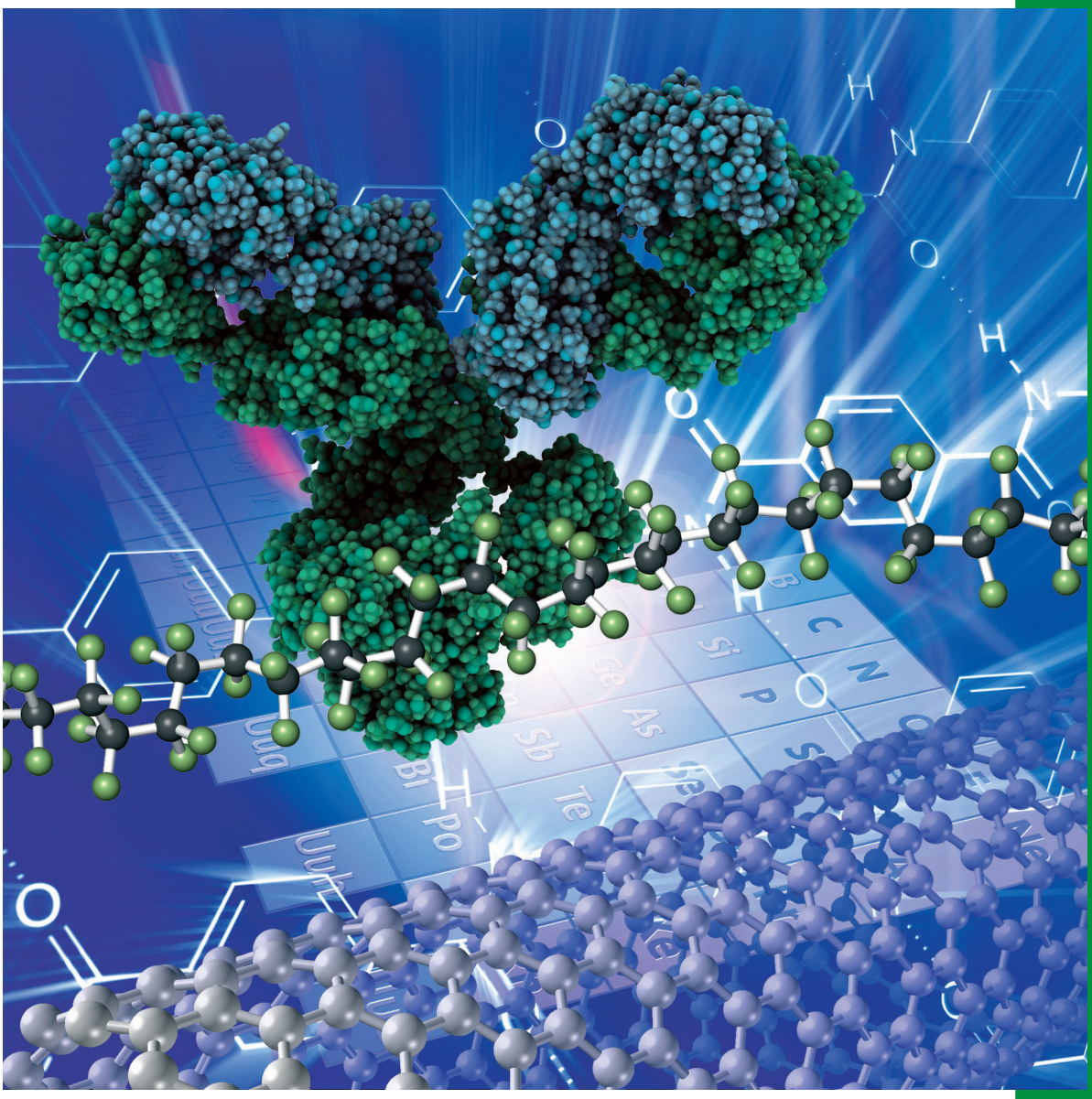

REPRINT

WILEY-VCH

ChemPubSoc Europe

DOI: 10.1002/slct.201900964

Chemistry SELECT Full Papers

Materials Science inc. Nanomaterials & Polymers

EDTA-Capped Iron Oxide Core-Corona System as Vehicle for Gene Delivery to Transform *E.coli*: Mimicking the Lipid Bilayer Environment

Ekta Shah,[a] Ashlesha Kadam,[b] Tina Jubin,[b] Rasheedunnisa Begum,[b] Pratik Upadhyay,[c] and Hemant P. Soni*[a]

EDTA-capped iron oxide nanoparticles (Fe_3O_4/*edta* NPs) were synthesized by simple wet chemical method and encapsulated with amphiphilic triblock copolymer Pluronic®F127 (Fe_3O_4/*edta/P*). The resulting 'core-corona' system becomes capable of condensing plasmid DNA (pDNA) and act as vehicle for cell transformation. As a proof-of-concept, *E.coli_DH5α* bacterial strain was selected. The plasmids like pBSKS and pUC18 having antibiotic resistance marker gene were eluted from the bacterial strain, purified and loaded on the synthesized nano-assembly. Green fluorescence protein tag was attached to pTX (pTX*gfp*) to confirm successful transformation. The gene transformation efficiency (TE) of the developed Fe_3O_4/*edta/P* vehicle was compared with traditional $CaCl_2$ mediated transformation as a positive control and naked pTX*gfp* was used as a negative control. PEGlation of Fe_3O_4/*edta* was also carried out and the TE of the resulting system was compared with as-synthesized Fe_3O_4/*edta/P*. This study demonstrates that Pluronic® F127 polymeric surfactant can be used to form stealth surface of the nanocarrier to solve Polyethylene Glycol (PEG) dilemma. The probable mechanism to explain the bacterial cell transformation is discussed.

Introduction

Delivery of foreign plasmid DNA (pDNA) or RNA into host cell nucleus is an important means of getting specific proteins synthesized in cells. This cost effective technique is equally important for the large scale industrial production of proteins as well as in the treatment of diseases like cystic fibrosis,[1] immune deficiency, haemophilia A, thalassemia, leukodistrophies and, cancers like B-cell malignancies caused due to gene mutation.[2] However, this is not an easy task to achieve as intracellular degradation of plasmids by nucleases would prevent their targeting to the nucleus or any organelle.[3–6]

The only viable solution to this problem is to insert the required pDNA or RNA in a vehicle (either synthesized or of natural origin) which can not only traverse the cell membrane but also sustain the integrity of the plasmid without being degraded by the cellular machinery. Viruses represent the ideal vehicle for this purpose.[7,8] In this context, many viral vectors like the retroviruses, lentiviruses, adenoviruses and adeno-associated viruses have been developed consequently.[9,10] However, they are beset with drawbacks like their breakdown by the developed immunity against them and carcinogenesis which restrict their recombination efficiency, limiting their use.[11,12] This calls for the development of safe and non-toxic non-viral gene delivery vectors. Non-viral vectors have, however, low transformation/transfection efficiency as they may not be able to sustain against multiple barriers (eg macrophage, serum endo-nucleases, filtration and exit through glomerular system etc.) that they come across during the journey in the cytosol. Lot of efforts has been made in the direction of development of safer and efficient non-viral vectors.[13,14] Amongst them, lipid based (liposomes)[15] and polymer based (polymersomes) are the major ones. For example cationic lipids like DOTAP (N-[1-(2,3-Dioleoyloxy) propyl]-N,N,N-trimethylammonium methyl-sulfate), DMRIE ((1,2-dimyristyloxy-propyl-3-dimethyl-hydroxy ethyl ammonium bromide), DOTMA (N-[1-(2, 3-dioleyloxy)propyl]-N,N,N-trimethylammonium chloride), DC-cholesterol etc. all having a hydrophilic cationic head group, hydrophobic long hydrocarbon chains and a linker group between the two, have the capability to condense DNA within the self-assembled lamellar bilayers called CL–DNA complex. This lamellar bilayer structure changes its phase to inverted hexagonal when it comes in contact with the negatively charged lipid (of endosomal membrane) leading to efficient release of DNA in the cytosol.[16] However, low delivery efficiency, poor stability and rapid renal clearance are again some of the drawbacks associated with these liposomal delivery vectors.[16,17] Synthetic or natural polymers having the capacity of self-assembly have also emerged as potential vectors. For example, poly-L-lysine (PLL) and its block copolymer with polyethylene glycol (PLL-b-PEG),[16–20] poly ethyl-

[a] *Dr. E. Shah, Dr. H. P. Soni*
Department of Chemistry, Faculty of Science, The Maharaja Sayajirao University of Baroda, Vadodara- 390 002, Gujarat, India
E-mail: drhpsoni@yahoo.co.in
hemant.soni-chem@msubaroda.ac.in
[b] *A. Kadam, Dr. T. Jubin, Prof. R. Begum*
Department of Biochemistry, Faculty of Science, The Maharaja Sayajirao University of Baroda, Vadodara- 390 002, Gujarat, India
[c] *Dr. P. Upadhyay*
Department of Pharmaceutical Technology, L. J. Institute of Pharmacy, Ahmedabad, Gujarat, India

Supporting information for this article is available on the WWW under https://doi.org/10.1002/slct.201900964

eneimine (PEI),[21 −24] PAGA (poly[α-(4-aminobutyl)-l-glycolic acid),[25] PAMAM (polyamidoamine) type dendrimers[26,27] etc. have all shown their capability to fuse covalently or electrostatically with DNA and act as non-viral gene delivery vectors. The protein like bovine serum albumin was also reported as delivery vehicle for pDNA transformation to *E. coli*_DH5α strain.[28] It exhibited ampicillin resistance subsequent to transformation with this developed delivery vehicle. Carbohydrate polymers such as chitosan and poly-β-cyclodextrin[29 −32] have also been considered for this purpose. However, issues related to efficiency and safety still remain as challenge necessitating further research in the field.

Gene transfer by bacterial transformation can be achieved through physical methods. For example, the cells can be made competent using electroporation, mild heat shock[33] and hydrogel exposure.[34,35] Hanahan *et al.* had shown that the bacterium *E. coli* can take up plasmid in double-stranded form. The plasmid forms a loop to pass through the lipid bilayer. This initial action is followed by a subsequent process of entry into the cell until the entire length of the plasmid passes through the membrane.[36,37] It has been observed that the trivalent cations, spermine and sperimidine, when used at specific concentrations, can condense plasmid DNA into spherical clusters.[38]

Transformation by applying magnetic field to obtain rapid contact between the vectors and target cells has been described by Luo and Saltzman in 2000.[39] For the purpose superparamagnetic Fe_3O_4 NPs are generally used. The advantage of using these NPs is that they immediately get magnetized in presence of magnetic field and demagnetized on removal of the field.[40]

Also, hydrophilic-lipophilic balance (HLB) within the carrier carrying the plasmid is very important to decide the stability of plasmid-vector conjugate in the intracellular environment. Generally, outer surface of the vector is PEGlated to increase the blood circulation and accumulation time. However, it reduces the cellular uptake due to hindrance between cell membrane and carrier known as 'PEG dilemma'.[41 −43] Hence, it is desired that the outer PEG layer of the developed nanocarrier should be detached before cellular entry. Pluronic® F-127 can become alternative for this. Pluronic® F127 ($EO_{102}PO_{78}EO_{102}$) is an amphilic triblock copolymer. Above CMC, its hydrophobic propylene oxide (PO) blocks self-assemble into the inner core while, hydrophilic ethylene oxide (EO) blocks form outer corona that result in the formation of stable polymeic micelle in the intracellular environment.[44,45] It has been observed that the incorporation of drugs into the hydrophobic PO core of these micelles increases the solubility, metabolic stability and circulation time during its journey towards the target.[45] However, very less studies are available showing the use of pluronic for gene delivery.[46] It was observed that pluronic block copolymers increase the expression of pDNA in skeletal muscle in mice.[47,48] The formulation, SP1017, made by mixing two different types of pluronics increases gene expression by 5–20 folds compared to naked DNA.[49]

The advantages of using pluronic for the formation of stealth outer surface as an alternative to PEG are: (1) being amphiphilic in nature, it is conducive to both drug/gene and intracellular environment prolonging the circulation time, (2) it has been observed that strong positively charged carriers are removed rapidly by the reticuloendothelial system (RES).[50] In case of pluronic, a weakly cationic character results due to oxonium ion formation with water protons or the sharing of the hydrogen in water by H-bonding.[51] Thus, the attractive interaction between this weak polycation and the negative cell surface synergistically enhances transformation and accumulation time. As a proof-of-concept, we demonstrate its application for prokaryotic cell transformation in the present study.

In our previous study, we had reported the synthesis of ethylene diamine tetra acetate (*edta*) capped Fe_3O_4 nanoparticles (NPs) encapsulated by using pluroic F-127 (Fe_3O_4/*edta*/*P*) and used as vehicle for drug delivery and as T1-T2 dual contrast agent for magnetic resonance imaging. In vitro cell viability, cytotoxicity and MTT assay (for k562 cell-line) proved that the developed magnetic vector is safe, non-toxic and capable of transfecting the cell. We had demonstrated the presence of inner-sphere and outer-sphere water responsible for added T1 contrasting ability along with innate T2 ability of the developed vehicle.[52]

In the present study, we report this developed 'core-corona' system as a vehicle for gene delivery. *E.coli* transformation was carried out using these superparamagnetic Fe_3O_4 NPs under the influence of a magnet. The advantage with regard to this magnetofection is that a competent cell preparation is not required. The objective of this study was to develop a transformation technique wherein potential iron oxide NPs acting as carrier of pDNA could transform bacterial host cells without making the cells competent by special techniques. For the purpose, plasmids like pBSKS (3 kb size with ampicillin resistance gene as selection marker) and pUC18 (2.68 kb size with ampicillin resistance gene as selection marker) were selected. These plasmids were eluted, purified, and utilized for loading on to the surface of Fe_3O_4 nanoparticles. Such gene loaded Fe_3O_4 nanoparticles were used to transform *E. coli_ DH5α*. Development of resistance to antibiotics was used as evidence to score successful transformation. Also, green fluorescence protein tag was attached to pTX as marker and, successful transformation of *E. coli_DH5α* strain by pTX*gfp* was confirmed by observing transformed cells under a confocal microscope. Also, the gene transformation efficiency (TE) of the developed Fe_3O_4/*edta*/*P* vehicle was compared with traditional $CaCl_2$ mediated transformation (which requires competent cells preperation) as positive control and naked pTX*gfp* was used as a negative control. PEGlation of Fe_3O_4/*edta* was also carried out and the gene transformation efficiency of the resulting system was compared with as-synthesized pluronic encapsulated Fe_3O_4/*edta*.

Results and Discussion

The synthesized iron oxide NPs were characterized by powder XRD to study their particle size, crystallinity and the phase (Figure 1a). The XRD patterns manifested predominant diffraction peaks at 2θ values 30.1, 35.15, 43.10, 53.50, 57.21 and 63.0

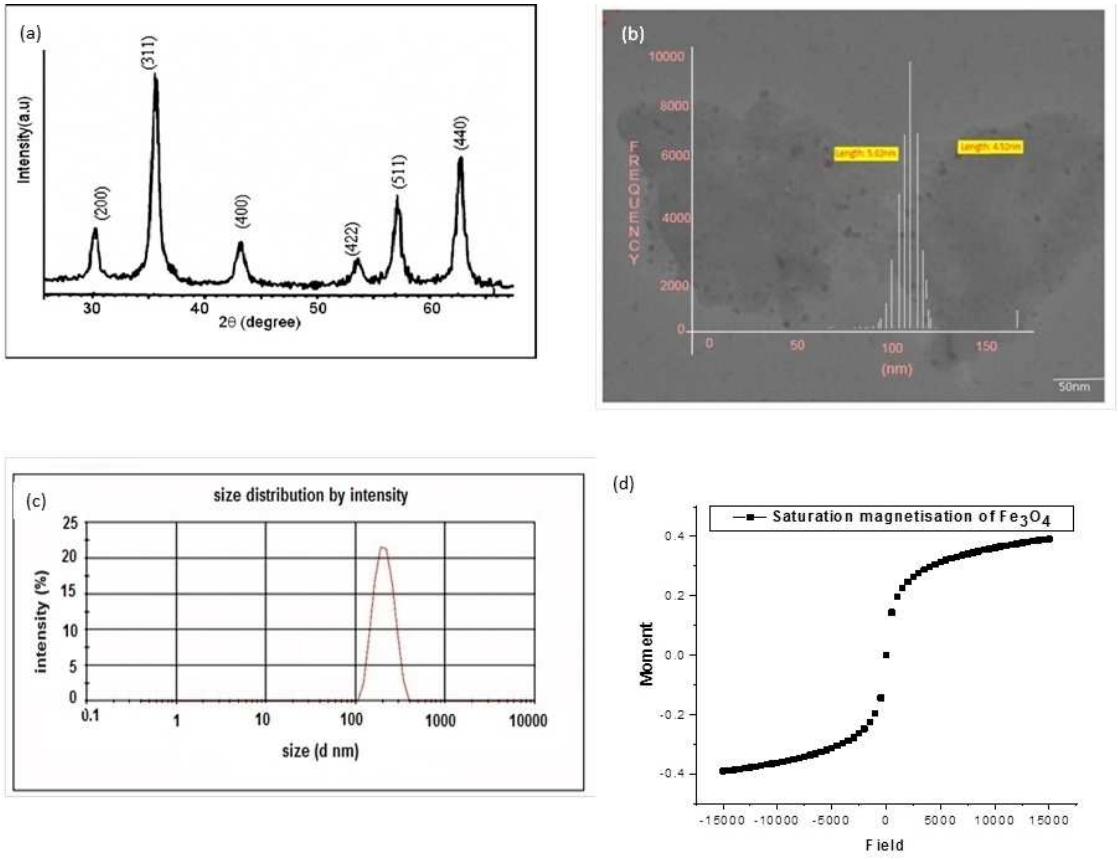

Figure 1. (a) XRD patterns of Fe_3O_4/*edta* NPs (b) TEM image and particle size histogram of as-synthesized Fe_3O_4/*edta/P* nanoparticles (c) DLS analysis of Fe_3O_4/*edta* /P NPs and (d) magnetization curve at room temperature for Fe_3O_4/*edta* NPs.

which correspond to the (200), (311), (400), (422), (511), and (440) planes respectively. These features indicate the magnetite phase with inverse spinel structure and peak positions indicate that coating of *edta* on Fe_3O_4 NPs as capping ligands does not affect the crystallinity and phase of the material. The particle size was calculated by the Debye-Scherrer formula ($L = 0.9\lambda / \beta \cos\theta$) and the FWHM (Full Width at Half Maximum) correspond to the major plane (311) which, is in the range of 56 nm.

Particle size was also measured by Dynamic Light Scattering (DLS) technique (Figure 1c). The mean hydrodynamic radius for Fe_3O_4/*edta* NPs was 232 nm with polydispersity index (PDI) 0.251. On addition of pluronic F127 surfactant the average particle size increases to 440 nm with a PDI 0.005. It can be observed (Table 1) that Fe_3O_4/*edta/P* NPs possess negatively charged surface with ζ value −23.87 mV and when bounded with pBSKS and pUC18, negative charge decreases to −14.73mVand −9.27 mV respectively. The emergence of charge on the surface is directly influenced by the presence of counter ions in the medium and the mode of crystallization. The negative charge on the surface of NPs is due to the presence of $^-$OH ions in the basic aqueous medium. During the crystal growth, $^-$OH ions as well as *edta* both act as capping ligands, however, $^-$OH ions are more prone to be adsorbed on to the surface while *edta* makes coordination with surface Fe (II/III) ions or H-bonds with surface oxygen.

Table 1. Zeta potential of Fe_3O_4 nanoparticles loaded with different plasmids.

Plasmid	Size of plasmid (kb)	Zeta potential (mV)
Blank Fe_3O_4/*edta/P*	-	-52.21
pUC18	2.68	-40.2
pTX*gfp*	11.2	-19.27.
pBSKS	3.0	-33.56

The size and shape of Fe_3O_4/*edta* NPs were further studied by TEM analysis. The TEM image shows almost monodispersed spherical particles with an average size of 5–10 nm (Figure 1b).

The discrepancy in particle size measured by XRD and by DLS and TEM was very well explained by Jain at al[53] DLS technique measures overall hydrodynamic diameter of the NP assembly resulting from hydration of Fe_3O_4/*edta* in aqueous media while crystallite size can be calculated from XRD. The shape of magnetization curve (Figure 1d) for Fe_3O_4/*edta* indicates superparamagnetic behavior of NPs in presence of magnetic field. The magnetization and coercivity of Fe_3O_4/*edta* NPs were 0.4 emu/gm and 0.4611 G (Hci) respectively. This property makes NPs suitable for delivering the cargo in the

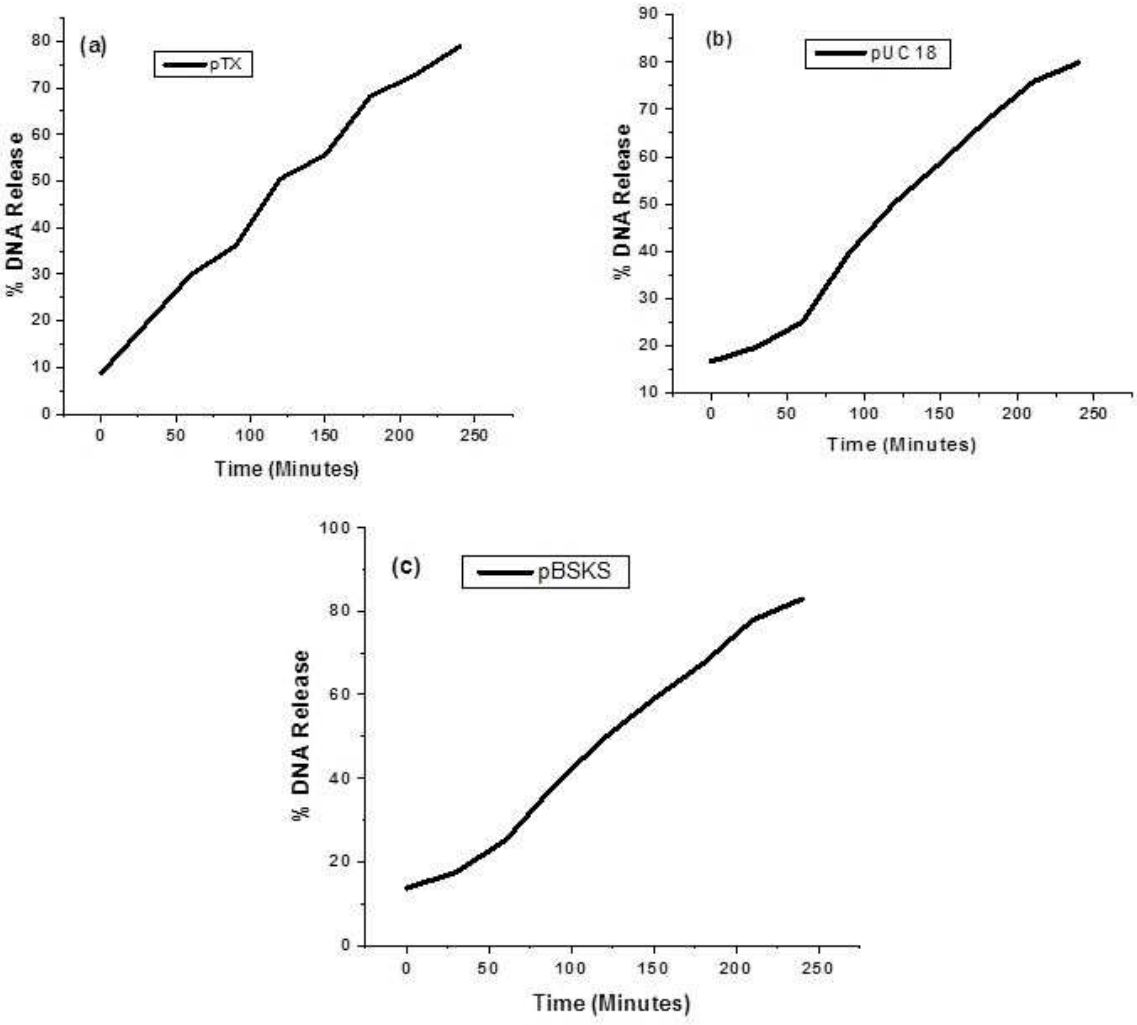

Figure 2. Release profile of (a) pTX*gfp* (b) pUC18 and (c) pBSKS loaded Fe_3O_4/*edta*/*P* NPs as vehicles.

cellular environment under the influence of magnetic field.[54–56]

To understand the interactions of the *edta* ligands with the surface of Fe_3O_4 NPs vibrational spectroscopy (FTIR) was carried out. Figure S1 show the FTIR spectrum of Fe_3O_4/*edta*/*P*. The absorption at 646 cm^{-1} corresponds to Fe–O stretching in Fe_3O_4 inverse spinel lattice. Absorptions at 1111 and 1156 cm^{-1} are due to the presence of block copolymer covering the surface of NPs and the $-CH_2-$ rocking vibrations of pluronic respectively. The vibration at 1623 $cm^{-1}$is due to carboxylate stretching.[53]

It can be observed from the Table 1 that on loading the plasmid and, as its size increases the surface charge reduces due to the interaction of surface coordinated molecules with the plasmid. This observation lead to the assumption that the circular plasmid may remain adsorbed near the periphery of inner surface due to H-bonding with entrapped water molecules or residual surface hydroxyl groups resulting in partial encapsulation of the surface by plasmid with reduction in negative charge. This is advantageous over the covalent interactions as it makes the release of plasmid easy without any mutation in the bacterial cell.

Three plasmids namely pBSKS, pUC18 and pTX*gfp*, having different sizes were isolated from *E.coli* culture and purified (Figure S2 and Table 1) to investigate their ability to transform *E.coli_ DH5α* strain using synthesized Fe_3O_4 NPs as delivery vehicle. Figure S3 shows the TEM images of the transformed cells.

Figure 2 shows the release profile of all the plasmid loaded on the Fe_3O_4/*edta*/*P* NPs in *E. coli_* DH5α bacterial cells in 250 min. It can be observed that the release profile is directly correlatable with the size of the plasmid. The pTX*gfp* having maximum size gets released in steps and maximum 75% gets released within 200 min. While pUC18 and pBSKS having almost the same size released in a single burst, almost 85% got released within 225 min. This demonstrates the steady and intact release of plasmids in bacterial cells.

For the confirmation of transformation, confocal microscopy of *E. coli _DH5α* strain was carried out. It can be observed from Figure 3 that *E. coli* harboring pTX*gfp* shows fluorescence

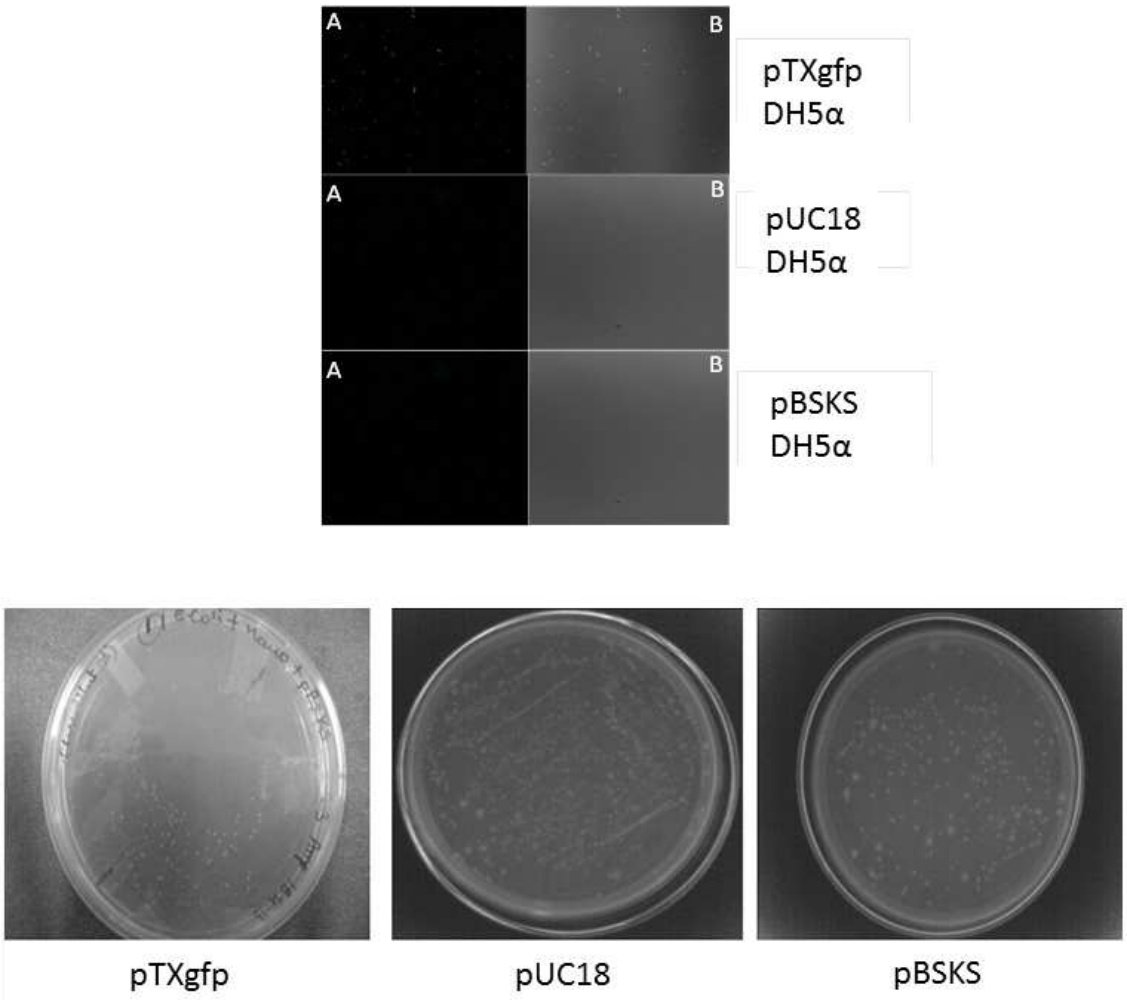

Figure 3. (Top) Confocal microscope images of *DH5α* transformed with pDNA. A-lane fluorescent field and B-lane merges of fluorescence and bright field **(bottom)** Growth of antibiotic sensitive *E. coli_DH5α* in diluted LB, containing ampicillin after 1 day incubation with plasmid loaded nanoparticles.

property while fluorescence was absent in other plasmids due to the lack of *gfp*. To confirm the transformation of *E. coli* with all pDNAs under study by using Fe_3O_4/*edta*/*P* NPs as vehicle, the transformed bacteria should demonstrate resistance towards antibiotics.

For assessing the same, transformed *E. coli DH5α* strain was grown in an ampicillin containing plates. It can be seen from Figure 3 (bottom) that the pDNA transformed colonies grew on ampicillin or kanamycin containing plates, antibiotics to which they were susceptible previously.

Transformation efficiency was compared with negative control (naked pTX*gfp*) and positive controls ($CaCl_2$ mediated transformation), and the results are shown in Figure 4.

Higher transformation efficiency was found in case of magnetofaction than $CaCl_2$ mediated transformation which requires competent cells preparation, suggesting pluronic encapsulated and *edta* capped iron oxide nano-carriers provide a better gene delivery system.

The TE of pTX*gfp* loaded on Fe_3O_4/*edta*/*P* and Fe_3O_4/*edta*/*PEG* systems were compared. It was found higher in case of system having stealth surface of Pluronic® F127 than that of PEG (Figure 5). This demonstrates Pluronic® F127 ability to form flexible and stealth surface surrounding the EDTA capped iron oxide nano-carriers for the efficient gene delivery.

Further, the transferred plasmid could again be isolated from these *E.coli* strain establishing the integrity of the plasmid during the transformation process (Figure S3). These results show retention of pDNA function (as seen in the figures). This substantiates the fact that the developed Fe_3O_4/*edta*/*P* could serve as promising candidates for successful gene delivery into prokaryotic cells.

Discussion

It is known that *edta* in free form can quench the divalent cations (Mg^{2+}), which are crucial co-factors for DNA polymerase or DNA repair enzymes, thereby resulting in the degradation of the plasmid. However, in present study, *edta* forms stable chelate with surface Fe ions. For this, it uses four carboxylate arms for making coordinate bonds together with two nitrogen

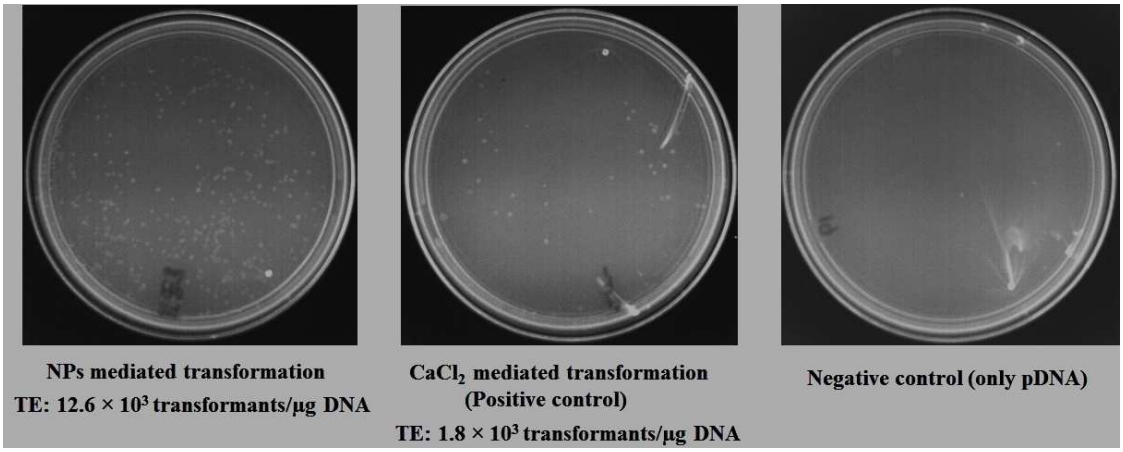

Figure 4. Transformation efficiency of pTX*gfp* loaded as-synthesized Fe_3O_4/edta/*P* NPs system (by magnetofaction), transformation by means of $CaCl_2$ and negative control.

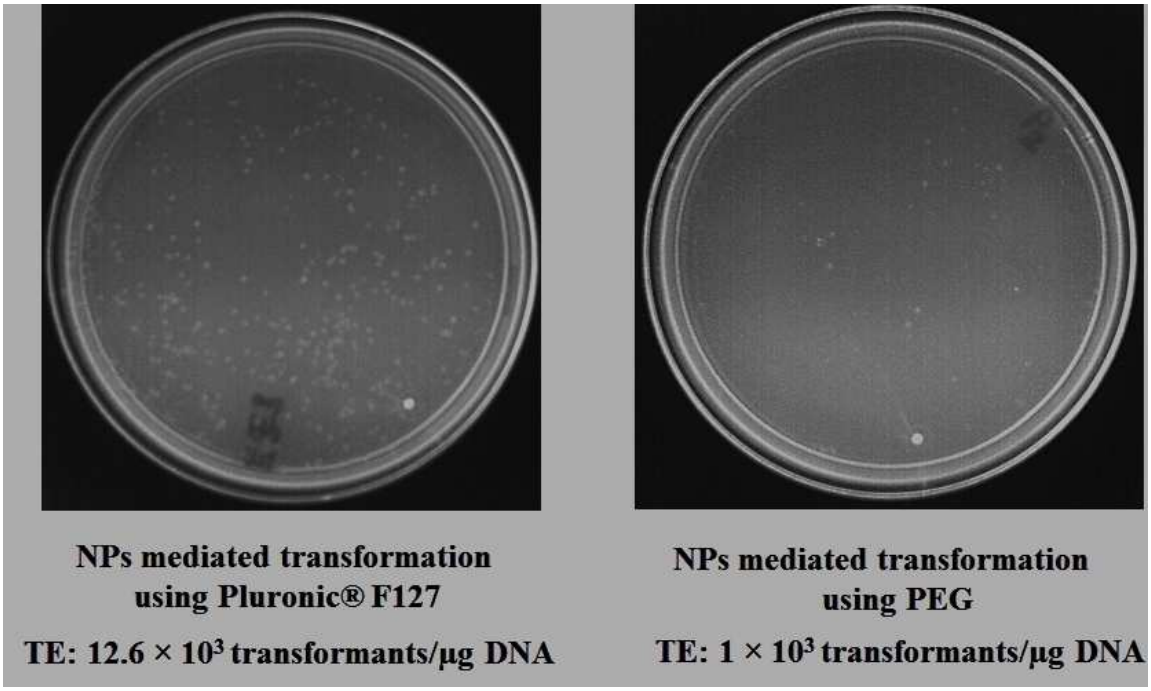

Figure 5. Transformation efficiency of pTX*gfp* loaded as-synthesized Fe_3O_4/*edta*/*P* and Fe_3O_4/*edta*/*PEG* system (by magnetofaction).

loan pair electrons, also confirmed from the FTIR study. Due to this, the outer 'zigzag' periphery of NPs becomes hydrophobic having two nitrogen atoms embedded with loan pair electrons can entrap water molecules by H-bonding (Figure 6). This could create the surface environment perfect for next pluronic layer. Pluronic® F127 having maximum number of EO units in a single block than those of PO units, possesses maximum HLB value compared to other type of pluronic systems (eg. Pluronic® P85 and Pluronic® L61).[45] This quality makes it compatible to interact with the hydrophilic outer layer of the cell membrane and can get easily engulfed into the cellular environment. During synthesis procedure, pluronic forms the exterior layer in such a way that its hydrophobic PPO blocks remain directed inwards towards the hydrocarbon parts of *edta* and its hydrophilic PEO blocks face outwards. This situation is similar to the lipid bilayer of the cell membranes having outer hydrophilic heads and inner sandwiched hydrophobic hydrocarbon chains. In contrast to the lipid bilayer, pDNA cannot be condensed by exterior pluronic layer of the presently synthesized 'core-corona' system due to its very weak charge. This proposed model was confirmed by using thermogravimetric techniques in our previous study, endorsing two types of water molecules, first near to the hydrophilic Fe_3O_4 surface having coordinated carboxylate ions in its vicinity and, second near to the exterior

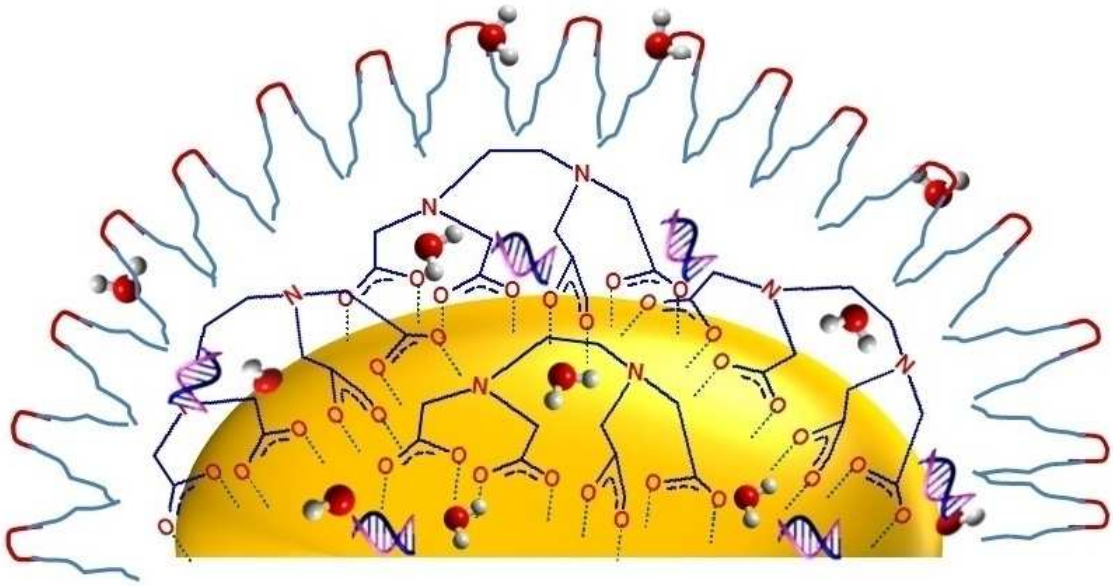

Figure 6. Cartoon showing a Fe_3O_4/*edta*/*P* magnetic gene delivery vehicle. Central hemisphere represents Fe_3O_4 nanoparticle surrounded by *edta* ligands (coordinate with surface Fe ions). The outer zigzag light blue lines correspond to hydrophobic PPO blocks while that of red to hydrophilic PEO blocks. Some water molecules can be seen entrapped near the ligand's nitrogen atoms by coordination bond while the polymeric micelle is surrounded by second sphere water molecules. Plasmid can be seen entrapped near inner surface water molecules and hydroxide ions.

pluronic hydrophilic PEO blocks.[52] The advantage of this kind of molecular architecture is that it can very well condense and stabilize the double stranded pDNA. Perhaps, PEG is not able to provide such kind of molecular environment results into the situation called 'PEGdilema'. Now, the position of pDNA within the carrier is crucial to determine its fate in the cytoplasm during its journey towards the nucleus. Once the vector-plasmid conjugate enters the cytoplasm (mostly through endocytosis), pDNA must be released before it enters the nucleus and expresses itself. Strongly bounded plasmids cannot be released easily from the vehicle and become more prone to be directed towards the lysosomes where it is digested. The weakly bounded plasmid delivered prematurely is destined for intracellular degradation by nucleases within minutes.[57,58] Figure S1 shows the FTIR spectra of pDNA conjugated Fe_3O_4/*edta*/*P* NPs, in comparison to that of blank Fe_3O_4/*edta*/P, with the carboxylate stretching peak near 1600 cm^{-1} being blue shifted up to 10 cm^{-1} and becoming sharp. This indicates that the strong binding of carboxylate ligands with the surface Fe ions, may be due to the insertion of negatively charged pDNA near the surface. The plasmid can be stabilized near the core due to either electrostatic interaction with the positively charged surface Fe ions or through H-bonding with the entrapped water molecules or with free surface hydroxyl groups, also corroborated from zeta potential measurements. The release profile of the plasmids selected for this study indicates sustained release with structural and functional integrity which is also expressed in antibiotic resistance study. This is possible only when stable condensation of pDNA takes place and supports our postulate regarding the position of plasmid inside the vehicle. Hence, the plasmid present in the inner core remains intact on detachment of stealth layer of pluronic in the intracellular environment.

Conclusion

Edta capped iron oxide nanoparticles were successfully synthesized by simple wet precipitation method. These NPs were employed as gene-delivery vehicles to load pDNAs such as pUC18, pBSKS and pTX18gfp carrying ampicillin resistance genes. Encapsulation of as-synthesized NPs by Pluronic® F127 triblock copolymeric surfactant provides stealth and flexible surface helps the vehicle to sustain in the harsh cellular environment leading to successful gene delivery with high transformation efficiency compared to traditional systems used for the purpose. From this study, it can be concluded that: (i) pDNA makes stable bonding with nanoparticles on its surface by intermolecular H-bonding or by entrapping inside cavities; (ii) greater the size of the plasmid, the faster is its release profile; (iii) pluronic like copolymeric surfactant which are capable to acquire 'mild' positive charge in the intra cellular environment can provide stealth and flexible surface to the delivery vehicle, at least in case of prokaryotic cells. More experiments are needed to establish this claim for eukaryotic cells in a large scale. Hence, iron oxide nanoparticles can serve as non-toxic, biodegradable and safe vectors to load a variety of genes of useful products like enzymes, proteins, peptides, hormones etc into bacterial cells. Such a carrier can also be used for delivering genes into eukaryotic cells and can be a potential candidate for use in gene therapy. This work may further be extended to fields such as bio-augmentation, DNA profiling, and development of biosensors.

Supporting Information Summary

Details of the experimental procedures, FTIR spectra of all synthesized nanomaterials with core-corona systems, Agarose electrophoresis of all plasmid isolated from *E.coli_DH5α* strain, TEM images of control cells as well as cells transfected by Fe_3O_4/*edta*/P loaded with pTXegfp, pBSKS and pUC18 are provided in supporting information.

Acknowledgements

HS and RB thank Science & Engineering Research Board (SERB), New Delhi, for supporting this work under a sponsored scheme (No.EMR/2016/007638). Also, thanks to Prof. A. V. Ramachandran for necessary suggestions and corrections in the manuscript.

Conflict of Interest

The authors declare no conflict of interest.

Keywords: Cell transformation · DNA condensation · Gene delivery · Non-viral vectors · SPIONs

[1] M. W. Konstan, P. B. Davis, J. S. Wagener, K. A. Hilliard, R. C. Stern, L. J. Milgram, T. H. Kowalczyk, S. L. Hyatt, T. L. Fink, C. R. Gedeon, S. M. Oette, J. M. Payne, O. Muhammad, A. G. Ziady, R. C. Moen, M. J. Cooper, *Hum. Gene. Ther.* **2004**, *15*, 1255–1269.
[2] T. Friedmann, *The development of human gene therapy.* Cold Spring Harbor Laboratories Press, NY, **1999**, pp. 729.
[3] C. M. Wiethoff, C. R. Middaugh, *J.Pharm.Sci.* **2003**, *92*, 203–217.
[4] P. S. Eder, J. D. Rene, J. M. Dagle, J. A. Waldereder, *Antisense Res. Dev.* **2009**, *1*, 141–151.
[5] E. Mastrobattista, A. M. Van Der, W. Hennink, D. J. Crommelin, *Nat. Rev. Drug. Discov.* **2006**, *5*, 115–121.
[6] M. E. Gore, *Gene Ther.* **2003**, *10*, 4 −4.
[7] S. Rauth, R. S. Kucherlapati, *J. Biosci.* **1984**, *6*, 543–567.
[8] W. F. Anderson, *Nature* **1998**, *392*, 25–30.
[9] M. A. Kay, *Nat. Rev. Genet.* **2011**, *12*, 316–328.
[10] F. Mingozzi, K. A. High, *Nat. Rev. Genet.* **2011**, *12*, 341–355.
[11] H. –S. Zhou, D. –P. Liu, C. –C. Liang, *Med. Res. Rev.* **2004**, *24*, 748–761.
[12] B. Gansbacher, *J. Gene. Med.* **2003**, *5*, 261–262.
[13] I. Lostalé-Seijo, J. Montenegro, *Nat. Rev. Chem.* **2018**, *2*, 258 −277.
[14] S. Senapati, A. K. Mahanta, S. Kumar, P. Maiti, *Signal Transduction Targeted Ther.* **2018**, 7.
[15] J. Buck, P. Grossen, P. R. Cullis, J. Huwyler, D. Witzigmann, *ACS Nano* **2019**, *13*, 3754 −3782.
[16] K. A. Whitehead, R. Langer, D. G. Anderson, *Nat. Rev. Drug Discov.* **2009**, *8*, 129–138.
[17] C. Lonez, M. Vandenbranden, J. M. Ruysschaert, *Prog. Lipid Res.* **2008**, *47*, 340–347.
[18] D. E. Olins, A. L. Olins, V. P. H. Hippel, *J. Mol. Biol.* **1967**, *24*, 157–176.
[19] U. K. Laemmli, *Proc. Natl. Acad. Sci.U. S. A.* **1975**, *72*, 4288–4292.
[20] M. A. Wolfert, E. H. Schacht, V. Toncheva, K. Ulbrich, O. Nazarova, L. W. Seymour, *Hum. Gene Ther.* **1996**, *7*, 2123–2133.
[21] U. Lungwitz, M. Breunig, T. Blunk, A. Gopferich, *Eur. J. Pharm. Biopharm.* **2005**, *60*, 247 −266.
[22] O. Boussif, F. Lezoualc'h, M. A. Zanta, M. D. Mergny, D. Scherman, B. Demeneix, J. P. Behr, *Proc. Natl. Acad. Sci. U. S. A.* **1995**, *92*, 7297–7301.
[23] W. T. Godbey, K. K. Wu, A. G. Mikos, *J. Biomed. Mater. Res.* **1999**, *45*, 268–275.
[24] L. Wightman, R. Kircheis, V. Rössler, S. Carotta, R. Ruzicka, M. Kursa, E. Wagner, *J. Gene Med.* **2001**, *3*, 362 −372.
[25] Y. –B. Lim, C. –H. Kim, K. Kim, S. W. Sim, J. –S. Park, *J. Am. Chem. Soc.* **2000**, *122*, 6524–6525.
[26] D. W. Pack, A. S. Hoffman, S. Pun, P. S. Stayton, *Nat. Rev. Drug Discov.* **2005**, *4*, 581–593.
[27] M. A. Mintzer, E. E. Simanek, *Chem. Rev.* **2009**, *109*, 259–302.
[28] J. Wagh, K. J. Patel, P. Soni, K. Desai, P. Upadhyay, H. P. Soni, *Luminescence* **2015**, *30*, 583–591.
[29] S. R. Popielarski, S. Mishra, M. E. Davis, *Bioconjugate Chem.* **2003**, *14*, 672–678.
[30] W. -F. Lai, *Biomaterials* **2014**, *35*, 401–411.
[31] R. Borchard, *Adv. Drug Deliv.* **2001**, *52*, 145–150.
[32] T. –H. Kim, H. L. Jiang, D. Jere, I. –K. Park, M. –H. Cho, J. W. Nah, Y. –J. Choi, T. Akaike, C. –S. Cho, *Prog. Polym. Sci.* **2007**, *32*, 726–56.
[33] M. T. Alegrea, M. C. Rodríguezb, J. M. Mesasc, *FEMS Microbiol. Lett.* **2004**, *241*, 73–77.
[34] N. Yoshida, T. Nakajima-Kambe, K. Matsuki, T. Shigeno, *Anal. Chem. Insights* **2007**, *2*, 9–15.
[35] E. Arkhangelsky, Y. Sefi, B. Hajaj, G. Rothenberg, V. Gitis, *J. Membr.Sci.* **2011**, *371*, 45–51.
[36] D. Hanahan, *J. Mol. Biol.* **1983**, *166*, 557–580.
[37] I. Koltover, T. Salditt, J. O. Radler, C. R. Safinya, *Science* **1998**, *281*, 78–81.
[38] J. Clark, J. Hudson, R. Mak, C. McPherson, C. Tsin, *Exp. Microbiol. Immunol.* **2002**, *2*, 68–80.
[39] D. Luo, W. M. Saltzman, *Nat. Biotechnol.* **2000**, *18*, 893–895.
[40] K. M. Krishnan, A. B. Pakhomov, Y. Bao, P. Blomqvist, Y. Chun, M. Gonzales, K. Griffin, X. Ji, B. K. Roberts, *J. Mat. Sci.* **2006**, *41*, 793–815.
[41] Q. Jin, Y. Deng, X. Chen, J. Ji, *ACS Nano* **2019**, *13*, 954–977.
[42] H. Hatakeyama, H. Akita, H. Harashima, *Biol. Pharm. Bull.* **2013**, *36*, 892–899.
[43] H. Hatakeyama, H. Akita, H. Harashima, *Adv. Drug Delivery Rev.* **2011**, *63*, 152–160.
[44] A. V. Kabanov, E. V. Batrakova, V. Y. Alakhov, *J. Control. Release,* **2002**, *82*, 189–212.
[45] A. V. Kabanov, P. Lemieux, S. Vinogradov, V. Alakhov, *Adv. Drug Deliv. Rev.* **2002**, *54*, 223–233.
[46] M.-M. Fan, X. Zhang, J. Qin, B. -J. Li, X. Sun, S. Zhang, *Macromol. Rapid Commun.* **2011**, *32*, 1533–1538.
[47] P. Lemieux, N. Guerin, G. Paradis, R. Proulx, L. Chistyakova, A. Kabanov, V. Alakhov, *Gene Ther.* **2000**, *7*, 986–991.
[48] C. W. Cho, Y. S. Cho, H. K . Lee, Y. I. Yeom, S. N. Park, D. Y. Yoon, *Biotechnol. Appl. Biochem.* **2000**, *32*, 21–26.
[49] V. Alakhov, E. Klinski, P. Lemieux, G. Pietrzynski, A. Kabanov, *Expert Opin. Biol. Ther.* **2001**, *1*, 583–602.
[50] M. Kanamala, W. R. Wilson, M. Yang, B. D. Palmer, Z. Wu, *Biomaterials* **2016**, *85*, 152–167.
[51] M. J. Rosen, X. Y. Hua, *J. Colloid Interface Sci.* **1982**, *86*, 164–172.
[52] E. Shah, P. Upadhyay, M. Singh, M. S. Mansuri, R. Begum, N. Sheth, H. P. Soni, *New J.Chem.* **2016**, *40*, 9507–9519.
[53] T. K. Jain, M. A. Morales, S. K. Sahoo, D. L. Leslie-Pelecky, V. Labhasetwar, *Mol. Pharmaceutics* **2005**, *2*, 194–205.
[54] T.-H. Shin, Y. Choi, S. Kim, J. Cheon, *Chem. Soc. Rev.* **2015**, *44*, 4501–4516.
[55] D. Ho, X. Sun, S. Sun, *Acc. Chem. Res.* **2011**, *44*, 875–882.
[56] M. H. Baghersad, S. Jamshidi, A. Habibi, A. Salimi, *ChemistrySelect* **2019**, *4*, 810–815.
[57] R. J. Mumper, J. Wang, S. L. Klakamp, H. Nitta, K. Anwer, F. Tagliaferri, A. P. Rolland, *J. Control. Release* **1998**, *52*, 191–203.
[58] N. Maurer, A. Mori, L. Palmer, M. A. Monck, K. W. C. Mok, B. Mui, Q. F. Akhong, P. R. Cullis, *Mol. Membr. Biol.* **1999**, *16*, 129–140.

Submitted: March 14, 2019
Accepted: June 28, 2019

Biol. Cell (2020) **112,** 1–16 DOI: 10.1111/boc.201900104

Research article

Insights into the functional aspects of poly(ADP-ribose) polymerase-1 (PARP-1) in mitochondrial homeostasis in *Dictyostelium discoideum*

Ashlesha Kadam, Tina Jubin, Rittwika Roychowdhury, Abhishek Garg, Nishant Parmar, Sayantani Pramanik Palit and Rasheedunnisa Begum[1]

Department of Biochemistry, Faculty of Science, The Maharaja Sayajirao University of Baroda, Vadodara, Gujarat 390002, India

Background information. Poly(ADP-ribose) Polymerase-1 (PARP-1) is predominantly a nuclear protein and involved in various cellular processes like DNA repair, cell death, development, chromatin modulation etc. PARP-1 utilizes NAD^+ and adds negatively charged PAR moieties on the target proteins. Over-activation of PARP-1 has been shown to cause energy crisis mediated cell death in which mitochondrial homeostasis is also affected. Moreover, the presence of mitochondrial NAD^+ pools highlights the role of *PARP-1* in mitochondria. The aim of present study is to understand the physiological role of *PARP-1* in regulating mitochondrial functioning by varying the levels of *PARP-1* in *Dictyostelium discoideum*. Intra-mitochondrial PARylation was analyzed by indirect immunofluorescence. Further, the effect of altered levels of *PARP-1* i.e. overexpression, downregulation, knockout and its chemical inhibition was studied on mitochondrial respiration, reactive oxygen species (ROS) levels, ATP production, mitochondrial fission-fusion, mitochondrial morphology and mitochondrial DNA (mtDNA) content of *D. discoideum*.

Results. Our results show intra-mitochondrial PARylation under oxidative stress. Altered levels of *PARP-1* caused impairment in the mitochondrial respiratory capacity, leading to elevated ROS levels and reduced ATP production. Moreover, *PARP-1* affects the mitochondrial morphology and mtDNA content, alters the mitochondrial fission-fusion processes *in lieu* of preventing cell death under physiological conditions.

Conclusion. The current study highlights the physiological role of PARP-1 in mitochondrial respiration, its morphology, fission-fusion processes and mtDNA maintenance in *D. discoideum*.

Significance. This study would provide new clues on the PARP-1's crucial role in mitochondrial homeostasis, exploring the therapeutic potential of PARP-1 in various mitochondrial diseases.

Additional supporting information may be found online in the Supporting Information section at the end of the article.

Introduction

Poly(ADP-ribose) polymerases (PARPs) catalyse the transfer of ADP-ribose moiety of NAD^+ to receptor proteins forming poly(ADP-ribose) (PAR) polymers. This post-translational modification affects a large

[1]To whom correspondence should be addressed (email: rasheedunnisab@yahoo.co.in)

Key words: *Dictyostelium discoideum*, Fission-fusion, Mitochondrial respiration, Poly(ADP-ribose) polymerase-1, Reactive oxygen species.

Abbreviations: ADPRT, ADP-ribosyl transferase; ADPRT1A KO, ADPRT1A knockout; ADPRT1A OE, ADPRT1A overexpression; ARH3, ADP-ribosyl hydrolase 3; BN-PAGE, blue native-PAGE; EXOG, exonuclease G; mtDNA, mitochondrial DNA; OCR, oxygen consumption rate; PARG, Poly(ADP-ribose) glycohydrolase; PARP-1, Poly(ADP-ribose) polymerase-1; PARP dR, PARP downregulation; SB, Sorensen's buffer; TEM, transmission electron microscopy; TFAM, transcription factor A.

array of proteins. The most abundant PARP, PARP-1 accounts for 85–90% of PARP activity in the cell. The function and localisation of other PARP family members are still unknown [Krishnakumar and Kraus, 2010]. PARP-1 is involved in various cellular processes like DNA repair, cell death, cell growth, development, chromatin modulation and so on [Rajawat et al., 2011; Jubin et al., 2017; Jubin et al., 2016a; Jubin et al., 2016b; Jubin et al., 2019a; Jubin et al., 2019b]. PARP-1 consumes maximum NAD^+, lowering 10–20% cellular NAD^+ pool within a few minutes of its activation [Houtkooper et al., 2010]. Most of the studies to date have focused on the nuclear role of PARP-1 while its presence in mitochondria is still debated. As mitochondria have been gaining a special attention in health and disease, it would be interesting to study if PARylation of mitochondrial proteins modulate mitochondrial activities such as electron transport, ATP production, mitochondrial DNA (mtDNA) maintenance, cell death and so on. Thus, it is important to explore the functional relationship between intra-mitochondrial PARylation and mitochondrial homeostasis.

The role of PARP-1 in mitochondria was documented with PAR accumulation in mitochondria, low mitochondrial membrane potential (MMP) and enhanced glycolysis by mitochondria targeted heterologous expression of catalytic domain of *PARP-1* [Niere et al., 2008]. It is not clear whether this dysfunction is due to the reduced cellular and/mitochondrial NAD^+ pools or a direct effect of PARP-1 on cellular energetics. Lai et al. [2008] reported both PARP-1 and PARylation events in mitochondria. Overexpression of PAR glycohydrolase (*PARG*) or ADP-ribosyl hydrolase 3 (*ARH3*) led to a reduction in mitochondrial PARylation and restoration of mitochondrial function upon PARP-1 activation [Lai et al., 2008; Niere et al., 2008]. Moreover, pharmacological inhibition and silencing of PARP-1 protected against the mitochondrial dysfunction and increased the respiratory reserve capacity in endothelial cells post exposure to oxidative stress [Modis et al., 2012].

PARP-1 is also implicated in mtDNA repair and maintenance. Rossi et al. [2009] showed interaction between PARP-1, DNA ligase 3 and mtDNA, suggesting that PARP-1 may be a part of mtDNA repair machinery. Also, PARP-1 was found to interact with mitochondrial transcription factor A (TFAM) and mtDNA repair enzymes, DNA polymerase gamma (Polγ) and Exonuclease G (EXOG). Interestingly, PARP-1 depleted lung adenocarcinoma cells exhibited mtDNA integrity under oxidative stress, suggesting PARP-1 negatively affects mtDNA repair [Szczesny et al., 2014].

Studies on pharmacological inhibition of PARP-1 suggest its role in cellular bioenergetics under nitrosative/oxidative stress and pathological conditions [Jagtap and Szabo, 2005; Giansanti et al., 2010; Sodhi et al., 2010]. Our previous studies also showed involvement of PARP-1 in stress responses like oxidative stress, UV stress and staurosporine induced caspase independent paraptotic cell death in *Dictyostelium discoideum* [Katoch and Begum, 2003; Rajawat et al., 2007; Mir et al., 2012; Rajawat et al., 2014a; Rajawat et al., 2014b; Mir et al., 2015]. *D. discoideum* is an evolutionarily conserved model organism showing the transition from unicellular (growth) to multicellular (development) forms in its life cycle [Katoch et al., 2002; Mir et al., 2007; Kawal et al., 2011; Begum and Saran, 2020]. Many *D. discoideum* genes are orthologous to human disease related genes thus making *Dictyostelium* a model organism to study mitochondrial diseases [Annesley and Fisher, 2009]. Hence, the present study is aimed to explore the link between PARP-1 and mitochondrial functions under physiological conditions in *D. discoideum.*

Results

Intra-mitochondrial PARylation

In line with the previous reports, though the majority of PARP-1 was localised to the nucleus, PARP-1 was also identified in mitochondria [Brunyanszki et al., 2014; Szczesny et al., 2014]. To validate the same, intra-mitochondrial PARylation was analysed in *D. discoideum* cells upon H_2O_2 exposure. Fluorescence microscopic observations confirmed intra-mitochondrial PARylation in 30 and 100 μM H_2O_2 treated control cells at 10 and 30 min, respectively (Figures 1A and 1B). Interestingly, *ADPRT1A* OE cells also showed intra-mitochondrial PARylation even under non-oxidant conditions (Figure 1C). PARP activity was found to be higher in 30 μM (10 min) ($P = 0.0007$) and 100 μM H_2O_2 (30 min) ($P = 0.0001$) treated control cells and *ADPRT1A* OE cells ($P < 0.0001$) as compared with the control

Figure 1| | Intra-mitochondrial PARylation

Intra-mitochondrial PARylation was seen in (**A**) 30 μM H_2O_2 treated control cells at 10 min. (**B**) 100 μM H_2O_2 treated control cells at 30 min. (**C**) 30 μM H_2O_2 treated *ADPRT1A* OE cells at 10 min. (**D**) 100 μM H_2O_2 treated *ADPRT1A* OE cells at 30 min; *ADPRT1A* OE cells showed intra-mitochondrial PARylation even under non-oxidant conditions whereas mitochondrial PARylation was not seen in H_2O_2 treated *ADPRT1A* OE cells. Green colour: PAR levels; red colour: mitochondria [MitoTracker (MTR)]; blue colour: nucleus (DAPI); fluorescent green colour: intra-mitochondrial PARylation. Scale bar: 10 μm; Magnification: 60×. (**E**) Densitometric analysis of PARP activity: elevated PARP activity was observed in 30 μM (10 min) and 100 μM (30 min) H_2O_2 treated control cells and *ADPRT1A* OE cells as compared with the control cells. Significant decrease in PARP activity was seen in 30 and 100 μM H_2O_2 treated *ADPRT1A* OE cells as compared with the untreated *ADPRT1A* OE cells at 10 and 30 min, respectively. Data are representation of three independent experiments. $^{***}P < 0.001$ as compared with the control; $^{\#\#}P < 0.01$ as compared with the H_2O_2 treated control; $^{\$\$\$}P < 0.01$ as compared with *ADPRT1A* OE.

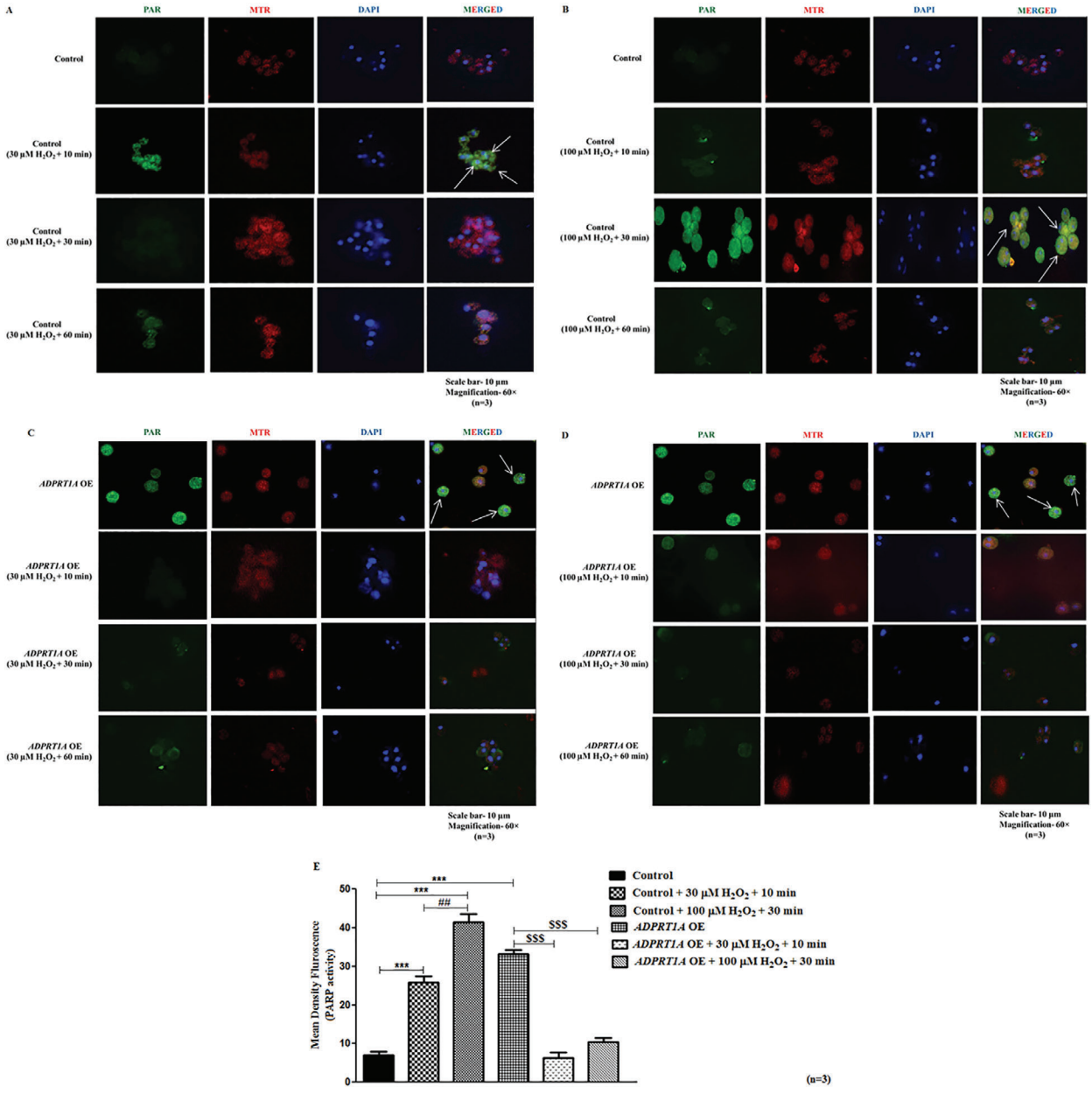

Figure 2| OCR studies

Significant reduction in complex I activity of (**A**) *ADPRT1A* OE, (**B**) *ADPRT1A* KO, (**C**) *PARP* dR and (**E**) 4 mM benzamide treated control cells was observed, whereas (**D**) no significant difference was seen in complex (I–IV) activities of 1 mM benzamide treated control cells as compared with the control cells. Data are representation of the SEM values of three independent experiments. $^{*}P < 0.05$ and $^{**}P < 0.01$ are as compared with the control; ns: non-significant.

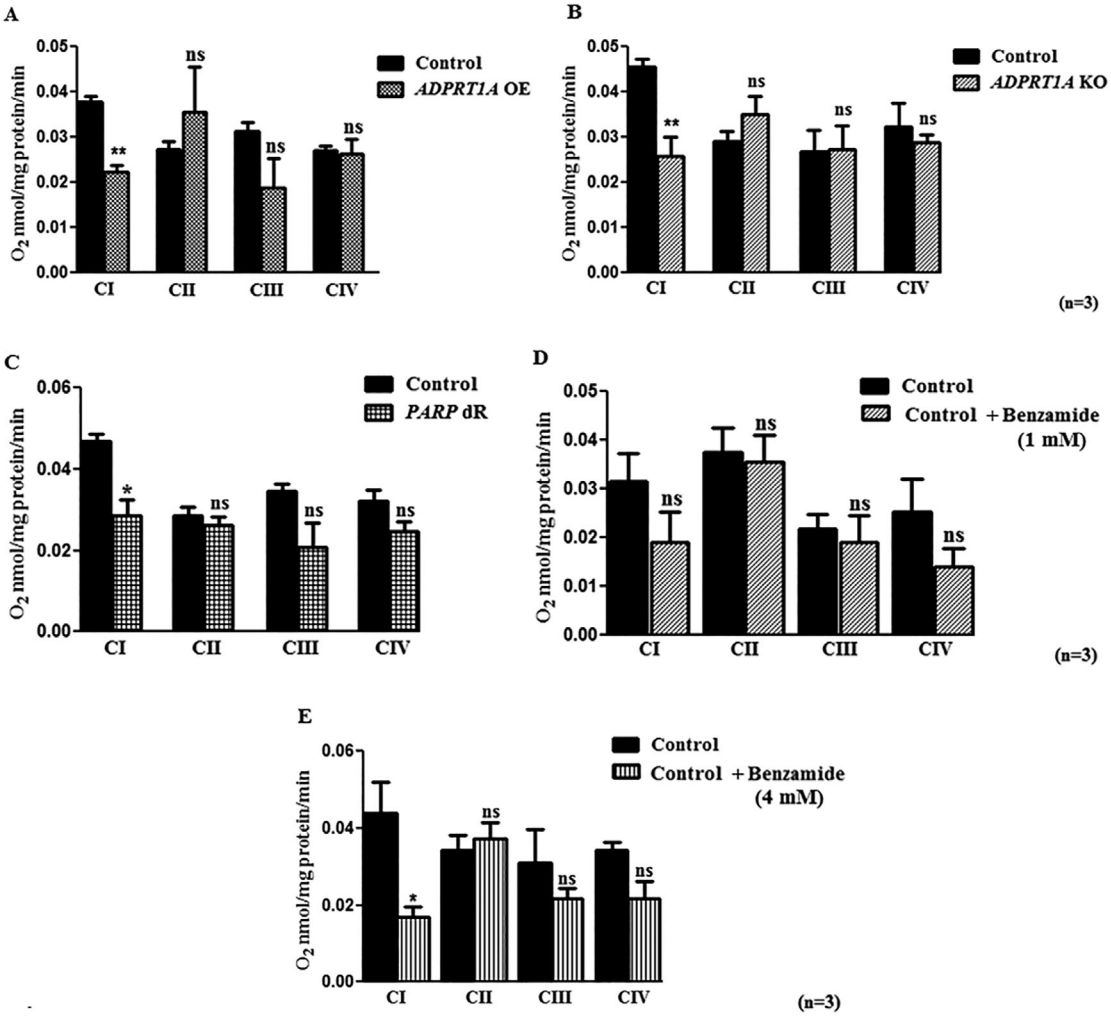

cells (Figure 1E). Moreover, significantly reduced PARP activity was observed in 30 μM ($P = 0.0001$) and 100 μM H_2O_2 ($P = 0.0001$) treated *ADPRT1A* OE cells as compared with the untreated *ADPRT1A* OE cells at 10 and 30 min, respectively (Figure 1E).

Analysis of mitochondrial respiratory capacity

The regulatory role of PARP-1 in mitochondria was assessed by estimating mitochondrial respiratory capacity in benzamide treated and *ADPRT1A* KO, *ADPRT1A* OE and *PARP* dR *D. discoideum* cells. Oxygen consumption rate (OCR) was measured in saponin permeabilised cells by Clark O_2 electrode. The decline in complex I activity was observed in *ADPRT1A* OE ($P = 0.0022$), *ADPRT1A* KO ($P = 0.0045$), *PARP* dR ($P = 0.0123$) and 4 mM benzamide treated control cells ($P = 0.0352$) (Figures 2A, 2B, 2C and 2E), whereas no significant difference was observed in complex (I–IV) activities in 1 mM benzamide treated control cells (Figure 2D) as compared with the control cells. These results indicate a possible connection between PARP-1 and complex I. Regulatory *PARP-1*

Figure 3| | ROS estimation by DCFDA dye

Significant increase in ROS levels was observed in *ADPRT1A* OE, *ADPRT1A* KO and *PARP* dR cells, whereas no significant difference was observed in 1 mM benzamide treated control cells as compared with the control cells. 30 μM H_2O_2 treated control cells were kept as a positive control. Data are representation of the SEM values of four independent experiments. ***$P < 0.001$ and *$P < 0.05$ are as compared with the control; ns: non-significant.

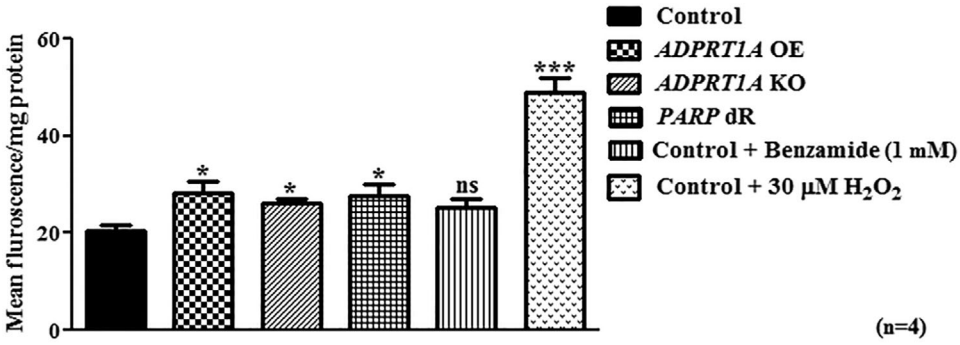

levels might be necessary for the optimum functioning of respiratory chain complexes.

Total cellular ROS levels

Complex I is known to be one of the major sites of reactive oxygen species (ROS) production [Hirst et al., 2008]. Hence, we monitored the ROS levels to know if there was any difference due to impaired complex I activity. Elevated levels of ROS were observed in *ADPRT1A* OE ($P = 0.0229$), *ADPRT1A* KO ($P = 0.0115$) and *PARP* dR ($P = 0.0369$) cells, whereas no significant difference was seen in benzamide (1 mM) treated control cells ($P = 0.0754$) compared with the control cells (Figure 3). Reduced complex I activity might be the cause for increased ROS levels in these cells.

Total ATP levels

To assess the functioning of mitochondria, cellular and mitochondrial ATP levels were estimated by HPLC. HPLC data showed diminution in cellular ATP levels in *ADPRT1A* OE ($P = 0.0095$), *ADPRT1A* KO ($P = 0.0221$) and *PARP* dR cells ($P = 0.0156$) and mitochondrial ATP levels in *ADPRT1A* KO cells ($P = 0.0272$) (Figure 4). Both cellular and mitochondrial ATP levels in 1 mM benzamide treated cells were comparable to control cells ($P = 0.0843$ and $P = 0.3485$). A decrease in complex I activity along with an increase in ROS levels suggest compromised total ATP production.

Analysis of electron transport chain assembly

Altered *ADPRT1A* levels affected mitochondrial respiratory activity. Various mitochondrial proteins along with electron transport chain (ETC) subunits were found to be subjected to poly(ADP-ribosyl)ation (PARylation) [Brunyzanski et al., 2016]. Thus, we further wanted to study the effect of altered *ADPRT1A* on the transcript levels by real time PCR and protein levels by BN-PAGE of the PARylated ETC subunits [Complex I: NADH Dehydrogenase subunit 7 (NAD7), NADH Dehydrogenase Ubiquinone 1 Alpha subcomplex subunit 9 (NDUFA9), NADH:Ubiquinone oxido-reductase core subunit V1 (NDUFV1) and NADH:Ubiquinone oxido-reductase core subunit V2 (NDUFV2); Complex V: ATP synthase Beta subunit (ATP5B), ATP synthase Gamma subunit (ATP5C1) and ATP synthase O subunit (ATP5O)]. Interestingly, *NDUFV1* transcript levels were found to be lower in *ADPRT1A* OE, *ADPRT1A* KO, *PARP* dR and 4 mM benzamide treated cells (Figure 5A). Reduced *NDUFV2* levels were found only in *ADPRT1A* KO and *NAD7* levels in *ADPRT1A* KO and 4 mM benzamide treated control cells (Figures 5B and 5C), whereas *NDUFA9* levels were low in *ADPRT1A* OE, *ADPRT1A* KO and 4 mM benzamide treated control cells (Figure 4D). *ATP50* levels were low in *ADPRT1A* OE and *ADPRT1A* KO (Figure 5G) cells. *ADPRT1A* OE exhibited elevated *ATP5B* and *ATP5C1* levels (Figures 5E and 5F), whereas *ADPRT1A* KO, *PARP*

Figure 4| | Estimation of cellular and mitochondrial ATP levels

(**A**) and (**B**) Significant reduction in cellular ATP levels was found in *ADPRT1A* OE, *ADPRT1A* KO and *PARP* dR cells, whereas a significant reduction in mitochondrial ATP levels was found in *ADPRT1A* KO as compared with the control cells. Non-significant difference was observed in 1 mM benzamide treated control cells as compared with the control cells. Data are representation of the SEM values of three independent experiments. $^{*}P < 0.05$ and $^{**}P < 0.01$ are as compared with the control; ns: non-significant.

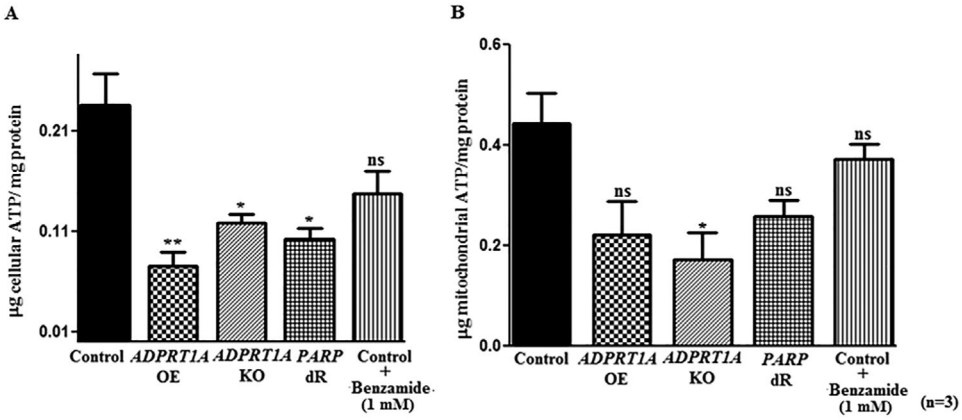

dR and 4 mM benzamide treated control cells showed decreased levels of *ATP5B* (Figure 5E). Thus, no significant difference in transcript levels of ETC subunits was observed in 1 mM benzamide treated control cells (Figure 5), whereas the transcript profiles of ETC subunits were different in *ADPRT1A* OE, *ADPRT1A* KO, *PARP* dR and 4 mM benzamide treated control cells, suggesting the role of ADPRT1A in the mitochondrial respiratory activity.

BN-PAGE is a powerful tool in identifying respiratory assembly defects [Van Coster et al., 2001]. As PARP-1 was found to be involved in maintaining mitochondrial respiratory capacity, the assembly of the ETC was analysed by BN-PAGE. Densitometric analysis of BN-PAGE gels exhibited reduced protein abundance of supercomplexes I+III+IV in *ADPRT1A* KO, *ADPRT1A* OE and *PARP* dR as compared with the control cells (Figures 6A and 6B); however, complex II levels were increased indicating ADPRT1A's role in respiratory complexes assembly and maintenance.

mtDNA content

PARP-1 is known to be involved in regulating transcription of the mitochondrial transcription factor A (TFAM) and its repair proteins such as exonuclease G (EXOG) and APEX nuclease multifunctional DNA repair enzyme transcript variant 1 (APE1) [Lapucci et al., 2011]. This specifies a potential role of PARP-1 in regulating the mtDNA content. To assess the same, mtDNA content was estimated in these cells. The mtDNA content was observed to be significantly lower in *ADPRT1A* OE ($P = 0.0033$), *ADPRT1A* KO ($P = 0.0423$) and 4 mM benzamide treated control cells ($P = 0.0105$), whereas non-significant change was found in *PARP* dR ($P = 0.2949$) and 1 mM benzamide treated control cells ($P = 0.3924$) (Figure 7).

Mitochondrial fission-fusion

The balance between mitochondrial fission and fusion is a major hallmark of an efficient mitochondrial quality function and optimised bioenergetic capacity [Westermann, 2012]. Hence, we further analysed the transcription profile of mitochondrial fusion gene, CLUstered A (*CLUA*) and fission genes [Dynamin A (*DYMA*), Dynamin B (*DYMB*) and mitochondrial cell division genes (*FSZA* and *FSZB*)] in these cells which were having compromised respiratory capacity. A significant decrease in *CLUA* transcript levels and an increase in *FSZA* transcript levels were found in *ADPRT1A* OE, *ADPRT1A* KO, *PARP* dR and 4 mM benzamide treated control cells (Figures 8A and 8B), whereas *FSZB* transcript levels were observed to be higher in *ADPRT1A* KO and 4 mM benzamide treated control cells (Figure 8C). Benzamide (1 mM) did not show significant difference in transcript levels of mitochondrial fission-fusion genes

Figure 5| | See Legend on next page

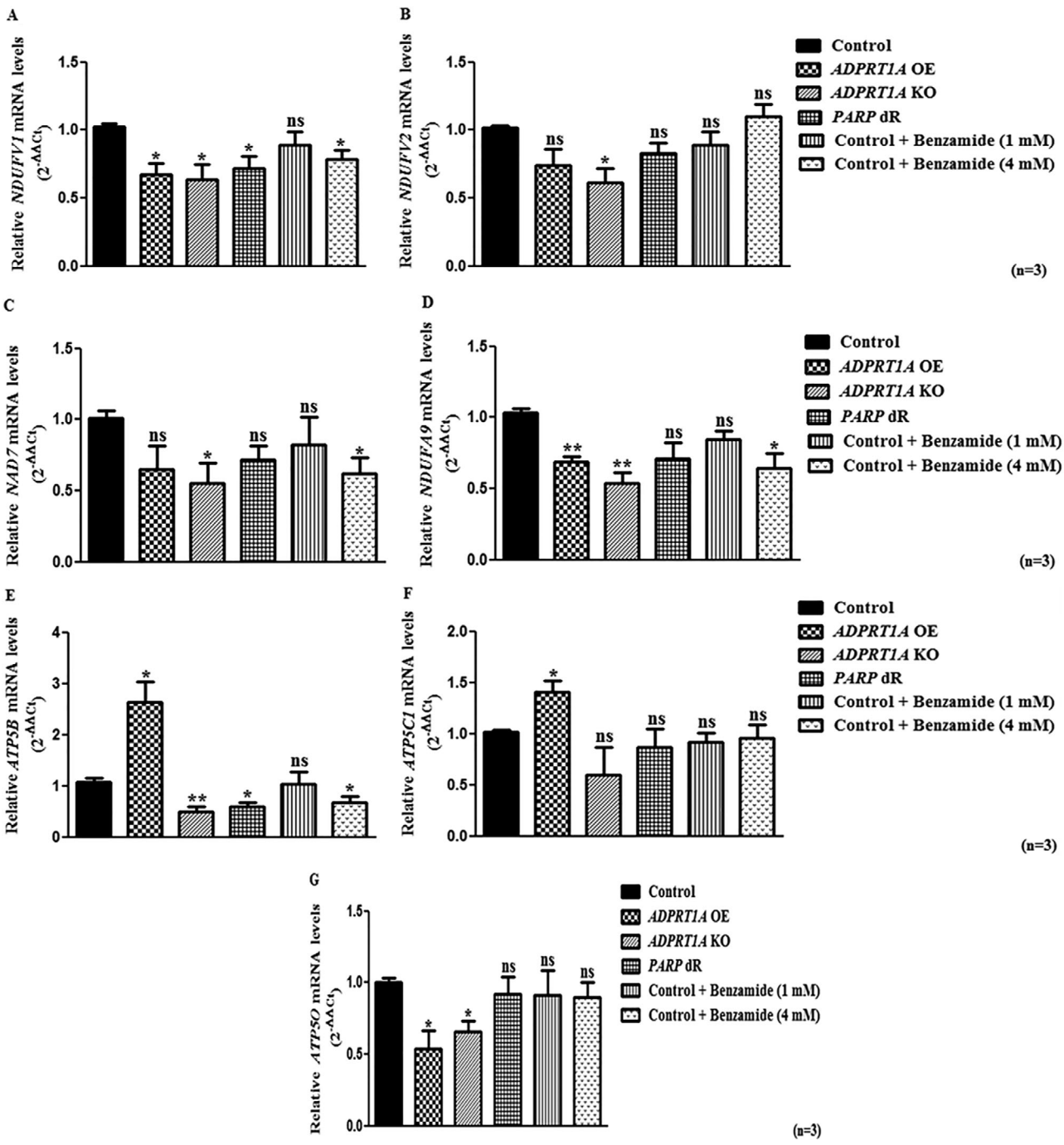

Figure 5| Gene expression analysis by real time PCR

Transcript levels of *NDUFV1, NDUFV2, NAD7, NDUFA9, ATP5B, ATP5C1* and *ATP5O* were analysed by real time PCR. (**A**) Significant reduction in *NDUFV1* levels were seen in *ADPRT1A* OE, *ADPRT1A* KO, *PARP* dR and 4 mM benzamide treated control cells as compared with the control cells. (**B**) Only *ADPRT1A* KO cells exhibited a drop in *NDUFV2* levels as compared with the control cells. (**C**) Reduced *NAD7* transcript levels were observed in *ADPRT1A* KO and 4 mM benzamide treated control cells, whereas no significant difference was observed in *ADPRT1A* OE, *PARP* dR and 1 mM benzamide treated control cells. (**D**) Significant decrease in *NDUFA9* transcript levels were detected in *ADPRT1A* OE, *ADPRT1A* KO and 4 mM benzamide treated control cells as compared with the control cells, whereas non-significant difference was seen in *PARP* dR and 1 mM benzamide treated control cells. (**E**) Increased transcript levels of *ATP5B* in *ADPRT1A* OE; decreased *ATP5B* transcript levels in *ADPRT1A* KO, *PARP* dR and 4 mM benzamide treated control cells were observed. (**F**) *ADPRT1A* OE cells exhibited elevated *ATP5C1* transcript levels as compared with the control cells. (**G**) Decreased *ATP5O* transcript levels were seen in *ADPRT1A* OE and *ADPRT1A* KO cells, whereas no significant difference was observed in *PARP* dR and benzamide (1 and 4 mM) treated control cells as compared with the control cells. Data are representation of the SEM values of three independent experiments. $*P < 0.05$ and $**P < 0.01$ are as compared with the control; ns: non-significant.

(Figure 8). Moreover, elevated *DYMA* transcript levels were found in *ADPRT1A* OE, *ADPRT1A* KO, and *PARP* dR cells as compared with the control cells (Figure 8D), whereas a non-significant difference in *DYMB* transcript levels were observed in all the cells (Figure 8E). These results indicate increased fission and decreased mitochondrial fusion processes upon change in *PARP-1* levels. The unbalanced mitochondrial fission-fusion processes in these cell types confirm the regulatory role of PARP-1 in mitochondrial function.

Mitochondrial morphology

Mitochondrial morphology is maintained by fission-fusion processes. Disruption in these processes results in altered number and size of mitochondria in a cell, hampering mitochondrial homoeostasis [Scott and Youle, 2010]. Hence, imbalance in fission-fusion processes led us further to analyse mitochondrial morphology. The higher mitochondrial number along with their smaller size and average surface area were observed in *ADPRT1A* OE, *ADPRT1A* KO and *PARP* dR *D. discoideum* cells as compared with the control cells (Figures 9A, 9B and 9C). This might be due to increased mitochondrial fission and decreased mitochondrial fusion processes. Increase in fission process may promote the segregation of defective mitochondria, facilitating their clearance by mitophagy for cell survival [van der Bliek et al., 2013].

Discussion

Although the nuclear role of PARP-1 has been well established, its presence in mitochondria is still in debate. Literature suggests that PARP-1 possibly enters mitochondria and interacts with inner mitochondrial membrane protein, mitofilin which is part of the MIA (Mitochondrial Inner Membrane Space Assembly) [Rossi et al., 2009]. PARP-1 activation leads to a reduction in cellular NAD^+ levels and eventual drop in cellular ATP levels [Szabo and Dawson, 1998]. As mitochondria have their own NAD^+ pool [Stein and Imai, 2012], it further raises the question of whether, PARP-1 also utilises mitochondrial NAD^+. Basal activity of PARP-1 contributes to the regulation of nuclear homoeostasis and cellular functions [Krishnakumar and Kraus, 2010]. PARP-1 gets activated in response to DNA damage, leading to chromatin remodelling and active transcription [Potaman et al., 2005]. Despite of remarkable progress in the field of PARP-1 biology, the physiological relevance of PARP-1 within mitochondria is still not clear. Hence, we have explored the possible role of PARP-1 in *D. discoideum* mitochondria by varying its levels using genetic methods, that is overexpression, knockout, downregulation and chemical inhibition by benzamide.

Along with nuclear presence of PARP-1, several studies have observed its existence in mitochondria. PARP-1 is also known to play various functions in cellular activities [Du et al., 2003; Rossi et al., 2009; Brunyanszki et al., 2014; Szczesny et al., 2014]. We have also shown intra-mitochondrial PARylation in *D. discoideum*, indicating PARP-1's presence in mitochondria (Figures 1A and 1B). Auto-PARylation of PARP-1 prevents its catalytic activity [Kauppinen et al., 2006]. In *ADPRT1A* OE cells, overexpression in due course leads to extensive auto-PARylation finally causing its inhibition. This could be the possible

Figure 6| BN-PAGE analysis

(A) Significant reduction in protein abundance was observed in the supercomplexes CI+III+IV in *ADPRT1A* KO, *ADPRT1A* OE and *PARP* dR; CIII+IV and CIII in *ADPRT1A* KO; CIV2 subunit in *ADPRT1A* OE, *ADPRT1A* KO and control + benzamide (1 mM). However, significant increase in CII protein was observed in *ADPRT1A* OE as compared with the control cells. Lane 1, Native Protein Marker; lane 2, *ADPRT1A* KO; lane 3, control; lane 4, *ADPRT1A* OE; lane 5, *PARP* dR; lane 6, control + benzamide (1 mM). (**B**) Densitometric analysis of BN-PAGE gels. Data are representation of the SEM values of three independent experiments. $^{*}P < 0.05$, $^{**}P < 0.01$ and $^{***}P < 0.001$ are as compared with the control; ns: non-significant.

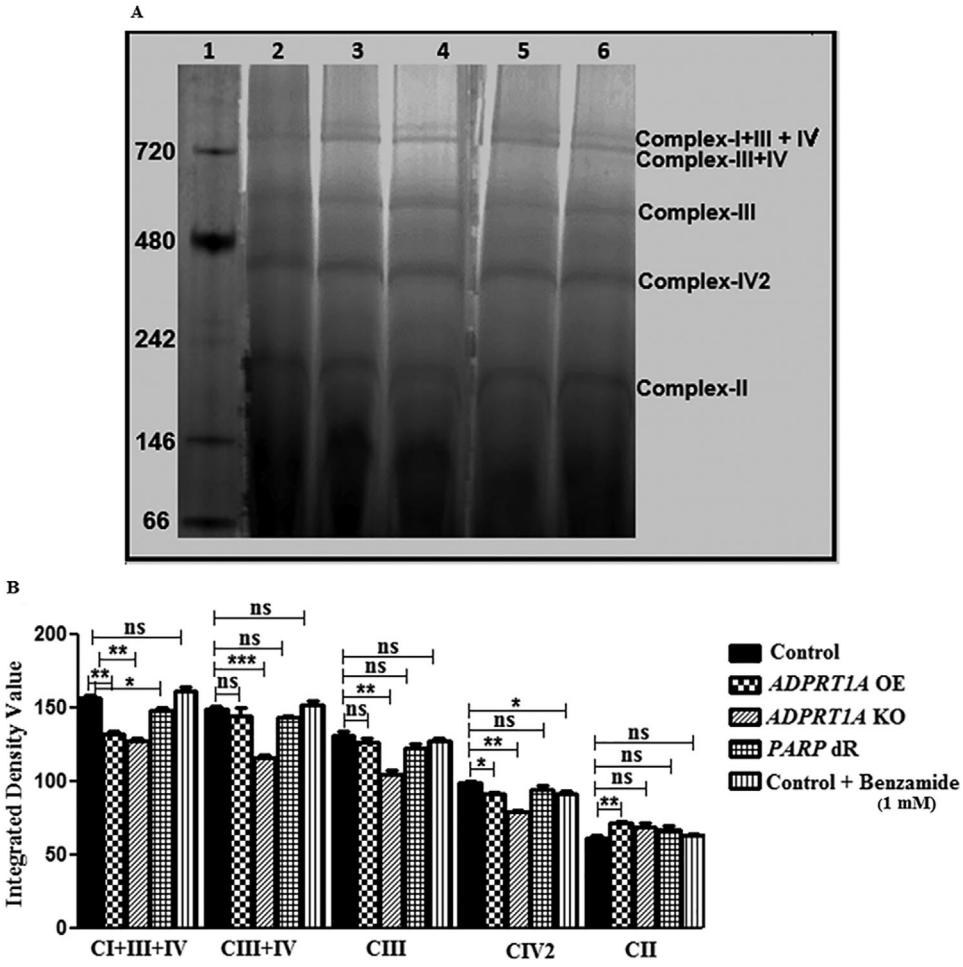

reason for the absence of PARylation in *ADPRT1A* OE cells upon H_2O_2 exposure (Figures 1C and 1D). The respiratory capacity of the cell depends on mitochondrial function. We have assessed the respiratory capacity in *ADPRT1A* OE, *ADPRT1A* KO, *PARP* dR and benzamide (1 and 4 mM) treated control cells. Reduced complex I activity was observed in *ADPRT1A* OE, *ADPRT1A* KO, *PARP* dR and 4 mM benzamide treated control cells (Figure 2). In addition to this, transcript levels of ETC complexes subunits and ETC complex assembly were affected in these cells (Figures 5 and 6), confirming the regulatory function of PARP-1 in mitochondria. Dysfunction in complex I activity results in elevated ROS levels and hence reduced total cellular ATP production [Sharma et al., 2011]. Impaired complex I activity in *ADPRT1A* OE, *ADPRT1A* KO and *PARP* dR cells led to an increase in ROS (Figure 3) and reduced cellular ATP levels (Figure 4). Supporting our results, overexpression of the catalytic domain of *PARP-1* exhibited a decrease in NAD^+ content and respiratory deficiency in HEK293 cells [Niere et al., 2008].

Figure 7| | mtDNA content by real time PCR

ADPRT1A OE, *ADPRT1A* KO and 4 mM benzamide treated control cells exhibited reduced mtDNA content, whereas no significant difference was observed in *PARP* dR and 1 mM benzamide treated control cells as compared with the control cells. Data are representation of the SEM values of three independent experiments. $^{**}P < 0.01$ and $^{*}P < 0.05$ are as compared with the control; ns: non-significant.

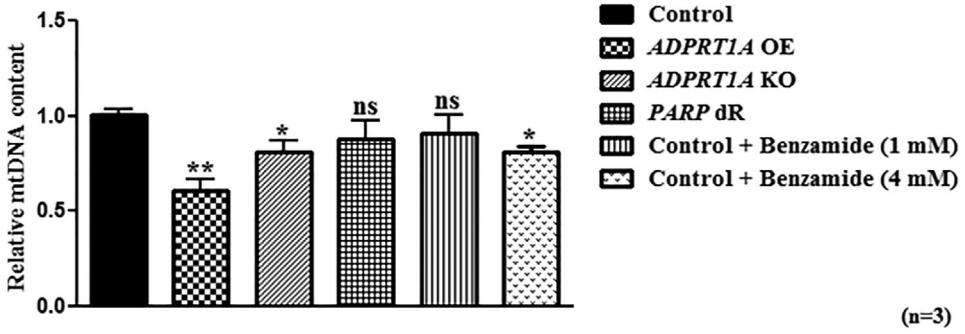

Zhang et al. [2018] observed *PARP-1* overexpression in Barrett's oesophagus (BE) which resulted in increased ROS levels. Moreover, BAR-T cells with knockdown of endogenous *PARP-1* using scrambled shRNA also displayed higher H_2O_2 levels, indicating PARP-1's protective role in BE [Zhang et al., 2018]. Impaired complex I might predispose the respiratory chain assembly to produce excess ROS due to stoichiometric or structural modifications in the ETC subunits by increasing interaction of oxygen with electron carriers [Pitkanen and Robinson, 1996]. We have also reported reduced ATP might be the reason for slower growth rate in *ADPRT1A* OE and *ADPRT1A* KO cells [Jubin et al., 2016b; Jubin et al., 2019b]. The MMP is generated by ETC and is essential for the synthesis of ATP [Sakamuru et al., 2016]. The loss of MMP might also be explained by elevated ROS in *ADPRT1A* OE cells [Jubin et al., 2016b].

The mtDNA encodes for essential components of respiratory complexes and defects in respiratory assembly can directly disrupt the mitochondrial functions. The transcription of OXPHOS genes is associated with mtDNA. Hence, we further analysed the mtDNA content. *ADPRT1A* OE, *ADPRT1A* KO and 4 mM benzamide treated control cells exhibited decreased mtDNA content (Figure 7), indicating the plausible role of PARP-1 in mtDNA maintenance. Our results are in line with the earlier studies suggesting a vital role of PARP-1 in mtDNA maintenance [Gilbertson et al., 1991; Rossi et al., 2009; Lapucci et al., 2011]. Hossain et al. (2009) showed the importance of PARP-1 activity for nuclear respiratory factor (NRF) -1 dependent activation and cytochrome c promoter activity, signifying PARP-1 acts as a key regulator of mitochondrial proteins [Hossain et al., 2009]. Moreover, suppression of *PARP-1* affected mtDNA integrity, expression of mitochondrial encoded respiratory complex subunits; NADH dehydrogenase 2 (ND-2), Cytochrome oxidase-1 (COX-1), cytochrome oxidase 2 (COX-2) and ATP production [Lapucci et al., 2011]. PARP-1 was also found to be localised at nuclear genes promoters encoding the mtDNA repair proteins; Uracil DNA glycosylase variant 1 (UNG1), mutY Homolog (MYH1) and APE1 and the mtDNA transcription factors (TFB1M and TFB2M), suggesting epigenetically regulated PARP-1 activity might be required for transcriptional activation of mitochondrial genes [Lapucci et al., 2011]. These findings suggest that PARP-1 can indirectly regulate promoter activity by poly(ADP-ribosyl)ating promoter-interacting proteins without direct binding to the promoter region itself.

Mitochondrial function is linked to its structure which is maintained by dynamic fission-fusion processes [Twig et al., 2008] and morphological changes in mitochondria have also been associated with mtDNA mutations [Hermann et al., 1998]. We have studied if variation in *PARP-1* levels affects the mitochondrial fission-fusion processes. We have found decreased transcript levels of *CLUA* and increased *FSZA* transcript levels in *ADPRT1A* OE,

Figure 8| | Mitochondrial fission-fusion genes expression analysis

Real time PCR analysis showed altered transcript levels of mitochondrial fission-fusion genes [(**A**) *CLUA*, (**B**) *FSZA*, (**C**) *FSZB*, (**D**) *DYMA*, and (**E**) *DYMB*] in *ADPRT1A* OE, *ADPRT1A* KO, *PARP* dR and 4 mM benzamide treated control cells as compared with the control cells. Data are representation of the SEM values of three independent experiments. $^{*}P < 0.05$ and $^{**}P < 0.01$ are as compared with the control; ns: non-significant.

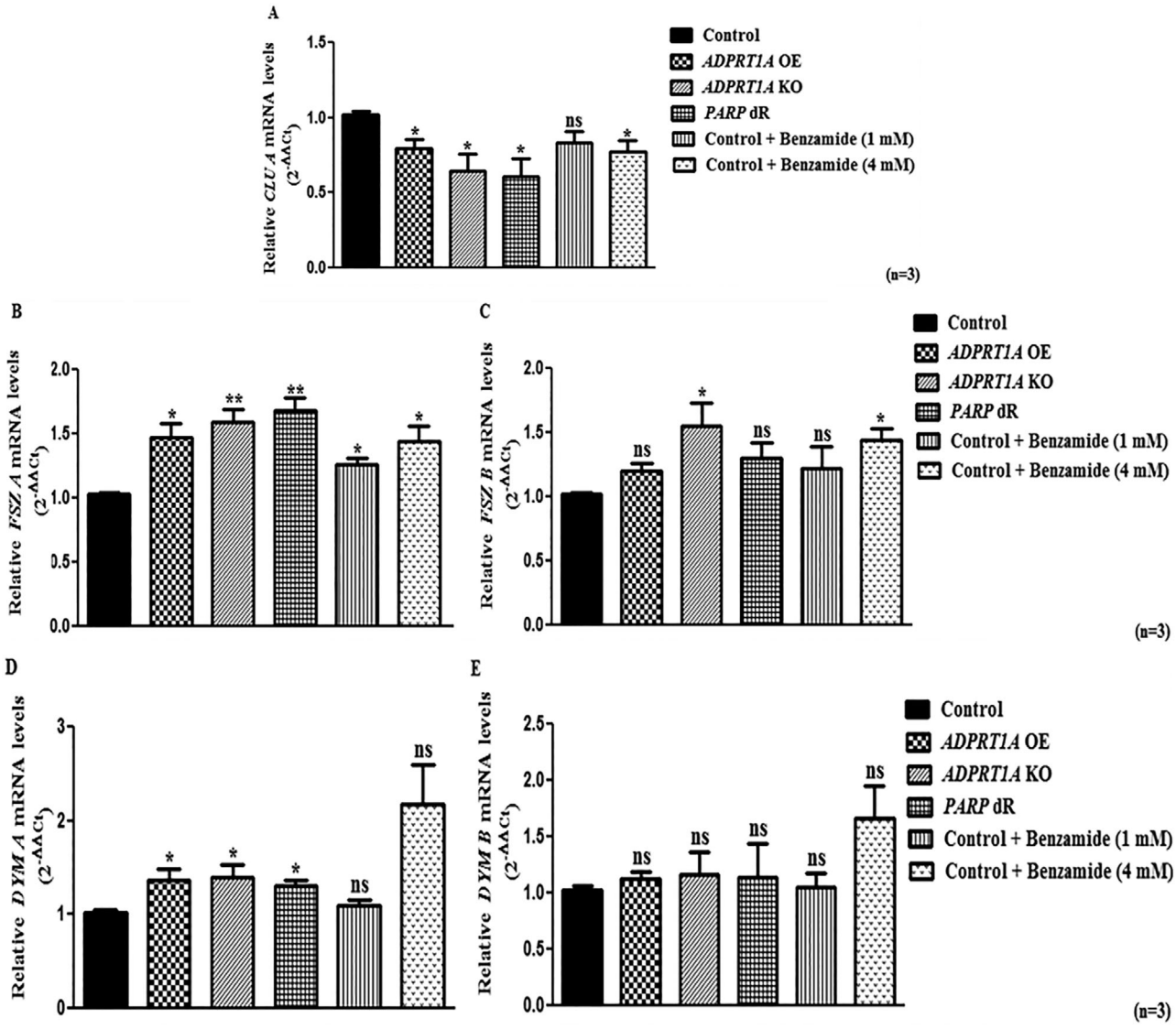

ADPRT1A KO, *PARP* dR and 4 mM benzamide treated control cells (Figure 8), suggesting less fusion and more fission of mitochondria which were confirmed by TEM analysis. Our TEM results showed increased mitochondrial fission resulting in a higher number of mitochondria in *ADPRT1A* OE, *ADPRT1A* KO and *PARP* dR cells along with less average surface area in *ADPRT1A* OE cells (Figures 9A, 9B and 9C). Mitochondrial fission and fusion are the opposing trends that are used to counter different levels of stress. Reduced fusion and/or increased fission usually occurs with high levels of stress [Gomes et al., 2011; Rambold et al., 2011]. Increased rate of fission may lead to mitophagy to salvage the damaged mitochondria and prevent cell death [Twig et al., 2008].

Figure 9| Analysis of mitochondrial morphology by TEM

(**A**) Representative electron micrographs showed compact and large mitochondria (shown by the red arrow) in control cells, whereas a small and higher number of mitochondria in *ADPRT1A* OE ($P = 0.0146$), *ADPRT1A* KO ($P = 0.016$) and *PARP* dR ($P = 0.0017$) cells. Scale bar: 1.0 μm. (**B**) A significant increase in the number of mitochondria was observed in *ADPRT1A* OE, *ADPRT1A* KO and *PARP* dR as compared with the control cells. (**C**) *ADPRT1A* OE cells ($P = 0.0405$) exhibited lower mitochondrial average surface area as compared with the control cells. $^{**}P < 0.01$ and $^{*}P < 0.05$ are as compared with the control; ns: non-significant.

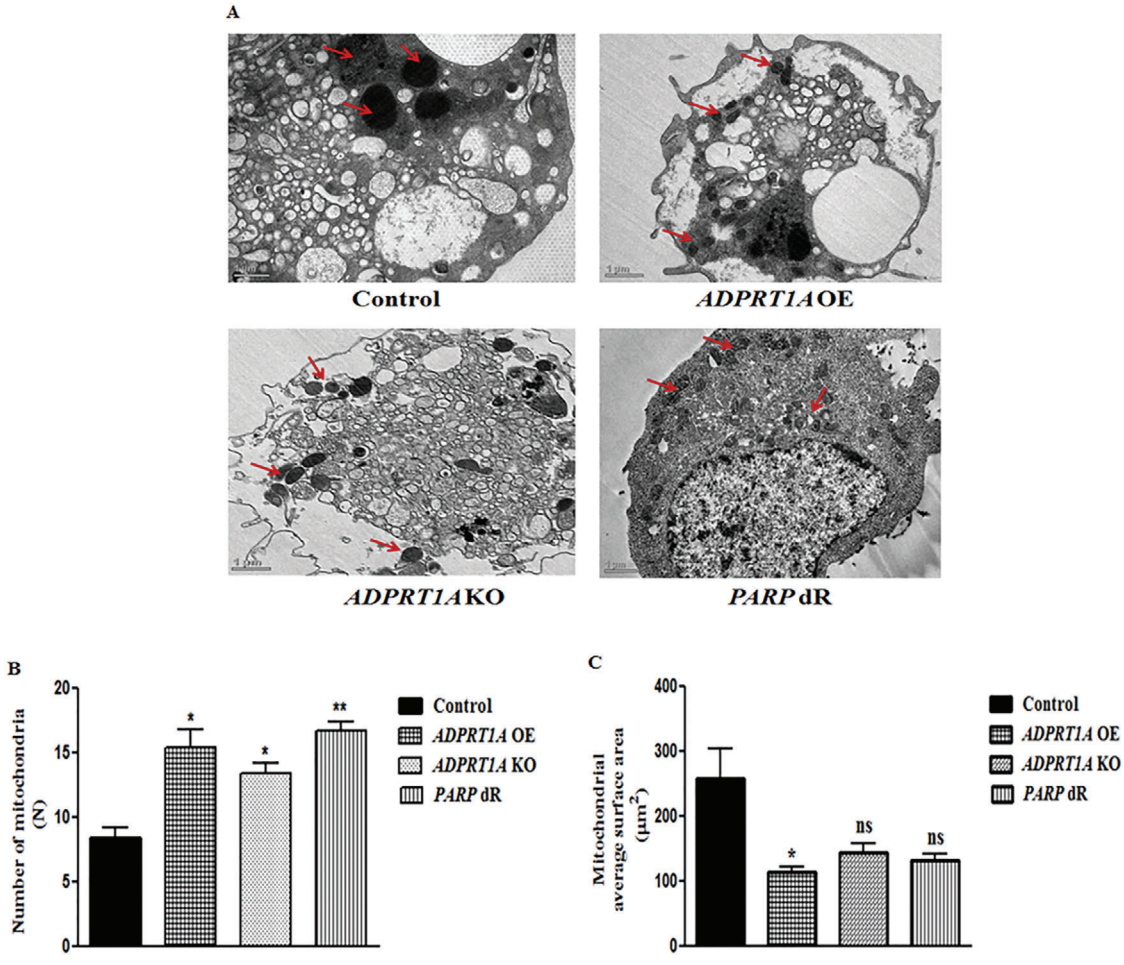

PARP-1 is PARylated by itself, PARP-2, and possibly by other PARPs. Auto-PARylation of PARP-1 inhibits its catalytic activity [Kauppinen et al., 2006]. In *ADPRT1A* OE cells, extensive auto-PARylation ultimately results in its inhibition. Nevertheless, *ADPRT1A* KO results are due to the reduction of *ADPRT1A* levels, signifying the role of ADPRT1A in mitochondrial homoeostasis. Thus, the effects generated due to *ADPRT1A* overexpression, knockout or downregulation may be similar. Moreover, deletion or overexpression of *PARP-1* may have a direct or indirect effect and/consequences on mitochondria which needs to be deciphered further.

Our novel findings in this study provide new clues on the PARP-1's crucial role in mitochondrial homeostasis of *D. discoideum* (Figure 10).

Conclusions

Overall, novel findings of the present study highlight the role of PARP-1 in mitochondrial respiration, ROS and ATP production, mitochondrial morphology,

Figure 10| | Effect of altered *PARP-1* on mitochondrial homoeostasis

The present study suggests presence of mitochondrial PARylation. Altered *PARP-1* levels and chemical inhibition of PARP led to compromised mitochondrial function, affecting oxidative phosphorylation, mtDNA pool and mitochondrial fission–fusion processes, demonstrating the physiological role of PARP-1 in mitochondrial homeostasis of *D. discoideum.* mt: mitochondrial.

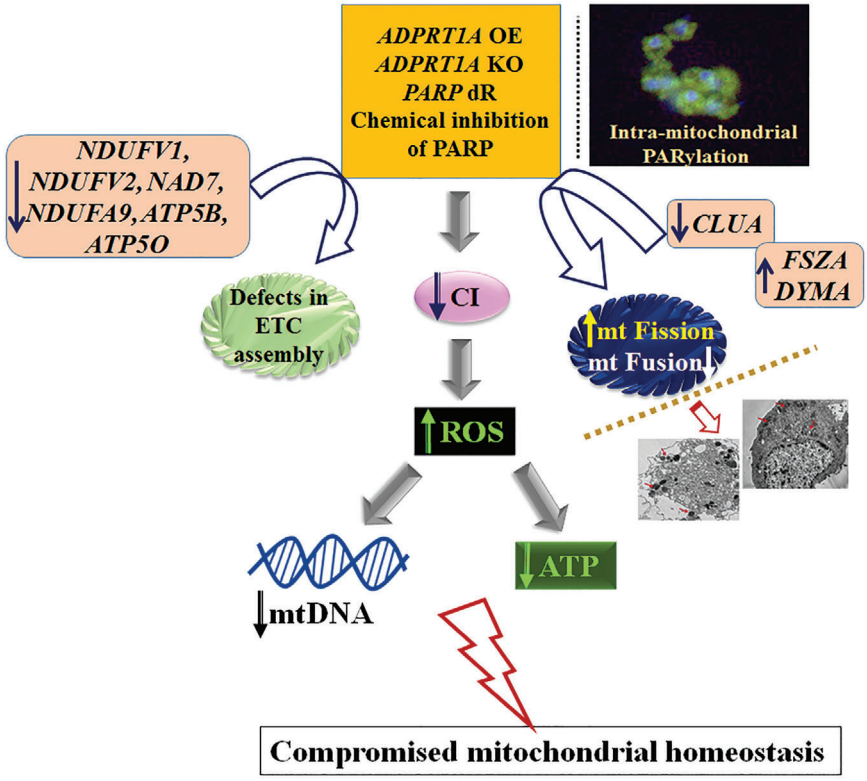

fission-fusion processes and mtDNA maintenance in *D. discoideum.* The intriguing findings of the present study would provide insights into the PARP-1's role in mitochondrial dysfunction, exploring a novel dimension to the multitasking roles of PARP-1. Nevertheless, further investigations are required to understand the underlying mechanism between PARP-1 and mitochondria to explore the therapeutic potential of PARP-1 in various disease conditions.

Materials and methods

Cell culture conditions

Dictyostelium discoideum AX-2 strain was grown in HL-5 medium, pH 6.5 with 150 rpm shaking at 22°C [Watts and Ashworth, 1970]. The *ADPRT1A* knockout (*ADPRT1A* KO) [Jubin et al., 2019a; Jubin et al., 2019b], *ADPRT1A* overexpressed (*ADPRT1A* OE) [Jubin et al., 2016b] and *PARP* downregulated (*PARP* dR) [Rajawat et al., 2011] *D. discoideum* cells were grown in HL-5 medium supplemented with 10 μg/ml blasticidin, 100 μg/ml geneticin and 20 μg/ml geneticin, respectively. PARP inhibition was done by treating *D. discoideum* cells with 1 and 4 mM benzamide for 12 h [Rajawat et al., 2007]. To elucidate the functional link between PARP-1 and mitochondria, downstream mitochondrial parameters were monitored in all *PARP-1* altered strains (*ADPRT1A* OE, *ADPRT1A* KO and *PARP* dR) and benzamide (1 and 4 mM) treated *D. discoideum* cells.

Intra-mitochondrial PARylation

As per our previous studies, higher basal poly ADP-ribosylation activity in *ADPRT1A* OE cells indicates higher endogenous PAR levels [Jubin et al., 2016b]. Hence, *ADPRT1A* OE *D. discoideum* cells were selected to investigate intra-mitochondrial PARylation. Intra-mitochondrial PARylation was analysed in control and *ADPRT1A* OE cells upon H_2O_2 treatment by indirect immunofluorescence using polyclonal rabbit anti-Poly(ADP-ribose) [PAR] (BD Pharminogen^{TM}) and anti-rabbit IgG (whole molecule) FITC conjugate (Sigma–Aldrich) at a dilution of 1:200. Mitochondria were labelled using 100 nM MitoTracker^{TM} Red (Thermo Fischer Scientific) dye. Cells were treated with 30 and 100 μM cumene H_2O_2 for 10, 30 and 60 min to analyse intra-mitochondrial PARylation

[Brunyanszki et al., 2014, Rajawat et al., 2014b]. Cells were observed by fluorescence microscope (Nikon Eclipse-Ti2) and images were taken. Mean density of fluorescence was plotted for quantification of PARP activity (PAR levels).

Estimation of oxygen consumption rate

OCR was estimated in saponin (5 mg/ml) treated *D. discoideum* cells [$\sim 12 \times 10^6$ of control, *ADPRT1A* OE, *ADPRT1A* KO and *PARP* dR and benzamide (1 and 4 mM) treated control cells] using Oxytherm Clark-type oxygen (O_2) electrode (Hansatech Instruments) containing respiration buffer (80 mM KCl, 0.1% BSA, 50 mM HEPES, 2 mM $MgCl_2$ and 2.5 mM KH_2PO_4; pH 7.2) as described in Kadam et al. [2020] and Finner and Newell [1987]. Respiratory chain complexes I-IV activities were measured using 100 mM pyruvate and 800 mM malate (complex I), 1 M succinate (complex II), 10 mM α-glycerophosphate (complex III), 200 mM ascorbate (complex IV) and protein concentration was estimated by Lowry method [Lowry et al., 1951]. Integrity of mitochondrial outer membrane in saponin-treated cells was assessed by impermeability to exogenous cytochrome *c* which was greater than 95%. All the chemicals were purchased from Sigma–Aldrich. The overall OCR is calculated by estimating the amount of oxygen (nmol) consumed per the time lapsed (min) per amount of protein present in the assay [Finner and Newell, 1987].

Estimation of intracellular ROS generation

The intracellular ROS levels were monitored by DCFDA (2'-7'dichlorofluorescin diacetate) dye (1 μg/ml). *D. discoideum* cells [$\sim 2.0 \times 10^6$ of control, *ADPRT1A* OE, *ADPRT1A* KO, *PARP* dR, benzamide (1 mM) treated control, and H_2O_2 (30 μM) treated control cells] were washed twice with 1× Sörensen's buffer (SB) [2 mM Na_2HPO_4+15 mM KH_2PO_4, (pH 6.4)] followed by addition of DCFDA dye and incubated for 15 min at 22°C with shaking. Cells were further washed with 1× SB and fluorescence intensity was measured by Fluorimeter (F7000; Hitachi), λ_{ex} and λ_{em} used for these studies were 480 and 525 nm, respectively [Myhre et al., 2003].

Estimation of ATP levels

Total cellular and mitochondrial ATP levels were estimated by HPLC in aliquots extracted with alkali [Leoncini et al., 1987; Kadam et al., 2017]. Mitochondria were isolated from *D. discoideum* cells [control, *ADPRT1A* OE, *ADPRT1A* KO, *PARP* dR and benzamide (1 mM) treated control cells] as described by Nagayama et al. [2008]. ATP levels were normalised with protein concentration which was estimated by Lowry method [Lowry et al., 1951].

Gene expression analysis by real time PCR

Total RNA isolation was done from *D. discoideum* cells [control, *ADPRT1A* OE, *ADPRT1A* KO, *PARP* dR and benzamide (1 and 4 mM) treated control cells] and transcript analysis was performed using gene specific primers by real time PCR using Light- CyclerH 480 SYBR Green I Master (Roche Diagnostics GmbH) in the LightCyclerH480 Real Time PCR (Roche Diagnostics GmbH). *RNLA* was used as an internal control. Fold change in transcript levels ($2^{-\Delta\Delta Ct}$) was shown graphically [Livak and Schmittgen, 2001]. Supplementary Table 1 contains the primer details of the genes analysed by Real Time PCR.

Estimation of mtDNA content

Total cellular DNA was extracted from *D. discoideum* cells [control, *ADPRT1A* OE, *ADPRT1A* KO, *PARP* dR and benzamide (1 and 4 mM) treated control cells] [Pilcher et al., 2007] and mtDNA was quantified by real time PCR (Roche Diagnostics GmbH) using the SYBR Green PCR Master Mix. mtDNA content was calculated by taking the ratio of mtDNA to the nuclear DNA (nDNA). The nuclear encoded gene, glyceraldehyde 3-phosphate dehydrogenase (*GAPDH*) and the mitochondrial encoded gene, cytochrome *c* oxidase subunit 1/2 (*COX1/2*) were chosen for mtDNA content estimation [Kim et al., 2007].

Blue Native-PAGE

Blue native-PAGE (BN-PAGE) was performed to analyse the assembly of mitochondrial respiratory chain complexes. Mitochondria were isolated from *D. discoideum* cells [control, *ADPRT1A* OE, *ADPRT1A* KO, *PARP* dR and benzamide (1 mM) treated control cells] and mitochondrial pellet were resuspended in solubilisation buffer (50 mM NaCl, 50 mM imidazole/HCl, 2 mM 6-aminohexanoic acid, 1 mM EDTA, pH 7) [Nagayama et al., 2008]. Amount of protein was quantified by Lowry method [Lowry et al., 1951]. Mitochondrial membrane was then solubilised using Triton X-100 (20%) and the samples were centrifuged at 20,000 g for 45 min at 4°C. Coomassie blue-G250 dye (5% in 750 mM 6-aminohexanoic acid) was added to supernatant to set detergent to Coomassie-dye ratio of 4:1 (g/g). This supernatant was subjected to BN-PAGE using 4–13% acrylamide gradient gels (with 1.0 mm sample wells) and run at 150 V for 2–3 h at 4°C as described by Jha et al. [2016].

Mitochondrial morphology

Mitochondrial morphology of *D. discoideum* cells (control, *ADPRT1A* OE, *ADPRT1A* KO, and *PARP* dR cells) was examined by transmission electron microscopy (TEM). Log phase cells were fixed with 2% glutaraldehyde in cold phosphate buffered solution, pH 7.2 at 4°C for 1 h and processed as described by Kosta et al. [2008] and Rajawat et al. [2014a]. Thin cell sections were obtained with a Reichert Ultracut E ultramicrotome, stained and observed under TEM (Morgagni 268D, FEI electron optics company Philips). Mitochondrial surface area was measured by using ImageJ software.

Statistical analysis

Data are presented as a mean and standard error of the mean or standard deviation as applicable. Statistical analysis was performed using GraphPad PRISM® 6, GraphPad software Inc. and Student's unpaired *t*-test was used to assess statistical significance for experiments with single comparison.

Author contribution

R.B., T.J .and A.K. designed the study. A.K., R.R., A.G., N.P., S.P.P. and R.B. conducted the study and acquired, analysed and interpreted the data. A.K. and R.B. drafted the manuscript. R.B., T.J., A.K., R.R.,

A.G., N.P. and S.P.P. critically reviewed and edited the manuscript.

Funding

R.B. thanks Council of Scientific and Industrial Research (CSIR), New Delhi [38(1383)/14/EMR-II] for financial support. We acknowledge Sophisticated Analytical Instrumentation Facility—All India Institute of Medical Sciences (SAIF-AIIMS), New Delhi for TEM facility. A.K. thanks CSIR, New Delhi for awarding Senior Research Fellowship (SRF).

Conflict of interest statement

The authors have declared no conflict of interest.

References

Annesley, S.J. and Fisher, P.R. (2009) *Dictyostelium discoideum* –a model for many reasons. Mol. Cell. Biochem. **329**, 73–91.

Begum, R. and Saran, S. (2020) Glimpses of dictyostelid research in India. Int. J. Dev. Biol. https://doi.org/10.1387/ijdb.190208 (In Press).

Brunyzanski, A., Olah, G., Coletta, C., Szczesny, B. and Szabo, C. (2014) Regulation of mitochondrial Poly(ADP-Ribose) Polymerase activation by the b-Adrenoceptor/cAMP/Protein Kinase A axis during oxidative stress. Mol. Pharmacol. **86**, 450–462.

Brunyzanski, A., Szczesny, B., Virag, L. and Szabo, C. (2016) Mitochondrial poly (ADP-ribose) polymerase: the wizard of oz at work. Free Radic. Biol. Med. **100**, 257-270.

Du, L., Zhang, X., Han, Y.Y., Burke, N.A., Kochanek, P.M., Watkins, S.C., Graham, S.H., Carcillo, J.A., Szabó, C. and Clark, R.S. (2003) Intra-mitochondrial poly(ADP-ribosylation) contributes to NAD1 depletion and cell death induced by oxidative stress. J. Biol. Chem. **278**, 18426-18433.

Finner, G.N. and Newell, P.C. (1987) GTP analogues stimulate inositol trisphosphate formation transiently in *Dictyostelium*. J. Cell Sci. **87**, 513-518.

Giansanti, V., Donà, F., Tillhon, M. and Scovassi, A.I. (2010) PARP inhibitors: new tools to protect from inflammation. Biochem. Pharmacol. **80**, 1869-1877.

Gilbertson, T.A., Scobey, R. and Wilson, M. (1991) Permeation of calcium ions through non-NMDA glutamate channels in retinal bipolar cells. Science **251**, 1613-1615.

Gomes, L.C., Di Benedetto, G. and Scorrano, L. (2011) During autophagy mitochondria elongate, are spared from degradation and sustain cell viability. Nat. Cell Biol. **13**, 589-598.

Hermann, G.J., Thatcher, J.W., Mills, J.P., Hales, K.G., Fuller, M.T., Nunnari, J. and Shaw, J.M. (1998) Mitochondrial fusion in yeast requires the transmembrane GTPase Fzo1p. J. Cell Biol. **143**, 359-373.

Hirst, J., King, M.S. and Pryde, K.R. (2008) The production of reactive oxygen species by complex I. Biochem. Soc. Trans. **36**, 976-80.

Hossain, M.B., Ji, P., Anish, R., Jacobson, R.H. and Takada, S. (2009) Poly(ADP-Ribose) polymerase 1 interacts with nuclear respiratory factor 1 (NRF-1) and plays a role in NRF-1 transcriptional regulation. J. Biol. Chem. **284**, 8621-8632.

Houtkooper, R.H., Williams, R.W. and Auwerx, J. (2010) Metabolic networks of longevity. Cell **142**, 9-14.

Jagtap, P. and Szabo, C. (2005) Poly(ADP-ribose) polymerase and the therapeutic effects of its inhibitors. Nat. Rev. Drug Discov. **4**, 421-440.

Jha, P., Wang, X. and Auwerx, J. (2016) Analysis of mitochondrial respiratory chain supercomplexes using blue native polyacrylamide gel electrophoresis (BN-PAGE). Curr. Protoc. Mouse Biol. **6**, 1-14.

Jubin, T., Kadam, A. and Begum, R. (2019a) Poly (ADP-ribose) polymerase (PARP-1) regulates developmental morphogenesis and chemotaxis in *Dictyostelium discoideum*. Biol. Cell **111**, 187-197.

Jubin, T., Kadam, A., Gani, A.R., Singh, M., Dwivedi, M. and Begum, R. (2017) Poly ADP-ribose polymerase-1: beyond transcription and towards differentiation. Semin. Cell Dev. Biol. **63**, 167-179.

Jubin, T., Kadam, A., Jariwala, M., Bhatt, S., Sutariya, S., Gani, A.R., Gautam, S. and Begum, R. (2016a) The PARP family: insights into the functional aspects of Poly (ADP-ribose) polymerase-1 in cellular growth and survival. Cell Prolif. **49**, 421-437.

Jubin, T., Kadam, A., Saran, S. and Begum, R. (2016b) Poly (ADP-ribose) polymerase1 regulates growth and multicellularity in *D. discoideum*. Differentiation **92**, 10-23.

Jubin, T., Kadam, A., Saran, S. and Begum, R. (2019b) Crucial role of poly (ADP-ribose) polymerase (PARP-1) in cellular proliferation of *Dictyostelium discoideum*. J. Cell Physiol. **234**, 7539-7547.

Kadam, A., Jubin, T., Mir, H. and Begum, R. (2017) Potential role of Apoptosis Inducing Factor in evolutionarily significant eukaryote, *Dictyostelium discoideum* survival. Biochim. Biophys. Acta Gen. Subj. **1861**, 2942-2955.

Kadam, A., Mehta, D., Jubin, T. and Mansuri, M.S., Begum, R. (2020) Apoptosis inducing factor: cellular protective function in *Dictyostelium discoideum*. Biochim. Biophys. Acta Bioenerg. **1861**, 148158.

Katoch, B. and Begum, R. (2003) Biochemical basis of the high resistance to oxidative stress in *Dictyostelium discoideum*. J. Biosci. **28**, 581-588.

Katoch, B., Sebastian, S., Sahdev, S., Padh, H., Hasnain, S.E. and Begum, R. (2002) Programmed cell death and its clinical implications. Ind. J. Exp. Biol. **40**, 513-524.

Kauppinen, T.M., Chan, W.Y., Suh, S.W., Wiggins, A.K., Huang, E.J. and Swanson, R.A. (2006) Direct phosphorylation and regulation of poly(ADP-ribose) polymerase-1 by extracellular signal regulated kinases 1/2. Proc. Natl. Acad. Sci. U.S.A. **103**, 7136-7141.

Kawal, A.M., Mir, H., Ramniklal, C.K., Rajawat, J. and Begum, R. (2011) Structural and evolutionary analysis of PARPs in *D. discoideum*. Am. J. Infect. Dis. **7**, 67-74.

Kim, H.L., Choi, Y.K., Kim, D.H., Park, S.O., Han, J. and Park, Y.S. (2007) Tetrahydropteridine deficiency impairs mitochondrial function in *Dictyostelium discoideum* Ax2. FEBS Lett. **581**, 5430-5434.

Kosta, A., Luciani, M.F., Geerts, W.J.C. and Golstein, P. (2008) Marked mitochondrial alterations upon starvation without cell death, caspases or Bcl-2 family members. Biochim. Biophys. Acta **1783**, 2013-2019.

Krishnakumar, R. and Kraus, W.L. (2010) PARP-1 regulates chromatin structure and transcription through a KDM5B-dependent pathway. Mol. Cell **39**, 736-749.

Lai, Y., Chen, Y., Watkins, S.C., Nathaniel, P.D., Guo, F., Kochanek, P.M., Jen-kins, L.W., Szabo, C. and Clark, R.S. (2008) Identification of poly-ADP-ribosylated mitochondrial proteins after traumatic brain injury. J. Neurochem. **104**, 1700-1711.

Lapucci, A., Pittelli, M., Rapizzi, E., Felici, R., Moroni, F. and Chiarugi, A. (2011) Poly(ADP-ribose) polymerase-1 is a nuclear epigenetic regulator of mitochondrial DNA repair and transcription. Mol. Pharmacol. **79**, 932-940.

Leoncini, G., Buzzi, E., Maresca, M., Mazzel, M. and Balbi, A. (1987) Alkaline extraction and reverse phase high-performance liquid chromatography of adenine and pyridine nucleotides in human platelets. Anal. Biochem. **165**, 379-383.

Livak, K.J. and Schmittgen, T.D. (2001) Analysis of relative gene expression data using real-time quantitative PCR and the 2(-Delta Delta C(T)) Method. Methods **25**, 402-408.

Lowry, O.H., Rosebrough, N.J. and Farr, A.L., Randall, R.J. (1951) Protein measurement with the Folin phenol reagent. J. Biol. Chem. **93**, 265-275.

Mir, H., Alex, T., Rajawat, J., Kadam, A. and Begum, R. (2015) Response of *D. discoideum* to UV-C and involvement of poly(ADP-ribose) polymerase. Cell Prolif. **48**, 363-374.

Mir, H., Rajawat, J. and Begum, R. (2012) Staurosporine induced cell death in *D. discoideum* is independent of PARP. Ind. J. Exp. Biol. **50**, 80-86.

Mir, H., Rajawat, J., Pradhan, S. and Begum, R. (2007) Signaling molecules involved in the transition of growth to development of *Dictyostelium discoideum*. Ind. J. Exp. Biol. **45**, 223-236.

Modis, K., Gero, D., Erdelyi, K., Szoleczky, P., Dewitt, D. and Szabo, C. (2012) Cellular bioenergetics is regulated by PARP1 under resting conditions and during oxidative stress. Biochem. Pharmacol. **83**, 633-643.

Myhre, O., Andersen, J.M., Aarnes, H. and Fonnum, F. (2003) Evaluation of the probes 2,7-dichlorofluorescein diacetate, luminol, and lucigenin as indicators of reactive species formation. Biochem. Pharmacol. **65**, 1575-1582.

Nagayama, K., Itono, S., Yoshida, T., Ishiguro, S., Ochiai, H. and Ohmachi, T. (2008) Antisense RNA inhibition of the b subunit of the *Dictyostelium discoideum* mitochondrial processing peptidase induces the expression of mitochondrial proteins. Biosci. Biotechnol. Biochem. **72**, 1836-1846.

Niere, M., Kernstock, S., Koch-Nolte, F. and Ziegler, M. (2008) Functional localization of two poly(ADP-ribose)-degrading enzymes to the mitochondrial matrix. Mol. Cell. Biol. **28**, 814-824.

Pilcher, K.E., Fey, P., Gaudet, P., Kowal, A.S. and Chisholm, R.L. (2007) A reliable general purpose method for extracting genomic DNA from *Dictyostelium* cells. Nat. Protoc. **2**, 1325-1328.

Pitkanen, S. and Robinson, B.H. (1996) Mitochondrial complex I deficiency leads to increased production of superoxide radicals and induction of superoxide dismutase. J. Clin. Invest. **98**, 345-351.

Potaman, V.N., Shlyakhtenko, L.S., Oussatcheva, E.A., Lyubchenko, Y.L. and Soldatenkov, V.A. (2005) Specific binding of poly(ADP-ribose) polymerase-1 to cruciform hairpins. J. Mol. Biol. **348**, 609-615.

Rajawat, J., Alex, T., Mir, H., Kadam, A. and Begum, R. (2014a) Proteases involved during oxidative stress induced poly(ADP-ribose) polymerase mediated cell death in *D. discoideum*. Microbiology **160**, 1101-1111.

Rajawat, J., Mir, H. and Begum, R. (2011) Differential role of poly(ADP-ribose) polymerase (PARP) in *D. discoideum*. BMC Dev. Biol. **11**, 14.

Rajawat, J., Mir, H., Alex, T., Bakshi, S. and Begum, R. (2014b) Involvement of poly(ADP-ribose) polymerase in paraptotic cell death of *D. discoideum*. Apoptosis **19**, 90-101.

Rajawat, J., Vohra, I., Mir, H.A., Gohel, D. and Begum, R. (2007) Effect of oxidative stress and involvement of poly(ADP-ribose) polymerase (PARP) in *Dictyostelium discoideum* development. FEBS J. **274**, 5611-5618.

Rambold, A.S., Kostelecky, B., Elia, N. and Lippincott-Schwartz, J. (2011) Tubular network formation protects mitochondria from autophagosomal degradation during nutrient starvation. Proc. Natl. Acad. Sci. U.S.A. **108**, 10190-10195.

Rossi, M.N., Carbone, M., Mostocotto, C., Mancone, C., Tripodi, M., Maione, R. and Amati, P. (2009) Mitochondrial localization of PARP-1 requires interaction with mitofilin and is involved in the maintenance of mitochondrial DNA integrity. J. Biol. Chem. **284**, 31616-31624.

Sakamuru, S., Attene-Ramos, M.S. and Xia, M. (2016) Mitochondrial membrane potential assay. Methods Mol. Biol. **1473**, 17-22.

Scott, I. and Youle, R.J. (2010) Mitochondrial fission fusion. Essays Biochem. **47**, 85-98.

Sharma, L.K., Fang, H., Liu, J., Vartak, R., Deng, J. and Bai, Y. (2011) Mitochondrial respiratory complex I dysfunction promotes tumorigenesis through ROS alteration and AKT activation. Hum. Mol. Genet. **20**, 4605-4616.

Sodhi, R.K., Singh, N. and Jaggi, A.S. (2010) Poly(ADP-ribose) polymerase-1 (PARP-1) and its therapeutic implications. Vascul. Pharmacol. **53**, 77-87.

Stein, L.R. and Imai, S. (2012) The dynamic regulation of NAD metabolism in mitochondria. Trends Endocrinol. Metab. **23**, 420-428.

Szabo, C. and Dawson, V.L. (1998) Role of poly(ADP-ribose) synthetase in inflammation and ischaemia-reperfusion. Trends Pharmacol. Sci. **19**, 287-298.

Szczesny, B., Brunyanszki, A., Olah, G., Mitra, S. and Szabo, C. (2014) Opposing roles of mitochondrial and nuclear PARP1 in the regulation of mitochondrial and nuclear DNA integrity: implications for the regulation of mitochondrial function. Nucleic Acids Res. **42**, 13161-13173.

Twig, G., Elorza, A., Molina, A.J., Mohamed, H., Wikstrom, J.D., Walzer, G., Stiles, L., Haigh, S.E., Katz, S., Las, G., Alroy, J., Wu, M., Py, B.F., Yuan, J., Deeney, J.T., Corkey, B.E. and Shirihai, O.S. (2008) Fission and selective fusion govern mitochondrial segregation and elimination by autophagy. EMBO J. **27**, 433-446.

Van Coster, R., Smet, J., George, E., De Meirleir, L., Seneca, S., Van Hove, J., Sebire, G., Verhelst, H., De Bleecker, J., Van Vlem, B., Verloo, P. and Leroy, J. (2001) Blue native polyacrylamide gel electrophoresis: a powerful tool in diagnosis of oxidative phosphorylation defects. Pediatr. Res. **50**, 658-665.

van der Bliek, A.M., Shen, Q. and Kawajiri, S. (2013) Mechanisms of mitochondrial fission and fusion. Cold Spring Harb. Perspect. Biol. **5**, a011072.

Watts, D.J. and Ashworth, J.M. (1970) Growth of myxamoebae of the cellular slime mould *Dictyostelium discoideum* in axenic culture. Biochem. J. **119**, 171-174.

Westermann, B. (2012) Bioenergetic role of mitochondrial fusion and fission. Biochim. Biophys. Acta **1817**, 1833-1838.

Zhang, C., Ma, T., Luo, T., Li, A., Gao, X., Wang, Z.G. and Li, F. (2018) Dysregulation of PARP1 is involved in development of Barrett's esophagus. World J. Gastroenterol. **24**, 982-991.

Received: 9 December 2019; Accepted: 15 April 2020; Accepted article online: 23 April 2020